HANDBOOK OF INDUSTRIAL REFRACTORIES TECHNOLOGY

Principles, Types, Properties and Applications

Reprint Edition

by

Stephen C. Carniglia

University of California, Davis
Davis, California

and

Gordon L. Barna

National Refractories & Minerals Corporation
Livermore, California

np NOYES PUBLICATIONS
Westwood, New Jersey, U.S.A.

Library of Congress Catalog Card Number: 92-4458
ISBN: 0-8155-1304-6
Printed in the United States

Published in the United States of America by
Noyes Publications
Fairview Avenue, Westwood, New Jersey 07675

10 9 8 7 6 5 4

Library of Congress Cataloging-in-Publication Data

Carniglia, Stephen C.
Handbook of industrial refractories technology : principles, types, properties, and applications / by Stephen C. Carniglia, Gordon L. Barna.
p. cm.
Includes bibliographical references and index.
ISBN 0-8155-1304-6
1. Refractory materials--Handbooks, manuals, etc. I. Barna, Gordon L. II. Title.
TP838.C27 1992
666'.72--dc20 92-4458
CIP

MATERIALS SCIENCE AND PROCESS TECHNOLOGY SERIES

Electronic Materials and Process Technology

DEPOSITION TECHNOLOGIES FOR FILMS AND COATINGS: by Rointan F. Bunshah et al

CHEMICAL VAPOR DEPOSITION FOR MICROELECTRONICS: by Arthur Sherman

SEMICONDUCTOR MATERIALS AND PROCESS TECHNOLOGY HANDBOOK: edited by Gary E. McGuire

HYBRID MICROCIRCUIT TECHNOLOGY HANDBOOK: by James J. Licari and Leonard R. Enlow

HANDBOOK OF THIN FILM DEPOSITION PROCESSES AND TECHNIQUES: edited by Klaus K. Schuegraf

IONIZED-CLUSTER BEAM DEPOSITION AND EPITAXY: by Toshinori Takagi

DIFFUSION PHENOMENA IN THIN FILMS AND MICROELECTRONIC MATERIALS: edited by Devendra Gupta and Paul S. Ho

HANDBOOK OF CONTAMINATION CONTROL IN MICROELECTRONICS: edited by Donald L. Tolliver

HANDBOOK OF ION BEAM PROCESSING TECHNOLOGY: edited by Jerome J. Cuomo, Stephen M. Rossnagel, and Harold R. Kaufman

CHARACTERIZATION OF SEMICONDUCTOR MATERIALS–Volume 1: edited by Gary E. McGuire

HANDBOOK OF PLASMA PROCESSING TECHNOLOGY: edited by Stephen M. Rossnagel, Jerome J. Cuomo, and William D. Westwood

HANDBOOK OF SEMICONDUCTOR SILICON TECHNOLOGY: edited by William C. O'Mara, Robert B. Herring, and Lee P. Hunt

HANDBOOK OF POLYMER COATINGS FOR ELECTRONICS: by James J. Licari and Laura A. Hughes

HANDBOOK OF SPUTTER DEPOSITION TECHNOLOGY: by Kiyotaka Wasa and Shigeru Hayakawa

HANDBOOK OF VLSI MICROLITHOGRAPHY: edited by William B. Glendinning and John N. Helbert

CHEMISTRY OF SUPERCONDUCTOR MATERIALS: edited by Terrell A. Vanderah

CHEMICAL VAPOR DEPOSITION OF TUNGSTEN AND TUNGSTEN SILICIDES: by John E.J. Schmitz

ELECTROCHEMISTRY OF SEMICONDUCTORS AND ELECTRONICS: edited by John McHardy and Frank Ludwig

HANDBOOK OF CHEMICAL VAPOR DEPOSITION: by Hugh O. Pierson

(continued)

Ceramic and Other Materials–Processing and Technology

SOL-GEL TECHNOLOGY FOR THIN FILMS, FIBERS, PREFORMS, ELECTRONICS AND SPECIALTY SHAPES: edited by Lisa C. Klein

FIBER REINFORCED CERAMIC COMPOSITES: by K.S. Mazdiyasni

ADVANCED CERAMIC PROCESSING AND TECHNOLOGY–Volume 1: edited by Jon G.P. Binner

FRICTION AND WEAR TRANSITIONS OF MATERIALS: by Peter J. Blau

SHOCK WAVES FOR INDUSTRIAL APPLICATIONS: edited by Lawrence E. Murr

SPECIAL MELTING AND PROCESSING TECHNOLOGIES: edited by G.K. Bhat

CORROSION OF GLASS, CERAMICS AND CERAMIC SUPERCONDUCTORS: edited by David E. Clark and Bruce K. Zoitos

HANDBOOK OF INDUSTRIAL REFRACTORIES TECHNOLOGY: by Stephen C. Carniglia and Gordon L. Barna

Related Titles

ADHESIVES TECHNOLOGY HANDBOOK: by Arthur H. Landrock

HANDBOOK OF THERMOSET PLASTICS: edited by Sidney H. Goodman

SURFACE PREPARATION TECHNIQUES FOR ADHESIVE BONDING: by Raymond F. Wegman

FORMULATING PLASTICS AND ELASTOMERS BY COMPUTER: by Ralph D. Hermansen

HANDBOOK OF ADHESIVE BONDED STRUCTURAL REPAIR: by Raymond F. Wegman and Thomas R. Tullos

Preface

Refractories are a family of technical ceramics. They manage industrial process heat, defying thermal and mechanical abuse and high-temperature chemical attack. Their technology is a saga of ongoing advancement and sophistication.

After describing representative hot processes, their vessels and demands, we commence by laying the foundations of thermal and mechanical integrity and of corrosion resistance. These qualities and the demands imposed are traced to contemporary refractory compositions and microstructures, from mineral-based to synthetics and from dense working refractories to lightweight insulating materials. Criteria are developed for their selection and use. All major refractory manufacturing methods are described, founded on material behavior in their unit operations. Modern configurations and techniques of installation are presented. The chemical, physical, and mechanical properties needed for refractory system design are catalogued, together with considerations of quality, reliability, and alteration in service.

We have drawn from both science and engineering in describing how refractories behave and how they are made and utilized. The resort to fundamentals is confined to what is relevant. The same is true of modern numerical computation methods: these are too lengthily derived for repetition here in full. The serious pursuit of any facet of the subject will require further reading.

To that end we have listed over five hundred technical references and about three hundred applicable patents. Preference has been given to the more recent publications, including expert review articles. Their bibliographies in turn should open up most of the further resources which the reader might need. This being the case, we have indulged in certain economies.

First, we have generally refrained from crediting authors by name in the text. The alternative would oblige us to enlarge the reference list about threefold. Second, we have omitted pictorial renditions of manufacturing plants, operating or test equipment and measuring instruments. Such views can not do justice to their variety and elegance. Third, we have consistently omitted illustrative photomicrographs. The literature is so rich with visualized microstructures as to reward its exploration far beyond the capacity of a few occasional examples. Journeys there in depth will immeasurably expand understanding in areas of each reader's preferred inquiry that we cannot anticipate.

We thank the suppliers of illustrations and data, credited in the text or figures and tables. In representing commercial refractories we have drawn largely from U.S. sources as a matter of convenience; but much additional information is taken from the international literature, providing balance. We thank the many colleagues, authors and tutors who have gone without citing, for background and enrichment whose sources are dimmed in memory. Substantive suggestions and encouragement have been received from others unnamed but remembered. Still others who have graciously endured our absence for several years on this project likewise know who they are. The Department of Mechanical, Aeronautical, and Materials Engineering of the University of California, Davis, is thanked for facilitating much of the library research and writing; and Anne Simmons at the University of Utah for typing the text.

Stephen C. Carniglia
Gordon L. Barna

NOTICE

Contents

Chapter I

Introduction

TECHNICAL PERSPECTIVES

An Enabling Industry

What sets homo sapiens apart is the ability to imagine and create. Our era boasts a storehouse of created means of improving the human condition that is at once thrilling and overwhelming. Yet like the fabled red shoes or the sorcerer's broom, discovery and invention will not stop. The arsenal still grows. This book addresses a small but vital segment of that arsenal, a segment that possesses its own unique technology.

How does this small segment so significantly serve?

Virtually every thing provided in an advanced society depends directly or indirectly, somewhere in its background, on manufacturing processes conducted at high temperatures. That goes for every thing we eat, drink, learn, use, wear, occupy or enjoy; for our work, our health and security, our mobility, our comfort and leisure. This thought deserves emphasizing because it is so little appreciated: the positive impact of high-temperature processes on modern life is all-pervasive.

The hot manufacturing processes we have in mind include the making, shaping or treating of metals, ceramics including glasses and cements, electronic materials, fuels, a host of organic and inorganic chemical products, and more. Whatever it is, if it is in any way altered from the natural state, its production may well include high-temperature processes. Now add the production of heat itself, for

conversion into mechanical work or electrical energy. Together, these are the makers of tangible wealth.

Industrial refractories make these hot processes possible and economical when metal containment cannot compete. Refractories are thus *enablers* or *facilitators* of our productivity. For hundreds of millenia before there were any useful metals, hot processing employed combustion as a source of heat and primitive refractories were used to contain fire. Only in the 19th century A.D. did electrical heat sources begin to invade processing. With that enlargement understood, we might encapsulate the place of refractories in industry as, *harnessing fire in the service of man.*

The refractories industry, all told, is relatively small. In the U.S. it amounts to some $1-2 billion of annual production, against several hundred $billion annual output of the industries it serves directly. By and large, its products do not themselves reach consumer markets nor even the awareness of the public. They are not very well known among technologists either, beyond those directly involved in their production and use. In these respects refractories are akin to catalysts: they are technical products performing an enabling function, but substantially out of sight. A recent publication calls refractories "the hidden industry."[1] Our mission here is to provide an authoritative view on their equally unadvertised contemporary technology.

Nature of Refractories and Their Duty

The Duty. The commonest duty of refractories is to contain high temperatures: to erect a solid barrier between hot "inside" and ambient or tolerable "outside." But that duty entails other obligations as well. Mechanical loads must be borne, of both mechanical and thermal origins, both at the service temperature and often through repeated temperature cycles. Criteria of heat transport per se apply: in most uses, the refractory must serve as a thermal insulator; less frequently, as a conductor of heat. In some areas of application, either electrical resistance or electrical conduction is called for.

But the greatest challenge to refractories occurs as they face hot, corrosive fluids. This is where metals are most often disqualified. Corrosive attack increases in severity with increasing temperature. Industrial fluids are furthermore rarely quiescent, usually rapid-flowing. Corrosive attack is thus further enhanced and augmented by erosion. Since many such fluids carry entrained particulates, abrasion must be borne as well. It goes without saying that any exterior metalwork must be isolated physically from the hot corrosive medium: joints in the refractory must be tight, and dimensional and phase stability are called for to prevent the development of leaks or "runout" as well as to retain mechanical strength.

Only a few of these considerations have to do with the function, or duty, of a refractory installation. About twice as many are considerations of its integrity: its reliability and durability in service. They are in summary:

Considerations of Function

Permeability	Electrical Conductivity
Thermal Conductivity	Cost (relative to
Heat Capacity	feasible alternatives)

Considerations of Integrity

Melting & Vaporization	Thermal Expansion
Dimensional & Phase Stability	Corrosion Resistance
Strength & Flow Properties	Erosion Resistance
Elastic Properties	Abrasion Resistance

The technology of each refractory application has to address all of these considerations simultaneously. The quantitative specifications and the relative stringency or importance of each one may vary widely from case to case, even from place to place in a given installation. Not all desired combinations of properties can be obtained by material selection. Best solutions are approached by comprehensive engineering design of each refractory system, which includes selection of materials, their types, forms, dimensions and configurations, system dimensions and configuration, methods of installation and support, and methods and schedules of patching, repair and maintenance. Installation methods include masonry construction, a variety of monolithic techniques, light-weight preform installation, and others. Refractory system design is multidisciplinary, including a detailed familiarity with each process or operation to be served as well as an intimate knowledge of the available refractory materials.

The Materials. Refractories are a category of technical ceramics. Industrial refractories are almost all complex combinations of high-melting crystalline oxides, plus a few carbides, carbon and graphite. Polycrystalline ceramics are characteristically brittle, and far less strong in tension than in compression. They are subject to considerable variability in strength, resulting from local variations in their microstructure and their lack of ductility. They exhibit high-temperature creep or plastic deformation, but almost always by a mechanism different from that operating in metals. Their mechanisms of conduction of heat and electricity are also different from those of metals. Their elastic moduli are generally quite high; this and their brittleness make them somewhat prone to failure under thermal stress and shock. Compositions can be chosen having selectively high

chemical resistance (but rarely immunity) to oxidizing or reducing agents, acids or bases, metals or salts, whether liquid or gaseous.

Shaped refractory objects are typically made by particulate forming processes. Their thermal maturing or sintering produces a wide variety of phase compositions and microstructural features. Most fired industrial refractories have experienced "liquid-phase" sintering; and for this and other reasons they contain porosity. Both the lower-melting intercrystalline phases and the porosity influence mechanical and thermal properties, and both have much to do with penetration by corrosive media. Only a few refractories are made essentially pore-free and without selective phase melting.

The variety of phase compositions and structures sought in refractory manufacture is thus greater than in metals, and in some ways different in kind. The manufacturing methods themselves are more varied, and mostly different in kind. The fundamental connections made between properties and structure are in some ways unique to nonmetallic materials. And finally, there is an intense concern with the preparation and characterization of particulate starting materials, of pivotal importance in ceramic synthesis but infrequently of any interest at all in metal manufacture. These starting materials are often minerals, as opposed to high-purity synthetic chemicals.

Thus the technology of refractory materials and their properties alone is itself a multidisciplinary matter. Refractory materials are best comprehended on a foundation of ceramic science and engineering or of materials science and engineering. Specifically, we shall be dealing mostly in inorganic chemistry, kinetics and thermodynamics; solutions and phase equilibria; the rudiments of nonmetallic crystalline and vitreous structure; the thermomechanical properties of solids including fundamentals of elasticity, plastic flow, and fracture; and concepts of heat, heat transport and electrical transport -- not to mention also, ceramic synthesis.

The Challenge of Product Quality

Processing of minerals faces inevitable variations in raw material composition. Processing of particulates faces inevitable variations in their sizing and size distributions. High-temperature processing of complex solid mixtures faces the inevitable variation of their final phase composition and microstructure. The compaction of particulates into formed shapes prior to firing is a further source of variability; this is telegraphed in turn to the firing operation and thence on to the product.

This description is by no means exhaustive, but its point is clear: refractory products risk variation about the mean of any of their properties or characteristics owing to a long chain of deviations from

material and process norms. These risks encompass such matters as finished dimensions and flatness, density and porosity, and all manner of inhomogeneities. Another roster of risks applies to unfired monolithic refractory preparations, such as their shelf-life, workability, installed density, dimensional change on heating in service, and a comparable list of potential inhomogeneities.

An installed refractory system tends to obey the rule of the weakest link; and this can apply not only to an inferior batch or lot but to a single masonry unit within any lot. A critical refractory installation is not superior unless all of it is superior. Meticulous attention to processing detail has to accompany the development of every advanced refractory product. But refractories are still ceramics, and some variability remains.

Later in this book we shall give attention to quality assurance (Q.A.) in refractories: to matters of product uniformity and reproducibility. It is not enough simply to identify and reject inferior finished units or lots; competitive profit margins cannot sustain a significant load of wasted product. Statistical approaches to head-end problem recognition, early process correction, and in-process verification can be very effective in Q.A. But even these techniques alone are not enough. The individual concern, involvement, and knowledgeability of the entire production workforce have to be mobilized. Given an unrelenting vigilance, the challenge of product quality can be met.

The Challenge of Chemical Alteration

As refractories are employed in many different processing operations, they face various performance demands in as many different chemical environments. Corrosion by the environment is trivial in only a few of these usages. Examples can be found in heat-treating and annealing furnaces and in ovens and air ducting.

In the much more typical case, corrosion is at least a significant if not a dominant factor in refractory serviceability and life. Ferrous metallurgy provides dramatic examples (about half of all refractory tonnage goes into the making and handling of molten iron and its alloys). Most nonferrous metal smelting and remelting operations similarly exemplify the importance of refractory corrosion. Most glass-making environments are by nature highly corrosive. Lime, cement, carbon, ceramic, and numerous inorganic chemical manufacturing processes also entail corrosion of their furnace or kiln linings to a greater or lesser degree. Likewise do steam plants, boilers, incinerators, and high-temperature stills. Most electrical heat sources as well as burners in industry are life-limited by corrosion. These examples add up to the lion's share of all industrial refractory consumption.

Corrosion of refractories is rarely a simple matter of recession of the "hot face" or working surface alone. Penetration to some depth into the refractory is a common occurrence. Reactive gases may permeate up to many inches of refractory thickness. Fortunately, gas penetration is usually down a temperature gradient such that the corrosion rate decreases exponentially with increasing depth. Reactive liquids or liquid corrosion products may similarly penetrate, to a depth ultimately limited by the temperature at which they freeze. This depth may be from a few millimeters up to several inches.

The refractory in service thus risks becoming significantly altered in its chemical and phase composition, over some appreciable thickness behind its working face. The remaining material lying behind this is in most cases essentially unaltered. The original refractory is in effect replaced by a duplex or two-layer system. The layer now facing the bulk of the hot corrosive environment has a new set of properties corresponding to its altered condition. These new properties may or may not include significantly decreased rigidity and hot strength as well as resistance to recession. Ordinarily, unless carefully planned for, they do. But chemical alteration also often works against dimensional and phase stability, this fact becoming unhappily evident upon thermal or even atmospheric cycling. The boundary between altered and unaltered layers or zones is particularly susceptible to shear failure in this situation, resulting in periodic loss of the altered material in slabs. But decrepitation within the altered layer itself by ratcheting apart of grains is also not uncommon. In the light of these more dramatic risks, an altered thermal conduction affecting the backside or "cold face" temperature may seem relatively trivial; but because of them it is not trivial at all. The loss of external metal support or containment due to overheating can be disastrous.

Opportunities to prevent corrosion and alteration thermodynamically in refractories are severely limited. But the kinetic control of alteration leaves room for some considerable variety and ingenuity of approach. In describing advanced refractories and their more demanding applications, we shall point out not only how altered properties affect their performance, but also how recognition and prediction of the modes of chemical alteration have been used to formulate still more remarkably corrosion-resistant materials.

HISTORICAL PERSPECTIVES

Refractory Materials in Retrospect

Refractories technology has evolved from early origins of uninformed trial-and-error, through the collection of more and more

experience permitting informed trial-and-error, to a time now when predictions can be made based on organized knowledge in both the central and peripheral fields. The making and testing of predictions in that way is the introduction of science into the creative process. But there is also an element of inspiration in invention, not to mention an element of courage. The overall historical progress of refractories, on the other hand, illustrates the power of a still further element as well: motivation, or the perceived need for change.

Millenia of Clay and Stone. The earliest baking oven found, in China, is said to have dated about 30,000 B.C. Baking ovens were common in the Middle East by 10,000 B.C. Natural rocks and clays served adequately as refractories for thousands of years from those beginnings, while ovens were wood-fired. The introduction of charcoal made little difference: temperatures could hardly have exceeded about 800°C. Convective-draft and forced-draft furnace designs, introduced around 4,000 B.C., raised maximum temperatures to about 1100°C and opened the Ages of Metals; but stone, clay, and fired clay ("firebrick") refractories still served.

Count off another 5,000 years, plus or minus. While porcelain was being made in China at 1350°C by about 600 A.D., water-powered bellows and vertical kiln designs were combined into the earliest metallurgical blast furnaces in Europe by about 1400 A.D. Fueled mostly by charcoal, these gave working temperatures around 1500°C. Iron could then be melted, treated and cast. Still there was no need for any refractories but fireclay and stone. Count off still another 400 years to the Machine Age and the Industrial Revolution.

The regenerative blast furnace, using pre-heated air, brought maximum temperatures up close to 1700°C in the mid-1830s and following. This type of furnace was first built of shaped blocks or stones of natural steatite (soapstone), which had been known as such and used for centuries. Stone and selected fireclays were by then in use all over the world for lower-temperature processes including glassmaking. While the very next new furnace invention to come would exceed the capability of those original refractories, it had not quite come yet. Nor had the durability demands of mass production.

Recall that by 1830 the Age of Science was already some 200 years old; the British Royal Society was founded in 1660. A diversified chemical industry existed. Steam power was in use, and electricity had been discovered. Extensive scientific knowledge was being put to use in sophisticated glassmaking and in ferrous and nonferrous metallurgy. Why was there yet no scientifically-based refractories technology? Simply put, there was yet no perceived need for radical change.

Entering the Twentieth Century. Refractories remained almost exclusively mineral-based until well into the 20th century, for that same reason. Yet their technologists, who were skilled in mineralogy, were paying attention. Metallurgists had been experimenting with acid and basic slagging practices since the Middle Ages, and had catalogued some of the benefits of each. Refractory artisans had correspondingly experimented with ganister and other nearly-pure silica minerals, and with magnesite, a predominantly $MgC0_3$ mineral which was calcined to Mg0. When the Bessemer steelmaking converter was invented in 1856, combining working temperatures of over 1600°C with corrosive acid slagging, "acid" silica refractories were all but ready. When the Siemens open hearth furnace followed in 1857 at even higher temperatures, and steelmaking went over in both cases to corrosive basic slagging, "basic" magnesite linings were soon introduced. Basic refractories made from dolomite (Mg0-Ca0) were developed during World War I, when the European magnesite supply was cut off from the Allies. Later, with the development of other mineral resources worldwide, magnesite reasserted itself.

Meanwhile, bonded carbon bricks were produced in England starting in 1863 and eventually found their way into the iron-smelting blast furnace as its working temperatures climbed still higher. They also went quickly into the Hall-Héroult cells for the production of aluminum (1886).

Lime had been made for some 5,000 years using clay and then firebrick kilns. Portland cement first called for an innovative refractory when rotary kilns were introduced after 1877. The first resistant linings were made of cement-bonded cement clinker. Later on, more durable commercial refractories returned to this industry.

Recuperative and regenerative furnaces originating in the newborn manufacture of steel in the 1850s were introduced into nonferrous metallurgy and glassmaking in the late 19th century. Fireclay refractories had to be superseded there, too. Magnesite linings were used in copper converters from 1909, and in the first modern glass tanks about ten years later. Electric arc furnaces were first tried for steelmaking in 1853, and became common after 1900. A 100-ton unit installed in the U.S. in 1927 employed a magnesite lining.

Three-phase arc furnaces were in place before 1950; it was only then that serious demands arose for more sophisticated refractories. In the same time frame, oxygen blowing was introduced into Bessemer and open-hearth furnaces in the 1940s. The basic oxygen furnace (BOF), a logical but inspired design outgrowth, literally took over steelmaking commencing in the late 1950s. Oxygen blowing, by its sheer dollar volume importance, impelled the

refractories industry for the first time to introduce *synthetic* materials into its products on a significant scale.

Coming of Age: Modern Refractories. This insistent call for higher-performance refractories coincided with the Age of Technology in America. All the supporting sciences and industries were in operation (though not necessarily tuned to the needs of refractories). Ceramics had grown substantially from craft to applied science. The American Ceramic Society had been founded in 1899, the British Ceramic Society in 1901. Oxide phase diagrams began to appear in the literature in the 1920s. The techniques of petrography were well developed, and the detailed mechanisms of refractory degradation and wear were beginning to be understood. American refractory producers had become largely reorganized, consolidated, and capable of performing their own research.[1] The tools of refractory synthesis and instruments of investigation were both burgeoning.

Synthetic industrial carbons were of course not new. Coke was first made commercially from coal in the 1860s, and from petroleum shortly thereafter. Synthetic graphite and silicon carbide appeared almost simultaneously at the turn of the century, following Acheson's self-resistance-heated electric furnace invention in 1896. These products, having properties quite unlike those of oxides, rapidly stimulated their own uses and markets.

Synthetic alumina, Al_2O_3, had been available since the Bayer process started feeding aluminum production about 1888. Synthetic magnesia, MgO, was first made from seawater in England in 1937 and in the U.S. in 1942, stimulated by wartime needs for magnesium. Zirconia, ZrO_2, had become available, also spurred by the military. Lime had been a major commodity for ages. A host of other chemicals were on hand for consideration as refractory components or as minor additives and bonding agents. The only important component of oxide refractories that has resisted any very considerable replacement by synthetics is silica, SiO_2. High-purity silica rocks and sands abound and are used in this industry as well as in glass formulation.

The use of synthetics in refractory manufacture has been enormously helpful; but mineral raw materials have been by no means displaced, nor should they be. Synthetics are not necessarily panaceas. They cost more, and that cost has to be justified. Some synthetic materials create severe problems in refractory processing, and new ways must be found to overcome these. Optimum results have often been achieved by combinations of synthetic and mineral raw materials, with creative inputs into their processing as well.

Innovation had not been lacking in the all-mineral-based product line, either, dating back well into the 19th century. Long

before the 1950s, firebrick formulations had incorporated relatively high-alumina and higher-purity beneficiated minerals such as kaolin, flint, mullite, kyanite, sillimanite, and andalusite. Diaspore and bauxite had been investigated and used. Basic refractories had encompassed magnesite-chrome and chrome-magnesite ("chrome" here referring to chromite ore), and some wholly-chrome compositions had appeared. Alumina-chrome formulations followed shortly. When it was discovered that Al_2O_3 actually injured the performance of SiO_2 refractories, a very low-alumina SiO_2 product was developed.[1]

Mixtures of clay with carbon had been used to line crucibles and ladles since iron was first poured; and silica bricks containing carbon were made in France in the 1860s. Since 1960 both the techniques and the compositions have changed dramatically. The use of carbon-bearing oxide refractories has literally mushroomed, starting with MgO+C. The first real impetus may have been provided by the BOF; but today there is hardly any advanced oxide refractory type that cannot be had either with or without added carbon or a carbon precursor for superior performance in specific applications.

Arc-fused refractory grain or aggregate had been made since the early 1900s, and fused-cast refractory bricks of several compositions followed in the '20s and '30s, notably of mullite, alumina, magnesia-alumina-silica, and alumina-zirconia-silica. More often than not, these products were made entirely from mineral raw materials.

In fact, all-mineral-based refractories remain today an important component of the product menu. The reasons: they are on the whole cheaper, they often perform admirably, and there are still many applications of lesser demand as well as those of critical demand for the highest levels of refractoriness and corrosion resistance.

The successful formulations containing synthetics as well as the enduring all-mineral-based refractories will be given attention in ensuing chapters. For now it suffices to note that when more sophisticated refractory compositions were needed, the technology responded. There has also been ample innovation in other areas besides that of composition alone. The monolithic refractory forms -- installed unfired by casting, tamping, trowelling, gunning and the like -- had ancient beginnings; but for centuries most refractory structures and then linings were of masonry construction. Monolithics gained a real foothold in the 1920s and '30s. Since then they have been greatly improved and multiplied, competing effectively in many areas where masonry was once sacred. Fiber refractories, of very low density and very high thermal insulating quality, also had their real start in the 1930s and have grown explosively in quality and

acceptance since then. These non-masonry refractory forms have revolutionized high-temperature practice in their user industries, substantially since the 1950s.

Furnaces in Retrospect

The challenge to every industrial plant is basically the same: to do its job efficiently and economically, and to endure. In large high-temperature facilities the forces encountered are massive and evident: the thunder of mills and machinery, the crash of tons of material charged into furnaces, the roar of flame, the pyrotechnic glare of pouring "hot metal" or the volcanic glow of incandescent solids, the smoke and smell of all things heated. Some of these forces are present even in quieter circumstances; others, less evident from outside, are insidiously at work as well. Chemical corrosion heads that list.

Well-designed furnaces and refractory systems bear those burdens and perform their duty. That they also endure is an engineering feat to be appreciated only by looking down the 800-foot bore of a running rotary cement kiln, or by watching the full operating cycle of a BOF, or by comprehending the chemistry that inexorably dissolves a glass tank. Today an iron-smelting blast furnace will run far in excess of five years without a major refurbishing, while sustaining operating temperatures approaching 2000°C and feed throughputs, day-in, day-out, exceeding 1,000 tons per hour around the clock.

Durability and reliability were not always so impressive. The devices and their materials of construction have both evolved over time. Contemporary furnaces will be illustrated in ensuing chapters. Some of their predecessors have been mentioned here; but a number of these may not be seen again -- at least, not operating. For the reader not personally familiar with the territory:

Figure I-1a is a brick "beehive." Though this figure recreates an English coking oven of ca. 1000 A.D., beehives were used widely from about 3000 B.C. well into the present century and for as disparate purposes as smelting ore and firing pottery and bricks. Some brickmaking still employs this fuel-efficient configuration.

Figure I-1b is a three-story Italian glass furnace also dating ca. 1000 A.D. These became much larger and more elegant later, but the basic design idea persisted until the advent of the glass melting tank in the 1870s. Ceramic shelving inside supported the fireclay pots in which each small glass batch was melted by the flame from below. The topmost level was used for annealing.

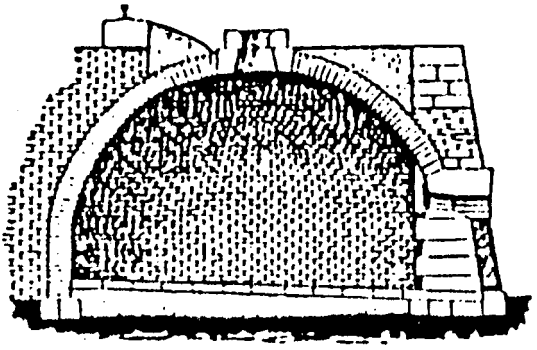

Figure I-1a Beehive Coking Oven, England, ca. 1000 A.D.
(reprinted from Ref. 2: C. Singer et al, eds., "A History of Technology," 1954-84, Oxford University Press, by permission)

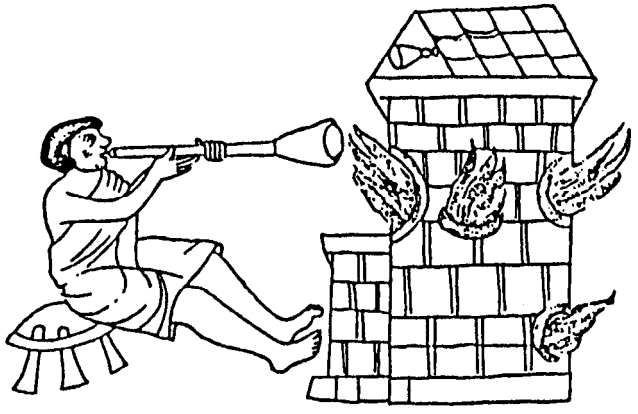

Figure I-1b Early Glass Furnace, Italy, ca. 1000 A.D.
(reprinted from Ref. 2, by permission)

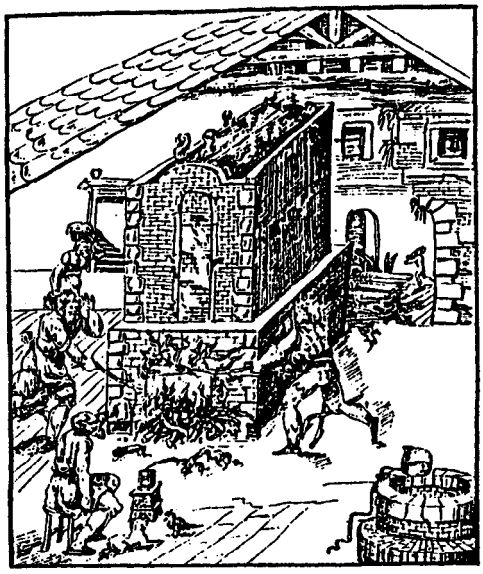

Figure I-2a Medieval Pottery Kiln, Europe, ca. 1550 A.D.
(reprinted from Ref. 2, by permission)

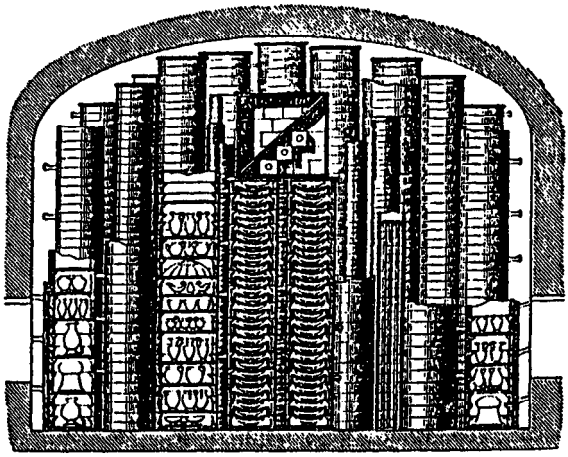

Figure I-2b Renaissance Porcelain Kiln, France, 17th Cent. A.D.
(reprinted from Ref. 2, by permission)

Figure I-2a depicts a medieval European pottery kiln in operation about 1550 A.D.: a two-story rectangular affair, stoked below and with the ware stacked above on an open refractory grate.

Figure I-2b, a much more advanced porcelain-ware kiln of 17th century Renaissance France, shows in section how the ware was then set on shelves, each shelf forming the top and bottom of stacked "saggers" or enclosing muffles. These isolated the ware from the products of combustion.

Figure I-3a is an array of "bottle" kilns in England, also of about 1700 A.D.; used for firing pottery. The tall profile and narrow neck are marks of progress in heat and draft management.

Figure I-3b is a conical type, an early Portland cement kiln dating ca. 1825. It had the iron banding that proved exceedingly practical for holding refractory structures together, but lacked the spring-loading that would be added later on.

Figure I-4 shows the evolution of the iron-smelting blast (i.e., forced-draft) furnace from the 1,500-1,000 B.C. "bloomery" that made the first iron matte, to the vertical and narrow-necked continuous-feed design of medieval Germany that stood architecturally unchanged for about 400 years, awaiting the advent of the pre-heated blast ca. 1830 A.D. Only the last of these four, using multiple mechanized bellows, could make castable iron.

Figure I-5a is a reverberatory (i.e., roof-radiating) "puddling" furnace of the 1780s, used to burn out some carbon from reheated iron by stirred contact with air and thus to convert brittle cast iron into malleable or wrought iron.

Figure I-5b, the next step in this particular progression, is the bottom-air-blown Bessemer converter such as made the first carbon steel in England in the 1850s. This opened the Age of Steel.

Figure I-5c is the reverberatory and regenerative open hearth furnace of the same time frame. This soon overtook the Bessemer converter and became the mainstay of world steel production for some hundred years. It was of excessively complicated construction, ultimately calling for a half-dozen different types of refractory brick and monolithics. A few open hearth furnaces are still in operation.

Figure I-6a is a foundry (i.e., remelt and casting) furnace of ca. 1765, used for iron but essentially like nonferrous metal casting furnaces as well. And finally,

Figure I-6b depicts a sulfide ore-roasting furnace of the early 1880s. This one was fed copper ore, but similar designs served for numerous other sulfides.

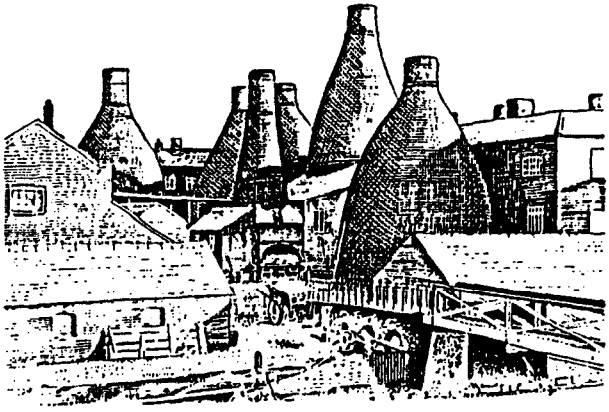

Figure I-3a Bottle Pottery Kiln, England, ca. 1700 A.D.
(reprinted from Ref. 2, by permission)

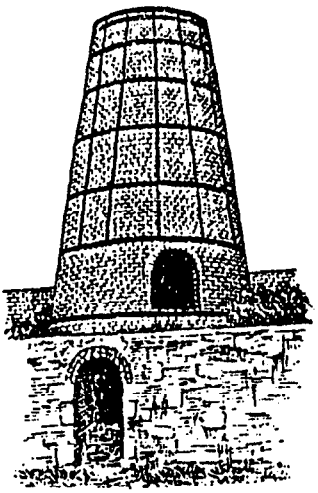

Figure I-3b Early Portland Cement Kiln, England, ca. 1825 A.D.
(reprinted from Ref. 2, by permission)

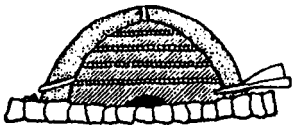

a

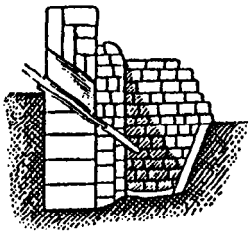

b

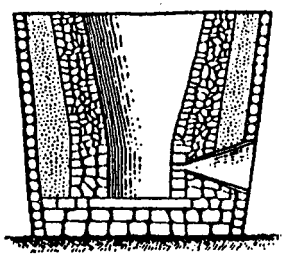

c

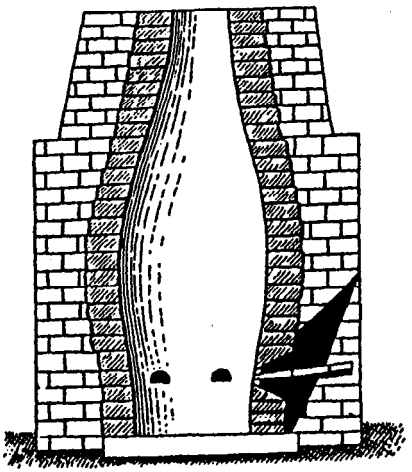

d

Figure I-4 Evolution of the Iron-Smelting Blast Furnace
a. Bloomery, Widespread, B.C. b. Catalan, Spain, Medieval
c. Osmund, Europe, Medieval d. Stückofen, Germany, ca. 1400 A.D.
(reprinted from Ref. 2, by permission)

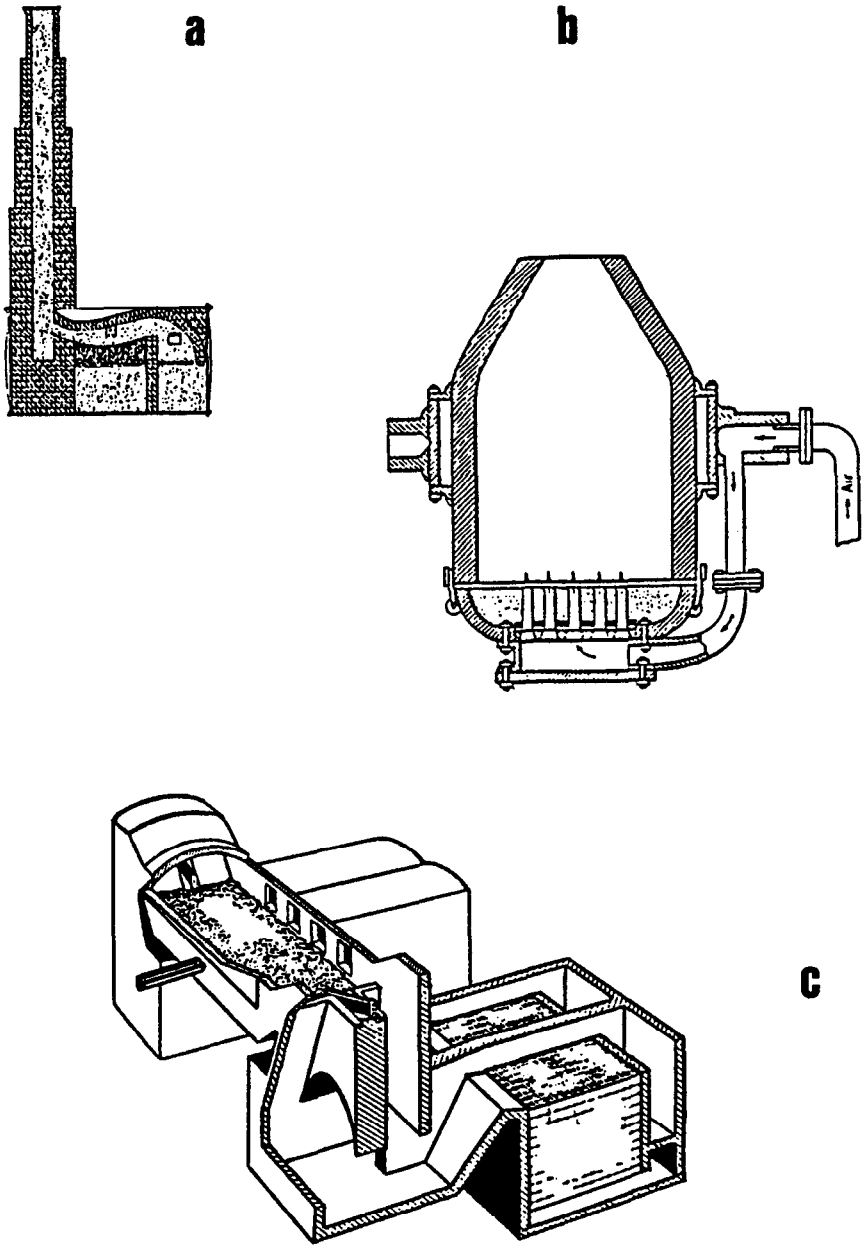

Figure 1-5 Early Steelmaking Furnaces
a. Puddling Furnace, ca. 1780 A.D. (reprinted from Ref. 2, by permission)
b. Bessemer, ca. 1850 A.D. (adapted from Ref. 3, by permission)
c. Open Hearth, 19-20th Cent. (adapted from Ref. 8, by permission)
(©American Iron and Steel Institute, by permission)

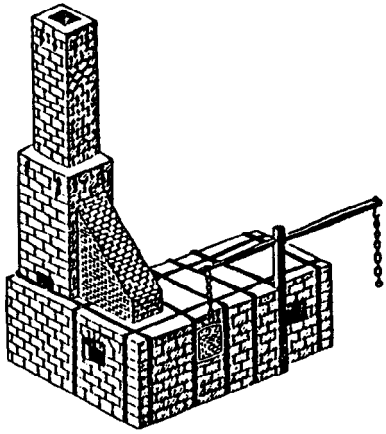

Figure I-6a Reverberatory Foundry Furnace, ca. 1765 A.D.
(reprinted from Ref. 2, by permission)

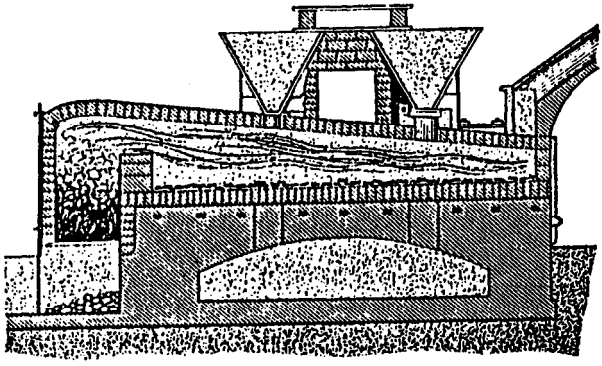

Figure I-6b Reverberatory Roasting Furnace, ca. 1880 A.D.
(reprinted from Ref. 2, by permission)

Resources Past and Present

The information base underlying refractories technology has grown exponentially. As to the prospect of still further technical advancement, it is a truism that discovery and invention in any era are built upon the achievements of their predecessors. Our vast information base can take much of the guesswork out of technical progress. But the element of inspiration is still present: no two persons, given nominally the same information and asking, "What if --?," will necessarily come up with the same ideas. However well-informed and rationally supported, "What if ---?" remains the key to creative imagining; and imagining is as crucial to incremental advancement as it is to earth-shaking new discovery.

That our predecessors over the ages asked this same question so imaginatively is a source of admiration and awe. It is remarkable how many modern technical concepts were thought of early-on, when structured knowledge and even adequate tools of inquiry were lacking. The historical sequence of discoveries, inventions and practices that fed and were fed by each other in the saga of high-temperature processing is encapsulated in Table I.1. We have constructed this table selectively (and no doubt with some important omissions), mostly by consulting the eight-volume Oxford set treating the history of all technology.[2] Other sources we have used for more contemporary history include that of Krause[1] and the monumental volume by Norton.[3]

The last-named work, though reportedly out of print, can still be readily found and contains much of the earlier technology of refractories that cannot be treated here in equal detail. Other English-language works of more recent issue include two by Chesters,[4,5] and those by Shaw[6] and by Gilchrist.[7] The Kirk-Othmer Encyclopedia[8] contains useful digests of many technologies. A large number of property and performance test procedures for refractories and other materials have been standardized, and are published annually in the standards of the American Society for Testing and Materials.[9] The Refractories Institute[10] is a rich resource of information provided by the industry itself.

The American Ceramic Society and publishing houses worldwide offer many pertinent reference works. Technical handbooks also abound. We hesitate to reduce all these to a suggested reading list as Norton[3] did in his time, for obvious enough reasons. We shall, however, document as much as possible of the specialized material presented in this book by references to the scientific and engineering journals and to the larger technical treatises. As those references are likely to be cited in more than one chapter, they are listed all together at the back.

Table I.1 Chronology of Discovery and Invention in the Harnessing of Fire

B.C.

$x \cdot 10^5$ Fire. Cooking pit (rock, sand lined).

$1 \cdot 10^5\pm$ Wheel. Drilling, grinding, polishing. Mortar and pestle.

$x \cdot 10^4$ Unfired clay utensils. Fiber-reinforced composite: clay + straw, grass, hair. Baked clay ware. Pit oven. Horse power.

$1 \cdot 10^4\pm$ Pottery. Pit oven common. Wood, peat, charcoal fuel.

5,000± Pulley. Weights and balances. Wheel milling.

4,000± Molded unfired bricks. Frit. Carbon (soot). Coal. Potter's wheel. Slip casting. Vertical pottery kiln (clay and rock). Baked, unvitrified ornamental glazes on rock.

3,500± Smelting: bronze, Cu, Ag, Au, Sn, Pb, Sb (stone crucibles). Baked masonry bricks. Lime. Caustic. Candles. Ore identification by color, hardness, luster, physical form.

3.000± Bronze casting, forging, work-hardening, annealing. Vitrified alkaline glaze (Na_2O-SiO_2). Blowpipe. Beehive pottery oven. Fireclay differentiated. Surface and underground mining. Written language.

2,500± Ag, Cu refining by solution/partition in liquid Pb. Lead distillation. Bronze tools. Horizontal pottery kiln: stone, block construction. Stone muffles. Molded glass.

2,000± Sexagesimal number system. Abacus. Copper extractive metallurgy perfected. Lead embrittlement of Cu known. "Lost wax" and open and closed-mold casting of metals. Downdraft kiln. Manual bellows. Oils, tars, bitumen known. Sulfur produced.

1,500± Iron smelting; $CaCO_3$ slagging (clay crucibles). Forging of Fe. Sn metallurgy complete. Bronze alloys produced. Large-scale metal casting. Pb-glazed pottery. Fe mining.

1,000± Fe annealing, quenching, pack-cementation carburizing. Fe tools. Advanced ferrous and nonferrous slagging, fluxing. Soldering, brazing, welding: bronze, Cu, Fe. Au-Cu alloys made. Brick oven construction. Grog used in baked brick.

500± Mathematics and geometry. Pottery clays differentiated by color. Clay slurries oeptized. Jiggering. String cutting. Lead silicate glaze. Glazed brick. Reduction firing; duplex firing. Continuous-feed furnace. Plaster, mortar, pozzolanic cement. Alum. Fractional crystallization: Pb-Ag. Modern mining: shafts, galleries, pillars. Mineral dressing: density separation, sizing, leaching.

Table I.1, continued

200± Trigonometry. Geometrical optics. Density measurement. Large-scale Fe casting. Fe tempering. Brass alloys made. Arsenic and Hg metallurgy. Red lead (Pb_3O_4) made. Ceramic muffles, saggers, pointed supports fabricated. Glass furnace design differentiated (firebrick construction). Fireclay glass-melting pots. Fe glass-blowing tube. Cast glass. Blown bottle-glass (soda-lime-silica). Low-quartz-high-quartz phase change known. Mechanical bellows. Rotary fan. Lifting machinery: ratchet, screw, bucket elevator, etc.

A.D.

200± Water wheel. Windmill. Water-powered impact mill. Brick-constructed horizontal pottery kiln. Roman hypocaust (first ceramic/gas heat exchanger). Glass annealing. Cast glass windows. Crystal (lead) glass. Cut glass: emery abresive. Alchemy: filtration, fractional crystallization, fractional distillation, refluxing, extraction, sublimation, calcination, combustion.

400± Many chemical reactions known. Numerous commercial chemicals. Brass and Zn commercial. Colored alkaline glazes: Cu(I,II), Fe(II,III), Pb, Fe-Pb. Stoneware produced (China).

600± Phlogiston inferred. Borax known. Window glass commercial. Kaolin glass-melting pots. Porcelain produced (China). Sb, Co, Mn glazes. Cu, Ag reduced over glaze. Shaft kiln (firebrick construction).

800± Au reduced on glass and glazes. Tin glaze (opaque white). Gunpowder and pyrotechnics.

1000± Glassblowing and its tooling fully developed. "Wax resist" ornamental glazing technique. Pb-glazed ornamental tile.

1200± Arabic numbers; modern mathematics and metrication. Eyeglasses. Density of metals codified. Hg amalgamation used in metallurgy. European stoneware. Salt glazing. Plaster of Paris. Water-powered bellows.

1400± Piston pump. Centrifugal fan. Water-powered bellows used in blast furnace (still firebrick). Fireclays differentiated by heat resistance. Cast iron produced. Mechanized foundry and forge. Hot drawing; rolling mill. Boring, drilling, cutting of iron. Assayer's balance. Three-story glass furnace fully developed and enlarged. Glass fritting practiced before melting. Tin-glazed majolica ware.

1500± Sand-glass timer. Sand-loading used in tensile test. Rod-reinforced composite concept. Pendulum. Mechanical clock. Printing press (screw press). Potash glass. Tin-plated iron. Pewter (Pb-Sn). Typemetal.

Table I.1, continued

1550± Steam-jet rotor (turbine precursor). Reverberatory furnace (firebrick construction). Foundry pouring pits. Clay molds wire/bar reinforced. Smelting and metallurgy codified, including diverse fluxes. Descriptive mineralogy codified. Melting points, solid and liquid properties catalogued. Transition from Alchemy to Chemistry commenced.

1600± Laws of motion. Telescope. Microscope. Bubble level. Nonius (i.e., Vernier). Fractography. Elastic properties. Radiant-color pyrometry. Solar furnace. Speculum (mirror) metal, Cu-Sn. Enclosed-muffle furnace. Tall chimneys (convective draft). Large furnaces differentiated: roasting, smelting, remelt, foundry, forge, heat-treating.

1650± Foundations of higher mathematics. Gas laws of chemistry. Chemical neutralization codified. Thermometer (alcohol). Barometer. Refractive index. Pb sheet poured & rolled. Lead shot. Plate glass. Nucleation/precipitation in glass by reheat: ruby glass (Au). Coking of coal. Coal-tar and pitch commercial. Thermostatted furnace. Bottom-tapped ladles and crucibles (fireclay-lined metal). Clay + charcoal refractories for metal remelt and pouring. New fuels: coal-gas, blast furnace off-gas, coke-oven gas.

1700± Steam boiler (firebrick lined). Steam-driven piston used in mining. Lime-cement concrete. Ceramic "bottle kiln" (firebrick construction). Porcelain and china wares (milled kaolin, marble, feldspars): Dresden, Sèvres, Chantilly, Limoges; England. Static electricity generator. Electrometer.

1750± Measurements: force, pressure. vacuum, velocity, sound, heat energy, latent heat, temperature, thermal expansion, dilatometry, electrical conduction and resistance, magnetic field. Calcined flint clay used in ceramic formulations. Wet ball milling using stone balls. Porous plaster of Paris used for slip-casting molds. Role of %C in iron and steel hardness understood. Crucible steel technology started (fireclay pots). Coal- and coke-fired furnaces feasible for iron and steel. Synthetic H_2 fuel. Continuous-feed conical blast furnace.

1775± Escapement clock; watches, chronometers. C removal from Fe by "puddling" process. Alloy steels: Cu and Ni. Multiple tuyeres; first basic brick in blast furnace. Steam engine. Steam power throughout all metallurgy.

1800± Chemical elements, symbols; atomic theory. atomic weights. Analytical chemistry. Chemical identification of minerals. Voltaic pile; D.C. electricity. Electrochemistry. Glass stirring and fining. Covered glass melting pots. Scientific glass coloring. German silver alloy (Cu-Ni). Internal combustion engine patented. Steam engine commercial. Steam locomotive and maritime vessels.

Table I.1, continued

1825± Electromagnetism; electric motor. Magnetoelectricity; electric generator; A.C. electricity. Galvanometer. Chemical-grade stoneware and porcelain. Portland cement concrete (vertical firebrick cement kiln). Blast furnace stoves (firebrick): preheated blast (steatite rock furnace construction). Tunnel kiln for ceramics (firebrick construction). Hg distillation furnace. Production of Pt metals and Cd, Co, Cr, Mn, Mo, Nb, Ti, and W.

1850± First and Second Laws of Thermodynamics. Iron-reinforced concrete. Multiple hearth Cu ore roaster (firebrick construction). Electric arc furnace. Induction furnace. Proliferation of ceramic kiln designs. Carbon refractory brick; SiO_2+C brick. Bessemer converter (silica brick, then magnesite brick lined). Regeneratively-heated open hearth steel furnace (magnesite lined). Petroleum fractional distillation. Fuel oil. Natural gas. First producing oil well (U.S.).

1875± Electromagnetic waves identified. Glass melting tank (magnesite brick lined). Rotary kiln for Portland cement (cement clinker lined). Hall-Héroult aluminum process (carbon block lined). Bayer process Al_2O_3. Alloy steels commercial: Mn, W-Mn, Cr, Ni. Superheated steam. Internal combustion engine practical. Refractory insulators: mica, zircon, glass, porcelain, etc. Gibbs Phase Rule. Petrographic (optical) microscope. Sieve (size) analysis of particulates. Centrifuge. Analysis and classification of clays. Full characterization of silica. Pyrometric cones.

1900± Quantum theory. X-rays generated; X-ray optics. Steam turbine. Venturi tube. Large electric motors. Diesel engine patented. Petroleum cracking. Graphite and silicon carbide produced (Acheson process). Basic refractory lined Cu converter. Chemical processing of ores and minerals proliferated. Incandescence understood. Resistance pyrometry. Photo- and thermoelectric emission; vacuum tubes ("valves").

1925± XRD crystallography. First oxide phase diagrams. Measurement and utilization of pH. Synthetic carbides and nitrides; ultrahard tooling. Pyrex borosilicate glass. Glass-metal sealing. Fiberglass. Continuous recuperative glass melting (firebrick checkers). Super-duty firebrick: mullite + Al_2O_3 phase compositions. Refractories containing zirconia ore concentrate. Insulating refractories. Particle packing theory. Micromeritics. Electric arc furnace practical. Arc-fused refractories. Liquid air and liquid O_2 commercial. Magnesia-chromite refractories. MgO from seawater (England). Emission spectrometer. Optical pyrometry. Polarography.

Table I.1, continued

1950± (partial) Chromatography. Mass spectrometry. Spectrophotometry. Digital counters; first computers. Superalloys (Ni-, Co-, Fe-base). Oxygen blowing in Bessemer and open hearth steelmaking. MgO from seawater (U.S.). Fiber refractories. Tunnel kiln dominant in ceramic and refractory production. Gas turbine. Nuclear fission. Continuous casting of steels. Float process (molten Sn) for plate glass. Basic oxygen process (BOP) and its furnace (BOF). Argon-oxygen decarburization process (AOD) for stainless steels. Electric arc furnace steel. Induction furnace steel processing. Vacuum processing of reactive metals. IR and UV spectrometry; XRF spectrometry; NMR devices. Electron optics: TEM, SEM, microprobe. Auger, Mössbauer, and other investigative tools. Dislocations imaged; theories of deformation and fracture; fracture mechanics. Junction transistor; solid state electronics. Maser and laser. Light- and laser-light-scattering devices. Sonic and ultrasonic devices. Porosimetry. Transducer and instrumentation explosion. Ultra-high-temperature and plasma generators. Proliferation of synthetic chemical processes. High-technology and synthetic oxide refractories introduced. Colloid chemistry advanced.

Chapter II

Foundations of Hot Processing

A REFERENCE CHAPTER

There are bodies of basic information to which the reader must refer from time to time, whether within the confines of this book or otherwise. The purpose of Chapters II and III is to fill these needs early. Here, after disposing of some elemental matters, we outline the temperature regimes and essential chemistry of some representative high-temperature industrial processes.

COMPUTATIONAL QUANTITIES AND CONVERSION FACTORS

Mensuration Units

Most computations presented in this volume will use metric units. The SI (Système Internationale) metric mensuration system and the cgs (centimeter-gram-second) system are compatible. The English system has also been long entrenched in refractories technology, however, and some practitioners continue to use or refer to those units.

Table II.1 facilitates conversion from one system to another. Each subtable is laid out such that all quantities in any one horizontal row are equal, and one of these is unity. The notation used in the table should be familiar: "3.048E+02" means $3.048 \cdot 10^{2}$ and "3.937E-08" means $3.937 \cdot 10^{-8}$, for example, while "3.281 E00" means 3.281.

Table II.1 Computational Units and Conversion Factors

LENGTH

ENGLISH			SI or CGS					
yards, yd	feet, Ft	inches, in	meters, m	centim., cm	millim., mm	microm., μm	nanom., nm	Ångstroms, Å
--1--	3.	36.	9.144E-01	9.144E+01	9.144E+02			
3.333E-01	--1--	12.	3.048E-01	3.048E+01	3.048E+02	3.048E+05	3.048E+08	3.048E+09
2.778E-02	8.333E-02	--1--	2.540E-02	2.540 E00	2.540E+01	2.540E+04	2.540E+07	2.540E+08
1.094 E00	3.281 E00	3.937E+01	--1--	1.000E+02	1.000E+03	1.000E+06	1.000E+09	1.000E+10
1.094E-02	3.281E-02	3.937E-01	1.000E-02	--1--	10.	1.000E+04	1.000E+07	1.000E+08
1.094E-03	3.281E-03	3.937E-02	1.000E-03	1.000E-01	--1--	1.000E+03	1.000E+06	1.000E+07
	3.281E-06	3.937E-05	1.000E-06	1.000E-04	1,000E-03	--1--	1.000E+03	1.000E+04
	3.281E-09	3.937E-08	1.000E-09	1.000E-07	1.000E-06	1.000E-03	--1--	10.
	3.281E-10	3.937E-09	1.000E-10	1.000E-08	1.000E-07	1.000E-04	1.000E-01	--1--

AREA

ENGLISH			SI or CGS		
sq. yds., yd^2	sq. ft, ft^2	sq. in, in^2	sq. m, m^2	sq. cm, cm^2	sq. mm, mm^2
--1--	9.	1.296E+03	8.361E-01	8.361E+03	8.361E+05
1.111E-01	--1--	144.	9.290E-02	9.290E+02	9.290E+04
7.716E-04	6.944E-03	--1--	6.452E-04	6.452 E00	6.452E+02
1.196 E00	1.076E+01	1.550E+03	--1--	1.000E+04	1.000E+06
1.196E-04	1.076E-03	1.550E-01	1.000E-04	--1--	1.000E+02
1.196E-06	1.076E-05	1.550E-03	1.000E-06	1.000E-02	--1--

TEMPERATURE (K=kelvin)

Celsius

$T^oC = T(K) - 273$

Fahrenheit

$T^oF = 1.8T^oC + 32$

Rankine

$T^oR = T^oF + 459.7$

VOLUME (Note: 1 ml ≅ 1 cm^3 and 1 liter ≅ 1000 cm^3)

ENGLISH			U.S. LIQUID		SI or CGS			
cu. yds., yd^3	cu. ft, ft^3	cu. in, in^3	gallons, gal	quarts, qt	cu. m, m^3	cc, ml, cm^3	cu. mm, mm^3	liters, l
--1--	27.	4.667E+04	2.020E+02	8.081E+02	7.646E-01	7.646E+05	7.646E+08	7.646E+02
3.704E-02	--1--	1.728E+03	7.482 E00	2.993E+01	2.832E-02	2.832E+04	2.832E+07	2.832E+01
2.143E-05	5.787E-04	--1--	4.330E-03	1.732E-02	1.639E-05	1.639E+01	1.639E+04	1.639E-02
4.950E-03	1.337E-01	2.310E+02	--1--	4.	3.785E-03	3.785E+03	3.785E+06	3.785 E00
1.237E-03	3.341E-02	5.774E+01	2.500E-01	--1--	9.463E-04	9.463E+02	9.463E+05	9.463E-01
1.308 E00	3.531E+01	6.103E+04	2.642E+02	1.057E+03	--1--	1.000E+06	1.000E+09	1.000E+03
1.308E-06	3.531E-05	6.103E-02	2.642E-04	1.057E-03	1.000E-06	--1--	1.000E+03	1.000E-03
1.308E-09	3.531E-08	6.103E-05	2.642E-07	1.057E-06	1.000E-09	1.000E-03	--1--	1.000E-06
1.308E-03	3.531E-02	6.103E+01	2.642E-01	1.057 E00	1.000E-03	1.000E+03	1.000E+06	--1--

TYLER AND U.S. STANDARD SIEVE (SCREEN) SIZES, by Mesh No., m

Tyler No.	U.S. No.	Opening mm	Opening in	Examples of Size Factor	Tyler No.	U.S. No.	Opening μm	Opening in
--	1/2-in	12.70	0.500		32	35	500	0.0195
--	3/8-in	9.52	0.375		35	40	420	0.0164
--	3	6.35	0.250		42	45	350	0.0138
4	4	4.76	0.185	x2 x2	48	50	297	0.0116
5	5	4.00	0.156		60	60	250	0.0097
6	6	3.36	0.131		65	70	210	0.0082
7	7	2.83	0.110		80	80	177	0.0069
8	8	2.38	0.093	x2 x2				
9	10	2.00	0.078		100	100	149	0.0058
					115	120	125	0.0049
10	12	1.68	0.065		150	140	105	0.0041
12	14	1.41	0.055		170	170	88	0.0035
14	16	1.19	0.046	x2 x2	200	200	74	0.0029
16	18	1.00	0.039		250	230	62	0.0024
20	20	0.84	0.0328		270	270	53	0.0021
24	25	0.71	0.0276		325	325	44	0.0017
28	30	0.59	0.0232	x2 x2	400	400	37	0.0015

Table II.1, continued (Refs. 11, 12, 13)

MASS

ENGLISH		SI or CGS	
tons, t_m	pounds, lb_m	kilograms kg_m	grams, g_m
--1--	2.000E+03	9.072E+02	
5.000E-04	--1--	4.536E-01	453.6
1.102E-03	2.205 EOO	--1--	1000.
1.102E-06	2.205E-03	1.000E-03	--1--

DENSITY

ENGLISH	U.S.	SI or CGS		
pcf, lb_m/ft^3	ppg, lb_m/gal	kg_m/m^3	g_m/cm^3	g_m/liter
--1--	1.337E-01	1.602E+01	1.602E-02	1.602E+01
7.481 EOO	--1--	1.198E+02	1.198E-01	1.198E+02
6.243E-02	8.345E-03	--1--	1.000E-03	--1--
6.243E+01	8.345 EOO	1.000E+03	--1--	1.000E+03

FORCE (Note: Std. gravitational accel. = 32.174 ft/s^2 = 9.8066 m/s^2)

ENGLISH		SI or CGS			
tons, t_F	pounds, lb_F	newtons, N	kilograms kg_F	grams, g_F	dynes
--1--	2.000E+03	8.897E+03	9.072E+02	9.072E+05	8.897E+08
5.000E-04	--1--	4.448 EOO	4.536E-01	4.536E+02	4.448E+05
1.124E-04	2.248E-01	--1--	1.020E-01	1.020E+02	1.000E+05
1.102E-03	2.205 EOO	9.807 EOO	--1--	1.000E+03	9.807E+05
1.102E-06	2.205E-03	9.807E-03	1.000E-03	--1--	9.807E+02
1.124E-09	2.248E-06	1.000E-05	1.020E-06	1.020E-03	--1--

PREFIXES USED WITH METRIC UNITS

10^1 = DEKA		10^{-1} = DECI	
10^2 = HECTO		10^{-2} = CENTI	
10^3 = KILO		10^{-3} = MILLI	
10^6 = MEGA		10^{-6} = MICRO	
10^9 = GIGA		10^{-9} = NANO	
10^{12} = TERA		10^{-12} = PICO	

STRESS OR PRESSURE (Note: 1 Pa = 1 N/m^2 and 1 N = 1 $kg_m m/s^2$)

ENGLISH		SI or CGS					CHEMICAL	
psf, lb_F/ft^2	psi, lb_F/in^2	pascals, Pa	bars, b	ksm, kg_F/m^2	dynes per cm^2	g_F/cm^2	atm	mm Hg
--1--	6.944E-03	4.788E+01	4.788E-04	4.882 EOO	4.788E+02	4.882E-01	4.725E-04	3.591E-01
1.440E+02	--1--	6.895E+03	6.895E-02	7.031E+02	6.895E+04	7.031E+01	6.804E-02	5.171E+01
2.089E-02	1.450E-04	--1--	1.000E-05	1.020E-01	1.000E+01	1.020E-02	9.869E-06	7.500E-03
2.089E+03	1.450E+01	1.000E+05	--1--	1.020E+04	1.000E+06	1.020E+03	9.869E-01	7.500E+02
2.048E-01	1.422E-03	9.807 EOO	9.807E-05	--1--	9.807E+01	1.000E-01	9.678E-05	7.355E-02
2.089E-03	1.450E-05	1.000E-01	1.000E-06	1.020E-02	--1--	1.020E-03	9.869E-07	7.500E-04
2.048 EOO	1.422E-02	9.807E+01	9.807E-04	10.	9.807E+02	--1--	9.678E-04	7.355E-01
2.116E+03	1.470E+01	1.013E+05	1.013 EOO	1.033E+04	1.013E+06	1.033E+03	--1--	7.600E+02
2.785 EOO	1.934E-02	1.333E+02	1.333E-03	1.360E+01	1.333E+03	1.360 EOO	1.316E-03	--1--

HEAT, ENERGY, OR WORK

ENGLISH		SI	CGS		PHYSICAL
$ft \cdot lb_F$	Btu	joule, J	mean cal	erg	eV
--1--	1.285E-03	1.356 EOO	3.239E-01	1.356E+07	8.463E+18
7.780E+02	--1--	1.055E+03	2.520E+02	1.055E+10	6.584E+21
7.376E-01	9.480E-04	--1--	2.389E-01	1.000E+07	6.242E+18
3.087 EOO	3.969E-03	4.186 EOO	--1--	4.186E+07	2.613E+19
7.376E-08	9.480E-11	1.000E-07	2.389E-08	--1--	6.242E+11
1.182E-19	1.519E-22	1.602E-19	3.827E-20	1.602E-12	--1--

POWER

1 watt, W = 1 $joule \cdot s^{-1}$
1 V·ampere = 1 $joule \cdot s^{-1}$
1 horsepower, HP = 746.0 W
1 Btu/s = 1054.6 W
1 Btu/s = 1.414 HP

WORKING DEFINITIONS OF SOME PHYSICO-CHEMICAL AND ELECTRICAL QUANTITIES

ATOMIC MASS UNIT, amu : $1.661 \cdot 10^{-24}$ g_m (also called "atomic weight" unit).
AVOGADRO'S NUMBER, n_A : $6.023 \cdot 10^{23}$ (per g-atom, g-mol, g-formula-weight).

ELECTRONIC CHARGE, $e^{\pm}$: $1.602 \cdot 10^{-19}$ coulomb.
COULOMB, C : Deposits $1.118 \cdot 10^{-3}$ g Ag or $3.293 \cdot 10^{-4}$ g Cu in aq.
FARADAY CONSTANT, F : $n_A \cdot e^{\pm}$; hence, $9.6488 \cdot 10^4$ coulombs/gram-equivalent.

AMPERE, a : 1 C/s (coulomb per second).
VOLT, V : Defined by, 1 V·C = 1 joule = 1 N·m = $1 \cdot 10^7$ ergs.
OHM, Ω : 1 V/a (volt per ampere).

BRIT. THERMAL UNIT, Btu: 1 lb H_2O x 1 °F; hence, 251.98 calories (mean).
CALORIE (mean), cal : 1 g H_2O x 1 °C; 4.186 joules or $4.186 \cdot 10^7$ dyne cm.

BOLTZMANN'S CONSTANT, k: $1.3804 \cdot 10^{-23}$ $joule \cdot K^{-1}$ or $8.620 \cdot 10^{-5}$ $eV \cdot K^{-1}$
GAS CONSTANT, R : $n_A \cdot k$; hence, 8.314 $J \cdot mol^{-1}K^{-1}$ = 1.986 $cal \cdot mol^{-1}K^{-1}$.

Sieve or Screen Sizes

The measurement of sizing of particulate solids by the use of standard sieves or screens is so important in refractories as to warrant inclusion of "Tyler and U.S. Standard Sieve Sizes" in Table II.1. Other sets of standard wire-mesh sieves are available in England, Germany, Japan and elsewhere; their descriptions can be accessed through local industrial sources.

It should be noted that the progression of standard sieves (designated by successive mesh numbers) is logarithmic as to size of opening. In the table, for example, we have marked off just one subset that progresses in size by a factor of 2. Every second mesh number differs by approximately $2^{1/2}$, and every adjacent mesh number by approximately $2^{1/4}$ or a factor of 1.18921. We shall deal with *subsieve* particle sizes, i.e., "-325m" or "-400m," including *colloidal* sizes ($\leq 1\mu m$), in later chapters.

Fundamental Physical Quantities

At the bottom of Table II.1 we have appended working definitions or numerical statements of a few fundamental quantities that will be employed repeatedly. As in all of Table II.1, recourse to current references and handbooks[11-13] should be made for quantities or units not listed.

Chemical Elements and Atomic Weights

Table II.2 lists all of the chemical elements which the reader may ordinarily expect to encounter. These are arranged alphabetically by *symbol.* Notable among the purposeful omissions are the rare earth elements, running consecutively from atomic number 59 to 71. We have also omitted the transuranium elements, though retaining U and Pu in recognition of their importance in nuclear energy.

Atomic weights are tabulated to two decimal places, which should suffice for most work in refractories. The sole possible exception is hydrogen, H: the reader may feel justified in taking its atomic weight as 1.007. The correct term is "atomic mass," and the unit in all cases is the a.m.u. of Table II.1.

Formula weights of compounds follow, given the chemical formulas known or supposed to apply. Avogadro's number of atoms (Table II.1) weighs the atomic weight numerically, but in grams; and that same number of "formulas" weighs the formula weight numerically but in grams. We shall use the term *mol* equally for either of these, dispensing with the terms "gram-atom" and "gram-molecule." The reader is of course free to use "kg-mol," "pound-mol," and "ton-

Table II.2 Chemical Elements and Atomic Weights (Ref. 11)

Symbol	Name	At. No.	Atomic Weight
Ag	SILVER	47	107.87
Al	ALUMINUM	13	26.98
Ar	ARGON	18	39.95
As	ARSENIC	33	74.92
Au	GOLD	79	196.97
B	BORON	5	10.81
Ba	BARIUM	56	137.33
Be	BERYLLIUM	4	9.01
Bi	BISMUTH	83	208.98
Br	BROMINE	35	79.90
C	CARBON	6	12.01
Ca	CALCIUM	20	40.08
Cb	(COLUMBIUM)	See Nb	
Cd	CADMIUM	48	112.41
Ce	CERIUM	58	140.12
Cl	CHLORINE	17	35.45
Co	COBALT	27	51.93
Cr	CHROMIUM	24	52.00
Cs	CESIUM	55	132.91
Cu	COPPER	29	63.55
F	FLUORINE	9	19.00
Fe	IRON	26	55.85
Ga	GALLIUM	31	69.72
Ge	GERMANIUM	32	72.59
H	HYDROGEN	1	1.01
He	HELIUM	2	4.00
Hf	HAFNIUM	72	178.49
Hg	MERCURY	80	200.59
I	IODINE	53	126.91
In	INDIUM	49	114.82
Ir	IRIDIUM	77	192.22
K	POTASSIUM	19	39.10
Kr	KRYPTON	36	83.80
La	LANTHANUM	57	138.91
Li	LITHIUM	3	6.94
Mg	MAGNESIUM	12	24.31
Mn	MANGANESE	25	54.94
Mo	MOLYBDENUM	42	95.94
N	NITROGEN	7	14.01
Na	SODIUM	11	22.99
Nb	NIOBIUM	41	92.91
Ne	NEON	10	20.12
Ni	NICKEL	28	58.69
O	OXYGEN	8	16.00
Os	OSMIUM	76	190.2_0
P	PHOSPHORUS	15	30.97
Pb	LEAD	82	207.2_0
Pd	PALLADIUM	46	106.42
Pt	PLATINUM	78	195.08
Pu	PLUTONIUM	94	244. ±
Rb	RUBIDIUM	37	85.47
Re	RHENIUM	75	186.21
Rh	RHODIUM	45	102.91
Rn	RADON	86	222. ±
Ru	RUTHENIUM	44	101.07
S	SULFUR	16	32.06
Sb	ANTIMONY	51	121.75
Sc	SCANDIUM	21	44.96
Se	SELENIUM	34	78.96
Si	SILICON	14	28.09
Sn	TIN	50	118.71
Sr	STRONTIUM	38	87.62
Ta	TANTALUM	73	180.95
Te	TELLURIUM	52	127.60
Th	THORIUM	90	232.04
Ti	TITANIUM	22	47.88
Tl	THALLIUM	81	204.38
U	URANIUM	92	238.03
V	VANADIUM	23	50.94
W	TUNGSTEN	74	183.85
Xe	XENON	54	131.29
Y	YTTRIUM	39	88.91
Zn	ZINC	30	65.39
Zr	ZIRCONIUM	40	91.22
R.E.	(RARE EARTHS)	Omitted	

mol" where large quantities of elements or compounds are appropriate.

HOT PROCESSING TEMPERATURES AND THEIR MEASUREMENT

As regards the usefulness of refractories, "hot" extends from well below 200°C to well above 2000°C. The vast majority of commercial applications entail process working temperatures between 200°C and 2000°C. Figure II-1, subdivided into two spans purely for convenience of display, gives by bars the approximate working temperature ranges of some twenty-five kinds of physico-chemical operations or processes. Before discussing those processes, let us focus first on temperature itself: its scales and methods of measurement.

Temperature Scales

The kelvin, celsius, Fahrenheit, and Rankine temperature scales are inter-related by the familiar equations grouped in Table II.1. The scales of Figure II-1 display °C and °F simultaneously; most refractories literature employs one or the other of these.

The graduated bar on the left edge of Fig. II-1 gives the approximate incandescent or radiant color of hot solids as a function of temperature, as detected by the eye. Since the intensity of incandescent radiation increases rapidly with increasing temperature and can be harmful to ophthalmic tissues, colors above orange or temperatures above 900°C must not be dwelt upon without eye-protective filters. The emissivity of different solids varies widely, as also do the circumstances of their enclosure and viewing background; so this *color-temperature scale* is quite inexact. Nevertheless, it has been of some industrial utility based on experience; and the visitor to a hot-processing installation can use it to estimate operating temperatures roughly at-a-glance.

Between the two temperature scales of Figure II-1 lies a column designated "Orton Cone No." The corresponding cone softening temperatures are taken from Orton product literature.[14] By no means are all Orton cones represented in the figure; nor, quite evidently, are their number designations linear with temperature. Although Orton cones are distributed worldwide, other manufacturers are also established in England, Germany, Japan, Brazil, and elsewhere. Their products and designations can be accessed through local sources.

Such standard *pyrometric cones* have long been employed in the ceramic and refractories fields. Like the silicate products they were developed to serve, they themselves are of complex silicate compositions but of rigorous specifications. They do not melt sharply, but soften and deform progressively under their own weight with increasing temperature. The progressive deformation depends on the temperature rise rate and, once commenced, continues even at fixed temperature. Thus these cones reveal a sort of time-temperature integral in a furnace or kiln. This kinetic feature is peculiarly adapted to the control of sintering of silicate minerals, ceramics, and classical refractories; hence the well-justified use of pyrometric cones in those industries, as well as the common characterization of softening temperature of refractories in terms of the *pyrometric cone equivalent,* or *P.C.E.* -- a representation of somewhat limited value as a service rating.

Orton standard cones are elongate triangular pyramids or tetrahedra. In use several cones of successive numbers are placed at an angle of 8° from the vertical, usually in shallow cavities in a supporting plate. When heated in oxidizing atmosphere at a fixed rate of 2.5°C per minute, a cone of a given number will bend over by about 160° of arc, more or less, at a reproducible softening temperature. Two series of Orton cones are available: a 2"-long series and a 15/16"-long series. The softening temperatures marked in Fig. II-1 are for the 2" series for cone nos. 022 to 10, inclusive, and for the 15/16" series for cone nos. 12 to 37, inclusive (underlined in the figure). In the correct jargon, a given temperature (e.g., 1015°C) has a P.C.E. of a given standard cone number (e.g., cone 06). Equivalencies generally accepted in the U.S. refractories industry will be mentioned later.

Temperature Measurement

For the more precise measurement of processing temperature per se and as a continuous variable, several types of instruments are at hand. The more common ones are described following.

Bimetallic Thermometers. The stainless-steel-clad dial-gauge bimetallic thermometer, operating on differential thermal expansion, is serviceable to about 600°C. Placement of the sensor is limited by length of stem. Precision is about 1/100 of full-scale. Response to temperature changes is slow, calling for from one to a few minutes to equilibrate. The most common industrial use of this very inexpensive instrument is in relatively low-temperature ovens and ducts, sensing wall or interior atmospheric temperatures at steady state.

Thermocouples. Operating on the Seebeck effect,[15] a closed wire loop comprised of two "halves" of different metals gives a

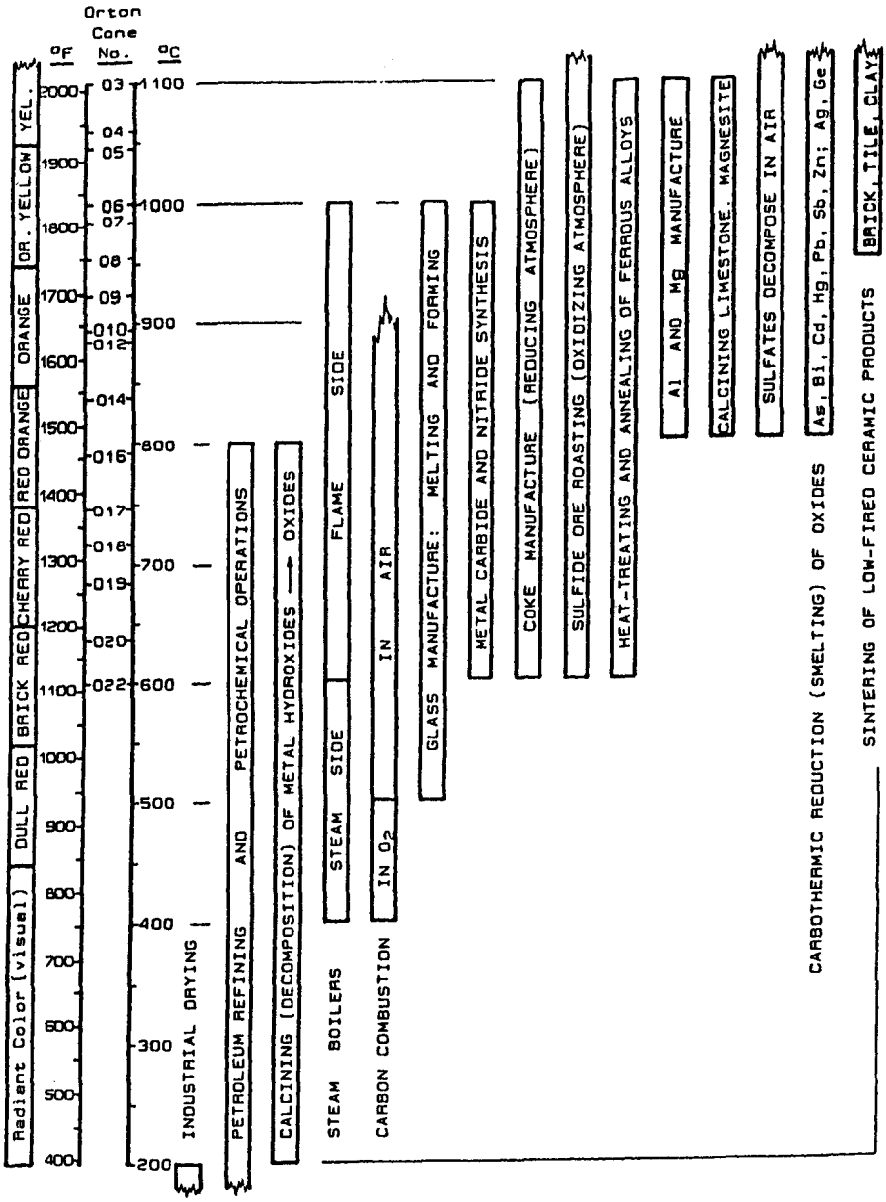

Figure II-1 Approximate Temperature Ranges of Industrially Significant Processes

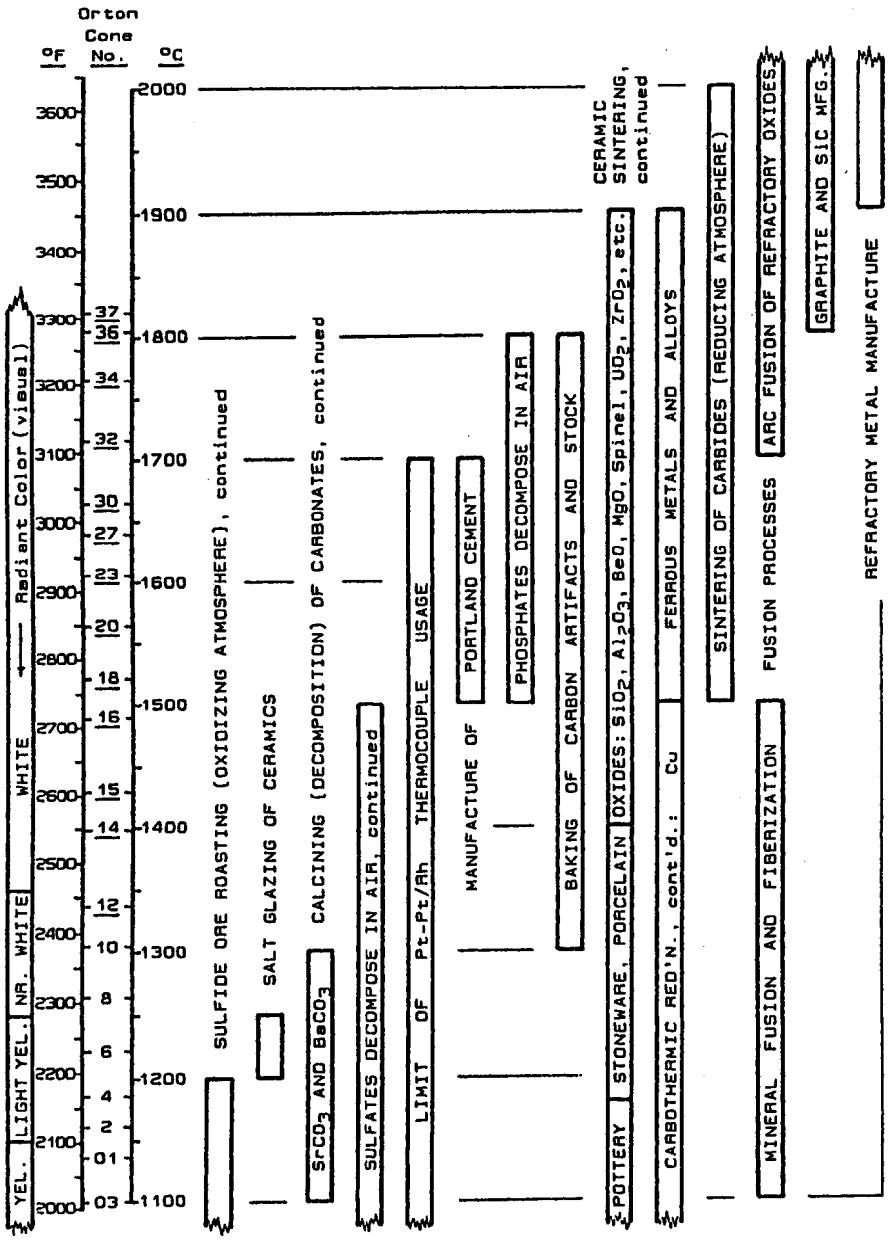

Figure II-1, continued

reliable electrical response to the temperature difference between their two welded junctions. A series of alternating wires of the same two metals, with the hot junctions bunched together and the cold junctions bunched together (but electrically insulated), is called a *thermopile*: its configuration increases the magnitude of the electrical effect (e.g., the zero-current EMF) and hence the sensitivity to a given ΔT between junctions. A suitable millivolt meter is inserted in one leg of the circuit, and in commercial instruments its readout is calibrated as ΔT. Or, commonly, with electronic amplification the response is continuously recorded and/or computer-processed.

Commercial instruments use selected pairs of metals known to be reliable and durable. Examples are chromel/alumel (base-metal alloys) and Pt/Pt-10%Rh or Pt/Pt-17%Rh. Each pair has its own Seebeck voltage, hence its own temperature calibration, supplied by the manufacturer. The Pt/Pt-Rh type is reliable only in an oxidizing or neutral environment, but in that case is serviceable to about 1700°C. This limit is shown by one of the labelled bars in Figure II-1, for comparison with the working temperatures of various processes. The chromel/alumel type is serviceable to some 1400°C, but becomes soft and corrosion-sensitive (hence vulnerable to loss of calibration) at that limit. All types are susceptible to condensation of reactive substances in flame or furnace environments, requiring periodic inspection. Absent these deteriorating circumstances, excellent precision in measured ΔT between junctions can be achieved: typically about 1/1000 of full-scale or better. For laboratory work, the cold junction can be immersed in ice/water at 0°C. For an ambient-temperature cold junction, that temperature is usually estimated and worked into the instrument calibration. Response to temperature changes is a little slow, calling for up to one minute to equilibrate. The Pt/Pt-Rh circuit is somewhat vulnerable to stray electromagnetic fields.

In practice the hot legs are typically ceramic-armored, leaving only the hot junction exposed. Leg lengths up to the order of ten feet are feasible; thus relatively remote sensing can be entertained. Thermocouple *pyrometry* of clean atmospheres is widely practiced; but embedment of hot junctions in precision-drilled cavities in solids also makes the method highly suitable for in-wall temperature measurement. An example of this use is the measurement of $\Delta T/\Delta z$ (z = depth) in a plane refractory wall at steady state, from which either the mean thermal conductivity, k, or the heat flux through the wall, J, is determined. Patched or pressed onto external steel shells, thermocouples can signal the onset of dangerous overheating. Armored hot junctions (electrically insulated within) make possible the pyrometry of corrosive liquids and gases under steady-state conditions. Laboratory uses are many, and cost is low.

Efforts have long been made to develop thermocouples for use above the limit of Pt. Refractory metal thermocouples (Mo and W alloys) have been used to well above 2000°C, but have not gained a wide reputation for reliability. A recently-introduced B_4C/carbon thermocouple is said to have overcome the reliability problem and to serve up to 2200°C. But its placement is limited by rigidity of its legs, and its use is expected to be confined to vacuum and inert-gas atmospheres where Mo and W alloys can also behave acceptably.

Optical Pyrometers. The hand-held "disappearing filament" visual incandescent-radiation comparator is the work-horse of the furnace room. It is sighted on any chosen area inside a furnace or kiln, while an optical system superimposes the image of a tungsten-filament lamp in the focal plane of the object image. The operator adjusts battery-powered heating of the filament until its image disappears, i.e., is neither less bright nor brighter than that of the object. In commercial instruments the filament-heating controller is graduated directly in radiant temperature.

In the hands of an experienced and careful operator, repeatability is good to 1° or 2°C. Precision depends on adherence of the furnace enclosure to "black-body" conditions, approach of the contents to isothermal, and absence of appreciable dust between instrument and object. Ideally, the precision about equals the repeatability. Time-temperature patterns can be accurately tracked. The useful range is from about 500°C to above 2000°C. Perhaps the only persistent drawback of this instrument is that it is manually operated.

Automatic optical pyrometers can also be had, however, at increased cost. In those the human eye is dispensed with. The intensity of radiation from the hot source is sensed at several specific wavelengths. The electronically-amplified output may be made use of in whatever way is desired.

Optical pyrometry can be used not only to measure and control furnace or kiln temperatures. In the conduct of planned experiments, it can help to optimize fuel usage, adjust kiln temperature profiles, balance cooling-air flow against combustion-gas flow, and otherwise improve the management of heat.

Infrared Pyrometers. IR pyrometers have basically the same capabilities as the "optical" type, except for their utility down to much lower temperatures and for the lack of any dependency on the human eye. All automatic instruments are relatively expensive, yet the amount of labor they displace is small. On this account, their use is not widespread except where continuous temperature data are needed; but the latter need is growing rapidly with automation of most types of furnacing equipment in industry.

PROCESS CHEMISTRY AND ENVIRONMENTS

We shall take up the processes of Figure II-1 in approximate order of increasing temperature, i.e., as their bars appear from left to right in the figure.

Industrial Drying

Drying of solids is dedicated to the evaporative removal of bulk or free H_20 and of physisorbed (molecular) surface H_20. Chemisorbed and chemically bound or combined H_20 are ordinarily in the form of hydroxide, -0H, which is removed at higher temperatures. But the distinction is sometimes hazy: for example, the *desiccation* or water loss of silicic acid hydrogel is progressive and continuous without interruption from ~100°C to ~700°C or even higher.

Granted a few such exceptions, free and physisorbed water are usually distinguished from chemisorbed and combined water by separated broad features of *differential thermal analysis* (DTA) and *thermogravimetric analysis* (TGA) curves. The former curves show loss of water by *endotherms* (regions of heat absorption), while the latter disclose the same by weight loss of the solid as H_20 is evaporated. The low-temperature DTA peak and TGA step both correspond to loss of free and physisorbed water. These features ordinarily begin in an air atmosphere below 100°C, and end by about 150°C. Given the freedom to overheat so as to speed the process in industry, we can bracket nearly all thermal drying in the interval from ~100°C to ~200°C.

This interval applies to the bed, or charge, of solid. The drying gas, usually either air or combustion gases, may be up to as high as ~700°C in cocurrent drying. A good example is the spray-drying of particulate solids, which are fed as an aqueous slurry through a disperser and sprayed into a hot gas. The exit temperature of both gas and solid, on the other hand, falls about in the interval given above. Many drying operations are countercurrent, wherein the gas entrant temperature about equals the exit temperature of the charge.

The entrant temperature of the drying gas may well determine whether a refractory lining is needed or whether a metal vessel may be exposed directly to the process. One consideration is heat loss: a refractory lining may be used simply as a thermal insulator. Unless the metal structure is of stainless steel, shell corrosion and contamination of the charge may be a further consideration. Refractory linings are often preferred simply to isolate the charge from a steel enclosure. Refractory corrosion rates are usually quite low because the temperature is low; but abrasion must be considered, along with possible contamination of the product by refractory dust.

In tray drying, where the charge never touches the enclosure, this consideration vanishes and friable insulating refractories serve admirably.

Petroleum and Petrochemical Processing

This category, at its lower-temperature end (nominally 100° to 400°C), encompasses a host of diverse purposes including polymer manufacture. Most organic chemical process systems are not very aggressive. Glass-lined steel vessels are in common use, even up to moderate pressures; stainless steel as well. Steel-clad or unclad plastic vessels (generally thermoset, or crosslinked polymers) can serve up to about 300°C. "Impervious" carbon equipment finds limited use over the whole temperature range, owing to its chemical inertness especially to chlorides and HCl. Except for this last case, the lower-temperature domain of petrochemical processing is not a domain for much refractories usage.

Petroleum refining, on the other hand, reaches up into temperatures and may entail aggressive chemicals such that organic polymers, glass, and bare steel sometimes cannot serve for containment. Crude oil is usually contaminated with some NaCl, and it contains small amounts of organic compounds of oxygen, nitrogen, sulfur, and of metals such as vanadium, nickel, and others. Its refining consists largely of (a) fractional distillation processes, and (b) catalytic chemical treatments designed to break down (i.e., "crack"), build up (i.e., polymerize), or rearrange the molecular structure (i.e., "reform," "isomerize," "akylate," etc.), in various of its hydrocarbon fractions. Stills and vacuum stills are for the most part made of steel. But high-pressure H_2 is a prominent chemical reagent used, e.g., in hydro-cracking and elsewhere, together with circulating solid catalysts that are abrasive. Refractory linings of cracking equipment provide the needed abrasion resistance, and their thermal insulation reduces steel shell temperatures so as to impede hydrogen embrittlement. Desulfurization and denitrification catalysts are also abrasive, and refractory linings can also protect their processing vessels against both wear and hydrogen attack. "Reforming" is an acid-catalyzed process calling for acid-resistant vessel linings or coatings.

The "bottoms" or residues from petroleum refining ultimately become commercial tars, pitches, asphalts, and coke. They tend to concentrate corrosive nonvolatile impurities. Their hot chemical treatment calls for resistance to acids and salts. But in all of these above refractory uses the processing temperatures are low relative to refractory melting points, and linings tend to be long-lived.

Calcining of Hydroxides

Calcining means heat-treating an inorganic solid well below its melting point, yet hot enough to effect either some desired chemical decomposition or else some desired degree of recrystallization and crystal growth. Here we have a case of the former: a decomposition described by the general equation,

$$M(OH)_x \rightarrow MO_{x/2} + x/2\ H_2O_{(g)}\ .$$

As a number of oxyhydroxides are important in industry, another general equation is written:

$$MO(OH)_x \rightarrow MO_{1+x/2} + x/2\ H_2O_{(g)}\ .$$

Another class of (partly) hydroxide compounds, or *hydrated* compounds, is comprised of the clay minerals. Their thermal decomposition by calcining can be illustrated here using a disarmingly simple representation of kaolinite:

$$Al_2Si_2O_5(OH)_4 \rightarrow Al_2Si_2O_7 + 2\ H_2O_{(g)}\ .$$

Examples of the first reaction that feed the refractories industry among others include the synthesis of alumina from gibbsite: $2Al(OH)_3 \rightarrow Al_2O_3 + 3H_2O_{(g)}$, and the synthesis of magnesia from brucite: $Mg(OH)_2 \rightarrow MgO + H_2O_{(g)}$. Examples of the second include the preparation of catalytically-active gamma-alumina from precipitated boehmite: $2AlO(OH) \rightarrow Al_2O_3 + H_2O_{(g)}$, and the synthesis of rutile pigment from precipitated titanyl hydroxide: $TiO(OH)_2 \rightarrow TiO_2 + H_2O_{(g)}$. Large amounts of calcined clays are produced by reactions analogous to the third equation above. Every one of these examples has up to a dozen individual analogs of industrial importance.

These decomposition reactions occur gradually with increasing temperature. A TGA plot of weight loss of the solid vs T is an S-shaped curve, rising gradually above a threshold temperature, then steeply, then tailing off to approach completion asymptotically at much higher temperatures. Different hydroxide compounds undergo decomposition over different temperature ranges, encompassed by the "Calcining of Metal Hydroxides" bar in Figure II-1.

To facilitate the escape of water vapor, the bed or charge is normally fed and rotated as particulate material. If melting is to be avoided, the temperature must be increased somewhat slowly since mixtures of the hydroxide and oxide may well melt lower than the former and the final temperature of the S-shaped decomposition curve often lies far above the hydroxide melting point. Na and K compounds as impurities (common in mineral feeds) especially

promote partial melting. Typical consequences of partial melting include caking and *agglomeration* (balling-up) of particles and their adherence to the walls of the vessel.

These chemical systems are relatively benign toward refractory linings. The most aggressive attack is by abrasion. A very small amount of agglomeration can be helpful, by building up a thin protective layer on the refractory wall whereby refractory abrasion is stopped off. Excessive buildup, on the other hand, is troublesome: its occasional spalling can send large undecomposed chunks into the discharged solid, and periodic shutdown may be required for scraping or *de-scaling* of the walls.

Steam Generation

Superheated steam is ubiquitous in industry, used by utilities to drive turbogenerators and by refineries and chemical plants as a source of process heat. A steam boiler consists of burners and an array of metal tubes facilitating thermal contact of pressurized water with a "cool" (i.e., slightly oxygen-deficient) flame; all surrounded by a refractory-lined enclosure. While thermal insulation is a primary function of the refractory, over long time intervals the chemical aggressiveness of combustion products becomes significant.

The gaseous combustion products CO, CO_2, H_2O, and air residues of N_2 and O_2 are familiar. We will deal later with the effects of CO on certain refractories. But with the possible exception of natural gas, inexpensive industrial fuels are also sources of accompanying alkali compounds (principally NaCl), sulfur compounds, and a spectrum of other inorganic salts. U.S. coals, for example, range from about 0.5% to the order of 5% sulfur by weight, and from about 5% to 10% or more of *ash* (nonvolatile inorganics). Heavy fuel oils are on the whole somewhat cleaner, but only somewhat. Furthermore, a yellow flame of whatever fuel origin contains fine particulate carbon or soot.

Volatile compounds (principally SO_2, chlorides, and alkalies) react and condense as liquids on the refractory walls and form low-melting solutions in the hot-face layer. Other ash components stick to these and substantially dissolve in them as well, all softening the refractory surface. Meanwhile, bombardment of the walls by carbon and ash particles (and also coal) abrades the softened refractory. Depending on location and local gas flow patterns, the result may be either eventual refractory wear or else excessive buildup, chemical alteration, and even spalling when the temperature is changed. Buildup of course predominates on the metal heat-exchanger tubes, which are coolest; and on floors, which collect everything that settles. These changes may be slow, but the demands for longevity placed on boiler refractories intensify their importance.

Carbon Combustion

Our concern here is not with the productive burning of a fuel, but with the limitations imposed on carbon and graphite as engineering materials by their susceptibility to burning: certainly a form of corrosion. As numerous oxide refractories for metallurgical processing contain particulate carbon, its loss by combustion is not trivial.

In air, particulate carbon burns rapidly commencing at roughly 500°C; in 0_2 at roughly 400°C; in $C0_2$, above 600°C. Combustion of C in CO is impossible, a fact pertinent to steelmaking; but the admission of air into hot steelmaking vessels lined with carbon-bearing refractories can be severely damaging in a short time. Similarly with respect to massive carbon or graphite used as resistive heating elements or as electrodes in arc furnaces: exposure to air or $C0_2$ or other oxidizing agents while hot is the principal cause of wear.

A word might be injected here concerning SiC, used in massive forms in its own right but also introduced into some oxide refractories in substitution for particulate carbon. Massive SiC can sustain temperatures of 1500°-1700°C in air without burning, and particulate SiC is only modestly less resistant. If survival in air were the only consideration, SiC would be the unhesitating choice. Other considerations do apply, however. They will be attended to later.

Glass Manufacture

If all the special glasses of industry were included, this bar in Figure II-1 would be much lengthened at both ends. Vitreous silica, for example, melts at 1723°C; and "water-glass" (a soluble sodium polysilicate) is made at room temperature. The tonnage silicate glasses are melted between about 500° and 1000°C, however. Superheating to as high as 1500°C or so is common in glass manufacture, for reasons given presently below.

The feed materials for commercial glasses include soda ash, Na_2C0_3; siliceous minerals ($Si0_2$ and various aluminosilicates); limestone, $CaC0_3$; potash, K_2C0_3, or sometimes lithium carbonate; sometimes magnesite, $MgC0_3$, or strontium or barium carbonate; sometimes borax, $Na_2B_40_7$; sometimes Pb0 or $PbC0_3$; and sometimes colorants. When a selected formulation is melted and stirred together, the carbonates decompose:

$$MC0_3 \rightarrow M0 + C0_{2(g)}, \text{ etc.};$$

and the product oxides dissolve in each other, forming one homogeneous liquid phase.

The silicate liquid is polymeric and viscous. If this were not so, it would crystallize out separate phases on cooling instead of undercooling in the *vitreous* (i.e., atomically disordered) state. Being viscous, it has to be heated well above its melting temperature in order for it to flow readily. Fluidity is needed for homogeneity of mixing, for the rise and expulsion of gas bubbles, and for pouring, fiberizing, etc.

Being in that sense superheated, the as-manufactured liquid is thermodynamically capable of dissolving some quantity of every other oxidic substance known, including its own component oxides. Nowhere else is it more universally certain that oxide refractories of containment (here called "glass contact" refractories) must necessarily dissolve in their charge -- and indefinitely over time, since in mass production the glass moves and is replenished continuously.

The concentration of alkalies (Na_2O, K_2O) in glass formulations is higher than refractories encounter in most other services; and akalies are notoriously aggressive toward oxide refractories. But the challenge does not end there. These alkali oxides are volatile at glassmaking temperatures, and uniquely so among the other glass components. Not only do they escape from the upper surface of the melt. Every CO_2 bubble that rises from the glass also carries in it a near-saturated partial pressure of M_2O gas, increasing the evolution rate.

The glass melting tank is thus an alkali distillery. The atmosphere above the liquid is enriched in alkalies alone, isolated from most other components of the melt. Now unimpeded by the viscosity of a liquid host, these corrosive gas molecules attack the sidewalls and roof of the glassmaking vessel. Since the heating gases are further used after passing over the glass melt, threading through a checkerwork of heat-exchanger bricks before being discharged, their entrained alkalies also attack the exhaust port, ducting, and the checker bricks themselves. In fact, a material balance can be struck in the entire containment system above the *glass line*, or meniscus:

$$M_2O_{\text{(deposited in refractories)}} = M_2O_{\text{(evaporated from the melt)}}.$$

Refractory alteration is inevitable. It is only a matter of time, or kinetics.

Metal Carbide and Nitride Synthesis

Refractory metal powders and some powder-metallurgical compacts are converted to carbides by diffusion-reaction with simultaneously-cracked light hydrocarbons, e.g.:

$$Ta + CH_{4(g)} \rightarrow TaC + 2\ H_{2(g)}$$

The hydrogen produced appears first as monatomic H, some of which enters the metal as hydride, pulverizing it. Carbon diffusion is usually quite incomplete, requiring subsequent heating to 1800°C or so for homogenization. Similarly, nitriding is often done by cracking ammonia gas on the metal, e.g.,

$$Ti + NH_{3(g)} \rightarrow TiN + 3/2\ H_{2(g)}$$

Nitriding is also conducted using N_2 instead of NH_3, calling for reaction temperatures up to the 1800°-1900°C region. This works neatly with formed powder compacts, since they are sintered at the same time.

These are air-free reactions, generally conducted in water-cooled metal equipment capable of sustaining vacuum as well as pressure. Electrical heating techniques are used, isolating the work thermally from the envelope as much as possible. These systems are not candidates for industrial refractories usage.

"Pack-cementation" carbiding is also practiced, involving embedment of a metal object in carbon black, often in a graphite enclosure and electrically-heated, in turn surrounded by much more powdered carbon in a larger metal box. The large excess of carbon reacts with any stray air, providing a bathing atmosphere of CO. It also provides thermal insulation, and in that sense may be regarded as a refractory. A special case of this kind is the manufacture of SiC, to be described later.

Coke Manufacture

There are many uses of coke, and accordingly numerous commercial grades, originating either in coal or in petroleum residues. The heaviest tonnage use of coke is as a reagent in the smelting of iron ore: step one in the making of all iron and steel.

The superficial chemistry of coke manufacture is about the same whether the feed is a coal or a petroleum residue. The general equation is:

$$C_xH_y \rightarrow x\ C + y/2\ H_{2(g)}$$

But on the way to this end, a host of volatile organic byproducts are evolved by complex pyrochemical mechanisms. These byproducts are (a) of considerable value, and (b) inadmissible into the environment. They are condensed and collected. Needless to say, the evolved hydrogen is valued too, at least as fuel. Other noncondensibles include C0 and some light hydrocarbons, also combustible: burning of the stack gases after removal of the condensible byproducts supplies more than enough heat to operate the coking process.

The equipment and the detailed manner of its operation vary with the type of feed. But it is evident that conditions have to be reducing, that is, air-free. Since combustion in air supplies the needed heat, coke ovens are *indirect-fired*, or *indirect-heated*. The vessel containing the charge must be hermetic, and its walls must be relatively conductive of heat. These refractory walls must be resistant to all manner of reducing organics and to coal or petroleum ash on their one side, and to combustion products (high in $C0_2$ and H_20) and much higher temperatures (to about 1400°-1500°C) on their other. Getting the charge in and coked and the product out again entails temperature and atmospheric cycling, not to mention severe abrasion. The double-walled equipment is architecturally complicated: provisions for periodic discharge and major maintenance and those for hermetic sealing are in conflict, and there are needs for numerous special refractory parts and seals. All of this must be accomplished at costs commensurate with the unit value of coke, which is very low.

The product of this operation is referred to as *green coke*, which still retains some greasy hydrocarbonaceous character. In many cases that product is calcined in a subsequent step at still higher temperatures. *Calcined coke* is flinty-hard and free-flowing, free of nearly all contained hydrogen and other volatiles, but still possessing a considerable content of ash or nonvolatile inorganics.

A separate bar for calcining of granular coke has not been included in Figure II-1. It would fill the temperature gap between Coking and Baking of Carbon, overlapping the latter. Coke is typically calcined in a reducing flame in rotary equipment, to about 1200°-1400°C. Anthracite, which is similarly prepared for making certain kinds of electrodes, is calcined far hotter: to as high as 1800°-2000°C in electrically-heated vertical kilns. In both of these cases the containing refractories face reducing conditions at variously high temperatures, combined with severe abrasion.

Sulfide Ore Roasting

Numerous of the transition metals (Fe series) and Group I' to V' metals of the Periodic System (e.g., Cu, Ag; Zn, Cd, Hg; Pb, As, Sb and Bi) occur in nature at least in part as commercially significant

sulfide ores. These ores are not *smelted* directly (i.e., reduced to metal); they are first *roasted* in air at temperatures mostly from about 600°C to 1200°C, to oxidize sulfide and replace it by oxide:

$$MS_x + 3x/2\ O_{2(g)} \rightarrow MO_x + x\ SO_{2(g)} \quad .$$

As sulfide ores are impure and accompanied by siliceous minerals, in roasting it is difficult to avoid partial melting. Roasting furnace refractories must withstand not only a sticky and agglomerating charge, but also the acidic attack of SO_2 gas. That gas must be trapped, giving rise to chemical scrubbing systems interpolated between furnace and stack. Scrubbers usually operate at much lower temperatures, and will not be singled out here.

Heat Treating and Annealing

This bar in Figure II-1 encompasses only ferrous-metal processing. As applied to nonferrous metals and to glass, it would be extended down considerably in temperature. Products ranging from ingots and billets to sheet and bar stock to finished articles are typically put through programmed heating and cooling for various adjustments of microstructure and/or internal stress relief. Interaction of the charge with refractories is close to nil; but combustion gases and the evolution of machining oils often have to be coped with. On a relative scale, the environment is not very aggressive to refractories. The user compensates for this by expecting them to be exceptionally long-lived.

Aluminum and Magnesium Manufacture

These two commercial processes are D.C.-electrolytic, using fused-salt electrolytes. For aluminum, the electrolyte is a low-melting composition of Al_2O_3, AlF_3, NaF, and minor additives: when molten, a solution of Al^{+3}, Na^+, O^{-2} and F^-. The electrode reactions taking place at about 800°C are,

$$\text{Cathode: } 2\ Al^{+3} + 6\ e^- \rightarrow 2\ Al_{(liq)}, \quad \text{and}$$

$$\text{Anode: } 3\ O^{-2} \rightarrow 3/2\ O_{2(g)} + 6\ e^- \quad .$$

That is, Al_2O_3 is consumed and periodically replenished. The aluminum is collected in a wide, shallow pool and periodically *tapped* (drawn off) while the cell runs continuously. A small amount of elemental Na is formed by the analogous cathode reaction of Na^+, dissolving in the Al. The liquid-metal pool is the cathode, contained in a shallow box of compacted carbon refractory with sidewalls either also of carbon or else of SiC. This electrically-conducting containment

must be resistant to liquid Al and Na, and to the fused oxide-fluoride electrolyte which lies on top of the metal pool.

Specially-formulated baked-carbon anode rods are used, developed empirically for maximum corrosion resistance. The 0_2 that is made anodically appears first as monatomic 0, which is effective in burning carbon. It is accompanied by a small amount of F and then F_2, formed by the analogous anode reaction of F^-. This attacks carbon vigorously. Thus the anodes are consumed continuously by corrosion; they are fed down mechanically to maintain constant anode-cathode vertical spacing. Granular Al_2O_3 feed maintains an overhead *skull*, or self-refractory; the lining of the upper part of the surrounding shell need be resistant only to 0_2 and F_2 gases and occasional splashes of the electrolyte. Once started, the Hall-Héroult cell maintains its operating temperature by the resistance (I^2R heating) of the working current. Local heating may run up to about 1000°C.

The metal product is collected either as liquid or as ingots and transferred to remelt furnaces for purification and alloying. These also run between the Al melting point of 660°C and about 1000°C. Remelting employs a molten added cover layer or *flux* of NaCl-KCl, which protects the liquid Al from air and also collects oxides and other impurities as a final floating *dross*. Hence, remelt furnace linings must be resistant to Al, alkali-metal chlorides, and miscellaneous fused oxychlorides in solution. They must also resist dissolving in and thus contaminating the aluminum, which is intolerant of impurities such as iron and silicon.

The Dow cell for making magnesium is operated somewhat similarly, and at similar temperatures since Mg melts at ~650°C. In this case the electrolyte is principally of molten $MgCl_2$, or Mg^{+2} and Cl^-. The electrode reactions are,

$$\text{Cathode: } Mg^{+2} + 2\,e^- \rightarrow Mg_{(liq)}, \text{ and}$$

$$\text{Anode: } 2\,Cl^- \rightarrow Cl_{2(g)} + 2\,e^- .$$

Thus the cell linings must be resistant to Mg metal, chlorides, and chlorine gas; and the last-named consumes the anodes. Remelt furnace linings for Mg have about the same exposure as those for aluminum, except for the identity of the molten metal.

Calcining of Carbonates

This bar in Figure II-1 starts with limestone and magnesite in the 800°-1100°C region, then continues with strontium and barium

carbonates in the 1100°-1300°C region. These processes are like the hydroxide decompositions discussed previously. The same type of S-shaped decomposition curve prevails, and the same precautions have to be taken to avoid melting.

The general equation for calcining of the alkaline-earth carbonates is:

$$MCO_3 \rightarrow MO + CO_{2(g)}, \text{ where } M = Mg, Ca, Sr, Ba.$$

Calcined magnesite, MgO, is a component of some refractories. Calcined lime is the largest-tonnage and most familiar product among these four. Strontium and barium oxides find uses in glassmaking and as chemicals. The oxides of Ca, Sr, and Ba are increasingly *basic*, or caustic. They also react increasingly vigorously with water or water-vapor to make their hydroxides (called *slaking*) and are increasingly soluble in water, in that order. MgO is the best-behaved of these as an engineering material, but is nonetheless chemically basic. It will slake in water:

$$MgO + H_2O \rightarrow Mg(OH)_2 \ ;$$

but this reaction of pure magnesia becomes more sluggish with increasing calcining temperature (hence increasing MgO crystal size and perfection). If impure magnesite is calcined hot enough (say, to about 1700°C), the MgO crystals become coated with silicates and thus also protected from the slaking reaction. Such a liquid-phase-sintered impure oxide is called *dead-burned.*

Refractory formulations calling for significant amounts of both MgO and CaO are often made in part of calcined dolomite, or *dolime.* Dolomite is a mixed mineral of $MgCO_3$ and $CaCO_3$; this introduces nothing new into the calcining reaction. But the product oxides are not very soluble in each other, and the CaO component of dolime remains subject to slaking even after high-temperature firing. Slaking is disruptive to any formed oxide body.

Refractory containment for the calcining of alkaline-earth carbonates has to manage temperatures up to ~1100°-1300°C. If calcining is extended on up to 1500°-1800°C to grow the oxide product crystallites, corrosion reactions on the refractory lining become much more important. These include reactions with the basic oxide products (e.g., MgO or CaO). Corrosion is augmented in intensity if silicates, alkalies, and iron are present in the oxides (common in calcined minerals), owing to the fluxing action and penetration of these liquid components. Abrasion is a major further factor.

Lime kilns in particular are very large and subject to some flexure, giving rise to significant mechanical loads on their linings. Finally, reaction products which pack into the interstices between bricks while hot cannot extrude out on cooling when a kiln is shut down for any reason. Spalling is a potential consequence. The performance demands placed on lime-kiln refractories are underscored by the low unit value of the product: long, trouble-free lining life is essential.

Decomposition of Sulfates

Between about 800°C and 1500°C, most sulfates decompose in air. A suitable representation is:

$$SO_4^{-2} \rightarrow O^{-2} + SO_{3(g)} \text{ (or, } SO_{2(g)} + 1/2\ O_{2(g)}).$$

Writing the equation in this way signifies that our concern is with sulfate as a minor additive or impurity (i.e., placed substitutionally in an oxide host); not as an identified bulk compound to be decomposed commercially, such as gypsum. Sulfates, sulfites, or organic sulfonates which ultimately behave in about the same way, are sometimes used as *binders* or *binder-lubricants* in the compaction of oxide refractories. Their decomposition is only mildly disruptive to the host, and transient. Refractories that are fired or that see service at 1500°C or above are not likely to be troubled by the presence of residual sulfur, even in trace quantities in crystallite boundaries.

This knowledge is also of some use in assessing the consequences of exposure of oxide refractory linings to environments rich in SO_2. Chemical combination with such linings is unlikely to be troublesome above about 1300°C. The sulfurous environment of coal-burning or heavy oil-burning flames, for example, is likely to be damaging to a refractory only below this range (see Steam Boilers); and sulfurous coke-oven atmospheres are also aggressive because the temperature is relatively low, not high.

One might well inquire why, this being the case, the deliberate oxidation of sulfide ores in the range 600°-1200°C yields gaseous SO_2 and condensed oxide products rather than condensed sulfites or sulfates (see Sulfide Ore Roasting). There are several reasons. One is that equilibrium can be swung over magnitudes by manipulating the partial pressure of SO_2 (or SO_3 or SO_2 and O_2). Another is that SO_2 and SO_3 are acids, and their greatest chemical affinity in condensed phases is with basic oxides: those of the alkali metals and alkaline earth elements. The sulfide ores that are successfully roasted to oxides are those whose oxides are relatively acidic -- of low affinity for SO_2 and SO_3. And finally, those roasting reactions are by no means quantitative. Some sulfur is virtually always left in the products.

Carbothermic Reduction of Oxides

This large family of *smelting* processes encompasses most of the metals of Groups I'-V' of the Periodic System -- usually referred to as the *nonferrous metals* --, and the *ferrous metals* based on iron. These terms are somewhat vague if unexplained, however: (a) there are many other nonferrous metals that either are not or cannot be reduced by carbon; and (b) of the ferrous elements which are capable of being directly produced carbothermically, only iron is so made. A brief overview of commercial extractive metallurgy may help orient the reader.

Figure II-2 is an abbreviated Periodic Table showing the elements of interest both in this connection and for general reference, giving the melting point of each in °C. Solid lines in the figure divide these elements into rough categories with terse descriptive names. Pertinent remarks concerning smelting of the elements in each category are given in outline form below.

Ferrous Metals

Fe - Carbothermically reduced.
Ni - Carbothermically reduced but distilled as $Ni(CO)_4$ (b.p. 43°C)
Cr, Mn, Co - Aluminothermically reduced (form carbides with C).

Semimetals

Ga, Ge, As, In, Sb - Carbothermically reduced.
C - Discussed previously here as Coke; also made as "carbon black", or soot.
Si - Aluminothermically reduced (forms a stable carbide with C).
B - Magnesiothermically reduced (reacts with both C and Al).

Low-Melting Metals

Zn, Cd, Hg, Sn, Pb, Bi - Carbothermically reduced.

Noble Metals

Cu, Ag (in part) - Carbothermically reduced. Much Ag is native.
Au and Others (Pt group) - Reduced with hydrocarbons or thermally. Also occur as native metals.

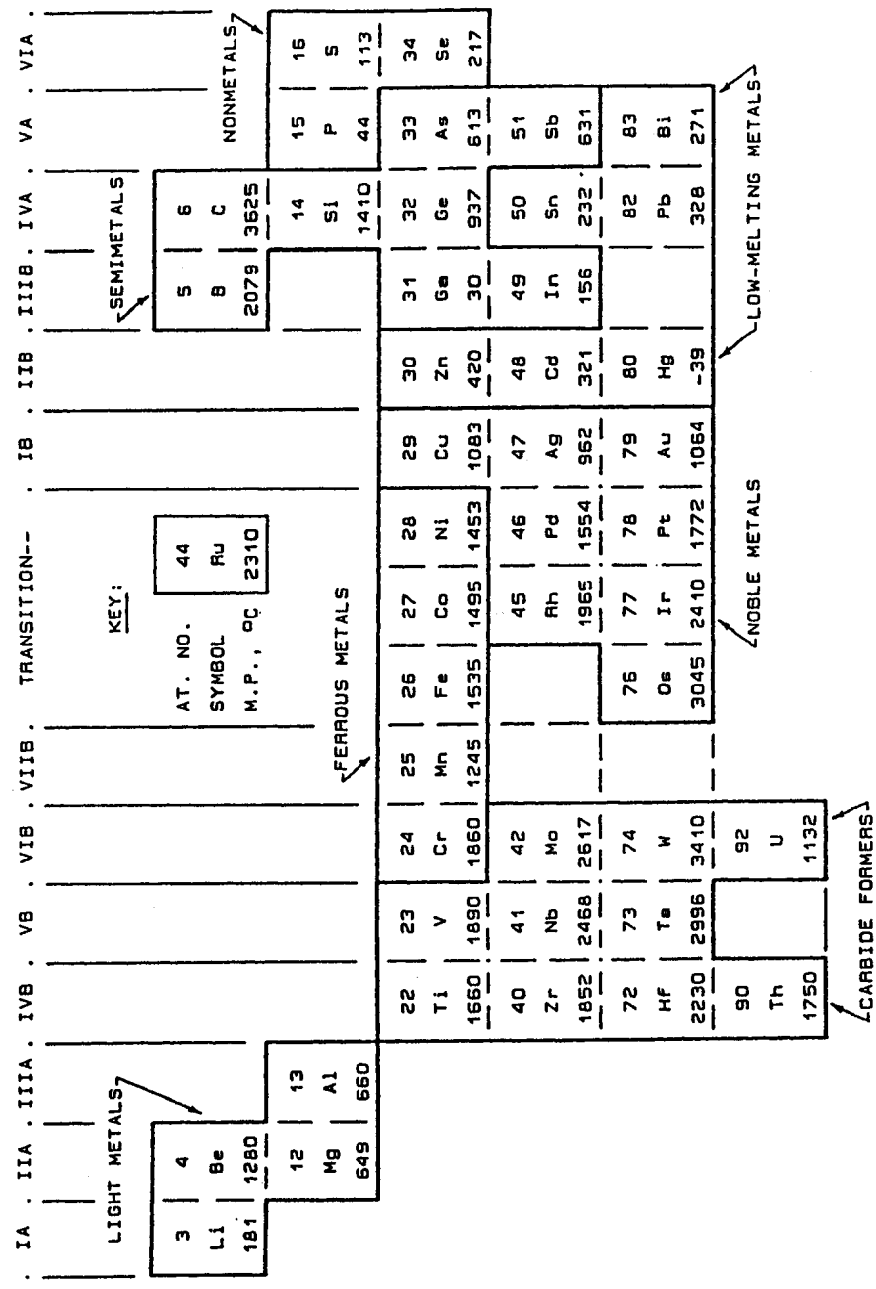

Figure II-2 Melting Points of the Elements, °C (Ref. 11)

Nonmetals

P - Carbothermically reduced.
S - SO_2 reduced by H_2S at low temperature.
Se - SeO_2 reducible by H_2Se or other mild reducing agents at low T.

Light Metals

Li, Be, Mg, Al - Electrolytically reduced; Al and Mg discussed previously. Others of Periodic Groups I and II (not shown) - Electrolytically reduced.

Carbide Formers (generally form stable monocarbides)

Mo - MoO_3 reduced by H_2 at 500°-1000°C.
Ti,W - Aluminothermically reduced.
V, Zr, Nb, Hf, Ta, Th, U - Halides reduced by H_2, Na, or K.

In this context, *carbothermic reduction* means high-temperature conduct of the following general reaction:

$$MO_x + x\,C \rightarrow M + x\,CO_{(g)} \quad .$$

Similarly, *aluminothermic reduction* is the high-temperature conduct of:

$$MO_x + 2x/3\,Al_{(liq)} \rightarrow M + x/3\,Al_2O_3 \quad .$$

And *halide reduction*, by sodium as example, can be illustrated by the following equation although fluorides or various double salts are used in some cases:

$$MCl_x + Na_{(g)} \rightarrow M + x\,NaCl \quad .$$

The reduction of halides is a relatively low-temperature operation, using metal containment and often in the form of sealed "bombs." Aluminothermic reduction amply supplies its own heat, once started: its equation above describes the well-known "thermite" reaction. Skull or self-refractory containment is most often employed within an outer steel shell. In both of these cases, if the product metal melting-point is exceeded a pool of metal collects at the bottom of the working volume; if not, either a powder or "sponge" is produced which must be subsequently consolidated (see later under Refractory Metal Manufacture). By disposing of these two extractive processes summarily here, we return to carbothermic reduction.

Nonferrous Metallurgy

With few exceptions, the ores and roasted ores in the Semimetals and Low-Melting Metals categories contain at least several of these elements, among which non-native or combined Ag may be found as well. Figure II-2 reveals that all of these metals are relatively low-melting (<1000°C), at least half of them so low that vapor-pressures at the smelting temperature are appreciable. Accordingly, (a) smelting equipment must be contrived to condense and recover volatile products, and (b) subsequent separation of individual metals can be effected by liquid- and gas-phase processes such as fractional crystallization, extraction, and distillation.

Copper lies on the edge of this nonferrous group. In Figure II-2 we have classified it with the Noble Metals, of which it is the least noble. It melts only some 100°C higher than the highest of the other nonferrous metals. Post-smelting separation of other elements from Cu includes the methods given just above, but also includes an aqueous electrolytic process yielding high-purity Cu (used mainly as an electrical conductor where the highest conductivity is needed). Copper smelting is a somewhat complicated sequence of operations, which will be treated separately in Chapter III.

Silicates accompany virtually all of the minerals of this group, making it possible to conduct the carbothermic smelting reaction, $MO + C \rightarrow M + CO_{(g)}$, such that the reagent "MO" is a component of a liquid phase. This is desirable: the other reagent, carbon (typically coke or even coal) is always solid, and solid-solid reactions are too slow. In some cases, *fluxing* or *slagging* chemicals are added to bring this liquefaction about. Smelting temperatures range from a low of about 1000°C for lead and others to a high of about 1600°C for copper, dictated far more by reaction rate considerations than by thermodynamics.

At least some of the metal product occurs in a heterogeneous mixture with the *slag* or *gangue*, comprised mostly of unreduced silicates and some excess unreacted carbon. Product recovery may entail reheating after crushing, as in the case of copper, or distillation as in zinc, lead, and other low-melting metal processing.

Containing refractories must resist the reducing action of carbon and CO gas, excessive penetration by the metals produced, alteration by SO_2 and by low-melting complex silicates (often including some alkalies), and in continuous processes the grinding and abrasion of a moving charge. Thermal stresses accompany all startups and shutdowns. Some of the operations are *direct-fired* or *direct-heated* by contact with combustion gases; others, *indirect-heated,* can intensify refractory corrosion and alteration since the bulk

of the refractory is then hotter than the working face and penetrating liquids cannot freeze. In the *blast furnace* form of smelting, a large excess of carbon is fed and is burned in injected hot air to generate the needed process heat. In the *reverberatory* form, hot combustion gases pass over a shallow bed of the charge and under a low overlying roof, which radiates much of its heat back into the bed.

Iron and Steel

Iron ores are smelted in huge, continuous-fed vertical blast furnaces. The coarsely-crushed charge, mainly a mixture of ore, limestone, and a large excess of coke, enters at the top and moves down by gravity as it is consumed and/or discharged at the bottom. Abrasion is ever-present. The smelting reaction depends on the particular iron oxide(s) in the ore, but is most often or predominantly:

$$Fe_2O_3 + 3\,C \rightarrow 2\,Fe_{(liq)} + 3\,CO_{(g)}\,.$$

This reaction and the decomposition of limestone,

$$CaCO_3 + C \rightarrow CaO + 2\,CO_{(g)}\,,$$

absorb heat. The necessary heat is supplied by the combustion of coke,

$$2\,C + O_2 \rightarrow 2\,CO_{(g)}\,,$$

using a blast of preheated air or O_2-enriched air injected near the bottom. The up-flowing gases are finally cooled by the incoming cold feed; exit-gas temperatures are in the region of 300°-500°C. The entrant air is preheated to some 800°-1100°C, and the maximum working temperature in between runs from about 1700° to 2000°C, depending on the operation. This is far hotter than necessary to melt iron (see Fig. II-2); superheating is dedicated to increasing the throughput rate. The CaO from the decomposed limestone reacts with silica and silicates in the ore, and all these melt together and partially dissolve the iron oxide. The liquid cascades down over the coke, facilitating the smelting reaction and dissolving more iron oxide on the way. On reaching the bottom this liquid, largely depleted of its iron oxide, forms a pool of molten siliceous slag lying atop and protecting the collected pool of liquid iron on the bottom or *hearth* of the furnace. Both liquid layers are periodically tapped, one going to further processing and the other to waste impoundment.

Outside the furnace stands a set of (usually, three) "stoves" containing checkerworks of heat-exchanger brick, in principle not unlike those used with glass melting furnaces. In rotation these are (a) heated by combustion of the blast furnace exit gas, which is largely CO; and then (b) used to heat a stream of air or enriched air

which is then fed into the blast furnace as described above, sometimes under elevated pressure.

It is typical of *recuperative* shaft furnaces, i.e., those which cool the outgoing gas with incoming feed, that a circulating load of volatile/condensible byproducts is carried within. The ironmaking blast furnace is one such. Its interior circulating load is comprised principally of alkalies (Na_20, K_20), some alkali halides (NaCl, KCl), and zinc, which are boiled out of the charge at the lower levels and rise in the gas phase, to be condensed at the cooler upper levels and then carried down again in the charge, ad infinitum. These corrosive agents of course also condense on the furnace walls, where they can be particularly aggressive at temperatures between about 500° and 1400°C.

In *regenerative* furnaces (i.e., those whose off-gas is burned to supply their own process heat), the off-gas is hardly a clean fuel. The blast furnace off-gas contains, in addition to some alkalies, other impurities of sulfur and phosphorus, some chlorides, and miscellaneous other volatiles. These occur partly as gases and partly as a fog of liquid droplets, together with a stream of entrained dust on which they condense also in part. Dust separation is practiced, but is incomplete inasmuch as immense volumes of gas must be processed in restricted space and time and with as little pressure drop as possible. Consequently the stoves and their associated equipment receive a cumulatively heavy load of most of these impurities in addition to the combustible C0 and residual N_2 gases.

The source of the sulfur and phosphorus mentioned above consists primarily of compounds of those elements present in the iron ore. Their carbothermic reduction to elemental S and P should be minimized, since those free elements are soluble in liquid Fe. As their oxides are acids, those oxides can be somewhat diminished in chemical reactivity toward carbon by reacting them with a base, namely Ca0. This is one of two reasons for maintaining a high $Ca0:Si0_2$ mol ratio in the feed. The other relates to the silicate component itself. As the $Ca0:Si0_2$ mol ratio is increased from near zero to about 2:1, on the whole the melting temperature increases a little; but the viscosity of the liquid decreases quite rapidly toward the latter limit. This is because the average length of silicate polymer chains decreases as the relative amount of Ca0 (which terminates those chains) is increased. The melting and solvent action and the transport properties of the molten silicate are all improved by reducing its viscosity; hence the smelting rate can be increased by supplying ample Ca0.

Basic slagging is thus generally identified with a high $Ca0:Si0_2$ ratio, as here. The optimum ratio is influenced by other elements present as well, and may be either greater than or a little less than

2:1. To depress the slag melting temperature, an addition of fluorspar, CaF_2, can be made along with limestone in the feed -- a practice much more used in steelmaking than in smelting iron.

The solubility of carbon in superheated molten Fe is very large. By the time this iron is poured and solidified as *pig-iron*, it still contains up to 10% or more of carbon by weight. It also still contains appreciable quantities of Si, S, and P; and depending on the original ore, it may contain other reduced ferrous metals of which Mn has been the most common and troublesome. The removal of these impurities lies at the heart of the making of steel. Regardless of the equipment and processes used, the principles are the same. Suppose the pig-iron has been remelted in a suitable furnace, or was delivered straight from the blast furnace as liquid without cooling.

The excess carbon is burned out, most often by injecting O_2 gas into the melt. This reaction produces enough heat to sustain the melt temperature, typically 1600°-1800°C:

$$2\ C(\text{in Fe}) + O_{2(g)} \rightarrow 2\ CO_{(g)}\ .$$

Silicon, sulfur and phosphorus are simultaneously oxidized by comparable reactions, yielding SiO_2, SO_2 and P_2O_3 in smaller quantities; and some Fe is oxidized as well, principally to FeO but also in part to Fe_2O_3. The oxidized impurities are chemically scavenged by the use of a basic slag, floating as a liquid or slush on top of the melt. The *slagging chemicals* added to the furnace are typically sand or other siliceous minerals, limestone and fluorspar, in ratios calculated to yield the desired basic $CaO:SiO_2$ ratio and the desired fluidity. Hence the oxidative removal of Si, S, and P from the metal charge is encouraged chemically.

But the chemical effect of basic slags on the removal of contaminating ferrous metals from the melt is relatively inhibiting. If their oxidation process is characterized by, for example,

$$2\ Mn\ (\text{in Fe}) + O_2 \rightarrow MnO\ ,$$

this oxide is more effectively scavenged by an *acid slag*, that is, one which is high in SiO_2 and relatively low in basic components such as CaO. The $CaO:SiO_2$ mol ratio would be typically closer to 1:1. Fluorspar need not be employed, as the melting temperatures of acid slags are lower than of basic slags. Manganese oxide reacts with an acid slag to yield dissolved manganous silicates. Thus "acid" steelmaking processes combine oxygen injection with acid slagging practice, and are dedicated as such to the removal of ferrous metal impurities from iron (see Figure II-2). Other elements in the same row of the Periodic Table, e.g., V and Ni, are also scavenged but not very effectively. Some Fe is also removed as FeO, but not much.

In fact, none of the above impurity removal processes is quantitative. Recent efforts to increase the effectiveness of steel purification have focussed on increasing the time of slag treatment and on starting it earlier, i.e., by conducting these processes in transfer ladles as well as in melting furnaces. If it is necessary to use both acid and basic processes, this must of course be done sequentially; and if both are conducted in the same vessel, the containing refractories are exposed to both kinds of slag in turn. When it is time to add other elements in the making of alloy steels, e.g., chromium, nickel, molybdenum, tantalum, titanium, vanadium, or etc., their mixing is hastened to limit their oxidation. In "aluminum-killed" steel, Al is added to remove CO and contained oxides rapidly, and the resultant Al_2O_3 goes to the slag.

This brief treatment covers the essential chemistry of iron and steelmaking, but not the variety of ways and of vessels in which these processes are carried out. The subject will be revisited later in those contexts. At this point it is evident that steelmaking refractories must withstand, up to exceptionally high temperatures: (a) vigorously stirred or poured "hot metal," its penetration, reducing action and erosion; (b) equally reducing CO gas (periodically interrupted by exposure to air during charging and discharge); (c) acidic and/or basic liquid slag attack, including its splashing, penetration, erosion and abrasion; (d) the thermal and mechanical shock of large-scale transfers of material; and (e) modes of heating and cooling and techniques of valving and of moving massive amounts of liquid about that have not yet even been touched on. If blast furnace refractory life can be measured in (say, 8 to 10) years, some batch-operated steelmaking refractories may last only a month, more or less -- and even then with repeated patching and repair in the meanwhile. More research is devoted to steelmaking refractories than to any other category. They survive far longer than they used to, by factors of 5 to 10 and more. But the challenge of steelmaking remains the severest combination of thermal, chemical and mechanical experiences to which refractories are routinely exposed.

Ingots and Billets

Metalmaking generally ends in the casting of ingots or billets, ready for processing into end-useable forms. This is true not only of the ferrous and nonferrous metals but also of aluminum and magnesium, discussed previously, and of still other metals we have chosen to omit. Ingot molds for the ferrous and comparably-melting metals are typically sand-lined, while refractory-lined lids (called *hot tops* in iron and steel) are used to prevent too-rapid freezing. Low-melting metals are usually cast in unlined steel molds. Again particularly in iron and steel, the ingot molds are arrayed in what is called the *pouring pit*: the area devoted to casting of pigs or ingots.

Continuous casting of billets is an alternative now widely practiced. A vessel of sufficient surge capacity receives liquid metal periodically while delivering it continuously from the bottom down through a water-cooled sleeve such that the liquid metal freezes into a rod. The rod is continuously withdrawn from below so that the freezing plane remains stationary. Exposure of the refractory lining of the surge tank is quite comparable to that in remelt furnaces. Bottom valving or gating presents stringent performance and reliability demands, while the chemical exposure of refractory stoppers and gates is more treacherous than that of the lower surge tank lining. These devices will be given special attention later.

Foundry Operations

Foundries are not given explicit acknowledgement in Figure II-1; but they are significant consumers of refractories. A *foundry* is an installation devoted to the casting of metals in end-useful shapes.

The remelt operation of a foundry is much like that of a metal manufacturer, except smaller in scale and usually conducted batchwise. But the casting molds add new variety to refractories usage beyond that of primary metalmaking. Sand molds are much employed; but so also are numerous other refractory materials and binders and parting aids. The performance criteria differ considerably from those of a wall lining, and so do the materials used.

Sintering of Oxidic Ceramics

This bar in Figure II-1 starts with brick, tile, and clay pottery, some sintering well below 1000°C, and goes on through stoneware and porcelain (still products of selected clays and minerals) to the sintering of more and more highly-purified oxides of successively higher melting points. The highest oxide processing temperatures run up to 1800°-1900°C. The forms of material sintered range from small aggregates of particles looking like sand or pebbles or rocks, up to compacted and shaped bodies from spark-plug insulators to clay pipe and ornamental urns and sculptures measured in feet. Refractory aggregates fall in the smaller category, formed refractory bricks and blocks in the larger. Their sintering temperatures range from about 1200° to 1900°C, depending on composition and intended temperature of use.

Sintering is the thermal bonding and consolidation of particulate materials into a relatively strong, rigid and cohesive mass, conducted without major melting so that the initial shape is substantially retained. *Solid-state sintering,* depending wholly on

solid-state diffusion, is reserved to the purest of substances, as for example a 99.99%-pure Al_2O_3. *Liquid-phase* sintering is vastly more common: a few percent (more or less) of the material melts, wetting, dissolving in and bonding the remainder together while that remainder persists as solid. This phenomenon may be unplanned, as it is in sintering most single compounds of ordinary purity. Or it may be quite deliberately undertaken as in the making of porcelain, bone china, stoneware, and the lower-fired clay products -- all of which depend on the viscous nature of molten silicates to retain their shape through firing. In fact stoneware to a degree, and porcelain and chinaware quite evidently, are *vitrified*: the molten silicate phase subsequently undercools as a glass and remains a substantially non-crystalline continuous phase in the final product, while the solid particles bonded by that phase can be readily detected by appropriate optical techniques. In other material systems, including some refractories, the molten phase may be far less viscous. Slumping is avoided by careful sizing of the solid particles and dense, high-pressure precompaction such that the liquid phase is restricted to very thin films.

In *reaction sintering*, advantage is taken of the atomic mobility that accompanies a chemical reaction between substances initially present, forming one or more new substances, to create new chemical bonds in the process -- ordinarily without actual melting but initiated by heating. A number of refractory formulations are thus *chemically bonded,* as will be detailed later on. *Hot pressing* and *hot isostatic pressing* are techniques for conducting sintering under pressure so that, as the heated mass becomes plastic, it is still more tightly consolidated. These operations call for special equipment, to be touched on later.

Finally to avoid misunderstanding, *cement bonding* should be mentioned here. This term is reserved in ceramics for low-temperature bonding mechanisms of which hydraulic cementing (the formation of -0H by hydration and the subsequent forming of M-0-M' bonds by splitting-out of water) is typical. Cement bonding may or may not have utility at high temperatures: Portland cement concrete, for example, is not a very refractory material. But a number of ceramic cements that set up at low temperatures, and are initially cured at low temperatures, go on through hot processing via either minor modification or other subsequent chemical reactions to create durable bonded structures. Cement-bonded refractories employ such added chemicals. Their final chemical bonding is often carried out in actual service, rather than via thermal maturing in manufacture.

Sintering is generally conducted in fuel-fired equipment, and direct-heated. If it is necessary to protect the charge (called *ware* in the case of formed ceramic artifacts) from the dust and soot and impurities in combustion gases, either an indirect-fired kiln is

contrived or the equivalent interior hardware is erected surrounding the ware. Such protective enclosures are called *muffles*. An enclosure surrounding only one or a few articles for firing is called a *sagger*; these may be stacked quite high, each one also providing mechanical support for its contents and thus preventing sagging under their accumulated weight. Refractories used for muffles and saggers need to be relatively conductive of heat, while those lining the kiln need to be relatively insulating. In any case, they are all exposed to combustion products.

Sintering of materials containing iron compounds (i.e., most unpurified minerals and especially common clays) proceeds at a lower temperature under reducing conditions than it does under oxidizing conditions, since ferrous (Fe^{+2}) compositions generally melt lower than ferric (Fe^{+3}). Thus, for fuel economy and/or for most effective consolidation and bonding, the programmed heating often includes a period of *reduction firing,* i.e., in a fuel-rich atmosphere. During that period soot is produced in the combustion flame, and of course all refractories in the equipment are then exposed to reducing conditions. A period of *oxidation firing* may follow before slow cooling is undertaken, whereby all refractories in the equipment experience chemical cycling of the atmosphere.

Volatile compounds and decomposition products are driven out of any impure mineral-based charge in the course of sintering. These volatiles may also come from added organic or inorganic lubricants, binders, cements or chemical bonding agents. As a general rule the most aggressive on the enclosing refractories are inorganic chlorides and HCl, alkalies, and to a lesser degree $S0_2$; but some heavy-metal compounds may be boiled out as well. Reaction and condensation of these volatiles on refractories are cumulative and can result in glazing, penetration and alteration -- ultimately, in swelling, warping or spalling or in failure of refractory joints. Temperature cycling of batch-operated kilns, and of interior hardware in any case, intensifies these consequences.

Ceramic Glazing

Glazing of bricks, tiles, and ceramic artifacts (even occasionally, of refractory bricks) can be regarded as a sort of variation on sintering. If the firing of enamelled metals is included, the process temperatures reach down into the low hundreds of °C; in other special cases, up to the vicinity of 1800°C. As regards the exposure of containing refractories, the principal added factor lies in the extended range of low-melting and volatile compounds that are used in glaze formulations. This wider range includes alkalies at concentrations even higher than those in commercial glasses; but also oxides of boron, selenium, antimony, lead, vanadium and molybdenum, as well as successively higher-melting oxides of cobalt,

tin, copper, iron, cadmium, manganese, titanium, zinc and chromium. Gas-phase transport of the more volatile of these adds to refractory attack.

We have included only one short bar in Figure II-1 that is at all illustrative of glazing. Extending from 1200°C to 1250°C, it is labelled, "Salt Glazing." The operation it represents is the infrequently-practiced one of opening a small kiln in that temperature range and throwing in a scoopful of salt, NaCl. The entire kiln interior is bathed in a cloud of NaCl vapor (b.p. 1413°C), which condenses to liquid by dissolving in and reacting with virtually everything oxidic -- especially, silicates. After a dozen or so repetitions of this brief operation, the kiln lining is found to be literally dripping with low-melting liquid corrosion products, though never heated above ~1250°C. This dramatic episode is described here to emphasize how voracious is refractory attack by alkalies and by chlorides even when these are present in only impurity amounts in other circumstances. Degradation may take longer in those other circumstances; but it nonetheless proceeds, even at temperatures reaching down well below 1000°C. Whenever it is feasible to avoid alkalies and chlorides in hot processing, it is worthwhile to do so for the sake of the containing refractories.

Portland Cement Manufacture

World tonnage producton of Portland cement exceeds that of iron and steel. A feed comprised principally of ground limestone and clay is heated in a direct-fired rotary kiln to well above a minimum temperature of 1500°C, causing the limestone to decompose and the resultant CaO to react with the alumina-silica clay. The product is a calcium aluminosilicate, of $CaO:SiO_2$ mol ratio about 3:1, containing impurity oxides principally of iron, titanium, magnesium, and some alkalies. The $Al_2O_3:SiO_2$ ratio has a considerable latitude, easily met by clays found in many localities.

In the hot zone the product sinters lightly, agglomerating into rough nodules of cement "clinker" which are subsequently pulverized. The sticky material builds up on the hot-zone refractory. The threat of alkaline attack limits refractory selection, but alteration is usually not deep. On the other hand, the large tubular steel shell (up to some 800 feet long) is subject to flexure, calling for high hot strength in the refractory and raising the risk of wedging by intrusion and packing of the cement into open joints. In the cooler zones of the kiln, flexure remains a challenge while corrosion is lessened; but over most of the length, abrasion is severe. Thermal stresses accompany shutdown and startup, as the working temperatures are high (to ~1700°C) and the dimensions are large (to easily 15-25ft. O.D.). Fortunately, the atmosphere is uniformly slightly oxidizing.

Phosphate Decomposition

Inorganic phosphates as additives are often favored in refractory formulations. They undergo durable chemical bonding reactions with the host oxides at temperatures as low as 1000°C. The polyvalent nature of the P atom leads to cross-link bonding in the host:

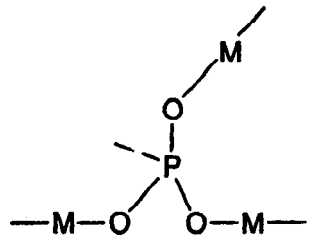

The oxides of P are relatively nonvolatile. The corresponding bar in Figure II-1 shows about where phosphate bonding is decomposed, progressively, and phosphorus oxides are vaporized: up to as high as about 1800°C. Atomic mobility in the host is so high at these temperatures that the decomposition of minor phosphates is not very disruptive. The bridging bonds shown above are readily replaced by M-O-M bonds and host crystal forces. Carbothermic reduction to elemental P goes at several hundred degrees lower temperature, but also without major disruptive effect of its own. The -O-P-O- bonded structure persists in a mildly reducing atmosphere almost as well as in air. Phosphate bonding is thus versatile. Its atom linkage is stable in -Si-O-Si- networks as well as in crystalline oxides, and stable over quite some range of temperatures and of atmospheres.

This view, just as the one taken previously for decomposition of sulfates, is limited to phosphate as a minor component. The decomposition of a bulk phosphate compound (e.g., of apatite or phosphate rock) is not conducted in this way at all, save for carbothermic reduction to elemental P. In that case the original solid structure is massively disrupted, but its preservation is of no purpose.

Carbon Baking

The raw material for making carbon stock (logs, bars, plates, rods), and less-frequently for making molded carbon shapes, is typically a selected grade of calcined coke, pulverized to a desired fineness or sizing. A liquid binder is admixed, generally a hot industrial pitch; then the hot mass is either pressure-molded or extruded and let cool, whereupon it becomes rigid. This is then to be baked: a rough equivalent of sintering.

The superficial chemistry of carbon baking is the same as that of Coke Manufacture, except (a) the material coked is now a small fraction of the total material present, and (b) a latitude of baking temperatures is available to develop within each carbon particle a structure ranging at will from somewhat disarrayed toward the regular lattice structure of graphite. The pitch binder becomes carbonized, bonding adjacent particles together by new -C-C- bonds; and its carbonizing shrinkage creates some porosity, or void spaces between particles. Somewhere above 1800°C baking temperature, the assemblage begins to exhibit properties comparable to those of graphite; so this arbitrary upper limit is taken in Figure II-1. If the baked carbon stock is to be graphitized subsequently, it may be baked as low as 1000°C; otherwise, to about 1300°C and up.

Carbon baking furnaces are very large rectangular double-walled (indirect-fired) brick structures, usually erected below ground level. The charge is laid in, separated and surrounded by powdered coke, and a refractory roof is laid on top. Burners in the outer walls supply the heating, which is continued for days since heat transport to the center of the charge is slow. Cooling is protracted for the same reason. Air is excluded from the charge by the brickwork, while the excess carbon within consumes any interior 0_2, providing a CO atmosphere for baking. Some of these furnaces are built in a ring of segments, operated sequentially around the circle.

Refractory exposure to this process is like that in coking, though byproduct gas levels are lower (except CO) and temperatures run much higher. Refractories exposed to 1600°-1800°C experience warpage and slumping, owing mainly to the reducing action of CO gas. Furnace walls and floors are rebuilt piecemeal.

Sintering of Carbides and Nitrides

Refractory carbide and nitride artifacts are sometimes sintered in the course of their synthesis, previously discussed, sometimes afterwards. As their melting points range from about 2000°C to well over 3000°C and they oxidize readily, sintering presents a severe challenge. In some cases this is met by electric heating in vacuum or inert atmosphere; in other cases by metal bonding of the refractory powder, i.e., by sintering of a lower-melting metal. In any event these special processes usually employ water-cooled metal containment and are not candidates for industrial refractories use other than of some graphite. Again, SiC is held out for individual treatment presently below.

Fusion of Oxidic Materials

As indicated in Figure II-1, there are two discrete types of oxidic fusion processes. That of the lower-temperature domain is devoted to

the melting of selected silicate minerals to make glasses. The molten material can be fiberized by spinning or by steam-blowing, in the same general manner as pertains to ordinary commercial glass. The fibrous material, though vitreous, is considerably more refractory than commercial glass fibers; its uses are primarily in low-mass, highly-insulating refractory forms.

Refractories of containment for this type of process are exposed to environments comparable to those of Glass Manufacture, but (a) alkalies are less prevalent in either the melt or the atmosphere, while (b) the processing temperatures exceed those of commercial glassmaking. The scale of operation is much smaller than that of glass. It can be effectively carried out batchwise, in simpler equipment.

The second type of fusion process is conducted either on mineral charges formulated to yield refractory silicate compositions, or on single or mixed synthetic refractory oxides. This is the process of *arc-melting*. It is invariably conducted batchwise on a small (e.g., ten-ton) scale. A two-phase current source is commonly used, the electrodes in "vee" configuration buried in the coarse-powder or granular charge. The molten product of progressively growing volume occupies the central region of the containing vessel, surrounded in all directions by a skull of unmelted charge. The outer containment is of refractory-lined steel. Water-cooled steel can serve for the roof, or a simple refractory-lined dome can be used. Provision is made for pouring the product into molds in the making of fused-cast refractories; or the fused mass can be allowed to solidify in place for later crushing. More modern methods are described in Chapter III.

The skull collects most of the vaporized byproducts. Refractory liners for pouring are subject to severe wear, of course; but otherwise thermal shock at startup is the most dramatic exposure. Operating temperatures can run as high as over 3000°C, though in that case typically on a still smaller scale. Quantity production of fused refractories is principally limited to ZrO_2 (m.p. 2700°C), MgO (m.p. 2850°C), Al_2O_3 (m.p. 2054°C), and lower-melting silicates.

Graphite and SiC Manufacture

Imagine a long, slender column of carbon logs, laid out horizontally and packed in a generous envelope of granular coke -- in turn covered all over and under with sand (silica) as a refractory thermal insulator. Butt a massive water-cooled graphite electrode against the column at each end. Now deliver a heavy, voltage-regulated electric current to the electrodes and through the column, which is then self-resistance-heated. This is the essence of Acheson's graphite and silicon carbide furnace of 1896. Only its peripheral

technology and detailed design have changed. The whole column is now usually contained in a long rectangular refractory box.

The current is at first concentrated in the relatively dense carbon core, which accordingly heats up most rapidly. At temperatures of 2000°-3000°C, the core graphitizes (i.e., crystallizes) and becomes more conducting. So does the carbon packed between logs, which is series-connected with them. Heat flows out radially from the axis by radiation and conduction, so that presently some of the surrounding coke is graphitized as well and the current path broadens. Some of the sand bed melts and reacts with the outer layers of carbon, producing a mixture of silicon oxycarbides and finally some SiC, which begins to conduct as these crystals grow. As a roughly cylindrical shell of SiC crystals is grown, the current path expands still farther and heat is generated over a still broader column. CO gas is a byproduct, escaping radially. At these extreme temperatures, SiO gas is also copiously generated. Some of this filters outward, cools, and eventually re-oxidizes; but some of it diffuses inward and reacts with graphite in the interior, producing more SiC.

The inferno is finally allowed to cool. The column is broken down and mechanically separated into its various component products: SiC of several sizings and purities, graphite powder or grain, and graphite logs; and outer layers composed of silicon oxycarbides, fused silica and unaltered sand, all heavily contaminated with impurities volatilized from the carbon fractions that were charged.

By varying the manner and geometry of laying up the column in the first place, one can direct the process predominantly toward graphite production or predominantly toward SiC. When graphite stock is the objective, a massive array of baked carbon logs is laid up, each one transverse to the furnace axis and well-separated by granular coke. This array is the principal conductor throughout the heating period. If SiC is the objective, only enough baked carbon or coarse coke is laid in to start the furnace, and SiC crystals ultimately become the principal conductor. The particulate graphite made in the process is rarely formed into logs, but finds other uses after being ground to powder.

Silicon carbide crystals so made are sized, mixed with binder, and pressed into blocks or other forms much as in the making of baked carbon. One family of SiC refractory products uses clay as binder, subsequently sintered for the final bond. Another family uses pitch as binder and is baked much like carbon products to carbonize the pitch. Still another family is made by admixing and compacting SiC and Si powders and carbiding or nitriding the Si as described previously. Other powdered bonding metals are used as well, e g.,

cobalt; in this case the bonding metal is sintered. The strongest forms of SiC are Si_3N_4-bonded or bonded by SiAlON, made by nitriding added Si and Al.

Small graphite logs can also be made individually by self-resistance heating of baked carbon in a much cleaner type of furnace. Here radiation shielding replaces the packings described above and the log touches nothing but graphite connectors at its ends. On a still smaller scale, a graphite tube serves as the resistor and articles to be graphitized are placed within the tube. Or, the graphite tube can serve as a susceptor for induction heating. All these systems are swept by inert gas, and all employ combinations of graphite and water-cooled metal construction.

Refractory Metal Manufacture

The refractory metals lie within the "Carbide Formers" category of Figure II-2. If we demand a melting point of 2000°C or higher to qualify, then the group is limited to Hf, Nb, Ta, Mo and W. Their smelting was disposed of previously as exceptions under Carbothermic Reduction. Here we assume that unconsolidated metals have been so obtained, and the problem of refractory metal manufacture then lies in how to make these metal powders into something massive and useful.

These metals are all highly electropositive, i.e., readily oxidized. Air and moisture must be scrupulously excluded in their processing. Their consolidation into massive metal is typically conducted in an atmosphere of dried H_2 or argon, though vacuum is suitable as well.

One method used consists of powder-metallurgical compaction and sintering. Typical temperatures are about the same as for Sintering of Carbides and Nitrides, ranging between about 1500° and 2300°C, achieved electrically. The other method consists of arc melting, using a consumable self-electrode fashioned powder-metallurgically as above. The second electrode is momentarily the bottom of a water-cooled copper crucible, but quickly becomes the refractory metal itself as the tip of the upper electrode melts, falls through the arc, and forms a pool which rapidly freezes adjacent to the copper. The crucible is initially charged with loose powder, which is also melted by the arc. These are small-scale batch operations, measured in pounds. They are not candidates for use of industrial refractories, except peripherally.

Further Information

For most of the hot processes discussed here the Kirk-Othmer Encyclopedia of Chemical Technology[8] will provide an additional level of detail, though generally not in a context of refractories usage. A practicing comprehension of each process, calling for extensive reading of its own specialized literature, is quite outside the scope of this volume. The intent of this chapter has been to address high-temperature processing only sufficiently to develop an appreciation of working environments for the refractories technologist. By including some hot processes which do not employ appreciable amounts of refractories, we have imparted some perspective to the subject as well. Chapter III will complete this general preparation for the detailed discussions to follow.

Chapter III

Foundations of Refractory Application

A SECOND REFERENCE CHAPTER

We now conclude the survey of industrial hot processing by describing the major types of equipment employed; and by delineating, within each device, the several areas or zones whose refractories are exposed to different environments in the same process. This will lay a groundwork of different performance demands in numerous specific and commercially important circumstances. How refractory systems are contrived to meet those demands will occupy the remainder of this book.

CONTEMPORARY HOT PROCESSING EQUIPMENT

Nomenclature and Classification

Devices used for heating and hot processing are variously called *furnaces*, *kilns*, and *ovens*. The distinctions among these are not always entirely consistent, however. A *furnace* usually achieves a molten charge or product, while a *kiln* is used for calcining or sintering. But most other hot solid-state processes are carried out in "furnaces" by common word usage: e.g., metal pre-heat, heat-treating and annealing operations. Likewise for most roasting and smelting processes, whether melting occurs or not.

Carbon products are properly baked in a *kiln*, but "baking furnace" or even "baking oven" is the accepted usage. An *oven* is a lower-temperature device, used, e.g., for drying or for glass

annealing; yet the "coke oven" runs up to ~1100°C and the carbon "baking oven" much hotter than this.

Numerous devices are called by none of the above, e.g., steam boilers, incinerators, stills, retorts, reactors, cracking towers. A *glass melting tank* is a horizontal furnace, but "tank" is in common use. Furnaces dedicated to other specific processing tasks like converting iron to steel or copper matte to blister copper are called *converters*. A *crucible* is a cup-shaped container placed or built within a furnace, its charge ultimately molten; a *cupola*, on the other hand, is a vertical shaft or cylindrical furnace, though its name is derived from "cup" and is the preferred, albeit arcane term.

Managing the charge within a hot vessel, or moving it when the operation is completed, calls for devices and techniques adapted to special needs. For the heating or sintering of ceramic ware, a wide variety of refractory articles used as shelves, supports, trays, setters, spacers, baffles, and enclosing muffles or saggers go by the collective name of *kiln furniture*. Hot solid products are transported by devices bearing self-explanatory names like "chute," "conveyor," "slide," "scoop," "car," etc.

Hot liquids are sometimes transferred direct from furnace to destination by gravity flow through *troughs* and *runners*. Vessels that are used to transport molten charges by carrying are called *ladles*. If the destination is a pouring pit where ingot molds are filled in rapid succession, the term *teeming ladle* is used. Ladles are mostly cup-shaped, lifted either by their external pivots or *trunnions* (especially if tilt-poured), or else by an upper flange (especially if bottom-poured). An exception to the common ladle shape is the low-formed *torpedo ladle*, used to carry the discharge of a blast furnace to a nearby steelmaking area. A *torpedo car* is such a ladle having its own wheeled undercarriage, riding on rails.

A cup-shaped transfer vessel which is not itself moved may not be called a ladle at all. An example, the bottom-poured *tundish*, is the surge vessel which feeds a continuous casting device. Bottom-poured vessels make use of a lower orifice together with a moveable *stopper* or *slide gate valve*.

Classification by Mode of Heating. Heating devices are discriminated by the nature of the heat source and heat-transfer method used, each one of which contributes uniquely to the chemical and thermal environment of refractories:

Fuel-Fired, or Combustion-Heated

Coal
Coke
Oil
Natural Gas
Syn.-Gas (various)
Hydrogen
Off-Gas (e.g., C0)
Internal Fuel (e.g., admixed coke)

Direct-Fired vs
Indirect-Heated (muffle type)
Countercurrent vs
Cocurrent (if the charge moves)
Down-Draft vs
Up-Draft (if applicable to a stationary charge)

Hot-Air-Heated (using separately indirect-heated air)

Electric-Heated

Resistance
Self-Resistance
Arc (single-phase or three-phase)
Induction
Microwave
Plasma (arc or inductively-coupled)

Classification by Operating Mode. Irrespective of the mode of heating, hot processing vessels are classified as *continuous*, or as *batch* operated or *periodic*. In *continuous* operation the feed and/or discharge may be either literally continuous or conducted in discrete increments; but the charge flows or is conveyed through the vessel, which itself operates essentially at steady state. In *batch* or *periodic* operation the vessel is fully charged, then heated to conduct its process, then cooled and/or discharged in entirety. The complete batch operating cycle in metal-melting processes is called a *heat*. Holding any charge for some time at a fixed high temperature is called *soaking*. Whether batch or continuous, the calcining or sintering of solids is often called *firing* or *burning*.

A hybrid operating mode, combining features of both continuous and batch modes, employs equipment made up of identical *compartments*. These are usually laid out in a ring. Combustion gases pass successively through all but one of these compartments, that one being idled for cool-down, unloading and reloading. Then the points of entry and exit of the heating gases are moved, to include that one compartment but to take the next one out of service. And so on, in rotation, around the ring. Each compartment is thus batch-operated in turn, while the equipment as a whole gains the benefit in fuel economy of continuous countercurrent operation. This hybrid mode is used in kilns and ovens, but infrequently since the architecture is necessarily complicated. An important special case is the two-unit or three-unit air pre-heater, mentioned in Chapter II in connection with glass manufacture and blast-furnace smelting.

Table III.1 Classifications of Hot Processing Equipment

CONTINUOUS	
VERTICAL	(Circular in plan view)
BLAST FURNACE	(Modified shaft: conic sections)
CUPOLA	(Cylindrical form of blast furnace)
SHAFT KILN OR CALCINER	(Cylindrical)
HEAT EXCHANGER	(Checker- or pebble-packed tower)
REACTOR	(Various chemical process vessels)
STILL OR RETORT	(Packed or unpacked, baffled, etc.)
SPRAY-DRIER OR -CALCINER	(Cylindrical plus conic section)
MULTIPLE HEARTH	(Several stages vertically stacked)
ELECTROLYTIC SMELTER	(Generally rectangular in plan view)
ROTARY	(Elongate revolving tube, inclined to the horizontal)
ROTARY KILN OR CALCINER OR DRIER	
HORIZONTAL	(Approx. rectangular in section)
GLASS MELTING TANK	(Elongate)
REVERBERATORY FURNACE	(Elongate; low roof or crown)
TUNNEL KILN	(Highly elongate)
HEAT-TREATMENT FURNACE	(Elongate)
DRYING OVEN	(Elongate)
STEAM BOILER	(Short: near square in plan view)
BATCH OR PERIODIC	
CIRCULAR, UPRIGHT	(Stationary or tiltable)
BASIC OXYGEN FURNACE: BOF or BOP	(Steelmaking process)
QUELLE-BASIC OXYGEN FURNACE: Q-BOP	(Steelmaking process)
ARGON-OXYGEN DECARBURIZATION FURNACE: AOD	(Alloy steels)
ELECTRIC ARC FURNACE: EAF	(Alloy steelmaking)
CORELESS INDUCTION FURNACE: CIF	(Steels and nonferrous)
BEEHIVE OR OTHER	(Kilns, including updraft and downdraft)
HORIZONTAL CYLINDER	(Non-revolving)
COPPER CONVERTER	(Smelter)
TUBE FURNACE	(All kinds)
RECTANGULAR	(Generally horizontal; various dimensions)
ACHESON FURNACE	(Elongate; graphite or SiC manufacture)
ARC-MELTING FURNACE	(Near square in plan view)
GLASS MELTING TANK	
REVERBERATORY FURNACE	
COKE OVEN OR COKING FURNACE	(Narrow in plan view)
CARBON BAKING FURNACE	
METAL REMELT FURNACE	(Nonferrous metallurgy; all kinds)
HEAT-TREATMENT FURNACE	
MISCELLANEOUS FURNACES	(Solar, plasma, vacuum, glo-bar)
SHUTTLE KILN	
BELL KILN	
ELEVATOR KILN	
DRYING OVEN	
MISCELLANEOUS SHAPES	
POTTERS' KILNS; LABORATORY AND TEST DEVICES	

Under each operating mode, numerous types of heating devices can be distinguished first by their characteristic geometry, then by how they are heated and operated in detail -- not to mention their working temperatures and processing purposes. In Table III.1 about forty different types are listed according to operating mode and geometry, for introduction to their nomenclature. Most of these will be described next, approximately in the order in which they appear in the table. Thanks are given to the suppliers of many illustrations to follow; each one will be referenced in the appropriate figure captions.

CONTINUOUS TYPES -- VERTICAL

Blast Furnace: Smelting of Iron

The Furnace. The chemistry of iron ore smelting is described under Iron and Steel in Chapter II. The *blast furnace*, a continuous, countercurrent, modified vertical *shaft* configuration in which that process is carried out, is depicted in Figure III-1. The ring of *tuyeres* near the bottom are the water-cooled nozzles through which pre-heated air is introduced. Their manifold is the annular "bustle pipe," surrounding the furnace and supported by the "mantle," and fed in turn from the "stoves" or air-blast pre-heaters (not shown). Below the tuyeres lies the *hearth,* whose floor and sidewalls form a crucible to contain the collected molten iron and slag. These liquids are tapped separately at two different levels.

In the *bosh*, which extends upward from tuyeres to waist, the shaft diameter increases. The reverse-tapered tall section above the waist is called the *stack*. This ends at the top in a short cylindrical section, through which the solid feed falls from the charging hopper. The hopper is fed and discharged in increments; it forms seals alternately above and below to prevent escape of the CO-rich off-gas. The short cylindrical section bears hard refractory "wear plates" which resist the abrasion of the falling charge of iron ore, limestone and coke.

The column of charge occupies about two thirds of the height of the vessel above the bottom. The remaining headspace provides for disengagement of the solids from the up-flowing gas. The whole vessel is encased in steel, the larger part of which is water-cooled. Over the entire bosh and about half the stack, a forest of copper cooling plates or iron "staves" of various designs project into the refractory lining from the shell; these too are water-cooled. The height of the structure, from base to hopper, ranges from the order of 60 to nearly 200 feet; the hearth I.D. ranges from about 20 to 50 ft. One of the largest of these vessels at this writing, an installation at Redcar on

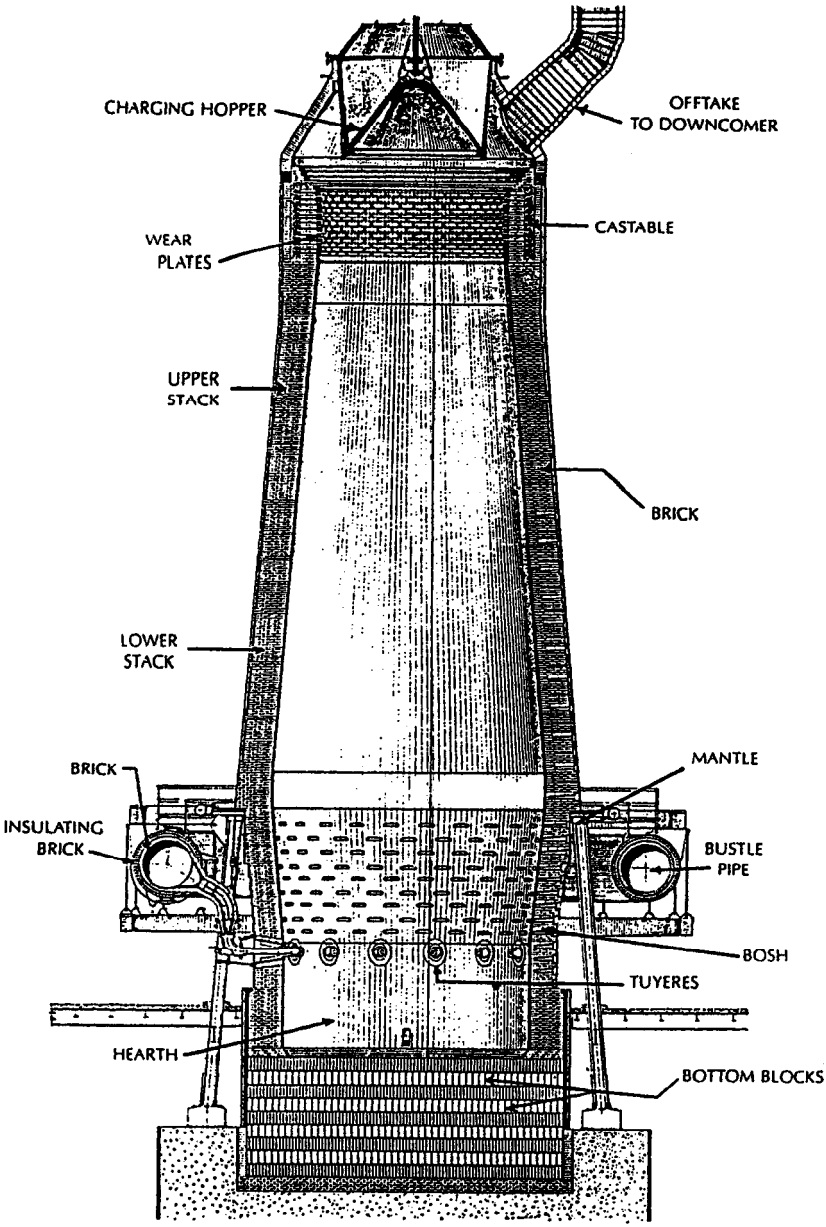

Figure III-1 Iron-Smelting Blast Furnace
(reprinted from Ref. 10, by permission)

the east coast of England, has an ironmaking capacity of 11,000 short tons per day.

Stoves. The combustible off-gas leaves the blast furnace via a port at the top, to the "offtake" and thence to the "downcomer" (not shown in Figure III-1). These are large ducts leading to ground level where much of the entrained dust is removed by lined cyclones. Then the gas is led by valved manifolding to one of three identical *stoves* in rotation, where it is mixed with air and burned.

A blast furnace *stove* is a tall chamber filled with an open *checkerwork* of refractory heat-exchanger bricks and with associated ducting, as depicted in Figure III-2. Until recently, blast furnace checkers were literally that: staggered arrays of bricks with a communicating labyrinth of open spaces between. The improved design now popular consists of fluted and parallel-bored hexagonal blocks, stacked in registry so as to provide a dense triangular array of parallel tubular passageways, each one the full height of the column. Each open tube is about 1.5" in diameter.

Each stove is operated reciprocally, in pairs of half-cycles. In the heating half-cycle, the blast furnace off-gas and air enter from the lower right of Figure III-2. Their combustion products rise in the duct and pass down through the checker, then out at the lower left. At the conclusion of this half-cycle, the top of the checker column is hottest: typically about 1200°-1400°C. The bottom is at about 800°-1000°C. Then the blast furnace off-gas is diverted to another stove, while the one now heated will be presently turned to its air pre-heating half-cycle.

In this second half-cycle, ambient air is pumped in at the lower left of the diagram and rises through the checker, where it is heated close to the uppermost brick temperature; then it flows down the duct and out at the lower right. From there it is ducted to the bustle pipe and thence to the tuyeres of the blast furnace. Three stoves thus cycled in rotation ensure an uninterrupted flow of hot air to the furnace. Elevated air pressure and oxygen enrichment are optional variations. The entire system is of course refractory lined.

Refractory Zones in the Blast Furnace. The principal refractory wall areas in this equipment and the typical range of conditions faced by each one are given in the table below. A number of local areas calling for special refractory fittings are omitted.

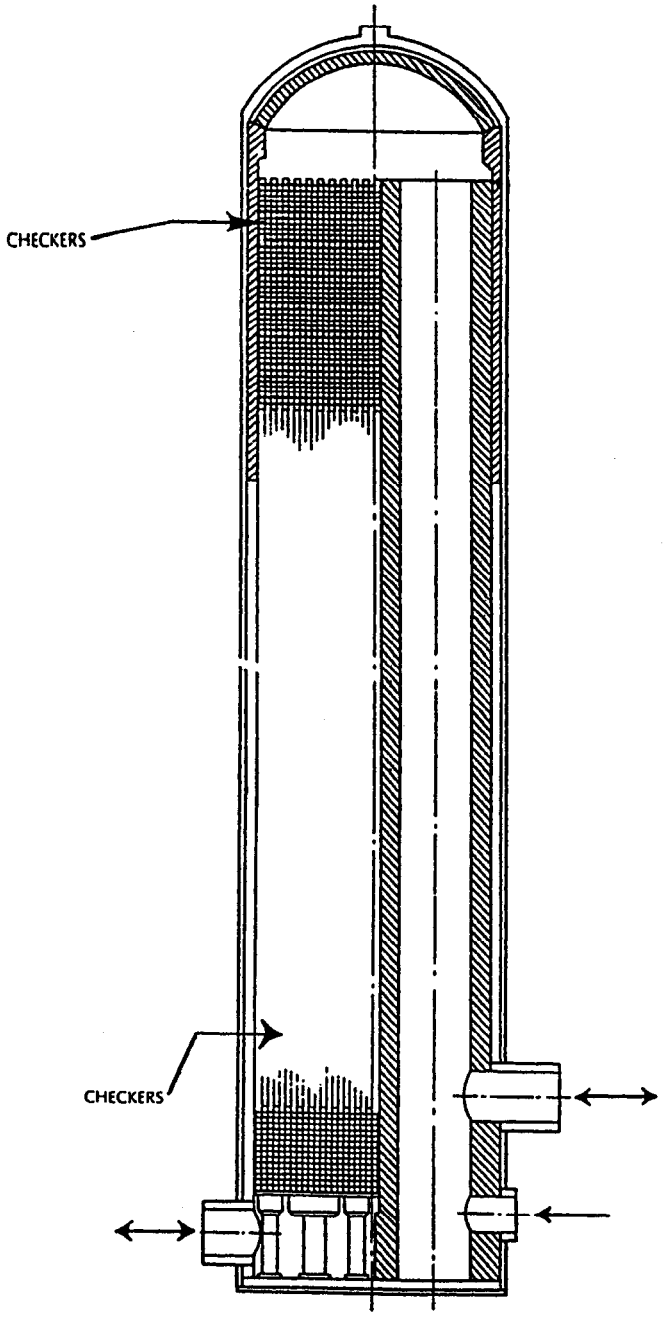

Figure III-2 Blast Furnace Stove (reprinted from Ref. 10, by permission)

Refractory Zone	Hot Face T, °C	Aggressive Environment	Erosion-Abrasion	Thermal Stress
Hearth Area	1400-1700	Fe,C,CO, slag	Minor	Minor
Bosh Area	1600-1900	Fe,C,CO, slag	Severe	Mod.
Waist Area	1400-1700	Fe,CO,Zn,slag	Moderate	Mod.
Lower Stack	1000-1400	Alkalies,CO,Zn,S	Moderate	Mod.
Mid Stack	600-1000	Alkalies,CO,Zn,S	Moderate	Minor
Upper Stack	300-700	CO, S, dust	Severe	Minor
Port Area	300-500	CO, S, dust	Severe	Minor
Downcomer	300-500	CO, S, dust	Moderate	Minor
Checkers:				
Upper	1000-1400	CO_2, SO_2	Minor	Severe
Lower	200-1000	CO_2	Minor	Severe
Blast Ducts	800-1200	Air	Minor	Minor
Bustle Pipe	800-1100	Air	Minor	Minor

Accessories and Peripherals. The *wear plates* just under the charging hopper receive brutal impact and abrasive forces, while the temperature at that level is low and relatively unchanging and corrosion is not a major factor.

Tuyere blocks surround and protect the tuyeres from undue exposure. Their frontal environment is much like that of the lower bosh: a combination of severe corrosive and abrasive forces, but at lower temperatures than are experienced above them.

Taphole refractories and their plugs must resist fast-flowing liquid metal and/or slag: intensely corrosive and erosive. They are subjected to severe thermal shock at each opening and closure. The demands for reliability are nonetheless critical.

Troughs and *runners* and their associated devices constitute a system of refractory-lined ditches through which metal flows from the blast furnace taphole to the point of loading of ladles. This system is exposed to both iron and slag at 1500°-1700°C, and to severe thermal shock at each onset of flow. A system of slag runners diverts separately-tapped slag from the furnace to a collection/disposal facility.

Torpedo ladles or *teeming ladles* transport hot metal respectively to a steelmaking area or to a pouring pit for the casting of pig-iron. Ladle linings experience both mechanical and thermal shock in charging and discharging, as well as corrosion by iron and slag at up to ~1700°C. In a shop where iron purification is begun in the torpedo ladle, the temperature may be even higher while added slagging chemicals and stirring increase the corrosiveness of the charge. A single ladle may carry as much iron as a steelmaking

furnace (up to some 250 tons or more), and is further subjected to mechanical jolting in transit. Provisions against metal leakage through the lining to the ladle shell are critically important.

Steelmaking ladles present more variety than do iron transporting ladles. They and the bottom-pouring devices that are common to both will be described later in conjunction with the steelmaking furnaces (BOF, Q-BOP, AOD, EAF and CIF of Table III.1).

Cupola: Iron Remelting

The *cupola* is a downrated and miniaturized blast furnace compared to the iron smelting vessel described above. It is a *remelt* furnace, used by some foundries to make gray castable iron, for example, from pig-iron and scrap. Coke is fed as fuel and limestone as a slagging chemical, but the charge is mostly metal. Air is fed through tuyeres from an annular manifold, generally without pre-heating since the peak temperature is only about 1650°C; so in the usual case there are no stoves.

The hearth of this furnace is retractable, well above ground. Access is had daily to the entire interior for patching and repair of the refractory lining, in contrast to the ironmaking blast furnace which must run for years without entry. While the cupola is a continuous furnace design, equipped for tapping of metal and slag, its daily interruption gives it the aspect of a batch furnace as well. Being so frequently exposed to air while hot, the lining materials are ordinarily limited to oxidic refractories. These linings experience about the same corrosive agents as occur in iron smelting, but at lower peak temperatures and on a vastly smaller throughput scale. Thermal shock is much more a factor, occurring daily. Severe abrasive wear is confined to the charging level (upper shaft), except for each day's startup.

Blast Furnace for Lead Smelting

The lead blast furnace contrasts with the ironmaking blast furnace in nearly every conceivable way. Lead melts at 328°C (Fig. II-2), its oxide not a great deal higher (886°C). The peak temperature in its blast furnace is only about 1200°C, and much of the construction may be of water-cooled cast iron or steel, unlined. Refractory linings are employed at least in the upper shaft or charging area for abrasion resistance, and in the hearth or crucible area below the tuyeres for resistance to collected molten lead and slag. Again the air blast is not pre-heated, hence there are no stoves. The entire structure from hearth to exhaust is only some 30-35 feet high. It is of *shaft* (i.e., fixed-I.D.) configuration.

The lead ore fed to this blast furnace, principally PbO from roasting of galena, PbS, generally contains several other nonferrous metal oxides as well as residual unconverted sulfides -- not to mention the ubiquitous silicates. Thus both the metal product and the slag are chemical misches. Both are relatively aggressive toward the refractory hearth or crucible lining. They are tapped separately.

Some of the lead is separated from the collected slag in a lined settling tank. Most of the metal product is tapped or siphoned from the blast furnace. Both of these fractions go together to a refractory-lined reverberatory refining furnace, in which air blown into the charge oxidizes As, Fe, Sb, Sn and other impurity metals. Their oxides float to the top and are skimmed off as *dross* for separate recovery by re-smelting. The linings of these peripheral vessels have to resist attack by molten Pb and by PbO-rich slags, but at temperatures of about 1100°C and down. The more noble metals, Ag and Cu, are extracted later from the molten lead.

Heat Exchangers and Reactors

Heat Exchangers. Refractory *heat exchangers* or gas *pre-heaters* are not necessarily cylindrical shafts, though the blast furnace stoves described above are an important example. The gas flow through the checkers is almost always vertical, as there. But the design can as well be square or rectangular, and in such case sets of like units may be conveniently laid out in line. Arrays of this latter geometry are built as adjuncts to the glass melting tank, and will be described and zoned presently in that connection.

A third, somewhat smaller-capacity heat exchanger type that has proliferated in recent decades is the continuous circulating *pebble-bed* heater. This employs uniformly-sized refractory spheroids whose small diameter (typically from about 3/8" to about 1") considerably diminishes thermal shock damage. One of several equipment designs is illustrated in the diagram of Figure III-3.

Reactors. *Chemical process reactors* likewise need not always be upright cylinders, but that geometry is common. A steel shell forms a complete enclosure. The typical refractory application is as lining of this shell, for either or both of thermal insulation and corrosion or abrasion resistance. But there are numerous ports and tubulations providing for feed and discharge, pressurization, internal heaters or stirrers, instruments, and access for maintenance. These may call for refractory gasketing and seals. Reactors are generally indirect-heated, but the working temperatures are usually such that this feature does not call for other very special refractory appurtenances. Thermal stress is minor in steady-state, continuous operation.

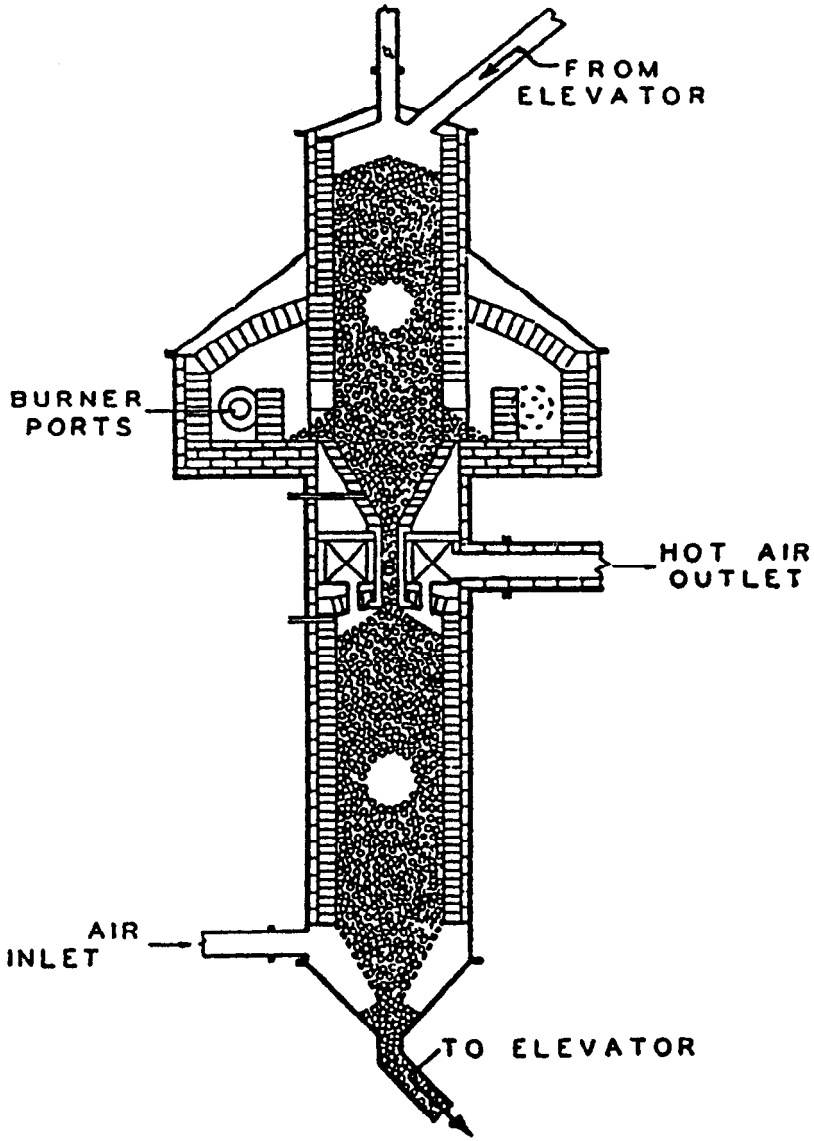

Figure III-3 Pebble-Bed Heater (from Ref. 3: F. H. Norton, "Refractories," 1949, McGraw-Hill, Inc., by permission)

The variety of both continuous and batch reactor usage in chemical processing defies reduction to any one illustrative design or one chemical environment. Nevertheless, refractory lining techniques have become fairly well standardized, as represented by practices in petroleum and petrochemical processing. That industry, touched on briefly in Chapter II, will be revisited later on.

Stills and Retorts: Zinc Smelting

Stills and *retorts* share with reactors and air heaters in being indirect-fired. The functional distinction between them is minor: properly, a *still* evaporates and re-condenses liquids without chemical change, while a *retort* conducts a chemical reaction or decomposition by heating and condenses a gaseous product of that reaction. Refractories are called upon where the chemical environment is aggressive, hence typically where the materials processed are inorganic. A representative case is in the smelting of zinc.

Zn, Cd, and Hg are in the Low-Melting Metals category of Figure II-2. These three metals are unique in that category in being exceptionally low-boiling as well. Their oxides, obtained by roasting of sulfide minerals, are variously higher-melting:

Metal	M.p., °C	B.p., °C	Oxide	M.p.,°C
Zn	420.	907.	ZnO	1975.
Cd	321.	767.	CdO	1520.
Hg	-39.	357.	HgO	500.

It is thus advantageous to conduct the carbothermic smelting of these oxides below their own melting points so as to minimize excessive volatility of the metal product; but it is kinetically impractical to smelt below the boiling points of the metals. Hence the use of a retort. Zinc is the largest-tonnage product among these three metals, and is produced in continuous retorts. The batch-operated retorts smelting other nonferrous metals are exposed to comparable chemical environments and are of basically the same materials of construction.

The continuous zinc retort is a tall, narrow brick vessel, slot-shaped in plan view, into which a hopper feeds a briquetted mix of powdered ore and excess coke or coal. The briquettes form a bed at the bottom. Heating to 1200°-1300°C is typically by a surrounding gas-fired furnace. Projecting from the upper walls of the retort, which is otherwise closed, are arrays of gently downward-sloping open-ended tubular condensers. Their outer extremities are cooled by ambient external air to about 600°C to condense the zinc from the

flowing mixture of generated zinc vapor and CO. The liquid product is collected continuously. The CO is likewise collected by manifolding, for use or disposition in accordance with environmental regulations. A residual siliceous gangue from the briquettes is periodically removed below the bed through a grate and underlying pit.

Most of the retort experiences only minor to moderate thermal stress at steady state. Absence of liquid slag in large amounts at the bottom is favorable for refractory life. The pervasive exposure is to CO gas and Zn vapor, and to liquid Zn in the condensers, plus volatiles from the bed which include considerable sulfur. Impermeability of the refractories of construction is a must, and they must be thermally conductive.

Aluminum Electrolytic Smelter

Fused-salt electrolytic smelting processes are inherently corrosive but, employing halides, are conducted for the most part at fairly low temperatures. Aluminum, the largest-tonnage metal so made, is something of an exception: (a) its smelting temperature is about 800°C, and (b) the compound consumed in its manufacture is its oxide, Al_2O_3. The melting point of this synthetic "ore" is depressed from 2050°C to about 600°C by the adroit use of the dissolved components AlF_3, NaF, and sometimes Li_20. The essential chemistry of the operation and an outline of its equipment are given under Al and Mg Manufacture in Chapter II. The pertinent zones in a Hall-Héroult aluminum cell are, starting from the bottom:

Collector Base	Upper Sidewalls
Cell Bottom	Roof and Ducting
Cell Sidewalls	Anodes

"Collectors" are a manifold of iron bars or pipes, used to spread the electric current from a copper buss across the entire bottom of the cell. Their "base" is a conducting refractory, rammed among the collectors and spreading the current uniformly over its area. The "cell bottom" extends this base up to a level surface on which lies the collected molten aluminum cathode and, on top of this, the molten electrolyte. The cell bottom and its sidewalls (roughly 1 foot high) define the dimensions of the cell: usually a long rectangle because several anodes penetrate down to it in a line. All these parts are of electrically-conducting refractory, seeing a fluid temperature within of about 800°C at steady state, and all surrounded by ambient-air-cooled steel.

The linings of the superimposed upper walls, the roof or shroud, and ducting are generally protected by the fresh unmelted "ore" feed and by copious dust; but they do see corrosive fluoride vapors and fog. Their inner faces range from about 500°C down. The

anodes complete the cell, being corroded most rapidly as described in Chapter II.

Shaft Kiln or Calciner

The recuperative feature of the continuous countercurrent blast furnace is repeated in less-elaborate equipment designed for solid-state (nonmetal) processing. In simplest concept, a refractory-lined vertical cylinder or *shaft* is fed a solid charge continuously from above, while a gating device meters the processed material out the bottom and thus controls the throughput rate. A ring of burners pierces the shell about one-third up; these are supplied both fuel and air or 0_2. Typically, the off-gas is reduced in pressure by exhaust fans so that additional ambient air is drawn in at the bottom. That ambient air serves both to cool the emerging hot solid and as secondary air for combustion. As the solid fed at the top likewise serves to cool the emerging off-gas, the system is fuel-efficient. The shaft can be divided roughly into three zones:

Upper 1/3 -- Charge preheat and off-gas cooling zone.
Middle 1/3 -- Hot zone or combustion zone or processing zone.
Lower 1/3 -- Product cooling and air preheat zone.

The solid material fed has to be relatively coarse and uniformly sized to provide passageways for the up-flowing gases; and it must retain substantially that same sizing throughout the process. "Relatively coarse" can range from about 1/4" pea-gravel to pelletized or nodulized agglomerates to pressed briquettes (~1" - 1.5") to 2" rock or so. Appreciable attrition carries a risk of plugging the gas channels as well as caking up the refractory walls with agglomerated dust. Too much melting within the charge, on the other hand, can cause its sticking together and to the walls, bridging and impeding the solid flow. A further constraint on the charge relates to volatile/condensible impurities, which can accumulate in the upper levels with resultant plugging and cementing action. Wet feed material is decomposed explosively, and cannot be used.

Materials which successfully avoid all of the above hazards would ordinarily confront the refractory lining with a minimum amount of corrosion; but most are borderline in this respect. Alkalies, chlorides, sulfates, and other volatile inorganics are the most troublesome of the common impurities. The next most pervasive attack on the refractories is abrasion. Thermal stress is moderate, assuming prolonged steady-state operation. See Sintering and Calcining in Chapter II for the processes conducted.

Synthetic periclase (MgO) grain or aggregate for refractories is sintered in this equipment, at a peak temperature of about 1900°C. So also is some synthetic alumina, at 1600°-1800°C. Magnesite is

calcined and sintered similarly, either using burners as described here or else co-feeding the mineral with coal and operating as a blast furnace. There the peak temperature is about 1500°-1700°C. Dolomite and limestone have also been fired in shaft kilns.

Multiple Hearth Furnace

Multiple hearth furnaces or calciners are used with granular feed materials that are free-flowing: generally from a few tens of μm to 1/4" or so in sizing. A typical drying and calcining use is for decomposition of hydrated inorganics or of carbonates (see Calcining of Hydroxides and Calcining of Carbonates in Chapter II). The multiple hearth is also occasionally used for roasting of sulfide ores; but through this or other types of chemical reaction the production of appreciable liquid within the bed could lead to excessive agglomeration and caking. The hearth furnace can not cope with a sticky bed.

A single hearth in this equipment is a level circular table, pierced at its center by a rotating vertical steel shaft. Attached to the shaft are rigid radial arms bearing downward-projecting fingers or rakes, called *rabbles*, which ride on or barely clear the hearth. Continuous rotation of the rabble arms turns the thin bed of charge over repeatedly; and it also moves the bed slowly in a circular or spiral path. A low overlying roof and a cylindrical outer wall complete the enclosure.

The *multiple hearth* is a set of several such units or *stages*, usually from three to five, stacked one atop the other and sharing the same axial steel shaft. Figure III-4 is an illustrative section. The axial shaft and rabble arms are water-cooled. The charge is continuously fed onto the uppermost hearth, and is ultimately raked by its rabbles around to open slots through which it falls to the next hearth below; and so on down the series until it is discharged from the lowest hearth onto an air-cooled conveyor. In most cases combustion gases enter between the lowest hearth and its roof, then pass upward through the slots to the next stage above, and so on, finally to exit through a port in the topmost roof. Heating is thus countercurrent. Each stage has a characteristic range of bed temperatures, highest at the bottom stage and coolest (i.e., recuperating) at the topmost. A maximum calcining temperature may be about 1500°C. Refractories are used to line hearths, roofs, and outer walls.

The chemical environments are not very aggressive except when heavy-metal sulfides are fed. Abrasion on the hearths is significant. Thermal stresses are minor to moderate at steady state. Thermal insulation is the primary duty of the refractories, plus resistance of the hearths to abrasion and to any chemical interaction

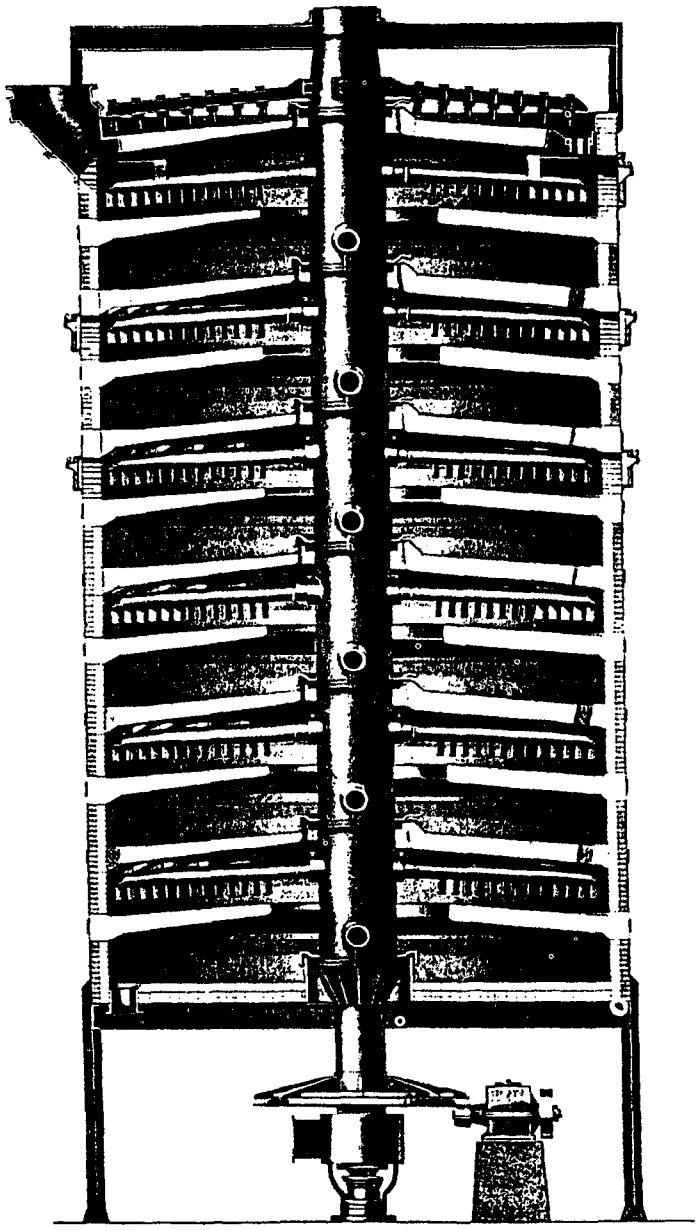

Figure III-4 Multiple Hearth Furnace
(adapted from Ref. 507, by permission)

of the charge. Volatile products (e.g., alkalies or SO_2) may slowly attack all refractory areas, especially around ports.

Spray-Drier/Calciner

The shell of this continuous equipment consists of a short, fat upright cylindrical section, closed at the top, with a conical section below. Hot air or combustion gas enters through a central port in the top with a baffle to prevent streaming; and the cooled gas exits at the bottom or apex of the cone. The fine-particulate inorganic material to be treated is prepared as a pourable aqueous slurry, generally between about 20% and 50% water. This is pumped under pressure up a vertical axial pipe which ends in a disperser located variously in mid-vessel. Two types of disperser are used: (a) a nozzle type, and (b) a high-speed rotating disc type. The slurry is by these means broken up into small droplets and sprayed in a designed pattern radially out into the vessel. The spray droplets are essentially flash-dried: their residence time in the vessel is measured in seconds before they too exit at the apex of the cone. Flow is predominantly cocurrent, but turbulent.

The resulting dried particles are aggregates measuring, at will, from about 20 to some 300 μm across. Also at will they may be only dried, or both dried and lightly calcined (see Industrial Drying and Calcining of Hydroxides, respectively, in Chapter II). A wide variety of materials are successfully dried in this manner; relatively few are calcined. Fuel efficiency is high. Outlet temperatures can range from the order of 150°C to the order of 500°C.

The chemical environment is usually benign, though humid. Refractory vessel linings are used to protect the shell and for thermal insulation. Thermal stresses are low at steady state, and abrasion is not severe. Caking of the product on the walls occurs in some cases, requiring periodic shutdown for de-scaling. Refractory practice is much like that in chemical process reactors.

CONTINUOUS TYPES -- HORIZONTAL

Rotary Kiln: Portland Cement, Lime, Coke, and More

Though Table III.1 places the rotary in a class by itself, here we shall use it to introduce a group of horizontal heating vessels.

The Kiln. The continuous *rotary kiln* is in simplest concept a long, slowly-rotating refractory-lined steel tube supported on several sets of driving and idling rollers. An overall view is given in Figure III-5. The feed end is elevated a little. The granular charge, which never fills more than about one-fourth of the diameter, executes a sort of helical motion by which it travels slowly down the kiln to the discharge end. There it passes over an annular lip and falls onto a cooled conveyor; or there may be slots in the shell at the discharge end, through which the product falls to a conveyor or silo.

A large burner is aimed axially from the discharge end. Commonly, ambient air is also aspirated there, serving both to cool the emerging product and as secondary air for the burner. The combustion gases pass up the length of the tube (i.e., countercurrent), are finally cooled by the incoming feed, and then exit at the up-hill end of the tube. One-third of the length, more or less, is the *hot zone* where processing is completed. This zone is displaced toward the burner.

The rotary kiln is versatile as to state of subdivision of the feed. Readily-airborne fine particles fix the lower size limit; fine-particle beds furthermore will often slide in the revolving tube instead of being turned over by it. The coarse size limit of the charge can be several inches; but in a mixture of coarse and fine material, the coarse tends to float on the upper surface of the bed and impedes uniform heating. At liquid-phase sintering temperatures, a coarse/fine mix can function as an unwanted nodulizer, the coarse material growing still larger by "snowballing" or accretion of fines on its surface. The best-behaved beds are of somewhat uniformly-sized spheroids or the crushed "gravel" or "rock" equivalent.

By virtue of its own dimensions, the rotary kiln can provide both extended residence times and enormous material throughput rates, up to well in excess of 100 tons per hour. The flow rate within the tube can be altered from place to place by (a) changing the diameter, or (b) providing an annular *dam* in the form of a projecting ring of refractory bricks in an otherwise-uniform lining. Projecting rows of lining bricks, parallel to the axis, can serve as *lifters* to ensure the rotation of a bed that otherwise tends to slide; also to move the bed along more rapidly.

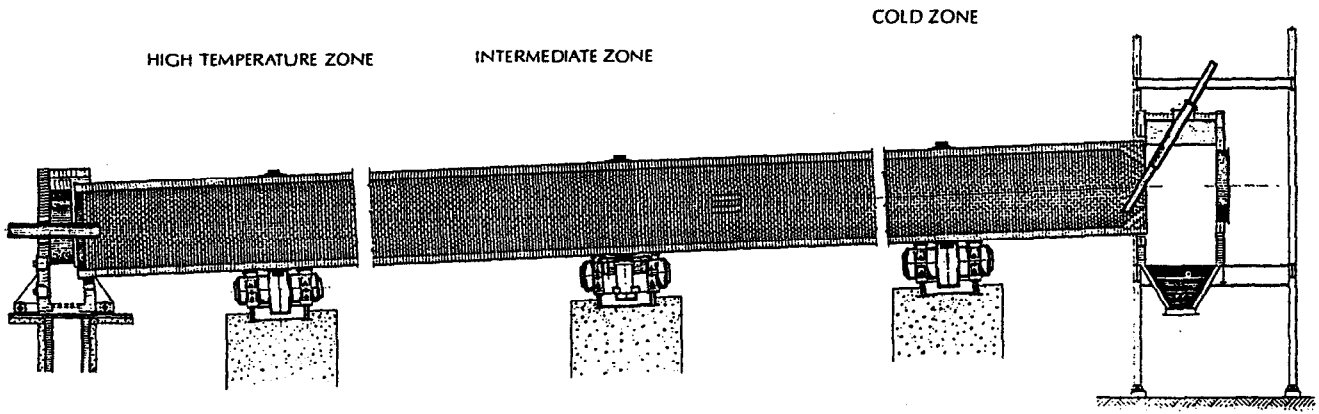

Figure III-5 Rotary Kiln (reprinted from Ref. 10, by permission)

Both mineral and synthetic materials are dried or calcined in rotary equipment, or dried and calcined in the same pass. When clays are so treated, they are usually fed as a wet cake or even a heavy slurry. The wet material cakes up in the course of drying, then becomes friable. It is common in that case to suspend heavy chains from the stationary feed-end closure, these chains dangling down some length of the kiln, to break up large clumps of the clay into manageable-sized agglomerates. The ultimate particles of clay are so fine as to be easily airborne, and their agglomeration is essential. Clays for use in refractories are variously calcined or sintered at hot-zone temperatures from about 500°C to over 1600°C.

Bauxitic minerals and synthetic aluminas are also variously calcined and/or sintered over about that same range of temperatures; likewise magnesite, dolomite, and limestone. For some several decades, formulated refractory aggregates comprised of mixed clays or clay and alumina, alumina or magnesia and chrome ore, and others have been agglomerated into pebbles or rocks or nodulized into spheroids, then pre-reacted and sintered in rotary kilns. These operations often push the firing temperature to its limit, which is about 1900°C. The products are then crushed and sized for refractory manufacture.

Rotary calcining of granular coke is a heavy-tonnage process, conducted up to about 1400°C using an oil- or coal-burning flame with inadequate air so as to provide an atmosphere predominantly of C0. But the largest-scale of all rotary calcining processes are those making lime and Portland cement. Kilns for these processes range, respectively, up to about 15 ft. dia. by over 400 ft. length and about 25 ft. dia. by 800 ft. length. Their peak hot-zone wall temperatures are respectively about 1500°C and 1700°C.

Portland Cement and Lime. The essential chemistry of these operations is outlined under Portland Cement Manufacture and Calcining of Carbonates in Chapter II. Portland cement manufacture is the more demanding on hot-zone refractories, as (a) the temperature is higher; (b) liquid-phase reaction sintering of the product is conducted, whereby both build-up and attack on the refractory are enhanced; and (c) volatile impurities are encountered, especially from the clay component of the feed. In the making of lime from limestones, the hot-zone temperature is maintained well above the decomposition temperature of $CaC0_3$ principally to cause recrystallization and crystal growth of the Ca0. In both processes abrasion is severe throughout, but more so at the feed end in the cement kiln owing to the common use of wet feed and dragging chains. Flexure of the shell in both cases demands high hot strength in the refractories, which compromises their thermal insulating properties and thermal stress resistance.

These kilns must do prolonged duty at steady state between lining repairs. For purposes of refractory specification, their zones are described as follows in rough fractions of the overall kiln length:

Feed end -- Drying zone (cement kiln); gas cooling.
Next 1/2 (±) -- Charge preheat and calcining; gas cooling.
Next 1/3 (±) -- Hot zone: charge reaction and/or sintering.
Outlet end -- Product cooling zone.

Coke Calcining. This operation is alluded to as a follow-on process under Coke Manufacture in Chapter II. Apart from the infamously abrasive nature of granular coke, the principal burden borne by the rotary kiln lining lies in the reducing atmosphere under which the calcination is conducted, over all wall temperatures up to 1400°C. The effect this atmosphere has on the softening of refractories containing iron oxides (i.e., mineral-based compositions) was mentioned under Sintering of Oxidic Ceramics in Chapter II. A still more potentially damaging effect occurs in the event of admission of air on shutdown, followed by a return to reducing conditions in the next ensuing campaign.

Glass Melting Tank

Glass manufacture encompasses numerous chemical formulations, melted at various temperatures and in several kinds of equipment. Only one of these vessels is continuous: the *glass melting tank.* In fact, simplified and somewhat smaller versions of this horizontal furnace are often operated batchwise. Still further downscaling is exemplified by the *glass pot*, and even by *crucible* melting of specialty glass batches. The smaller vessels are successively more regarded as disposable, i.e., shorter-lived under corrosive attack; and of course they represent much smaller-volume glass production. But their refractory exposures are basically the same as those in the glass melting tank. This latter equipment, by virtue of its large size, long expected life, and continuous flow, exemplifies the most severe demands on glassmaking refractories. The chemistry of glass attack on its refractory containment is outlined under Glass Manufacture in Chapter II.

Figure III-6a is a schematic plan view of the cross-fired glass melting furnace, while Figure III-6b is a somewhat-enlarged section at a burner station and through the adjacent regenerative air pre-heaters, or checkers. The tank itself may be easily up to 50-60 ft. long, and about half as wide.

The Furnace. The melting tank is a rectangular refractory box about 3-4 ft. high. The granular feed materials are charged and mechanically stirred in at one end, where melting and the evolution of CO_2 are most concentrated. Much of the length of the tank is devoted

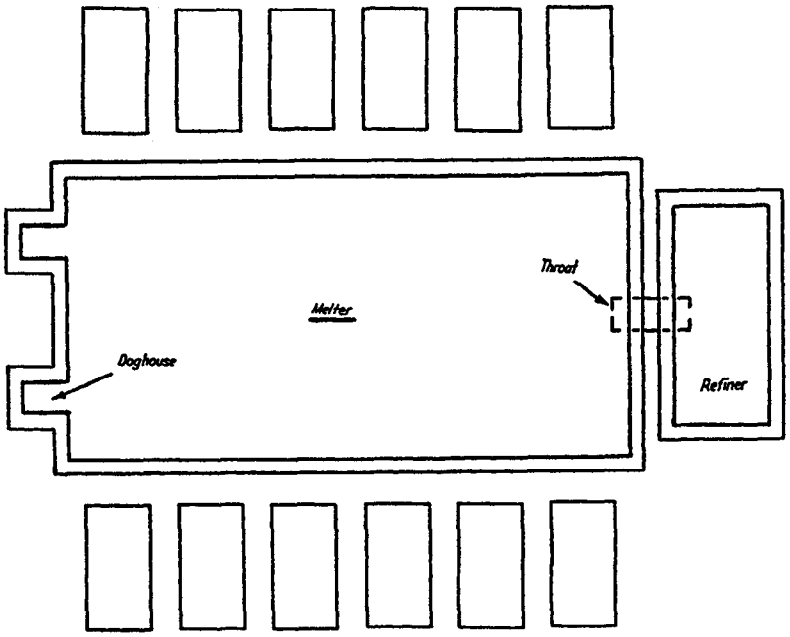

Figure III-6a Schematic Plan View of Glass Melting Tank

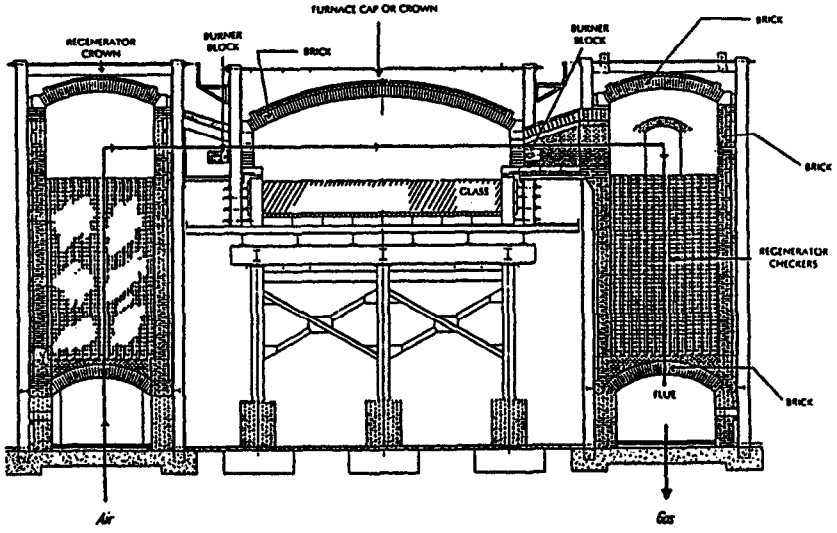

Figure III-6b Section of Glass Melting Tank and Checkers
(adapted from Ref. 10, by permission)

to achieving uniformity of the glass temperature and composition. At the opposite end is a constriction or *throat*, containing a *weir* under which the glass flows to the *refiner* section. Homogenizing is completed there, plus the removal of any retained CO_2 bubbles by passing gas in much larger bubbles up through the melt: a process called "fining." The refiner discharges to a *forehearth* (not illustrated), from which the liquid is taken for forming by sheet casting, molding, blowing, fiberizing, etc. The commonest products are sheet, plate, tableware and bottles.

Glass contact refractories, of which the tank itself is constructed, must be of oxidic composition. Carbons and carbides (and even chrome-containing oxidic formulations) would release dark-colored particles into the melt by corrosion or otherwise; and glass products in general can tolerate neither the color nor the presence of undissolved particulates (called *stones*). Platinum metal tank linings have been used, mostly in small batch-heated vessels, balancing the high initial cost against extremely long life; but this use is rare. Such a soft metal lining (m.p. 1772°C) is of course backed by a refractory.

The furnace, of which the melting tank forms the bottom, is of direct-heated and reverberatory design comprised of *breastwalls* (i.e., sidewalls) and a low overlying, radiating roof or *crown*. This last term denotes arch construction. It could well replace the word "roof" used previously in this chapter for other types of furnaces, and it will be used henceforth when applicable.

In the cross-fired design, which is common, the upper sidewalls are pierced by rows of opposed pairs of oil or gas burners and large exhaust ports or flues. Figure III-6a depicts six of these pairs and their associated checkers in a 40-foot furnace. The refiner section and forehearth at the discharge end are separately heated by arrays of small burners, but are some 200°C lower in temperature than the main melting chamber.

Checkers. Figure III-6b shows that each pair of burners, flues, and *checkers* or regenerative heat exchangers is a symmetrical set. The heavy arrow in the diagram, from "Air" in to "Gas" out, depicts one half of a reciprocal operating cycle. In this half, the regenerator on the left has been heated and ambient air is pumped up through it. The left-hand burner is in operation, supported by this air which has become pre-heated to 1100°-1200°C. The flame is at roughly 1800°-2000°C, heating the glass to 1500°-1600°C maximum working temperature. The combustion gases exit via the right-hand flue in the figure at some 1600°-1700°C and pass down through the right-hand regenerator, heating it. At the conclusion of this half-cycle, the top of the heated checker is at about 1500°C, the bottom at least 800°C.

Then all flows are precisely reversed, with the right-hand burner operating. This reversal occurs about three to four times per hour.

The checkers themselves are rectangular lattice-works of refractory brick with communicating open spaces between for passage of the air and combustion gas. They are about 15-20 feet high, much less tall than blast furnace stoves. Their open spaces are much larger than in the latter (here, up to 6" or so across) to accommodate massive dust and alkali deposition. Otherwise, and except for the prevailing chemistry, they are comparable to those stoves.

A description of contemporary glassmaking must not omit to mention the use of *electric heating*: inserting molybdenum or other inert electrodes at opposite ends of a tank and driving a current through the molten glass. This practice is usually limited to smaller tanks. It rarely eliminates burners, owing to the potential consequences of a power failure. But it can either augment (i.e., "boost") or replace routine burner operation, and it can eliminate the need for checkers. There are other advantages in temperature control and in cleanliness of operation, which become especially important in making lower-tonnage glasses such as high-strength fibers, lead crystal, optical glass, and specialty borosilicates.

Refractory Zones in the Glass Melting Furnace. Long refractory life is at a great premium in continuous glassmaking. The furnace is expected to run some three to five years or more without interruption for major rebuilding or repair. Yet the several environments within differ markedly. In Chapter II a distinction was made at the "glass line" or meniscus. In the industry this is usually called the *metal line*, by analogy with metal melting. Owing to the lapping action of the liquid due to stirring, and to the confluence of both gas-phase and liquid-phase attack, the metal line itself is a focal zone of corrosion. Undercutting immediately below it has also been a common experience, associated with a liquid-corrosion phenomenon called *upward drilling*. On the other hand, in the tank walls and bottom there is little temperature cycling: even the charging of cold raw materials is continuous. Thermal stresses in the tank arise almost solely from the steady-state ΔT across walls and bottom, the outsides of which are generally forced-air-cooled.

By contrast all refractories above the metal line face a different chemistry, but always coupled with thermal cycling due to the reciprocal operation of the burners and gas flow. If oil is used as fuel, its ash becomes a part of the chemical and erosive environment. Temperature cycling is of course especially severe in the checkers and flues, in addition to the massive condensation of dust and alkalies.

The simple zoning table below omits about a dozen local areas in the furnace and its appurtenances, omitting their special nomenclature as well. It does not, however, omit any signally important features of the refractory environment.

Refractory Zone	Hot Face T, °C	Aggressive Environment	Erosion-Abrasion	Thermal Stress
Melting Tank:				
Bottom, Walls	1400-1600	Glass	Moderate	Startup
Metal Line	1400-1600	Glass, alkalies	Moderate	Startup
Throat	1300-1500	Glass	Moderate	Startup
Refiner Tank:				
Bottom, Walls	1200-1400	Glass	Moderate	Startup
Breastwalls	1400-1600	Alkalies, dust	Severe	Mod.
Upper End Walls	1400-1600	Dust, alkalies	Moderate	Mod.
Upper Sidewalls	1400-1700	Dust, alkalies	Severe	Mod.
Ports & Flues	1100-1700	Dust, alkalies	Severe	Severe
Burner Blocks	1100-1600	Dust, alkalies	Moderate	Severe
Furnace Crown	1500-1700	Alkalies	Moderate	Severe
Regen. Crown	1100-1600	Dust, alkalies	Moderate	Severe
Regen.Walls	500-1200	Minor	Minor	Mod.
Checkers:				
Top	1100-1500	Dust, alkalies	Severe	Severe
Bottom	200-900	SO_2 from oil	Minor	Severe
Regen. Ducts	200-900	Minor	Minor	Severe

Reverberatory Furnace: Copper Smelting and Refining

The Copper Smelting Process. It has been mentioned that most nonferrous metal ores are comprised of mixtures of several recoverable metals. Copper ores are no exception. The lead blast furnace and the zinc retort, previously described, illustrate processes in which the separation of metals substantially follows after the primary smelting or reduction. The smelting of copper sulfide ores is quite the reverse: the bulk of accompanying metal separations is conducted prior to the final reduction to copper. In Chapter II we deferred the treatment of this more complex process, which entails about a half-dozen steps all told. As the *reverberatory furnace* figures

importantly in the sequence, a view of the overall process here will serve to put that equipment in perspective.

Omitting preliminary ore dressing conducted at low temperatures, the standard smelting of copper sulfide ores follows the scheme shown below:

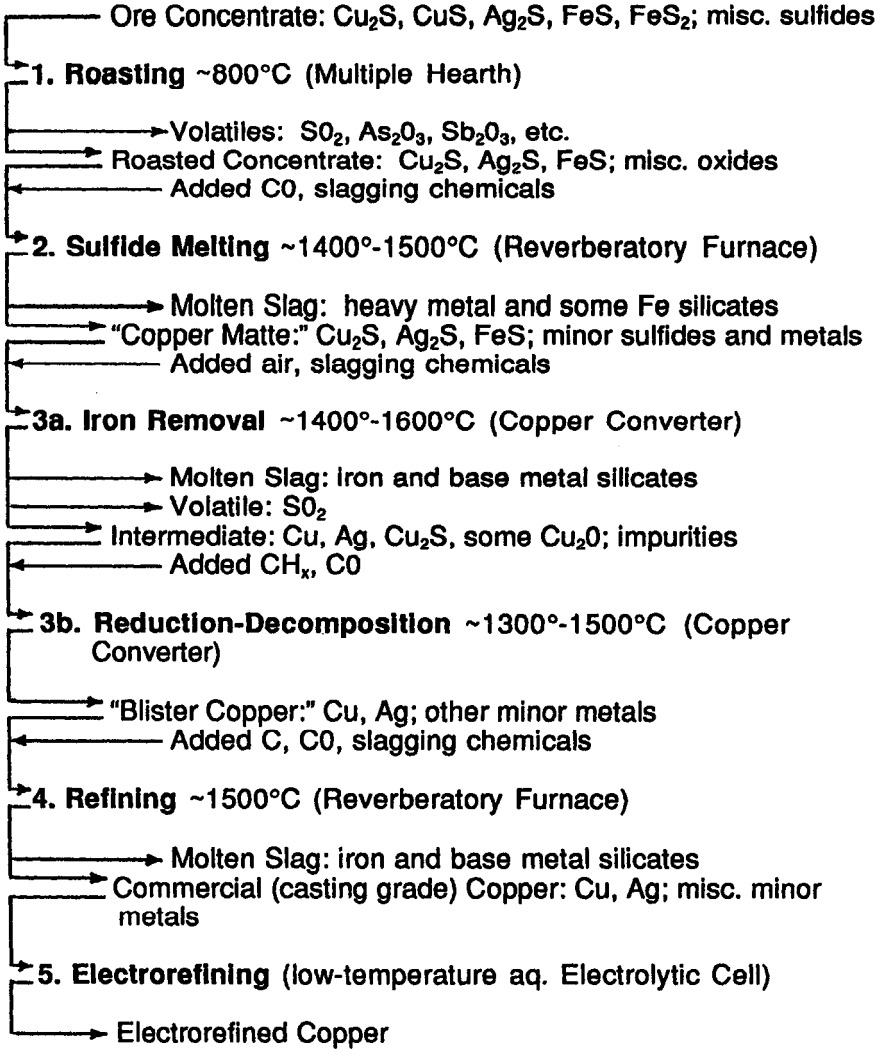

Step 1, Roasting, falls within the description of the direct-fired *multiple hearth* furnace given previously. Its low temperature and the oxidizing potential of the flame are threaded between limits such that the more stable sulfides remain unaffected, principally only volatile oxides are produced, and only very minor melting (due to other

oxides) occurs within the bed. This is a special low-silicate case of the chemistry of Sulfide Ore Roasting given in Chapter II, in that some of the sulfides present are not oxidized at all.

Step 2, Sulfide Melting, typically uses powdered coal or oil as fuel in a neutral flame. The *reverberatory furnace* is employed. Siliceous slagging chemicals (limestone and sand or equivalent) are added. The temperature and processing conditions are again threaded between limits such that now additional metal oxides are formed and go into the slag, while only the most stable sulfides are retained. The latter are melted together in a liquid layer which underlies the liquid slag. The two layers are tapped separately and cooled, the mixed sulfide product being called "copper matte." Basic slagging practice is usual.

The two parts of Step 3 are conducted sequentially in the *copper converter*, to be described later as a batch-operated vessel. Iron Removal is achieved there by blowing air through the molten charge, sufficient to oxidize principally iron which then joins the molten slag as mixed silicates. After the slag is tapped off, sufficient carbon or hydrocarbon is added to create a mildly reducing atmosphere in the Reduction-Decomposition step. Here the reduction to liquid copper (plus silver, etc.) is completed by decomposition of the sulfide. Small amounts of $S0_2$ left dissolved in the molten metal come out of solution on cooling and freezing; hence the name "blister copper" given to this crude product.

The oxidative part of the copper converter operation employs either acid or basic slagging practice, depending on the shop. Basic slagging predominates. Acid and basic slagging practices and their chemical rationale are described under Iron and Steel in Chapter II. The definitions and criteria are similar here.

Step 4, Refining, employs another *reverberatory furnace,* usually air-blown at first. Basic slagging chemicals are again added, including soda ash. The combustion atmosphere is finally mildly reducing. The purpose is consolidation and further refining of the metal. The commercial-grade copper product may be cast into ingots or billets or finished shapes; or into anodes for Step 5, Electrorefining. We shall not discuss Step 5 here, though it is of great importance in making high-purity Cu and in recovery of byproduct Ag.

The reverberatory furnace refining of Step 4 is in essence a copper remelt operation. With little modification it is also used to recover scrap Cu, either alone or melted together with blister copper. And it is used in foundries to melt ingots for casting. As either a refining or alloying or simply a *remelt furnace*, the reverberatory design is also used elsewhere in both ferrous and nonferrous metallurgy where metal volatility is not a major problem, e.g., in iron,

lead, tin, and aluminum. Oxidic copper ores (principally mixed carbonates or silicates) can also be smelted by coke in this type of equipment; use of the vertical blast furnace for this purpose is rare.

The Reverberatory Furnace. Though designs vary considerably in detail, this horizontal vessel is basically a shallow trough-shaped hearth lying under a low-arched radiating crown. Steel framing and support are rarely all-enclosing. The furnace is always direct-fired, sometimes from one end, sometimes by several burners. It may be charged through several ports in the crown, or through only one. It may be either continuous or batch-operated, being in the former case quite elongate in shape (e.g., 25± by 140± feet). Its really distinguishing features are the shallowness of its melted charge and the correspondingly large upper surface area of that charge, across which both heat and chemical reagents and products pass.

Figure III-7 shows such a furnace as employed in Step 2 of the copper-smelting scheme given above. Its main features are repeated in all like furnaces: a hearth exposed to molten metal and slag of chosen composition; crown, end and sidewalls bearing the corrosion-erosion of coal or oil (or gas) flame, ash, dust, and volatiles from the charge; exhaust ports where abrasion is especially concentrated; and charging doors experiencing thermal stresses upon each opening and closing. In continuous operation, taphole appurtenances are periodically shocked and exposed to hot metal and/or slag. In batch operation, discharging exposures are similar though less frequent, while the entire vessel interior sees wide temperature swings and atmospheric cycling.

The vessel depicted in Figure III-7 runs at some 1400°-1500°C in the bed, with the crown, wall and port areas a hundred °C or so higher. The blister-copper refining furnace falls in about the same temperature regime. For refining other nonferrous metals the working temperatures are generally lower. Sulfurous fumes are important corrosives in the copper smelting operation, while they are all but absent in subsequent refining, remelt and foundry usages. In copper matte furnaces, frequent shutdowns for refractory repair are the rule; the life of a roof lining, for example, is measured in months.

The temperatures listed in the zoning table below are typical for the reverberatory furnace making copper matte, and close for refining blister copper. They are not far from those experienced in the Glass Melting Furnace in corresponding zones. Here, however, checkers are absent. The off-gases of metallurgical reverberatory furnaces are burned independently, for waste-heat recovery with larger units and at least for pollution control with the smaller. The refractory corrosion chemistry here is of course unique to copper smelting; but the relative intensity of corrosive attack in the several zones is about equally applicable to other nonferrous metal systems.

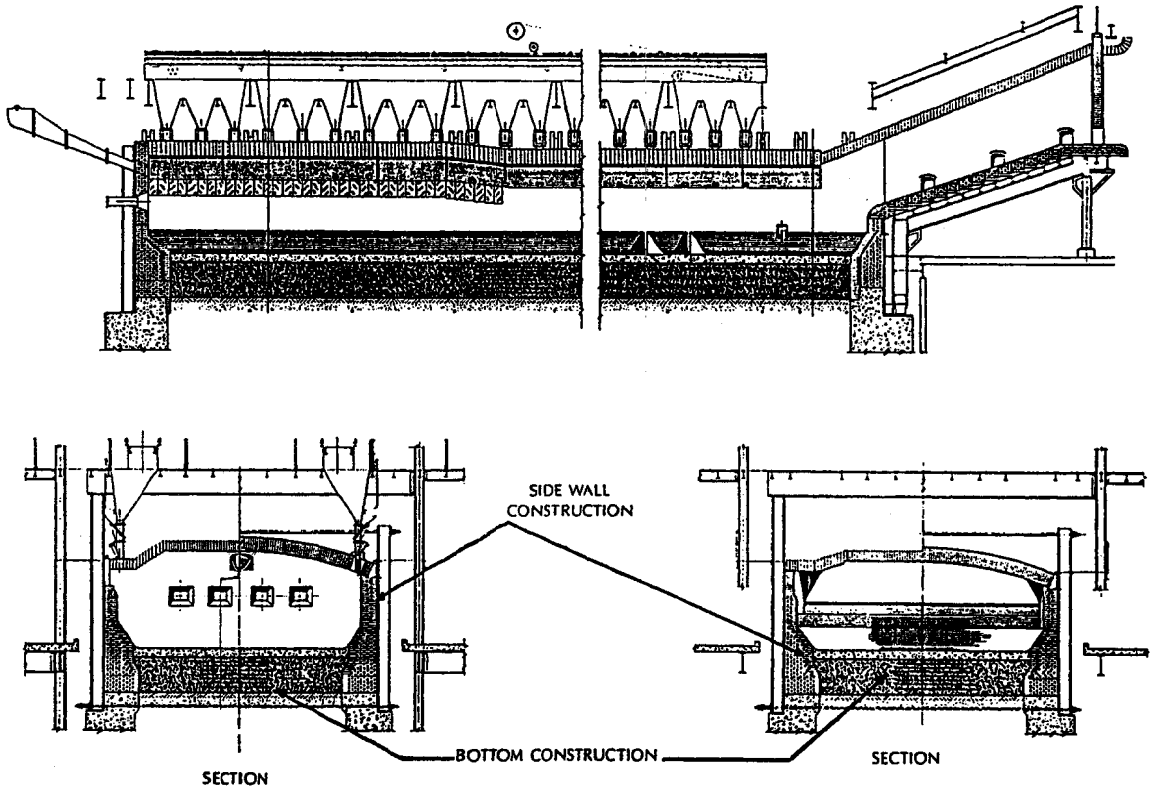

Figure III-7 Copper Reverberatory Furnace
(adapted from Ref. 10, by permission)

This table will thus serve as a general guide for most reverberatory furnace usage. We are, further, not distinguishing here between continuous and batch operations, which result in differences in refractory practice only in very local details.

Refractory Zone	Hot Face T, °C	Aggressive Environment	Erosion-Abrasion	Thermal Stress
Hearth	1400-1500	Cu_2S,Cu,slag	Moderate	Minor
End, max.	1600-1700	Slag, dust, fumes	Moderate	Moderate
End, exhaust	1400-1600	Slag, dust, fumes	Severe	Minor
Sidewalls	1400-1700	Slag, dust, fumes	Moderate	Minor
Exhaust Port	1400-1600	Dust, fumes	Severe	Moderate
Roof	1500-1700	Dust, fumes	Moderate	Minor/Mod.
Charging Door	800-1500	Dust, fumes	Moderate	Severe
Taphole & Plug	400-1500	Cu_2S,Cu,slag	Severe	Severe

Tunnel Kiln: Ceramic Sintering

The *tunnel kiln* is to formed ceramic artifacts what the rotary kiln is to their granular raw materials: a versatile, fuel-efficient, continuous countercurrent sintering furnace of up to many hours' residence time and up to huge throughput capacity. It is used for repetitive mass-production firing anywhere in the composition and temperature ranges and in most of the product size range described in Sintering of Oxidic Ceramics in Chapter II. It is a mainstay of production of fired refractory bricks and blocks; but its annual output of glazed and unglazed whitewares, china, and many other commercial clay and synthetic ceramic products is much greater.

As the name implies, a *tunnel kiln* is a long stationary horizontal tube of roughly rectangular cross-section. It is operated at steady state while carloads of the ware to be fired are pushed into one end in line and extracted, one at a time, from the other end. A view illustrating its common features is given in Figure III-8. Its typical construction starts with a straight and level steel railway set in a rigid base, running the entire length of the kiln plus appurtenances. The *kiln cars* moving on these rails have wheeled steel undercarriages and pushing and mating provisions all designed to ensure a smooth, jerk-free ride and precise alignment of each car relative to the others and to the kiln sidewalls.

Each car top is a square or rectangular refractory platform which (a) forms one short segment of the hearth of the furnace; (b) supports the ware and kiln furniture comprising the *setting* (i.e.,

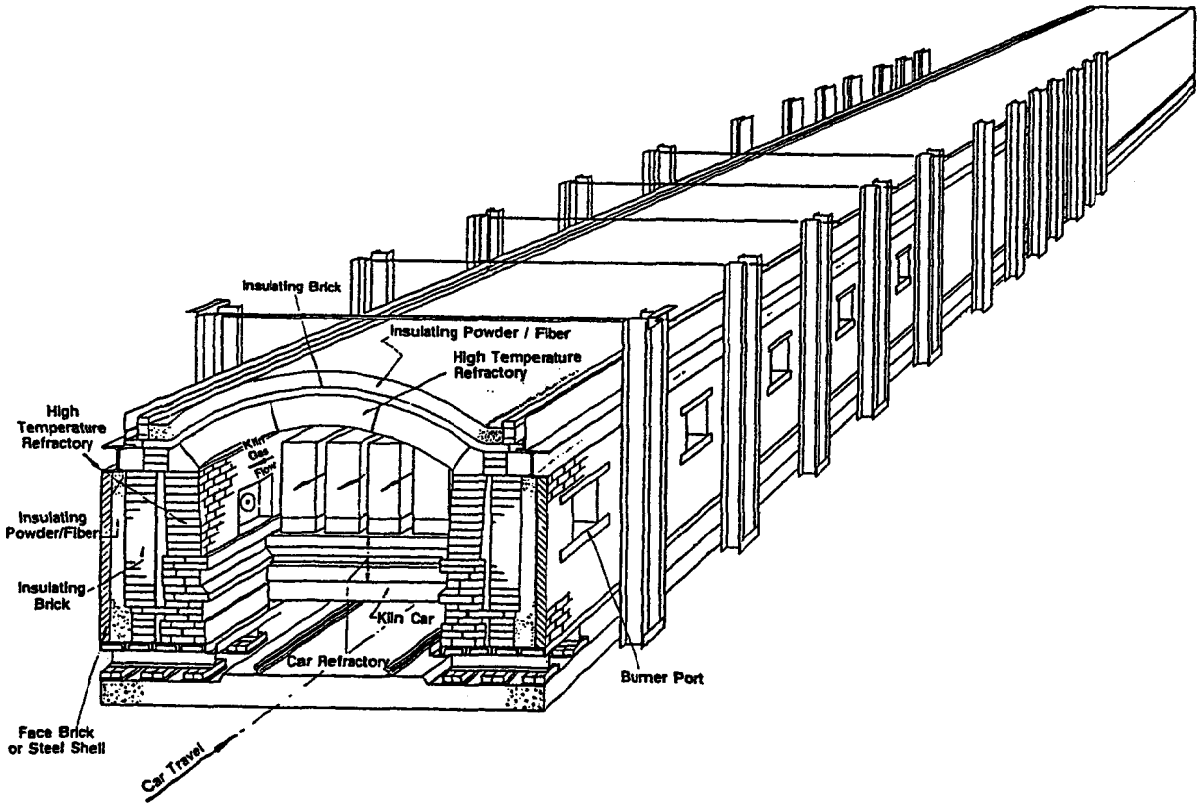

Figure III-8 Tunnel Kiln (reprinted from Ref. 10, by permission)

increment of the charge) on that car; and (c) forms seals both fore-and-aft with the tops of other cars and side-and-side with the kiln walls. These platforms and their seals thus divide the tube into an upper working chamber and a lower forced-air-cooled chamber that protects all steel undercarriages, wheels and rails. As working temperatures permit, the seals range from a simple abutment or rubbing fit to key-and-slot designs to others constructed partly of metal. One such can be seen in the lower left of Figure III-8: a steel blade riding in a "U"-shaped steel trough filled with sand.

The kiln walls are of free-standing refractory brick construction. The roof is usually a low arch or crown. Freedom from distortion and creep over long operating periods is a must. As the figure shows, external steelwork is limited to that necessary for mechanical support. Some kiln designs are modular, with refractory seals between segments. A one-car-length air-lock chamber is added at each end, to accommodate each incoming car yet to be fired and each emerging car of fired ware. The overall kiln length ranges from well under 100 feet to some 500-600 feet. Inside dimensions of the working chamber are likewise variable, running up to some ten to 14 feet wide and at least as high.

A great premium is placed on thermal insulation in all the refractory components, as the heat-leakage area of the tunnel shape is many times that of a compact shape. On the other hand, thermal transients in the kiln proper are at a minimum in prolonged steady-state operation; and since the ware is in only gas-phase communication with the enclosing refractory, corrosive attack is far less severe than is experienced in metallurgical melting furnaces. Expected refractory life is correspondingly measured in years: typically, three to five or more. But the principal life-limiting factor is still corrosion and alteration.

Unlike the rotary kiln, the tunnel kiln is capable of considerable variety of designed-in temperature and atmosphere profiles down its length. Gas flow is in general countercurrent to the movement of the cars. But (a) the placement of multiple burners (up to six or eight or more) along each sidewall, (b) adjustment of their fuel and primary air or 0_2 supply, and (c) the provision of secondary air and exhausting of combustion products through ports located over the length of the furnace, are all independent variables of design and operation. Ambient air is typically metered-in near the discharge end in such manner as to cool the fired ware slowly, while this air is preheated for combustion. The hot zone or sintering zone may itself be subdivided into oxidizing and reducing sub-zones, while its temperature profile and overall length are fitted to the sintering kinetics of the ware. The heating ramp or gradient at the feed end is likewise subject to precise design, which includes a head-end drying zone in some cases. In any event, the incoming ware efficiently cools the bulk of the

exhaust gases. These recuperative features yield high fuel efficiency. Oil or gas is the preferred fuel.

The kiln operating parameters and the geometry of the car settings have to be optimized together for uniformity of gas flow and of sintering of each piece of the ware, also for fuel consumption and throughput rate. "Close" settings risk underfiring of artifacts placed toward the center and overfiring of those nearest the periphery or top. "Open" settings call for careful design and often for custom kiln furniture. When well executed, they yield superior fired quality. After optimization, the emphasis is on reproducibility over prolonged production campaigns, at which the tunnel kiln excels.

Contemporary clay products manufacture has made significant strides in such areas as (a) use of robotics in setting of cars, (b) setting once only for both drying and firing, and (c) reduction of the mass of both cars and kiln furniture by the use of advanced design and advanced refractory materials. A more sweeping innovation in some plants has been use of the *roller hearth* to eliminate kiln cars altogether. Meanwhile, improvements in insulating refractories and their installation have markedly reduced heat leakage out through the kiln proper. Computer-automated kilns are the rule.

Refractory Zones in the Tunnel Kiln. Any one kiln has a distinct set of temperature zones down its length, applicable to the sidewalls and crown:

Drying Zone (optional; exit-gas down to 100°C±)
Preheat Zone (gas cooling down to 200°C±)
Hot Zone or Sintering Zone (incl. optional reduction firing)
Product Cooling Zone (to 200°C±; air preheat)

But the many different articles and compositions that are fired preclude giving any typical zone lengths or temperatures. Hot zone temperatures, for example, may be as low as about 1000°C for firing common clay products or up to a maximum near 1900°C for some synthetic refractories and ceramic products, or anywhere in between. The variety of approaches to sintering and the various gas-transported chemical exposures of tunnel kiln hot zone refractories are sampled in Chapter II. Glazing, also summarized there, adds further aggressive chemicals to the hot zone and preheat zone environments. Since gas velocities are high -- up to some 50 linear feet per second --, erosion and abrasion are generally present, particularly at ports, baffles, and other areas of turbulence and impingement.

A number of other refractory accessories should be mentioned. Burner blocks, especially including catalytic burners, see very high flame temperatures and velocities. Refractory seals and gasketing

are needed. Duct linings external to the kiln usually experience less demanding conditions. Refractory closures surrounding the air-locks at the ends similarly see lower temperatures and little chemical corrosion; but they must be moveable or flexible, and they are by no means immune to dust exposure. Finally, car tops and kiln furniture experience the entire gamut of kiln conditions in every pass, unlike the stationary parts of the kiln; and they receive mechanical abuse between passes. Yet these accessories must be re-useable many times.

In spite of the wide range of tunnel kiln uses and operating environments, refractory design in each case falls within some relatively systematic guidelines. We will show later how these guidelines are developed and applied.

Heat-Treatment Furnaces: Metals and Glass

Horizontal rectangular-shaped heating vessels are of course prolific. In the *heat treatment* category we can conveniently collect together all such chambers dedicated to the sub-solidus heating of metals. The annealing and crystallization of glasses and the baking of glass enamels might as well be included here too. The highest-temperature chambers are used to prepare metal ingots or billets for subsequent hot shaping, for example by rolling, pressing, forging, drawing, etc. For steels this means heating uniformly to some 1100° to 1400°C. The unalloyed-metal melting points given in Figure II-2 make it plain that this temperature range is neither the maximum nor the minimum for this type of operation; but it certainly is the commonest. The older soaking pit has largely given way to continuous automated billet-heating furnaces.

As solid-state heat treatment is taken to include the development or healing of microstructure and the relief of stress in metals, glass, and enamels, the working temperatures encountered move generally down from the above case. Corrosiveness of these operations on the enclosing refractories likewise moves down from modest to trivial. So also does thermal stress. In none of these processes does the work touch the enclosure; so abrasion is absent as well.

Refractory usage and usage criteria are best regarded in this category primarily as functions of the working temperature. The following temperature ranges are arbitrary and a little indistinct at the edges; but they will do. The coded entries under refractory usage are intended to mean: I -- thermal insulation; C -- chemical-resistant containment or support; H -- electrical resistance heating.

Temp. Range, °C	Heating Method	Typical Atm.	Typical Refractory Usage: Roof, Walls	Floor	Interior Equipment
<500	Fuel	Combustion	I	I	-
500-1000	Fuel	Combustion	I	I	-
1000-1500	Fuel	Combustion	I	I, C	C
>1500	Electric	Inert	-	-	H, C

The 1000°-1500°C range encompasses steel billet reheating for hot forming, wherein protective fluxes or slags are often retained as measures against excessive oxidation of the metal. Hence there is some exposure of refractories to chemical corrosion. The highest range, >1500°C, exemplified by refractory metal processing, typically makes a step change to electric heating in inert atmosphere or vacuum and in much smaller equipment, as was pointed out in Chapter II. In fuel-fired vessels there are of course exhaust ports, flues and ducts; but the vessel wall lining materials chosen will generally serve those locations as well.

Drying Ovens: Ceramic Ware

The drying of inorganic solids has already been mentioned as a technical function of spray driers, multiple hearths, and rotary kilns. It should be noted that all of those high-throughput devices operate on particulate or granular feeds. The tunnel kiln may include a head-end drying zone for formed ceramics; but such a provision is often defeated by the extremely long drying times and low temperatures required by bodies of appreciable mass or wall thickness. It is common in ceramic and refractory manufacture for the drying of *green* (i.e., wet) formed ware to be conducted as a separate unit operation.

The principle of the continuous tunnel kiln is quite appropriate for this drying purpose. Heated-air *tunnel driers* are in widespread use, taking up to several racks or cars abreast as well as in line. Drier temperatures permit the use of metal, enamelled, and even polymeric (or polymer-coated) racks, shelves, conveyors, etc., in place of the typical conveyance design of a high-temperature tunnel kiln.

The necessity for careful time-temperature programming of small batches in ceramic drying often calls for batch-operated *drying ovens* rather than the continuous tunnel. These ovens are simple rectangular chambers, gently swept by steam-heated air or air-diluted combustion gases. Waste gases can be used, if clean, and if provisions are made for close temperature and humidity control. Indirect radiant heating is common too. Microwave drying has been investigated but is not in extensive use. "Open" setting of the ware on

cars destined to enter a tunnel kiln for firing is an option often taken to avoid setting twice.

It is well to recall here the distinctions made under Industrial Drying in Chapter II among the several types of water contained in wet porous bodies. The temperature ranges of water evolution can significantly overlap. As some formed bodies are excessively weak when green, it is not at all uncommon to see ceramic wares ambient-air dried for long periods on shelves or on warm floors, before being placed in a drier or kiln. Depending on the state of desiccation at which sufficient strength is developed for further heating, programmed oven drying may then be omitted entirely or conducted, at will, up to 100°C or 150°C or 200°C before firing. Considerable shrinkage is experienced in these early desiccation stages; slow drying is necessitated in order to minimize thermal and "dryness" gradients within the ware, which would otherwise lead to flaws and cracking.

Refractory linings for drying ovens and tunnels have the sole purpose of thermal insulation of the peripheral walls and roof. Their process environment can be likened to that in the <500°C group under Heat Treatment Furnaces immediately preceding: namely, exceptionally benign. Fiber refractories, even glass wool, serve well in these situations.

Steam Boilers

It is arguable whether the preponderance of *steam boilers* are horizontal or vertical in architecture. They come in both styles. Fuels burned in steam boilers range from lump to granular to powdered coal, to oil, to natural or synthetic gas, to process off-gas or other combustible wastes. Units come in a wide range of sizes and of patented engineering designs. Only one of many boilers -- an oil-fired model -- is shown cutaway in Figure III-9 to illustrate its typical compactness.

Boilers are likewise compact in the temperature range of their operation. In fact, from the refractory viewpoint the most significant variable is the fuel, from which all the corrosives and abrasives in the chamber are derived (see Steam Generation in Chapter II). When industrial or municipal wastes and trash are burned, the unit is called an *incinerator.* Incinerators, like coal-burning units, must provide an ash pit and ash removal hopper at the bottom. They add severe abrasion to the refractory environment. The corrosives unleashed by burning wastes may be in about the same chemical class as those from coal, but they are far higher in lb/Btu or in kg/kJ. Incinerator linings accordingly go down frequently for repair, while industrial and utility boilers can run without major rebuilding for a decade or better.

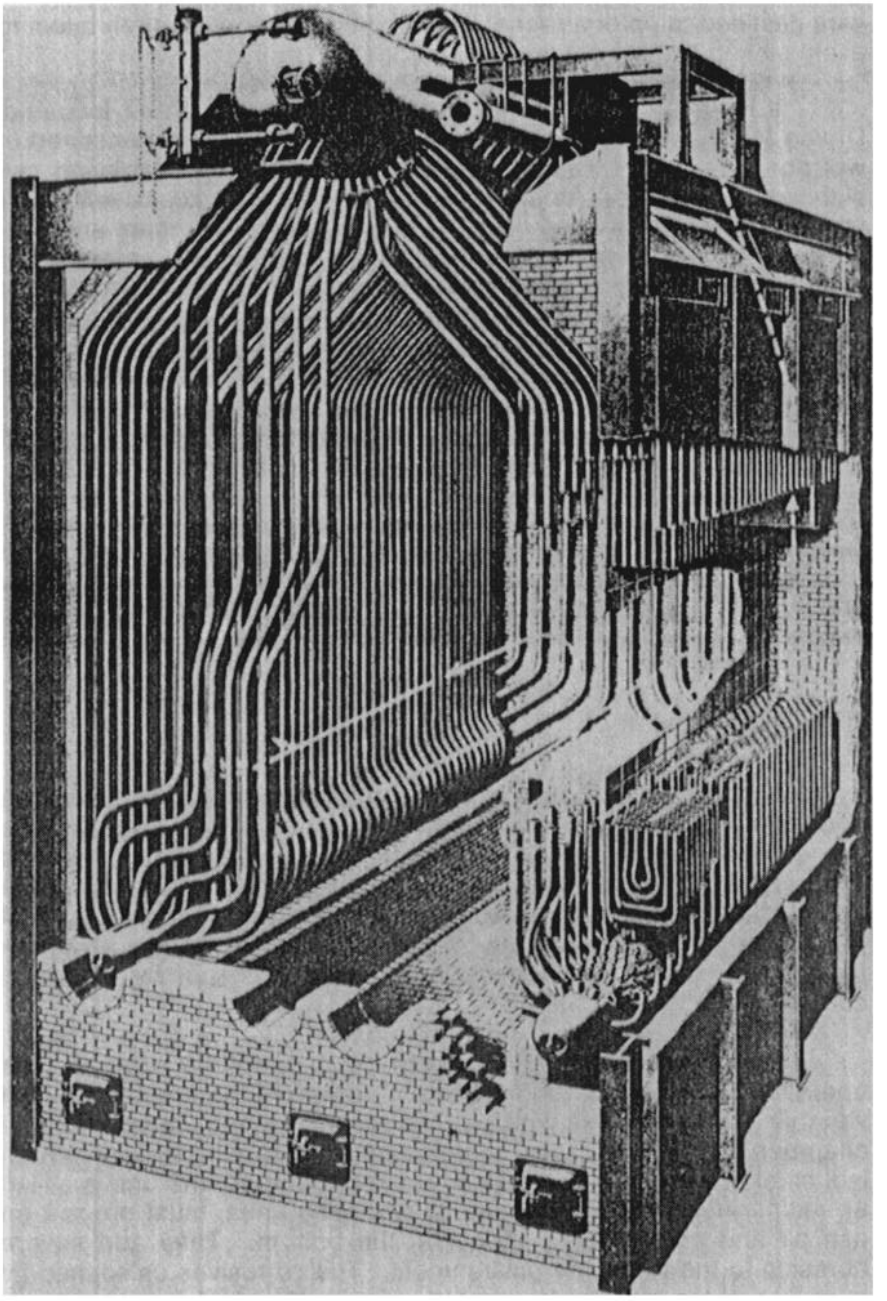

Figure III-9 Steam Boiler (reprinted from Ref. 10, by permission)

Design of the insulating walls has much improved refractory life as well as fuel efficiency. Modern boiler walls use water-cooling within their refractory insulation, in such manner as to cool the refractory significantly as well as to pre-heat the water on its way to the boiler tubes. While burner-block or fire-box wall temperatures may reach 1500°C or so, most of the vessel is far cooler, as represented in Figure II-1.

Zoning for purposes of refractory practice recognizes the following areas, though not all are present in every boiler:

Ash Pit and Hopper	End Walls and Roof
Grate and Fire-box	Recuperative Sidewalls
Burner Block	Floor

Refractory usages are highly individualized, however. These area designations only point broadly toward characteristic refractory exposures within the steam boiler. Each one is approached by boiler engineers in too many ways to be given justice here. One marked change from earlier practice, however, is the use of monolithics -- especially in conjunction with water cooling.

BATCH TYPES -- CIRCULAR

Steelmaking: Oxygen Blowing

Modern commercial steels can be classified in terms of carbon content in weight-%:

Very High Carbon	1.25-2.25	Medium-Low Carbon	0.10-0.25
High Carbon	0.75-1.25	Low Carbon	0.04-0.10
Intermediate Carbon	0.50-0.75	Very Low Carbon	0.01-0.04
Medium Carbon	0.25-0.50	Alloy Steels (approx.)	0.01-1.25

Of the prominent impurity elements left in iron by the blast furnace, the minimum levels achievable in making steels used to be about 0.04% each for C, P and S and about 1% each for Si and Mn. With the advent of *oxygen blowing* and sophisticated slagging practices in steelmaking, these specifications began to be lowered. In current times, especially for certain alloy steels, goals have been set close to 0.01% in respect to each one of these elemental impurities.

The essential chemistry of dissolved-impurity removal from Fe is given under Iron and Steel in Chapter II. The two methods usually invoked together are (a) batch oxidation using 0_2, and (b) scavenging of the resultant oxides by chemical reaction with a specified acidic or basic slag. The origins of modern vessel geometry go back to the

Bessemer converter of Figure I-5b. Oxygen blowing of molten iron has not only made possible much higher-purity and lower-carbon steels than were previously achievable. It has also greatly accelerated the operation, by virtue both of higher oxidant concentration and of higher temperatures. Finally, it avoids the unwanted nitriding that accompanies the use of air.

Basic Oxygen Furnace

Given a charge of molten iron, 0_2 gas can be delivered into it either from above or from below. In the *basic oxygen furnace* or *BOF*, depicted in Figure III-10a, the former is the case. The 0_2 injection is best described by going through all of the steps of a *heat* in turn. Take for example a 300-ton vessel, and imagine its trunnion axis perpendicular to the plane of the figure.

In the first step the empty vessel is rotated counterclockwise about 20°, and roughly 100 tons of scrap steel is dropped onto the "charge pad" area. This is followed by some 200 tons of molten blast furnace iron, then by the basic slagging chemicals: sand if necessary, limestone or quicklime, dolime, fluorspar, and ore or mill scale, all metered by weight. Chemically these are: $Si0_2$, $CaC0_3$ or Ca0, Mg0+Ca0, CaF_2, and $Fe0+Fe_20_3$.

Once charged, the vessel is rotated upright and a water-cooled, refractory-armored tube or *lance* is inserted down through the mouth. Lance designs and practices vary. For now it is sufficient that this is the means of injecting 0_2 down into the hot metal. This "top blowing" operation takes about 15 minutes, during which time the temperature of the charge rises, usually ending somewhat above 1700°C. The evolution of C0 gas from within the charge churns it violently, intermixing the molten slag and metal, making a voluminous froth and splashing it well up on the sidewalls or "barrel." The atmosphere above the charge is principally a $C0-C0_2$ mixture, containing small amounts of $S0_2$ and other volatile oxides and much dust. It is exhausted through a moveable hood and ducting, not shown.

On conclusion of the "blow," the lance is withdrawn and the vessel is tilted clockwise about 90°, so that the hot metal pours out the taphole while the overlying slag is restrained by the cone. Ordinarily the vessel is then rocked back and forth so as to coat the upper walls with slag as much as possible; finally it is turned all but upside-down to pour out the slag. If no lining repair or maintenance is to be performed, the BOF is then ready for the next heat. The total elapsed time is about 30 minutes.

Given frequent repair, BOF lining life in the U.S.A. generally varies from ~1000 to over three thousand heats. The average is

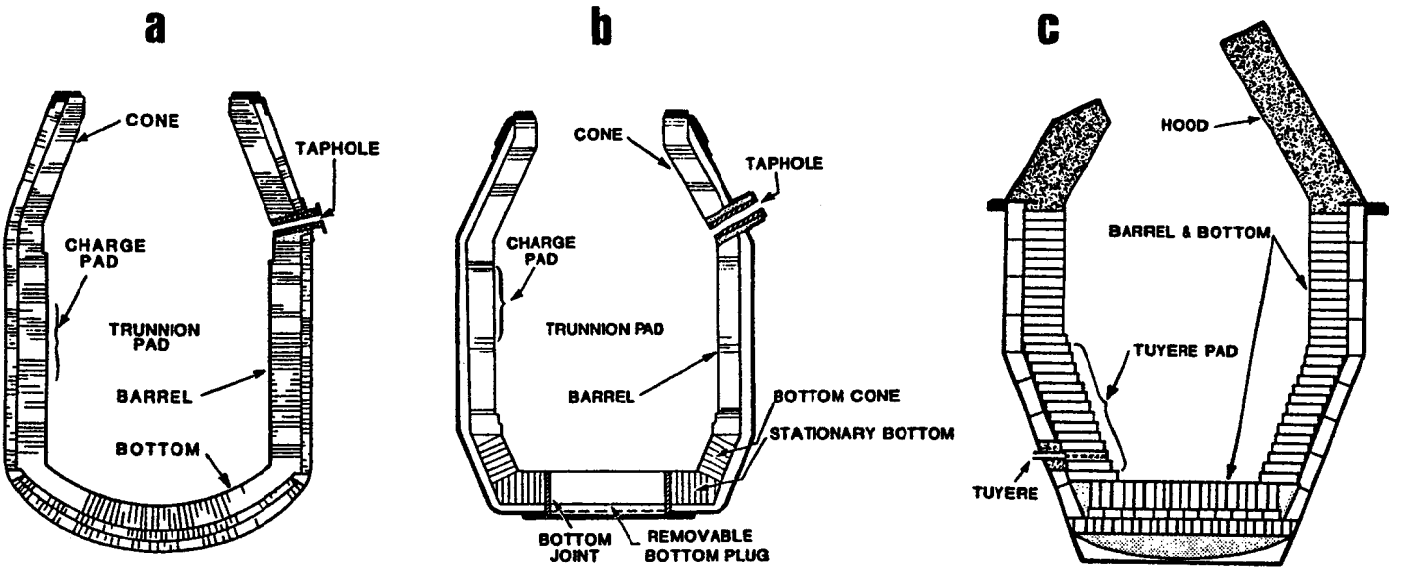

Figure III-10 Oxygen-Blown Steelmaking Vessels
a. Basic Oxygen Furnace b. Quelle-Basic Oxygen Furnace
c. Argon-Oxygen Decarburization Furnace
(courtesy of National Refractories & Minerals, Inc., by permission)

about 2500. Carbon steel is the principal product of the BOF, but some of its output goes on to further processing ending in alloy steels. It makes far more steel than any other vessel: 59 million tons in the U.S.A. in 1989.

Quelle-Basic Oxygen Furnace

The "bottom-blown" version of the basic oxygen process or BOP is known by several designations, principally *OBM* in Europe and *Q-BOP* in the U.S. and Japan. A generic representation of its vessel is given in Figure III-10b. A bottom plug is shown in the figure, "removable" because it is typically quite short-lived. There are two basic types of bottom plug: (a) dense refractory, through which an array of vertical tuyeres penetrate; and (b) porous, permeable refractory which serves as an oxygen diffuser. Again we are omitting details; it suffices for now that 0_2 is injected up through the bottom.

The conduct of a Q-BOP heat runs the same course as that in the BOF, except there is an option if tuyeres are used: powdered slagging chemicals (e.g., Ca0) can be aspirated into the 0_2 stream and delivered directly into the molten charge, improving the efficiency of P and S removal and reducing the loss of Fe0 to the slag. The blow is accordingly a few minutes shorter than in the ordinary BOF. Tuyeres of concentric design also provide for surrounding the 0_2 stream with a hydrocarbon coolant, e.g., methane, thus helping to control the temperature rise during the blow. The bottom-blowing technique was originally developed to treat high-phosphorus iron, but it is by no means limited to that use alone.

Argon-Oxygen Decarburization Furnace

The *AOD* vessel is also bottom-blown, employing tuyeres; but Figure III-10c shows these entering horizontally through a lower cone wall instead of vertically through a bottom plug. Characteristically, this vessel is charged only with molten iron or steel, hence the absence of a "charge pad." Its distinguishing feature is that it is blown with mixed 0_2 and Ar, in ratios variable at will through the course of the blow. The tuyeres may also be used to introduce powdered slagging chemicals. The AOD process was developed primarily to make stainless steels, but it is now in much broader use, even in foundries. The vessel runs from a few tons capacity up to about half the charge of a typical BOF. Its peak temperature runs up close to 1800°C.

The argon diluent facilitates throttling the flow of 0_2 without decreasing the churning action of the gas. In fact, the AOD process is the most turbulent of the three described here, and for that reason alone the most corrosive. To make matters worse, some shops have employed dual slagging in the course of each heat: first acid, then basic. Linings of AOD vessels last about one-tenth as long as do BOF

linings. A further contributing reason for this discrepancy is that hot patching and maintenance procedures that work in the BOF are not very effective here, owing to the extreme turbulence of the AOD process. New refractory patches are rapidly washed away.

Permutations and Combinations

Combined top-and-bottom blowing is practiced, using either a porous bottom plug (e.g., "LBE") or bottom tuyeres (e.g., "LD" or "LD-KG") together with a lance. Some shops have converted their bottom-blown (Q-BOP) vessels to horizontal tuyeres. Some have combined 0_2 blowing by lance (BOF) with the feeding of solid chemicals through the same tube; others have tipped the lance with a porous refractory gas diffuser like that of a porous bottom plug. It is hardly beyond reason in this era of change to predict still wider proliferation of designs, or a single design enabling the user to operate in any chosen combination of ways; even perhaps water-cooling of portions of the steel shell, as has proven effective in other types of furnace.

Refractory Zones in Oxygen Furnaces

The principal refractory areas in the three main types of oxygen steelmaking vessels are designated by the legends in Figures III-10a, b, and c. The principal omissions there are the BOF lance and its details, and the details of the Q-BOP bottom plug. Lance refractories including optional porous diffuser tips can be selected without undue regard for their life: replacement does not shut down the furnace. The Q-BOP plug can hardly be regarded as expendable, on the other hand: its removal and replacement is disruptive at best, and while in place it had better not develop a severe hot-spot or run-out. Tapholes see high-velocity metal and some slag; the main concern there is maintenance of a constant diameter. Fairly rapid rebuilding techniques have been developed so that tapholes are not life-limiting on their vessels as a whole. Nevertheless, durability is at a premium.

For the remaining fixed wall areas, efforts are made toward realizing a common service life over the whole vessel. These efforts include: (a) choice of refractory composition and type; (b) variation of lining thickness according to the corrosiveness of its environment; and (c) use of automated, rapid, remote hot patching and repair techniques between heats. Wear profiles are now routinely scanned by an automated laser sensing device, whose output can be directly programmed into the refractory gunning controller so that patching is completed quickly, effectively, and economically. The further coating of vessel walls with slag at the conclusion of each heat has been mentioned; but the trunnion area cannot be reached in that manner, and reliance has to be placed on the other life-prolonging methods.

Typical cycle environments in the several lining zones are tabulated below. The furnace atmosphere reverts to oxidizing (air) on every turn-down. References here to "slag" are to basic slag; but the AOD case can be an exception.

Refractory Zone	Max. Hot Face T, °C	Aggressive Environment	Erosion-Abrasion	Thermal Stress
Lance (lower)	Virtually	Fe, slag, etc.; turb.	Severe	Severe
Cone or Hood	all areas	CO, CO_2, dust	Moderate	Mod.
Taphole Area	in BOF	Fe, slag, gas, dust	Severe	Severe
Upper Barrel	& Q-BOP	Splash, gas, dust	Moderate	Mod.
Trunnion Area	see up to	Bathed: Fe, slag	Moderate	Mod.
Charge Pad	~1700°C.	Ditto plus impact	Severe	Severe
Lower Barrel		Fe, slag, etc.; turb.	Severe	Severe
Bottom Cone	In AOD	Ditto	Severe	Severe
Tuyere Areas	all areas	Ditto	Severe	Severe
Fixed Bottom	see up to	Fe, slag; turb.	Severe	Severe
Bottom Plug	~1800°C.	Ditto	Severe	Severe

Electric Arc Furnace: Alloy Steelmaking

The *electric arc furnace*, or *EAF*, is the second-highest producer of steel in the U.S.A. It made 35 million tons in 1989. Though it is a mainstay of alloy steel manufacture, it also makes carbon steels and is used in foundries; and it sees much use as a melting furnace, feeding the AOD for alloy steel refining. It has become classified according to power consumption, roughly related to operating temperature: ultra-high power (UHP), high power (HP), and low power (LP). It is versatile as to size and as to feed, receiving scrap and blast furnace hot metal or the output of an oxygen furnace. It may be fed some coke, and either acid or basic slagging may be used. In the U.S. the latter predominates. Top blowing (lancing) with O_2 is sometimes practiced, though the addition of iron ore (Fe_2O_3, etc.) is usually employed for oxidation of carbon, silicon, phosphorus and sulfur without blowing at all. The vessel is discharged by tilting, either by use of a spout alone or through a taphole. It virtually always employs 3-phase alternating current.

EAF designs and operating practices are presently in a state of flux. Figure III-11 illustrates a common refractory-lined vessel and its top. In recent years, however, water-cooled steel sidewalls have greatly reduced their lining thickness; and water-cooled roofs have eliminated refractories altogether from all but an enlarged "delta" section enclosing the electrode guides. The graphite electrodes (presently, coated) must of course be electrically insulated from each other; delta-section refractories have no evident alternative. Elsewhere, especially in UHP furnaces, still further design evolution is forecast.

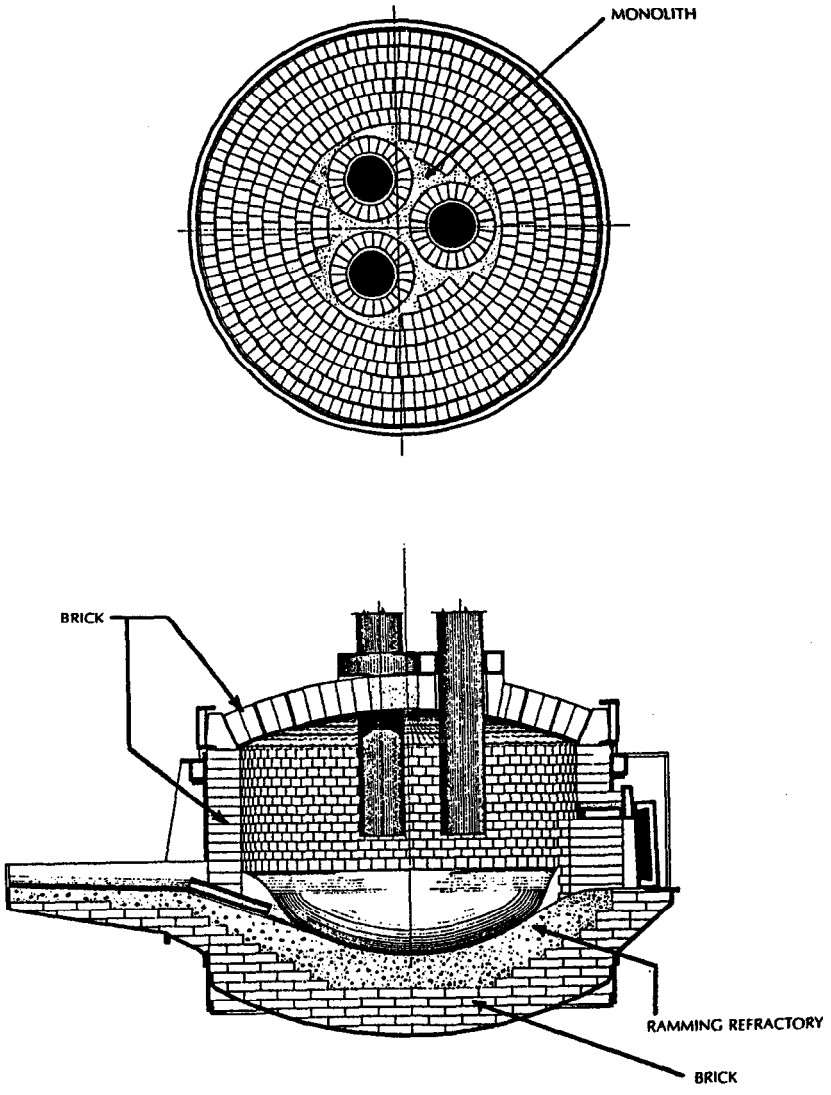

Figure III-11 Electric Arc Furnace, Steelmaking
(reprinted from Ref. 10, by permission)

The heating arcs pass from one electrode to its neighbor, in rotation, through the melt. Although this creates turbulence and metal-slag mixing, the EAF has a much better defined *slag line* (i.e., meniscus) than is typical in the BOP, Q-BOP, and AOD furnaces. The slag line is located at the lowest sidewall, just above its junction with the bottom or hearth lining. Below this level, refractory exposure is primarily to metal and slag; above it, to splash, CO-CO_2, and dust, and also to direct radiation from the arcs. "Hot spots" occur in sidewall areas where this radiation is most intense. Except for these areas, the sidewalls and bottom see common maximum steelmaking temperatures of about 1700°C with basic slagging, about 1600°C with acid slagging. Upper refractory sidewalls and roof run progressively a little cooler; but their water-cooled steel construction has now changed all that.

The course of a steelmaking heat in the EAF is about the same as in the O_2-blowing furnaces. Alloying elements Cu, Ni, and Mo may be added before heating, as these are not burned out of the melt. Ferrosilicon or ferromanganese may be added late, to "kill" or deoxidize the steel. Alloying elements such as Cr, Al, Ti, and Zr, which oxidize readily and would be lost to the slag, are added in the transfer ladle after the heat is concluded.

Refractory Zones in the EAF. The refractory temperatures and chemical exposures listed in the table below are typical for alloy steelmaking with basic slagging. For acid slagging or for foundry use, take off about 100°C in each area.

Refractory Zone	Max. Hot Face, T, °C	Aggressive Environment	Erosion-Abrasion	Thermal Stress
Roof:				
Delta Section	1600	CO, CO_2, dust	Moderate	Moderate
General	1600	CO, CO_2, dust	Moderate	Moderate
Electrode Coating	2000	Fe, slag, etc.	Severe	Severe
Sidewall:				
Upper	1700	CO, CO_2, dust	Moderate	Moderate
Hot Spots	1800	Splash, gas, dust	Moderate	Severe
Lower	1700	Bathed: Fe, slag, etc.	Severe	Moderate
Slag Line	1700	Fe, slag, etc.; turb.	Severe	Severe
Bottom	1700	Fe, slag, turb.	Severe	Severe
Taphole and Plug	1700	Fe, slag, turb.	Severe	Severe
Spout	1700	Ditto	Moderate	Severe

"Taphole plug" in the list above is giving way to the slide gate valve, which offers continuous control of the pouring rate and a precise shutoff. Modern hot maintenance of the bottom and slag line areas, and greatly improved monolithic basic refractories combined with water-cooled steel, are responsible for EAF campaigns now many-fold longer than used to be realized between major relinings.

Coreless Induction Furnace: Utility Melter

The *CIF* has the cleanliness of a laboratory device, yet a broad size range and flexibility for production. Little wonder it is used widely as a melting, alloying, and foundry furnace, ferrous and nonferrous alike. Ideally suited for vacuum and controlled-atmosphere melting, the induction furnace is much used for metal de-gassing and for the preparation of high-quality alloy steels -- not to mention copper and nickel base alloys and others. It is not a large-scale, mass-production melter, nor is it appreciably used for chemical refining. Its slag is of the nature of a floating protective covering and flux for impurities, rather than a reagent to be churned into the metal as is the case in the primary steelmaking furnaces.

The *coreless induction furnace* consists in essence of (a) an external, water-cooled helical copper conductor, carrying alternating current ranging at will from line frequency up to kilohertz or even megahertz frequencies; (b) a thermally-insulating, non-suscepting and impermeable refractory crucible fitting closely against the coil; and (c) a metal charge placed in the crucible. The charge becomes the "core" or susceptor and is heated by induced eddy currents within. Once the charge is molten, resistance to the eddy currents produces mechanical stirring. Figure III-12a is a sketch of a 20-ton line-frequency unit. It shows that, with provision of a magnetic yoke surrounding the coil, the entire assembly can be encased in a steel shell. That shell then forms the enclosure permitting vacuum or controlled-atmosphere operation. Figure III-12b is a cutaway rendition of the commercial unit.

The only refractory zone of note in such a furnace is the crucible. Apart from the qualities listed above, this crucible obviously must not crack and leak in service. For a furnace cycled repeatedly between ambient and some 1650°C and subjected to corrosion by steel and slag, that is a tall order.

Steelmaking Ladles

Torpedo ladles and teeming ladles were introduced previously here as accessories to the iron-smelting blast furnace. The use of ladles is implicit, as well, with every other liquid-metal processing device we have described. In steelmaking ladles, change and the prospect of further change are the rule at this writing.

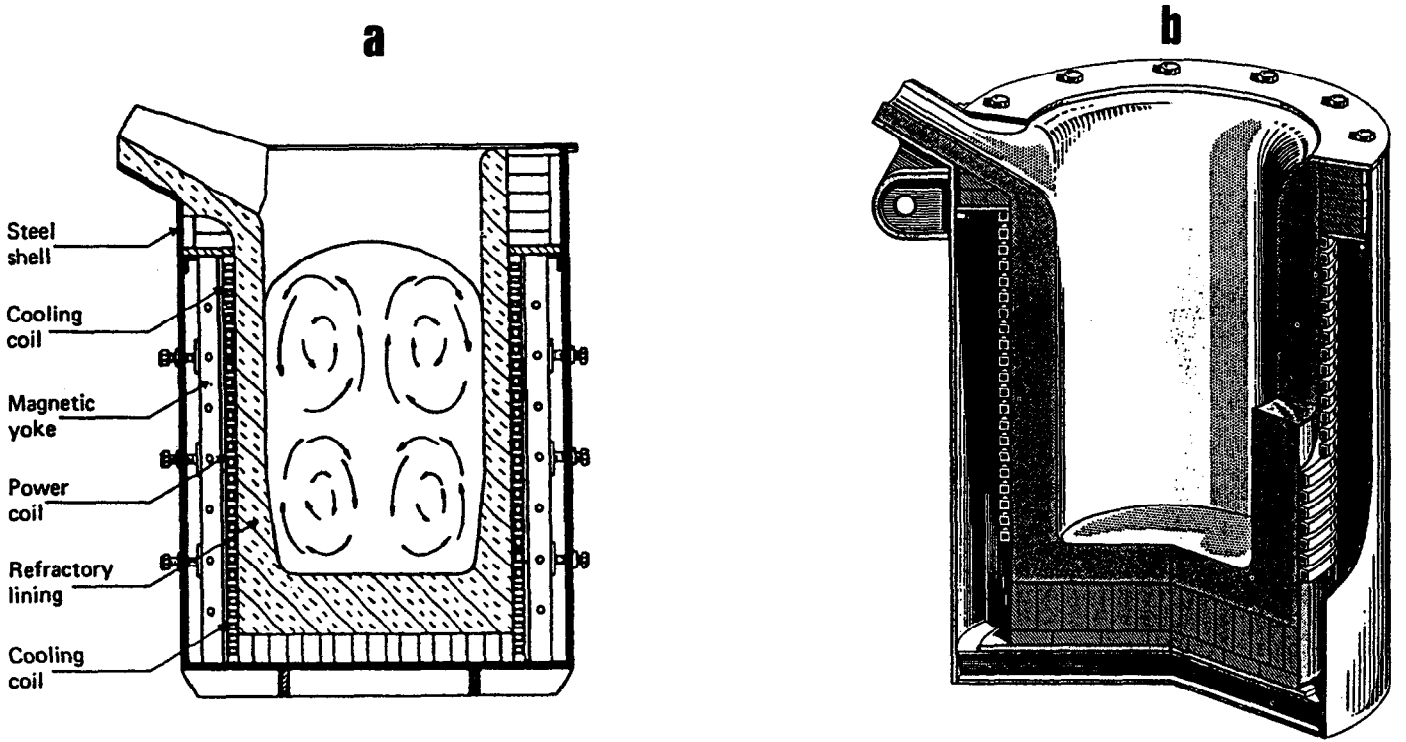

Figure III-12 Coreless Induction Furnace, Steel Melting
a. Section (reprinted from Ref. 8, by permission)
b. Cutaway (courtesy of National Refractories & Minerals, Inc.)

Bottom-Pouring Ladles. Classical ladle designs are not likely to disappear, particularly in small shops and foundries. The simplest form is a cup with a pouring lip or spout, discharged by tilting. But to avoid delivering slag, it is necessary to pour metal from the bottom.

Figure III-13 shows three types of bottom-pouring ladles. The tilting "teapot" in the upper right is otherwise like all tilt-poured spout configurations: (a) the metal stream is not precisely directed, and (b) shut-off timing is uncertain. The "bottom pour" ladle in the upper left of the figure is better described as the *stopper rod* type; this has been a standard configuration in iron and steelmaking for decades, as it answers both of the above faults of spout pouring. It has been used in torpedo ladles and teeming ladles for iron and in all their counterparts for steel transfer and casting. The same concept of course applies to the taphole and plug used for discharging furnaces.

However, this concept has limitations too. For one, the metal delivery rate through a fixed-diameter orifice depends on the hydrostatic head in the vessel. For teeming ladles, an ideal refractory orifice would be one which enlarges by wear such as to maintain constant metal flow while the ladle empties. It is not easy to create and reproduce a ceramic material that is so obliging; but efforts to do so generated a second drawback: uneven orifice wear, often resulting in inability of the stopper to re-seat. Modern nozzle, taphole, stopper and plug refractories have been improved so that reliable re-seating is now expected; but the price is a slow wear rate of the orifice. The variable pouring-rate consequences can be abided in operator-controlled plants and foundries. However, the incentives for computer-driven automation in iron and steelmaking are great; and automation calls for controllable pouring rates.

Enter the *slide gate valve*, shown at the bottom of Figure III-13. This device has been evolving since about 1970, and will no doubt see still further improvement. It consists basically of two fixed, parallel refractory plates with a space between, and a sliding plate filling that space. It is clamped across the bottom nozzle of the vessel, holes in the two fixed plates being aligned with the nozzle orifice. The sliding plate, or *gate*, bears a corresponding hole for discharge and a blank or solid area for shutoff. Precise hydraulic positioning of the sliding gate can provide controlled flow of hot metal at any rate from zero to maximum. With sensing and programmed positioning controls, the slide gate valve can serve an automated plant. Large ladles, running up to several hundred tons capacity, now use the slide gate almost exclusively. Slide gates are also being fitted to the tapholes of steelmaking furnaces.

All steel ladle refractories must withstand corrosive attack at up to about 1700°C. An upper slag line (filled level) and a lower slag line

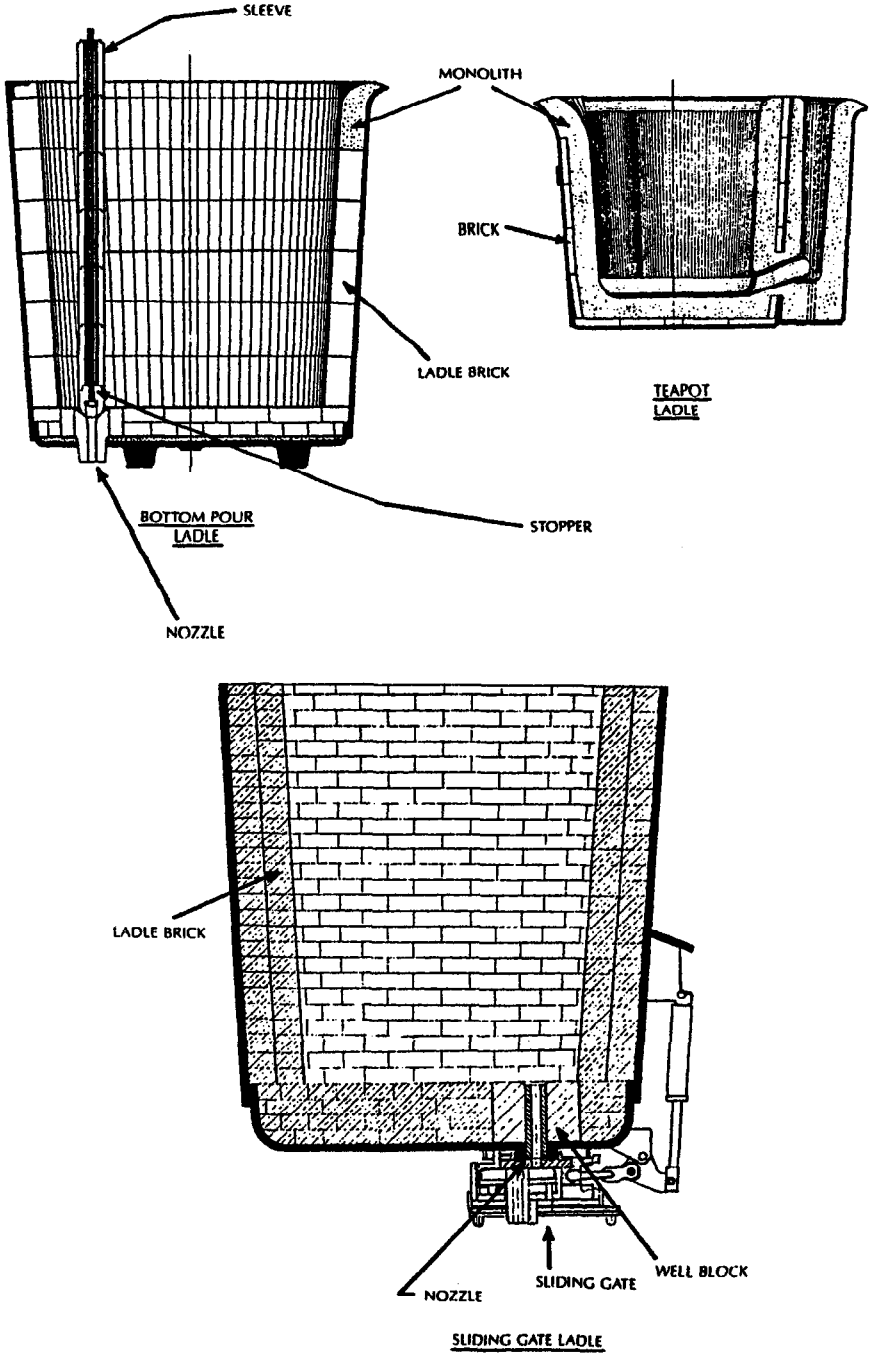

Figure III-13 Examples of Metal Pouring Ladles
(reprinted from Ref. 10, by permission)

(discharged level) are foci of corrosive wear. The refractory must not shrink from the shell over some ten to one hundred temperature cycles, nor crack under the thermal shock of being filled; and it must endure much mechanical abuse. The nozzle and its surrounding block take intense erosive forces, while the stoppering and gating devices do likewise. The ladle-discharging system is repeatedly subjected to thermal shock as it is operated. Slide gate parts must in addition be exceedingly hard and wear-resistant, and surfaced to very close tolerances. But now there is still more.

Ladle Metallurgy. The 1980s saw gathering momentum in ladle practices that could not have been entertained only a couple of decades before. These practices are taking the refining of iron and the making of alloy steels out of conventional furnaces and into their ladles. "Clean steel," a watchword for high purity and freedom from inclusions, is one incentive; another is the most economical use of time, process energy, labor, and fixed capital equipment.

Steel processing now quite commonly starts in the torpedo ladle, where desulfurization is carried out with much more reliance on slag chemistry than on blowing: slag $CaO:SiO_2$ mol ratios up to about 10:1 are in use. Phosphorus removal is more difficult at that early stage; but other combinations or sequences of ladle and furnace treatment are sure to evolve. These are addressing both the chemical differences in iron ores worldwide and the mix of steels needed by world markets.

Numerous argon bottom-bubbled (i.e., stirred) ladle designs have appeared, combined with top blowing and either or both of top and bottom slag-chemical injection. Generally these call for higher ladle temperatures, i.e., about 1750°C. In a counterpart of the EAF, a complete water-cooled roof assembly, with electrodes, is lowered over a ladle and run just like a fixed installation but lifted off again at the end of a heat. Vacuum degassing is being conducted in ladles as well as in furnaces.

For the most part, this technological turbulence will alter the product mix of the refractories industry without necessarily calling for new materials that have not already been placed on the want list. *Ladle metallurgy* has, however, accelerated research into more corrosion-resistant refractories in the present era, as it has intensified the exposure of ladle refractories to corrosion along with the traditional demands made upon them.

Continuous Casting of Steel

The last steelmaking device we shall catalog here is the *continuous casting* device. The process is dubbed *concast* in the industry. It has counterparts in all major nonferrous metals as well.

The economy of continuous casting over pouring-pit casting is enormous, and the billet quality obtained is higher. The concept was introduced in Chapter II. Here the equipment is illustrated in Figure III-14, in which attention is called to the *tundish* and its metal delivery and casting system.

Figure III-14a is a schematic overview of the whole operation, showing the processed steel in black. A transfer ladle is placed in position at the top. A "ladle shroud" (vertical refractory tube) is affixed under its slide gate valve, by means of which hot metal is delivered intermittently to the tundish immediately below. This procedure keeps the tundish, a much smaller surge reservoir, always nearly full. Below the tundish is the "tundish shroud," another tube, whose lower extremity is submerged in the steel which it delivers continuously down into a water-cooled copper mold. The mold starts the process of solidification of the steel as the latter flows and is then drawn down by sets of rolls. Between the underside of the mold and the first set of rolls are water sprays (not shown) which play directly on the steel and continue its solidification from the outside in. Additional sets of rolls bend and then straighten the now-solid billet so that it moves horizontally onto a roller table, where it is cut into lengths.

Figure III-14b is a faithful representation of the continuous casting mold itself, and its ingenious operation. Here the tundish is at the top, and its submerged pouring tube or "tundish shroud" is highlighted in black for orientation.

It is seen that a *mold powder* is fed into the top of the mold, and that this floats on the upper surface of the molten steel. Mold powder is a *flux*: some of it melts on top of the steel, protecting the latter from the air. Thermal insulation by the powder prevents the top of the metal pool from freezing; so bits of refractory or slag in the steel can rise to the top, where they are dissolved in the molten flux and hence removed.

Next it should be noticed that there is an annular gap between the downward-moving steel and the copper mold. This gap is filled by the molten flux, flowing down from above. The mold oscillates vertically to drag the flux down and spread it evenly in the annular space, where it serves as lubricant as well as heat path for the now-freezing steel. As the flux exits below with the moving steel, more of the mold powder melts on top.

Without mold powder, the steel would freeze directly onto the copper, jamming the process. Mold powder may be the only product of the refractories industry that is formulated to melt rather than not to melt. In honor of this uniqueness, we shall not refer to mold powder again in later pages. But its vital use is a delicately-balanced one in which numerous properties of the material are critical: its melting

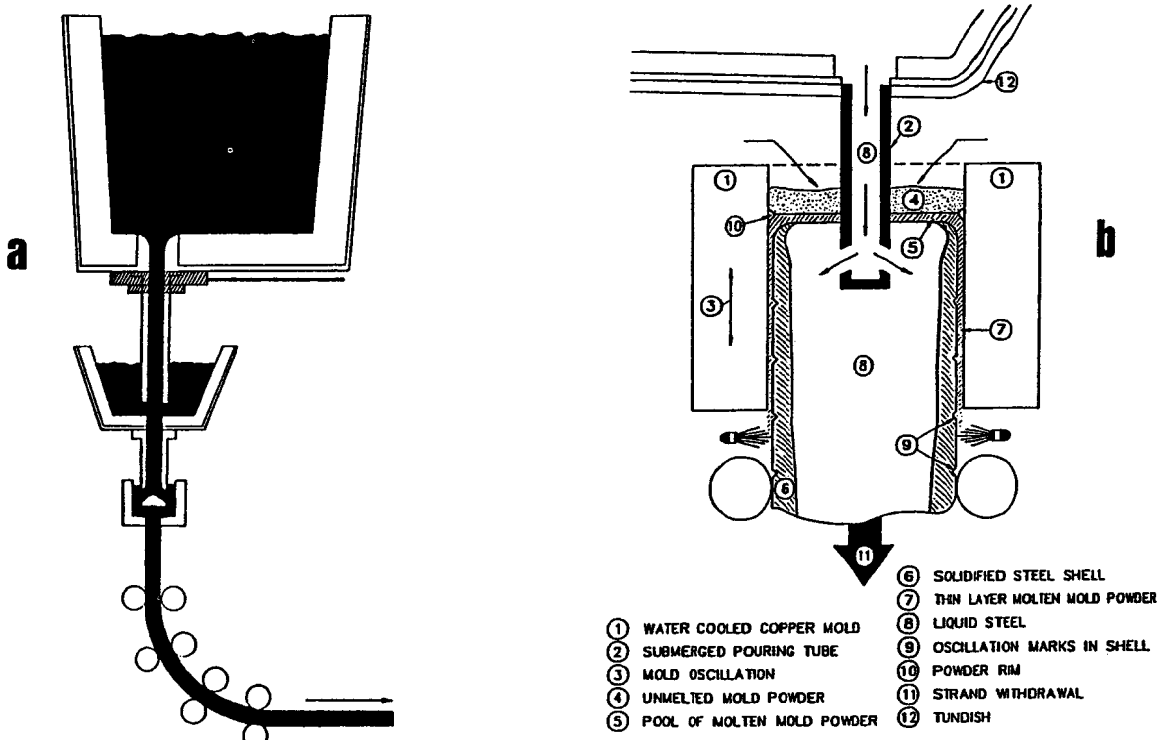

Figure III-14 Continuous Casting of Steel
a. System View (adapted from Ref. 10, by permission)
b. Detail View (courtesy of National Refractories & Minerals, Inc.)

range, solid and liquid thermal conductivity, heat of fusion, liquid viscosity and solvent power for other oxides. Since different steels are cast at different temperatures and since billets of different dimensions are needed, there is not one mold powder but a family of mold powders. The conceptual brilliance of continuous casting and the cooperating skills of its execution are a fitting note on which to close these descriptions of steelmaking, the largest single user of refractories.

Copper Converter

Earlier in this chapter a standard copper smelting flow scheme was presented. The operation has been streamlined by some later equipment designs; but consolidated processes address the same chemical objectives in basically similar ways. Meanwhile the *copper converter* will most likely persist where it is already in place, and it continues to illustrate refractory exposures in hot processing that are as perennial as copper. It will be recalled that the converter receives copper matte (Cu_2S, FeS, etc.) from a reverberatory melting furnace, and converts this batchwise in two steps to crude blister copper. The latter then goes to another reverberatory furnace for refining.

The converter is pictured in Figure III-15. It is seen to be a small (≤100 ton Cu capacity) closed-ended refractory-lined tube, bearing a generous charge-and-discharge port, an end burner, exhaust port, and a row of closely-spaced horizontal tuyeres for air-blowing. Its charge includes a prescribed silicate slag, usually basic. After charging, the vessel is heated to a maximum of about 1600°C and air-blown. At this temperature copper oxides are substantially unstable; partial oxidation of Cu_2S produces crude Cu, some Cu_20, and $S0_2$ gas. Silver is reduced. FeS, on the other hand, is oxidized to $S0_2$ and iron oxides which dissolve in the slag, making a corrosive iron-rich composition. Slag and metal are churned by the injected air, reaching up about half the diameter of the converter. Then they settle and separate. The slag is poured off by rotating the vessel; then the converter is returned upright.

A picturesque alchemical method used to be employed for the second part of the heat.[3] Today the same end is ordinarily achieved with a reducing (i.e., C0) atmosphere and/or suitable heavy hydrocarbon or coke injection. Any remaining Cu_2S and Cu_20 react:

$$Cu_2S + 2\ Cu_20 \rightarrow 6\ Cu + S0_2.$$

In the mildly reducing environment the decomposition of residual compounds to copper is completed, and the metal product is poured off. The entire cycle takes about six hours, though it has been shortened and the temperature raised somewhat by using 0_2-enriched air in the blow.

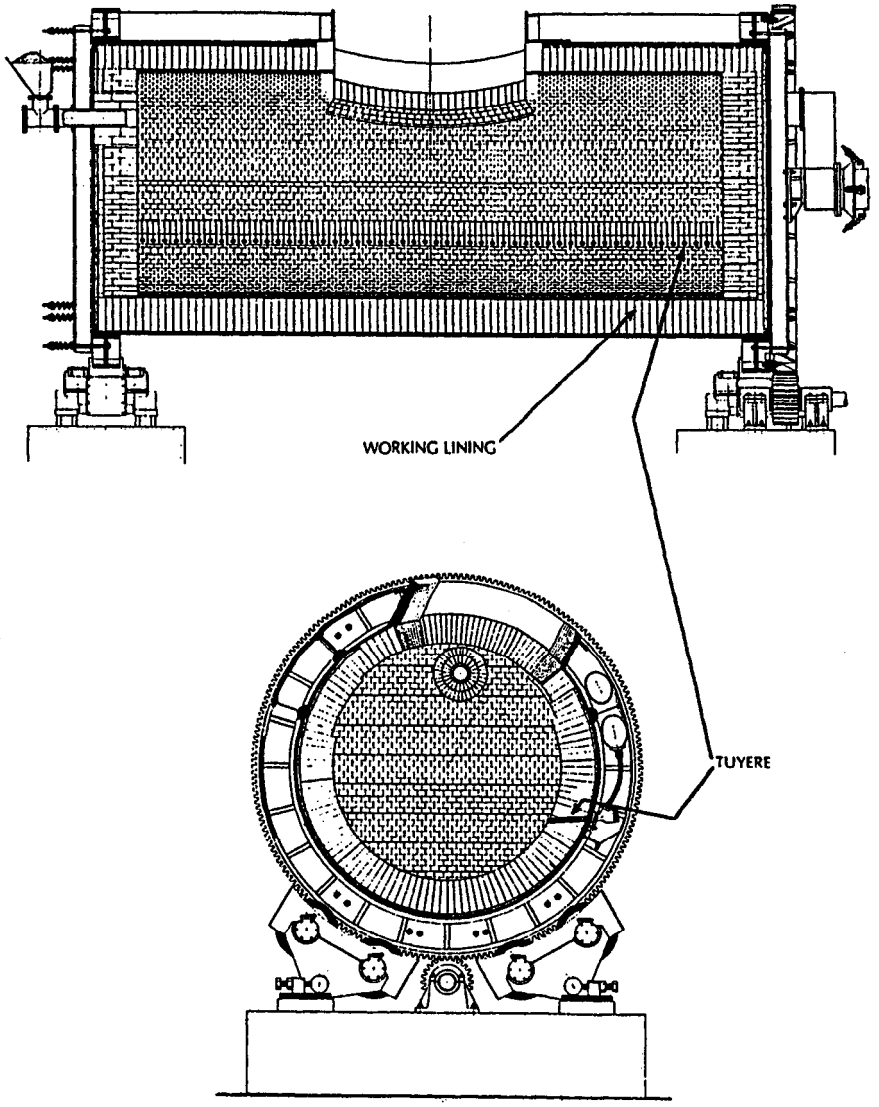

Figure III-15 Copper Converter
(reprinted from Ref. 10, by permission)

Refractory corrosion is most severe around the tuyeres; next, generally in the lower semicircle due to molten slag contact. The atmospheric cycling between oxidizing and reducing has to be recognized in refractory selection. The copious evolution of SO_2 generates corrosion problems mainly in the gas-handling system outside the converter. Copper smelters often still run sulfuric acid plants as the least costly means of getting rid of that SO_2, in tonnage amounts up to three times the amount of copper produced. The trend in new installations is now to smelt copper electrolytically at low temperatures, eliminating the several successive SO_2-generating steps and their costly air-pollution problem.

BATCH TYPES -- RECTANGULAR

Reverberatory Furnace: Basic Open Hearth

Batch-type reverberatory furnaces go back a very long way: to the "puddling" furnace of Figure I-5a, the foundry furnace of Figure I-6a, and the roasting furnace of Figure I-6b, for example. In describing the contemporary reverberatory furnace in copper smelting earlier in this chapter, we pointed out that this device has important uses in several other areas of nonferrous metallurgy too. We further suggested that the continuous and batch versions have much in common. There is no need to revisit the batch version explicitly here. But there is one exception, with which the refractories technologist should have some acquaintance.

That exception is the *basic open hearth* steelmaking furnace. This was the mass-production tool of the emerging Age of Steel, supreme in the industry for a century ending in the 1960s. It was the only major reverberatory metallurgical furnace to be heated regeneratively. It is still in use today, here and there, but waning. In that sense it is still a contemporary furnace, though hardly modern. It cannot make anything approaching "clean steel." Efforts to revitalize it by air or oxygen lancing have met with mediocre success at best: true to the reverberatory design, its bed is too long and too shallow. In the U.S. in 1989, 4.5 million tons of O.H. steel were made: under 5% of total production.

The cutaway sketch of Figure I-5c will serve for illustration, as that figure portrays a 20th-century open hearth. Recalling the cross-fired glass melting tank of Figure III-6, the open hearth is fired reciprocally in the same way except end-for-end. Its two alternating burners can be seen in Fig. I-5c, as well as its two sets of checkers -- the near set cutaway and the far set covered. The entire length of its bed is exposed by the cutaway; only the far edge of the radiating crown can be seen. The four rectangular openings on the right side

are charging doors. The trough on the left side emerges from a taphole.

The furnace is charged with scrap and with blast-furnace iron. A basic slag is added, but containing a significant amount of iron ore. Ferrous oxide from the slag is soluble in molten iron, and this quality is made use of for decarburizing because the access of air as oxidant is too limited. The reaction is,

$$FeO + C \rightarrow Fe + CO_{(g)}.$$

This is the same reaction used in the electric arc furnace, but there the temperature near the arcs is much higher and stirring is much more effective. Whereas the copper converter slag starts low in iron oxide and ends high, the open hearth slag starts high and ends low; but on average both are quite penetrating. The open hearth bed, being ill-stirred, shows the most sharply-defined slag line of any primary steelmaking charge, with equally sharply-defined corrosive attack on the lower furnace walls.

Above the slag line, the open hearth and the glass melting furnace have much in common as to refractory exposure. Their frequencies of reversal of the firing direction are comparable. Their operating temperatures, including those of the checkers, are comparable. Their bed temperatures are comparable. While the glass furnace atmosphere is enriched in alkalies, that in the open hearth is high in ash owing to the use of dirty fuels: typically heavy oil or heated tar.

As compared with the BOF which replaced it, the basic open hearth is at best a maker of medium-low carbon steel and an inefficient desulfurizer. Its elapsed time for a heat averages about 8-10 hours, vs about 30 minutes for a comparable-sized BOF. Though its bed temperature is 100°C lower and its refractory corrosion is accordingly slower, per ton of steel produced its refractory consumption is greater.

Refractory zones in the basic open hearth have been long since established and material selection in each zone standardized. Hot patching and repair between heats is helpful to refractory life; but the elongate dimensions of the open hearth are not favorable for repair, compared to the compact dimensions of the BOF. Refractory improvement for the open hearth, like this vessel's use in world steelmaking, has waned. Yet for some time to come, relining and repair will still be called for.

Arc Furnace: Oxide Melting

Small *arc furnaces* for batch melting of oxides have habitually been of rectangular shell construction; but cylindrical forms are hardly uncommon. Their industrial role is described under Fusion of Oxidic Materials in Chapter II.

This type of furnace is singled out again here, not so much as a consumer of refractories but because of its increasing use in their manufacture. That continuing increase may be projected into the future, with the lion's share of growth devoted to melting the single or principal oxides zirconia, magnesia and alumina and the compounds $MgO{\cdot}Cr_2O_3$, $MgO{\cdot}Al_2O_3$ and $3Al_2O_3{\cdot}2SiO_2$. Furnaces are accordingly gaining both in size and in power density, with increasing emphasis on rapid tilt-pouring and minimum down time between heats. Three-phase systems now dominate this segment of furnace use. Figure III-16 illustrates a modern high-powered furnace installation capable of repeatedly melting ZrO_2 or MgO batches of the order of 10-15 tons each.

In the furnace design illustrated, the shell is water-cooled, unlined. The skull and surrounding granular material and a heel of molten oxide are kept in place from heat to heat. The skull forms a crucible of fairly stable size, which is refilled for each new batch. The furnace roof is subjected to intense radiation from the arcs; this heating and its suddenness are met with water-cooled steel swingaway roof construction. Water cooling of refractory insulators around the electrodes completes this critical part of the furnace construction.

The most dramatic refractory exposure in this arc furnace is that of the pouring spout. Its preheating during the course of the melting cycle lessens the thermal shock it receives on pouring; yet the temperature exposure during the pour itself, up to some 3000°C, has to cause severe wear. Pouring spouts in these furnaces are now often just skull-protected extensions of the water-cooled shell, eliminating formed refractory parts that are rapidly expendable. Casting molds are typically of water-cooled steel as well. In short, the processor buys electric power instead of refractories.

Coke Oven: A Crude Retort

A paramount concern in coking of coal or petroleum residues is economy. Coke Manufacture should be consulted in Chapter II. In laying out a facility, the operator must consider the logistics of moving huge amounts of feed materials and hot product; also of collecting and processing immense volumes of gaseous byproducts. The common layout is in a long line, between parallel railways.

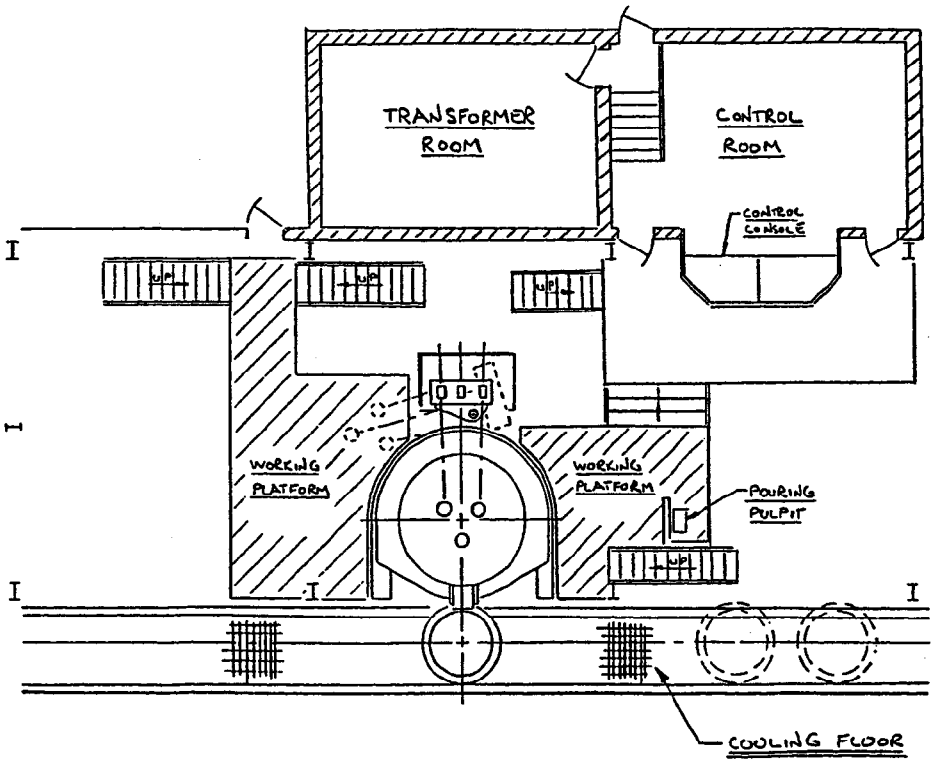

Figure III-16 Arc Furnace Layout, Oxide Melting
(courtesy of Ref. 16, by permission)

In the line, narrow rectangular or slot-shaped *coke ovens* -- better described as *retorts* -- are alternated with even narrower flues through which the indirect-heating gases pass. These cavities share common refractory walls, such that each flue heats ovens on either side and each oven is heated by flues on either side. Even though the maximum coking temperature is only about 1100°C (combustion-gas temperature only 1400°-1500°C), regenerative heating is employed for fuel economy. Rows of checkers and manifolding for air and gas lie underground, below the line of ovens. The fuel gas is part of the noncondensible part of the oven overhead product; the remainder of the noncondensibles is burned elsewhere in steam boilers or for process heat .

The oven overhead, consisting of the volatile byproducts of coking, is taken by refractory-lined manifolding above the entire line, off to a condenser and then a distillation plant for separation of the condensibles. The uncondensed fraction (principally H_2, CO, and light hydrocarbons) is utilized as described above.

The oven roofs contain charging doors, used for batch filling and then sealed before coking. If the common oven/flue walls are called sidewalls, then the narrow end walls of each oven are removable panels, taken off for discharge. These too have to be hermetically sealed in place for the coking. The entire array is of intricate architecture, calling for a host of brick shapes, monolithic and sealing refractories, and a complex of ducts and valving. All of this must be exceedingly long-lived to warrant its initial cost.

If the refractory zones are characterized by individual geometry and architectural function, they are many indeed. A smaller number are distinguished by their process environments. Oven walls experience highly reducing H_2- and CO-rich atmospheres during coking, with air-oxidation, thermal stress and abrasion accompanying discharging and charging. The oven/flue dividers must in addition be thermally conductive. Checkers and their enclosures see thermal stresses attendant on cycling; and combustion liners experience H_2O-rich gas at the maximum operating temperature of about 1500°C. The byproduct offtakes and manifolds have to manage the oven atmosphere and dust at high velocity, at temperatures up to 1100°C. All external walls have to be thermally insulating. Impermeability of all refractories is a must, as is dimensional stability through many cycles.

The product of coking, it will be recalled, is then in part calcined. The rotary kiln for this purpose has been described previously in this chapter. Other forms of calciner are used too; their refractory exposures are much like that in the rotary.

Carbon Baking Furnace

The essential features of the indirect-fired *carbon baking furnace*, as well as the nature of its charge and the process it conducts, are described under Carbon Baking in Chapter II. Though geometrical designs vary, the common layout is a large, room-like rectangular brick box with double walls where heating gases surround the interior structure and its contents. A given charge, or lot, of carbon stock is all fired to a common temperature; but successive loadings of the same furnace may be taken to different temperatures. Generally, such a furnace is fired to temperatures between 1200° and 1500°C. Smaller furnaces may go as high as approaching 1800°C. Furnaces with the latter capability are much less common, and shorter-lived.

The principal difference among the refractories employed relates to the maximum temperature of use. Divider walls again have to be thermally conducting, outside walls insulating. The CO-rich atmosphere within the box is powerfully reducing. Though the furnace is cooled some before unloading, exposure of the refractories to air while hot is usual. Mechanical abuse in unloading and loading is also common; but in between, the operating characteristics are those of an indirect-fired batch kiln. The difference is, the contents are carbonaceous instead of oxidic.

Batch or Periodic Kilns: Ceramic Sintering

The continuous ceramic-firing tunnel kiln was treated earlier in this chapter, and referenced to the section in Chapter II entitled Sintering of Oxidic Ceramics. Both of those discussions now serve as background for the description of *batch kilns*, many of which are essentially rectangular in shape.

Batch kilns and their predecessor ceramic ovens antedate the tunnel kiln by millennia. But they have survived in coexistence with it, and numerous types of batch kilns still serve the needs of firing unglazed and glazed ceramic ware -- even, firing refractories. A technical or economic preference for batch firing in production can occur, for example, when a plant or operation:

(a) Is too small to justify the tunnel kiln capacity or investment;
(b) Entails small lots of different products requiring kiln re-programming;
(c) Requires time-temperature-atmosphere programs ill-fitted to the tunnel kiln;
(d) Entails wares too large or too various for tunnel kiln setting; or
(e) Entails excessive refractory corrosion, requiring frequent kiln shutdown for repairs.

The term *periodic kiln* is used preferentially for designs utilizing kiln cars similar to those of the tunnel kiln. But "periodic" seems also to be synonymous with "batch" for all types. Cars enter a periodic kiln on rails, but there the journey stops. Advantages are that the setting and unloading are done outside, and such a kiln does not have to be cooled sufficiently for human entry between cycles. A disadvantage is that the car platform (or, e.g., a "square" array of four of these) must form a seal with the kiln shell, isolating the working volume above from an air-cooled plenum below. An alternate arrangement available for firing clay products provides for the platform and its setting to be prepared on a car topped with rollers, and then pushed off into the kiln on a *roller hearth* within. The platform still becomes the true hearth.

All batch car-kilns are front-loaded. In the commonest type, called the *shuttle kiln,* after loading the front wall is closed by moveable refractory-lined doors. In the *bell kiln*, the entire shell (except floor) is lifted up for loading, then lowered over the car(s) and ware for firing. In the *elevator kiln*, the shell is permanently set high above the floor; the kiln base and its contents, once loaded, are lifted hydraulically up into the shell. Car removal is the reverse of entry.

All three of the above types, if designed without a lower plenum, can be charged without the use of cars: that is, with the setting laid on a permanent hearth. In this case, as well as in top-loaded kilns, there is latitude for a variety of geometries including those circular in plan view. One of the oldest, though now used infrequently, is the *beehive*, pictured in Figure I-1a. Granted it requires a complex of brick shapes for its construction, the beehive is essentially free-standing. Cylindrical and rectangular kilns employ external steel framework support. The former are typically dome-roofed, the latter arch-roofed or in some cases may possess a suspended roof.

Batch kilns can have free space above the setting, unlike the tunnel, because the heating gases are not constrained to horizontal motion. This latitude permits various sizes and shapes of ware to be fired in successive batches. Permanent-hearth kilns furthermore can enjoy a considerable variety of interior architecture, ranging for example from indirect-fired (muffle) designs to *updraft* and *downdraft* and radiating direct-fired designs intended to achieve uniformity of heating throughout the chamber.

Like the tunnel kiln, batch kilns are generally oil- or gas-fired. Unlike the tunnel, too many have lacked any provision for recuperative or regenerative heating. The pebble-bed air pre-heater such as that depicted in Figure III-3 is an appropriate heat-recovery device because it is continuous and does not require gas/air flow reversal. Such an addition can as much as halve fuel consumption.

Irrespective of external geometry, some batch-type kilns are ganged together or else subdivided within as *compartment kilns,* and are operated in the hybrid batch/continuous mode described in the first section of this chapter. That arrangement also gives good fuel economy, but is not used for the highest-temperature equipment.

Batch-heated units have historically suffered economically because the mass of the vessel including its refractories -- or more properly, the heat storage capacity thereof -- was large compared to that of the ware being heated and then cooled. Rarely was so much as half of the combustion heat used productively in heating the ware, and this fraction could be as low as one-fifth. Though the majority of the wasted heat went up the stack, the next largest portion was pumped into kiln walls, roofs, floors, cars, and other fixed heat sinks; only to come out slowly during cooling, sometimes profitlessly extending the cooling period required before personnel could enter.

Concerted efforts by the ceramic producers and dramatic progress made in insulating and low-mass refractories useable up to some 1600°C have taken much of the mass -- and a great deal of the thermal mass -- out of batch kilns and cars. Fuel savings up to 50% and better have been realized in non-recuperative systems. Other benefits include relief from the effects of thermal cycling on rigid brickwork, and from unnecessarily-prolonged firing and cooling times. The basic means of making such improvements have been in place for 20 to 30 years and are now being extensively exploited. Incremental improvements continue to be made.

Refractory zoning in direct-fired batch or periodic kilns is essentially simple: the entire interior sees the maximum firing temperature of the particular use, and all of it sees roughly the same thermal transients and the same atmospheric and corrosive history. Burner blocks are an exception, running hotter. "Bag walls," making the first deflection of the combustion gases in a downdraft kiln, also run hotter. Exhaust ports suffer increased corrosion-erosion by virtue of gas turbulence and velocity effects. Kiln furniture always has special considerations, such as concentrated loads. In muffle kilns and in saggers, heat-transfer walls have to be thermally conducting and are hotter on the combustion-gas side than on the side facing the ware. As in the tunnel kiln, firing may be conducted to a maximum temperature ranging from as low as about 1000°C to as high as about 1900°C. Also as in the tunnel kiln, the firing of refractory bricks and blocks includes the highest temperature demands. The corrosive atmospheres of glaze firing may fall more to the batch kiln than to the tunnel, because refractory damage is there more confined.

In illustrating batch kilns, it is best to represent concepts because there are so many units differing in size, shape, and details of construction. Figure III-17 schematically illustrates two

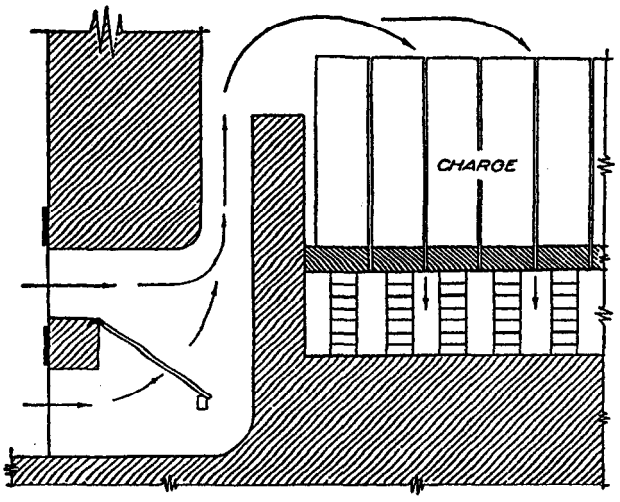

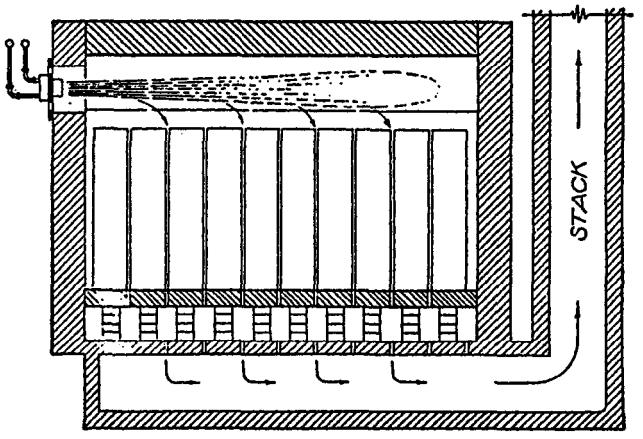

Figure III-17 Two Downdraft Kiln Designs
(reprinted from Ref. 3, by permission)

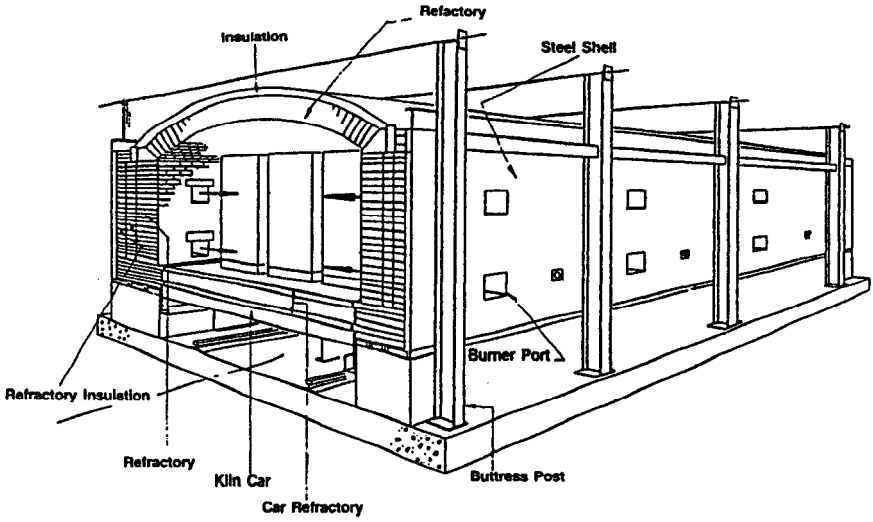

Figure III-18a Shuttle Kiln, Door Removed
(adapted from Ref. 10, by permission)

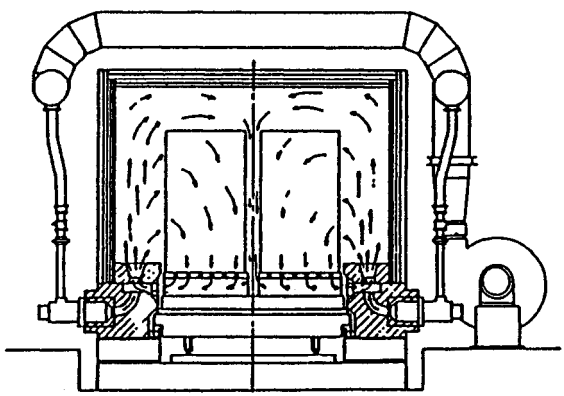

Figure III-18b Patented Downdraft Shuttle Kiln Design
(courtesy of Ref. 17, by permission)

classical stationary downdraft concepts, one with a bag wall and one fired overhead. Figure III-18a portrays a standard form of shuttle kiln (door removed), a high-capacity workhorse of the ceramic industry. And Figure III-18b is a schematic section of a shuttle kiln incorporating downdraft firing. What defies illustration but must be given recognition is the pervasive use of instrumental sensing and programmed electronic control of kilns in the ceramic industry. Automation is making them into powerful tools of repetitive high-quality production.

OTHER REFRACTORY APPLICATIONS

In these pages we have sampled hot processing equipment and illustrated its uses in industry, but in neither case exhaustively. As to uses, we have omitted numerous other operations knowing that a comprehension of those included will convey principles of refractory application that are transferable elsewhere. We have chosen illustrative uses from the dramatic and challenging to the mundane in respect to refractory selection. But refractory applications are not limited to our sampling.

As to types of processing equipment, we have made no effort to be encyclopedic. We have not even given explicit observance to every equipment type listed in Table III.1, especially not to all of the batch types. The reader will recognize their incidental inclusion under the corresponding continuous-type headings. We have further omitted whole classes of electrically-heated devices, an endless array of art potters' equipment, and whole spectra of laboratory preparative, investigative and testing tools. The use of refractories in every one of these deserves mention; yet to compile a comprehensive catalog of hardware would surely, in the reader's interests, pass the point of diminishing returns. Omissions from this chapter imply no disregard, but rather a certainty that potent similarities will be found by the reader between those devices omitted and those included.

A genuine dilemma arises, on the other hand, regarding still further categories of application of refractory materials. If beta-spodumene or zirconia or silicon nitride performs duties in heat engines, those are refractory applications. The nose cone of a guided missile has to be refractory or it could not serve there; likewise the launching pad of a space vehicle installation and the protective tiles on the vehicle itself. Intumescent fire-resistant polymers and ablative hypersonic-vehicle coatings are assuredly refractory, becoming carbon in service. If heat rejection is a refractory function, add the selective-reflectance coatings on space satellite skins.

Ceramic abrasives and machine tools glow orange-hot on the job, a testimony to their refractoriness. Advanced high-strength

filament-reinforced composites contain at least one refractory component, such as carbon or silicon carbide. Those two substances are also serving as legs of a high-temperature thermocouple. Graphite has had a pivotal role in nuclear power generation, as have also the refractory fuels uranium carbide and uranium dioxide. Refractory materials provide military armor and nuclear hardening.

Zirconia, a semiconductor, measures the oxygen content of automotive exhaust gases. Alumina contains the combustion catalyst that ensures their passing environmental regulations. Alumina also insulates the electrodes of a hot spark plug, while chromia in situ prevents superalloys from burning up in an aircraft turbojet. Every one of these examples recollects more.

In truth, refractory materials are both fascinating and limitlessly useful. Yet this book cannot be allowed to ramify so limitlessly. The danger of adhering to our proscribed subject, however, is that it is from distant technologies that some of the best new ideas will come for refractory improvement. As we now proceed to construct the technology of industrial refractories from where we have been, the reader is admonished to keep another eye on what may yet be possible.

Chapter IV

Principles of Thermal Stability

MELTING POINTS OF SUBSTANCES

The Tammann Temperature

The melting temperatures of refractory compounds are important for several reasons. First, diffusion of atoms or ions in a solid, generally by complex lattice vacancy migration,[15] depends exponentially on temperature. Vacancy diffusion in ionic compounds becomes significant only above about 3/4 of the absolute melting point.

Some aspects of *corrosion* are rate-limited by diffusion in the host material. If corrosion limits the life of a refractory, that life may in principle be extended incrementally by choosing a higher-melting composition -- all other things being equal. Another diffusion controlled process is *plastic flow*. Below about 3/4 of its absolute melting point, a crystalline compound is likely to remain sensibly non-plastic, or elastic, under mechanical load. Above that rough temperature limit, which is called the *Tammann temperature*, time- and load-dependent plastic flow or *creep* may be expected, leading to such consequences as *creep-rupture* (i.e., mechanical failure at low load) and/or permanent deformation remaining on re-cooling. Still another diffusion-controlled process is *sintering*, usually exhibiting an attendant shrinkage.

A further property which tends to correlate with the melting point is resistance to thermal *decomposition*. Other properties do too, their values changing markedly above the Tammann temperature. Included are the *transport properties* such as thermal and electrical

conductivity. Even the heat capacity or specific heat is likewise affected.

Microstructural Definitions

Different regions in a refractory microstructure may melt at markedly different temperatures. The majority of industrial refractory materials are heterogeneous mixtures. That is, they are comprised of more than one *phase.* The regions or volumes of each phase are separated from one another by thin boundaries. A single phase is by definition a homogeneous region (or, collectively, all of the like homogeneous regions in a body). Two classifications of solid phases are recognized: *solutions* (i.e., of continuously-variable chemical composition within limits), and *substances* (i.e., elements or compounds, of relatively fixed compositions represented by chemical formulas). A single-phase solid region ordinarily will contain many *orientation boundaries*, between crystallites whose lattices are oriented differently but which are of like composition. These boundaries are distinguished from the *phase boundaries* in heterogeneous materials, across which step changes in composition occur.

Solutions, being capable of continuously variable composition, exhibit variable properties. Here we shall start with *substances*: mainly, compounds. To the degree that the composition is fixed, the bulk properties of a compound are relatively fixed and reliable. Refractories are often contrived to present one or two compounds to the hot environment as the primary barrier(s) to corrosion. Thus one or two compounds may be the *major phase(s).* The melting point of each such phase is the first of several indicators of how it will behave, thermally, chemically, and mechanically, at high temperatures.

Oxide Melting Points

Simple Oxides. The roster of binary oxide compounds provided by nature is indicated in Figure IV-1, which lays these out in an abbreviated Periodic Table. The melting point of each is given in °C.[11] There may be an error in the m.p. of V_2O_5 (trivial because we shall exclude it). That of ZrO_2 is for the hafnia-free compound, whereas the ZrO_2 usually encountered contains about 15% HfO_2 in solid solution and melts at about 2700°C. PuO_2 is not included; its m.p. is probably close to that of UO_2. Some of the listed melting points are reported within brackets as large as ± 25°C, reflecting mainly uncertainties as to chemical purity. Nevertheless, the most refractory oxides make themselves clearly evident in Figure IV-1.

Complex Oxides. Of all the ternary oxide compounds that are possible, only a few are comparably high-melting. Only the ten most refractory of these are listed below:[11]

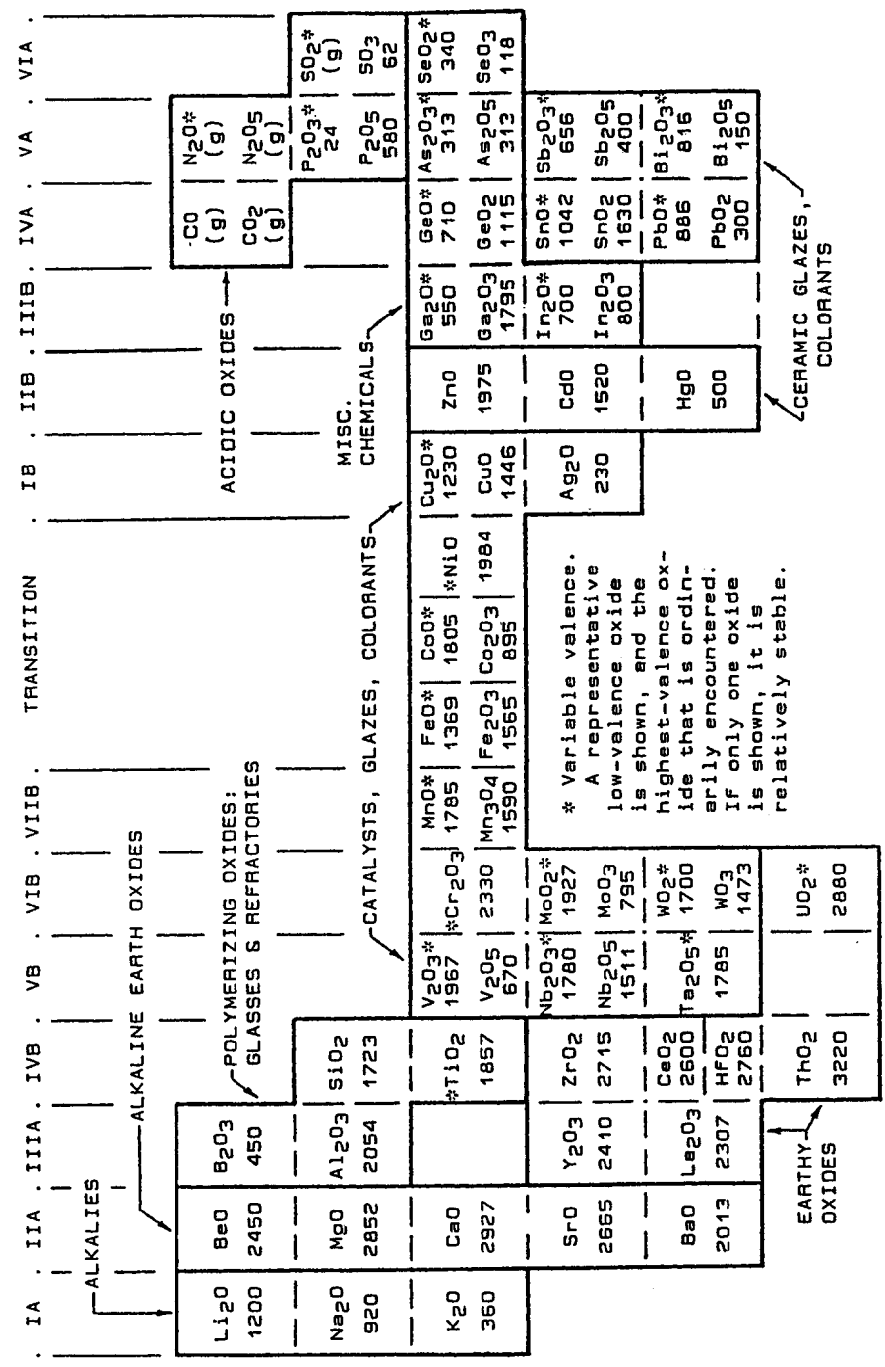

Figure IV-1 Melting Points of Simple Oxides, °C (Ref. 11)

Name	Formula			M.p., °C
Magnesium aluminate	$MgAl_2O_4$	or	$MgO{\cdot}Al_2O_3$	2135
Magnesium chromite	$MgCr_2O_4$	or	$MgO{\cdot}Cr_2O_3$	2380
Iron (-ous) chromite	$FeCr_2O_4$	or	$FeO{\cdot}Cr_2O_3$	~1700
Forsterite	Mg_2SiO_4	or	$2MgO{\cdot}SiO_2$	1910
Dicalcium silicate	Ca_2SiO_4	or	$2CaO{\cdot}SiO_2$	2130
Zircon	$ZrSiO_4$	or	$ZrO_2{\cdot}SiO_2$	2550
Dialuminum silicate	Al_2SiO_5	or	$Al_2O_3{\cdot}SiO_2$	1868
Mullite	$Al_6Si_2O_{13}$	or	$3Al_2O_3{\cdot}2SiO_2$	1920
Calcium zirconate	$CaZrO_3$	or	$CaO{\cdot}ZrO_2$	2550
Calcium titanate	$CaTiO_3$	or	$CaO{\cdot}TiO_2$	1975

Magnesium aluminate and the others grouped with it here will be recognized as *spinels*. Iron chromite (e.g., as chromite ore) has a place in this list because of its role in stabilizing iron in refractories against disruptive oxidation-reduction cycling, to be discussed later. Calcium titanate will be recognized as *perovskite*; it and the zirconate (which is not a perovskite) will be evaluated later on. Dialuminum silicate is the principal constituent of the minerals andalusite, kyanite, and sillimanite. Mullite and zircon will become even more familiar.

Free Energy Criteria: Chemical Stability. Any given compound can be imagined as made directly from its elements, as for example alumina:

$$2\,Al + 3/2\,O_{2(g)} \rightarrow Al_2O_3$$

If this equation is read in reverse, it represents the *decomposition* of alumina, an unwanted event in its use as a refractory. The Gibbs free energy change* for this type of chemical reaction as written is called the *free energy of formation*, symbolized ΔG_f. A large negative value of ΔG_f indicates a large driving force for compound formation, hence a high resistance of the compound to thermal decomposition. For the comparison of oxides, a rough indicator will suffice. This can be obtained by using the standard* ΔG_f at room temperature, written $\Delta G°_{f,298}$: a quantity readily available in reference tables.[11]

But we want to assess the stabilities of oxides of different formulas, viz., MO vs M_2O_3 vs MO_2. Instead of taking $\Delta G°_{f,298}$ per mol as it is tabulated, we must take it per *equivalent*: of Al_2O_3 above, for example. The total number, n, of mols of electrons transferred from

---

*Chemical thermodynamic quantities will be used more rigorously later on.

Al to O in the above equation is 6, hence one mol of Al_2O_3 is n = 6 equivalents, and the thermodynamic quantity we want is $(\Delta G°_{f,298})/6$. The reader will note that for simple oxides of formula MO, n = 2; while for MO_2, n = 4; etc.

It is intuitive that chemical stability should increase, on the whole, with increasing melting point. Figure IV-2 is a plot of $(-\Delta G°_{f,298})/n$ vs $10^4/T_m$ (where T_m is m.p. in K), demonstrating this rough correlation for a large number of binary oxides and some of the ternary oxides just considered. The dashed line cutting across the correlation band is an arbitrary but reasonable one, dividing "acceptable" refractory compounds above it from "unacceptable" ones below. The latter are thus disqualified by the combined criteria of both melting point and chemical stability. Fortuitously, the oxides of most metals exhibiting multiple valences (Fig. IV-1) are thereby disqualified. We are spared having to examine the still further problem of their susceptibility to oxidation and reduction between valences.

Other Considerations In Selection. Among the acceptable oxides of Fig. IV-2, it is convenient to disqualify some for miscellaneous other reasons:

BeO - Exceedingly toxic dust
ThO_2, UO_2 - Radioactivity
BaO, SrO - Slaking susceptibility (a concern about CaO as well)
La_2O_3, Y_2O_3, CeO_2, HfO_2, ThO_2, UO_2 - Cost (also BaO, BeO, SrO)

"Cost" in isolation is certainly a relative matter. A compound eliminated as too costly today may be acceptable in a different economic framework tomorrow. Or, eliminated from general use, it may still find application in special technical circumstances. A good current example is zirconia. Even zircon was little used in this field much before the 1960s, and ZrO_2 not until well into the '70s, on account of cost. Now both are well-known refractories.

Nonoxide Melting Points

The elements grouped in Figure II-2 as Carbide Formers provide a family not only of refractory carbides, but also of borides and nitrides. The atoms B, C, and N are very small, and the bonds they form in interstitial compounds are substantially covalent. Each small interstitial atom bonds typically to three or four nearest-neighbor metal atoms, yielding high-melting and stable compounds.

Carbon is well known as forming two- and three-dimensional atomic networks by covalent bonding. Boron, nitrogen, and silicon atoms share this capacity. A second family of refractory nonoxides is comprised of small-atom compounds among selected pairs of these.

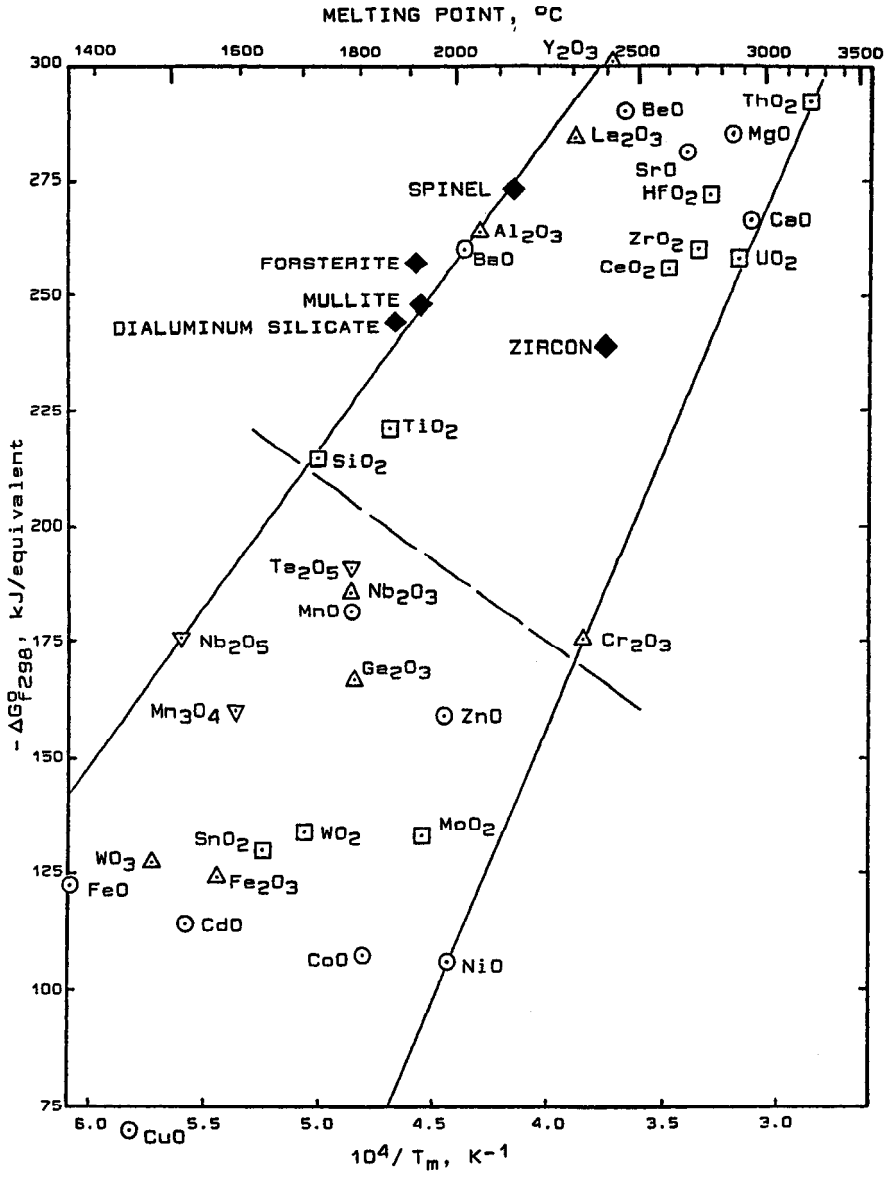

Figure IV-2 Correlation of Oxide Melting Points with Std. Free Energies of Formation per Equivalent (Ref. 11)

To a limited extent, even aluminum participates in such compounds of principally covalent nature. The ability of these small atoms to substitute for one another results in some mixed compounds such as carbo-nitrides, and even more complex compositions such as the SiAlONs; and it underlies the interest in nitride-bonded carbides and carbide-bonded nitrides as sintered powder-metallurgical products. While acknowledging these extended families, we shall here confine our cataloguing to the simple binary nonoxide compounds and to carbon. Their melting points below are taken from Ref. 11:

Parent	Carbide		Nitride		Boride	
	Formula	M.p.,°C	Formula	M.p.,°C	Formula	M.p.,°C
B	B_4C	2350	BN	~3000s		
C	Graphite	~3650s				
Si	SiC	~2700s	Si_3N_4	<1900s		
Hf	HfC	~3890	HfN	3305		
Nb	NbC	3500	NbN	2575	NbB_2	~2900
Ta	TaC	3880	TaN	~3360	TaB_2	~3000
Th	ThC_2	~2660			ThB_6	2195
Ti	TiC	~3140	TiN	2930	TiB_2	2900
U	UC,UC_2	~2370	UN	~2630	UB_2	2365
W	W_2C,WC	~2860			WB_2	~2900
Zr	ZrC	3540	ZrN	~2980	ZrB_2	~3200

The notation "s" in the table means "sublimes." One usually expects some other lower-temperature restriction on the use of these substances; only for Si_3N_4 will volatility be taken to be limiting.

Any of these substances may find utility in special technical circumstances;[18,19] but for the most part the broader ranges of refractory application are identified with the small-atom group. Except for the interstitial compounds of titanium, the interstitials as a family are on the whole very dense and very expensive. We shall excuse them from further interest here on those grounds, realizing again that changing times or new discoveries may alter attitudes about cost and application.

Summary: Melting Points of Refractory Substances

From the foregoing sections, we now have a manageable list of oxides and nonoxides that may be fit candidates for appearance as major phases in industrial refractories. This consolidated list is recapitulated in Table IV.1, which includes the melting point of each substance in both °C and °F and also gives the approximate Tammann temperature in °C. The substances in each category are

Table IV.1 Melting Points of Refractory Substances (Ref. 11)

NAME	FORMULA	M.P. °C	M.P. °F	TAMMANN TEMP, °C
OXIDES				
LIME; CALCIA	CaO	2927	5300	2130
PERICLASE; MAGNESIA	MgO	2852	5165	2070
BADDELEYITE; ZIRCONIA	ZrO_2	2700	4890	1960
ZIRCON; ZIRC. SILICATE	$ZrO_2 \cdot SiO_2$	2550	4620	1850
CALCIUM ZIRCONATE	$CaO \cdot ZrO_2$	2550	4620	1850
CHROMIC OXIDE; CHROMIA	Cr_2O_3	2330	4225	1680
MAG. ALUMINATE; SPINEL	$MgO \cdot Al_2O_3$	2135	3875	1530
DICALCIUM SILICATE	$2CaO \cdot SiO_2$	2130	3865	1530
CORUNDUM; alpha-ALUMINA	Al_2O_3	2054	3730	1470
CALCIUM TITANATE; PEROVSKITE	$CaO \cdot TiO_2$	1975	3585	1410
MAG. CHROMITE; CHROME SPINEL	$MgO \cdot Cr_2O_3$	1950	3540	1400
MULLITE	$3Al_2O_3 \cdot 2SiO_2$	1920	3490	1380
FORSTERITE; DIMAG. SILICATE	$2MgO \cdot SiO_2$	1910	3470	1370
DIALUMINUM SILICATE	$Al_2O_3 \cdot SiO_2$	1868	3395	1340
RUTILE; TITANIA	TiO_2	1857	3375	1330
SILICA; CRISTOBALITE	SiO_2	1723	3135	1230
IRON CHROMITE; CHROME ORE	$FeO \cdot Cr_2O_3$	1700	3090	1210
NONOXIDES				
CARBON; GRAPHITE	C	3650[s]	6600[s]	2670
TITANIUM CARBIDE	TiC	3140	5685	2290
BORON NITRIDE	BN	3000[s]	5430[s]	2180
TITANIUM NITRIDE	TiN	2930	5305	2130
TITANIUM DIBORIDE	TiB_2	2900	5250	2110
CARBORUNDUM; SILICON CARBIDE	SiC	2700[s]	4890[s]	1960
BORON CARBIDE	B_4C	2350	4260	1700

[s] -- Sublimes

arranged in order of decreasing melting point. Their common names are also given. Later we shall both expand and whittle that list. In the meanwhile, it will serve as a sufficient basis for considering the thermal stability of refractory *mixtures*.

MELTING OF OXIDE MIXTURES

Compositional Notation

The simple binary compound formulas of Table IV.1 serve a useful function for describing mixtures: that of *components*, or the set of simplest *end-member compositions* of which the compositions of mixtures are made up analytically. In that table those formulas were used to represent compound *phases*, however, and this dual usage can be confusing. The context should explain which is meant.

The ternary compound formulas in Table IV.1 were given in "dot" form in anticipation of this section. The dot connecting two *component* formulas signifies an *addition compound* of them, in the mol ratio(s) given by their coefficients. Dot formulas may contain any number of *components* in a compound *phase*. If a dot formula is used instead to represent a *component*, this must be done knowledgeably and for reasons.

Solid-solution phases are represented in either of two ways: (a) by specifying their *components*, or (b) preferably, by specifying the *compounds* that are dissolved in each other. In either case the formulas are connected by hyphen(s). When one compound's phase identity is retained and another is a solute in it, the host compound formula is often given followed by "ss" for "solid solution," instead of naming both.

Heterogeneous mixtures are described unambiguously. The *phases* contained are designated as above and connected by "+" signs. It is wrong to describe a heterogeneous mixture by the formulas of its components, and wrong to connect its phases by hyphens.

However, one last notation adds confusion again. A *material system* consists of some set of *components,* each of whose proportions is simultaneously variable between zero and 100%, the constraint being only that their sum is always 100%. A "material system" is thus a framework for inquiry and response as to what phases are present. It asserts no phases by itself. It is described by naming all of its *components*, connected by hyphens. To avoid confusion with solid-solution phase notation, here the word "system" should accompany.

The rules in the above five paragraphs are illustrated below, each in turn, by examples of notation using the following formulas:

MgO	$MgO{\cdot}Al_2O_3$
Al_2O_3	$3Al_2O_3{\cdot}2SiO_2$
Cr_2O_3	$2MgO{\cdot}SiO_2$
SiO_2	$2MgO{\cdot}2Al_2O_3{\cdot}5SiO_2$

1. *Individual Components of Which Mixtures Might be Made:*

   MgO Al_2O_3 Cr_2O_3 SiO_2

2. *Individual Compound Phases (i.e., of fixed composition)*:

   All of the above, viz.: periclase; alumina; chromia; silica; spinel; mullite; forsterite; and cordierite. Note that the last four are made up of members of the first four acting as *components*.

3. *Individual Solid-Solution Phases (i.e., homogeneous mixtures):*

Al_2O_3-Cr_2O_3	(these happen to be completely miscible)
MgO-$MgO{\cdot}Al_2O_3$	or periclase-spinel ss (host named first)
$MgO{\cdot}Al_2O_3$-MgO	or spinel-MgO ss (host named first)
$3Al_2O_3{\cdot}2SiO_2$-SiO_2	or mullite-SiO_2 ss (host named first)

4. *Two or More Phases Together (i.e., heterogeneous mixtures):*

$MgO+2MgO{\cdot}SiO_2$	or periclase + forsterite (no ss)
MgOss$+MgO{\cdot}Al_2O_3$ss	or periclase ss + spinel ss
$Al_2O_3+3Al_2O_3{\cdot}2SiO_2$	or alumina + mullite (no ss exists)
$3Al_2O_3{\cdot}2SiO_2+SiO_2$	or mullite ss + silica

5. *Material Systems (phases present are not specified):*

Al_2O_3-SiO_2 system	(binary)
MgO-Al_2O_3-SiO_2 system	(ternary)
MgO-Al_2O_3-Cr_2O_3 system	(ternary)
MgO-Al_2O_3-Cr_2O_3-SiO_2 system	(quaternary)

With the language of mixtures in hand, we can begin to address refractory materials in their complexity. Mixtures of non-oxides can profitably be set aside here, to be picked up later as necessary.

Phase Equilibria; Phase Diagrams for Mixtures

If some given number of components of fixed identity are ground up and mixed together in fixed proportions, if they are kinetically able to do so they will approach an *equilibrium* state (i.e., a state of minimum free energy). That state will be comprised of some number of phases and the composition of each, all determined by nature if the temperature and pressure are also fixed independently. If we change any one of the independent variables (temperature, pressure, and overall composition or proportioning of the components), nature may change the equilibrium *phase composition* (number and compositions of phases). A moment's reflection should confirm that, for each overall composition, if the number of phases and the composition of each are determined by nature, then the proportion or relative amount of each phase is fixed as well. Furthermore, if one of the phases is liquid (i.e., molten), a *melting temperature* will appear among the variables.

These are general statements about phase equilibria. A durable guiding principle is the *Gibbs Phase Rule*. That rule underlies all empirical descriptions of specific phase equilibria and provides their scientific disciplining. We shall not use it here per se because it is already incorporated into the data we shall be consulting. The interested reader can find it in any reference work on materials science [15] or on phase equilibria.[20,21]

All specific phase equilibria are determined empirically, in the laboratory, using materials felt to be of reasonable reference quality at the time of the work. Comprehensive determinations are reported graphically in standardized forms, called *phase equilibrium diagrams* or simply *phase diagrams*. Their collections, e.g. for metals in the "Metals Handbook" of ASM[20] and for nonmetallics in "Phase Diagrams for Ceramists" of the American Ceramic Society,[21] total in the thousands. Modern refractories and an understanding of their high-temperature behavior depend on the information contained in phase diagrams. How these diagrams are determined, constructed, read and interpreted is explained in Volume I of Ref. 21, also to a lesser but basically adequate extent in Ref. 15. There are numerous other good resources.

Most oxide phase diagrams have been determined under a fixed total pressure of 1 atm., and under a chemical atmosphere (i.e., oxidizing or reducing potential) such that the valences expressed by the formulas of the components are reasonably stable. In the majority of cases this means determined in air. Use of such diagrams for refractories facing environments of other chemical potentials can sometimes be risky, because some oxides can become distinctly metal-deficient or oxygen-deficient without losing their crystal or

phase identity. These ion-deficient modifications must certainly exhibit modified phase equilibria, about which there is not much literature. Alteration by oxidation-reduction will be treated in Chapter V.

Two-Component Mixtures

Completely Miscible Solids. Among binary mixtures of refractory oxides, the system Al_2O_3-Cr_2O_3 is unique in that these two solid oxides are soluble in each other in all proportions. That is, all compositions are single-phase at equilibrium. This system is a classic case of the Hume-Rothery Rules[15] at work, and a classic "near-ideal" solution in both the solid and liquid states. The melting temperatures move almost linearly with composition from 100% Al_2O_3 to 100% Cr_2O_3.[21] It is quite reasonable to infer that in more complex systems containing these two components, if an alumina phase exists it will likely dissolve chromia. It cannot be supposed that these two oxides will have like phase diagrams with all other oxides. However, there is an expected large solid-solution region in the ternary system Al_2O_3-Cr_2O_3-Fe_2O_3,[21] and this can figure in the stabilization of iron-containing refractories (Chapter V).

Eutectic Systems. If two solids do not react but have limited solubility in each other, yet are mutually soluble in the liquid state, their phase diagram is of the simple *eutectic* type. This is quite common. An example is the CaO-MgO system, which is reminiscent of magnesite-dolomite refractories but idealized as to chemical purity. Its phase diagram[21] is given in Figure IV-3a: a temperature vs composition diagram from 100% MgO on the left to 100% CaO on the right, with the abscissa scale marked in wt.-% CaO. The ordinate (temperature) scale is in °C. This diagram is uncluttered enough that it can be used to review some important features. For this purpose the letters *a-i* and *L* and some dashed lines have been penned in.

The uppermost curve *c-a-e-d* is the *liquidus*, bounding the single-phase liquid field *L* above it. Two single-phase solid-solution fields are shown: the "MgOss" field bounded by the left vertical edge (100% MgO) and by the curve *c-b-f-h*; and the "CaOss" field bounded by the right vertical edge and by the curve *d-g-i*. This curve *d-g-i* represents saturated solutions of MgO in the host solid CaO at all temperatures from 1600°C to the m.p. of CaO; and the curve *c-b-f-h* represents saturated solutions of CaO in the host solid MgO at all temperatures from 1600°C to the m.p. of MgO. The segments *c-f* and *d-g* are called *solidus* curves.

Imagine an infinite number of horizontal line segments in the diagram, each one parallel to segment *f-g* and to segment *a-b* and, like them, extending from one single-phase boundary to the next nearest one. Those are *tie lines*. Tie lines connect pairs of single-

phase compositions that are in equilibrium with each other at the same temperature. In the composition field occupied by a tie line itself, no phase compositions are possible at all at its temperature. Any overall system composition lying in this forbidden phase field is the weighted average of the two single-phase compositions at the tie line extremities, each one multiplied by the relative amount of that phase present in the system.

In Figure IV-3a the "forbidden" phase fields are three in number: the roughly rectangular area bounded by *h-f-g-i-h* and the two roughly triangular areas bounded respectively by *c-e-f-c* and by *d-e-g-d*. Overall system compositions lying in those fields are *heterogeneous* mixtures, each composed of two phases in equilibrium whose identities are printed on the diagram in those respective areas.

There are three distinctive equilibrium points on the liquidus, called *invariant points* (at fixed pressure). These are *c* (100% MgO at its m.p.), *d* (100% CaO at its m.p.), and *e*, the minimum-melting cusp, called the *eutectic point*. The system composition at *e* is about 66 wt.-% CaO, 34% MgO. Its melting point is 2370°C. At each of these three points, the liquid freezes to a solid of the same overall composition and the freezing point (which is also the m.p.) does not change over the course of the process of transition. At point *e* the reason for this is unique: the liquid of this composition freezes to a pair of solids, compositions *f* and *g*, but in such relative amounts that the composition of the remaining liquid never changes. This pair of solids in that ratio is called the *eutectic solid*.

At no other overall composition in the CaO-MgO system is the freezing or melting temperature invariant. This circumstance results from the horizontal separation of the solidus from the liquidus on either side of point *e* and above it. That is, for any system composition other than those of points *c*, *d*, and *e*, the liquid first freezes to a single solid phase which is richer in one of the end-member components than the liquid is. The remaining liquid, being depleted in that component, freezes at a lower temperature. And so on, over a range. And conversely, quite precisely in reverse, over the course of melting.

As example, take the overall composition at point *a*, which is 40% CaO, 60% MgO. Slowly cool the liquid *L* of that composition from 2800°C down. At 2600°C (point *a*), freezing starts; but the first solid composition is that of point *b*, about 7% CaO, 93% MgO. The liquid composition becomes richer in CaO, hence freezing lower. Freezing progresses at steadily decreasing temperatures along the curve *a-e*, until the last body of liquid to freeze does so at point *e*, at 2370°C, yielding the eutectic solid phases of compositions *f* and *g*.

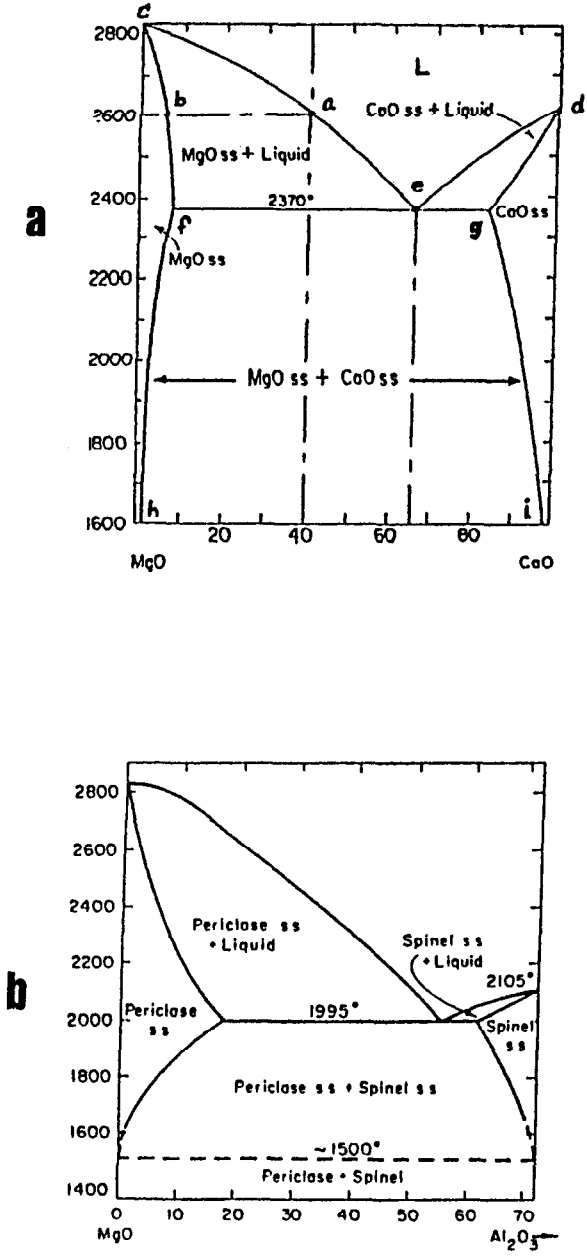

Figure IV-3 Binary Oxide Phase Systems
a. Ca0-Mg0 System b. Mg0-Spinel System
(reprinted from Ref. 21, by permission)

Now it is time to assert the viewpoint of refractories over the metallurgical viewpoint: What will happen progressively with increasing rather than decreasing temperature? If the overall system composition is that of *a*, it is certain from the above that melting will commence at 2370°C and will be completed at 2600°C. But the focus of concern in refractories is on the *onset* of melting Liquid first appears here at 2370°C, not at the 2850°C that we associated with MgO melting in Table IV.1. But how damaging will that be to the integrity of a 60MgO-40CaO refractory? That is, how much liquid will appear just barely above 2370°C as a result of eutectic melting, before the melting temperature even starts rising? This can be answered using the *Lever Rule*.[15,21]

> The Lever Rule states that the ratio of amounts of two phases in equilibrium is the inverse of the ratio of the "lever arms" connecting their respective compositions to the overall system composition.

The lever arms needed can be obtained from either %CaO or %MgO; the abscissa scale of %CaO in Fig. IV-3a is convenient. In the present problem the right-hand or "eutectic liquid" lever length (*e-a*) is (66-40) on that scale or 26. The left-hand or "remaining MgOss" lever length (*a-f*) is (40-9) at 2370°C, or 31. Their ratio is 26/31; its inverse is 31/26 or 1.19:1. This is the ratio of the masses of those same two phases. The fraction of the original material which has melted minutely above 2370°C is thus 1.19/2.19 or 0.544 or 54.4%. So far as mechanical integrity is concerned, this 60MgO-40CaO composition is completely destroyed by eutectic melting at 2370°C.

The reader can readily confirm that *all* overall compositions between 66% CaO (point *e*) and 9% CaO (point *f*) will commence melting at 2370°C; but the amount of liquid obtained at that temperature will decrease from 100% of the original solid to zero. Only if the original composition is <9% CaO (i.e., within the single-phase MgOss field) will melting commence higher; but if the temperature is gradually raised, the amount of liquid will again increase.

In a fired refractory this gradually-increasing fraction of liquid commences to weaken and finally to separate phase boundaries, destroying more and more of the interfacial bonding that gave the assemblage its mechanical integrity. Creep at liquid-containing temperatures takes the form principally of viscous flow between particles rather than of plastic deformation of crystals: after all, 2370°C is but little above the Tammann temperature of magnesia (2070°C, Table IV.1). The onset of eutectic melting is the threshold of a temperature-dependent progression that ends in the material's coming substantially unglued while still appearing to be solid. Pyrometric cones (Chapter II) demonstrate this progression dramatically and visibly.

Compound Formation. Figure IV-3b represents a portion of the MgO-Al_2O_3 system,[21] in which the compound $MgO \cdot Al_2O_3$, or spinel, is formed at equilibrium. This diagram has been cut off at the stoichiometric composition of spinel, namely at about 72.2% Al_2O_3 component and 27.8% MgO component by weight. The remainder, from 72.2% to 100% Al_2O_3, has simply been ignored. This liberty illustrates a prerogative of the reader, too: if there are one or more compounds within a binary system of components, that system can be subdivided into two or more subsystems. Here the subsystem retained lies between 100% MgO and 100% spinel. Its mate, deleted here, lies between 100% spinel and 100% Al_2O_3. Their phase equilibria are utterly independent of one another except where they join.

This binary subsystem has all the features of the CaO-MgO system discussed above; but its eutectic melting temperature is only 1995°C, compared with the pure MgO melting point of 2850°C and Tammann temperature of 2070°C. The onset of melting in the heterogeneous composition range MgOss + spinel ss is accordingly at 1995°C. The corresponding eutectic in the range spinel ss + alumina (not shown) melts at 1860°C.[21]

The MgO-$MgO \cdot Cr_2O_3$ binary subsystem is very similar to Fig. IV-3b, having its eutectic similarly placed and melting at 2325°C.[21] It can be safely inferred that the ternary system MgO-Al_2O_3-Cr_2O_3 could be treated in this same composition range as a binary system MgO-$MgO \cdot R_2O_3$, where "R_2O_3" is defined as Al_2O_3 and Cr_2O_3 in the same phase. The onset of melting will occur between 1995° and 2325°C, depending on the mol proportions of Al_2O_3 and Cr_2O_3 present in "R_2O_3."

Figure IV-3c shows the system Al_2O_3-SiO_2.[21] This phase diagram gives a first glimpse into the melting behavior of silica, fireclay, and fireclay-alumina refractories. The 1595°C eutectic begins to explain why early fireclay refractories in the 30%- to 60%-alumina (by weight) classes had much in common, and why the later 70%-alumina class (virtually all mullite at equilibrium) was much higher-melting. The same eutectic also explains why just a few percent Al_2O_3 in silica injured the performance of that acid refractory. Pure silica melts at 1723°C, which is borderline for high duty (see Fig. IV-2); but as little as 9% alumina reaches the 1595°C eutectic, and most compositions between 1% and 9% Al_2O_3 would commence melting at that same temperature. With the further m.p. depressing effect of other impurities present in mineral-based compositions, thermal performance would be still lower.

c

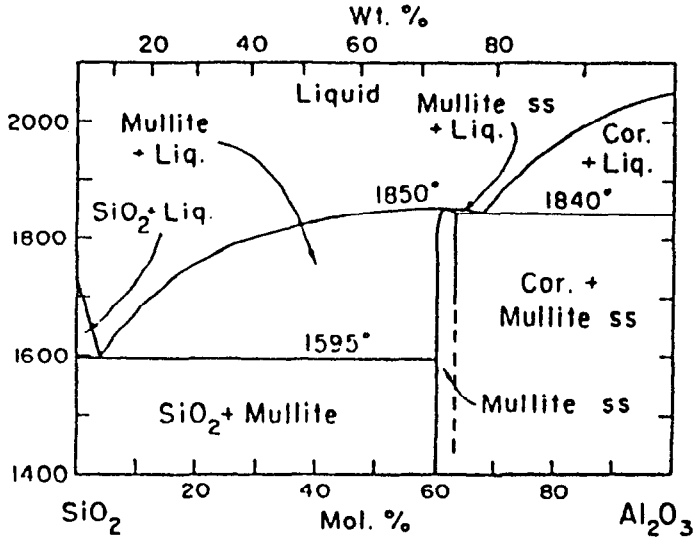

d

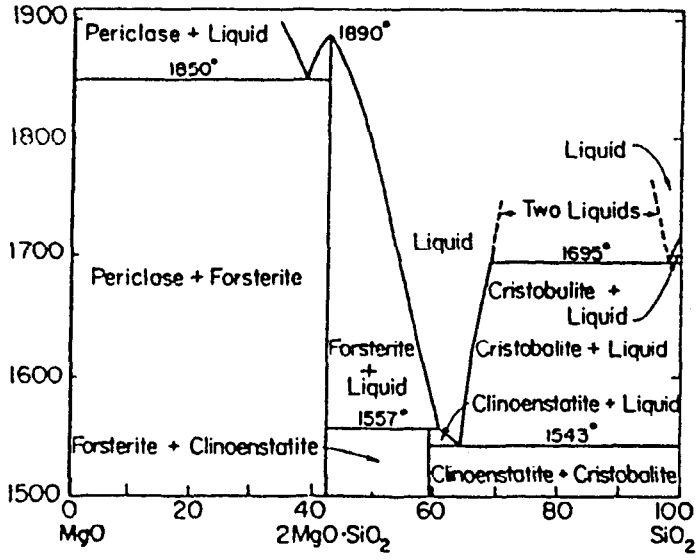

Figure IV-3, continued
c. Al_2O_3-SiO_2 System d. MgO-SiO_2 System
(reprinted from Ref. 21, by permission)

The "high-alumina" refractories, above 70% Al_2O_3 by weight, are seen in the diagram to pass over the maximum m.p. of mullite and into the two-phase region corundum + mullite ss, whose melting is governed by the second eutectic at 1840°C. Again, impurities in minerals will degrade this somewhat; but it can be seen why high-alumina refractories have been able to take over much of the high-temperature duty of silica.

Noted in passing: on this diagram, $Al_2O_3 \cdot SiO_2$ is no high-temperature compound at all, but is an undifferentiated composition in the two-phase field SiO_2 + mullite below 1595°C and in the two-phase field mullite + liquid above 1595°C. Yet it is listed as a compound in Table IV.1. Why it is not present in Figure IV-3c will be discovered before this chapter closes.

As a final graphic example of binary eutectic influences on the onset of melting, consider the MgO-SiO_2 system described in Figure IV-3d.[21] Two intermediate compounds are shown: forsterite, $2MgO \cdot SiO_2$ (listed in Table IV.2), and clinoenstatite, $MgO \cdot SiO_2$. The high-silica compositions in this system are not of interest in constructing refractories. What is striking here is to compare the periclase + forsterite eutectic at 1850°C with the melting point of periclase, 2850°C; but then further to contemplate the clinoenstatite + SiO_2 eutectic at 1543°C. True, there is an intervening *peritectic* feature;[15,21] but most overall system compositions in the forsterite + clinoenstatite field nonetheless commence melting at 1543°C. A magnesite-based refractory sufficiently contaminated with silica could see its potential melting of MgO at 2850°C degraded to an actual incipient melting at temperatures from 1000° to 1300° lower.

The system CaO-SiO_2 is not far different from the above, as to phases. It contains four intervening compounds between 100% CaO and 100% SiO_2.[21] The first compound, $3CaO \cdot SiO_2$, shares with CaO in being subject to low-temperature slaking. Following the next one, $2CaO \cdot SiO_2$ (listed in Table IV.1 at 2130°C m.p.), a peritectic and then a eutectic appear, the latter melting at 1460°C. A final eutectic appears between $CaO \cdot SiO_2$ and SiO_2, melting at 1436°C.

Three-Component Mixtures

If the two-component liquidus is a line, the three-component liquidus is a surface. The two-component liquidus has been seen to contain one or more eutectics. With three components each eutectic becomes a low-melting valley or groove, climbing or descending gradually in temperature as it moves in composition. From place to place in a ternary system, these valleys meet at *ternary eutectics*, which are invariant points. These are the minimum melting points in three components.

The same horizontal displacements between liquidus and solidus as were seen in two components cause liquid compositions, in the course of freezing, to move first downhill in temperature to a eutectic valley and then down the valley to its ternary eutectic. Precisely the reverse occurs on melting as the temperature of a solid mixture is gradually raised. Melting commences at or close to a ternary eutectic composition, then the liquid composition moves up a valley and finally climbs out of the valley to meet the overall system composition when melting is complete. Peritectics are present too, but we can again safely ignore them in seeking minimum melting points.

For evident thermodynamic reasons, freezing can never progress uphill (in temperature) on the liquidus surface, nor can melting progress downhill. Temperature maxima -- domes or crests or ridges in the liquidus -- lying between a given overall system composition and a eutectic valley thus cannot be traversed in the progress of either melting or freezing.

The features of phase equilibria that are needed to comprehend three-component melting are thus embodied in a topographical or contour map of the liquidus surface. Only one of these maps is chosen for display here.

The MgO-Al_2O_3-SiO_2 System. The phase diagram (liquidus map) for this system is given in Figure IV-4.[21] The system composition is laid out on triangular coordinates, in wt.-%. To find the composition of any point in the field requires a straightedge, as for example to identify point *A*, penned in at the lower left. To find its percent SiO_2, using the outer tics as a guide, lay the straightedge through the point and parallel to the side *opposite* the SiO_2 corner. Then on either outer border, count up tics (and interpolate) from that opposite side to the straightedge. Every tic is 10%. For the percent MgO, lay the straightedge parallel to the SiO_2-Al_2O_3 side and count tics likewise; and so on. The composition of point *A*, thus found, is 60% MgO-30%Al_2O_3-10% SiO_2. The unfamiliar reader should confirm this.

Now note the eutectic valleys, which are heavy lines bearing occasional arrowheads marking their downhill slopes in temperature. Sets of eutectic valleys form boundaries around *primary crystallization fields*, each with the name of a compound phase printed in it. Phase names are keyed to their formulas in the list at the upper right. The phase named in each field is the first one to crystallize if a molten liquid of any composition within that field is slowly cooled.

Tracing the progress of freezing is then easy. First, find a very small circle in the diagram labelled with the formula of that named phase. In the case of point *A*, its field is "periclase," and the compound phase "MgO" is at the lower left corner. Now if MgO freezes

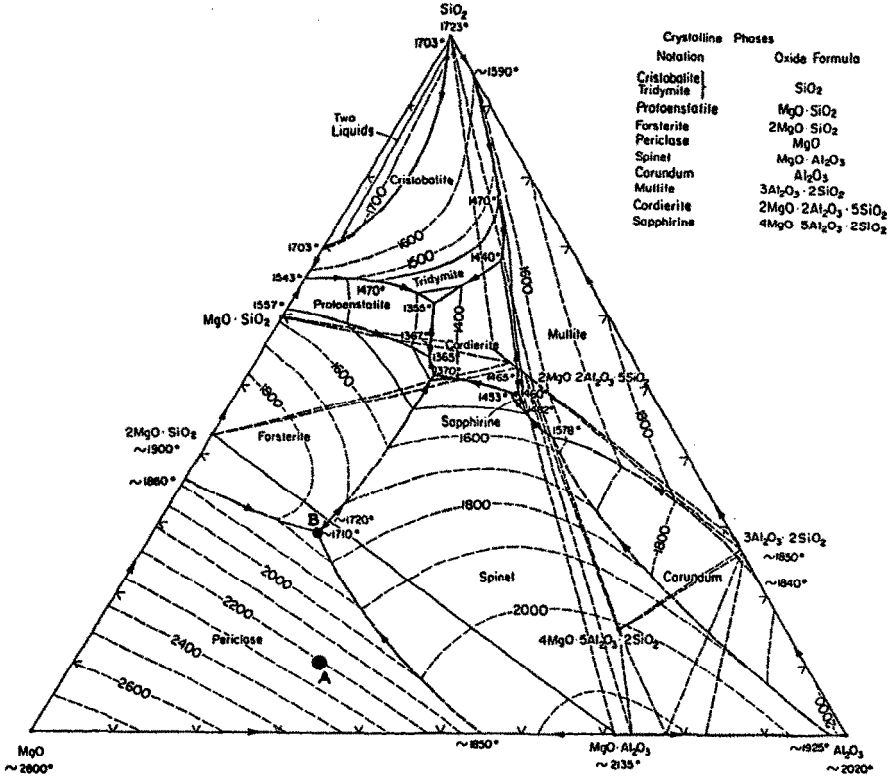

Figure IV-4 Ternary Phase System MgO-Al_2O_3-SiO_2
(reprinted from Ref. 21, by permission)

first, the composition of the liquid must move directly away from "MgO" as freezing progresses. Accordingly, lay the straightedge across both *A* and "MgO" and draw a line from *A* away from "MgO" until a eutectic valley is encountered.

At that intersection two fields adjoin: "periclase" and "spinel." Locate "$MgO{\cdot}Al_2O_3$" in the diagram. Now both MgO and $MgO{\cdot}Al_2O_3$ will commence freezing, in such ratio that the composition of the remaining liquid stays in the valley and moves down it to its ternary eutectic. The letter *B* has been penned in to identify this. Thenceforth in the progress of freezing, the remaining liquid composition is unchanging while MgO, $MgO{\cdot}Al_2O_3$, and $2MgO{\cdot}SiO_2$ (forsterite) crystallize simultaneously at a constant 1710°C until the liquid is exhausted.

Starting with a given overall composition and tracing the progress of freezing is on the whole advisable if one wants to describe the progress of melting. Practice makes perfect. For now, only a few further remarks will suffice concerning this particular ternary system.

Clay minerals exhibit Al_2O_3:SiO_2 mol ratios between 0 and 1/2, and MgO:SiO_2 ratios mostly between 0 and 2. Thus fireclay refractories fall much in the higher-silica part of this triangle. Andalusite, kyanite, and sillimanite are all nominally $Al_2O_3{\cdot}SiO_2$, with %MgO→0. Hence the clay-aluminas and high-alumina refractories tend to hug much of the right side of the triangle. These are the areas whose ternary eutectics may be informative as to the onset of melting in alumina-silica types of refractories. The top corner area likewise relates to silica refractories.

Each ternary eutectic in the diagram occurs at the junction of three fields. These locations and the minimum melting points are:

$MgO{\cdot}SiO_2 + 2MgO{\cdot}2Al_2O_3{\cdot}5SiO_2 + SiO_2$	1355°C
$MgO{\cdot}SiO_2 + 2MgO{\cdot}2Al_2O_3{\cdot}5SiO_2 + 2MgO{\cdot}SiO_2$	1365°C
$MgO{\cdot}Al_2O_3 + 2MgO{\cdot}SiO_2 + MgO$	1710°C

The CaO-Al_2O_3-SiO_2 System. CaO is a component of a few clays and other mineral raw materials for refractories, and tramp gypsum and limestone are common in the earth. The phase diagram for the CaO-Al_2O_3-SiO_2 system[21] gives some insight into the effect of replacing MgO by CaO in aluminosilicates. In this three-component system there are five ternary eutectics, none of which melts as high as 1350°C. The lowest-melting is at 1170°C.

The CaO-MgO-SiO_2 System. This system has a peculiar relevance to basic refractories, i.e., those made principally from

magnesite or seawater periclase. Its phase diagram shows six ternary eutectics.[21] Four of these are somewhat clustered in the high-silica composition region (i.e., $MO:SiO_2 \leq 1$), all melting between 1320° and 1375°C. One is in the region $MO:SiO_2 = 1.5$, melting at 1430°C; and one joins the fields $MgO + 3CaO{\cdot}2SiO_2 + 2CaO{\cdot}SiO_2$, melting at 1790°C. Designing about this last-named eutectic figured importantly in an improvement of basic steelmaking refractories in the early 1970s.

Ternary Systems Containing Iron Oxides. Numerous clays contain ferric oxide as a component, and are accordingly red. Fireclay refractories made from them may be from tan to brick-red depending on what clays are used and in what proportions. Here we take only an introductory glimpse into the effects of iron on the onset of melting: once in the ferric state and once in the ferrous, i.e., under reducing conditions.

The $CaO-Fe_2O_3-SiO_2$ system may be compared with the $CaO-Al_2O_3-SiO_2$ system highlighted above. Its phase diagram[21] indicates that every field in the triangle leads to one of three ternary eutectics, all melting between 1204° and 1216°C. The overall system composition can control only the amount of liquid formed in this temperature region, and how rapidly that amount increases with increasing temperature.

In the $FeO-Al_2O_3-SiO_2$ diagram,[21] on the other hand, all fields in the system lead to a single ternary eutectic melting at 1088°C. This might be compared with the 1170°-1345°C eutectics in the $CaO-Al_2O_3-SiO_2$ system and with the 1355°-1710°C eutectics in the $MgO-Al_2O_3-SiO_2$ system, above.

Ternary Systems Containing Na_2O. Finally it should be noted that alkalies have long crept into the composition of mineral-based refractories. Though they are largely eliminated today, a few examples of minimum melting points in systems containing Na_2O will readily illustrate the motivation for their removal.

The $Na_2O-Al_2O_3-SiO_2$ system[21] exhibits two ternary eutectics melting at 1062°C, so located that they pertain to nearly all $Al_2O_3-SiO_2$ compositions containing Na_2O even at impurity levels (i.e., few-%). Three other eutectics between 732° and 760°C would relate to environmental exposure of refractories to alkalies: they pertain to fields of about 1:1 $Na_2O:Al_2O_3$ ratio and higher. The most rational comparison to be made for now is between the 1062°C eutectics at low soda and that of the pure mullite + silica system at 1595°C.

A portion of the $Na_2O-Fe_2O_3-SiO_2$ system[21] shows eutectics of 955°, about 800°, and 760°C. And in the system $Na_2O-FeO-SiO_2$,

minimum-melting temperatures of 703°, 667°, and <500°C are found. This last and lowest pertains to alkali- and iron-contaminated silica refractories under reducing conditions, but again at only impurity levels.

Higher-Order Mixtures

A few four-component oxide equilibrium systems have been worked out, for the most part covering only selected subsystems. Not only is the experimental work excessively tedious; presentation in two-dimensional drawings requires exceptional creativity.

One such system that comes very close to representing real mineral-based refractories is the CaO-MgO-Al_2O_3-SiO_2 system. Its sole departure from reality is in the absence of any iron oxide, alkalies, and titania which appear in a number of clays. A gratifyingly informative mode of presentation is reproduced in Figure IV-5.[21] This is a set of liquidus maps of the pseudoternary system CaO-MgO-SiO_2 prepared for successively increasing fixed values of $\%Al_2O_3$. The published series of diagrams stops, however, at $35\%Al_2O_3$; this leaves most of the spectrum of fireclay refractories undescribed. It is hoped this series will one day be completed.

So far as they go, these diagrams introduce no remarkably different eutectic temperatures of which we should take note. In any event, those we have catalogued in the preceding sections suffice to give a convincing and quantitative picture of the melting behavior of mixed-oxide refractories. Of the major refractory families, we have omitted only the ZrO_2-containing system. That gap will be filled presently.

Summary: Onset of Melting in Refractory Mixtures

We have sampled oxide phase diagrams sufficiently in this chapter to demonstrate that the occurrence of eutectics is common if not universal, and that eutectics dictate the onset of melting as temperature is increased. Our sampling of available phase diagrams is far from complete; numerous others remain to be consulted.[21] Their importance in understanding the progressive thermal softening, weakening, and ultimate destruction of refractories cannot be overstressed. It should be clear that the maximum feasible service temperature of a refractory has to be confined by: (a) its lowest germane eutectic and the melting temperature thereof; (b) how much liquid is produced at that temperature; and (c) how rapidly the amount of liquid increases with increasing temperature above this. The viscosity of the liquid vs temperature must also figure. But these three enumerated properties, all derivable in principle from phase diagrams and the Lever Rule, provide a powerful start toward describing the thermal stability of refractory materials.

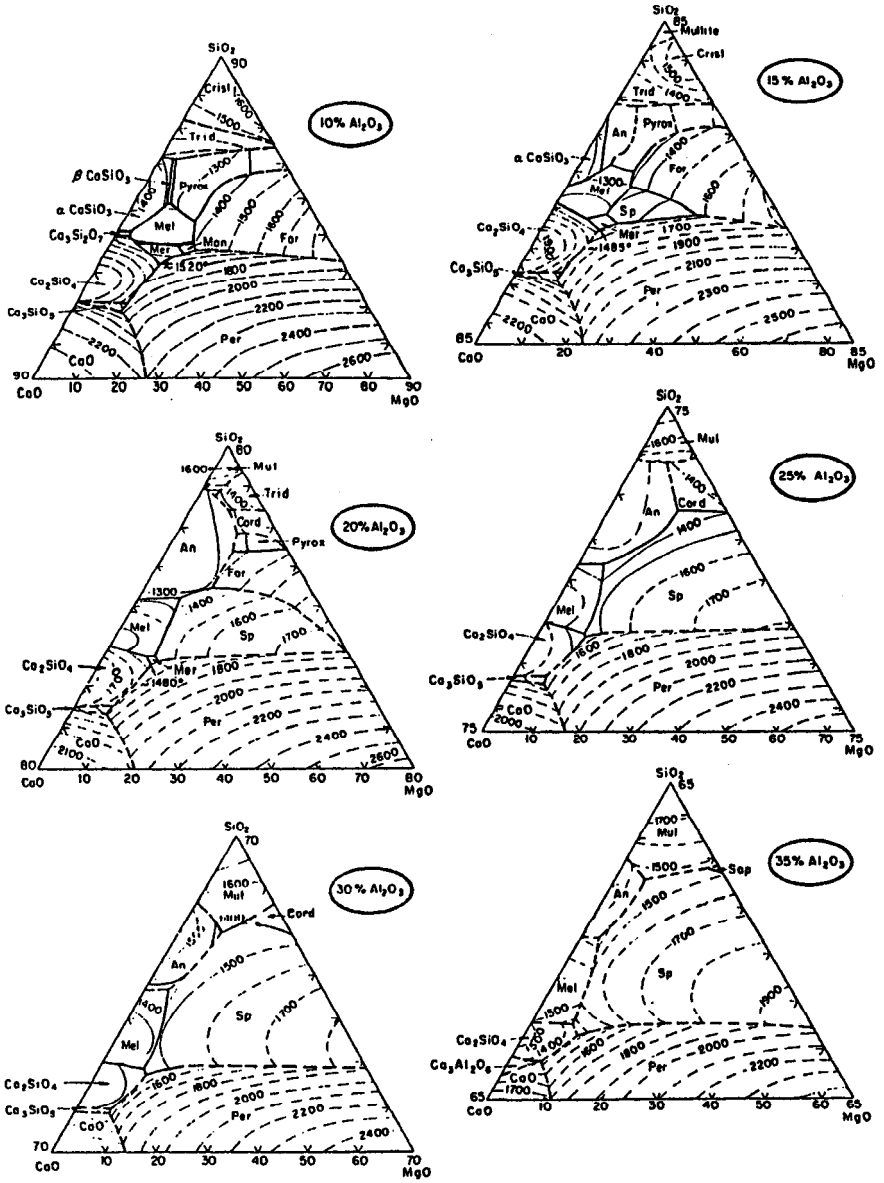

Figure IV-5 Quaternary Phase System Ca0-Mg0-Al_2O_3-SiO_2
(reprinted from Ref. 21, by permission)

Our sampling has encompassed only the components CaO, MgO, Al_2O_3, SiO_2, Fe_2O_3, FeO, and Na_2O. That sampling is summarized in Table IV.2, which compares the melting temperatures of various binary and ternary eutectics with the melting points of the pure parent compounds and with the Tammann temperatures of those compounds. The successive lowering of melting temperatures in going from one- to two- to three-component systems is clearly seen. The specific effects of the components Fe_2O_3, FeO, and Na_2O are further seen to be dramatic.

Some important detail and some accuracy of representation have been sacrificed in constructing Table IV.2, in the interests of a concise summary of general correlations and trends. Nevertheless this table is eminently useful, and it will be referred to later. Here it also introduces a further shorthand notation for phases and components that is commonly used in the industry. This notation is defined in the box at its top.

Mixtures of Oxides with Nonoxides

If two substances are not measurably soluble in one another in either the liquid or the solid state, nor react chemically, the melting of each is quite unaffected by the presence of the other. This condition can be stated somewhat more generously. First, "substances" can be replaced by "material systems." Further, if one of these is molten at some temperature while the other is not, yet the latter is not soluble in the former, their phase diagrams up to that temperature are also indifferent to each other's presence. A separate inquiry must be made into oxidation-reduction reactions between them; this is reserved to Chapter V. Here it is assumed that redox reactions are absent.

This condition of *immiscibility* is common for mixtures of material systems that are respectively (a) metallic, (b) covalent, and (c) ionic in their chemical bonding. The oxidic systems we have been describing are all predominantly ionic, or at least highly polar. The nonoxides such as listed in Table IV.1 are substantially covalent, tending toward nonpolar. The third group is the elemental metals. As a general rule we can take oxide phase diagrams as being unaffected by admixing an oxide system with either (a) high-melting metals or (b) the nonoxides of Table IV.1 -- or for that matter, with both at once.

This observation underlies the successful admixing of carbon or carbides into oxidic refractories, for example, as well as the juxtaposition of oxide bricks with carbon or silicon carbide bricks in a furnace lining. Metal wire reinforcing has also been incorporated into oxide refractories. Lacking redox reactions, such juxtaposed material types are basically compatible. The admixed formulations are properly referred to as *composites*. Many composite refractories have

Table IV.2 Minimum Melting Temperatures of Some Refractory Material Systems (Refs. 11, 21)

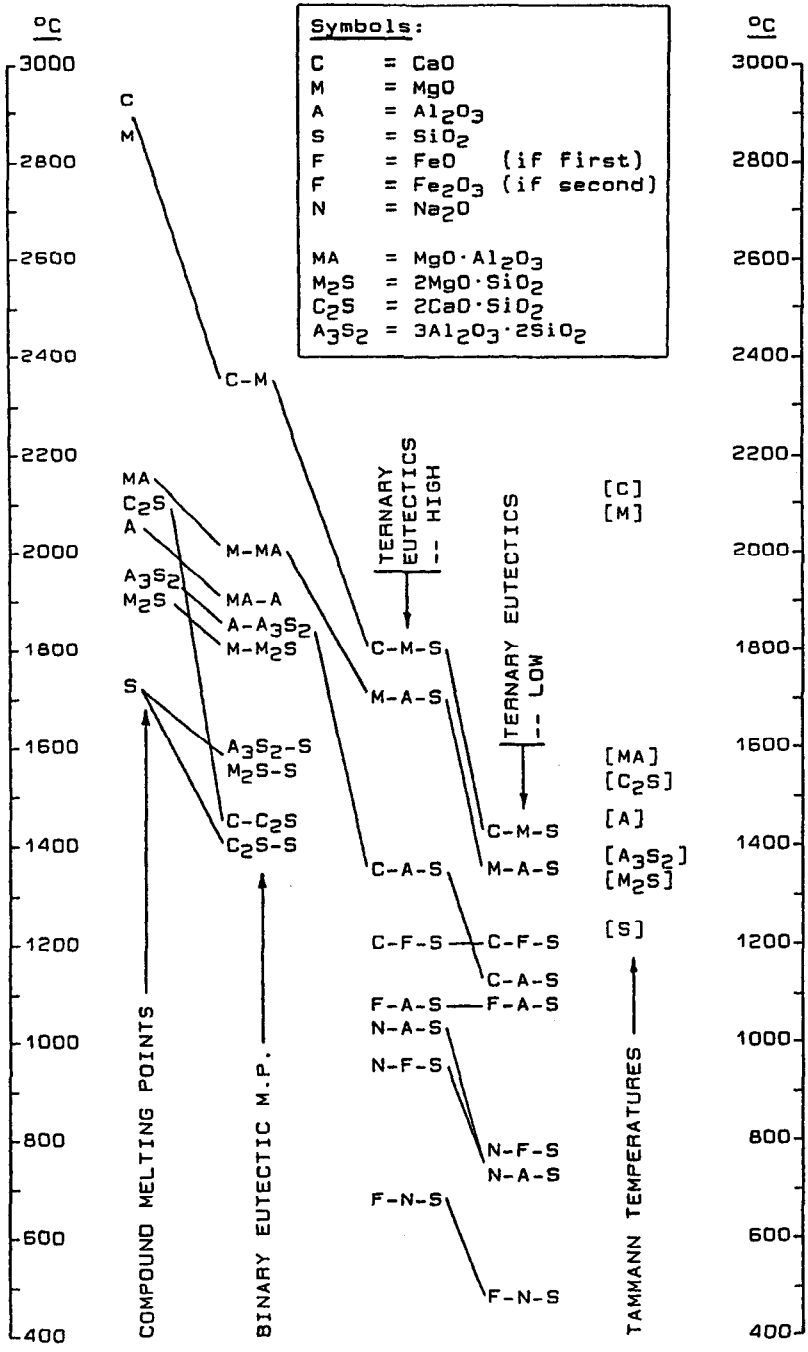

been able to combine favorable properties while masking the unfavorable. It is favorable that they are heterogeneous but without consequent new and still lower-melting eutectics.

MICROSTRUCTURAL INTEGRITY

Polymorphs; Solid-State Transitions

Some substances exist in two or more crystal forms and undergo solid-state transitions from one to another at fairly specific temperatures. Each crystal form or lattice type is a different phase of the same substance, and the set of them are called *polymorphs.* An example in metallurgy is iron; examples in ceramics and refractories are silica and zirconia.

If the densities of two such phases are markedly different, one crystallite in a polycrystalline assemblage which undergoes the transition from one phase to the other will then occupy a greater or lesser volume to which the remainder cannot accommodate. Such volume changes are also often *anisotropic,* i.e., dimensionally of unequal magnitudes in different directions. Crystallite or phase boundaries can be subjected to immense compressive, tensile, or shear forces in either case. If microcracks ensue, they are subject to successive extensions if the temperature is cycled through that of the transition: a process called "ratcheting."

Another possible kind of transition is the decomposition of a ternary compound to its component solid oxides. Zircon and dialuminum silicate need to be examined in this regard.

In still another kind of solid-state phase transition, exemplified by titania and alumina, the "high-temperature" phase is the more stable one at all temperatures and the transition is not reversible. Comparable changes are found in the devitrification of glasses and the crystallization of stable high-temperature phases from amorphous or ill-crystallized forms. An example of this latter type is the graphitization of carbon.

An interesting change, between alpha- and beta-SiC, is effected more by mechanical shear forces than by thermal energy. Another "diffusionless" transition (i.e., one not requiring nucleation and growth of new crystals) is that between tetragonal and monoclinic zirconia. The first of these is accompanied by virtually no volume change, while that of the second is very large and disruptive.

All told, among the twenty-four refractory substances listed in Table IV.1, eight exhibit some kind of change of phase as listed

above. Not all of these changes are properly called "transitions," and not all the phases so related are properly called "polymorphs." What is most important to refractories is the volume change. We shall catalog all eight cases, as the reader is likely to encounter them and should know which changes are destructive.

Refractory Phases and Phase Changes

Irreversible Changes: Alumina and Titania. Alpha-alumina, or corundum, is of hexagonal crystal type. It is the thermal end-product of three recognized series of "transition" aluminas,[22] which are made from various hydrated origins at low temperature. Corundum is the thermodynamically stable form at all temperatures above ambient. All of the phase changes leading to it are irreversible, and most are somewhat sluggish, occurring progressively over some range of increasing T. The transition alumina series, their origins, and their approximate unidirectional transition temperatures in °C are:

[Boehmite, AlOOH]	450	gamma	600	delta	1050	theta	1200 alpha
[Bayerite, $Al(OH)_3$]	200	rho	300	eta	850	theta	1200 alpha
[Gibbsite, $Al(OH)_3$]	250	chi	----------		900	kappa	1200 alpha

Volume shrinkages aggregating up to some 20% accompany these changes and even the intermediate heating of each phase.[22] These changes are typically realized in calcining and sintering of particulates, but sometimes in sintering of formed refractories before use. Alpha-alumina, once it is recrystallized at some 1600°-1800°C, is stable indefinitely.

The common low-temperature (metastable) form of TiO_2, called anatase, is also typically derived from a hydrated origin: titanyl hydroxide, $TiO(OH)_2$. Between about 700° and 900°C, depending on purity, anatase goes over sluggishly and irreversibly to rutile which is the thermodynamically stable form at all temperatures.[8] Both phases are tetragonal. The volume shrinkage in the transition is of the order of 10%, but again is ordinarily realized in the calcining of particulates where it does no permanent harm. Rutile is then dimensionally stable.

Irreversible Changes: Carbons and Graphites. The graphite crystal is hexagonal, but is unlike most others in that the center of each hexagon is unoccupied. Thus each basal plane remotely resembles chickenwire rather than a dense triangular network of atoms. In a region of crystal perfection, successive basal layers are stacked A-B-C-A-B-C. That is, some atoms of each layer lie under the "pockets" in the overlying hexagons, and every third layer is in a like position except for their perpendicular separation. All other forms of carbon are metastable.[8]

The organic compounds of which most industrial carbons are made include aromatics and condensed aromatics, in whose "ring" molecules the hexagonal net of the basal graphite layer is already started. Pyrolysis builds on these hexagonal nuclei, so that carbons contain some (molecularly small) planar regions of hexagonal atomic order. But disorder is the general rule, taking the forms of (a) large ragged and buckled rings in the basal "plane" together with branching chains of atoms out of that plane; (b) large distances, nonparallelism and rotational disorder between "planes;" (c) stacking faults even where planar segments are parallel; and (d) bits of extra planes.

The thermally activated solid-state progression from carbon to graphite is energetically very difficult and hence very sluggish. Large volume shrinkages accompany this progression, involving both the consolidation of void spaces between crystallizing regions and condensation of the crystallizing structures themselves. "Carbon" is not a defined phase, as it is made in many ways and at many different temperatures; so the progression itself is not a phase transition and cannot be simply characterized. The shrinkage into well-ordered crystallites is not mechanically destructive to a carbon body, however, as it typically progresses at 2000°-3000°C;[8] but it does produce porosity which cannot be substantially collapsed by sintering, as no liquid phase or intergranular lubricant exists. The progression is irreversible.

Some carbons, e.g., made from aliphatic organic precursors and hence lacking in hexagonal ring nuclei, persistently resist effective graphitization. Some carbon blacks that were once fog droplets of heavy aromatic oils develop their "basal planes" as concentric onionskin shells. These tend to persist through graphitization, yielding unique microstructures. Thus there can be almost as many "graphites" as there are types of carbon precursors.

"Vitreous carbon," made by careful pyrolysis of certain preformed thermosetting organic polymers, has the substantially random three-dimensional atomic network of glass. It is the only form of carbon which lacks any granular or crystalline microstructure and hence grain boundaries. As it is very costly to make, it is never willingly graphitized. It is truly impermeable to liquids. "Impermeable" granular carbons and graphites will be described in Chapter VI.

Crystalline diamond should be mentioned here to complete the roster of carbon forms, but it has no conventional refractory uses. At ordinary pressures it too is metastable with respect to graphite, but the transition is not willingly carried out.

Diffusionless Changes: Silicon Carbide. Alpha-SiC is variously of hexagonal and rhombohedral crystal types, the differ-

ences arising from different stacking sequences of otherwise-identical atom layer planes. Beta-SiC is cubic, again seen as an unique stacking sequence of the same. Though beta-SiC is thermodynamically more stable by a slim margin, the two phases coexist readily over a wide temperature range. Their densities and thermal expansions are all but identical. The transition from one to the other can be effected more by high-shear processing (e.g., extrusion forming or hot working) than by simply heating or re-heating alone. This transition consists of the shear displacement of successive layer planes in the crystal, nucleated about favorable sets of stacking faults and then growing out by successive short-range movements of atoms. The temperatures at which the transition to beta is carried out are in the sintering range, but a clear crossover in stability at some fixed transition temperature has not been demonstrated.[8]

Owing to the high temperature and the near-zero volume change of this transition, it is harmless to the mechanical integrity of massive SiC bodies. Their use as engineering materials rarely approaches 2000°C; hence SiC bodies in service retain their crystal identities whether alpha, beta, or mixed.

Decompositions: Zircon and Dialuminum Silicate. The phase diagram for the system ZrO_2-SiO_2 is shown in Figure IV-6a.[21] In this figure the overall composition of zircon, $ZrSiO_4$ or $ZrO_2 \cdot SiO_2$, falls in the two-phase field ZrO_2 + liquid at all temperatures from about 1680° to 2250°C, and likewise on up to the liquidus above at about 2400°C. In fact, the figure suggests that $ZrSiO_4$ disappears as a stable phase somewhere about 1550°C by the decomposition reaction,

$$ZrSiO_{4(s)} \rightarrow ZrO_{2(s)} + SiO_{2(s)} \quad .$$

The Al_2O_3-SiO_2 phase diagram of Figure IV-3c[21] gives no acknowledgement at all of the compound Al_2SiO_5 or $Al_2O_3 \cdot SiO_2$. A possible implication in that case is that dialuminum silicate decomposes below the lower extremity of the figure, 1400°C, by:

$$3\,Al_2SiO_{5(s)} \rightarrow 3Al_2O_3 \cdot 2SiO_{2(s)} + SiO_{2(s)} \quad .$$

One may infer in both cases that there is a temperature-dependent crossover in the thermodynamic stability of the addition compound with respect to its decomposition products. A reversible change of phases would occur at the temperature of the crossover: each of the above reactions would occur as written above its equilibrium temperature, and the reverse of each would occur below.

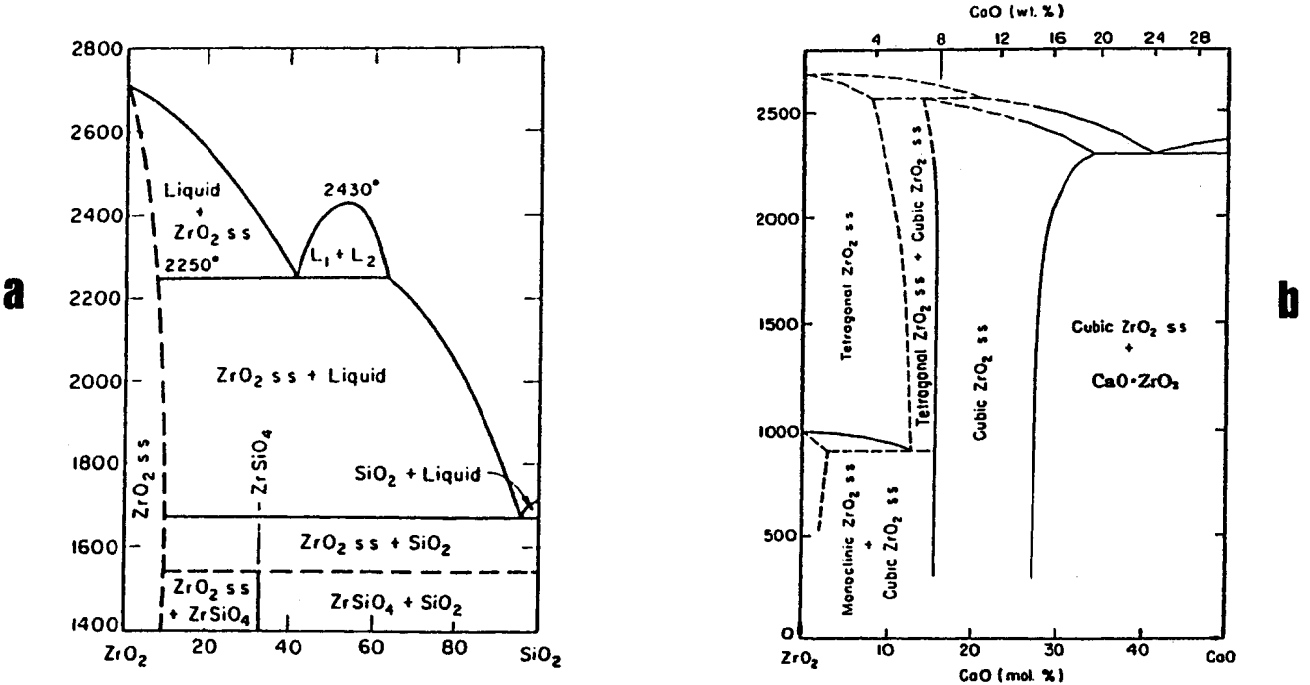

Figure IV-6 Two Binary Phase Systems Containing ZrO_2
a. SiO_2-ZrO_2 System b. CaO-ZrO_2 System
(reprinted from Ref. 21, by permission)

Since the reagents and products are all solids in each case where equilibrium is supposed to occur (~1550°C and <1400°C, respectively), the question of ΔV of these reactions looms.

The answer is surprisingly simple. Tabulated Gibbs free energy data[23] show that there is no reversal at all in the sign of ΔG for either of the above reactions, up to the temperature of appearance of a molten phase. Both zircon and dialuminum silicate are stable, but by a narrow margin which is relatively constant with temperature. When a liquid phase appears, however, by virtue of its solution composition the chemical activities of both of the liquid components are reduced and ΔG then becomes negative. The above reactions will both proceed as written only when the product $SiO_{2(s)}$ is replaced by an appropriate descriptor of the silicate liquid.

In plain English, this means that zircon and dialuminum silicate decompose only in conjunction with *melting* and not at any lower temperature. In the presence of liquid, any concern with ΔV of the decomposition reactions vanishes.

Disruptive Changes: Zirconia. Figure IV-6b, the phase diagram for the system $CaO\text{-}ZrO_2$,[21] shows the one-component system ZrO_2 along its left vertical edge. The tetragonal-monoclinic phase change at 1000°C may or may not be quite correctly represented in the light of current knowledge; but that is not important here. This is a diffusionless transformation, occurring over about a 100° range. Its volume change, $V_{mono.} - V_{tet.}$, is about 7% and mechanically destructive. Refractories and ceramics containing appreciable ZrO_2 phase could not be successfully made until a cure was found for this fault.

As Figure IV-6b shows, however, a solid solution of some 8 wt.-% or more of CaO in ZrO_2 has a cubic crystal structure all the way from room temperature to the melting point, uninterrupted by any solid-state phase change. Lime-stabilized cubic zirconia ss phase at about 8% CaO is extensively used in refractories and ceramics.[24-28] Its peritectic and adjacent eutectic points indicate that the onset of melting will be just a little under 2300°C, vs 2700°C for pure ZrO_2. But the 8% CaO composition, by the Lever Rule, yields very little liquid at the eutectic temperature. MgO also stabilizes cubic zirconia.

A few other dissolved oxides have the same effect on ZrO_2, but none so inexpensively. One of these, Y_2O_3, figures in the transition-toughened partially-stabilized zirconia ceramics called "PSZ." The partially-stabilized concept plays no role in refractories, as its toughening function[29] diminishes and disappears with increasing temperature up to only about 800°C or less.[30]

Disruptive Changes: Silica. The one-component system SiO_2 is a remarkably complex phase system all by itself. Figure IV-7, prepared from data in several sources,[3,11,21] presents the solid silica phases and their transitions in the context of crystal density rather than of phase equilibria. The latter are incorporated, however. By showing the intervening thermal expansions (expressed as density), the figure puts the volume changes of the several phase transitions in perspective. As a rough rule of thumb, any reasonably rapid transition entailing a volume change of the order of 1% or more has to be considered dangerous in the temperature range of elastic behavior: microstructural damage will likely ensue.

In order of thermodynamic stabilities with increasing temperature, the principal crystalline phase types in silica are quartz (hexagonal, stable to 870°C); tridymite (rhombohedral, stable from 870° to 1470°C); and cristobalite (tetragonal and cubic, stable from 1470° to 1723°C, the melting point). Vitreous silica is metastable and has the relatively random polymeric network structure of the liquid, "frozen in" by undercooling.

The three crystalline phases all have extended temperature ranges over which they are metastable. They all undercool. Their transitions to their respective higher-temperature forms are sluggish. It is difficult enough to transform quartz to tridymite or crystobalite, requiring heating in the 1450°-1700° range and preferably at the upper end, including preferably by melting. It is impossible in a short time to transform tridymite or cristobalite to quartz by cooling, as the latter is not stable except below 900°C. By then, kinetic barriers are too high.[3] Vitreous silica can interchange with tridymite and cristobalite at high temperatures, and will devitrify slowly even down to about 1000°C. That is the approximate upper service limit of this otherwise unique and useful material. Mixtures of vitreous and crystalline silicas are unstable for the reasons given below.

Once undercooled, every one of the crystalline silicas undergoes one or more transformations at very low temperatures above ambient. These are all diffusionless transitions, requiring only simple shear or rotational displacements within the host crystal. They relate to various ways in which the tetrahedral Si atom and its surrounding oxygen atoms can be arrayed regularly in space. The transitions are all fairly rapid and reversible, in spite of the fact that they all occur well below the Tammann temperature of SiO_2 (Table IV.1). The nomenclature of the various forms connected by these transitions is laid out in Figure IV-7. Tridymites II, III, and IV are not labelled in the figure, but the reader will locate them readily.

The volume changes of all transitions are tabulated in the figure. It is seen that the rapid high-low-cristobalite and high-low-

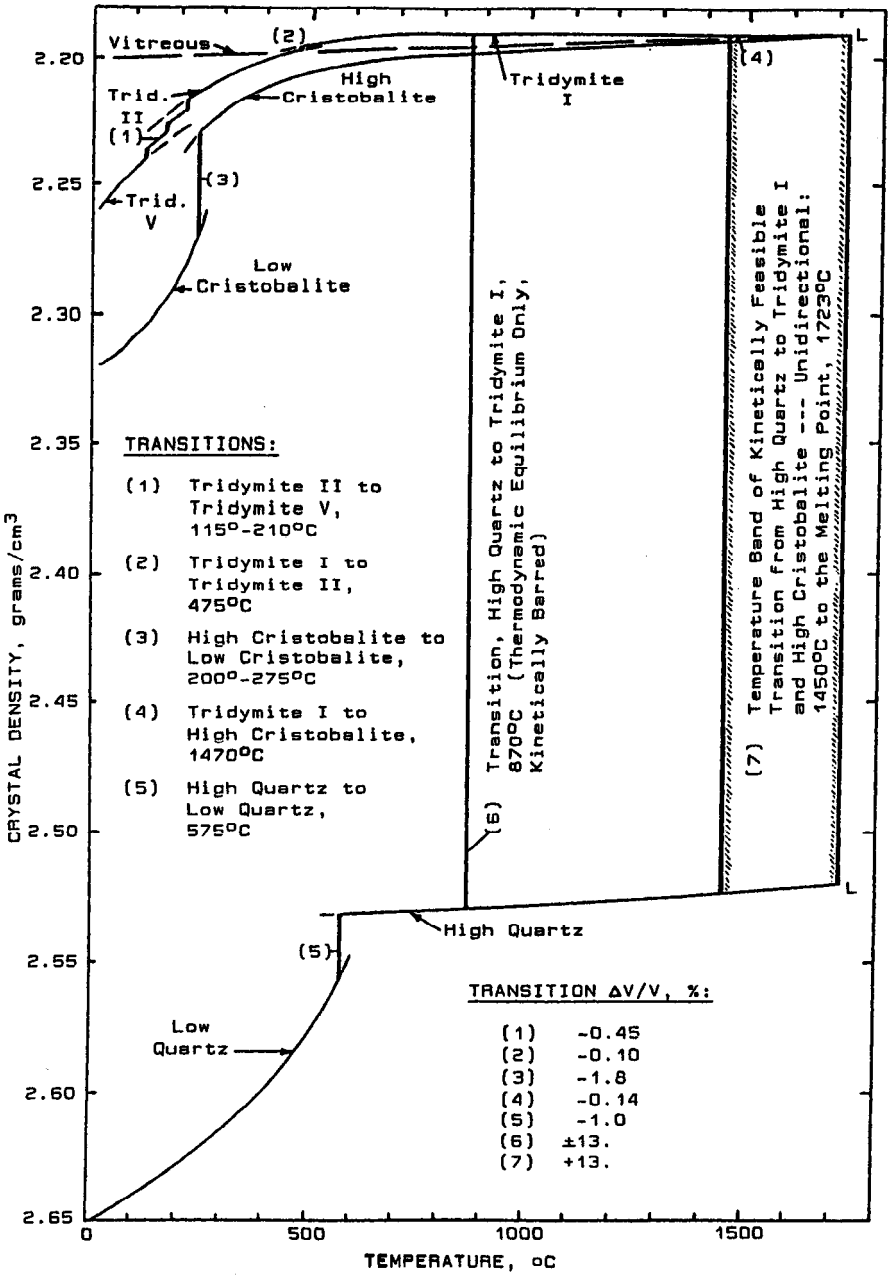

Figure IV-7 Phase Transitions and Densities of SiO_2 (Refs. 3, 11, 21)

quartz transitions are clearly in the disruptive range, while the tridymite II-III-IV-V transitions could be as well.

These low-temperature transitions have plagued "acid" silica refractories in both manufacture and use, since the beginning. No solute oxide has even partially relieved the problem, least of all promising a cure such as is provided by CaO in ZrO_2. The consequences of these transitions ramify to a lesser extent into all heterogeneous silica-containing refractories as well: a large group of products. The implications and defensive measures are too numerous to belabor here. They will be brought up later and references will then be made back to this important figure.

Thermal Anisotropy

Some refractory compounds are subject to disruptive intercrystalline debonding even without a change of phase. These are compounds whose crystallites exhibit thermal expansion *anisotropy*: unequal $\Delta L/\Delta T$ in the several crystallographic directions.

Consider a boundary segment joining two crystals of mutually perpendicular crystallographic orientation. Upon some rise in uniform bulk temperature ΔT, one of these anisotropic crystals will expand linearly along the boundary by a larger ΔL and the other by a smaller ΔL. The result is a *dimensional mismatch* along the boundary, or a *boundary shear strain*. In the general case, the amount of this strain depends on the relative orientations of the conjugate crystals and of the boundary, which are statistical parameters in a sintered body. This strain is also directly proportional to (a) the difference in thermal expansion coefficients in the two perpendicular crystallographic directions, or the *degree of anisotropy*; (b) the length of the boundary segment, which is on average proportional to the *crystallite size*; and (c) the magnitude of the ΔT experienced.

If the span of ΔT lies in the range of elastic behavior of the material, then only two responses are possible. Either the strain falls within the elastic limit and is withstood without damage; or its corresponding stress exceeds the local boundary shear strength and partial debonding of the boundary results. The sign of ΔT does not matter to this process. In fact, mechanical damage often results on cooling from the plastic temperature region where stresses have been relieved. Once microcracks have been started, they can be extended by cyclic repetitions of the ΔT experience, by what we have previously called "ratcheting."

All crystal types other than cubic exhibit some degree of thermal expansion anisotropy. Crystallographic notation is described sufficiently in Ref. 15, or in any reference work on this subject.[31] Here it is necessary only to flag the anisotropic phases among those listed

in Table IV.1, adding just a few others that may yet be of interest. The following table, giving the approximate ratio of mutually-perpendicular crystallographic thermal expansion coefficients, has been compiled from several sources.[3, 8, 11, 15, 32] Where thermal expansion data are lacking, the crystal type is given.

Formula	Th. Exp. Ratio	Formula	Th. Exp. Ratio	Formula	Th. Exp. Ratio
Al_2O_3 (hex.)	1.09:1	$Al_6Si_2O_{13}$(rhomb.)	1.3:1	AlN(hex.)	1.18:1
Cr_2O_3(hex.)	1.30:1	Al_2SiO_5	(non-cub.)	B_4C	(rhombohedral)
Fe_2O_3(trig.)	1.26:1	$CaAl_2O_4$	(monocl.)	BN	(hex.)
MgO(cub.)	1.00:1	Ca_2SiO_4	(monocl.)	C(graph,hex.)	>1.5:1
SiO_2(qtz.,hex.)	1.58:1	$Ca_2Al_2SiO_7$	(non-cub.)	C(carbon)	(imp.hex.)
(vitr.)	1.00:1	$CaTiO_3$	(rhomb.)	C(vitr.)	1.00:1
TiO_2(rutile)	(tetr.)	$CaZrO_3$	(monocl.)	SiC(alpha)	(hex.)
ZrO_2(monocl.)	1.50:1	$FeCr_2O_4$(cub.)	1.00:1	SiC(beta,cub.)	1.00:1
ZrO_2-CaO(cub.)	1.00:1	$MgAl_2O_4$(cub.)	1.00:1	TiB_2	(hex.)
		$MgCr_2O_4$(cub.)	1.00:1	TiC(cub.)	1:00:1
		Mg_2SiO_4	(rhomb.)	TiN(cub.)	1.00:1
		$Mg_2Al_4Si_5O_{18}$	(non-cub.)		
		$ZrSiO_4$(tetr.)	1.68:1		

All of the substances whose expansion ratios are itemized as >1:1 above are vulnerable to some local debonding upon temperature cycling. Notable among these as major phases of refractories are alumina (Al_2O_3), low quartz (SiO_2), mullite ($Al_6Si_2O_{13}$), zircon ($ZrSiO_4$), and graphite. Others that are also susceptible include forsterite (Mg_2SiO_4), boron carbide and nitride, granular carbon, and TiB_2.

Two materials long used as load-bearing kiln furniture are cordierite ($Mg_2Al_4Si_5O_{18}$, m.p.~1500°C) and SiC. In the former, though the ratio of thermal expansion coefficients is probably large enough, the mean coefficient is inordinately low as will be catalogued presently. Cordierite is typically life-limited by creep rather than by anisotropic ratcheting. In SiC, though the hexagonal alpha phase has exhibited long cycle lifetimes in service, more recent products that are predominantly beta (i.e., cubic) are reputedly even more durable.

In anticipating possible mechanical damage in refractories due to thermal anisotropy, reduction of the above tabulated data to quantitative rules is frustrated by several circumstances. One of these is that this phenomenon rarely acts alone. A second cause of debonding is considered next.

Differential Thermal Expansion

The foregoing pertains to orientation boundaries in a single phase. A precisely parallel phenomenon pertains to phase boundaries joining two dissimilar phases. Taking this phenomenon in isolation, the first criterion for phase-boundary shear is a difference in thermal expansion coefficients of the two conjugate phases. Anisotropy of either phase is a secondary matter. In all other respects, the entire description of the preceding phenomenon carries over here without change.

The table below is compiled from thermal expansion data given in Vol. 13 of Reference 32 This table gives for various pairs of phases the dimensional mismatch or calculated shear of a boundary segment at room temperature (20°C), on the assumption that the boundary and conjugate rigid crystals were strain-free at 1000°C. The boundary shear is given as the *shear displacement* in nanometers that would occur at *either end* of an unsupported boundary segment, per micrometer overall length of segment.

Phase Boundary	$\Delta L/L$, nm/μm	Phase Boundary	$\Delta L/L$, nm/μm
$Al_2O_3+Al_6Si_2O_{13}$	1.67	$Mg_2Al_4Si_5O_{18}+Mg_2SiO_4$	4.62
$Al_6Si_2O_{13}+SiO_2$	0.70	$Mg_2Al_4Si_5O_{18}+Al_6Si_2O_{13}$	1.35
		$Mg_2Al_4Si_5O_{18}+SiO_2$	0.65
$MgO+MgCr_2O_4$	3.27		
$MgO+MgAl_2O_4$	2.39	$ZrO_2+ZrSiO_4$	1.16
$MgAl_2O_4+Al_2O_3$	0.28		
		$ZrSiO_4+Al_6Si_2O_{13}$	0.04
$MgO+Mg_2SiO_4$	1.07	$ZrSiO_4+SiO_2$	0.67

It matters little that the calculational method is naive: compared to the typical atomic diameter of some 0.2-0.3 nm, most of these dimensional mismatches are enormous. Phase boundary microcracking can be anticipated in almost all cases.

Thus the great majority of heterogeneous refractory materials are susceptible to microcracking by either or both of thermal anisotropy and differential thermal expansion. In fact, the resulting microstructural deterioration typically starts in the original manufacture of bricks and blocks, upon their first cooling after firing. It is then potentially continued under thermal cycling.

Internal microcracking results in a modest irreversible macroscopic volume increase, which can become appreciable if ratcheting occurs. The tensile strength of a sintered body is profoundly affected. The compressive strength is less so, though

susceptibility to shear spalling under compression is increased. The macroscopic elastic modulus and the thermal and electrical conductivity are appreciably diminished. All of these properties will be treated in later chapters. Effects of microcracking on the susceptibility of refractories to corrosive attack will be addressed in Chapter VI.

It may well be asked why the susceptible refractories are not reduced to sand in cyclic service. There are several contributing reasons. First is the almost universal encounter of microcracks with *porosity*. A crack terminating in a pore loses continuity with other cracks. It is well known that the development of large continuous cracks by linking up of microcracks (such as, e.g., in spalling) decreases with increasing pore volume fraction.[38-41]

Another mitigating fact is that the lengthening of isolated microcracks is to some degree self-limiting: the remaining bonded length of boundary segments becomes shorter, diminishing the cumulative dimensional mismatch and hence shear stress at its ends. Still another, pertaining to the region near the hot face, is that thermal healing of cracks accompanies periods of heating within the plastic or liquid-containing temperature range.

In cases of necessity, the refractory user has responded by reducing the frequency and magnitude of temperature transients. A notable example is in the use of silica refractories, wherein both the thermal anisotropy of quartz and the ΔV of the high quartz - low quartz transition (Figure IV-7) are damaging. By processing adaptations, furnace and kiln operators have greatly extended the life of these refractories by keeping them always above the transition temperature.

Differential Thermal Expansion in Composites

Here the term "composite" is restricted to mixtures of oxides with nonoxides. The commonest example in refractories is the "MgO+C" type. Numerous basic refractories containing one or both of carbon and graphite particles are on the market.[42-44] Clay-alumina and high-alumina refractories containing these particulates as well as SiC are also plentiful.[45-48]

The principal reason for constructing these composites is to improve corrosion resistance of the refractory (Chapter VI). But minute hard particles placed in the grain boundaries of oxide ceramics have been known for at least a half century to influence their tensile strength and toughness. In more recent times, toughening of ceramics by the use of fibrous reinforcement has received increased analytical attention,[29] though also antedated for decades by the

experimental use of chopped wire and then of "whiskers" (small fibrous single crystals) as inclusions. Some refractories have been made incorporating short-fiber reinforcement.[49-52]

In "MgO+C" type refractories the oxide grains are bonded interfacially by the carbon, which is made by pyrolysis in situ. In fiber-reinforced types, the toughening sought must also arise from interfacial bonding surrounding the inclusions, which is created at high temperatures in the course of sintering. Here we take a brief view of interfacial bonding in refractory composites as they are cooled from the temperature of their synthesis down to ambient.

A sufficient model is of a single particle of inclusion completely surrounded by the oxide host. If the volume shrinkage of the host exceeds that of the inclusion, the boundary between them will be increasingly compressed with decreasing T and accordingly strengthened. If the inclusion is fibrous, even if differential linear shrinkage in the axial direction should cause some unbonding of the interface, radial compression contributes to a potent frictional force resisting pullout of the fiber.[29] Conversely, if the volume shrinkage of the inclusion sufficiently exceeds that of the surrounding host, the interface may fail in tension leaving the two phases essentially unbonded. Frictional forces resisting pullout of a fiber are thereby also lessened or eliminated.

Thus the thermal stability of refractory composites depends not only on differences in linear and volume coefficients of thermal expansion. It becomes crucial, which phase's coefficient is the larger. Anisotropy matters as well but will be ignored here. The following table gives the pertinent parameters computed from data in Vol. 13 of Ref. 32, for some representative composite systems cooled from an assumed stress-free condition at 1000°C down to ambient (20°C). The "Δ" quantities are the *mismatch* in the unconstrained dimensions of the two conjugate phases at room temperature. For the volume and radial mismatch, "c" indicates compression and "t" indicates tension across the boundary. The length mismatch $\Delta L/L$, applicable to axial shear of fiber interfaces, is again given in nm at each end of a boundary per μm of length. The one case shown of an "Fe" inclusion is indicative for chopped wire reinforcing: most steel alloys including stainless have thermal expansion coefficients within ±15% of that of iron. Where "C" is shown for carbon as inclusion, averaged data for (anisotropic) graphite have been used.

Host	+	Inclusion	Larger Coefficient	ΔV/V, %	ΔR/R, nm/μm	ΔL/L nm/μm
MgO	+	C	MgO	c2.86	c9.54	4.77
Al_2O_3	+	C	C	t1.26	t4.21	2.10
MgO	+	SiC	MgO	c2.66	c8.86	4.43
Al_2O_3	+	SiC	Al_2O_3	c1.06	c3.52	1.76
Mullite	+	SiC	Mullite	c0.05	c0.18	0.09
Zircon	+	SiC	Zircon	c0.03	c0.10	0.05
MgO	+	Fe	Fe	t0.46	t1.54	0.77
ZrO_2	+	TiC	TiC	t0.10	t0.30	0.15
Spinel	+	TiC	Spinel	c0.40	c1.34	0.67

Carbon as a bonding agent in MgO is compatible in spite of the above, as the inclusion is quite porous and compliant. Carbon or graphite in high-alumina refractories risks becoming unbonded on cooling, but these composites rarely call on the inclusion as a bonding agent. Silicon carbide adapts well to several oxidic hosts whether it is included as particles or as fibers. Titanium carbide fibers may provide a better thermal expansion match than does SiC for some higher-expansion oxides such as ZrO_2 and $MgAl_2O_4$, as shown. Indeed, TiC is also better matched to MgO than is SiC. In a dense MgO+SiC (e.g., fiber-reinforced) system some local microcracking of the MgO might be anticipated, since the host is placed in circumferential tension about the inclusion by the large differential shrinkage.

Steel wire reinforcing of MgO appears from the data to risk tensile unbonding of the interface; but oxidation of the wire may result in a structurally stable system. Most other oxidic hosts would part from steel wire on cooling, by a much larger tensile mismatch. Fiber-reinforced composite refractories, if they are not too costly, may well follow rational guidelines such as these.

Thermal Stress and Shock Resistance

Steady-State Temperature Differentials. A simple origin of thermal stress in a refractory wall or layer lies in its functions of thermal insulation and conduction. In either case a ΔT or (T_2-T_1) exists between the hot face and the cold face of the wall or lining at steady state. Unrestrained solids, heated isothermally, expand reversibly in dimensions with increasing temperature by an amount expressed by the *linear coefficient of thermal expansion.* Close to the same expansion is experienced when one part of a body is hotter than another, even though these parts communicate elastically with each other. In that case the body becomes dimensionally deformed.

The equation which both defines and uses the linear coefficient of thermal expansion is:

$$dL/L = \alpha dT \quad ;$$

or, on integrating:

$$\Delta L/L_1 = \bar{\alpha}(T_2-T_1) \quad .$$

But $\Delta L/L_1$ is recognized as linear strain, ε, which in the elastic temperature range is:

$$\varepsilon = \Delta L/L_1 = \sigma/E \quad .$$

In these equations, α is the coefficient of thermal expansion. This is a property of each material composition, but it varies with temperature. Hence $\bar{\alpha}$ appears as a suitable average of α between temperatures T_1 and T_2. The strain is ε; and the imposed stress required to remove that strain is σ while E is the *Young's modulus* of elasticity of the material.

A number of engineering problems at steady state are approached using the above equations, or combining them to yield:

$$\sigma = E\,\bar{\alpha}(T_2 - T_1) \quad .$$

For example, if a cylindrical wall is installed stress-free at room temperature but is then operated at hot-face temperature T_2 and cold-face temperature T_1, σ above represents the restoring stress (applied or internal) that maintains the geometrical relation between inner and outer circumferences. If there is sufficient external restraint, as e.g. by a steel shell, there could be a net zero internal circumferential stress at the refractory cold face while the circumferential stress σ at the hot face would be compressive. Lacking any external restraint, the hot-face circumferential stress may be about $+\sigma/2$ (compressive) and the cold-face stress about $-\sigma/2$ (tensile).

A similar differential expansion occurs in the axial direction of the cylinder, of course. Consideration of its restraints, simultaneous with the circumferential, transforms the problem into one of *biaxial* stresses parallel to the hot and cold faces; but the above equality persists. Maximum compressive or tensile stresses in different refractory materials are seen to be proportional to their respective thermal expansion coefficients and their Young's moduli. But still another stress mode also pertains.

Take a straight flat wall of cold-face length L_1, for easy visualization. If

$$\Delta L/L_1 = \bar{\alpha}(T_2 - T_1) \ ,$$

then:

$$\Delta L/Z = L_1 \cdot \bar{\alpha}(T_2 - T_1)/Z \ ,$$

where Z is the thickness of the wall and $(T_2-T_1)/Z = dT/dz$ is the *temperature gradient* across the wall. Now $\Delta L/Z$ is recognized as the shear strain, γ, which in the elastic temperature range is:

$$\gamma = \Delta L/Z = \tau/G \ .$$

Here, τ is the corresponding shear stress and G is the *shear modulus* of elasticity. Combining these last two equations, one obtains:

$$\tau = L_1 G \ \bar{\alpha}(dT/dz) \ .$$

This equality also persists when biaxial stresses in the wall faces are recognized. It shows that the shear stress (which acts parallel to the wall faces) is proportional to the thermal expansion coefficient and the shear modulus of the material, but also to the lineal wall dimensions and to the temperature gradient across the wall. These proportionalities also apply in cylindrical, spherical, and other wall geometries.

The appearance of the lineal wall dimension L_1 in the above equation is the single overriding reason for the historical use of masonry construction in refractory installations of any appreciable size and thickness. Centuries ago the sizing of refractory bricks and blocks to avoid shear failure (or alternatively, excessive warping) was approached empirically. Now it is confirmed analytically.

Once brick construction has been decided upon for a cylindrical furnace lining, then it is illuminating to return to the equation:

$$\sigma = E \ \bar{\alpha}(T_2 - T_1) \ .$$

As was noted, σ in this equation can be regarded as the difference between circumferential tensile stresses on the cold face and compressive stresses on the hot face. If externally unconstrained, bricks are prone to separate toward the cold face by tensile failure of their mortared joints. If sufficiently constrained, they experience the full compressive circumferential stress σ at the hot face.[53,54] In small

sections, brittle materials under compressive load fail in shear along crack paths making angles variously near 45° with the principal axis of compression, for well-understood reasons.[15] Thus if a lining failure occurs, the patterns of cracking observed give a strong indication of the design cause. Compensations in lining design can take numerous forms, such as (a) changes in overall brick dimensions (including in Z, affecting ΔT); (b) use of dual linings (working lining plus insulating backup, markedly reducing ΔT in the former): and (c) providing tapered spacings between bricks, with or without various kinds of fillers or pads, such that these gaps become closed but without excessive compressive loads when the steady-state operating ΔT is established.[56,57] The gaps open up again on cooling, of course, but re-close on re-heating.

Properties appearing or implied in the sets of equations above include the tensile, compressive, and shear failure strengths, the elastic moduli E and G, and the coefficient of thermal expansion, α. Among these, the last-named is the only one that is essentially microstructure-insensitive, i.e., intrinsic to composition. It also varies over an exceptionally wide range from substance to substance, hence becoming a useful and proportional index of susceptibility to failure under thermal stress.

Temperature Transients. Steady-state thermal stresses were described first here because their analysis is relatively straightforward. But substantially larger stresses arise in service in consequence of a rapid rise or fall of the hot-face temperature of a refractory wall, lining, or other component. When such transients are extremely large and rapid, the consequence is referred to as thermal shock; but thermal stress and thermal shock are the same phenomenon, and there is no boundary between one and the other.

A rapid rise in hot-face temperature may occur when any furnace or kiln is started up. Other rapid temperature increases accompany the filling of furnaces, ladles, troughs and runners with hot liquid metal; the opening of a gate valve or taphole for metal or slag discharge; and the closing of a port or door in a hot furnace after it has been open for a time. Still another example is in the reciprocal operation of regenerative heat exchangers. Rapid chilling accompanies the shutdown of a furnace or kiln or the turn-down of an oxygen-blown steelmaking vessel; the opening of a charging door or port; and again the reciprocal operation of any hot processing device.

The onset of a temperature transient is marked by a large change in the heat flux, J, at the refractory hot face after some near-steady-state condition may have been in effect. The instant response in the material is a correspondingly large change in dT/dz at the hot face, together with a time-dependent change dT/dt. Heat flow at steady state is governed by the *thermal conductivity*:

$$J = -k(dT/dz) \quad ,$$

where J is heat flux in joules sec^{-1} m^{-2} or equivalent units, k is the thermal conductivity in compatible units, and dT/dz is the local temperature gradient (e.g., in the thickness direction of a refractory wall). But when the temperature of each volume element of the refractory also changes with time, the *heat capacity* or *specific heat* is simultaneously involved. J, which in a simple steady-state case is constant with both position and time, becomes in the transient case a function of both: $J = J_{x,y,z,t}$. The material property required in the transient case is the *thermal diffusivity*, δ, defined by:

$$\delta = k/(c \cdot \rho) \quad .$$

Here k is thermal conductivity, c is specific heat, and ρ is density. All of these quantities will be catalogued in later chapters; suffice it for now to note that every one is a function of temperature.

Finite-interval methods of numerical (i.e., computer) analysis make possible the position- and time-dependent description of temperature transients, even in unconventional geometries, if the material is reasonably homogeneous.[53-58] The solutions have certain characteristics in common, which may be generalized as shown schematically in Figures IV-8a and b. For simplicity we use only the position coordinate z, from z = 0 (hot face) to z = Z (cold face).

In both figures an *initial* (i.e., pre-transient) steady-state wall condition is depicted, showing constant dT/dz < 0 at time t < 0. At time t = 0 a step change is made in the heat source exposed to the hot face, giving an increased J in Figure IV-8a and a decreased J in Figure IV-8b. The source of the transient is idealized, such that a *final* steady-state wall condition is approached asymptotically as $t \rightarrow \infty$.

Several schematic temperature profiles are shown in each figure, as might be recorded instantaneously at successively increasing times, $t_1 \ldots t_5$, after the step change in the hot-face environment. The slope at any point on each curve is the gradient dT/dz at that point. The steepest branches of these curves are seen to increase in absolute slope with decreasing elapsed time; but the slopes never become infinite. The curves engage progressively smaller thicknesses of material with decreasing time. One could as well mark off an absolute ΔT on the steep branch of each curve, noting that this ΔT increases with time especially early-on in Fig. IV-8a and actually goes through a maximum early-on in Fig IV-8b.

Heating Transients. It is clear from Figure IV-8a that a refractory panel or wall, constrained at its cold face and abutted under the initial steady state condition, will experience large biaxial compressive stresses nearest the hot face upon a heating transient.

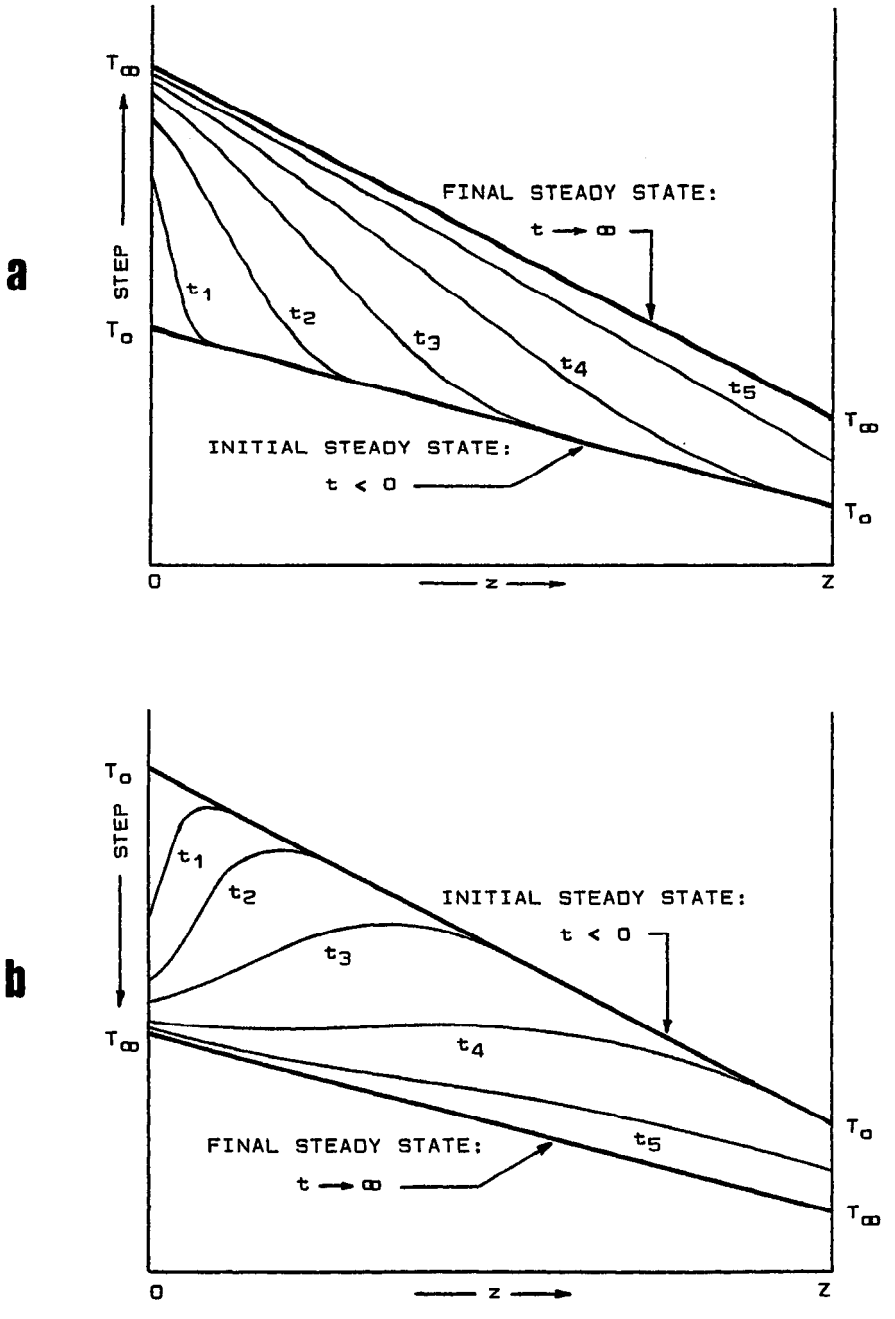

Figure IV-8 Schematic Temperature Transients Imposed on a Refractory Wall
a. Heating Transient b. Cooling Transient

As the ΔT of the hot curve branches increases with time, the compressive stress σ_c does too, by:

$$\sigma_c = E\,\bar{\alpha}\Delta T \quad .$$

If the compressive strength is exceeded at any point in time, cracking will occur; in general this will be at some time $t > 0$. As previously mentioned, failure in compression is by shear at a preferred 45° to the compressive forces; this shear initiates near the hot face and near the edges of each single brick, typically taking off corners. In a monolith it will typically take out wedge-shaped *spalls*.

Meanwhile, shear stresses parallel to the hot face are also at work, by:

$$\tau = LG\,\bar{\alpha}(dT/dz) \quad .$$

As the transient dT/dz is very large and occurs very early, shear cracking parallel to the hot face is also expected even in bricks where L (the hot face dimension) is small. But shear cracking reduces the remaining effective L, so that this type of crack may not progress all the way across a brick. Compression of a monolith, on the other hand, can combine parallel shear with 45° shear, taking out slabs.

Cooling Transients. The reversal in sign of dT/dz near the hot face, seen in the curves of Figure IV-8b, places the hot face in biaxial tension relative to the bulk of the refractory in a cooling transient. Since the ΔT of the hot-face curve branches increases and then goes through a maximum with time, the tensile strength of the material is likely to be exceeded a short time after the transient is initiated, by :

$$\sigma_t = E\,\bar{\alpha}\Delta T \quad .$$

Cracking in tension starts at the hot face and progresses parallel to z; but as cracks grow in a brick they readily interact with the shear stresses and may turn out to the side at some depth. A monolith, on the other hand, may simply *craze* (form a network of cracks) on the hot face. In that case cracking stops at some depth, leaving the material intact except for occasional subsurface interactions that may take out small plugs. Owing to installation and curing stresses, surface cracks in a monolith can join into erratic lines running considerable lengths across a hot face; but again, the material tends to remain intact unless there is a subsurface bonding flaw or *lamination* (typically occurring in repairs or patching). Then isolated slabs may become detached.

Once cracking arrays are started under either a heating or a cooling transient, they are most often extended under *repetitive*

thermal cycling.[36,37,59,60] Thus mechanical damage tends to be cumulative. Standardized thermal stress tests and ratings of refractories[9] take this cumulative quality into account; but its prediction from first principles is quite unreliable.[29] Here we must continue to address thermal stress and shock resistance in terms of the first large transient experienced.

Index of Thermal Stress and Shock Resistance. In transients the prevailing dT/dz was long ago shown to be proportional to the inverse square root of the thermal diffusivity,[3] while the derived stresses remain related to dT/dz by the coefficient of thermal expansion just as in the steady-state case. But when $\delta = k/(c \cdot \rho)$ is computed for various oxidic compounds (i.e., all of low k), and then the square root taken, the numerical results fall consistently in a narrow range. It follows that under transients as well as at steady state, the only pertinent material property that ranges widely and is at the same time substantially microstructure-independent is the thermal expansion coefficient, α.

Thus α is a sufficient index of thermal stress and shock resistance of refractory phases. But it should be observed that all of the other matters of microstructural integrity discussed in the preceding sections also apply to behavior under single and repeated thermal stress. Real refractories accordingly do not lay themselves out neatly in order of thermal stress resistance, indexed precisely by α or any combination of easily-measured properties. Features of microstructure that increase thermal cycling resistance are (a) high porosity; (b) microcracks; and (c) low bonded area between crystals, i.e., under-sintering. It is intuitive that all of these increase local compliance and the energy of fracture in a material. But despite years of attempts to describe the toughening of brittle materials by microvoids,[61-64] no really adequate quantitative expression of the relationships has emerged.[29,36] These enumerated features have been incorporated empirically.

A convenient way of representing α for present purposes is to plot the reversible percent linear expansion, $100 \cdot \Delta L/L_o$, vs temperature from room temperature up. Here L_o is measured at T_o = 20°C. The equation to be plotted is:

$$100\Delta L/L_o = 100\ \bar{\alpha}(T - T_o) \quad .$$

One of the best compilations of such reference data is in Vol. 13 of the multi-volume set, "Thermophysical Properties of Matter," published by Plenum Press in 1970.[32] Selected data from that source are plotted in the above fashion in Figures IV-9a and b and in Figure IV-10. The two-branched curve for quartz in Figure IV-9a does not incorporate the volume change of the low quartz - high quartz transition; that

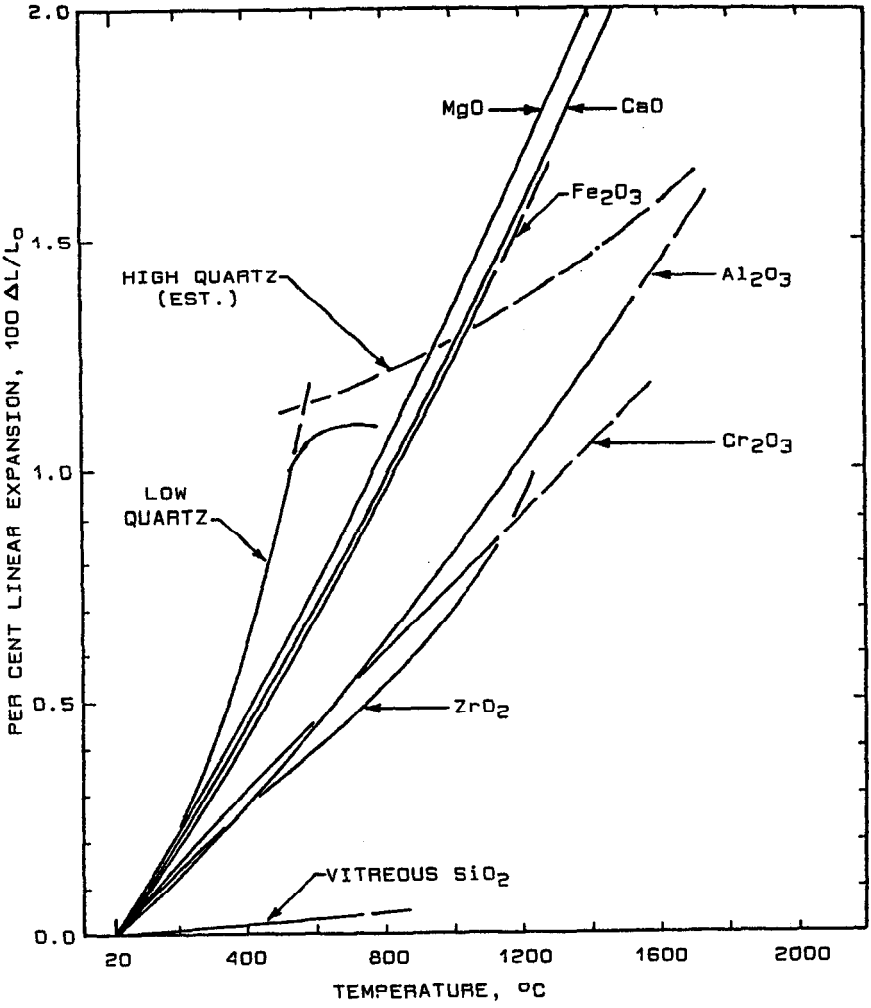

Figure IV-9a Thermal Expansion of Simple Oxides (Ref. 32)

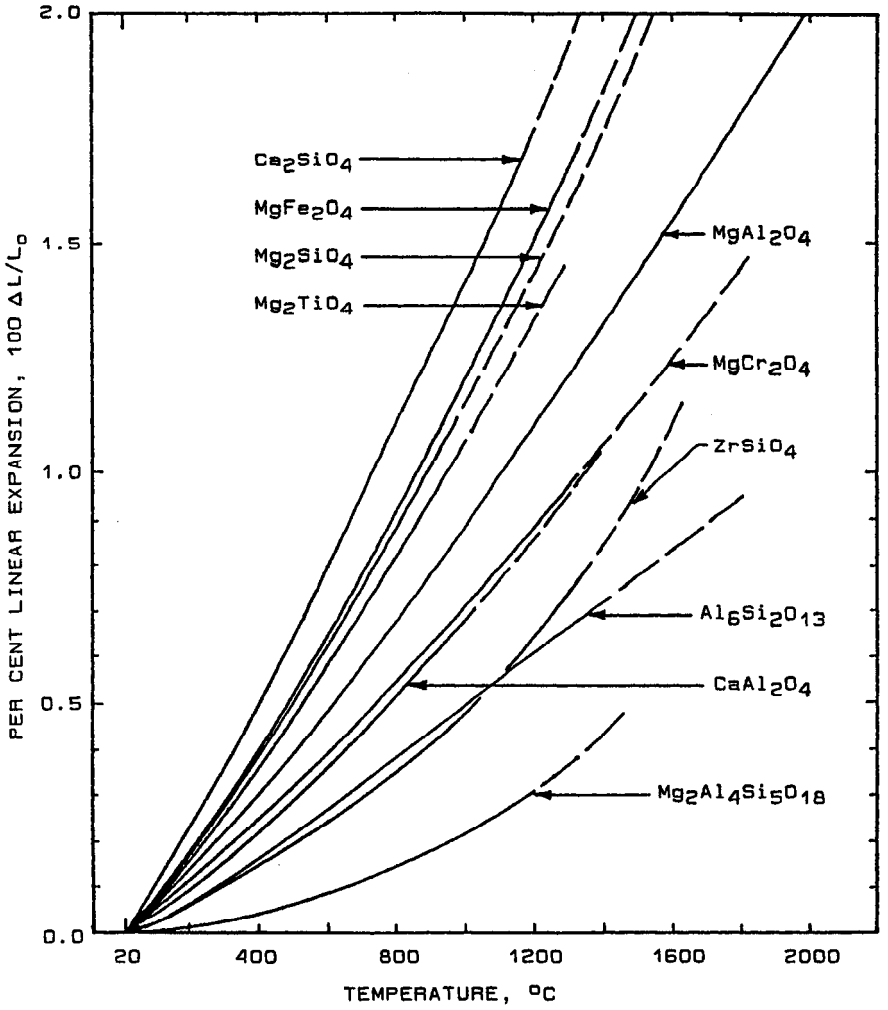

Figure IV-9b Thermal Expansion of Ternary Oxides (Ref. 32)

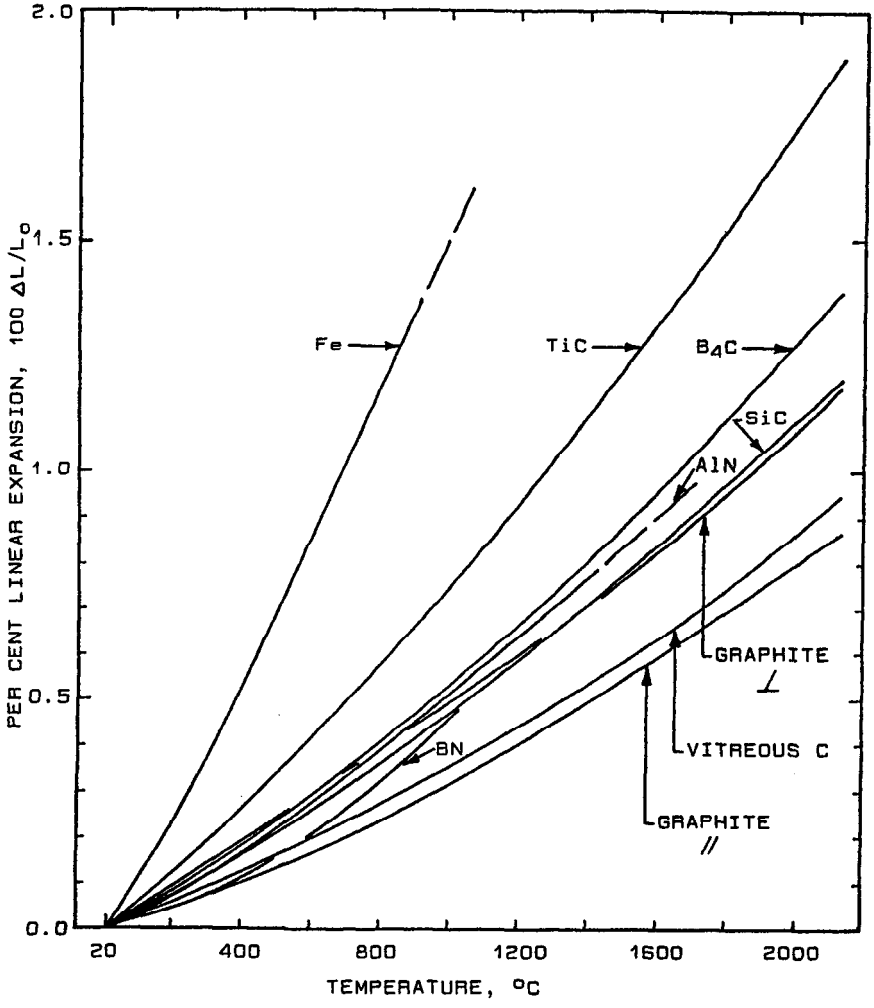

Figure IV-10 Thermal Expansion of Nonoxides (Ref. 32)

feature is better displayed in Fig. IV-7. But here the exceptionally large thermal expansion of low quartz is placed in perspective by plotting it alongside that of other oxides on the same ordinate scale.

Low quartz and the alkaline earth oxides MgO and CaO are judged from Fig. IV-9a to be prone to failure under thermal stress and shock. By contrast, high quartz and vitreous silica are adjudged to be thermal-stress-resistant. Beta-spodumene, a crystalline lithium aluminum silicate (not shown), also exhibits near zero expansion up to ~1000°C.[65] Figure IV-7 shows that high cristobalite and tridymite I share this quality if their transitions are ignored.

The top four curves of Figure IV-9b are quite comparable to those for MgO and CaO. Striking familial similarities in Figures IV-9a and b are those between Fe_2O_3 and $MgFe_2O_4$, Al_2O_3 and $MgAl_2O_4$, Cr_2O_3 and $MgCr_2O_4$, and ZrO_2 and $ZrSiO_4$. These last two appear relatively thermal-stress-resistant up to about 1000°C. Mullite, $Al_6Si_2O_{13}$, is comparable but without such a limitation on T. Calcium aluminate, $CaAl_2O_4$, is included in Figure IV-9b as this is a cement-bonding phase much used in high-alumina refractories; its expansion is seen to be compatible with those of Al_2O_3 and the important spinels. And finally in that figure, the low expansion of cordierite, $Mg_2Al_4Si_5O_{18}$, suggests high thermal stress resistance.

On the other hand, the *nonoxides* of Figure IV-10 are all relatively good conductors of heat. Thus in spite of the high thermal expansions of a few of these, all are relatively resistant to thermal stress and shock. Graphite is here represented by two curves, showing the expansion respectively perpendicular and parallel to the preferred orientation of graphite basal planes in polycrystalline products. It is very difficult to prepare an industrial carbon or graphite which is not significantly anisotropic.

The lowest thermal expansions in these three figures are exhibited by vitreous silica, cordierite, vitreous carbon, silicon carbide, graphite -- and granular carbon by inference. The first two are both limited to about 1000°C service in air, but cordierite is far cheaper to produce. Vitreous silica, while occurring as an incidental constituent of high-silica refractories, is synthesized as a pure single-phase material only for special technical purposes on account of its high cost. Vitreous carbon has the same limitations. Silicon carbide continues to see increasing use in severe thermal stress situations in spite of relatively high manufacturing cost, as it combines a number of valuable properties.

The roster of cheap oxidic refractory compounds exhibiting low thermal expansion is disappointingly short. Where dense oxide refractories are required for corrosion resistance, a deficiency in their stability under thermal stress and shock usually has to be abided. By

controlling their thermal stress environments, however, users have often been able to adapt to this fault. For high-corrosion applications such as steelmaking, the trend in refractory formulation is to improve corrosion resistance even at a sacrifice in thermal stress resistance. That trend is microstructural as well as compositional, moving toward higher chemical purity, toward lower and finer porosity, and toward more effective sintering or bonding of refractory phases.

Permanent Deformation

There are ample engineering uses of the thermal expansion coefficient in respect to *reversible* expansion and contraction of refractories.[36,37,53-60,65] These uses have not been emphasized here because they are simple and familiar. The phenomena in this chapter, by contrast, all represent risks that a refractory may sustain irreversible microstructural changes on exposure to thermal excursions. Additional to such consequences as mechanical weakening or possible fracture, these *irreversible* changes usually result in *permanent deformation* upon a return to room temperature. In brief review, the most important of these phenomena and their potential consequences are:

Phenomenon	Occurs Under	Potential Consequences
Partial Melting	Hi T	ΔV; Plastic Distortion, Creep
Recrystallization, Devitrif.	Hi T	Microcracking, ΔV
Solid Phase Change	ΔT	Microcracking, Ratcheting, ΔV
Anisotropic Exp./Contr.	ΔT	Microcracking, Ratcheting, ΔV
Differential Exp./Contr.	ΔT	Microcracking, Ratcheting, ΔV
Thermal Stress, Shock	ΔT	Cracking, ΔV, Fracture

Not all of these phenomena occur in every refractory; nor is each one necessarily inescapable, given latitudes in the compositional and microstructural design of each refractory material. But these materials have to meet criteria of refractoriness, corrosion resistance, strength, thermal conductivity, cost, etc., all at the same time. Compromises are the rule. From the user's point of view, first of all a given refractory must be fit for its duty, which may include setting limits on some of the above phenomena individually. Beyond this, the permanent deformation sustained in service is somewhat negotiable, so long as it is not indefinitely cumulative. To this end standard tests have evolved, which measure the permanent or irreversible deformation occurring under specified test conditions but do not concern themselves with which phenomena contribute to the net result. One such type of standard test is called the "reheat change."[9] Its output is expressed as percent linear change after heating and then cooling.

If the "reheat" test conditions relate to those of use, then the test results can be interpreted in terms of refractory performance. A considerable reheat shrinkage, for example, means that a brick lining will pull away from its steel containment and/or will open gaps in its mortared joints. Consequences in a rotary kiln or a steelmaking furnace can be readily foreseen. Reheat shrinkage of a monolithic refractory preparation could disqualify it for lining a coreless induction furnace, or for patching purposes where it is intended to match the expansion and contraction of a seasoned lining. A reheat expansion could be equally unfortunate for patching, while in a new lining an excessive reheat expansion might forewarn of compression-spalling problems.

Modern refractories can be formulated to meet reheat change specifications. Permanent shrinkage can be minimized, for example, by using pre-sintered particles of the major phase(s) and by sizing and packing these under high pressure so that they are in extensive mutual contact. Then shrinkage of the minor phase(s) in sintering of the mixture cannot cause the major phase(s) to shrink appreciably.

Linings for ladles present a still further challenge, however. Chapter III pointed out that special provisions are required to prevent hot metal from penetrating the lining and reaching the steel shell. Yet the repeated thermal shock of filling a ladle is intense, and cracking of the lining has to be expected. The challenge is to keep the lining in compressive contact with the shell, so that cracks remain closed while temperatures are high.

Ladle linings are installed in firm contact with the shell, but at ambient temperature. Comparing the thermal expansion curve for Fe in Figure IV-10 with those for oxides in Figures IV-9a and b, it is seen that on first heating the shell will part from the refractory unless a permanent expansion can be added to the reversible thermal expansion of the latter. A positive reheat change is called for.

This was achieved for many years, and still is, by including in monolithic clay and clay-alumina refractory formulations a so-called *bloating clay.* Bloating clays contain organic matter which foams and swells in the course of heating, before ceramic bonding of the clay-derived oxides sets in. Their deficiency in this for steelmaking ladles is, however, that the hot face sees liquid metal at 1500°-1600°C or higher while the back side is much cooler. This range is too wide for thermal sintering throughout the thickness. If enough sintering occurs at the cold face to bond the refractory there, too much melting occurs at the hot face. Alteration and freeze-thaw cycling in the hot layers will then shorten the refractory life and presently lead to a general shrinkage that reverses the original swelling.

In a brilliant material redesign, modern monolithic steel ladle refractories are formulated to swell on initial heating but are *chemically bonded* rather than thermally sintered. Much higher-melting compositions than clays alone can be used, including MgO-based "basic" linings and high-alumina "acid resistant" linings. Phosphate chemicals are among those chosen for bonding. Curing at the cold face sets up the material there, while at the hot-face temperature the chemical bond reverts slowly to oxide bonding but without melting. The original positive reheat change is thus preserved, and lining life is greatly extended. These refractories can face hot metal at the 1700°C now required in steelmaking.

When such a ladle is emptied and cooled, it is true that the steel shell then places the refractory cold face in elastic compression. But the steel and the cold face cycle over a span or ΔT of only some 400°C or so, while the hot face cycles over a span some three times as large. The hot face itself is accordingly in tension when cold and in compression when hot: ideal conditions for the retention of hot metal and for keeping cycling damage to a practical minimum.

It is appropriate to close with a positive observation on all of the aspects of thermal stability discussed here. These once gave rise to refractory performance limitations before which the technologist stood largely helpless. Today they are sufficiently understood to be designed-around when necessary, and in the best cases to be harnessed for effective product selection and design. On the more sobering side, nonetheless, is that the microstructural features favoring a refractory's ability to withstand aggressive thermal experiences are on the whole unfavorable to its corrosion resistance. We shall proceed next to develop the compositional and microstructural bases for meeting the *chemical* environments of hot processing.

Chapter V

Principles of Corrosion Resistance: Oxidation-Reduction

IMPORTANCE OF CORROSION

Working refractories are differentiated above all else by their thermal stability and corrosion resistance. Corrosion most often determines refractory life, and often enough sets the temperature limit on the contained process. Control of corrosion motivates or tempers nearly every modern working refractory improvement.

For these reasons we take up high-temperature corrosion and corrosion resistance in the next three chapters, before listing the product line in Chapter VIII. Corrosion resistance is a matter not only of refractory phase composition but importantly of microstructure. We shall develop the fundamentals in these three chapters, illustrating each with examples of real refractories and real applications. We start here with redox alteration.

GIBBS FREE ENERGIES

One way to anticipate corrosion reactions of refractories is to employ some established thermodynamic properties of their compounds. The necessary definitions and methodology are reviewed first; then a number of applications of thermodynamics to significant refractory exposure and consequences will be described.

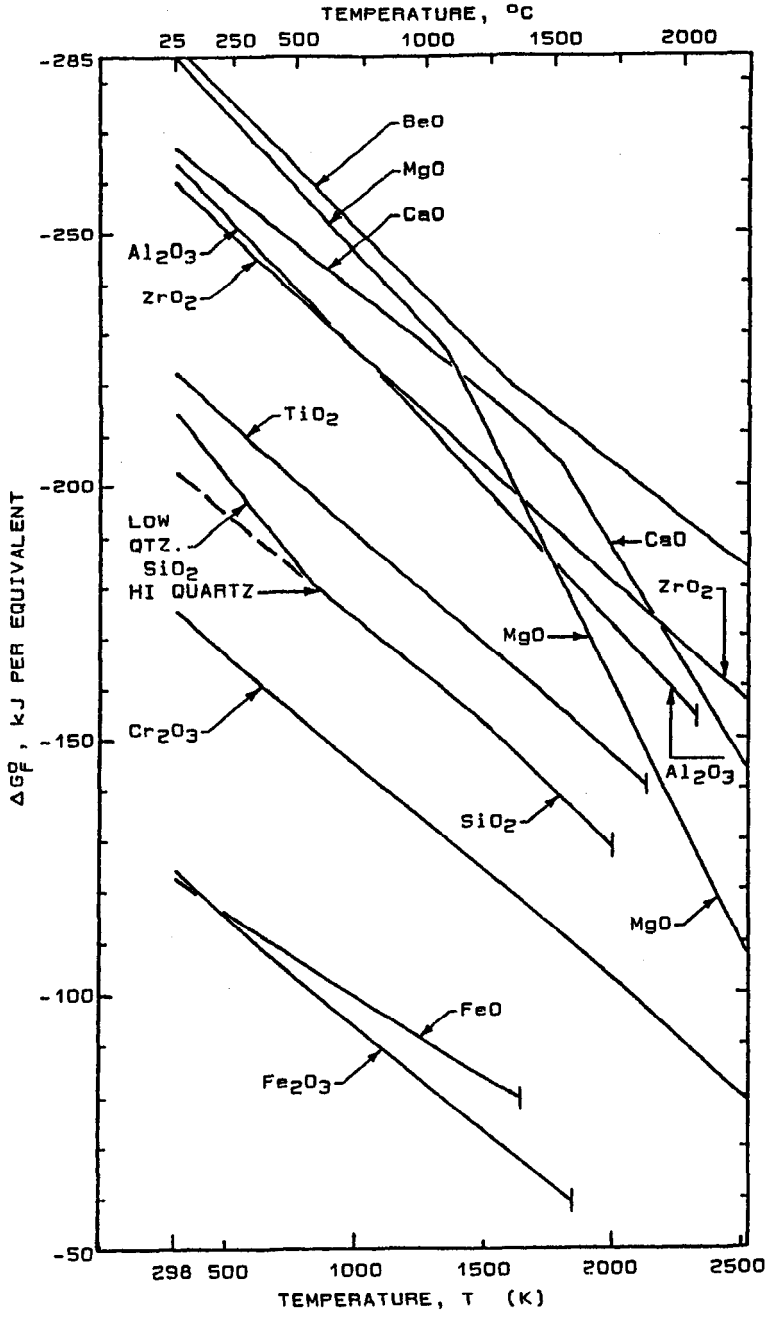

Figure V-1a Free Energies of Formation of Simple Oxides vs T, per Equivalent (Ref. 23)

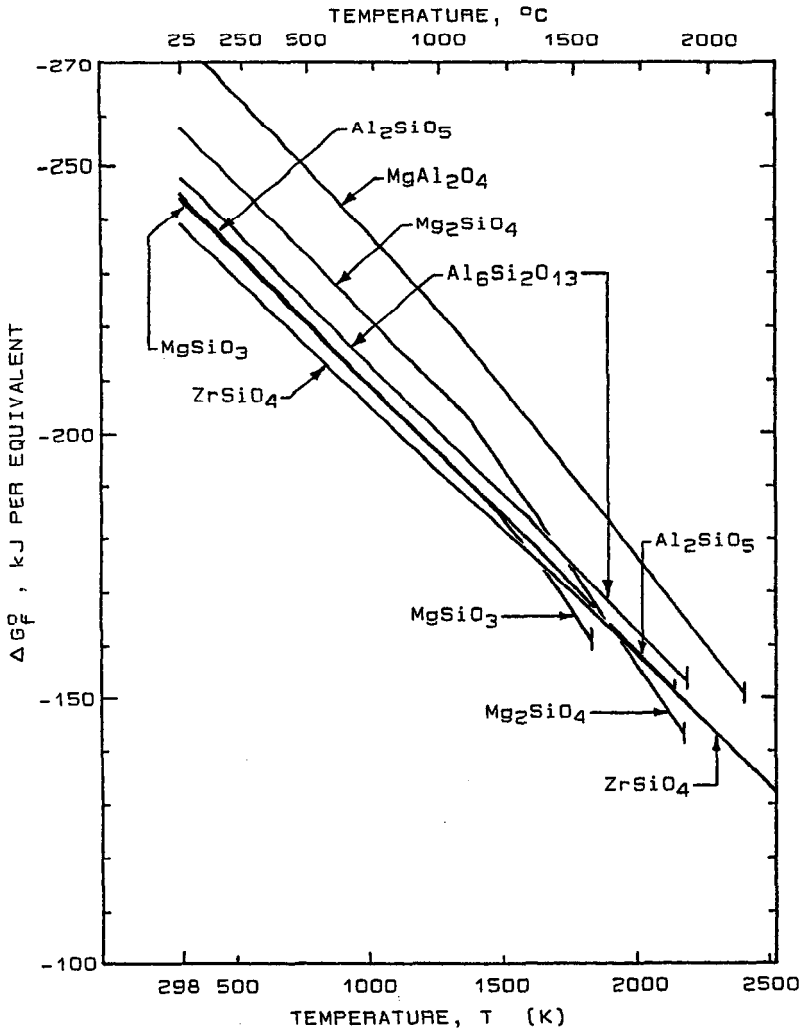

Figure V-1b Free Energies of Formation of Ternary Oxides vs T, per Equivalent (Ref. 23)

Standard Free Energies of Formation of Compounds

The quantity $\Delta G°_{f,298}$ was introduced in Chapter IV and in Figure IV-2. This is the *standard free energy of formation.* It is the total energy difference, expressed in kilojoules, between *one mol* of a compound and the corresponding amounts of its elements at the same temperature. If $\Delta G°_f < 0$ the compound is the more stable, and conversely. To call ΔG_f "standard," by the "°" sign, is to say that the compound and its reagent elements are all in their "standard states" at the designated temperature, namely: (a) the stable crystalline solid if below its m.p.; (b) the pure liquid if above its m.p.; and (c) the "ideal" gas at 1 atm. partial pressure if above its b.p. A constant total pressure of 1 atmosphere is also assumed.

Our first object here is to present $\Delta G°_f$ for refractory compounds at all temperature of interest. Figures V-1a and V-1b display these quantities. Once again we show $\Delta G°_f$ *per redox equivalent* rather than per mol. The basis for this choice is the equation,

$$-\Delta G° = nFE° \qquad \text{or} \qquad E° = -\Delta G°/nF \ ,$$

in which n is the number of redox equivalents per mol of compound and F is Faraday's constant (see Table II.1). Thus $-\Delta G°_f/n$ is proportional to $E°_f$, which is the standard driving force for the formation reaction in volts -- an intrinsic quantity permitting the direct comparison of compounds of different formulas.

Figure V-1a is a plot of $-\Delta G°_f/n$ vs T for simple binary oxides. The ordinate scale is reversed so that the most stable compounds are uppermost. The principal reason for the downward slope in all cases is that $0_{2(g)}$ is a reagent in all cases and its pV product increases linearly with T. This is reflected in its own G°. The "knee" in the curves for Mg0 and Ca0 occurs at the metal boiling-point, reflecting a change in standard state of the metal and a further pV effect of $Mg_{(g)}$ and $Ca_{(g)}$ at temperatures above that change. The bar terminating most of the curves signifies the m.p. of the compound.

Figure V-1b is a like plot for a number of ternary oxidic compounds. As most of them are silicates, note that these are all more stable than $Si0_2$ and all but $MgSi0_3$ are higher-melting.

Apart from giving direct comparisons of thermal stabilities, the free energy of formation *per equivalent* introduces more risks of misuse than it does conveniences. For all remaining purposes we recommend $\Delta G°_f$ in the conventional units. An abbreviated reference table of standard free energies of formation vs T (K) is given as Table

Table V.1 Free Energies of Formation of Oxides vs Temperature (Ref. 23)

	M.p., K	n[a]	$-\Delta G_F^\circ$, kJ/mol, AT TEMPERATURE T (K)										
			298	400	600	800	1000	1200	1400	1600	1800	2000	2400
Al_2O_3	2327	6	1582.3	1550.3	1487.4	1424.9	1361.4	1295.1	1229.2	1163.7	1098.5	1033.7	(liq.)
BeO	2723	2	574.7	564.1	543.3	522.6	501.8	481.1	460.3	439.6	423.9	408.3	377.1
CaO	3200	2	533.0	524.7	508.8	493.2	477.6	461.2	444.1	427.3	407.8	374.0	307.5
Cr_2O_3	2603	6	1053.1	1025.6	972.6	920.9	869.8	819.3	768.9	718.4	667.8	616.8	508.8
Fe_2O_3	1838	6	743.6	715.8	662.8	611.7	562.2	512.7	463.3	414.4	365.7	(liq.)	
MgO	3125	2	569.0	557.9	536.3	514.9	492.8	469.6	444.3	402.7	361.5	320.7	239.9
SiO_2 (LOW QTZ.)		4	856.5	834.1	790.2	735.2	(Tr. ~873K)						
" (HI)	1996	4	810.4	792.8	761.2	728.6	695.8	661.6	627.7	590.6	551.1	(liq.)	
TiO_2	2130	4	889.5	870.6	834.1	798.2	762.8	727.5	691.9	656.6	621.6	586.1	(liq.)
ZrO_2	2988	4	1039.7	1020.1	981.9	944.3	907.1	870.1	832.9	796.4	760.4	724.5	650.0
$Al_6Si_2O_{13}$	2193	26	6441.9	6312.5	6058.4	5806.3	5551.4	5289.2	5028.5	4769.4	4504.8	4236.6	(liq.)
Al_2SiO_5	2143	10	2444.5	2394.0	2294.7	2196.4	2097.2	1995.7	1894.8	1794.6	1691.7	1587.0	(liq.)
$MgAl_2O_4$	2408	8	2182.1	2148.5	2066.1	1984.4	1900.8	1813.4	1724.3	1619.6	1515.8	1412.9	1209.9
Mg_2SiO_4	2183	8	2057.9	2017.2	1937.5	1858.4	1778.4	1696.6	1611.2	1493.7	1373.9	1252.7	(liq.)
$MgSiO_3$	1830	6	1462.1	1432.3	1374.0	1316.1	1257.9	1199.0	1138.4	1061.8	982.2	(liq.)	
$ZrSiO_4$	2673	8	1909.5	1870.4	1794.0	1718.6	1644.0	1570.1	1496.3	1423.0	1346.7	1268.2	1109.3
CO_2	Gas	4	394.4	394.7	395.2	395.6	395.9	396.2	396.3	396.4	396.4	396.4	396.3
CO	Gas	2	137.2	146.3	164.5	182.5	200.2	217.8	235.1	252.2	269.2	286.0	319.2
$Fe_{0.95}O$	1642	2	245.2	238.1	224.9	212.2	199.5	186.5	173.5	160.8	(liq.)		
H_2O	Gas	2	228.6	223.9	214.0	203.5	192.6	181.5	170.1	158.7	147.2	135.6	112.3
H_2S	Gas	2	33.4	37.4	44.4	51.0	41.3	31.4	21.5	11.7	1.8	-8.0	-27.6
SO_2	Gas	4	300.2	299.5	300.4	303.7	289.0	274.4	259.8	245.3	230.9	216.4	187.7
SO_3	Gas	6	371.1	362.3	342.8	327.2	294.0	260.9	228.0	195.4	162.8	130.4	65.9
SiO	Gas	2	127.3	136.4	153.8	170.8	187.4	203.6	219.6	235.3	247.4	256.7	274.7
NH_3, NO_x	(N_2O, NO, N_2O_3, NO_2, N_2O_5): All negative (i.e., unstable) above about 400K.												

NOTES: a- Number of equivalents per mol.

V.1. The JANAF Tables[23] were used to compile these data in kJ/mol, from which Figures V-1a and b were derived.

It is important to note that Table V.1 gives $-\Delta G°_f$. This avoids the nuisance of negative signs on nearly all the data. The table is divided into three groups of compounds: (a) binary refractory; (b) ternary refractory; and (c) non-refractory. Within each group the order is alphabetical by formula. The data for high quartz are sufficient for cristobalite at the highest temperatures, as their free energies are close.[23] The TiO_2 data are for rutile, the Al_2O_3 data for corundum.

The third group is comprised mainly of gases prominent in refractory use environments (Chapters II and III), plus $SiO_{(g)}$ and $Fe_{0.95}O_{(s)}$ (loosely called "FeO" or "wüstite"). A fourth group is implicit: $\Delta G°_f$ for every free element in its standard state at every temperature is *zero.*

Free Energies of Reaction

Standard Free Energies of Reaction. The notation $\Delta G°$, without subscript f, is the free energy change of a specified chemical reaction whose correct equation has been written, and all of whose reagents and products are at standard state. Showing the temperature in K as subscript is an option: $\Delta G°_T$ or $\Delta G°_{2000}$, etc.

Values of $\Delta G°_T$ are easily obtained. As example, take the reaction:

$$3\ MgAl_2O_4 + 7/2\ SiO_2 \rightarrow Al_6Si_2O_{13} + 3/2\ Mg_2SiO_4\ .$$

The rule for computing $\Delta G°_T$ from standard free energies of formation is:

$$\Delta G°_T = \Sigma\, \Delta G°_{f,T}\ (\text{products}) - \Sigma\, \Delta G°_{f,T}\ (\text{reactants}).$$

Applied to the above chemical equation, this means:

$$\Delta G°_T = \Delta G°_{f,T}\ (Al_6Si_2O_{13}) + 1.5\ \Delta G°_{f,T}\ (Mg_2SiO_4)$$

$$- 3\ \Delta G°_{f,T}\ (MgAl_2O_4) - 3.5\ \Delta G°_{f,T}\ (SiO_2)\ .$$

Transferring the coefficients of the chemical equation into the $\Delta G°_T$ *equation* has to be comprehended rationally before proceeding. It is universally required.

The lowest-melting substance involved in this reaction melts at 1996K. Let us take for the first T of inquiry, 1800K. From Table V.1, we then have:

$$\Delta G^\circ_{1800} = -4504.8 + 1.5(-1373.9) - 3(-1515.8) - 3.5(-551.1\ ) = -89.4\ \text{kJ}.$$

It should be clear that ΔG° *is for the chemical equation as written in mols.* Here it is only coincidentally per mol of mullite formed. Since it is <0, the reaction as written is spontaneous at 1800K.

It is calculated for this same reaction that $\Delta G^\circ_{1600} = -84.0$; $\Delta G^\circ_{1400} = -75.5$; $\Delta G^\circ_{1200} = -78.3$; and $\Delta G^\circ_{1000} = -81.3$ kJ. The unfamiliar reader may want to confirm these.

Free Energies and Rates of Reaction. The standard ΔG° for a chemical reaction does not yield much information by itself. The next sections will show how it is more effectively used. However, we must digress here to emphasize that *free energies of reaction do not necessarily dictate reaction kinetics.* One of numerous troublesome examples is in the formation of mullite refractories by firing mixtures of clays or silicas with bauxite or alumina. A good enough simulation is:

$$3\ Al_2O_3 + 2\ SiO_2 \rightarrow Al_6Si_2O_{13}\ .$$

Using the data of Table V.1 at 1800K, we have:

$$\Delta G^\circ_{1800} = -4504.8\ - 3\ (-1098.5) - 2\ (-551.1) = -107.1\ \text{kJ}\ .$$

At lower temperatures ΔG° for this reaction remains a large negative number. Yet refractory syntheses aimed at mullite as a major phase typically fall far short of complete reaction unless the raw materials are sintered together at very high temperatures with copious liquid phase present, or else are fusion-reacted. Mullite simply does not nucleate and grow readily from solids. Similar kinetic difficulties accompany the formation of crystalline silica and the refractory spinels $MgAl_2O_4$, $MgCr_2O_4$, etc., by solid-state reactions even in the presence of some liquid phase.

Nonstandard Free Energies of Reaction. Inquiries about corrosion reactions have to deal with substances that are not in standard states. Examples are (a) substances in solution, and (b) gases at other than 1 atm. partial pressure. A fundamental thermodynamic relationship is:

$$\Delta G_T = \Delta G^\circ_T + RT\ln Q\ ,$$

where ΔG_T is the free energy change of a reaction involving at least one substance in a nonstandard state, and ΔG°_T is now familiar. R is the gas constant (see Table II.1) and Q is an *activity quotient* which we shall next define. But first let us transform natural ln to $\log_{10}$ and incorporate that conversion factor with R numerically:

$$\Delta G_T = \Delta G°_T + 0.01914\ T \log Q, \quad \text{for } \Delta G \text{ in kJ.}$$

The algebraic definition of Q is best given using an utterly generalized chemical equation, written with capital letters representing formulas and lower-case letters representing their coefficients. Q is a function of their chemical *activities*:

$$\textit{Reaction}: \quad uU + vV + ... \rightarrow xX + yY + ... \ ;$$

$$\textit{Quotient, Q}: \quad Q = [(a_X)^x(a_Y)^y....] / [(a_U)^u(a_V)^v....] \ .$$

It remains only to specify the chemical activity of each substance, a_X etc., by use of the following guidelines. If a participating substance X is:

1. In its standard state, $a_X = 1$;
2. A gas (above its b.p.), a_X = its partial pressure p in atm.;
3. A solvent or host, a_X ~ its mol fraction;
4. A solute, a_X ~ its concentration as fraction of the saturation value.

The above equation for nonstandard ΔG_T is used when $\Delta G°_T$ is known and *every activity is known or can be estimated.* As example, suppose a silica refractory wall has a hot-face temperature of 1527°C or 1800K and is exposed to a process atmosphere of 90% C0, 10% $C0_2$ (1 atm. total). An inquiry can be made as to reduction of $Si0_2$ to $Si0_{(g)}$:

$$Si0_2 + C0_{(g)} \rightarrow Si0_{(g)} + C0_{2(g)} \ .$$

An allowable-recession-rate calculation suggests that a partial pressure of $Si0_{(g)}$ of 10^{-3} in the furnace atmosphere is tolerable. The question asked is, Under these conditions will ΔG of this reaction be positive or negative?

First one obtains $\Delta G°_{1800}$ using Table V.1. This is, -247.4 (for Si0) -396.4 (for $C0_2$) + 551.1 (for $Si0_2$) + 269.2 (for C0), or +176.5 kJ. Then all the given activities are collected: $a_{Si0} = 1{\cdot}10^{-3}$; $a_{C02} = 0.1$; $a_{Si02} = 1$; $a_{C0} = 0.9$ (call 1.). From these and the chemical equation above, $Q = (0.1{\cdot}10^{-3})/(1{\cdot}1) = 1{\cdot}10^{-4}$; and finally, $\Delta G_{1800} = 176.5 + 0.01914{\cdot}1800{\cdot}\log 10^{-4} = 176.5 - 137.8 = +38.7$ kJ. This result being >0, the above reaction is spontaneous *in reverse* at $p(Si0) = 10^{-3}$ atm.; hence that partial pressure will never be reached at 1800 K.

Free Energies and Chemical Equilibrium

By far the most powerful use of thermodynamics in assessing refractory corrosion entails *equilibrium* calculations. Given $\Delta G_T = \Delta G°_T + 0.01914\ T \log Q$ from the preceding section, equilibrium occurs at some unique set of nonstandard conditions under which $\Delta G_T = 0$. That is, there is no driving force for reaction in either direction. If $\Delta G_T = 0$, then:

$$-\Delta G_T° = 0.01914\ T \log K \qquad \text{or} \qquad \log K = -52.25\ \Delta G°_T/T.$$

The numerical factors here are given for $\Delta G°_T$ in kJ. *K is the numerical value of Q at equilibrium.*

Given a chemical reaction of inquiry at a selected T, (a) its $\Delta G°_T$ is first obtained from data in Table V.1; (b) *K* which is the equilibrium value of Q is then determined numerically from $\Delta G°_T$ and T by the equation above; and (c) the algebraic expression of Q as a quotient of activities is determined by the chemical equation for the reaction. It is necessary only to fix or estimate enough of those activities to solve numerically for the remainder, setting Q = *K*.

We shall illustrate this computational process once. In the section above we found $\Delta G°_{1800} = +176.5$ kJ for the reaction $SiO_2 + CO \rightarrow SiO_{(g)} + CO_2$; and we found ΔG_{1800} for a specified full set of activities. If instead we want to describe equilibrium for that reaction at 1800K, with $\Delta G°_{1800}$ in hand we solve for *K*:

$$\text{Log } K = -52.25 \cdot 176.5/1800 = -5.1234, \qquad \text{or} \qquad K = 0.75 \cdot 10^{-5}.$$

The algebraic form of Q (hence of *K*) is, from the chemical equation,

$$Q = K = 0.75 \cdot 10^{-5} = (a_{SiO} \cdot a_{CO2})/(a_{SiO2} \cdot a_{CO}) \quad .$$

The activity of SiO_2 is still taken as unity in this problem, and those of the participating gases are their partial pressures. Now there are two options: (a) The ratio $p(CO)/p(CO_2)$ may be taken as about 10 as was given previously, and the above equation solved for p(SiO) at equilibrium:

$$p(SiO) = 0.75 \cdot 10^{-5} \cdot 10. = 7.5 \cdot 10^{-5} \text{ atm.}$$

(b) Or, the solution can be generalized as $p(SiO) = 0.75 \cdot 10^{-5} \cdot [p(CO)/p(CO_2)]$ and plotted vs that *ratio* of partial pressures as an independent variable. Modern instrumentation makes possible the reliable CO and CO_2 analysis of furnace atmospheres, such that p(SiO) at equilibrium can be realistically computed.

This equilibrium value of p(SiO) is the *maximum value* attainable in the furnace atmosphere by the given reaction at 1800K. From this and the vessel geometry and gas flowrate, the *maximum* possible SiO_2 recession rate can be computed. Equilibrium calculation methods like the above will be used repeatedly in the following sections.

REFRACTORY ALTERATION BY OXIDATION-REDUCTION

The majority of productive thermodynamic equilibrium calculations for refractory corrosion apply to oxidation-reduction or redox reactions. Some of the most important examples follow.

Redox Reagents In Combustion Atmospheres

For fossil-fuel combustion products, the equilibrium partial-pressure ratios of a number of substances in the atmosphere can be computed from the free energy data in Table V.1. This has been done for CO, CO_2, O_2, H_2, H_2O, H_2S and SO_2, all of whose redox equilibria are simultaneously inter-related. The results are shown in the composite logarithmic plot of Figure V-2. The C:H ratio of the fuel is open. The fuel:air ratio is also an independent variable.

The ratio of partial pressures of CO to CO_2 is used here as ordinate. Its range is bounded at the high-air extremity by an arbitrary envelope of residual O_2 partial pressures lying between 0.1 atm. and 0.01 atm. (i.e., 10% and 1% O_2). The reducing extremity occurs when elemental carbon appears (in kinetic contact with the atmosphere at equilibrium). This could mean copious soot or a blast furnace bed of coke, for example. At this extremity the partial pressure of CO alone becomes an independent variable. A generous envelope of its values is given in the figure between 1 atm. and 0.1 atm.

The absolute amount of H_2O present is another independent variable; but the equilibrium ratio of partial pressures of H_2 to H_2O bears a fixed relationship to the $CO:CO_2$ ratio. So also does the absolute value of $p(O_2)$ remaining.

The dashed curves describing the ratio of partial pressures of H_2S to SO_2 are independent of the total sulfur analysis; but further useful information is concealed there. First of all, from Table V.1 it is easily shown that SO_3 is unstable in the gas phase at all temperatures above 1000K and at all $p(O_2)$ up to at least 1 atm. It is also provable that elemental sulfur is unstable above 1000K in moist gas, disproportionating to H_2S and SO_2. The equilibrium ratio $p(H_2S)/p(SO_2)$ depends on the absolute value of $p(H_2O)$, though not

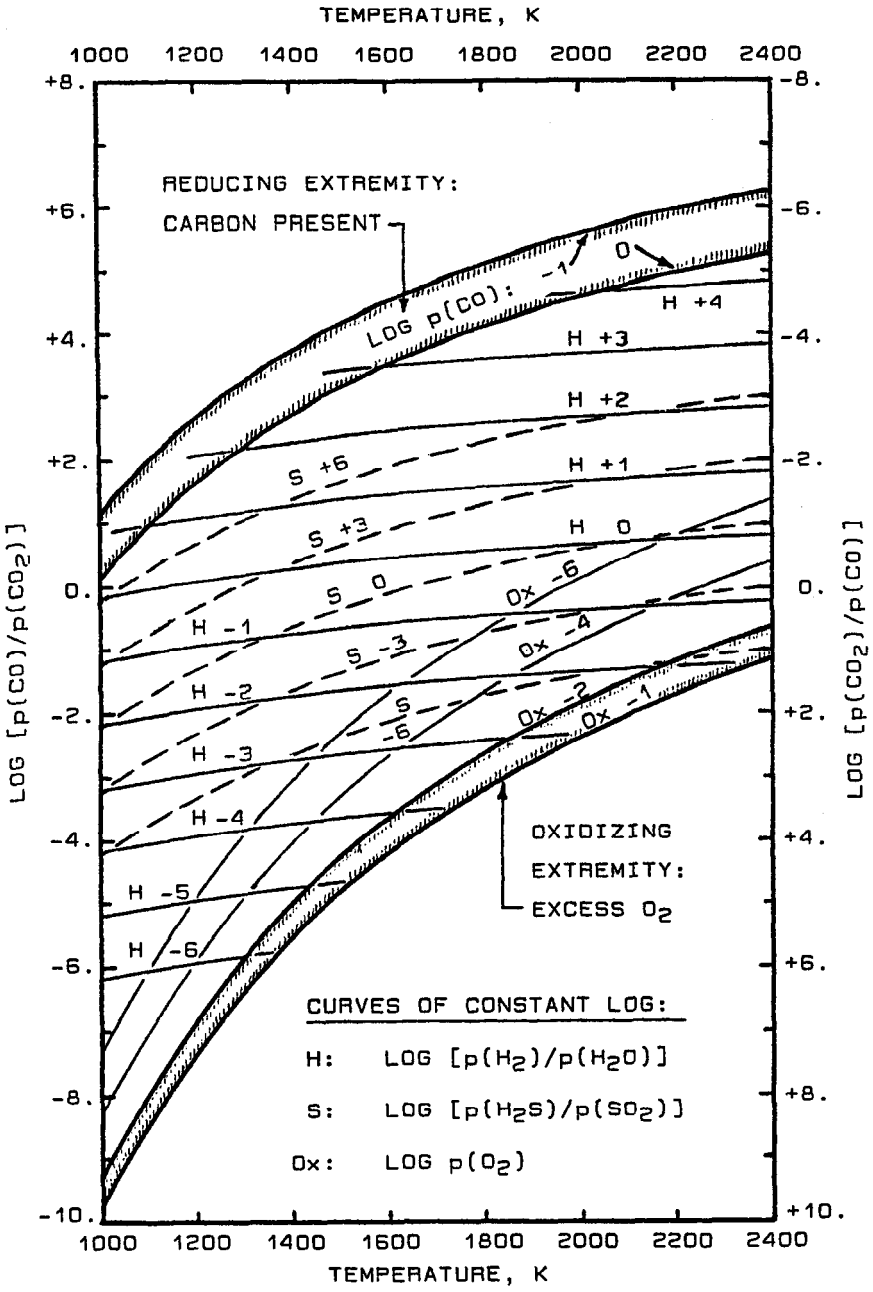

Figure V-2 Equilibrium Ratios of Gas Partial Pressures in Combustion Atmospheres (data from Ref. 23)

very sensitively on the log scale plotted. To avoid clutter, the dashed curves labelled "S" in Figure V-2 were determined at one reasonable fixed value of $p(H_20)$: namely, 0.1 atm.

All of the curves in the figure are isobars of a sort, or *contours.* The index number given on each curve is the logarithm of its designated function of partial pressures. Though it is true that furnace atmospheres are not static and sometimes are not at equilibrium, these curves are of much value in understanding and predicting the redox alteration of refractories.

Reduction-Decomposition of MgO and SiO_2

MgO. The evaporation of elemental Mg by reduction of MgO has long been of concern as a potential mechanism of recession of basic refractories. Historically the question first had to do with a juxtaposition of magnesite bricks with carbon blocks.[3] But the extensive use of particulate-carbon-containing MgO refractories in steelmaking vessels adds the possibility of internal self-destruction near the hot face to that of reduction by environmental CO or other reagents in the BOF, AOD, and EAF or elsewhere.

Figure V-3a presents pertinent equilibrium curves. The topmost curve represents the equilibrium,

$$MgO + C = Mg_{(g)} + CO_{(g)} ,$$

at an assumed p(CO) = 1 atm. The activity quotient Q for this equation can be written,

$$Q = [p(Mg) \cdot p\,(CO)] / [1 \cdot 1] .$$

Its equilibrium numerical value *K* was determined vs T by the methods of this chapter and then expressed as p(Mg) by imposing the condition p(CO) = 1.

That topmost curve is alarmingly steep, showing p(Mg) at about 10^{-3} atm. at 1500°C and about 0.1 atm. at 1700°C. Fortunately for the refractory in service, several factors mitigate the anticipated Mg evaporation rate: (a) mass transport is impeded by slag and other factors affecting diffusion;[66] and (b) much of the Mg vapor apparently reoxidizes within the refractory,[67] either at lower temperature behind the hot face or upon encountering a less-reducing atmosphere and slag-borne oxidizing agents (e.g., FeO or Fe_2O_3) at the hot face. Nevertheless, the susceptibility of MgO to reduction certainly limits its service temperatures in contact with carbon. They must not be appreciably higher than they are now in steelmaking.

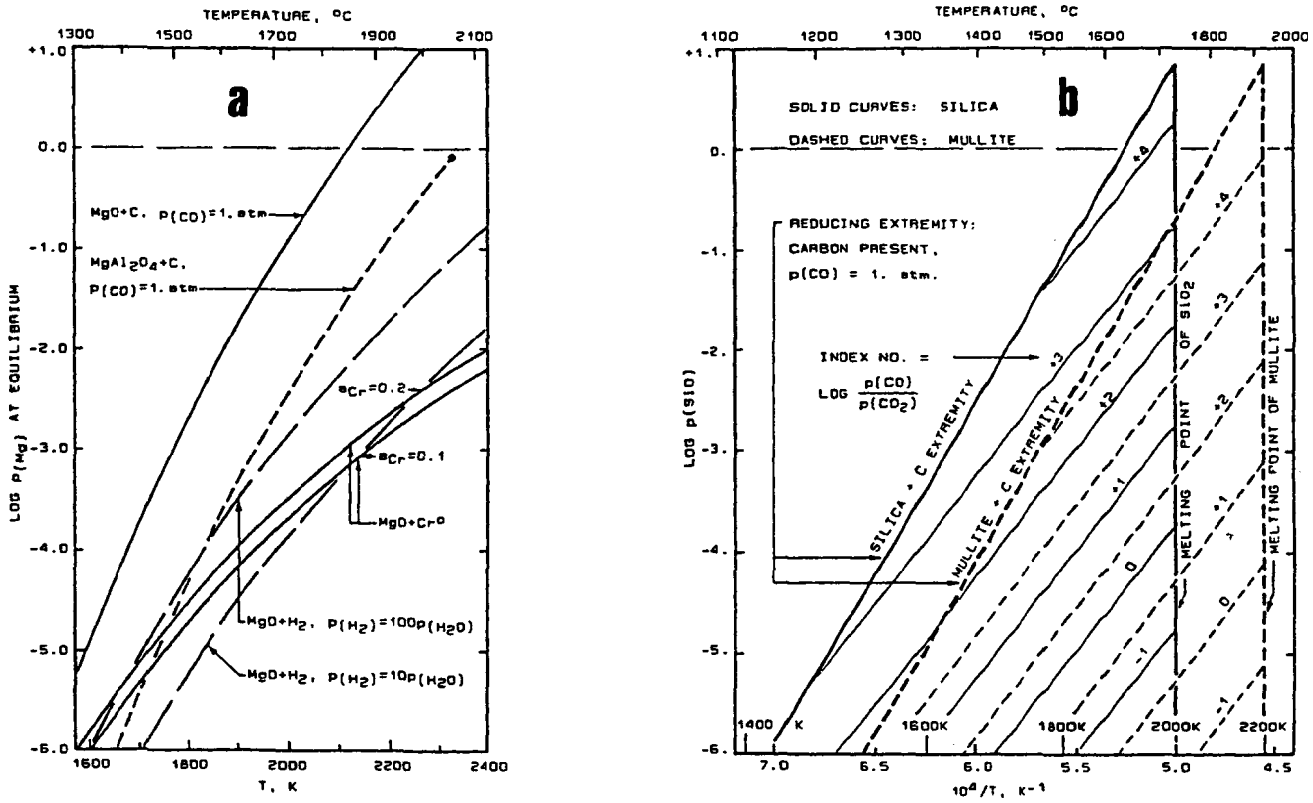

Figure V-3 Reduction-Decomposition Equilibria Yielding: a. Mg(g); b. Si0(g)

The second, dashed curve in Figure V-3a illustrates how this susceptibility can be diminished by replacing MgO by a stable spinel. $MgAl_2O_4$ gains about 200°C over MgO at equal p(Mg). $MgCr_2O_4$ (not shown) is roughly comparable.[68]

The remaining curves represent less-powerful reducing environments than carbon. The two for reduction of MgO by H_2 correspond in H_2/H_2O ratio to curves "H +1" and "H +2" in Figure V-2, from which the simultaneous $CO:CO_2$ ratios are found there by inspection.

The two curves labelled "MgO + Cr" are for the equilibrium,

$$4\ MgO + 2\ Cr = 3\ Mg_{(g)} + MgCr_2O_4\ ,$$

in which chromium is in liquid solution in iron in the manufacture of stainless steel. The two chromium activities in the figure are intended to bracket reality in molten SS.[68] Reduction of MgO by SS appears not to be a problem at reasonable process temperatures, a conclusion agreeing with experience.

SiO_2. Reduction of silica by carbon or CO can produce $SiO_{(g)}$, $Si_{(l)}$, or $SiC_{(s)}$. Below the melting point of SiO_2, for kinetic reasons only $SiO_{(g)}$ appears. A few pages back we found $p(SiO) = 0.75 \cdot 10^{-5} \cdot p(CO)/p(CO_2)$ at 1800K; but a broad display over practical ranges of all the independent variables is needed. Figure V-3b contains such a display, on coordinates differing from those of V-3a. Consider first only the solid curves in this figure, which describe the equilibrium:

$$SiO_2 + CO_{(g)} = SiO_{(g)} + CO_{2(g)}\ .$$

The temperature scale is linear in 1/T, on which scale all of the logarithmic functions of Figure V-2 have now become linear and regularly spaced. Only one reducing extremity is transferred to Fig. V-3b from Fig. V-2: that for p(CO) = 1 atm. in the presence of carbon. The sloping solid curves are of log p(SiO) vs $10^4/T$, each curve being indexed to a single contour value of log $[p(CO)/p(CO_2)]$ or "reducing power" of the atmosphere. The m.p. of SiO_2, 1723°C or 1996K, is taken to close the figure.

Silica is seen to be susceptible to reductive decomposition by carbon at temperatures well below those for MgO. But by including the $CO:CO_2$ ratio as an independent variable, Figure V-3b gives still more information. If $p(SiO) = 10^{-3}$ atm. is taken as an allowed equilibrium limit, for example, a horizontal line at this value gives many combinations of decreasing $p(CO)/p(CO_2)$ with increasing temperature, all of which yield this same equilibrium pressure of SiO gas.

The family of dashed curves in Figure V-3b is the corresponding set for the equilibrium of mullite with CO-CO_2 atmospheres:

$$1/2\ Al_6Si_2O_{13} + CO_{(g)} = 3/2\ Al_2O_3 + SiO_{(g)} + CO_{2(g)}\ .$$

Note that the temperatures of equal p(SiO) differ by about 200°C between SiO_2 and mullite; this is similar to the gain between MgO and $MgO{\cdot}Al_2O_3$ seen in Figure V-3a. Silicates found in basic refractories have been investigated likewise.[66]

Still another redox reaction of silicate refractories occurs in the containment of molten aluminum. This powerful reducing agent, operating at, say, 800°C or near 1100K, may reduce silicates to elemental Si. Free silicon is solid at 800°C (m.p. 1420°C); but in this system it goes into dilute liquid solution in the Al at much-reduced chemical activity. A model equation for the reaction might be:

$$3\ Al_2SiO_5 + 4\ Al_{(l)} \rightarrow 5\ Al_2O_3 + 3\ Si\ (\text{in liq. Al}).$$

Thermodynamic treatment of this reaction indicates a considerable driving force that is not greatly diminished if dialuminum silicate in the equation is replaced by mullite. Yet some silica-containing refractories perform well in this service. Interfacial kinetic reasoning has to be invoked, which will be discussed in Chapter VI under Liquid Metal Containment.

Oxidation-Reduction of Iron Oxides

FeO-Fe_2O_3 Equilibria. Iron oxides as impurities in refractories have been alluded to before. Chapter IV dealt with their effects on melting behavior. Elsewhere we have referred to harmful atmospheric oxidation-reduction cycling, which has to do instead with *dimensional instability* of solids containing iron oxide components.

Iron possesses three oxides with selected properties as tabulated below:

Iron Oxide	Crystal Type	Formula Wt., g	Density, g/cm³	Molal Vol., cm³	Vol. in cm³ Per Mol Fe
FeO	cub.	71.85	5.7	12.6	12.6
Fe_3O_4	cub.	231.55	5.18	44.70	14.90
Fe_2O_3	hex.	159.70	5.24	30.48	15.24

These oxides are formed stepwise from iron in successively more-oxidizing atmospheres. Magnetite, Fe_3O_4, has to be recognized; but

we choose to ignore it here on grounds of (a) its volume per mol Fe, which is close to that of Fe_2O_3; and (b) its existence in only a narrow band of oxidizing power of the atmosphere, i.e., its rough equivalence to FeO + Fe_2O_3 in equilibrium.

What is most noteworthy in the table is in the last column. The unit volume change at room temperature between FeO and Fe_2O_3 is 15.24/12.6 ≅ 1.21 or an increase of over 20%. The change from FeO to Fe_3O_4 is not far behind, at about 18%. There is little virtue in refining these numbers at high temperatures by invoking differences in thermal expansion; this magnitude of volume change persists.

In Chapter IV under Microstructural Integrity it was observed that solid-state volume changes of the order of 1% can be damaging if they occur rapidly and in the nonplastic temperature range of the host. This present order-of-magnitude-greater volume change results in microstructural breakdown. Where in the range of atmospheric oxidizing or reducing power does it occur?

This question can be answered by exploring chemical equilibria such as the following:*

$$Fe_2O_3 = 2\,FeO + 1/2\,O_2 \quad ; \qquad Q = K = [p(O_2)]^{1/2}$$
$$Fe_2O_3 + CO = 2\,FeO + CO_2 \; ; \qquad Q = K = [p(CO_2)/p(CO)]$$
$$Fe_2O_3 + H_2 = 2\,FeO + H_2O \; ; \qquad Q = K = [p(H_2O)/p(H_2)]$$

That is, if we obtain each *K* numerically, then imposed atmospheric values of Q larger than each will favor single-phase Fe_2O_3 and values of Q smaller than each will favor single-phase FeO. Only at Q = *K* will FeO and Fe_2O_3 coexist. And cycling of the atmospheric composition between larger and smaller values of Q will produce the destructive volume change -- if kinetics cooperate.

Descriptions of these equilibria are contained in Figure V-4. Some Fe-FeO equilibria are included as well; those should be ignored for now. The right-hand ordinate scale is not equivalent to the left, but is selected independently to display the O_2 equilibria over a convenient range. Recalling from Figure V-2 that all of these gas-phase equilibria are simultaneously connected, we can address the equilibrium ratio of CO_2 to CO alone.

---

*We assume thermodynamic data for FeO and Fe_2O_3 will serve for the corresponding silicates. This approximation is not bad.

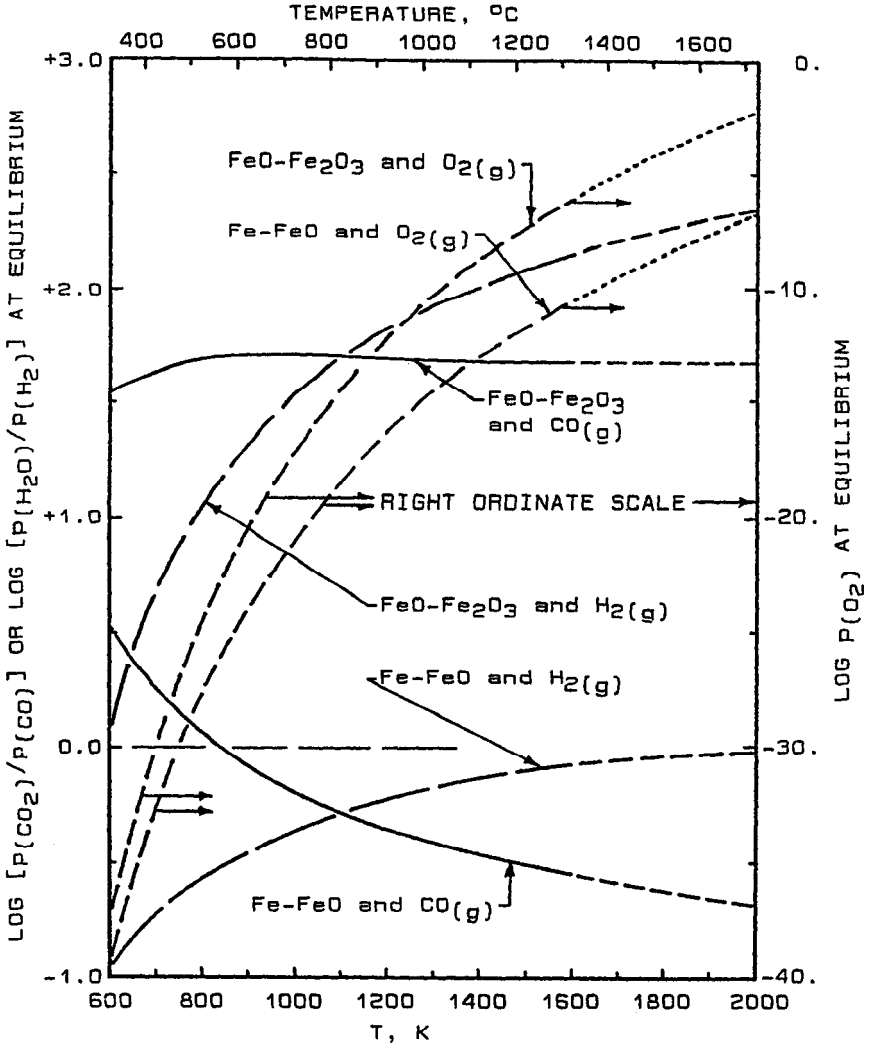

Figure V-4 Ferrous-Ferric Oxide Redox Equilibria

That equilibrium curve, labelled "FeO-Fe_2O_3 and $CO_{(g)}$" in Figure V-4, lies at a nearly constant value of log [$p(CO_2)/p(CO)$] of about +1.65 over the whole temperature range of interest -- i.e., above 500°C or 773K. This value on the right ordinate scale of Figure V-2 falls on the inner oxidizing extremity (1% O_2) at about 2073K or 1800°C. Thus fuels burned in a small excess of air for maximum heat yield and flame temperature, or hot air itself, will oxidize FeO to Fe_2O_3; and almost any degree of reducing flame or atmosphere will reduce Fe_2O_3 to FeO -- kinetics permitting.

Consequences. Atmospheric cycling is avoided in kilns and furnaces that are always fired with an oxidizing flame. There, Fe_2O_3 is stable. In such situations fireclay and clay-alumina refractories thrive, up to their softening temperature limitations and barring other forms of corrosive attack.

Vessels that are operated reducing, on the other hand, are bound to reduce ferric oxide in their refractories to FeO. In this service fireclays may soften at the hot face or not, depending on the prevailing temperature. But reducing gases can penetrate well into the depth of a porous refractory wall and also generate FeO at nonplastic temperatures within. On subsequent exposure to air, the FeO is reoxidized and grains of the material may be ratcheted apart. And so on, cumulatively, cycle by cycle. For fireclays the temperature range of most severe damage is probably from about 500°C to 1000°C. Below this rough range the redox reaction becomes increasingly sluggish, while above it there is eventually sufficient plastic compliance to abide the volume change without debonding of grains.

It is immediately apparent why clay ceramic wares that are put through a period of reduction firing are deliberately reoxidized at the sintering temperature before cooling (see Sintering of Oxidic Ceramics, Chapter II). Reoxidation of FeO with a liquid phase still present will not debond the ceramic structure, whereas it is potentially destructive upon cooling.

It might seem from the above that fireclay refractories should be excluded wholesale from reducing service. Not so. There are numerous possible mitigations: the amount of iron oxide in the composition; the frequency, temperature and pace of redox cycling; glazing of the hot face (cutting off the entry of gases); partial re-healing due to temperature cycling; partial rebonding due to slag penetration; and so on. Fireclays are avoided in a number of reducing scenarios, but by no means all.[69,70]

Nor is redox cycling harmful only to fireclays. Interesting phenomena occur where there is but little silica component. In basic

refractories (e.g., magnesite, or slag-penetrated periclase) FeO goes into solution in the hot MgO host in which it is very soluble.[21] This solid solution is called "magnesiowüstite." On reoxidation, Fe_2O_3 is not soluble in MgO but can react with it to form magnesium ferrite spinel, $MgFe_2O_4$. The iron is said to "exsolve" (i.e., come out of solution) as $MgFe_2O_4$. The volume change still prevails, and mechanical damage ensues, with each redox cycling.[71]

In high-alumina refractories it is Fe_2O_3 that goes into solution in the host, but not so stably.[21] On reduction, FeO comes out. Again there is cycling damage because the volume change still prevails.

Countermeasures. A solution to these problems was conceived decades ago: providing from a significant to a major amount of a chromite spinel phase in the refractory as a host for iron oxides.[72-80] In basic refractories this takes the form of a solid solution: $(Mg,Ca,Fe)(Cr,Fe)_2O_4$. Though the chemistry is complex, changes in the Fe^{+3}/Fe^{+2} ratio can be accommodated without change of phase nor appreciable volume change, and without appreciable FeO ever entering the associated MgO phase. In high-alumina refractories the spinel might be better represented as $(Mg,Ca,Fe)(Cr,Fe,Al)_2O_4$; but the principle is the same. The products can be simply described as MgO+chromite and Al_2O_3+chromite refractories, though other phases are also present.

The concept was, and is, carried out by admixing chrome ore (principally $FeCr_2O_4$) with the respective other oxide and then reaction sintering. In a newer embodiment, arc-fusion is used to ensure complete reaction among other purposes. Though there are a host of such products, not all performing alike, this concept greatly improves the microstructural integrity of both high-alumina and basic refractories in redox cycling when iron oxide is present.

Catalytic FeO: Disintegration by CO

The interested reader might want to use the CO and CO_2 data of Table V.1 to compute the equilibrium value of $p(CO_2)$ in the disproportionation reaction,

$$2CO_{(g)} = C_{(s)} + CO_{2(g)} \ ,$$

as a function of temperature, assuming p(CO) = 1 atm. In a hot reducing flame, the equilibrium $p(CO_2)$ is very small. When the gas cools somewhat, equilibrium then requires that the above reaction proceed as written, raising $p(CO_2)$ and precipitating carbon. But if carbon is not already present as nuclei, the reaction does not go. There is a kinetic barrier.

Ferrous oxide in reduced refractories is a surface catalyst for this reaction, however. The reaction proceeds only on the iron oxide surface,* causing carbon to grow on it. This is a nuisance on an external surface. But far worse, the CO penetrates and reacts on the interior pore walls as well, where eventually the carbon product wedges the refractory crystallites apart, destroying the structure.[81-83]

The reaction runs out of thermodynamic driving force by about 1000°C; most damage from it has been seen between about 400° and 800°C. Thus, this phenomenon about coincides in temperature with the ratcheting due to FeO-Fe_2O_3 cycling described above. The two are distinctly different, however: FeO-Fe_2O_3 ratcheting arises from redox cycling of the atmosphere, while CO disintegration occurs in a highly reducing atmosphere under a steady-state fall in gas temperature. As practical problems, they share a common solution: remove iron oxides as components of refractories. Since that solution is not economical, both problems continue to be in evidence with mineral-based refractories. Chromite formulations have helped some with CO disintegration, but have not eliminated it.

Reduction of FeO to Fe

Figure V-4 also deals with the reduction of FeO to Fe in a refractory setting. Droplets of iron are occasionally seen under the microscope in MgO+C refractories after service in the AOD vessel, for example.[68] They occur only near the hot face where MgO, C, slag, and porosity coincide -- but removed from possible access of iron from the furnace charge. That is, these Fe droplets are formed in situ. A good estimate of p(CO) at their location is ~1 atm., and a good estimate of the temperature of their formation is about 1600°C or 1873K.

Now locate the curve in Figure V-4 labelled "Fe-FeO and $CO_{(g)}$." This curve represents the equilibrium,

$$FeO + CO_{(g)} = Fe_{(l)} + CO_{2(g)}; \qquad Q = K = p(CO_2) / [p(CO) \cdot a_{FeO}] .$$

The curve intersects T = 1873K at log $[p(CO_2)/p(CO] = -0.57$, computed on the assumption $a_{FeO} = 1$. But FeO is presumably in solution. A reasonable minimum for its activity is of the order of 0.1, as there has

---

*There is evidence that a thin layer of iron carbide is formed on the FeO surface, and this may be the catalyst. On the other hand, if FeO were not catalytic, its carbiding probably could not proceed. Iron oxides are well-known redox catalysts.[83]

to be enough iron at the site to be detected. At $a_{FeO} = 0.1$, log $[p(CO_2)/p(CO)]$ would be -1.57 at the FeO-Fe equilibrium.

This equilibrium range -0.57 to -1.57 at T = 1873 K is found in the upper middle of Figure V-2. The prevailing conditions inside the AOD refractory, however, are: C present, p(CO) ≅ 1 atm. These conditions lie on the inner reducing extremity of Fig. V-2, where log $[p(CO_2)/p(CO)]$ <-4. Free energies thus confirm ample driving force for the reduction of FeO to Fe, even with the former dissolved in slag at reduced activity.

The reduction of FeO to $Fe_{(l)}$ is not felt to be important to MgO+C refractory life. Its worst aspect is the carbon it consumes, but the amount of this consumption is very small compared to the loss of carbon in the MgO+C reaction and its further loss by air oxidation during turn-down of steelmaking vessels.[84]

Reduction of TiO_2 and ZrO_2

TiO_2. The technical usefulness of rutile as a refractory is limited to the pure compound in relatively oxidizing environments. It melts at about 1857°C. As such it has little advantage over silica and none over mullite, while it is more costly than these.

In combination with silica, there is a eutectic at 10% TiO_2 melting at 1540°C.[21] In fired clays, where TiO_2 is an impurity component in more intricate chemical systems, its melting-point depressing effect is a nuisance; the resistance of pure TiO_2 to molten slags and glasses is likewise poor because of the existence of low-melting complex silicates.

As to reduction in furnace atmospheres, there is a stepwise series of oxides starting with rutile, going through Ti_3O_5 to Ti_2O_3 and then to TiO. Their melting points and binary eutectic melting points all remain within a fairly narrow band;[21] but the eutectic melting temperature of the reduced oxides combined with silica or silicates can be expected to plummet. Furthermore, the room-temperature volumes per mol of Ti are: TiO_2, 18.76 cm^3; Ti_2O_3, 15.63 cm^3; TiO, 12.96 cm^3. Exceedingly disruptive volume changes accompany their transitions.

There are some published $\Delta G°_f$ data for the lower oxides of Ti.[23] But every oxide phase here has a very wide composition range (i.e., metal and/or oxygen deficiency),[21] such that use of the data for equilibrium calculations is risky. It is certain that reduction to lower valences occurs in high-temperature furnace atmospheres. The destructive volume changes and the increased susceptibility to

melting and corrosion accompanying these reductions do not have to be abided: sufficient other and cheaper oxides are available.

Accordingly, rutile may be encountered as a refractory in limited special circumstances; but as a significant component of refractories for relatively broad usage, titania substantially eliminates itself. We may also delete $CaTiO_3$, for most of the same reasons.

ZrO_2. Zirconium has no lower oxide; and ZrO_2 is all but thermodynamically immune to reduction by the atmospheres of Figure V-2. In these respects ZrO_2 is not different from Al_2O_3 or CaO. In one other respect it is remarkably different, however. ZrO_2 exhibits an even greater range of oxygen deficiency than does TiO_2.[21] Its composition, ZrO_{2-x}, depends on the reducing power of its environment. Zirconia also becomes Zr-deficient in highly oxidizing atmospheres. It can thus be either a p-type or an n-type semiconductor,[15] depending on $p(O_2)$. Its use as an O_2-sensor in hot combustion gases is founded on its semiconducting properties.

Reduction within its single-phase composition limits should alter some of the properties of ZrO_2 as a refractory. Nonstoichiometric oxides generally sinter at lower temperatures than do their stoichiometric counterparts, reflecting increased vacancy diffusion and hence a decreased Tammann temperature. Whether reduced zirconia is any more susceptible to corrosion reactions with, say, molten silicates than it is in the fully oxidized state is not certain. Both ZrO_2 and $ZrSiO_4$ (including AZS) do well in reducing service in the 1600°C regime,[85-90] as they do also in oxidizing service.[24,25,91,92] In only one peripheral case was silicate slag attack reportedly worsened by reducing conditions;[93,94] this was leaching of the CaO from ZrO_2-CaOss, resulting in destabilization of the cubic phase.

Thermodynamics and Kinetics of Nonoxide Corrosion

Free energy tables exist[23] for some carbides, nitrides, borides and silicides; but the redox chemistry of nonoxide refractories can be appreciated largely without their help. These materials are immune to reduction. Without exception, on the other hand, they are subject to high-temperature oxidation. It is as true of these substances as it is of metals that corrosion and oxidation are essentially synonymous.

Carbon and other nonoxides can be very durable as refractories if they are protected *thermodynamically* against oxidation. One example is in the blast furnace, where an overwhelming mass of coke in the charge ensures a reducing atmosphere. In the Hall-Héroult cell the reducing potential is set by the molten aluminum and the several-volt negative electrical bias imposed. Other examples will have been recognized in Chapters II and III.

Kinetic control of oxidation is exemplified by the use of carbon in chemical equipment running below 500°C; and of carbon and carbides at high temperatures using inert-gas sweeping or vacuum. The oxidation of C in particulate-carbon-containing refractories is limited kinetically by buildup of the product CO pressure in the immediate pores, the gas holding back the entering oxidizing agents even as it diffuses out to the nearby refractory hot face.[66,84] In some of the current carbon-bonded magnesias, powdered elemental Si or Al is distributed in with the carbon.[74,95-99] Not only is the metal oxidized in preference to carbon; its oxide tends to fill the porosity and isolate the carbon from further oxidizing-gas and liquid intrusion. Other "deoxidants" have also been tried.[100-102]

Finally, a form of kinetic control known in metal corrosion as "protection" or "passivation" is also in effect in a few nonoxide refractories. Oxidation of SiC and of refractory silicides such as $MoSi_2$ yields a protective glassy surface coating, predominately of SiO_2. These refractory materials thrive in oxidizing atmospheres but in limited temperature ranges: SiC, for example, is best protected between about 900°C and about 1500°-1700°C. It must not, however, be simultaneously immersed in liquid silicate slags, risking the dissolving and washing away of the protective layer. The recent surge in use of SiC as kiln furniture in whiteware kilns exploits the unique properties of this material in the absence of slags. Those properties include, among others, resistance to both oxidizing and reducing atmospheres. Carbon, which is not self-protected against oxidizing agents, can be given some measure of protection by an applied coating of a glass-forming oxidic refractory.

Other Redox Reactions

A few additional treatments of redox reactions in the literature should be acknowledged. One[103] examines the oxidation of steel spacers that are sometimes placed between refractory bricks as a means of accommodating thermal expansion (see Chapter IV). It also describes the interaction of the resultant iron oxide with the refractory.

Another[104] is a comprehensive thermodynamic analysis of the effects of blast furnace environments on both slag and refractory components. Under the extremes of temperature and reducing conditions in the blast furnace, the array of reduced products that have to be considered is wider than we have described. This paper is commended to those who must deal with blast furnace chemistry in detail.

The use of chopped SS wire and of SiC particles or whiskers as mechanical reinforcement in refractories was mentioned in Chapter IV. Air oxidation of stainless steel can be inferred from

Ref.103; the maximum service temperature of SS reinforcement is thereby limited to about 1350°C. Reactions of SS wire with CO and with H_2O gas at lower temperatures have also been examined.[81] A study of oxidation of SiC reinforcement in alumina and other refractories has been made,[105] illuminating its effects on the interfacial bond.

Coal-gasification process chemistry includes high temperatures, high reducing potential, and voraciously aggressive slags. In addition to CO disintegration at low temperatures, described above,[81-83] the high-temperature reduction of refractory components including Al_2O_3 and Cr_2O_3 has been studied thermodynamically.[106] Products examined include $Al_{(g)}$, $AlO_{(g)}$, $CrO_{(g)}$, and various carbides of Al and Cr. Alumina- and chrome-containing refractories are not fully comprehended without an awareness of these reduction reactions.

Nor can the high-temperature oxidation of Cr_2O_3 be safely ignored. Particularly in the presence of alkalies, refractory chromites can be oxidized in part to toxic chromates (i.e., Cr^{+6}). The alkali chromates (e.g., Na_2CrO_4, $Na_2Cr_2O_7$) are water-leachable, presenting an environmental contamination risk if chrome-containing linings are dumped after high-temperature service. The rotary Portland cement kiln lining is one example. An introduction to the pertinent redox chemistry and consequences may be found in References 107 and 108, among other sources.

The refractories technologist may well encounter still other redox reactions in the course of field experience or through postmortem examination of spent refractories. This chapter should provide a sufficient groundwork for their recognition and evaluation.* We shall return briefly to this subject in Chapter VII, after considering some further and more common refractory corrosion mechanisms.

---

*A number of the corrosion reactions of this chapter would be advantageously treated by the partial-molal thermodynamics of solid solutions.[66] We have ignored that approach, as have most workers, because of the lack of established thermodynamic data appropriate to high-temperature solid-solution systems. This is an inviting area for future research.

Chapter VI

Principles of Corrosion Resistance: Hot Liquids

LIQUID PENETRATION AND DISSOLUTION-CORROSION

Infrequently is there much concern for corrosive interaction between two solids in contact, unless their reaction yields a fluid product serving as a mass transport medium. The refractory-lined vessels of Chapter III, on the other hand, are called upon to contain hot liquids. In that case, convective and diffusional transport of components of the liquid to the lining is relatively rapid. Corrosive components consumed in reaction can be replenished, and corrosion can continue over time.

Examples of such hot process liquids are metallurgical slags and fluxes; nearly all manufactured glasses; liquids formed in hot chemical operations such as combustion, ore roasting and Portland cement manufacture; and the majority of metals obtained by smelting. We shall examine their corrosion of refractories by mechanisms other than oxidation-reduction, but with incidental comments on redox involvement when appropriate.

We commence this examination by disposing of "acid-base neutralization:" a traditional concept of nonmetal interactions that is embedded in the lore of refractories.

Acid-Base Series of Oxides

Acidic

N_2O_5
SO_3
P_2O_5
SO_2
P_2O_3
N_2O_3
CO_2
As_2O_5
B_2O_3
As_2O_3
V_2O_5
SiO_2
Sb_2O_5
V_2O_3
Sb_2O_3
TiO_2
SnO_2
Bi_2O_5
SnO
ZrO_2
H_2O
ZnO
Bi_2O_3
PbO
Fe_2O_3
Co_2O_3
Cr_2O_3
Al_2O_3
CuO
FeO
CoO
NiO
MnO
CdO
BeO
MgO
CaO
BaO
Li_2O
Na_2O
K_2O

Basic

The chemical concept of acids and bases emerged historically along with the development of glass science and of systematic metallurgical processing. Silicate glass compositions seemed to fall within a prescribed range of percent "network formers" (principally SiO_2, B_2O_3, and Al_2O_3), and a range of percent "modifiers" (principally CaO, MgO, Na_2O, and K_2O). The first group is relatively more or less acidic, the second group clearly basic.

Metallurgical slags became characterized early-on as acidic or basic in connection with the (opposite) character of the metal oxides they were intended to sequester by chemical reaction. Modern slag compositions are found -- depending on the shop and the purpose -- over a considerable range from acidic (high-SiO_2) to basic (high CaO: SiO_2 ratio).

Finally, a number of gas-phase oxidic chemicals were catalogued in Chapters II and III as products of named hot processes. Apart from their possible redox reactions with refractories, the next most obvious way in which each of these substances can be characterized is by its degree of acidity or basicity. Examples are CO_2, SO_2, Na_2O and K_2O.

On this page we present an extended reference series of binary oxides, in approximate order from most acidic to most basic. The melting point of each is given in Figure IV-1. A single precise criterion for high-temperature acidity and basicity of all compounds is lacking; so formulas lying close together in this list are of uncertain relative order. Some reversals occur with temperature. The order toward the ends of the list is reliable, however: from SiO_2 up among acids and from MgO down among bases.

In the list the oxides SiO_2, ZrO_2, Al_2O_3 and MgO are in bold type, to single them out as important phases in refractories. Silica is in fact the most acidic oxide that is also high melting; and

magnesia is the most basic oxide that does not necessarily react destructively with atmospheric moisture or CO_2 at low temperatures. These are the prototypical "acid" and "basic" refractories. Although in the industry alumina is the prototypical "neutral" refractory, on a room-temperature chemical scale zirconia is precisely neutral and alumina is slightly basic.

"Acid" and "basic" refractories were originally conceived to face acidic and basic environments, respectively, on the quasi-chemical reasoning that opposites react most energetically while like oxides do not react. For anticipating refractory corrosion, this argument has proved on the whole to be naive. A few contrary examples follow: (a) MgO does not form compounds with ZrO_2, yet it reacts with the less-acidic Al_2O_3, Cr_2O_3, Co_2O_3 and Fe_2O_3; (b) the melting points of the reaction products of SiO_2 with Al_2O_3, MgO and Na_2O fall in that order, while those oxides are increasingly basic; and (c) while mullite is slowly attacked at 1500°C by molten glass (call SiO_2), it is not harmed at all at this temperature by the increasingly acidic CO_2 and SO_2.

Thus while occasions may arise when this acidity-basicity series will yield useful information, by itself it has limited predictive value regarding corrosion by hot process liquids.

Current View of Corrosion by Liquids

We describe common non-redox interactions of refractories with liquids by the word *dissolution*, i.e., including chemical reaction but not limited to it.[109] As to the Acid-Base Series of Oxides, for example, if its opposite members may react energetically to form compounds, its like members may simply dissolve in each other. We have to be far more concerned in either case with whether the product is *liquid* or *solid* at the prevailing temperature.

The importance of the physical state of the interaction product lies in the fact that continuing corrosion must be mass-transport-limited. The dominance of uniform corrosion of the macroscopic surface, which in metals is the rule, is more the exception in refractories. The rule in porous refractories is that corrosion is an accompaniment of *penetration* into connected networks of voids.[109] Now if the interaction product is a solid, formed in the interior, all convective and capillary processes bringing the reagents into contact are shut down at this solid barrier. Diffusion rates through it are quenched by orders of magnitude relative to those prevailing in the liquid. Reaction energies lose significance if the reagents are brought together at infinitesimal rates. In the event a liquid is produced, on the other hand, penetration and interaction can continue.

Penetration without dissolution is not corrosion. Dissolution without penetration is superficial. Between these extremities there is room for much mischief.

Avenues of Liquid Corrosion

Features of Microstructure. Consider a refractory wall whose hot face is maintained at some high, steady-state temperature at which it is stable in the absence of corrosion. Now bathe the hot face in a process liquid. The table below lists the several kinds of microstructural features that can exist in the refractory, that are presented to this environment. These features are arranged in order of increasing characteristic path cross-sections for liquid penetration and interaction:

Microstructural Feature	Continuous or Discontinuous	Characteristic Path Width
Refractory Crystal	Discontinuous	0.2 - 0.5 nm
Orientation Boundary	Continuous	0.5 - 2 nm
Phase Boundary	Continuous	1 - 5 nm
Segregated Impurity	Discon./Contin.	1 - 50 nm
Unbonded Boundary	Discontinuous	1 - 50 nm
Chemical Bond or Matrix	Continuous	>> 5 nm
Liquid Boundary Film	Discontinuous	>> 5 nm
Connected Porosity	Continuous	>>10 nm
Open Joint, Crack, or Gap	Continuous	>1000 nm

The *refractory crystal* is a unit of the one or more principal phases chosen to provide thermal stability and corrosion resistance in the material. It may be up to ~1 cm in size if arc-fused, otherwise from a few hundred μm down. The path dimensions for its surface invasion are literally atomic.

Orientation boundaries are narrow but not quite atomically narrow even if free from impurities. Even in this ideal state they run some 25% lower in atom density than the conjugate crystals, being riddled with vacancies, stacking faults, charge faults, atom holes, and lattice strain.[110]

Phase boundaries, even if postulated likewise free from impurities, are probably on average still somewhat thicker, atomically less dense, and crystallographically more disordered because they join crystals of different phases in haphazard orientations.

Segregated impurities occur in all the above boundaries in reality, and thicken them by up to a magnitude.[110] Generally this domain will be considerably lower-melting than the conjugate

crystals, and susceptible to much more rapid dissolution-corrosion. It will likely be above its own Tammann temperature at the hot face.

Unbonded boundaries, narrow voids between crystallites, occur due to the previous thermal history of the material, anisotropy of thermal expansion and contraction, and differential shrinkage after sintering. Some individual crystallites or groups of crystallites are incompletely sheared apart by internal boundary stresses. The resulting discontinuous microcracks generally communicate with pores.

A *chemical bond* may have been provided for in the refractory formulation. Examples are various sulfates or phosphates; chromates (of dwindling use owing to toxicity); colloidal silica; various cements, etc. Their distribution within the solid mass is hardly uniform: they tend to accumulate in the larger spaces between particles. Ideally they would bond particles together uniformly, everywhere, by almost atomically close chemical bridges after curing or firing; but the reality is often clustered and sometimes even discontinuous. Bonding films are in some cases lower-melting than the major phases. They may be likened in distribution to segregated impurities, but are much greater in volume.

A bond between crystals may on the other hand be formed by one or more minor indigenous phases. Typically these will have been partially or completely molten in the course of refractory manufacture, re-freezing as fine crystals and glasses after sintering. We shall call their domain the continuous *matrix* in a refractory microstructure. As to its thickness, this can easily exceed those of segregated impurities and "chemical bonds," reaching dimensions readily seen by optical microscopy. The matrix communicates intimately with the porosity.

Liquid films may or may not occur in boundaries near the hot face on account of the service temperature alone. If they do, they are portions of impurities, bond chemicals or matrix which have remelted. If so, they had better be discontinuous or else viscous. Diffusional transport in them is much accelerated over that in solids.

Connected porosity originates in the imperfect packing of particles; in the evaporation/decomposition of additives; and in shrinkages accompanying the reaction, melting and recrystallization of constituents of a refractory in its manufacture. This intricate network of communicating voids interpenetrates with the above-described boundary solids. Though pore networks are sometimes modelled analytically as tubular, almost every imaginable cross-section can be found somewhere. Cross-section dimensions range over orders of magnitude, from as little as 1 nm up. Most porosity in refractories

ranges in "diameter" from the order of 5 nm to ~5 μm -- even larger in foamed insulating materials.

The total volume of connected porosity is measured (for example) by a standard ASTM method called *apparent porosity*.[9] This method in essence employs capillary filling of the entire void volume with water and expresses the total water sorption as volume per cent. "Dense" or working refractories (other than fuse-cast) range in apparent porosity from the order of 5% to perhaps 30%.

Open joints, cracks, or gaps in a refractory wall or lining can originate in its installation, design and support together with its service history. We have called these "continuous" in that their length dimensions are typically well upwards of 1 cm -- beyond the dimensions of microstructure.

Patterns of Penetration. The above descriptions and dimensions form a rational basis for anticipating the typical relative rates and extents of intrusion into a refractory by corrosive liquids, and their consequences:

Microstructural Feature	Liquid Intrusion		
	Rate	Extent	Consequence
Open Joint, Crack, Gap	Very Rapid	Full	Liquid Filling
Connected Porosity	Rapid	Progressive	Liquid Filling
Unbonded Boundary	Rapid	Local	Liquid Filling
Liquid Film	Less Rapid	Local	Interdiffusion
Chemical Bond or Matrix	Moderate	Progressive	Debonding
Segregated Impurity	Moderate	Progressive	Debonding
Phase Boundary	Slow	Hot Face	Deep Grooving
Orientation Boundary	Very Slow	Hot Face	Grooving
Refractory Crystal	Slowest	Hot Face	Surface Recession

The first four features listed are the avenues by which a penetrating liquid reaches the immense number of structurally vulnerable solid features: up to some 10^{12} of these per cm^3. Penetration and filling of the porosity by capillarity produces a relatively uniform "front," moving in gradually from the hot face and remaining on the whole somewhat parallel to it. That penetration establishes the overall pace of corrosion, i.e., its increasing depth into the refractory with time.[109]

The next two listed features are the vulnerable ones. They are solid regions; their invasion has to be by *dissolution*.[109] This attack, proceeding down slot-shaped paths confined by crystallites on either

side, advances orders-of-magnitude more slowly than in voids. But the average distance between connected pores in boundaries is only of the rough order of 1μm. Dissolution processes need advance only very short distances before joining to debond the conjugate crystals.

The last three features listed in the table are equally exposed to the penetrating liquid; but their resistance to invasive dissolution is the highest among all features present. Recall that the two boundary types in this group were described as "clean" and hence are of rare existence; real (impure) boundaries between crystallites generally fall in the vulnerable group. These last three features are thus conveniently reduced to one: the refractory crystals. Those crystals may be hardly corroded at all, in the interior, in the time required for their debonding. Only at the exposed hot face itself is the coarse-crystalline refractory grain or aggregate subject to appreciable surface recession, aided by liquid velocity effects and added erosion and abrasion.

Both physical penetration and chemical invasion are favored by effective liquid-solid *wetting* and by low *viscosity* of the liquid. Yet the liquid viscosity is substantially dictated by the operation being contained. In general in the liquid state, (a) silicate slags and glasses are the most viscous, but exhibit a wide range depending on chemical composition and temperature; (b) simple oxidic compounds are less so, tending toward decreasing viscosity with decreasing valence or coordination number of the metal ions present; and (c) halides and elemental metals are the least viscous. Quantitative viscosity data for molten chemicals are hard to come by, and no comprehensive compilations are known.

Six Factors in Corrosion Resistance

Out of all the above observations, one can identify two groups of controllable factors influencing refractory dissolution-corrosion by liquids. These act and interact together. Discussing them severally is at best artificial, yet can aid the understanding of how they are managed. These six factors are:

Penetration Factors	Dissolution Factors
Freezing of the Penetrant	Resistance of the Bond or Matrix
Porosity and Pore Sizing	Extent of Intercrystalline Bonding
Wetting and Non-Wetting	Nature of the Grain or Aggregate

The next sections will take each of these up in turn.

FACTORS GOVERNING PENETRATION

Freezing of the Penetrant Liquid

Freezing and Penetration Depth. Process slags, fluxes, glasses, and melted process chemicals are of known and usually designed composition. Their freezing temperatures and temperature ranges are accordingly determined in principle: see Phase Equilibria and Phase Diagrams in Chapter IV. Available phase diagrams rarely duplicate the multi-component composition of real hot processing liquids, but they usually come close enough to yield useful information about freezing.

Figures VI-1a and b, for example, are liquidus maps of the CaO-MgO-SiO_2 and CaO-FeO-SiO_2 systems, respectively.[21] On each one, two composition regions have been schematically marked off. The region in the lower left (CaO-rich area) represents *basic metallurgical slags,* though in Figure VI-1a there is no iron oxide and in neither figure does fluorspar appear. Nevertheless, it is readily surmised that basic steelmaking slags may often float as a slush (part solid, part liquid) on the molten metal. When a BOF is rocked between heats to coat the walls with slag, the solid (i.e., high-CaO) component of this slush tends to remain while the liquid component runs off. It is this more refractory solid component that adds protection to the lining.

Oxygen-process steelmaking slags of lime:silica ratio >2:1 run low in iron oxide and are fairly well approximated by Figure VI-1a. The ternary eutectic at ~1790°C marked in the figure is depressed to ~1600°C by fluorspar, but remains fairly closely under the process temperature. By contrast, a basic slag of CaO:SiO_2 mol ratio <2:1 is seen in the diagram to lead to much lower-melting eutectics. In a vessel lining of a given negative ΔT behind the hot face, the latter slag can thus penetrate much farther than the former before reaching a temperature at which it freezes completely. For more reasons than this, basic O_2-process slags are best kept at CaO:SiO_2 ratios above 2:1. But the general rule illustrated here is that *the pertinent eutectic temperature of a slag determines its maximum liquid penetration depth into a refractory lining,* given the temperature profile of the latter.

Basic slags in nonferrous metallurgy usually run high in iron oxide and are better approximated by Figure VI-1b. The figure indicates that low-melting eutectics are in effect, though whether these are actually reached depends on Lever Rule calculations that we shall leave to the interested reader. The basic copper-converter

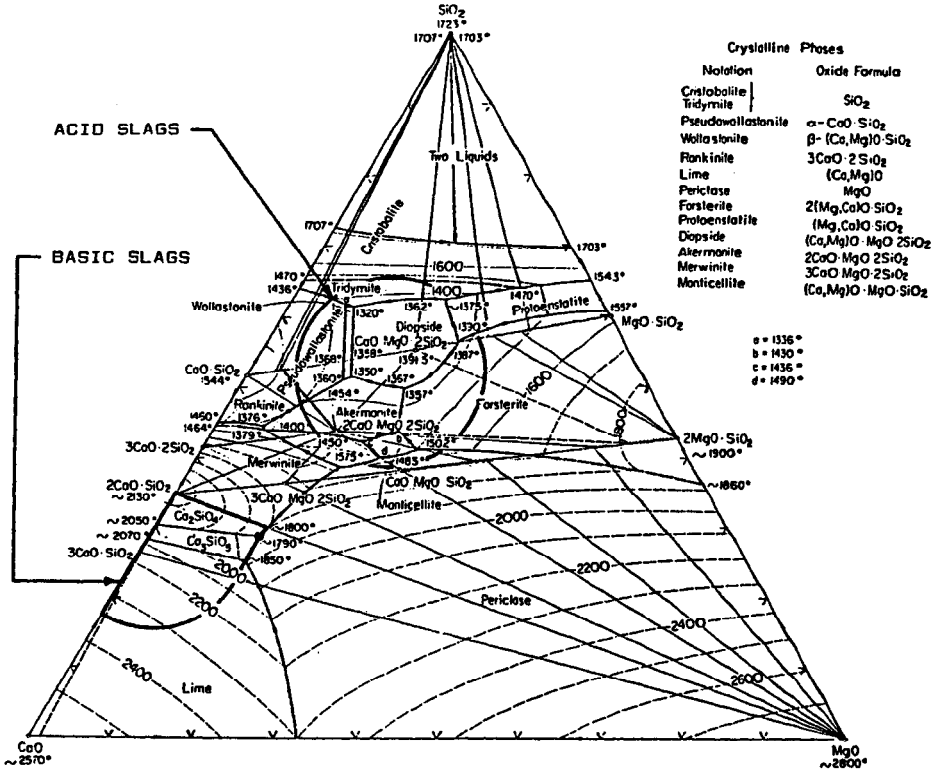

Figure VI-1a Low-Iron Slags in the Ca0-Mg0-Si0$_2$ System
(adapted from Ref. 21, by permission)

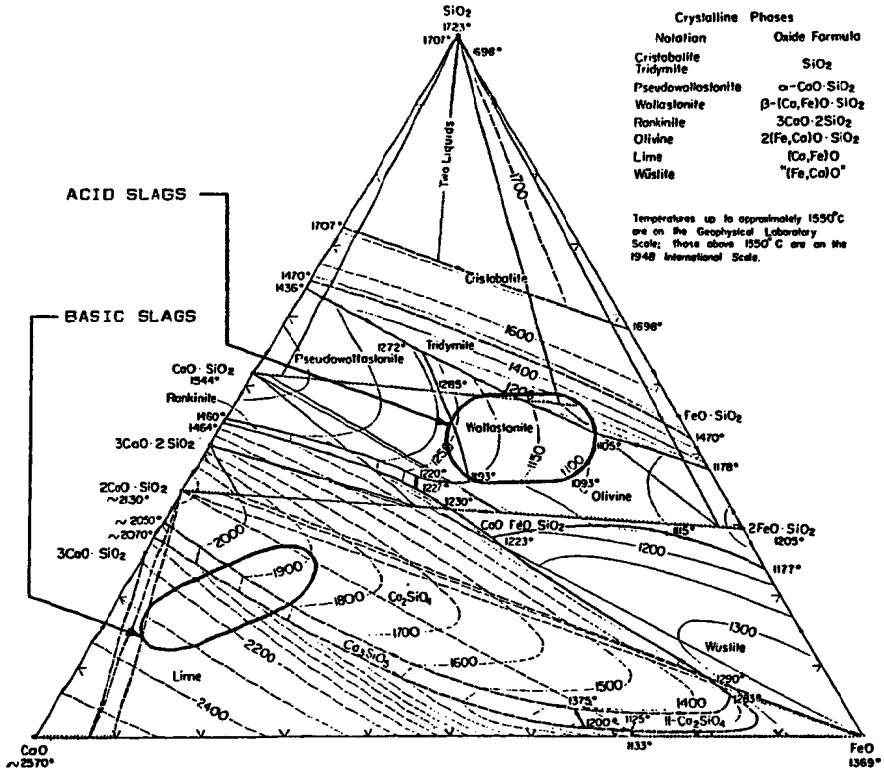

Figure VI-1b High-Iron Slags in the Ca0-Fe0-Si0_2 System
(adapted from Ref. 21, by permission)

slag falls in this category, as did also the basic open hearth steelmaking slag -- at least, early in each heat.

The second areas marked off in Figures VI-1a and b, for *acid slags,* cover most other slag compositions used in metallurgical smelting. Though the primary phase fields differ markedly depending on whether MgO or FeO is emphasized, the pertinent eutectics are all low-melting: in the 1300°C-1350°C region in Fig. VI-1a and the 1100°C region in Fig. VI-1b As iron oxide is prevalent in nonferrous metal ores and slags, the latter figure is the more indicative. On the other hand, acid slagging practice in argon-oxygen steelmaking is better represented by Fig. VI-1a. The reader interested in the system CaO-MgO-FeO-SiO_2 will find a partial phase diagram in Reference 21, as well as a map of the system FeO-MgO-SiO_2.

In Figure VI-2a, which is the FeO-Al_2O_3-SiO_2 phase diagram, [21] a penned-in circle indicates compositions illustrative of *coal ash.* The pertinent ternary eutectic, to the left in the diagram, is at 1038°C. As coal ash also contains appreciable alkalies, its melting actually commences much lower -- perhaps about 800°C or below. A refractory facing a reducing coal-burning flame is not immersed in this liquid, but it is certainly spray-coated. The liquid is quite penetrating, and its relatively high iron as well as alkali content should be remembered. The oxidized Fe_2O_3-Al_2O_3-SiO_2 system melts considerably higher.[21]

Fuel oils, being crudely distilled products, have a somewhat different *oil ash* (not shown). The silica content is comparable and alkalies are present, but the iron oxide content is low. On the other hand, oxides of vanadium and titanium tend to take its place. Oil-burner ash probably melts starting at about 1000°-1100°C reducing, and at about 1300°-1400°C oxidizing.[21]

Another important process liquid is the iron-smelting *blast furnace slag.* Its approximate "exit" composition range is indicated by the oval penned in on the CaO-Al_2O_3-SiO_2 phase diagram of Figure VI-2b.[21] This exit slag contains only a few percent FeO, permitting the use of this diagram. Owing to the high operating temperature of the blast furnace, alkalies are almost entirely distilled out. Allowing for impurities not represented in this diagram, the melting and freezing range of blast furnace slag at the taphole is estimated from the figure at about 1200°-1700°C. Subtract about five hundred °C up in the shaft, where the %FeO and Na_2O are much higher.

The other area, marked off by the circle in Figure VI-2b, represents the approximate composition range of *Portland cement.* The onset of melting shows there at ~1400°C, while the cement manufacturing operation at about 1700°C is seen to be far short of the

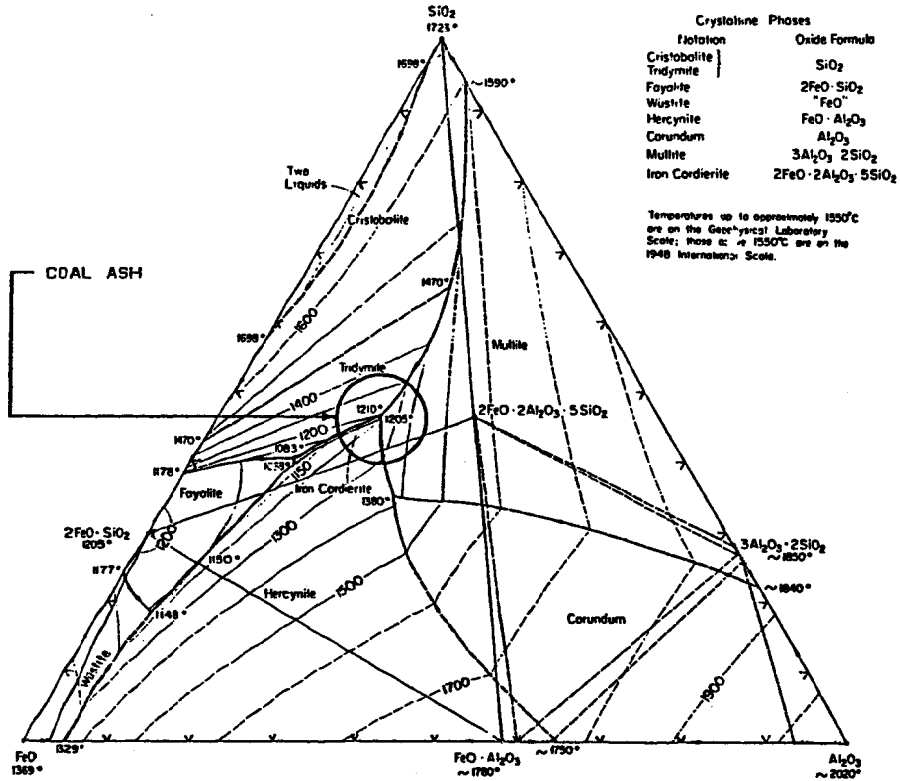

Figure VI-2a Coal Ash in the FeO-Al_2O_3-SiO_2 System
(adapted from Ref. 21, by permission)

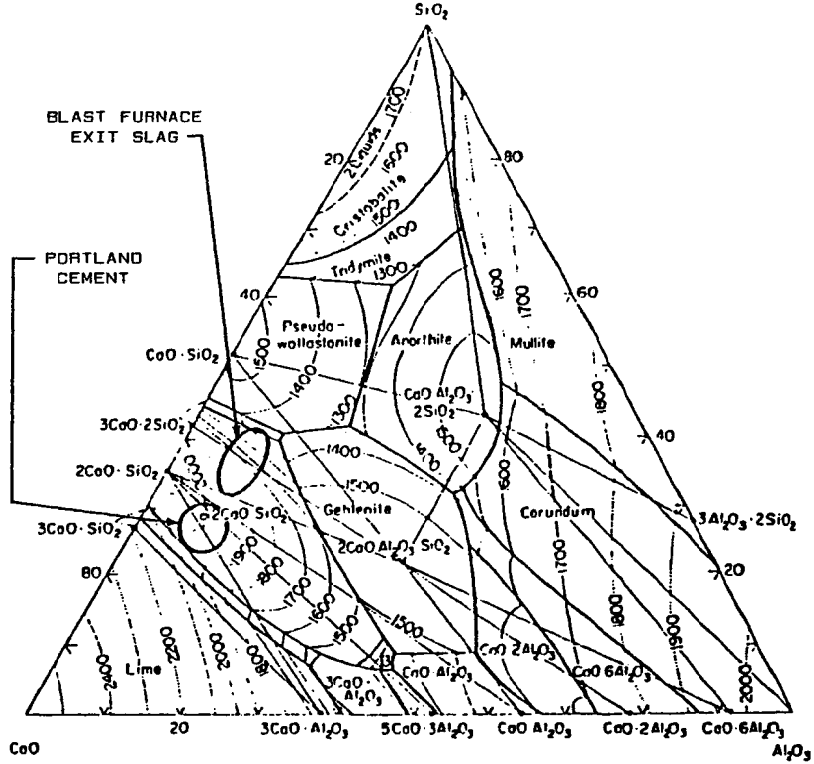

Figure VI-2b BF Exit Slag and Portland Cement in the $CaO-Al_2O_3-SiO_2$ System
(adapted from Ref. 21, by permission)

temperature required for complete melting. The liquid component of the cement clinker does penetrate the hot-zone refractory; but (lacking appreciable alkalies) it soon freezes within the ΔT of the kiln lining.

We shall not display phase diagrams illustrative of *glass* manufacture. Glasses, which do penetrate porous refractories, undercool in the metastable vitreous state within the ΔT of glass melting tank walls; so equilibrium (crystalline) phase diagrams are not very helpful. Current glass contact refractories make this omission of little moment, as will be seen presently.

Finally, the penetration and corrosion of refractories by *molten chlorides* has to be acknowledged. We shall do without displaying phase diagrams relative to the freezing of liquid halides. These diagrams are amply available;[21] the reader interested in halide systems can acquire the needed information without difficulty. For mileposts, NaCl melts at about 810°C, KCl at about 780°C, and the minimum-melting mixture (~50-50 by weight) melts at about 660°C.[21]

Freezing and Refractory Slabbing. A classical phenomenon associated with freezing of a penetrating and aggressive liquid is *slabbing,* also called *peeling* or *chemical spalling* of the refractory. Given a negative ΔT across a wall or lining, with time the liquid penetration front approaches the depth at which the liquid finally freezes. This moving front is a surface, roughly parallel to the hot face. Recall that debonding of crystals by dissolution has to follow this penetration in time; in any event it is a thermally-activated process which slows markedly with increasing depth (i.e., decreasing T). Hence the weakened zone of a refractory is less deep than the penetrated zone.

Now let this refractory cool, e.g. in shutdown of a furnace or between heats in a converter. Then place it on duty again, restoring the steady-state operating temperature and ΔT. As to the intruded liquid, this is freeze-thaw cycling, with a ΔV accompanying each change of phase. A common view is that this ΔV subjects the refractory to a shear strain parallel to the hot face. Failure occurs where the refractory is weakened but not yet plastic, namely within the penetrated zone, close to but not at the penetration front. Field observations confirm this. Slabs of the refractory are dislodged: a stepwise repetitive recession that greatly exceeds the rate of hot face surface removal. Typical depths of penetration at which slabbing occurs are from about 1/2" to well over 2", or from ~1 cm to well over 5 cm, in a wall or lining backed by a steel shell.

It may be arguable whether freeze-thaw cycling is necessarily the cause of slabbing. The same liability to shear under thermal transients was described in Chapter IV under Thermal Stress and

Shock Resistance, in the absence of liquid penetration. But it is certain that weakening of the refractory by dissolution is crucial to slabbing failure. Observations of this wear mode go far back historically. Except for those specifically designed to prevent it, no refractory type has been immune.[86,111-119]

Manipulation of Freezing. The magnitude of the steady-state dT/dz in a refractory lining clearly affects the maximum possible depth of liquid penetration. But there is little liberty to manipulate this temperature gradient in the favorable direction by modification of the refractory. In fact, the risk is rather the reverse. For example, the designer considering an insulating backup lining must beware that a diminished ΔT across the working lining will result, with an accompanying increase in both the depth of liquid penetration and the rapidity of invasive weakening. With sufficient depth of penetration, structural slumping may follow.

The composition of the liquid might be changed, by virtue of the refractory components that it dissolves, in such a way as to increase its minimum eutectic freezing temperature. This has been achieved once. But among all of the process liquids represented in Figs. VI-1a, b and VI-2a,b there appears to be no second opportunity. In the one case on record (ca. 1970), basic slags penetrating MgO refractories were altered from a $CaO:SiO_2$ mol ratio <2 to a ratio >2 in situ by providing a high lime content in the matrix of the refractory.[119] As was mentioned in connection with Figure VI-1a, the pertinent ternary eutectic is changed accordingly. A $CaO:SiO_2$ mol ratio >2 (weight ratio >1.87) remains a virtue in MgO refractories, but basic steelmaking slags no longer need this chemical alteration. Now they too are >2, by design.

Other phenomena can affect the penetration rate through freezing, however, without changing the pertinent eutectic. One example occurs in A-Z-S (alumina-zirconia-silica) and other refractories containing zircon.[88-91,120-125] In Chapter IV and Figure IV-6a, it was found that when this phase is melted (now including by dissolution) some ZrO_2 is left as solid. This high-melting solid may protect the underlying zircon, or, if entrained in the liquid, can obstruct pore passageways against further penetration.

Similar pore blockage effects occur in very-high-alumina refractories comprised of Al_2O_3 + mullite.[126-135] Dissolution in an aggressive liquid raises the $Al_2O_3:SiO_2$ ratio of that liquid, enabling an alumina-rich phase to precipitate out earlier as the ΔT across the refractory is traversed in penetration -- even if the Al_2O_3 + mullite eutectic is not brought into play in the liquid itself. This same quality is attributed to spinel ($MgAl_2O_4$) in both basic and high-alumina refractories,[136-143] and notably to chrome spinels ($MgCr_2O_4$ and ss) in

basic refractories.[72,73,141,144-151] Chromia as a component in aluminas and alumina-silicas has a similar effect.[77-80,129,151-153] Recent phase diagram work in the $MgO-Al_2O_3-Cr_2O_3-Fe_2O_3$ system[154] and the $CaO-MgO-Al_2O_3-SiO_2$ system[155] has helped rationalize some of these phenomena.

A common way of thermally controlling liquid penetration and invasion is by brute force: namely, to employ water cooling behind or within the refractory. This device was mentioned in Chapter III in connection with the blast furnace, tuyeres and oxygen lances, arc furnaces for steel and for oxide melting, and steam boilers. It is almost always an option. Water cooling is employed in many other situations not called out explicitly there, including reportedly in the BOF.[156] At the very least it lowers the temperature of thermally-activated corrosion. Most often it is designed to freeze the otherwise-penetrating liquid on the refractory hot face, creating a protective solid skull. The price paid includes the initial cost of intricate heat-transfer and plumbing systems as well as safety provisions, and often also the day-in, day-out cost of wasted process heat. The economic trade-off generally favors water cooling only after all possible measures of improving the refractory have been exhausted.

Porosity and Pore Sizing

Porosity and Penetration Rates. It should be realized from the foregoing that a hot process liquid, as it intrudes into the porosity and down the temperature ramp in a refractory wall, may crystallize out some of its own highest-melting component progressively as it goes. Upstream dissolution of the refractory augments this process. If equilibrium is in effect, at each penetration depth z the liquid remaining will be at a composition lying on its liquidus at the corresponding temperature T_z. At least two conflicting consequences make a quantitative statement of pore penetration kinetics difficult: (a) the effective pore size may decrease due to solid deposition out of the penetrant, even as it may be increased by matrix dissolution; and (b) the viscosity of the liquid may either increase or decrease with depth as the composition changes, even as it is increased with a fall in temperature. A further matter is the degree of wetting of the solid by the liquid, which is a knowable function of temperature but also depends on the changing liquid composition. Still another is that dT/dz, which might have been nearly single-valued over the refractory thickness Z before penetration, has to differ appreciably in the penetrated zone but by an amount which is difficult to compute.

Under these circumstances a single comprehensive mathematical model of pore penetration kinetics has not been forthcoming. Nevertheless, some qualitative assertions can be made.

If wetting is effective, the capillary penetration of pores by molten slag is driven by its surface tension, s, and resisted by its viscosity, η, times its linear shear rate. For a pore segment of "averaged" diameter $\bar{d}$ and "averaged" angular orientation relative to z (the thickness direction in a refractory wall), one inserts the geometrical factors necessary to obtain a capillary pressure difference Δp_c driving the liquid and a corresponding Δp_r resisting its flow in the z direction. These are:

$$\Delta p_c \propto s/\bar{d} \qquad \text{and}$$

$$\Delta p_r \propto (\eta\tau^2/\bar{d}^2)z(dz/dt) \ ;$$

where τ, called the "tortuosity factor," relates the distance travelled by the liquid through a devious succession of pores to the equivalent straight-line distance parallel to z.

Setting these two quantities equal and rearranging, one is able to write both the rate of advance of the liquid-filled "front," dz/dt, and its "parabolic time-law" integral.[90,109] These are:

$$dz/dt/ \propto (1/\tau)(s\bar{d}/\eta)^{1/2} \quad \text{and} \quad z^2 \propto (s\bar{d}/\eta\tau^2)t + C \ .$$

If further we define v as the volume penetration in cm^3 of liquid per cm^3 of refractory body, assuming all porosity is filled up to the advancing penetration front, then:

$$dv/dt \propto (P/\tau)(s\bar{d}/\eta)^{1/2} \quad \text{and} \quad v^2 \propto (P/\tau)^2(s\bar{d}/\eta)t + C \ ,$$

where P is the apparent porosity.[9]

Rigorous equations are not warranted since dT/dz is not incorporated and s and η are unstated functions of T and liquid composition, hence of z. In addition, as pointed out in the previous section, owing to deposition of solids in the pores the effective diameter $\bar{d}$ changes with T, t, and z.[90] One effort has been made to incorporate a variable $\bar{d}$,[157] but without avail to the present purpose.

Thus, we can infer only the correlations expressed in the above proportionalities. These have been fairly well upheld by experiment.[90,109,158] One study confirmed the proportionality of liquid permeability (a volumetric property) to P;[159] and another demonstrated the expected dependency of corrosion rate on slag viscosity.[160]

The separate dependency of penetration rate on pore size alone can be tested only in the laboratory. In working refractory manufacture, virtually all of the processing means available to reduce pore diameter diminish both the apparent porosity and the mean pore size simultaneously. Thereby another benefit is realized, relating to intercrystalline boundary invasion, as follows.

At fixed porosity P, the mean distance $\bar{x}$ between pores is directly proportional to $\bar{d}$. Hence pore size refinement alone is accompanied by an equal proportionate decrease in the distances over which boundary invasion by the liquid must progress before this process can link up to debond conjugate crystals. On the other hand, from the relation,

$$P \propto \bar{d}/\bar{x} \quad ,$$

a proportionate decrease in both P and $\bar{d}$ would leave $\bar{x}$ unchanged. A fractional decrease in P greater than that of $\bar{d}$ would actually increase the inter-pore distance $\bar{x}$. In addition, the local reservoir of liquid saturating the penetrated zone decreases precisely with decreasing P. This means its total dissolving or debonding capacity decreases, because the liquid can dissolve components of the refractory only until it becomes saturated in those components.

Countermeasures. These arguments all rationalize corrosion consequences that have been known qualitatively for decades: *the resistance of a refractory to penetration by liquids is improved by reducing its apparent porosity* -- other things being equal. There is of course an accompanying penalty, which has been equally long known: thermal stress resistance is diminished. The relative virtues of this trade-off have become better differentiated with time, such that higher porosity is still preferred where corrosion is not critical but denser versions of the same refractory have become preferred in corrosive situations. Needless to say, as the apparent porosity of a refractory is reduced toward zero, its susceptibility to slabbing is confined and then eliminated.

Some cases in point are: (a) the evolution of "high-fired" super-duty and high-duty firebrick, whose apparent porosities run some one-fifth to one-third less than those of the standard products; (b) the evolution of chemically-bonded high-alumina refractories, both brick and monolith -- especially silica-bonded, phosphate-bonded, and cement-bonded formulations -- , achieving porosities from one-fifth to two-thirds below those of their "direct-bonded" counterparts; and (c) the increasing use of arc-fused grain and of fusion-cast refractories. The latter type approaches zero apparent porosity in periclase, alumina, A-Z-S and zirconia bricks, among others.

Impervious Carbon. A special case of importance for lower-temperature processing pertains to the use of carbon equipment -- vessels, ducting, condensers, linings, etc. -- in hostile chemical environments. Synthetic rubbers and hydrocarbon polymers, for example, are resistant to numerous chemicals including aqueous salts and some acids, but are severely temperature-limited. Carbon equipment can carry this same chemical resistance up to considerably higher temperatures: to about 500°C, or even higher if protected against air oxidation from the outside. This temperature capability bridges between the aqueous domain below and the nonaqueous processing domain above. Carbon can withstand organic environments as well as inorganic.

But ordinary carbon products, made and baked as described in Chapter II, are highly porous and permeable. Water or organics penetrate the porosity and can "wick" or "weep" through a carbon wall. Gases can likewise pass through. Deterioration of the carbon might not follow, depending on the prevailing chemistry; but the function of containment is clearly not served.

"Impervious" or "impermeable" carbons are made starting out in the conventional way; but then the near-net-shape article is repeatedly re-impregnated with pitch and re-baked, until it meets pertinent specifications of apparent porosity or permeability. Synthetic resin impregnation and curing cycles are now conducted as well. The cost rises with the number of successive treatments, but practical penetrability can be reduced to zero by this means.

Wetting and Non-Wetting

The vertical angle made by the edge of a stationary body of a liquid with the flat surface of a solid, known as the *wetting angle*, is of immense importance to the penetration of porosity in that solid by that liquid. In the foregoing we have assumed wetting, characterized by a wetting angle <90° and in fact close to 0°. "Non-wetting" combinations, characterized by a wetting angle >90°, also occur and give entirely different penetration patterns.

A very low wetting angle signifies that the molecules (or ions, or atoms) of the liquid are attracted more to those of the solid than they are to each other. The meniscus made in a pore channel in that case is concave, and the surface tension of the liquid generates the equivalent pressure driving the liquid into the channel. This pressure increases with decreasing pore size, because the ratio of a channel circumference to its cross-section area is proportional to 1/d. Wetting angles of around 90° provide essentially no driving force for pore penetration, while with still further increasing angle the meniscus becomes increasingly convex and a resistance to penetration

develops. This resistance again increases with decreasing void diameter.[90,109]

A few model liquid-solid systems have been studied.[161] But the measurement of wetting angles at high temperatures is not easy, and no comprehensive cataloguing is known for systems of interest in refractory penetration broadly. General rules apply well enough, however, and will suffice here. On the whole, *liquid metals do not effectively wet either oxidic or non-oxidic refractories,* and *liquid oxides and halides do not effectively wet most nonoxide refractories.* Another way of putting this is that *wetting is most effective when the kind of chemical bonding* (viz., ionic or nonpolar-covalent or metallic) *is the same in both the liquid and the solid.*

As there are gradations in kinds of chemical bonding, there are varying degrees of wetting between the extremes of the above rules. Furthermore, for any given liquid-solid combination the wetting angle changes appreciably with increasing temperature,[161] or with a change in the gaseous environment. These effects are not always predictable, least of all quantitatively. Nevertheless, the general rules italicized above provide useful guidelines for empirical trial.

Some of the most strikingly corrosion-resistant refractories are those which have been selected in accordance with these rules. One further observation is in order before those refractories and their uses are described. For evident chemical reasons, a refractory which is not readily wetted by a given process liquid also tends kinetically to resist dissolution by that liquid. Hence a low or near-zero rate of penetration due to non-wetting can be accompanied by a low rate or extent of debonding of crystals even where there is liquid-solid contact. Choice of a refractory material that is sufficiently non-wetted is a sure cure for slabbing. The most important non-wetting cases are taken up in the next four sections.

Liquid Metal Containment

Molten metals are readily contained in a wide range of refractory materials. In metallurgical processing it is the slag or flux or dross that penetrates and corrodes; the metal itself is sufficiently non-wetting as to penetrate only large gaps, cracks and holes, rarely much of the connected porosity. Even cracks and brick joints whose faces are compressed together are protected from capillary penetration by this non-wetting characteristic.

That is fortunate indeed for metals technology, as cracking of refractories in service is common (see Microstructural Integrity in Chapter IV). Metal seepage by capillarity in crucibles, molds, ladles, induction furnaces, and hearths would otherwise be enormously

costly and dangerous. Furthermore, submerged mechanical closures such as taphole plugs, stopper valves, and slide gate valves could not otherwise function reliably.

It is also fortunate that the corrosive interactions between molten metals and refractories are almost entirely limited to oxidation-reduction. Only a few metal-refractory combinations are disqualified by the prospect of reaction. These disclose themselves readily by the use of free energy data.[23]

Dissolving of a refractory component or reaction product in the liquid metal can occur. One example, namely carbon, is rendered trivial in carbothermic smelting wherein this element is already provided in quantity as a reagent. Only in subsequent metal purification and handling are carbon refractories likely to be disqualified.

Another example brought up in Chapter VI is silicon. By redox reaction of refractory silicates with molten aluminum, silicon can be delivered into solution in that metal in unacceptable concentrations. This prospect would seem to disqualify the whole range of aluminosilicate as well as zircon refractories for aluminum containment. Not so, in part because of the relatively non-wetting quality of the metal-refractory interface, as explained following.

Take zircon as example. Reaction of the refractory surface with aluminum,

$$4Al_{(l)} + 3\,ZrSiO_4 \rightarrow 3\,ZrO_2 + 2\,Al_2O_3 + 3\,Si\ (in\ Al)\ ,$$

depletes the surface of its SiO_2 component but leaves the solid ZrO_2 skeleton intact. Now if the aluminum were to wet the solid, it could pursue the remaining SiO_2 component down into the crystal lattice and continue to react.

But the aluminum cannot penetrate, and the above reaction soon becomes solid-state diffusion-limited, i.e., all but stops. Since mullite reacts in the same way, leaving in place an Al_2O_3 surface skeleton, aluminosilicate refractories of >80% Al_2O_3 also enjoy this essentially kinetic protection against desilication by molten Al. Iron oxide impurity provides a similar scenario, dissolving as Fe in Al.

Thus liquid aluminum is variously contained in its commercial processing by mullite or high-alumina refractories, by zircon or A-Z-S, by carbon, and by silicon carbide; even by firebrick if it is to be subsequently purified of its Si and Fe contaminants. Likewise for magnesium. For higher-melting and less chemically active metals, e.g., copper and the ferrous metals, add to this list an array of basic

refractory products and upgrade the firebrick to high-duty or super-duty. Most nonferrous metal processing employs from high-alumina to fireclay refractories for containment. The blast furnace hearth, protected against oxidation, is often made of carbon blocks. The coreless induction furnace, dealing with high-quality metal charges, tends to use synthetic single-oxide refractories to avoid contamination: MgO, Al_2O_3, or $ZrSiO_4$. The indirect-heated zinc-smelting retort, having to deal with vapor leakage as well as liquid metal, is now most often constructed entirely of dense silicon carbide. Chemically speaking, simply to contain liquid metals is not very demanding.

Special Features. Three special features of metal intrusion in refractories deserve mention, however. One relates simply to penetration. Under a hydrostatic head, replacing capillarity as the driving force,[163,163] liquid metals may penetrate rapidly and deeply into submerged crevices and sometimes even into the coarser porosity of a refractory. Intrusion is aided by the very low viscosity of liquid metals. This is not "aggressive" attack, as by itself it is not responsible for oxide refractory corrosion or chemical alteration. It does not signify wetting. In masonry construction, hydrostatic intrusion is countered by (a) providing sufficient refractory thickness and ΔT to ensure that the intruding metal will freeze within the wall; (b) use of large blocks to minimize the number of joints to be penetrated; and (c) use of a multi-layer brick layup with the joints staggered, to interrupt the passageways. These design measures can be seen in large furnace hearth construction, e.g., in the blast furnace of Figure III-1.

The second feature has given rise historically to the labelling of some metals as chemically "aggressive" to oxidic refractories -- especially to firebrick. In such submerged refractories exposed to liquid metal alone, after service an altered zone is usually found, typically low-melting and containing the ion of that metal. Such "aggressive" metals include copper and most of the other carbothermically-smelted nonferrous elements. They all exhibit low-melting mixed silicates.

These are in fact not aggressive metals. They do not wet oxidic materials more effectively than do other metals. They do not appreciably invade or dissolve in refractories as metals (i.e., in the zero valence state). The first step leading to the observed penetration and alteration is invariably their *oxidation*, after which the phenomena observed in the refractories are quite properly attributed to their "slag" components (viz., oxides and/or silicates). It is these oxidized species that are aggressive.

All liquid metals can contain, in solution, greater or lesser amounts of their own oxides. For exaggerated examples, see the Ti-O and Zr-O phase diagrams in Reference 21. A dissolved metal oxide is readily given up from the metal into solution in a refractory silicate host. Other sources of submerged-metal oxidation include the atmosphere (viz., CO_2, SO_2, O_2) in the porosity of the refractory. This is a replenishable source, transported by gas diffusion. Other oxidizing agents may be present in the refractory itself: Fe_2O_3, for example. All hot oxidic refractories are semiconductors, and it is not necessary for the Fe_2O_3 to touch the liquid metal to oxidize it. In fact, FeO-Fe_2O_3 couples located variously throughout the refractory can serve catalytically to reduce O_2 wherever they are and to oxidize the liquid metal where it is, at some considerable distance, by diffusion. Countermeasures include (a) replacement of the high-silica, high-iron fireclay type of refractory by a low-iron alumina + mullite type,[126-134,164,165] and (b) reduction of the refractory porosity.[77,117,134,135]

The third noteworthy feature of metal-containing refractory corrosion is a more-or-less uniform hot face recession below the metal line in vessels and its exaggerated extent at the metal line itself. Here there is typically stirred or convective contact of a large body of metal with its slag and also with the refractory hot face. The metal is a vehicle of *transport* of (a) its own dissolved oxide, and (b) particles of entrained slag, from its upper slag interface to the refractory walls and bottom of the vessel.

Below the metal line this transport is slow compared to that of direct slag contact. The deep and rapid slag penetration characteristic of slabbing is absent. Yet the debonding of surface crystals or grains of the refractory proceeds at the hot face as metal oxide and slag are delivered to it from the metal. The loosened surface grains can then be dislodged by the metal movement (corrosion-erosion) and/or by the scrubbing action of entrained particles (corrosion-abrasion). Chemical dissolution of the surface grains is not absent, but ordinarily it is slower than their debonding. Nonuniform flow patterns in the liquid metal result in nonuniform refractory recession. Analysis of the latter has in some cases (particularly in O_2 and Ar blowing) resulted in measures taken to correct the former.

At the metal line there is a marked transition to direct contact of the wetting slag with the refractory, accompanied by increased depth of its penetration and increased intensity (rate and extent) of surface-grain debonding. In stirred cases there is also increased agitation of the liquid at the surface, by lapping or wave action. Increased recession of the refractory accompanies each of these changes in the environment. The typical wear profile at this level is horizontal gouging, accentuated by abrasive scrubbing by the agitated solid

constituents of the slag. In fact, this is usually and properly referred to as *slag-line* corrosion. Defensive measures include the use of dense, high-fired oxidic refractories or, in some cases, a resort to nonoxides on which these slags are non-wetting.

Non-Wetted Refractories: Massive Nonoxides

Other than with liquid metals, the roster of inexpensive refractory substances that resist wetting by hot process liquids is very short. The degree of that resistance varies with the environment, such that the conditions of successful use are also confined. Even within those limitations, however, wetting-resistant materials have had telling economic impacts on the processes that can use them. The principal materials in evidence are carbons, graphites, silicon carbide, and zirconia. It seems probable that a few more nonoxides may become competitive in time. For special uses of some interstitial compounds, see Refs. 18 and 19; and for hot-pressed BN, see Refs. 74 and 166.

Massive carbon, graphite, and SiC are resistant to wetting and reaction by molten chlorides, alkalies (M_2O and MOH), and silicates. This property can be diminished in two ways. One is by oxidation, which yields a silica skin on SiC and a partial monatomic surface oxide layer on C. Thus wetting is minimized by maintaining reducing conditions. The other interference is a matter of refractory phase composition. Early C and SiC formed products were clay-bonded and sintered, yielding a continuous aluminosilicate matrix between crystals. That matrix is penetrated and attacked; hence these products were not recognized as particularly resistant. Today's carbon is all carbon (though still porous). Today's refractory silicon carbides are reaction-bonded by Si_3N_4 or SiAlON and are dense, strong, non-wetted and inert.

The corresponding inability of the nonoxides to react chemically with process liquids is immensely important. Lacking attack on intergranular impurities, neither penetration nor dissolution is appreciable. This is one reason why immersed carbon and graphite electrodes are durable. Together with thermal stress resistance and mechanical strength, this is why silicon carbide refractories have taken over the blast furnace shaft lining. There a constant refluxing rain of alkalies and chlorides multiplies the corrosiveness of the reducing ferrous-lime-silica slag.[72,74,112,167,168] Carbon is also in use, though sometimes coated,[144] in circumstances where its oxidation can be controlled such as in the blast furnace and cupola hearth and in a few types of crucibles. It would be a natural choice for some of the high-alkali environments of glassmaking, were it not for its susceptibility to oxidation.

SiC is much more kinetically oxidation-resistant, but loses its non-wetted character progressively with surface oxidation. SiC tends to be used either under reducing conditions or where exposure to liquid slags is minimal. An example mentioned previously is the zinc retort. Several other nonferrous metallurgical retorts are also built of SiC. This chemically resistant material is now beginning to be used against the notoriously aggressive but reducing slags of waste incinerators.[169,170] Its wetting resistance underlies its use as lifters and as monolithic coatings in cement kilns.[171,172]

Nonoxide Composites

The earliest historical carbon composite refractories, made of clay with charcoal, then natural graphite, were developed quite empirically. Probably at first it was found that these lining materials enhanced the reduction or smelting of iron and inhibited its reoxidation. That is, they had a *reagent* function. Sophisticated smelting methods have largely obviated that function. The conceptual transition of the 20th century was to *wetting resistance*, hence resistance to slag penetration. The modern oxide+C or oxide+SiC composite refractory is intended to exploit the wetting resistance of nonoxides. But it uses these materials in particulate form in such manner as (a) to extend this non-wetting quality to an oxidic host; and (b) to enhance the oxidation resistance of the nonoxide kinetically by enveloping it in that host.

Magnesia-Base. Two types of composite basic refractories developed for the BOF are illustrative of these materials. The simpler type, used in the "charge pad" of Figure III-10a, consists of a conventionally fired MgO refractory brick which is then vacuum-impregnated with a hot (liquefied) industrial pitch. It is then installed. In the atmosphere of the BOF, restricted diffusion into and out of the porosity inhibits oxidation of the pitch and then of the carbon which results from its pyrolysis (i.e., coking) in service. That pyrolysis commences at the hot face and works gradually back toward the cold face in successive heats of the vessel.[115] The carbon retained inside the pores of the MgO provides the non-wetting barrier to slag penetration,[115] while the ceramic bonding of the host itself affords strength and abrasion resistance.

The second type, called "pitch-bonded" or "tar-bonded," starts with a size-graded mix of particles of a pre-fired and dense MgO refractory grain. The particles are thoroughly coated with hot pitch in a suitable mixer; then the slightly tacky mix is pressed into bricks and let cool. Except for a mild thermal curing treatment sometimes used, called *tempering*, these bricks too are installed unfired. Pyrolytic decomposition of their pitch to carbon is begun in the carefully-conducted *burn-in*, or first heat-up of the BOF. This coking also works

gradually back toward the cold face in successive heats.[115,173] In this case the bond or matrix between the particles of MgO consists rather exclusively of carbon -- grading back toward the cold face as partially decomposed pitch. There is no "ceramic bond" except that at the hot face itself, comprised of the intruding slag and some MgO resulting from reoxidation of vaporized Mg.[67] That fluid bond has inappreciable strength, but it does help to isolate the carbon.

Prior to the use of these composite refractories, the BOF had experienced severe slabbing. The first and largest contribution to service life made by both of these composite types was the elimination of slabbing -- a direct consequence of the resistance of carbon to wetting by CaF_2-CaO-MgO-FeO-SiO_2 slags.[115,174] Penetration went from inches to millimeters.

Most of the variations subsequently made on the original MgO+C composites have been in the second type. Their purposes have been principally: (a) to increase the amount and density of the carbon contained; (b) to decrease the dimensions of the pore or void spaces left after carbonization; and (c) to improve the protection given to the carbon by the surrounding oxidic material. Included in this evolution was the parallel development of alumina refractories containing particulate SiC, as well as additions of graphite to both the MgO and alumina compositions. Variables of manufacture of this once simple pitch-bonded composite now include at least:

Oxidic Grain
- Composition and Pretreatment
- Size Distribution
- Inorganic Additives

Organic Liquid
- Pitch, Synthetic Resin
- Pretreatment
- Solvent or Thinner

Particulate Nonoxide
- Solid Resin
- Graphite
- Silicon Carbide

Particulate Deoxidants
- Silicon
- Aluminum
- SiAl Alloy

Composite basic bricks of these two essential types -- the fired-impregnated type for high wear areas and the organic-bonded type for use there and elsewhere -- are the masonry linings of choice for virtually all of the O_2-blown and Ar-stirred basic steelmaking vessels of Chapter III. Basic composites sometimes also serve in the lower sidewalls and bottom of the EAF,[44,76,175,176] and in some torpedo ladles[74] and other ladles and ladle furnaces.[96,177-182] Their oxidic grain is essentially of three origins: (a) seawater periclase; (b) magnesite; or (c) dolomite or magnesite-dolomite (of considerable popularity in Europe and Britain).[97,177,178,181,183-185]

Except in the burned-impregnated type, the use of pitch alone has all but vanished: it was found early-on that slag resistance increases with increasing %C,[179,186] and the incorporation of graphite in amounts yielding up to about 19%C after pyrolysis is common.[43,187] This addition permits optimizing the amount of pitch for use solely as a carbonaceous binder, leading to a desired minimum of porosity and pore size after coking.[84,96,186] The use of phenolic resins and other organic polymers in place of pitch as a binder has now also become commonplace.

Many but not all pitch-bonded basic composites now contain a "deoxidant" metal powder, whose purpose is to protect the carbon further against unwanted hot oxidation. Reports are plentiful of the use of one or both of Al and Si powders or of a powdered brittle alloy of both,[74,95,96,98,179] claiming decreased refractory recession rates that well warrant the additional cost. The Si-Al alloy is the most convenient to use.[95,98] Powdered Mg has been tried but is extremely dangerous to handle. An additive of BN was favorably reported;[100] and several additional refractory metals and compounds have been studied as deoxidants.[101,102]

Alumina-Base. Alumina-base composites of the modern era started in the 1950s with an alumina + graphite plastic (i.e., trowellable) patching mix, renowned over the industrial world as "Helspot." Most of the developments in alumina composites since then have also been in monolithics. In addition to the Al_2O_3 + graphite type, a number of other graphite mixes have been reported including mullite,[188] andalusite,[189,190] A-Z-S,[191] and even zirconia.[74] But a concurrent development has incorporated particulate SiC with aluminous hosts, either alone or together with added graphite.[46,105,172,192] A concensus favors about 15% nonoxide, yielding not only excellent slag penetration resistance due to the non-wetting quality of SiC but also a marked improvement in thermal stress resistance.[46,192] The latter is due to toughening and strengthening by the hard-particle inclusions. Zircon and ZrO_2+Al_2O_3 grains with SiC and graphite have also been reported favorably.[86]

These SiC composite castables have been developed so far primarily in Japan. In some the use of phenolic resin binder is reported;[193-195] castables are generally either chemical- or cement-bonded otherwise. Successful applications of such composites include numerous corrosive-abrasive and thermal shock situations, e.g. in blast furnace tapholes, troughs and runners (where the chemical treatments of steelmaking are started); torpedo and other ladles; tundishes, nozzles, and concast valve parts.[45,47,48,74,86,191-201] The table given above serves as a framework for the formulation of all types of composites.

Miscellaneous. We conclude this introduction to wetting-resistant nonoxides by acknowledging a final category of monolithics: one in which the oxidic grain is absent. The typical formulation uses carbon or graphite or silicon carbide as grain, and often pitch or pitch plus solvent as binder. Since no built-in protection is afforded against major-phase oxidation, carbon materials in this category are limited to low-temperature or reducing service. One such example is an expansion-joint filler, used between the flooring blocks of the Hall-Héroult cell. Another is a rammed surface flooring of that same cell. Chemically-bonded SiC monolithics are used for their wetting resistance as mentioned previously above,[172] and for their resistance to abrasion. More uses of nonoxide monolithics will surely follow.

Non-Wetted Oxides

The only oxidic substance that has been credited with any appreciable non-wetting quality toward oxidic liquids is ZrO_2.[3] This compound has been found to be remarkably resistant to molten glasses and to their combined or separated alkalies (Na_2O, K_2O). It is the ultimate glass contact refractory, paying its way by durability despite its high cost.

Zirconia is also the highest-melting and one of the most thermodynamically stable (hence kinetically resistant) of all commercial refractory oxides. Its chemical durability has to be attributed in part to these qualities. In fact, if its resistance to wetting alone were sufficiently pronounced and persistent, it would not need in addition to be essentially non-porous. ZrO_2 really came into its own as a superior glass contact refractory when it became available as a nonporous arc-fused and cast or rebonded product.[24,27,91] In glass melting tank walls and bottoms, it has helped to eliminate the uneven wear profiles formerly experienced, associated with liquid velocity and scouring effects and with "metal-line" corrosion due to the combined action of glass and free alkalies. It is exceptionally effective against borosilicate glasses.[24]

The continuous glass tank operator now has at least three excellent glass contact refractories from which to choose, depending on the aggressiveness of the glass and the operating temperature. These are, in order of increasing durability and increasing cost: (a) rebonded fused-grain zircon or A-Z-S (zircon + mullite phase composition); (b) fused-cast A-Z-S; and (c) fused ZrO_2. The last-named is lime-stabilized, of course, as described in Chapter IV. Cooler areas of the glass tank, e.g., the forehearth, can employ less-expensive alumina refractories; but a ZrO_2+Al_2O_3 brick composition has shown superior resistance in contact with molten high-lead and -borate glazes and enamels,[129] which are aggressive at lower temperatures.

The very basic slags now employed in the torpedo ladle in "clean steel" manufacture are often spiked with Na_2O via soda ash addition. Zirconia bricks made with and without SiC and graphite have been used to line this vessel.[86] Other zirconia brick products used in basic steelmaking include a ZrO_2+dolime type for ladles[87] and ZrO_2+CaO formulations for tundish linings;[93,94] and a ZrO_2 lining brick is used in the coreless induction furnace operating up to 2000°C.[202] Castables made with and without graphite have been used for tundish nozzles and concasting parts.[28,74,191] A review of ZrO_2 refractory uses is included in Reference 121.

FACTORS GOVERNING DISSOLUTION

We now turn from matters concerned primarily with liquid penetration of the void space -- viz., freezing, porosity, and wetting -- to the kinetics of invasion of the refractory solid matter. Dissolution of the bond or matrix between crystals or grains of the major phase(s) causes their gradual debonding, while dissolution of the major-phase crystals or grains themselves is inherently slower and hence usually apparent only on the refractory hot face. It is helpful first to review briefly how these two solid domains are developed in a refractory; and in the process, to build working definitions of their descriptive terms.

Refractory Grain and Matrix

A *grain* or *aggregate* is the first line of defense against corrosion. It is distinguished by (a) its preponderance in the refractory phase composition (i.e., a major phase, selected from Table IV.1), and (b) its relatively coarse sizing and crystallite size. Since such particles may be either single-crystal or polycrystalline, use of the word "grain" as synonymous with "crystallite" is discouraged; the literal use of *crystal* or *crystallite* is preferred in that strict sense.

In most corrosion-resistant refractories the preparation of the grain or aggregate is carried out as a separate set of unit operations, including either sintering or fusion. This coarse, dense material is then typically crushed, ground, separated by screens into contiguous size fractions, and re-constituted into *graded* sizes as part of the refractory *mix*. The terms *grain* and *aggregate* are used for this coarse or graded material, or any size fraction of it above an arbitrary minimum -- at any stage of its processing -- including in the final fired or bonded product, where it persists.

The *matrix* is that portion of the final consolidated solid that separates and yet bonds the grain or aggregate particles. In

conventional ceramic processing, the *matrix* portion of the dry mix is composed of very fine particles of the major phase(s), together with any other finely-divided solids that may be added to modify its composition or for purposes of chemical or cement bonding. In the final product, any impurities that are rejected in processes of reaction or crystallization also turn up in the matrix. Hence the distinctions previously made here among "matrix" (the inclusive term), "bond," and "segregated impurities" are options used to emphasize their origins.

There are a few niceties of language that are not always observed. Since "aggregate" implies "polycrystalline," this word is improperly used for a single-crystal grain. The term "matrix" might not be appropriate for impurity or other minor phases occurring in orientation boundaries in the interior of a polycrystalline grain, if more-voluminous phases separate the grains themselves. In a fused-cast refractory, however, this intercrystalline material may be either "matrix" or "segregated impurities" depending on point of view. As a fused-cast product is not crushed and reconstituted, there is no other matrix. The large as-frozen crystals are the grain.

Finally, there are still other types of refractories in which the major phases are not manufactured separately as grain. In firebrick, for example, it is common to include in the mix a proportion of *grog*, which consists of crushed and sized previously-fired brick. Ordinarily, grog is chemically almost indistinguishable from the remainder of the finished brick, differing only in density by virtue of its having been fired twice. It is included in the mix primarily to control firing shrinkage. In finished firebrick it is common not to identify a "grain" at all, though there will be major and minor phases. In alumina-silica products that are >70% Al_2O_3, an alumina phase might or might not be included in the mix as a separately-made grain. If not, alpha-Al_2O_3 and mullite might be principal fired phases, but again a "grain" would not be identified.

Rebonded zirconia and A-Z-S refractories typically contain a (fused) grain and a matrix; and the MgO-chrome, chrome-MgO, and Al_2O_3-chrome types likewise are made using a pre-reacted (fired or fused) grain and a matrix. Major-phase $MgAl_2O_4$ spinel grain is similarly pre-reacted, crushed, and reconstituted with a matrix. Single-phase MgO, Al_2O_3 and zircon refractories are all made using separately-densified grain, while silica may be made either way.

Manufacture of nonoxide refractories is described under their own headings (Carbon, Graphite, or Silicon Carbide) in Chapter II. Grains of graphite or SiC, when used in a mix, are generally single-crystal.

Matrix Composition

It is far simpler to characterize the grain or aggregate in a refractory than to give the chemical or phase composition of the matrix from first principles. The variables of impurity and its location, additives used, particle sizing, the manner of bonding (viz., fusion, sintering, or solid-state reaction), temperature-time history and rate of cooling, for example, produce infinite variety in the matrix even when the overall refractory composition is given. The nearest accurate approach would be to describe the high-purity and equilibrium case; but this case is a rarity.

To illustrate, Figure VI-3 is a simplified simultaneous pictorial representation of nearly all of the common oxidic refractories made. Six "single-component" compositions are depicted at the corners of the hexagon. If pure, their matrices would be of the same composition, differing from the grain at most in crystallite size; and they would melt sharply at the temperatures given under their component (and phase) designations. Other "single-phase" refractories located variously in the diagram are spinel (MA); chrome spinel or picrochromite (MCr); forsterite, Mg_2SiO_4 (M_2S); mullite (A_3S_2); dialuminum silicate (AS); zircon (ZS); and calcium zirconate (CZ); not to mention two sets of alumina-chrome solid solutions.

"Two-phase" refractories are represented by the bold line segments connecting their end members in the diagram. An infinite number of these compositions are possible, depending on position along each bold line. If the overall composition is roughly midway between the end members, then both are major phases. But whether both are "grain" would depend on details of manufacture. In any event, if pure the equilibrium matrix would contain the eutectic solid (i.e., the last-to-freeze), and would first melt at the binary eutectic temperature marked on the diagram (taken from Chapter IV). If the overall refractory composition is near one of the end members, that one is the major phase and the other one (in addition to the eutectic solid) is likely to be found in the matrix.

But impurities and additives and departures from equilibrium alter this picture markedly. Take, for example, silica impurity in otherwise-pure magnesia. Silica is rejected from MgO in its crystallization. In a non-equilibrium matrix, pseudoenstatite, $MgO{\cdot}SiO_2$ (MS), may be found along with forsterite (M_2S). If lime is present, also rejected from the MgO crystals, then the non-equilibrium matrix may also contain C_2S or CS or CMS, all also shown in Figure VI-3 as a sampling of its variety. The phase diagram of Figure VI-1a adds still more possible matrix phases in the $CaO\text{-}MgO\text{-}SiO_2$ system. In alumina-silica matrices, a vitreous component is also quite commonly seen.

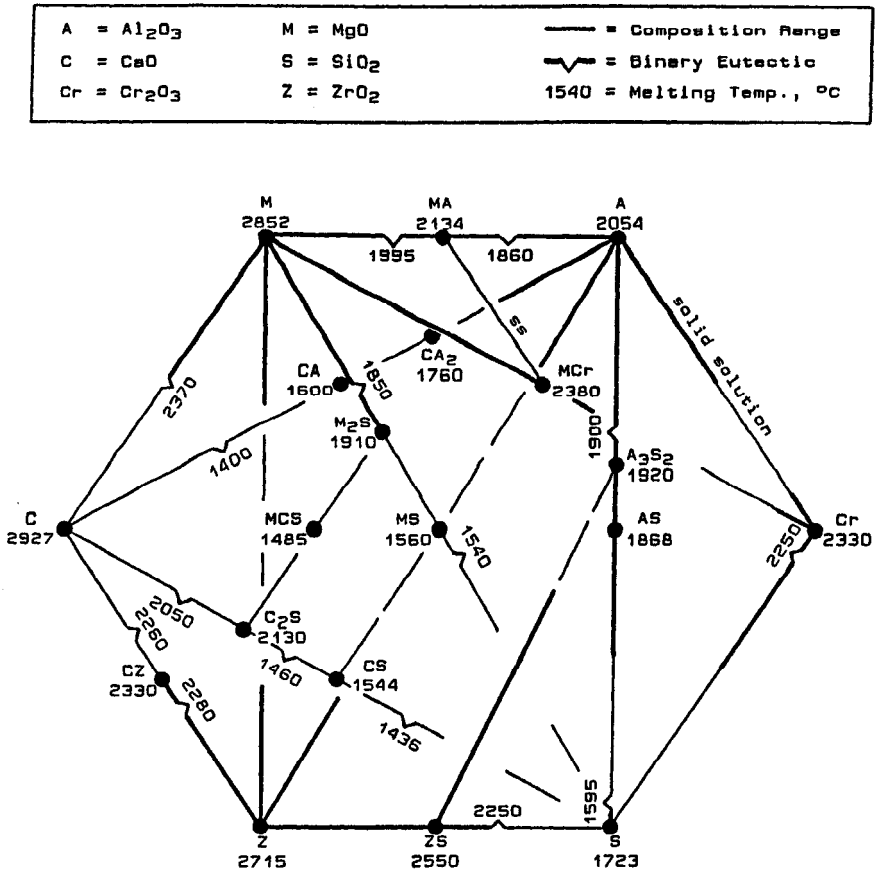

Figure VI-3 Monary and Binary Phase Representation of Common Oxidic Refractories

Bonding chemicals and the still further common impurities of iron oxide, titania, and alkalies have not even been touched here. These also turn up substantially in the matrix. Though estimating its phase composition in advance is all but futile, the governing eutectic melting temperatures displayed in Table IV.2 give some indication of what may be expected in matrix melting temperature. As a general rule, the lower-melting matrices are the more rapidly attacked by invading liquids.

Resistance of the Matrix to Dissolution

In addition to approaches addressed previously, it remains possible to increase the kinetic resistance of a matrix to dissolution by altering its composition so as to raise its own minimum eutectic melting temperature. That done, the matrix should also be well crystallized, i.e., as close as possible to its equilibrium phase composition.

One embodiment of the above advice would be a true single-component oxide ceramic, i.e., without a matrix per se. That approach is, however, (a) relatively expensive, and (b) useful only in limited circumstances of service: see, e.g., the effect on thermal stress and shock resistance (Chapter IV). Nonetheless, a growing number and quantity of refractories are approaching this embodiment. Arc-fused and cast refractories are coming close. Just how close is now more a matter of deliberate design for performance than of cost. But fused-cast refractories can not best serve the vast majority of applications, important though they are in the ones they do serve.

Purity. Given a matrix which is not to be eliminated, an obvious approach to its upgrading is via *chemical purity.* But a fetish simply with overall purity is not often cost-effective. Chapters IV and V and Table IV.2 make it clear that the removal of specific impurities -- to wit, Na_2O, K_2O, Fe_2O_3, and even CaO or Al_2O_3 in some circumstances -- can be far more telling. The alkalies are at the basic end of the Acid-Base Series of Oxides, and these are readily leached out of most hydrated minerals by dilute acids. As clays are generally washed with water before use anyway, the added cost of acid washing is not substantial. Iron oxide and titania in clays are another matter. Their control is best approached by selecting low-iron natural or beneficiated clays, e.g., kaolins -- or by resorting to synthetic chemicals in part or in whole.

Another case in point is bauxite as a source of Al_2O_3. The lowest-iron commercial bauxites in the U.S.A. are not low enough in Fe_2O_3 to make superior refractories. Synthetic alumina costs more, but is worth it if an upgraded matrix is wanted.

Basic refractories of mineral origin have to contend especially with SiO_2 and Fe_2O_3 as impurities: tramp silicates and iron minerals in magnesite are the rule. Beyond selection among mineral deposits and the use of beneficiation, the option of synthetic sea-water magnesia is available. One choice may be justified for making MgO+C composites; the other might be better suited for magnesia + chrome refractories wherein the chrome ore is contaminated. Makers of seawater periclase + chrome refractories feel it is better to reduce the total silica by improving one constituent even if the other must be abided. Though chrome ore is regularly beneficiated, its synthetic counterpart is too expensive for routine use.

Options as to purity also exist for zircon and zirconia. Selected zircon sands, like silica sands, are quite pure enough to use directly. Baddeleyite, a zirconia mineral concentrate, has also been much used as ZrO_2 in spite of up to some 10-15% of contaminants. But synthetic ZrO_2 is also readily available at higher cost.

Some other impurity considerations are self-evident. Water-soluble salts, especially chlorides, must be thoroughly washed out of both mineral and synthetic raw materials. Organic residues may be useful or not, as will be noted later on; but their ultimate burnout in a refractory does leave porosity. Other decomposables like carbonates and sulfates have to be watched in processing.

Matrix Additives. A second way of increasing the melting temperature of the matrix is by chemical addition rather than subtraction. Finely-powdered *matrix additives* are included in the initial refractory mix, with the intention that they shall dissolve when the matrix melts on firing. These may include powders of a major phase, e.g., MgO or Al_2O_3. Reactive forms (e.g., low-temperature calcines or other chemical precursors) are often preferred. Additives in general include one or more components that are already expected to appear in the matrix and are used to alter their ratios. An example touched on previously is lime for adjustment of the $CaO:SiO_2$ ratio in MgO refractories; another is alumina, used in clay-alumina refractories to raise the matrix $Al_2O_3:SiO_2$ ratio -- apart from their incorporation as components of the major phases.

It will be recognized, of course, that raising the matrix melting temperature by whatever means raises the sintering temperature required in refractory manufacture. The matrix serves as a *flux* in sintering, by melting well below the m.p. of the principal phase(s). That function extends to facilitating the formation and crystallization of principal phases themselves, e.g., mullite or spinels or cristobalite mentioned in Chapter V. The present objective appears to work against that fluxing function, and it does. Indeed, some matrix additives have been used deliberately as *fluxes* or *mineralizers*, for

example lime in silica refractories and clay or silica with lime in alumina refractories. The logic of reducing or eliminating such additives for improved corrosion resistance is compelling. But the consequence that the sintering temperature will go up is inescapable.

Reformulation. There are numerous unsubtle cases as well, that are arrived at by wholly new product formulation. In these a higher-melting matrix is accompanied by a changed major-phase composition, making it difficult to sort out the causes of improved performance. Yet the higher-melting matrix has to be important in its own right. One example previously touched on is the historical progression in percent Al_2O_3 starting with fireclays, that is today almost a continuum from about 30% to about 95%. But other compositional features figure as well, e.g., the %CaO, %SiO_2, and %Fe_2O_3 at fixed %Al_2O_3,[128] or the optional inclusion of Cr_2O_3.[78,80,153] The role of $MgAl_2O_4$ spinel in matrix improvement in basic refractories is powerful,[141,155] yet quite overshadowed by the effects of chrome spinel ss.[72,73,140,141,203,204] Zircon, A-Z-S, and zirconia refractories provide still other examples.

Bond Chemicals and Cements; Monolithics

The last kind of matrix additive in this context is comprised of *bond chemicals* and *cements*. These are included here not necessarily because they upgrade the matrix but because they can at least avoid downgrading it while retaining the advantages of low-temperature sintering. They are chemicals in a sense foreign to the refractory composition, but which react with crystals of the principal phases in such manner as to form chemical bridges between them. In an idealized view these bridging bonds might be taken to replace and eliminate the matrix, hence our use of the term "bond" separate from "matrix" in this chapter. But in reality the matrix (comprised of indigenous phases) and segregated impurities are both hard to get rid of, and a *chemically-bonded* or *cement-bonded* refractory exhibits a complex of bridging bonds in which major-phase crystals and other components of the intercrystalline mass are all involved.

The desired chemical bonding is established by thermally activated chemical reactions taking place without coherent melting and at temperatures conveniently below those of liquid-matrix sintering. The process, called *reaction bonding* or *reaction sintering*, was introduced under Sintering of Oxidic Ceramics in Chapter II. The stability of phosphate bonding, which is used in high-temperature applications,[134,135,205-211] was described under Phosphate Decomposition in that same chapter. Phosphate bonding starts at about 200°C and up. Sulfate bonding is also used, but at lower service temperatures: see Decomposition of Sulfates in Chapter II.

Cements differ from other bond chemicals in that they set up hydraulically, by hydration reactions, at room temperature. The commonest by far are a family of calcium aluminate cements.[212-214] The products, comprised of cement-bonded refractory components, are castable *refractory concretes*.[77-80,89,125,140,199,213-219] With gradually increasing temperature, the cementing hydrates decompose by loss of H_2O; then a progression of overlapping phase changes takes place, but with a gap at about 400°-700°C in which bonding is weak. Above 700°C there is not just one bonding reaction but a series of them.[22,214,220] The end product at highest temperatures can be regarded as approaching a solid solution of CaO in Al_2O_3, i.e., it does not decompose harmfully. Some grades of calcium aluminate cement contain considerable iron oxide and are low-melting. The grade used for maximum temperature and corrosion resistance is essentially iron-free.[22,214] It is most used in high-alumina refractories.

Chem-bonded and cement-bonded refractory bricks, blocks, and other preformed shapes are usually made and fired by the manufacturer.[74,132,138,140,191,199,221] But almost the entire spectrum of high-performance monolithic refractories owe their very existence to bond chemicals and cements. These monolithic products are installed unfired; and owing to the usual ΔT across the lining thickness, they experience curing or bond-forming temperatures in service over a wide range but never exceeding the hot-face temperature. Their corrosion resistance nonetheless often closely matches or exceeds that of fired brick of the same nominal composition: a tribute to the strength of phosphate and calcium aluminate chemical bonding and to decades of research in dense product formulation.

These materials are used to form or build up whole linings by wet casting,[48,164,215,222] by vibratory casting,[124,206,223-226] by ramming,[76,134,135,165,227] and even by gunning.[228,229] The mixes and installation techniques developed for patching, repair and rebuilding of linings between heats or in mid-campaign have afforded up to manifold increases in the on-line time of vessels.

Though numerous installation techniques are used for repair, the most exciting advances have been made in gunning. Including composite as well as oxidic mixes, monolithics are available for wet (cold) gunning,[133,230-233] and now for torch and plasma flame-gunning.[74,184,233,236-239] Virtually any steel-shelled vessel can be advantageously lined with monolithics, and some operators are beginning to plan for the feasibility of "infinite" vessel life between complete relinings. At this writing, monolithics account for about 50%

of all refractory tonnage in the U.S.A.; roughly the same in Japan; and somewhat less but rapidly rising in western Europe.

Two other types of bond chemicals might be mentioned in passing. One is a chromate type, usually aqueous CrO_3. This is a toxic chemical, and its use has been discontinued in the U.S. It is very effective, however, first forming bridge bonding by Cr^{+6} and subsequently becoming ceramic-bonded as Cr_2O_3 or chromites. The second type is comprised of a few chloride salts, which bond by forming oxy-chloride linkages with the host refractory. These as a group are low-melting, and thus they may downgrade a refractory matrix. Although still employed occasionally, chloride chemicals are not found in corrosion-resistant refractories used at high temperatures.

Colloid Processing

A matrix defect of calcium aluminate cemented high-alumina castables was discovered years ago.[240] So much CaO component is introduced into the refractory by the cement that low-melting CaO-MgO-Al_2O_3-SiO_2-Fe_xO_y eutectics are formed by invading acid slags. Phase diagrams[21] as well as postmortem examinations[240] leave no doubt that this is so (though the same matrix composition is not defective with respect to low-iron basic slags). Awareness of this fault has stimulated a groundswell shift in castable technology that is fundamentally important, not only in its own right but because it presages like changes elsewhere in refractory manufacture. First, "low-cement" castable products appeared.[133,151,152,241-250] Improved corrosion resistance was found, supported by direct comparisons of low-cement with normal-cement products.[117,251] So-called "ultra-low" and "zero-cement" castables were made as well,[240-242,245,249] culminating philosophically in an Al_2O_3 refractory without any foreign additives at all.[252] These castables also exhibited superior corrosion resistance over their predecessors.

Many of these improvements in performance were realized while sacrificing some refractoriness of the matrix, not increasing it. Attention was given instead to the chemistry of the *interaction product.*

What is fundamentally important in this evolution is that calcium aluminate has been replaced in its function by *colloidal silica*[117,133,253-258] or by *colloidal alumina*,[133,259-262] or both. Colloidal silica has been on hand for millenia as volcanic ash. But a wide variety of synthetic silicas are now available, ranging at will in particle size and reactivity and in most cases quite pure. Colloidal aluminas or their chemical precursors are also well known industrial or developmental products. Clays are natural colloids, and the

principles of their processing are not new. But the price of synthetic colloidal oxides is another matter. Their investigation and use had to await a favorable economic climate.

Colloid particles are very fine: by definition, about 1μm or less in diameter, in many cases much less. Their surface areas become enormous: the geometric surface of a silica sphere of 1μm diameter is about 2 m^2/g, varying as 1/d. At 10 nm diameter this becomes 200 m^2/g, not counting any internal pore surfaces. The chemical bonding of surface atoms is distorted; reactivity is greatly increased.

Colloidal zirconia and magnesia and hundreds of more complex oxidic particles have been made, mostly between about 20 and 200 nm in diameter. A burgeoning literature on colloid processing exists in the field of ceramics. The prospect looms for refractory synthesis using colloidal bonding agents that ultimately differ chemically in no way from the host crystals or grains, or that differ in designed and selected ways rather than by what nature supplies. Colloid synthesis of formed refractories could possibly produce the ultimate corrosion-resistant matrix. Whether it can do so at an affordable price is speculative; but investigations are already under way.[263,264] The cost may well not exceed that of arc melting and casting.

Extent of Intercrystalline Bonding

If the dissolving power of an invading liquid is finite, then in the interests of impeding the debonding of refractory crystals it is logical to provide the largest possible field for the liquid to have to plough. That is, a maximum feasible bonded area of the refractory crystals is desirable.

Extensive bonding comes from sufficient sintering at sufficient temperature, or from use of sufficiently reactive bonding chemicals well distributed among the refractory grains. The usual way to diminish porosity, after careful sizing and compaction of a mix, is to sinter it sufficiently. If major-phase synthesis and crystal growth are to be completed thermally, sufficient liquid-phase sintering and hence bonding of those crystals should take place at the same time. If a matrix has been formulated to be significantly high-melting, intercrystal bonding or sintering has to be given special attention to compensate for that adjustment.

Thus the manufacture of a corrosion-resistant refractory will typically culminate in a carefully chosen thermal or chemical provision for achieving the maximum feasible bonding of its major-phase crystals or grains. Among the several products of the same composition class made by each manufacturer, ordinarily one or more

will have been developed for use in benign chemical environments while one or more will have been optimized for durability in corrosive situations. In the case of fired brick, the resistant type will be higher-fired in accordance with this principle, and fired well above the temperature of use.[41] Since any or all of the other factors in resistance to corrosive liquids may be observed at the same time, higher firing is only one of a number of ways in which these sets of otherwise-like refractories are discriminated. Only rarely, as in standard-fired vs high-fired high-duty or super-duty firebrick, is the firing temperature the sole apparent distinction in their manufacture.

Nature of the Grain or Aggregate

Composition. Suitable major-phase compositions for the making of grain are well represented in Table IV.1 and, for oxidic refractories, in Figure VI-3. The chemical and phase composition of grain is selected to be as kinetically resistant as possible to the corrosive liquid at the intended hot-face temperature. Non-wetting options are explored first. Other than a high melting point, the remaining criteria for selection start with an examination of solubility of grain components in the liquid, solubility of liquid components in the solid, chemical reactions occurring between them, and melting temperatures of the solutions or products -- all by reference to available phase diagrams (Chapter IV and Figures VI-1a,b, VI-2a,b, etc.[21]). At this point in time those examinations have long since been made, and there is a wealth of field experience to go on as well. Norms of chemical purity have evolved. Matters of stability under thermal gradients and transients have also been evaluated (see Microstructural Integrity in Chapter IV). Besides the technical constraints, the cost of a grain has to be weighed against its durability. Grain, matrix, and porosity are of course a cooperating set, and in practice no one of them can be considered alone.

Crystallinity. Whether single-crystal or polycrystalline, a separately-manufactured grain must be fully reacted and well crystallized (i.e., coarse-crystalline) to realize its inherent corrosion resistance. Arc-fusion of oxides answers that challenge well but expensively. Sintering takes more patience. A typical relation of mean crystallite size $\bar{d}$ to time at fixed sintering temperature is,

$$\bar{d} = At^{1/n} + B \quad ;$$

where t is time, n lies between 2 and 3 and tends toward 3 for liquid-phase sintering, and A and B are constants. It is easily shown that $t^{1/n}$ soon becomes a very slow-moving function of t; so if crystals are to be grown in reasonable time, the sintering temperature must be high. The coefficient A in the equation above is a thermally-activated term, $A = a \exp(-E_a/RT)$, increasing rapidly with temperature.

As the most corrosion-resistant grains are high-purity and single-phase, e.g., MgO or Al_2O_3, etc., the preparation of these as coarse-sized, dense, well-crystallized materials presents a dilemma in their subsequent rebonding. After all, the matrix composition used for that rebonding is just another (but controlled) wetting and invasive liquid at the temperature of sintering. A corrosion-resistant grain is thus also resistant to effective thermal rebonding. This dilemma reaches its peak in *direct-bonded* refractories, in which no foreign matrix chemicals are used in the mix. These products are potentially very corrosion-resistant, but they must be carefully and thoroughly sintered.

Sizing. Chemical bonding is frequently carried out in bricks in lieu of unaided sintering, just as it is in monolithics. But in either case only the external or geometric surface of each grain is engaged by the rebonding reactions in manufacture, whether that grain is single-crystal or polycrystal.[266] Thus the size of the major-phase particles presented to the corrosive medium in service can be made quite large -- up to some 1/4" or 6 mm -- , even if the crystallites of which they are composed are much smaller. Large sizing of a dense grain or aggregate impedes dissolution because only its external or geometric surface can be reached by the corrosive liquid, and that external surface area is inversely proportional to the size of the grain.

Such a coarse-sized grain or aggregate will indeed be attacked only slowly at the hot face of a refractory. But if such a grain were monosized: (a) it could be only poorly bonded to other like grains, (b) a large volume of comparably coarse-sized porosity would exist between grains, and (c) the bonding matrix would be severely exposed to the penetrating corrosive liquid. Using rigid spheres as an idealized model of grains, for example, if these are monosized (even if perfectly packed) each hot-face surface grain is in point contact with at most only nine other like grains and the unsintered pore volume is 26%. For real crushed but equiaxed grains and real packing this void volume goes up to about 32%, with an average pore diameter of some 10% of the grain diameter. Not only are penetration and matrix dissolution encouraged. The surface grains, being bonded to each other at so few points of contact, are vulnerable to mechanical dislodging by erosion, abrasion, or impact. The bulk strength of the refractory is low for the same reason.

By the use of *graded* grain sizing, the number of nearest-neighbor particles and hence points of bonding contact can be increased by up to one-hundred-fold compared to this monosized model. The unsintered porosity can be reduced to below 5%, with the average pore size and the thickness of matrix films markedly reduced as well. Both strength and abrasion resistance are increased. These are all consequences of improved packing density of multi-sized

particles in the mix. The interstices between largest particles are occupied by smaller ones, and so on successively, from the *top size* to the *bottom size* of the graded grain. If a typical top size in large bricks is about 1/4" or 6 mm, the bottom sizing may be 100m or 200m or 325m, for example, as chosen by the manufacturer. These mesh sizes are respectively about 150, 75, and 44 μm diameter (see Table II.1). Size distributions between these limits are optimized empirically,[186] but within guidelines that will be presented later on. Major-phase particle sizes smaller than the selected lower grain limit are generally considered part of the matrix.

Since the surface:volume ratio of the grain particles increases as their size decreases, the smaller particles are successively more vulnerable to corrosive-liquid attack. A working refractory hot face in service eventually consists mainly of the largest grains, as the smaller ones dissolve and recede; but the embedment of the large surface grains is so firm in a graded system that they are able to resist mechanical removal. Remaining in place, they protect the underlying grains and matrix against erosion and abrasion and against stirred chemical attack. Thus, compromising the corrosion resistance of the grain somewhat by the use of graded sizing improves the resistance of the grain-matrix-pore system as a whole.

In monolithic refractory mixes the latitude for coarse sizing of the grain is sometimes sharply curtailed. Castable refractory concretes can run about as coarse as brick products; but gunning mixes and trowellable plastics, for example, are under other constraints. The grain sizing in every monolithic mix must be developed to meet its own individual set of criteria, related to its installation and intended use. These criteria include texture,[233] rheology,[262,267-272] working life,[207,254] adhesion,[232,236] chemical or cement bonding, corrosion resistance, and permanent dimensional change, to name a few. The same is true of mortars, used to fill the interstices between bricks and to bond them together in masonry construction. Mortars, having to be of creamy texture for installation, employ particle sizes mostly in the subsieve range, viz., -325m (read, "less than 325 mesh"). Thus in monolithics and in mortars the resistance of major phases to liquid attack at the hot face may be further compromised by their finer sizing.

It is well to recall, however, that hot face recession by grain dissolution can become life-limiting on a refractory only when penetration and matrix invasion are sufficiently minimized -- not to mention other modes of wear or failure such as thermal stress and shock fracture, cyclic ratcheting, and redox alteration. In optimizing monolithics and mortars, accepting restrictions on their maximum grain sizing has not much compromised their overall performance.[273]

When a coarse top size is permissible, then there is latitude for simultaneously optimizing (a) the composition, crystallinity, and sizing of grain or grains; (b) the composition, microstructure, and quantity of matrix; (c) the nature and technique and completeness of intergranular bonding; and (d) the porosity if not pore sizing. That multivariable optimization is the task of the manufacturer, for every working refractory product in every corrosive application.

In Chapter VII we shall complete this most important topic by examining refractory interactions with gases and gas-entrained particulates. Again, that separation is solely for our convenience. There will be cases of simultaneous exposure to both corrosive liquids and gases. While we shall not treat combined exposures exhaustively, in general the principles developed in Chapters V and VI will lead to the best material choices for those cases as well. Where exposure is solely to gases and dusts, reference to Chapters V and VII alone will sometimes lead to more economical yet technically satisfactory material selection.

Chapter VII

Principles of Corrosion Resistance: Hot Gases and Dusts

ATMOSPHERIC PENETRATION AND CONDENSATION

Refractory sidewalls, roofs, ducting, heat exchangers, and muffles exemplify exposures to hot gases and dusts. Kiln and steam boiler linings likewise entail corrosive atmospheric exposures without a liquid bath at the same time. Among the vessel descriptions in Chapter III, zoning tables are included which make distinctions between refractory exposure to liquid (e.g., slag or glass) below and predominantly to gases and dusts above. It is quite common that a change in refractory specification occurs near that boundary.

Both similarities and differences exist between atmospheric and liquid-phase corrosion. Entrained particulate matter will be taken up last. A distinction must be made between dust and fog; we shall treat the latter briefly as an extension of the former.

Gas Penetration by Diffusion Through Pores

There are striking parallels between corrosive-gas penetration into a porous refractory and reactive-gas penetration into a porous, surface-active solid catalyst. It is unprofitable here to seek quantitative solutions. But for qualitative use a simple equation can be adapted from the catalyst literature[274] relating gas diffusion kinetics to the characteristics of connected porosity. This equation applies to unidirectional steady-state diffusion in a flat porous wall of thickness Z, at some fixed temperature T:

$$\Phi = (D_b \cdot \bar{G}_d P/\tau)(-dp/dz) \quad .$$

Here, Φ is the flux of the diffusing species in mols per unit wall area per unit time. D_b is the bulk value of the diffusivity of that gas in some host gas at that T, and $\bar{G}_d$ is the suitably-averaged value of a function G_d which gives the actual diffusivity in a pore of diameter d: $D_d = D_b \cdot G_d$. This function G_d is non-linear, but decreases from a value of unity for large pores to about $G_d \propto d$ in small pores, where it may range from 10^{-1} to 10^{-3} or so. Then it goes steeply to zero for molecularly-small pores.[274] P is the volume fraction of connected porosity, or 0.01 times the volume percent apparent porosity;[9] and τ is the "tortuosity factor," related to the devious diffusion paths through a porous medium but somewhat more intricate than that.[274] Common values of τ range between about 2 and 5, ordinarily increasing somewhat with decreasing porosity.

The derivative dp/dz is itself negative; p is the partial pressure of the diffusing species, highest at the working face of the refractory (i.e., at z = 0) and tending toward zero with increasing depth due to consumption of that species by corrosive reaction. The derivative dp/dz is not constant with z (hence neither is Φ), but we need not be concerned with its evaluation for present purposes. It suffices here to observe how Φ varies with porosity and with average pore size.

The flux Φ_o at z = 0 is of course proportional to the *volume* rate of gas penetration; there is no linear advance of a "front" as was observed previously for liquids. Φ_o is, however, equal to the integrated steady-state gas consumption rate per unit area in the interior of the wall. From the equation above and the given descriptions of its terms, Φ_o varies (a) about proportionately with the apparent porosity, and (b) though not linearly, in positive correlation with the average pore diameter as determined by $\bar{G}_d$.

These are qualitatively the same relationships as were shown under Porosity and Pore Sizing in Chapter VI for liquid penetration by mass flow -- though matters of wetting and non-wetting are absent here. There are some aspects of gas corrosion which can alter the pore characteristics with time, as will be discussed presently. These and the gradient dT/dz across a refractory wall disclose the above isothermal equation to be an oversimplification; but its correlations are valid. There are also close similarities between gas penetration of crevices, cracks, and microcracks and the penetration of these same features by liquids, again excepting any dependency here on wetting.

Two phenomena distinguish corrosive gas diffusion into refractories from liquid penetration. One is that the driving force for the former at steady state is the pressure gradient due to consumption of the gas by reaction. On that account, it is reasonable to characterize gas penetration broadly as less rapid in *mass* terms than that of wetting liquids. The other distinction is that reaction does not

necessarily commence at the hot face. On both accounts the *depth* of penetration by gases can be much greater in some circumstances than that by liquids.[70,81,82,108,275,276]

Heat-Exchanger Profiles

The scenario implicit in the above is of a wall whose working face is bathed by a rapid-flowing gas parallel to it and of sensibly constant composition: typical for furnace and kiln walls and roofs and fairly close for ducts. Still another relationship in the catalyst field can be borrowed for heat exchangers. Here the gas flows progressively over a large refractory surface in "packed tower" configuration. At each level in the tower part of the corrosive component of the gas moves into the porosity of the solid and is consumed, and the remaining part passes along to the next level. The partial pressure p_o of that component ("o" for "outside the solid") thus falls with the distance or height, h, traversed by the gas through the tower, commencing wherever the corrosion process begins.

Equations relating p_o to h in an analogous catalyst bed or tower are roughly exponential in form at constant temperature, but depend on the "kinetic order" of the consuming reaction.[277] A simple isothermal equation for kinetic order of unity is adapted for use here as:

$$p_{o2} = p_{o1} \exp [(h_1-h_2)/k] \ ,$$

where $h_2 > h_1$, h_1 is the height at which gas consumption begins, p_{o1} is "initial," p_{o2} prevails at height h_2, and k is a constant. Again it is not profitable to seek quantitative solutions: matters of kinetic order, of boundary-layer mass transfer coefficients, and of actual temperature variation with h and time interfere. It suffices to infer that corrosion of the refractory heat-exchanger packing or checkerwork is intensely concentrated close to height h_1 and then falls off in quasi-exponential fashion with increasing h. Field evidence of this is in hand for $h_1 = 0$ in glass checker bricks removed after service:[278] severe damage was sustained in the topmost foot or so of a downflow tower.

Permeation Rates

The *permeability* of a porous refractory to gases is also sometimes of interest, in connection with leakage through a wall to the exterior or opposite side. Cases in point are a muffle, or a kiln or retort wall that is not encased in steel. If part of the gas reacts with the solid, equations can be developed to handle the simultaneous processes but are specific to each given case. The case of *nonreactive* gases can be treated more generally.

The simplest permeation equation is of the same form as that for diffusion:

$$\Phi = (D'\bar{G}_d P/\tau)(-dp/dz) \quad .$$

But here D' becomes, at steady state, an averaged permeation coefficient for the gas components present. Its most important dependency is on the gas viscosity, which is a function of composition, pressure, and temperature. The other terms in the equation are as defined above. Some fractionation by molecular weight occurs, which we are ignoring here.

In simple permeation, dp/dz is constant with z and can be replaced by $(p_e-p_o)/Z$. Here, p_e is the exit value and p_o the entrant (or, initial) value of the total pressure of the permeating gas, and Z is again the wall thickness. In common situations there is enough sweeping of the exterior or exit side of the wall that p_e may be taken as zero. This simple model has obvious limitations with respect to real systems; but the separate effects of p, P, $\bar{G}_d$ and τ on Φ remain about as shown.

The conclusion for permeability is thus sensibly the same as for diffusion: *gas leakage as well as diffusion through a refractory wall is diminished by decreasing its apparent porosity and pore size*; and (though rarely practical) by increasing the wall thickness. An important pertinence of the above equation in the reverse sense is in computing the pressure drop, p_o-p_e, in porous diffusers, used e.g. for O_2 or Ar blowing of steelmaking vessels (Chapter III). Those open-celled refractory materials have large porosities and large pore sizes, whereby both $\bar{G}_d$ and τ approach unity; and the use of a single-component gas simplifies the determination and use of D'. Then $\Phi = -D'P\cdot\Delta p/Z$.

An alternative isothermal permeability equation, entirely compatible with the above but used in a standard measurement method of ASTM,[9] is:

$$Q/A = (K/\eta)\cdot(\Delta p/L) \quad .$$

Here Q/A is the gas flow or permeation rate in cm^3 (measured under standard conditions) per second per cm^2 of specimen cross-section; η is the gas viscosity in centipoise; $\Delta p/L$ (L equivalent to our Z) is the absolute pressure drop through the specimen in atm./cm; and K, the coefficient of permeability, is in darcys. The *darcy* is a unit of permeability such that K = 1 darcy when Q/A, η, and $\Delta p/L$ are all unity. This equation and its terms will be commonly found in the engineering literature of permeation; but it omits the relations of permeability to porosity and pore size given by our preceding

equation in Φ. It is thus less informative as to microstructure. The coefficients K/η and D' are clearly equivalent; but they are by no means numerically equal, as their units differ.

Condensation-Corrosion by Gases

Interaction Processes. Again for the time being we shall set aside redox reactions in gas corrosion. That done, there remain three possible modes of interaction of a gas with the external and internal surfaces of a refractory. First, if the gas is condensible (referred to as a *vapor*), in the course of penetration of the porosity and moving down the temperature gradient in a wall, the gas may literally condense or liquefy progressively. Second, the gas may condense by virtue of dissolving in the refractory; and third, it may condense by virtue of reacting chemically to form one or more new compounds. These three possible modes, in the order given, are progressively more energetic and rapid and hence are progressively more concentrated into a narrow band in the porous solid. The one mode open to liquids but impossible for gases is to dissolve components of the refractory directly. For that reason we have called gas-phase corrosion *condensation-corrosion,* as opposed to the term *dissolution-corrosion* used for liquids.

Once condensation has occurred, however, the basic criteria for liquid corrosion apply. Liquid interaction products are the hallmark of corrosive gases. If liquid products occur, they will be wetting; but their penetration via the porosity will be paced by the gas diffusion and condensation rate, not by capillarity from an external reservoir. Thus rapid slabbing is absent in gas-exposed refractories.

Invasive debonding by liquid interaction products observes the reactivity distinction between refractory matrix and grains as described in Chapter VI. But again this tends to be paced by the gas penetration rate or slow rate of generation of liquid, in the absence of appreciable capillary flow. Even liquid interaction products tend to protect the underlying solid somewhat, however, so that the depth into the refractory at which maximum gas reaction rates occur tends to increase with time. Eventually the depth of alteration becomes large. But in the most aggressive cases, blinding of the hot-face pores with liquid occurs early and the most dramatic alteration is concentrated there. Reaction at depth then becomes paced by diffusion through liquid-filled pores near the hot face.

This concentration of liquid products at macroscopic surfaces causes severe local melting by dissolution, especially in crevices. Mortared joints between bricks are particularly vulnerable in this respect, as mortars tend to be more reactive than well-sintered bricks. In contrast with the blinding of pores, low-viscosity liquids condensed

in mortared joints tend to run out of the crevices by gravity, at once carrying out dissolved mortar and exposing the crevices to further condensation. This gravitational flow is most marked in vertical brick joints in sidewalls, and quite generally in roof joints. Attack is most severe with liquids of lowest viscosity, hence with alkalies and chlorides.[279] It is not uncommon for otherwise-sound bricks to fall out of a roof eventually in such service, requiring shutdown for repair to avoid a massive collapse. Temperature is a major factor, both in reaction kinetics and in its effect on liquid viscosity.

Sulfur dioxide, usually from combustion, gives good examples of most of the condensation-corrosion patterns found in refractory interiors. Its condensation is essentially the reverse of the Decomposition of Sulfates, discussed under that heading in Chapter II.

Unaccompanied by appreciable alkalies, SO_2 reacts with oxidic refractories in accordance with the Acid-Base Series of Oxides (Chapter VI). Condensation-reaction occurs with CaO in refractories at about 1400°C and down; with MgO at about 1100°C and down; with Al_2O_3 or ZrO_2 at much lower temperatures, about 600°C and down; and inappreciably at all with SiO_2. Given the refractory type and a hot-face temperature above the appropriate limit, SO_2 penetrates the porosity but does not condense until (with a negative ΔT across a wall) that limiting temperature is reached. Refractory alteration in that case occurs well inside a wall instead of at the hot face, while other corrosive gases may attack the latter region. This separation of corrosive reactions has been seen, for example, in oil-fired boiler linings.[70,280]

When alkali vapors are present with SO_2 at the same time, e.g. Na_2O, the condensation of Na_2SO_4 starts at still higher temperatures and overlaps with SO_2 attack on the refractory. Liquid Na_2SO_4 appears in this case at some 1600°C and down. Examples are seen in the cement kiln hot zone,[108] in coal processing,[203] and emphatically in glass furnace checkers.[178,275,276,278,281] Checkers, it will be recalled, operate over a large $\Delta T/\Delta h$ and dT/dt as well, so that the spectrum of condensation products is ultimately spread out, including by chromatographic redistribution (i.e., vaporization-recondensation) in cycling.[92,281,282]

Condensed liquids fill the porosity and engage in debonding of the refractory. They may experience freeze-thaw cycling, and if solidified may create thermal expansion mismatches with the host. The typical consequences are weakening, softening, swelling, and finally even slabbing.[70,108,217,280,281] These are additional to the surface-concentrated effects of dripping and brick separation mentioned previously above.

Corrosive Gases. In compiling a summary list of corrosive gases, the Acid-Base Series of Oxides is a good place to start. That Series should be reviewed (Chapter VI). The strongest acids and bases at its extremities are volatile, and these react with the chemically opposite components of the atmosphere and of oxidic refractories.

Oxides of nitrogen are infrequently encountered in quantity, but nitrate interaction products are low-melting. SO_2 and SO_3 form liquid sulfates in restricted temperature regions, the former by simultaneous oxidation to SO_3 in the process of condensing. Sulfite products are generally unstable at hot process temperatures. Phosphorus oxide vapors produce relatively high-melting phosphate reaction products (Chapter II), and are generally considered to be noncorrosive on that account. They are also rarely encountered as gases, usually as minor components of liquid slags. The same is true of B_2O_3: it is generally met as a component of liquid silicates, infrequently as a free gas.[92] CO_2 is commonly met as a gas, but carbonate reaction products are thermally unstable above about 700-1000°C (Chapter II). CO_2 is frequently an agent of redox corrosion, however. CO, equally commonly met, has no addition reactions with solid oxides and is restricted to redox corrosion alone. Volatile oxides of arsenic are encountered in some nonferrous metal operations, and are corrosive. This recounting covers the top of the Acid-Base Series down to SiO_2, below which volatile species generally do not occur.

The volatile basic oxides of the Series are the alkalies, K_2O and Na_2O, and their corresponding hydroxides, KOH and NaOH. Though encountered as components of process liquids, these are also distilled out as gases in the blast furnace, in glassmaking and Portland cement manufacture, and in other comparably high-temperature processes such as in steel and in the sintering and fusion of refractory oxides and ceramics. Their reaction products with containing refractories are almost always low-melting.

Even more volatile and more corrosive than the alkalies are the chlorides. The identity of the chlorides boiled out of an inorganic process liquid depends on the cations that are present; so does the temperature at which vaporization occurs. Alkali chlorides are by no means the most volatile. HCl gas is encountered in acidic systems, and may be accompanied or followed by others as temperature increases. Condensation of chlorides in refractories typically produces liquids, but these products are most often oxychlorides: solutions of refractory oxides (including silicates) in chloride hosts. Chloride ion also dissolves substitutionally in refractory oxides, lowering their melting temperatures.

A summary list of corrosive gases and vapors is:

Acidic Oxides	B.p.,[11] °C	Basic Oxides	B.p.,[11] °C	Volatile Chlorides	B.p.,[11] °C
N_2O_5	47	Na_2O	1275	HCl	-84
SO_3	45	NaOH	1390	BCl_3	12
SO_2	-10	KOH	1320	$SiCl_4$	58
CO_2	-79	K_2O	(1200)	$AlCl_3$	178
				$SbCl_3$	223
				$ZnCl_2$	732
				$PbCl_2$	950
				$CdCl_2$	960
				$NiCl_2$	973
				$MgCl_2$	1412
				NaCl	1413
				KCl	1500

Process gases are usually accompanied by fogs and dusts of more complex composition; the roster of real corrosive agents is not so simple as this table suggests. Products of combustion, often including coal ash or oil ash, are part of the direct-fired corrosive environment.

Countermeasures. Methods of resisting condensation-corrosion by gases are substantially the same as those marshalled against hot process liquids. Even non-wetted refractory compositions are useful, not because wetting is a factor in gas penetration but because a non-wetted surface is also relatively resistant to reaction, whether with a liquid or with its vapor. The reduction of porosity, an achievement mainly of the 1970s and following, has greatly improved gas-phase corrosion resistance.

Upper sidewall and roof refractory compositions are usually chosen from the same broad family used to resist the corresponding process liquid. Exceptions are made for the fact that gas-phase corrosion is slower, if less-expensive refractory types can therefore serve adequately long. Other exceptions are made for special situations including gas-fog-dust mixtures, local temperature differences, and local velocity and impingement patterns resulting in abrasion.

In general, basic refractories (almost always containing chrome ore) are used where atmospheric exposures are alkaline-to-neutral and hot face temperatures are highest.[108,178,203,276,281] The hot zones in copper furnaces and cement kilns and the uncooled sidewalls of electric arc steel furnaces are examples, and the uppermost zone of glass checkers. Where exposures are neutral to acidic and temperatures are highest, high-alumina, zircon, A-Z-S, and mullite refractory types are employed.[28,92,275,281,282] The use of silica "acid" refractories in furnace and kiln roofs, once almost

universal, has given way to these higher-temperature types to such an extent that silica bricks are no longer manufactured in quantity in the U.S.A. Super-duty silica still makes good crowns, however.

As operating temperatures lessen, high-alumina refractory applications expand into alkaline exposures and then give way successively to super-duty, high-duty, and regular fireclay products at successively lower cost.[69,870,275,280-282] A classic example of this progression of usage, from basic to alumina and alumina + mullite and on to the several grades of fireclay refractories, occurs in tunnel and periodic ceramic-firing kilns as their hot face temperatures decrease from ~1850°C to <1000°C -- depending on the products being fired and the zoning in each different kiln.

One reason why the highest-temperature oxidic refractories have lapped successfully into each others' environmental domains is that they have become better made -- purer, much less porous, and better bonded -- and hence more corrosion-resistant across the board. Indeed, there are relatively few corrosive applications today in which only one type of working refractory can survive competitively. This is a good thing: other qualities are required as well, whose specifications vary from one installation to another. Thermal stress resistance, redox cycling resistance, thermal conductivity, hot strength, and abrasion resistance are examples of these other considerations. The process operator has some breadth of choice among the several characteristics that are most critical.

Gas Corrosion by Oxidation-Reduction

It is appropriate to close the subject of gas corrosion by returning briefly to redox reactions. Gases are ubiquitous instruments of oxidation and reduction, and their ability to reach over large distances from their point of generation or release adds a spatial dimension to their corrosion phenomena.

Most of the reactions described under Redox Alteration in Chapter V involve gaseous reagents; but not all of the gases which may be faced by refractories are catalogued there. First, an important group of condensible vapors is comprised of the volatile chemical elements. These ordinarily appear along with their liquids in smelting or other reducing chemical process operations. They are most likely to be found among the low-melting elements in Figure II-2. But still others turn up in metallurgy as alloying elements, or elsewhere in chemical and device applications. They too have to be handled hot. A table of twenty more-or-less volatile elements is provided below, in alphabetical order by symbol, giving the m.p. and b.p. of each in °C.[11] This table omits the low-melting elements gallium, germanium, indium and tin, all of which boil close to or above 2000°C.

Element	M.p., °C	B.p., °C	Element	M.p., °C	B.p., °C
As	---	615s	Na	98	880
Ba	850	1140	P	44	280
Bi	271	1560	Pb	328	1620
Ca	845	1240	S	113	445
Cd	321	767	Sb	631	1380
Cs	29	670	Se	217	688
Hg	-39	357	Sr	800	1150
K	62	760	Te	452	1390
Li	186	1336	Tl	302	1460
Mg	649	1107	Zn	420	907

Whether an element in this list will be encountered as a vapor depends on the temperature of a relevant process operation. A gas-exposed refractory for the operation may be in the form of a crucible, still, retort, kiln, furnace, or associated plumbing, whose first obligation will be to prohibit vapor leakage. Its second obligation will be to survive reduction and to withstand alteration by the product of oxidation of the metal vapor. Inquiries as to redox reactions must encompass not only refractory major phases, but also their minor and impurity components.

Each such inquiry consists of: (a) proposing a valid chemical redox equation and the physical state of each substance therein, including solutions; (b) estimating the chemical activity of each substance; (c) acquiring the $\Delta G°_f$ data for each, either from compilations such as the JANAF Tables[23] or from the literature of the substance; and (d) using the equilibrium thermodynamic techniques given in Chapter V to assess the postulated reaction. It should be noted that, at any temperature between the m.p. and the b.p., a liquid and its vapor at the equilibrium vapor-pressure are equally at standard state, for which the activity a =1. Thus exposure of a refractory either to a liquid or to its saturated vapor is thermodynamically the same.[83] The differences lie in transport mechanisms and kinetics.

The second set of gaseous redox reagents encountered by refractories is comprised of the "permanent" oxidizing and reducing gases. These were incompletely sampled in Chapter V as Redox Reagents in Combustion Atmospheres. The fuller table below presents the most common oxidizing and reducing gases, respectively. Each set is given in approximate order of decreasing thermodynamic power.

Oxidizing Gases	Reducing Gases
NO_x	["Active" Metals & Carbon]
Cl_2	NH_3
0_2	H_2
HCl	C_xH_y
CO_2	CO
H_20	[Common Metal Vapors]
SO_2	H_2S

Except for Cl_2, HCl, and the metal vapors, the reduced products of the oxidizing gases and the oxidized products of the reducing gases are themselves volatile and go back into the local atmosphere after reaction. That is, with these named exceptions the damage done to a refractory by redox corrosion is almost solely the result of valence alteration of the refractory composition itself. Sufficient examples of that damage are given in Chapter V.

Certain of these oxidized and reduced pairs of gases can carry out a further *kinetic* function in corrosion. This is to supply an alternate path for solid-state reactions which otherwise would soon stop due to parting of their solid-solid interfaces.[283] The MgO+C reaction in composite basic refractories, for example, may proceed as,

$$MgO + C \rightarrow Mg_{(g)} + CO_{(g)} ,$$

only until the reagents lose contact. Recall, however, that the atmosphere in the BOF is a CO-CO_2 mixture which fills the pores of the refractory. Now the sequence,

$$MgO + CO_{(g)} \rightarrow Mg_{(g)} + CO_{2(g)} \quad \text{and}$$

$$CO_{2(g)} + C \rightarrow 2\,CO_{(g)} ,$$

can replace the former solid-solid reaction. The sum of these two is exactly the former equation; and their thermodynamic equivalence to it in terms of the equilibrium $p(CO_2)/p(CO)$ ratio can be readily demonstrated from the data in Table V.1. All that is necessary is that the gases be confined together in a small space (e.g., pores), reasonably isolated from the external atmosphere. In the blast furnace, the FeO+C reaction is similarly facilitated by CO on a huge scale -- though a liquid-solid mechanism is also in effect there.

Countermeasures. The available methods of controlling or slowing redox corrosion have all been mentioned previously. These include, in addition to limited allowable process modifications of temperature and atmospheric exposure: (1) selection of refractory

compositions that are resistant to reduction or to oxidation; (2) elimination of oxidizible-reducible minor refractory components or impurities, e.g., Fe_2O_3 and TiO_2; and (3) inhibiting the entry of the corrosive gas and exit of gaseous products, e.g., by decreasing porosity and pore size or by glazing or coating of the working face or back face of the refractory. (4) Sacrificial additives have also been mentioned.

The most difficult and damaging redox environment remains the cyclic one, for example the alternation of refractory exposures to process CO and to ambient air. The most effective defense that has ever been devised is removal of the unnecessary half of this cycle by the process architect.

DUSTS: DEPOSITION AND ABRASION

Hot process dusts originate in feed materials, but also importantly in the grinding action of moving solids within heated vessels. A further source is evaporation-condensation from process chemicals, while the combustion of inexpensive fuels always yields some dust and may produce soot (carbon dust) in addition. A number of such cases were called out in Chapter III. Dusts have two characteristic effects on refractories.

Deposition: Scaling and Caking

Industrial process dusts are often accompanied by fog and by gases which condense on refractories. These accompanying liquids facilitate the gradual accretion of solid particles on the working surfaces. The resulting build-up can be variously a hard *scale*, or a somewhat porous, lightly-sintered *cake*, or (typically downstream and cooler) simply a pile of powder. In some less-obvious cases, dust, fog, and condensing gases all fuse together to create an invasive liquid -- an extension of condensation-corrosion.

Solid build-up on refractory surfaces tends to seal off the porosity and is a deterrent to chemical corrosion. This is often welcomed. In large masonry installations, however, the deposition of hard scale in crevices together with temperature cycling or mechanical flexing can eventually fracture and even dislodge bricks. Since scaling and caking of walls may be unacceptable to a particular process, periodic de-scaling operations may be carried out which themselves are mechanically damaging to the working lining. These operations include the firing of explosive charges and/or projectiles as in rotary kilns, and the use of air chisels or pneumatic hammers as

in shafts and rotaries, for example. The net consequence may be life-shortening.

Finally, there are a number of geometrical situations in which solid build-up in inaccessible places actually terminates the life of a refractory installation or component. A dramatic example of this has been in glass checkers,[281] whose passageway dimensions have now become much enlarged by re-design to allow for their gradual constriction by caking. The effect of build-up on the transfer of heat from gas to refractory has to be figured in as well, requiring overdesign of the checker height.

Scaling, caking, and the accumulation of dust are operational problems which call for operational design adaptations. There is little latitude for refractory compositional countermeasures. In some instances, refractory hot-face glazing in manufacture has provided a smooth surface to minimize dust adhesion. But on the whole this approach can work only where simultaneous chemical corrosion is minor. By contrast, refractory selection does play some defensive role against the second characteristic mode of dust attack: abrasive wear.

Abrasive Wear

Lacking protective deposition or build-up, *abrasion* of the refractory working face by dusts often contributes to wear. This mechanical mode of recession is familiar in all materials wherever solid particulates are entrained in rapidly-moving fluids. Abrasive wear depends on the impinging particle size, shape, hardness, mass and velocity; on the inertia and viscosity of the entraining fluid; on the presence of intervening films; on the refractory surface geometry and texture; and on the angle of impact. Abrasion is frequently an accompaniment and aggravator of corrosion, as has been mentioned. Its severity is hard to predict; but throats, ports, flues, elbows, valves, angular shapes, surface roughness, and similar sites of high gas velocity or turbulence are most vulnerable.

Apart from the streamlining of ducting design and the limited use of glazing for smooth texture, the simple refractory property of most importance in abrasion resistance is *hardness*. The following table gives room-temperature hardness values from Ref. 11 for most of the crystalline refractory substances listed in Table IV.1, plus one or two others of interest. Within each group (oxides and nonoxides, respectively), these are listed in approximate order of decreasing hardness on the Mohs scale,[8] which is a relative scratch-hardness scale from 1 (talc) to 10 (diamond). Where data were not given,[11] estimates have been made by analogy and placed in parentheses.

Substance		Mohs Hardness	Substance		Mohs Hardness
Corundum	Al_2O_3	9	Silicon Carbide	SiC	9.5
Spinel	$MgAl_2O_4$	7.5-8	Boron Carbide	B_4C	9+
Zircon	$ZrSiO_4$	7.5-8	Titanium Carbide	TiC	(9+)
Chrome Spinel	$MgCr_2O_4$	(7.5-8)	Titanium Nitride	TiN	9+
Mullite	$Al_6Si_2O_{13}$	(7.5)	Titanium Boride	TiB_2	(8)
Dialuminum Silicate	Al_2SiO_5	7-7.5	Carbon (various)	C	(4-6)
Silica (quartz)	SiO_2	7	Graphite	C(gr.)	2+
Forsterite	Mg_2SiO_4	7	Boron Nitride	BN	2
Cordierite	$Mg_2Al_4Si_5O_{18}$	7			
Zirconia	ZrO_2	6.5			
Titania (rutile)	TiO_2	6-6.5			
Magnesia (periclase)	MgO	6			

There is no known compilation of hardness data at high temperatures. However, each of these substances probably retains its hardness tolerably well up toward its Tammann temperature (Table IV.1). To put these values in perspective, sintered periclase at hardness 6 is used in the charge pad area of basic oxygen steelmaking furnaces, while high-alumina at 9 or SiC at 9.5 does high-wear duty in most other metallurgical furnaces receiving heavy charges of scrap or ingot and ore. Those are severe impact applications, calling critically for matrix toughness in addition to grain hardness. In dust-abrasive exposure, resistance of the matrix to mechanical undermining is also about as important as grain hardness; high-purity, high-density, high-fired, high-melting compositions are the most durable. Those are the same characteristics that impart corrosion resistance; so an excellent refractory for the one is likely to be excellent for the other as well. Experience suggests that nitride-bonded SiC may be the number one abrasion-resistant refractory at this time, either cold or hot. But it is not entirely oxidation-proof. Alumina tops the list of oxides in a wide variety of abrasive applications. Yet whether or not chemical debonding of the working face accompanies abrasion, the matrix may well govern refractory selection.[117,208,224-226]

CONCLUSION: PRINCIPLES OF WORKING REFRACTORY CONSTRUCTION

Chapters V-VII together relate the major considerations and material characteristics that qualify industrial refractories for duty in corrosive environments. The materials which actually face or enclose those environments are the *working refractories*. In illustrating the principles of their construction, reference has been made to nearly every chemical and phase composition and every microstructural type

that is commonly encountered. These concepts of refractory construction have been developed in relation to the *phenomena* by which products survive or excel. It remains to re-group working refractory products under the *classifications* used in the industry -- such as might be found in a manufacturer's catalog. These and some important features of each class will be summarized in Chapter VIII.

Another whole category of like materials is comprised of the thermally insulating refractories. Their conditions of use are on the whole much less corrosion-intensive. Insulating refractories will be described and classified in Chapter IX. Then the selection of lining materials for the equipment of Chapter III will be addressed, followed in turn by examination of other properties required for use in engineering design.

Chapter VIII

The Working Refractory Product Line

CLASSIFICATION OF WORKING REFRACTORIES

Overall Chemical Composition and Systems of Components

Several thousand brand-name refractories are made by some 160 manufacturers in the U.S.A. alone. Adding in some 300 firms in all Europe, 80 in Japan, 30 in the Soviets, and estimating some 250 elsewhere including Canada, Latin America, the Middle East, India, China, Australia, and all of Africa, the 800 or so refractory manufacturers worldwide probably put out about 8,000 different named products.

These products can be sorted down into a few dozen material classifications, that are at least in a philosophical state of flux at this writing. Certainly up to 1950, commencing when the industry was more into tons than technology, two salient thrusts of refractory classification were toward product standardization and application. In the ensuing decades those two thrusts have become increasingly obliterated. More and more products are now being custom-developed or tailored together with their installation methods for specific usages. These are high-value-added items rather than tonnage commodities. They may disregard traditional constraints as to chemical composition or raw material sources. Their advent and variety have necessitated a new look at the purposes of classification.

In the same time frame the number of pertinent technical publications has multiplied enormously. An emerging purpose of refractory classification is the establishment of an agreed-upon

nomenclature for worldwide *database* construction.[284] A schema that is in accord with this purpose has been suggested by the International Standards Organization, ISO.[285] Its core is based on overall chemical composition. The refractory classifications acknowledged by ASTM[9] are not in conflict with that set, though they may be somewhat fewer.

In this book we have evolved the refractory product line out of the principles of thermal stability (Chapter IV) and corrosion resistance (Chapters V-VII). The core of that evolution lies in Figure VI-3, which deals with qualified major oxide phases and their binary eutectics. That figure likewise creates no disharmony with the ISO schema. But if a purpose of classification is to provide compositional compartments in which every known refractory can find an unambiguous place, no published system seems yet quite sufficient.

Retaining our own thread of logic, we make up these needed compartments out of n-component material systems, readily associated with n-component phase diagrams. The maximum value of n we can represent pictorially is 3. Figure VIII-1 accordingly displays the same end-member oxides of Fig. VI-3, but in a compact fashion incorporating their *3-component systems*. Ignoring the appendage at its top, this figure is a basal-plane projection of a regular octahedron, in which six simple component oxides occupy the corners of the overlying (bold) and underlying (dashed) basal-plane triangles. These two basal-plane equilateral triangles are facets of the octahedron representing, respectively, the ternary systems MgO-Cr_2O_3-SiO_2 and CaO-Al_2O_3-ZrO_2. The remaining six facets appear in projection as isoceles. The uppermost of these is the ternary system CaO-MgO-Al_2O_3. To its left can be seen the triangle CaO-MgO-SiO_2; and so on, continuing counterclockwise: CaO-SiO_2-ZrO_2, Cr_2O_3-SiO_2-ZrO_2, Al_2O_3-Cr_2O_3-ZrO_2, and MgO-Al_2O_3-Cr_2O_3.

Six end members can occur in a total of 20 ternary sets. To display the remaining twelve requires constructing the three major diameters of the octahedron. Only one of these has been drawn in Figure VIII-1: it is the dashed line joining Al_2O_3 with SiO_2. Now connect these two end members with the MgO corner to give the triangle MgO-Al_2O_3-SiO_2. In like manner the same diameter, Al_2O_3-SiO_2, can be connected alternatively with the corners Cr_2O_3 or ZrO_2 or CaO, giving a total of four ternary systems. Each of the remaining two diameters (not drawn) accounts for four more ternary sets. For every triangle implicit in the diagram a ternary liquidus map exists in principle; and binary phase diagrams exist for each of the sides of each triangle.[21]

Figure VIII-1 thus has the capacity to represent six monary, fifteen binary, and twenty ternary refractory material systems, all referred to knowable phase diagrams. It more than suffices for the contemporary oxidic refractory product line, lacking provision only for

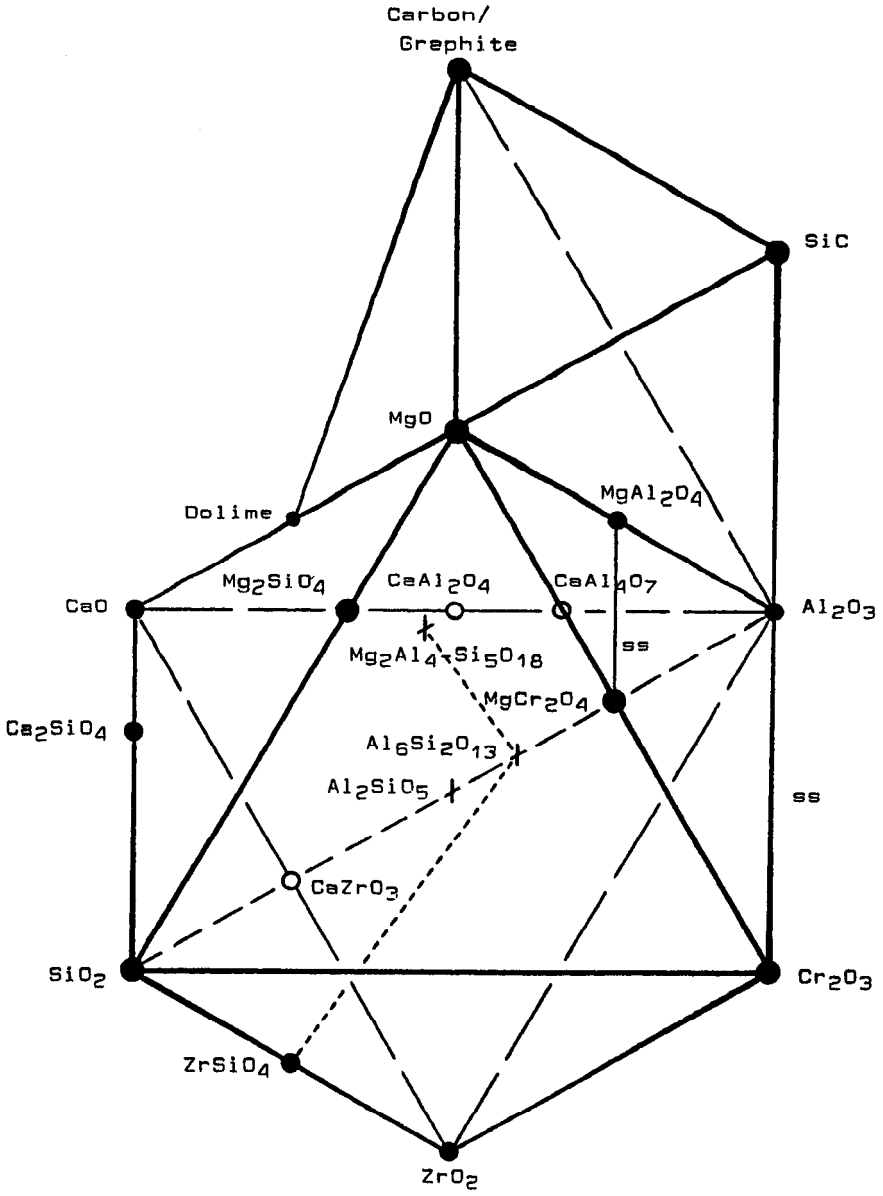

Figure VIII-1 Octahedral Representation of Ternary Refractory Material Systems

some "special" compositions of limited use such as rutile (TiO_2), beta-spodumene ($LiAlSi_2O_6$), beta-alumina ($NaAl_{11}O_{17}$), lanthana (La_2O_3), ceria (CeO_2), hafnia (HfO_2) and urania (UO_2).

Mineral compositions are suggested by the figure though not represented literally, as mineral formulas and impurities can run the number of components up to well above three. Examples sufficient for now include, on a fired basis: kaolinite (near $Al_2Si_2O_7$); andalusite/sillimanite/kyanite (near Al_2SiO_5); pyrophyllite, called "roseki" in Japan (near the silica-rich composition $Al_2Si_4O_{11}$ in the system SiO_2-Al_2O_3); serpentine (near $Mg_3Si_2O_7$ in the system MgO-SiO_2); olivine (near $Ca_xFe_{2-x}SiO_4$, suggested by Ca_2SiO_4); and soapstone or talcite (near $Mg_3Si_4O_{11}$ in the system MgO-SiO_2).

The triangle MgO-Al_2O_3-Cr_2O_3 in the figure includes the magnesia-chrome, chrome-magnesia, alumina-chrome, and chromite refractories, but imperfectly since all of these are made using chrome ore (near $FeCr_2O_4$). Yet it does discriminate their synthetic counterparts.[72,141,149]

One compound shown in a ternary field in the figure, marked by a "+" point, is cordierite ($Mg_2Al_4Si_5O_{18}$). A dotted line connecting this with mullite ($Al_6Si_2O_{13}$) denotes a family of 2-phase compositions that can be made between these. One such mixture has reportedly raised the maximum use temperature (about 1000°C for cordierite alone) to ~1430°C.[286]

The other dotted line in the figure connects zircon ($ZrSiO_4$) with mullite. But numerous refractories fall elsewhere in the Al_2O_3-ZrO_2-SiO_2 or A-Z-S triangle.[91,92,120,125] Other examples are a binary SiO_2 +$ZrSiO_4$ monolithic;[123] several zircon + roseki monolithics[90,233] falling on a line (not drawn) between $ZrSiO_4$ and $Al_2Si_4O_{11}$; a family of 2-phase ZrO_2+$ZrSiO_4$ mixtures;[121] and a ZrO_2+Al_2O_3 composition.[129] There are also several monary zircon refractories of record,[88,89,122,219,287,288] as well as monary ZrO_2.[24,27,85,202] Thus the 3-component A-Z-S triangle and its binary and monary subsystems are peppered with commercial and research products. The alumina-silica binary system, still used for classification, has become so overcrowded that it is helpful to employ ternary descriptors both to segregate products and to understand their behavior. Examples are the MgO-Al_2O_3-SiO_2, CaO-Al_2O_3-SiO_2, and Al_2O_3-Cr_2O_3-SiO_2 triangles.

Before resolving Figure VIII-1 with the existing ISO classifications, it is time to point out the appendage at the top of the figure. This appendage consists of a tetrahedron and added plane demarking the further monary material systems "carbon and/or graphite" and "SiC"; the binary composite systems of each of these with MgO and with Al_2O_3; the further binary composite "dolime + C";

and the ternary systems MgO-dolime+C, MgO-Al_2O_3+C, Al_2O_3+SiC+C, and MgO+C+SiC (not presently used). Suggested by the appendage but not drawn in to avoid clutter are some further composite refractory types of record: ZrO_2 + C;[74] ZrO_2 + Al_2O_3 + SiC + C;[86] A-Z-S + C;[191] ZrO_2 + $Al_6Si_2O_{13}$ + C;[199] $Al_6Si_2O_{13}$ + SiC + C;[188] Al_2SiO_5 + C;[189] and the numerous clay + graphite products that have been on the market for decades.

Also omitted from the figure are further single-phase nonoxides presently of limited use, such as BN, AlN, Si_3N_4, TiC, TiB_2, etc. Those are here treated as "specialties."

Table VIII.1 gives the principal ISO composition classifications of refractories,[9,284,285] and resolves these with the ternary and lower-order material systems of Figure VIII-1. The indicated correspondences employ all or part of four ternary systems: (a) CaO-MgO-SiO_2; (b) MgO-Al_2O_3-SiO_2; (c) MgO-Cr_2O_3-SiO_2; and (d) Al_2O_3-ZrO_2-SiO_2. At the lower left in the table are six more ternary oxidic systems from Fig. VIII-1 that are followed by cited references. Refractories falling in these systems are assignable into ISO classifications with difficulty; yet the references attest to their existence. The final ten listed ternary systems represent the further capacity of Figure VIII-1.

The burden rests upon the technologist to recognize the established classifications,[9,284,285] as these embody the official terminology of the industry. But any effort to be more than empirical in relating the behavior of refractories to their compositions has to start with their systems of components and their applicable phase diagrams. Some further subclassifications may also be helpful.

Subordinate Classifications

Accepted usage now prefers that bricks, blocks, and other forms made by the manufacturer be called *shaped* refractories, while what we have previously here called "monolithics" be referred to as *unshaped*. This latter term is the more inclusive, also taking in preparations used as mortars or other joining and filling materials, as coatings, and as refractory glazes, for example. Unshaped preparations are further sometimes used by the manufacturer, sometimes by the customer, to make shaped artifacts.[74,132,138,140,164,191,199,221] The earlier use of the term "specialties" to mean unshaped preparations is now considered poor form.

Beyond the important *shaped* and *unshaped* categories, there seems to be no universal agreement on any further set of refractory classifications.[9,284,285] Creation of a subordinate system answering our own purposes becomes an option, exercised in Table VIII.2.

Table VIII.1 ISO Refractory Classifications and Three-Component Material Systems

ISO CLASSIFICATIONS (Adapted from Ref. 284)	CORRESPONDING MATERIAL SYSTEMS FROM FIGURE VIII-1
Basic	
MAGNESITE	MgO; CaO-MgO-SiO_2
DOLOMITE	CaO-MgO-SiO_2
MAGNESITE-CHROME	MgO-$MgCr_2O_4$-SiO_2
CHROME-MAGNESITE	MgO-Cr_2O_3-SiO_2
CHROMITE (Ore)	$FeCr_2O_4$ (by analogy)
SPINELS (Non-Cr)	MgO-$MgAl_2O_4$; $MgAl_2O_4$-Al_2O_3
FORSTERITE	MgO-Mg_2SiO_4
CORDIERITE	$Mg_2Al_4Si_5O_{18}$-$Al_6Si_2O_{13}$-SiO_2
OLIVINE	$(Ca,Fe)_2SiO_4$ (by analogy)
CALCIA	CaO
Alumina, Fireclay, Siliceous, & Silica	
HIGH ALUMINA (I)	Al_2O_3; Al_2O_3-$Al_6Si_2O_{13}$
HIGH ALUMINA (II)	$Al_6Si_2O_{13}$-$Al_2Si_2O_7$
FIRECLAYS	$Al_2Si_2O_7$-SiO_2-$MgSiO_3$
SILICEOUS	SiO_2-$Al_2Si_2O_7$-(Mg,Ca)O
SILICA	SiO_2; SiO_2-$Al_2Si_2O_7$-(Mg,Ca)O
Ca ALUMINATE	$CaAl_2O_4$-Al_2O_3-SiO_2
Special Materials	
CARBON & GRAPHITE	Carbon/Graphite
ZIRCON	$ZrSiO_4$; Al_2O_3-ZrO_2-SiO_2
ZIRCONIA	ZrO_2; ZrO_2-Al_2O_3; ZrO_2-(Mg,Ca)O
SILICON CARBIDE	SiC
OTHER CARBIDES, etc.	("specialties")
Oxide-Carbon Mixtures	
MgO + CARBON	CaO-MgO-C (& analogies)
Al_2O_3 + CARBON	Al_2O_3-C (& analogies)
No Classification	Al_2O_3-SiC-C (& analogies)

OTHER TERNARY OXIDIC SYSTEMS

CaO-Al_2O_3-SiO_2	(117,128,133,165,217,218,232,240,280)	CaO-MgO-Al_2O_3
Al_2O_3-Cr_2O_3-SiO_2	(77-80,128,129,151-153)	CaO-Al_2O_3-Cr_2O_3
MgO-Al_2O_3-Cr_2O_3	(154)	CaO-Al_2O_3-ZrO_2
CaO-MgO-Cr_2O_3	(74,289)	CaO-Cr_2O_3-SiO_2
CaO-MgO-ZrO_2	(87,93,94)	CaO-Cr_2O_3-ZrO_2
Cr_2O_3-SiO_2-ZrO_2	(273)	CaO-SiO_2-ZrO_2
		MgO-Al_2O_3-ZrO_2
		MgO-Cr_2O_3-ZrO_2
		MgO-SiO_2-ZrO_2
		Al_2O_3-Cr_2O_3-ZrO_2

Note: There are no evident ISO classifications in these areas.

Table VIII.2 Subordinate Refractory Classifications

SHAPED REFRACTORIES
(bricks, blocks, special shapes)

Forming Methods

- PLASTIC MOLDING
- EXTRUSION
  - Cold
  - Hot
- UNIAXIAL PRESSING
  - Cold
  - Hot
- ISOSTATIC PRESSING
  - Cold
  - Hot
- FUSION CASTING
- RAMMING, CASTING, etc.
  (by use of UNSHAPED formulations opposite)

Grain Structures

- FUSION-CAST
  - Single-Phase
  - Multi-Phase
- REBONDED
  - FUSED GRAIN(S)
    - Single-Phase
    - Multi-Phase
  - SINTERED GRAIN(S)
    - Simple
    - Pre-Reacted
  - IN-SITU REACTION
  - OXIDE + NONOXIDE COMPOSITE
  - REINFORCED COMPOSITE

Bonding Mechanisms

- FUSION (fused-cast)
- DIRECT-BONDED
- LIQUID-PHASE SINTERED
- REACTION BONDED
  - Chemical or Colloid
  - Cement
  - Organic Carbonization
  - Gas-Solid Reaction

Porosity

- NEAR-ZERO (fused-cast)
- LOW
  - Corrosion Resistant
- MODERATE
  - Thermal Stress Resistant
  - Impregnated Composite
- PERMEABLE
- INSULATING

UNSHAPED REFRACTORIES
(monolithics, coatings, mortars, etc.)

Installation Methods

- Joining, Coating, Glazing
  - DIPPING
  - SPRAYING
  - TROWELLING
  - GUNNING (see below)
- Linings, New or Rebuild/Repair
  - PLASTIC MOLDING
  - TROWELLING
  - RAMMING/TAMPING
  - CASTING
  - VIBRATORY CASTING
  - SLINGING
  - GUNNING
    - Cold
    - Hot
    - Fusion
      - Flame
      - Plasma
- Bricks, Blocks, Tubes, Sheets, etc.
  - RAMMING/TAMPING
  - CASTING
  - VIBRATORY CASTING

Grain Structures

- FUSED GRAIN(S)
  - Single- or Multi-Phase
- SINTERED GRAIN(S)
  - Simple or Pre-Reacted
- IN-SITU REACTION
- OXIDE + NONOXIDE COMPOSITE
  - Deoxidant
- REINFORCED COMPOSITE

Bonding Mechanisms

- REACTION BONDED
  - Chemical or Colloid
  - Cement
  - Organic Carbonization
- LIQUID-PHASE SINTERED
- FUSION (fusion gunned)

Porosity

- NEAR-ZERO (fusion gunned)
- LOW -- Corrosion Resistant
- MODERATE
  - Thermal Stress Resistant
  - Explosion Resistant
- PERMEABLE
- INSULATING

This table introduces a group of *forming methods* for making shaped artifacts, and a group of *installation methods* for unshaped materials. Those will be discussed later. For now it should be noted that each anticipated forming or installation process can considerably influence the granulometry, texture and rheology as well as the chemical constituents of a refractory mix -- hence its ultimate fired phase composition and microstructure.

The various *grain* characteristics are listed next in the table. The terms are by now mostly familiar, with the possible exception of "in-situ reaction" product(s). That term is included for major crystalline phases that are developed concurrent with their thermal bonding, as opposed to grains that are separately prepared and sized for inclusion in a mix. It applies especially to mineral-based refractories such as are made directly from clays.

Inclusion of "reinforced composites" as a type of granular structure implies a separately-prepared particulate or fibrous reinforcing material, mixed with the other constituents and ultimately bonded by firing. Many hard inclusions are possible, of which few have yet been developed to the commercial product stage in refractories. The purpose is invariably to improve thermal stress resistance by imparting toughness to the consolidated mass (Chapter IV).

Other than with SiC,[46,74,189-192] most reported work in refractory composite reinforcement has been with chopped stainless steel wire. The two disadvantages of SS previously noted are its large thermal expansion coefficient and its susceptibility to oxidation at high temperatures. Nevertheless, SS wire reinforcement has been favorably regarded.[49-51,240,290,291] No doubt other reinforcements will find acceptance in time.

Table VIII.2 next lists the *bonding* mechanisms that are employed in refractories, each one initiated by appropriate heating. "Organic carbonization" pertains to carbon-containing products made with pitches, tars, or other natural or synthetic polymers or resins[97,179,181,182,190,193-195,199,298-303] and matured in a reducing environment.[115] "Gas-solid" bonding reactions occur in certain shaped nonoxides, e.g., SiC with which finely powdered Si or Al or SiAl alloy is admixed. The mixture is heated in dry N_2 or NH_3 gas, etc., to create a bond of Si_3N_4 or AlN or SiAlON.[168,304] "Colloid" reaction bonding is established in unshaped refractories (Chapter VI), whereas for brick manufacture its inclusion in the table is presently a statement of faith. Selection of a mode of bonding affects both the constituents of a refractory mix and the phase composition and microstructure of its fired matrix.

The *porosity* category at the bottom of Table VIII.2 was shown to be of signal importance in Chapters IV-VII. It is one of the main distinctions between working refractories and backup refractories for service under corrosive conditions. Other than via fusion, porosity is controlled cooperatively by (a) the size distribution of grain; (b) the amount, chemical nature and sizing of each of the matrix constituents of the mix; (c) details of the forming or installation process employed, including the rheology of the then-plastic mass and the shear and other forces involved in its compaction; and (d) the entire post-forming thermal experience to which the refractory is next subjected, which may impart both shrinkages and swelling or expansions to various of its constituents.

"Permeable" and "insulating" levels of porosity are to be discussed in Chapter IX. Occasionally, such porous materials are used as working refractories in special circumstances.[162,292-294] One means of creating large porosity is to incorporate particles of a combustible material (e.g., sawdust or porous resins) into the mix, and to burn these out in firing.

It must be appreciated that the connected porosity comprises the only avenues of escape of gases evolved in the first heating of a green refractory. Gases are evolved by numerous physical and chemical processes, a few of which are described under Industrial Drying, Calcining of Hydroxides, and Calcining of Carbonates in Chapter II. Dense refractory formulations require great care in their initial drying and heating to avoid building up excessive internal gas pressures. But monolithics, which are first heated in actual service, are vulnerable to the heat-up conditions of that service. Castables lining blast furnace troughs and runners, for example, have been known literally to explode[200] on first exposure to molten iron. Likewise in ladles. Hence the inclusion of "explosion resistant" unshaped refractories appearing under Porosity in Table VIII.2. One way of meeting this explosion hazard has been to incorporate in the mix a fibrous yet highly porous organic material, of the nature of chopped yarn or hollow straw but of finer dimensions.[295] These fibers per se provide initial gas escape paths; then on subsequent burning out, they leave some relic porosity in the ceramic host. Other approaches are taken too, such as to use sensibly dry ram-castable or vibratory-castable formulations to lessen the amount of gas generated in first heating.[124,240-242,245,249,250,296,297]

Summary. Table VIII.2, in summary, provides a classification framework additional to that of Table VIII.1. It enlarges upon the connections between refractory behavior and the critical features of phase composition and microstructure by emphasizing how those features are developed in manufacture.

In the remainder of this chapter a beginning is made toward assessing the fitness of working refractories for different applications by considering their maximum service temperatures, thermal stress resistance, and corrosion resistance class-by-class.

MAXIMUM SERVICE TEMPERATURES

It is easily agreed that the *maximum service temperature* or *MST* of a refractory implies a noncorrosive environment, but it is difficult to agree further. Hot mechanical properties may well limit service temperature in load-bearing situations; yet there is no "standard" load-bearing situation. As an alternative definition of the MST, consider the hot face of a vertical refractory wall whose temperature falls rapidly toward the cold face; and require only that the hot face layer (a few mm thick) shall not flow appreciably under its own weight. An MST so defined may be of limited practical utility. But the MST will not often be employed as a design property in any event. It is simply a consistent indicator of refractoriness.

Chapter IV dealt in depth with the *onset* of melting, as indicated by phase equilibrium diagrams. Given a valid phase diagram and a refractory composition falling therein, it is possible to determine, at equilibrium, the percent liquid in that body at every temperature above the onset of melting. Two problems of interpretation arise, however: (a) equilibrium is not assured in most cases; and (b) the viscosity of the liquid is not known, and if it were, could hardly be transformed confidently into terms of flowing or not flowing "under its own weight." The fundamental ideas of Chapter IV do indeed underlie the MST, but do not suffice to compute it.

Enter a practical approach: *measure* something that approximates the MST. That is the "pyrometric cone equivalent."

Alumina-Silica Products: The Pyrometric Cone Equivalent and the MST

The P.C.E. Standard pyrometric cones[14] were introduced under Temperature Scales in Chapter II. Their use to determine the *pyrometric cone equivalent* or *P.C.E.* of a refractory is standard laboratory procedure C24 of ASTM,[9] with a long history of practice and experience behind it. Following is the gist of the procedure.

To determine the P.C.E. of a fireclay or clay-rich refractory,[9] one forms or cuts it into the size and shape of a standard pyrometric cone. One then stands this on a plaque with an appropriate set of standard cones, heats them all together at 2.5°C per minute in oxidizing atmosphere, and identifies the one standard cone with

which the specimen bends over most similarly at the equivalent temperature of that cone. That standard cone's number is the P.C.E. of the refractory. The corresponding temperature is given in Fig. II-1.

A rough estimate of the maximum surface strain rate as the specimen bends over double under its own weight in this procedure is of the order of 0.01 (cm/cm or in./in.) per minute; and the maximum cumulative surface strain is of the order of 0.2. This large total strain, experienced without tearing, is evidence of a very high per cent liquid at the P.C.E. temperature (probably well upwards of 50%) and of viscous flow of that liquid as the mechanism of deformation. Refractories of much lesser silicate content will deform with much less liquid present, but a liquid of lower viscosity. Their specimens tend to tear in the course of bending over. In such case a P.C.E. is not reportable.[9]

MST from P.C.E. Measurement of the P.C.E. of a fireclay product is reproducible, given sufficient care. But its dependence on appreciable viscous flow violates our definition of the MST. On account of its historical origins, the P.C.E. will be found commonly listed in fireclay and clay-alumina refractory data sheets, while the MST is rarely listed. A reasonable approximate working relationship between them is (up to about 60% Al_2O_3 by weight):

$$MST = T_{PCE} - 150. \ *$$

Here each term is in °C. By this equation a specimen in pyrometric cone configuration would take about two weeks or more at the steady-state MST to bend over double. A few mm thickness of a refractory hot face, supported from behind, will not flow appreciably under its own weight at this temperature.

Above about 60% Al_2O_3 the temperature of onset of melting rises toward the P.C.E. temperature and the above equation eventually does not apply. The MST need never be below that of the onset of melting, as there can be no viscous deformation if no liquid is present. This latter limit on the MST is in full effect at about 70% Al_2O_3 and above, i.e., where the phase system of the refractory changes from SiO_2 + mullite to Al_2O_3 + mullite (Figure IV-3c).

Softening of Alumina-Silicas. The alumina-silica refractories at issue fall under the "Alumina, Fireclay, Siliceous, and Silica"

---

*The given equation corresponds to an activation energy for viscous flow of about 10^3 kJ/mol and a strain rate at the MST of about 10^{-5}/min, computed at a P.C.E. temperature of 1800K or 1527°C in pyrometric cone configuration.

group in Table VIII.1. Here we shall follow the industry practice of giving the approximate bounding values of wt.-% Al_2O_3 (fired basis), together with the ordinary name designations. Up to about 45% Al_2O_3, clays are virtually the sole constituents, including kaolins. From about 50% to about 85% Al_2O_3, typically andalusite, sillimanite, kyanite or bauxite and then synthetic Al_2O_3 is included with clays in the mix. The fired compositions lie close along the Al_2O_3-SiO_2 binary system (major diameter) of Figure VIII-1, but they include up to about 10% of other oxides at the 25% Al_2O_3 level and a few percent of other oxides at 85% Al_2O_3. The other oxides present in clays are typically 0-2% MgO+CaO, 2-5% Fe_2O_3+TiO_2, and about 1-3% Na_2O+K_2O, with the first of each pair predominating. From phase diagrams[21] the temperature of onset and completion of melting can be estimated, while the measured P.C.E. and its temperature are available in product literature and the MST is estimated by the above guidelines. Ordinarily a P.C.E. is not determined at all, or only approximately, above about 70% Al_2O_3; but reasonable extrapolation is possible on up to 100%. Some rounding-off and smoothing is employed in the following table, which accordingly presents average P.C.E. and MST ranges for a large number of commercial products. Numbers in parentheses are estimates.

	Melting		Orton	P.C.E.		Est.	
	Onset	Final	P.C.E.	Temp.		MST	
	°C	°C	No.	°C	°F	°C	°F
25% Al_2O_3 Low Duty Firebrick	(740)	(1730)	27	1640	2984	(1490)	(2715)
30% Al_2O_3 Med. Duty Firebrick	(800)	(1760)	29	1659	3018	(1510)	(2750)
35% Al_2O_3 High Duty FB	(860)	(1785)	31	1683	3061	(1535)	(2795)
40% Al_2O_3 Super Duty FB	(940)	(1800)	33	1743	3169	(1570)	(2860)
45% Al_2O_3 Clay-Alumina	(1060)	(1815)	34-35	1775	3227	(1610)	(2930)
50% Al_2O_3 Clay-Alumina	(1200)	(1825)	35	1785	3245	(1635)	(2975)
60% Al_2O_3 Clay-Alumina	(1460)	(1840)	36	1804	3279	(1660)	(3020)
70% Al_2O_3 Mullite	(1680)	(1850)	37-38	1830	3326	(1735)	(3155)
80% Al_2O_3 High-Alumina	(1810)	(1870)	(39)	(1860)	3380	(1810)	(3290)
85% Al_2O_3 Alumina	(1830)	(1945)	(40)	(1880)	3416	(1830)	(3325)
90% Al_2O_3 Alumina	(1870)	(1990)	--	(1908)	3466	(1870)	(3400)
95% Al_2O_3 Pure Alumina	(1920)	(2025)	--	(1950)	3542	(1920)	(3490)
100% Al_2O_3	2054	2054	--	(2054)	3729	(2050)	(3720)

Figure VIII-2 is a plot of these data for alumina-silica and alumina refractories from 25% Al_2O_3 to 95% Al_2O_3. The solid points represent measured P.C.E. temperatures; the open circles are estimated extrapolated values. The curve of maximum service temperatures has a small inflection in the vicinity of mullite (70% Al_2O_3) and the Al_2O_3+mullite eutectic. Its lower-Al_2O_3 inflection follows that of the P.C.E. curve above it, which in turn apparently reflects a steep climb of the liquidus temperature out of a eutectic valley in the region of 35-45% Al_2O_3. This inflection in the P.C.E. curve recommends refractories of 45% Al_2O_3 (super-duty firebrick) by a considerable temperature margin over those of lower Al_2O_3 content.

The MST curve of Figure VIII-2 up to about 70% Al_2O_3 may be used as guidance for the selection of fireclay and clay-alumina refractories in noncorrosive applications, simply according to the anticipated hot-face temperature. That curve has been confirmed in the field at 70% Al_2O_3: an advertisement run in the U.S. in 1990 announced that a fused-rebonded mullite kiln lining had passed 20 years' life at 1700°C hot-zone temperature.

High-Alumina and Alumina-Chrome Refractories

Above 70% Al_2O_3 the MST curve is best estimated by estimating the temperature of onset of melting. This curve is of diminishing value for application because these increasingly costly refractories are little used in noncorrosive service. Since the MST relates to refractoriness of the matrix, however, it does have value in connection with corrosion resistance (Chapter VI).

Figure VIII-2 shows a rapid increase in the estimated MST of high-alumina refractories with increasing Al_2O_3 content, from about 1810°C at about 80% Al_2O_3 to about 1920°C at 95% Al_2O_3 and extrapolated close to 2000°C at 98-99% Al_2O_3. The curve presumes that the difference is largely SiO_2, some Fe_2O_3 and well under 1% Na_2O. Virtually all of the "alumina" monolithics fall in this range, most of them at 85% Al_2O_3 and above. As to the MST, it matters relatively little whether the product is direct-bonded, phosphate bonded, or "ultra-low" CA cement bonded.

Synthetic alumina-chromia ss refractories run higher in MST than the aluminas by about 50°C. The more common "alumina-chrome" (i.e., chrome ore) products[77-80,128,129,151-153] may vary widely in % Al_2O_3 and % Cr_2O_3, but on the whole do not suffer in MST for being iron-contaminated. The added refractoriness due to the Cr_2O_3 component[21] compensates for the iron oxide (actually present as a spinel ss). At equal percent Al_2O_3 the alumina-chrome formulations can run up to ~50°C higher in MST than the corresponding alumina-silica products, rarely lower.

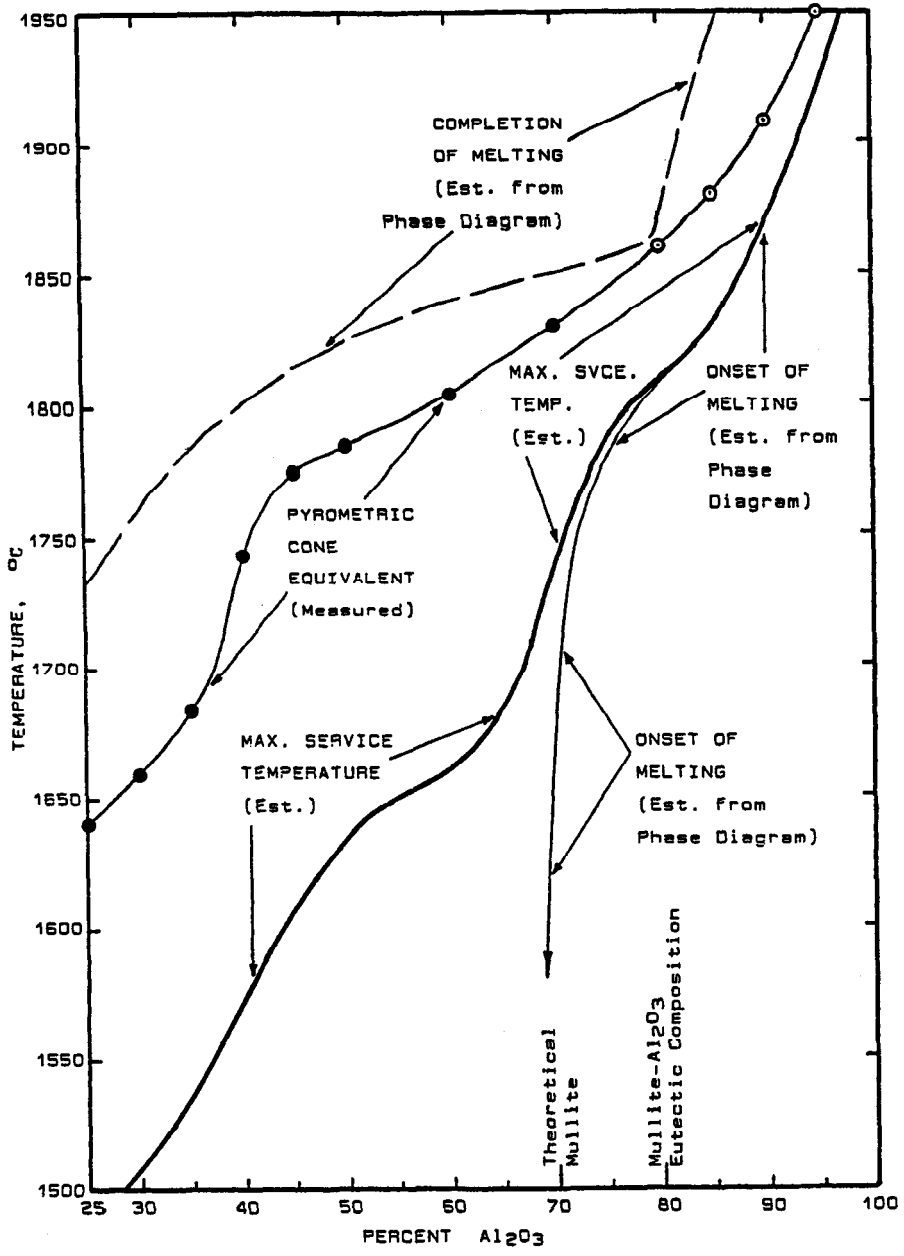

Figure VIII-2 P.C.E. and MST of Fireclay and Higher-Alumina Refractories

Silica Refractories

In classical silica refractories as developed for early steelmaking duty, impurities are usually held to about 5% maximum. If lime is used as a flux for sintering, then the binary SiO_2+$CaSiO_3$ eutectic governs initial melting at 1436°C[21] and the MST is close to 1550°C. Alumina impurity is tolerable to a few percent, so that if no flux is added but sintering is conducted well above 1600°C, an MST of about 1600°C can be achieved.[21] At still lower total impurity levels a fused and direct-rebonded sodium-free silica can realize an MST close to 1650°C.

This last-named high-purity rebonded silica refractory, called "super duty" silica, became an ASTM standard brick (type A under C416[9]) with a specified 0.5% maximum of Al_2O_3+2·Na_2O impurity. In steady service up to 1650°C its silica goes over to cristobalite, leaving only a very small fraction of very viscous Al_2O_3-SiO_2-rich liquid. Superior hot strength or creep resistance results. It is further resistant to alkali vapor attack: the alkali-altered surface liquefies but does not diffuse rapidly into the interior. These properties propelled super duty silica into glass furnace superstructures as well as open hearth steel furnaces. It is still found in the tops of blast furnace stoves and in glass furnace roofs.

The SiO_2 phase transformations described in Chapter IV and Figure IV-7 have to be remembered, however. These include the devitrification of vitreous silica, which separately limits its service temperature to roughly 1000°C.

Basic Refractories: Periclase, Magnesite and Dolomite

Turning now to the "Basic" refractories category of Table VIII.1, seawater periclase needs to be distinguished from burned magnesite. We shall ignore Calcia momentarily, owing to its tendency to slake at room temperature. The refractories of this section fall nominally within the ternary system CaO-MgO-SiO_2 (Figure VI-1a), and those of mineral origin are further modified by Fe_2O_3 impurity.

Seawater periclase products are quite pure MgO, running typically around 98-99%. Iron oxide contamination is low: less than 0.5%, typically about 0.3%. The seawater source gives a small B_2O_3 contamination, which is usually counted as SiO_2 but has a depressing effect on the matrix melting temperature. Silica impurity is usually ~0.3% unless SiO_2 is added for bonding. CaO is comparable, but may be adjusted deliberately to maintain a CaO:SiO_2 mol ratio above 2.0 (Figure VI-1a). In that case matrix melting starts at ~1790°C, but the maximum service temperature can approach 1900°C owing to the small amount of impurity present. With chemical bonding by silica,

the MST is closer to 1800°C. If the $CaO:SiO_2$ ratio in the matrix is let fall below 2.0 (wt. ratio 1.87), the MST drops to about 1600°C.

Burned magnesite refractories are considerably less pure than synthetic periclase, running at best about 95% and typically about 90% MgO, sometimes even lower. Their several percent SiO_2 increases the amount of matrix, but the initial melting temperature is again subject to control by fixing the $CaO:SiO_2$ ratio. Iron oxide contamination is up to an order of magnitude higher than in synthetic periclase, however; this reduces the MST to below 1850°C at best, with the onset of matrix melting below 1700°C. If the lime:silica ratio is below 2.0, the MST falls to as low as 1450°C.

Manipulating the lime:silica ratio can be done with any convenient source of lime, of which dolomite (nominally $CaCO_3 \cdot MgCO_3$) is a plentiful example. Dolomite deposits in fact range in composition from dolomitic limestone (CaO:MgO >1) to dolomitic magnesite (CaO:MgO<1). As there are enormous deposits of dolomite in some areas of the world where high-quality magnesite is scarce -- notably, for example, in western Europe -- it is tempting to make basic refractories of dolomite alone.[87,97,181,183-185,227,305] But mixtures of dolomite with magnesite may also be employed to yield any desired CaO:MgO ratio between the extremes.[177,178]

Figure VI-1a shows some gain in matrix melting temperature as the $CaO:SiO_2$ ratio is increased well above 2.0. But the compound $3CaO \cdot SiO_2$ is about as prone to slaking as is Portland cement, and above a 3:1 ratio free CaO appears. In this region of matrix composition, CaO also dissolves in MgO at equilibrium (Fig. IV-3a), altering the grain chemistry. Since a saturated MgO-CaOss contains CaO at unit chemical activity, the grain itself becomes subject to slaking. Hence with gradually increasing CaO content, fired basic refractories become subject first to matrix deterioration and then to both matrix and grain decay by slaking while "on the shelf." Using round numbers for illustration: a basic refractory containing 5 wt% SiO_2 passes the tricalcium silicate matrix composition at 14% CaO and becomes lime-saturated in the grains at a total CaO content of about 21%, whereas a burned 1:1 dolomite is about 55% CaO by weight. Thus the amount of free lime in the latter is very large. An estimate of its MST, allowing for the effect of iron impurity, is very close to that of seawater periclase, 1800°-1900°C. Managing its critical slaking susceptibility remains a severe challenge, however.[178,306]

Chrome-Containing Basic Refractories

By accepted practice, Magnesite-Chrome in Table VIII.1 contains more than 50% MgO, fired basis; Chrome-Magnesite contains less than 50% MgO; and a Chromite refractory is made from essentially all chrome ore (nominally $FeCr_2O_4$).[9] Because so much

iron is introduced in chrome ore, the binary systems MgO-$MgCr_2O_4$ and $MgCr_2O_4$-Cr_2O_3 of Figure VIII-1 and their ternary systems with SiO_2 inadequately represent the real materials. Furthermore, the variety of chrome ore deposits and concentrates adds to the variety of magnesias, from periclase to magnesites and even dolomites, to give a complex chemical family.

Inspection of a large number of commercial product data sheets leads to the conclusion that the MST is insensitive to the per cent chrome ore per se; somewhat sensitive to the total SiO_2 and CaO contents; and somewhat sensitive to the manner in which the grain is made (e.g., fused or pre-reacted) and to rebonding. For products made using periclase, the apparent MST ranges between about 1800°C and >1900°C; and without magnesia (i.e., chromite refractory), between about 1650°C and 1850°C.[72,144-151,154]

Forsterite and Olivine

Forsterite basic refractories (Table VIII.1) lie close to the binary MgO-Mg_2SiO_4 system of Figures VIII-1 and IV-3d. They must be kept on the MgO-rich side of the forsterite composition (i.e., ≥ 58 wt.% MgO) to ensure that the MgO-Mg_2SiO_4 eutectic at 1850°C governs initial melting. If appreciable CaO is admitted into the composition, then a ternary eutectic at 1357°C governs melting (Figure VI-1a). That prospect limits both the manufacture and use of forsterite refractories. Since these materials are typically made from magnesite and silica, other impurities such as iron oxide work against any exceptional refractoriness: in the best case the MST is probably close to 1800°C. Such a product made from magnesite and clay would run afoul of a ternary MgO-Al_2O_3-SiO_2 eutectic at 1365°C (Figure IV-4), besides risking alkali contamination.

Magnesia-rich compositions in the MgO-Mg_2SiO_4 system, best regarded as forsterite-bonded MgO, have also been made to facilitate low-temperature sintering of magnesite. The same binary eutectic at 1850°C governs melting.

Olivines (Table VIII.1) are mineral-derived refractory compounds, of limited interest. They are a family of $(Ca,Mg,Fe)_2SiO_4$ solid solutions. The most familiar olivines are $(Ca,Fe)_2SiO_4$, whose liquidus map is included in the ternary CaO-FeO-SiO_2 system.[21] That field is dominated by minimum-melting compositions at 1093° and 1115°C, suggesting an MST not greater than about 1200°C and probably lower. We shall lose track of olivine as a refractory henceforth.

Cordierite and Soapstone or Talcite

Cordierite, $Mg_2Al_4Si_5O_{18}$ or $2MgO{\cdot}2Al_2O_3{\cdot}5SiO_2$, is hardly a basic refractory although it has been so listed in Table VIII.1 after Reference 284. Formulated from clays, it is neither pure nor necessarily a single-phase refractory as-made. Its equilibrium phase field is included in Figure IV-4. The pure compound melts at about 1550°C, but its primary crystallization field is dominated by a ternary eutectic at 1355°C. Considering impurity effects, its MST may be between 1350° and 1400°C. As mentioned earlier, its isothermal use under load as kiln furniture is limited to the vicinity of 1000°C by considerations of creep.

The reported raising of that latter limit to ~1430°C, by a formulation of cordierite + mullite[186] falling on the dotted line drawn in Figure VIII-1, may stir up interest in this two-phase system. Evidently the MST was thereby raised as well. Cordierite has long suffered in kiln furniture applications for its low softening temperature, which this new formulation could conceivably remedy.

Soapstone or talcite, $Mg_3Si_4O_{11}$ or $3MgO{\cdot}4SiO_2$ (fired basis), is today only an echo of history. Once it was commonly used, being a soft natural stone capable of easy shaping into fitted blocks. It occurs as the hydrate, $Mg_3Si_4O_{10}(OH)_2$. On thermal decomposition of the hydrate, the oxidic composition given by the formulas above exists as a metastable relic structure. Heated near its melting temperature, the relic goes over to protoenstatite plus silica:

$$3MgO{\cdot}4SiO_2 \rightarrow 3\ MgSiO_3 + SiO_2\ .$$

The phase diagram of Figure IV-4 indicates a binary eutectic between these two phases, melting at 1543°C. This minimum melting point explains why soapstone survived so long, historically, into the Iron Age. Its MST is about 1550°C. By the time of the Age of Steel, it was doomed as a metallurgical refractory. Now it is all but forgotten.

Magnesium and Calcium Aluminates

Magnesium aluminate spinel, $MgAl_2O_4$, is a very refractory compound in its own right, melting at 2135°C. It has been studied and set aside more than once in both the refractories and technical ceramic fields, principally because it is so hard to synthesize as a single phase by reaction sintering. Now with the two capabilities of arc fusion and of colloid synthesis, perhaps it will be re-evaluated.

The MgO-$MgAl_2O_4$ eutectic melts at 1995°C (Figure IV-3b), while the $MgAl_2O_4$-Al_2O_3 eutectic melts at 1860°C.[21] The spinel has a marked solid-state solvent capacity for either MgO or Al_2O_3; it should

be a good bonding agent for either one. In fact, there seems to have been more interest over the years in spinel-bonded magnesia [136,137,141,203,204,307] and in spinel-bonded alumina[143] than in single-phase refractory spinel.[142] The pure synthetic single-phase spinel should have an MST close to 2100°C. A two-phase $MgO+MgAl_2O_4$ refractory should exhibit an MST near 2000°C, and a two-phase $MgAl_2O_4+Al_2O_3$ refractory about 1850°. By arc fusion, refractory grain synthesis from selected mineral raw materials should yield products almost as high-melting. The use of spinel as a host for particulate carbon composites is of potential interest, as pointed out in Chapter V.

Two calcium aluminates are shown along the binary $CaO-Al_2O_3$ system in Figures VIII-1 and VI-2b. The CA compound melts at about 1600°C, the CA_2 compound about 1750°C.[21,214] But these on melting dissolve more Al_2O_3, a process which continues indefinitely in an excess of alumina, and the melting temperature continues to rise. As we are interested only in high-purity CA cement[214] and only in its use in high-alumina refractories, we can be satisfied that coherent melting of the cement in these systems does not occur other than fleetingly. As stated earlier, the ultimate fate of CA cement in an alumina host at the highest temperatures is a solid solution of CaO in Al_2O_3. There is no clear MST for the cement, short of that of the alumina. Reactions with silica are another matter, discussed toward the end of Chapter VI.

Zirconia and Zircon

These refractories, listed under "Special Refractory Materials" in Table VIII.1, now deserve a place in a regular category. Their place in the A-Z-S triangle and elsewhere in Figure VIII-1 was pointed out early in this chapter. Yet the number of possible combinations of ZrO_2 and $ZrSiO_4$ with still other phases has not begun to be exhausted.

The zircon-rich and zirconia-rich areas of the $Al_2O_3-ZrO_2-SiO_2$ phase system are relatively simple.[21] Stoichiometric $ZrSiO_4$ exhibits a binary eutectic at 2250°C, giving a silicate liquid in equilibrium with solid ZrO_2 as discussed in Chapter IV and shown in Figure IV-6a. Compositions much richer in SiO_2 than $ZrSiO_4$ melt remarkably lower. Along the $Al_2O_3-ZrO_2$ binary system there are no intermediate compounds, only a simple eutectic melting at about 1860°C. A ternary peritectic appears at about 54% Al_2O_3, 28% ZrO_2, 18% SiO_2, melting at about 1790°C and leading toward the SiO_2 corner at 1700°C. The ZrO_2-mullite tie line is governed by a 1780° eutectic valley, and the $ZrSiO_4$-mullite tie line by a 1750° valley. These last two lead slowly downhill toward SiO_2. Thus in either the ZrO_2-mullite system or the $ZrSiO_4$-mullite system, to keep the MST in excess of 1800°C requires staying close to the composition of the zirconium

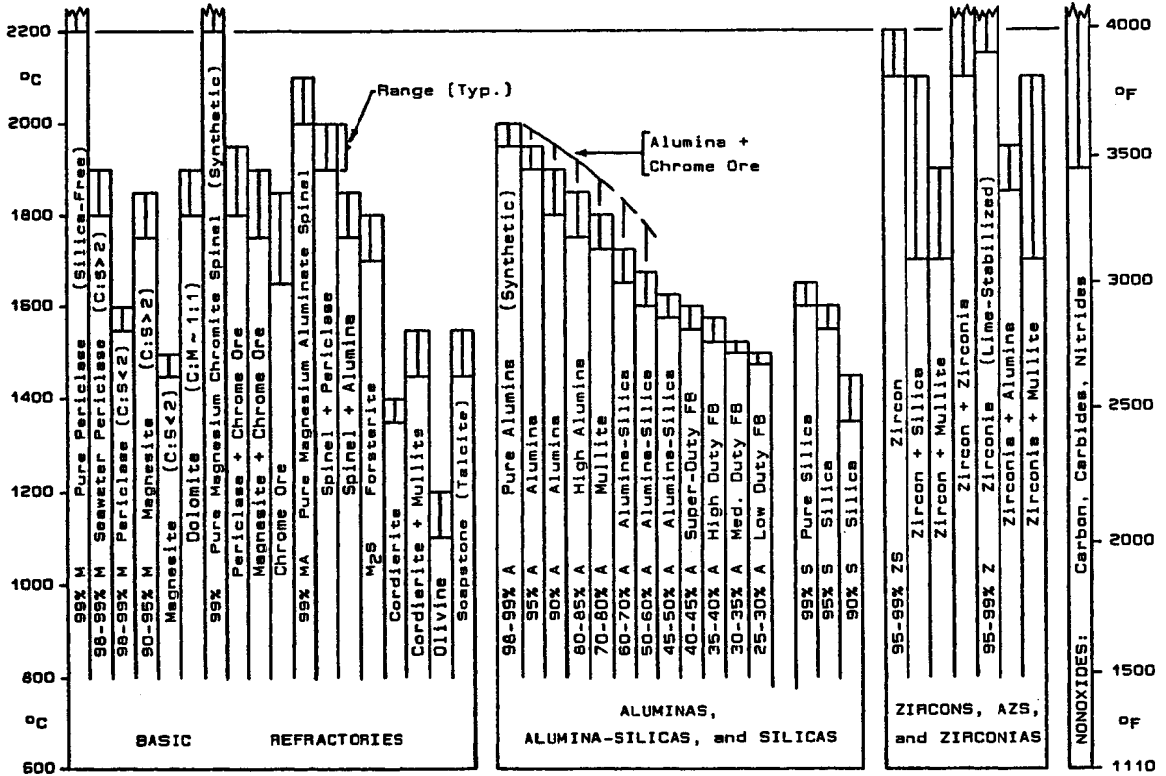

Figure VIII-3 Maximum Service Temperatures of Commercial Refractory Types

compound. Yet nowhere in the entire triangle is the MST below about 1700°C, lacking contamination by iron or alkali impurities or Ca0.

Nonoxides

Carbon and the carbides, nitrides, etc. listed in Table IV.1 are most commonly employed as single substances. Accordingly, the MST is near each tabulated melting point. In most cases this means well in excess of 2000°C.

MST Summary

The foregoing estimates of the MST for commercial working refractories are summarized in bar chart form in Figure VIII-3. The sequence from left to right conforms to the sequence of ISO classifications given in Table VIII.1. Some purity and composition distinctions have to be made in this figure; the code letters following the percentages given in the bars follow the same shorthand component notation introduced in Chapter IV, namely M = Mg0, C = Ca0, A = Al_2O_3, S = SiO_2, Z = ZrO_2, etc.

The temperature range identified at the top of each bar, scaled in °C and °F, is intended to correspond to the range of commercial refractory compositions that fall within the descriptors of the bar. There is an additional uncertainty in the estimation itself; this should be within ±50°C in most cases.

Qualification of a refractory type for noncorrosive service is one use to which these data may be put. This use is limited. Furthermore, if the entire thickness of a refractory wall is at or near the hot face temperature, as for example in muffles and kiln furniture, the MST will overstate its temperature serviceability on account of creep. Where this property is attributable to the matrix, corrosion life and refractoriness tend to correlate positively. Examples visible at a glance in Figure VIII-3 are found in the aluminas, magnesias, zircons and zirconias of about equal MST (~1800°-1900°C), which now serve to some degree interchangeably in each others' traditional territories of chemical exposure.

THERMAL STRESS RESISTANCE

Assessment of Thermal Stress Resistance by Refractory Type

Quantitative rules for the resistance of refractories to thermal stress are elusive. In Chapter IV the best index of vulnerability that could be found for a single phase was the coefficient of linear thermal

expansion, α. If a thermal transient is described in terms of a change in heat flux J into a surface, then the vulnerability to thermal stress cracking was shown also to depend in an inverse way on the thermal conductivity k or on the thermal diffusivity, $\delta = k/(c\rho)$. Thermal expansions are plotted in Figures IV-7, IV-9a,b and IV-10. Accounting for differences in k or δ between oxides and nonoxides as groups, the characteristic thermal stress sensitivities of single-phase refractories mentioned in Chapter IV are adapted in the following table:

	Oxides		Nonoxides	
Insensitive				
	Vitreous Silica	(≤1000°C)	Vitreous Carbon	
	beta-Spodumene	(≤1000°C)	Granular Carbon	
	Cordierite	(≤1000°C)	Graphite	
	High Quartz	(≥ 600°C)	SiC	
	High Cristobalite	(≥ 600°C)	BN	(≤ 1200°C)
	Tridymite I	(≥ 600°C)	B_4C	
	Mullite (moderately)		TiC (moderately)	
Moderately Sensitive				
	ZrO_2 (cub.)	(≤1200°C)		
	$ZrSiO_4$	(≤1400°C)		
	Cr_2O_3			
	Al_2O_3-Cr_2O_3ss		Typ. High Mol. Wt.	
	$MgCr_2O_4$		Carbides and	
	$MgAl_2O_4$		Nitrides	
	$CaAl_2O_4$			
	Al_2O_3			
	MgO			
Sensitive				
	Mg_2SiO_4			
	Fe_2O_3			
	$MgFe_2O_4$		None	
	CaO			
	Low Quartz	(≤ 550°C)		

In each group an effort has been made to list substances in order of increasing thermal stress sensitivity; but unequal macroscopic dimensions and microstructural features can change the order. Magnesia is rated better here than in Chapter IV by virtue of its thermal conductivity, which is very high among those of the refractory oxides.[74] The thermal k of SiC is among the highest of the nonoxides.[32] Numerical values of k will be given in a later chapter.

The above order represents the relative sensitivity to a single thermal transient. The first or "insensitive" group are also insensitive to repetitive temperature cycling within the ranges given. But the

cycling experienced in the field usually goes well below 600°C unless special operating precautions are taken. In such case the several forms of silica listed are susceptible to disruptive phase change (Figure IV-7) and then to the high thermal stress sensitivity of low quartz and of tridymite V. For these reasons silica refractories are mechanically unstable unless maintained above about 600°C.

With diminishing content of SiO_2, the severity of damage ultimately diminishes. The common fireclays derive much of their thermal stress resistance from high porosity, while giving clear evidence by aberrations in thermal expansion curves[3] that the SiO_2 phase changes are distorting and microcracking the structure as the temperature passes through the 500°-600°C region. Some ratcheting can follow. High-fired high-duty and super-duty fireclays (40-45% Al_2O_3 by weight) begin to relieve this phase-change sensitivity by separation of their SiO_2 crystals, but microcracking still occurs.

This progression with increasing percent Al_2O_3 defies quantifying because of the range of metastable phase compositions and particle sizes exhibited by different commercial clay-based products. But as the mullite phase composition (70% Al_2O_3) of clay-alumina refractories is passed and SiO_2 substantially disappears, the unique phase instability of that constituent disappears as well. In this composition range the clay-alumina refractories join all other oxidic types in becoming governed by common concepts of thermal stress resistance.

For each of the phases classed as "moderately sensitive" and "sensitive" in the preceding list, it is intuitive that progressively less-intense thermal excursions, repeated progressively more times, may eventually result in mechanical failure by cumulative growth and linking up of microcracks. It is also true that few real refractories are made solely of one of these phases, whether by virtue of impurities alone or by deliberate use of matrix-bonded and multi-phase formulations. In Chapter IV it was emphasized that virtually all real refractories are accordingly subject to microcracking at the outset. If the oxidic refractory product line is substantially described by the forty bars of Figure VIII-3, then at least thirty-five of those types are assuredly born microcracked.

By manipulating the selection and sizing of major-phase grains, the chemical nature and amount of matrix, and the thermal history of manufacture, it is possible to create a wide range of intensity (i.e., frequency and/or characteristic length) of microcracking in nearly any refractory type. However, the art of characterization does not include a reliable means of describing microcracks, and for this reason a good predictive model relating microcracking to thermal cycling resistance is not in hand.[29,36] It is clear that microcracking is

helpful, and that the mechanism is by increasing the energy of fracture.[36] But microcracks do also initiate failure.[35-37]

The further freedom to manipulate *porosity* in refractories rests on a somewhat sounder foundation: resistance to thermal cycling increases monotonically with increasing apparent porosity, without reference to the phase composition. The final degree of freedom is represented by refractory *composites*, wherein carbon bonding apparently works by virtue of the compliance of porous carbon while SiC and SS wire reinforcements have relatively well-understood toughening effects.[29]

The consequence of these several microstructural degrees of freedom is that the phase composition of multi-phase oxidic refractories is confounded with microstructure in thermal cycling behavior. Rating of refractories by composition class alone has to admit of many exceptions. The current literature is replete with multi-phase formulations that are accorded high resistance to thermal cycling without sacrificing density, for example:

	Oxidic	**Carbon-Bonded**
Basic	Mag-Chrome,[34,276,281]	Magnesia[74]
	Magnesia-Spinel[34]	Dolime[178]
	Magnesia-Forsterite[308]	Mullite[188]
	Magnesia-Mullite[308]	Andalusite[189,190]
	Cordierite-Mullite[286]	A-Z-S[191]
		Zirconia[74]
	Alumina-Chrome[77]	Zirconia-Mullite[199]
	Alumina-Mullite[275,309]	
	Alumina-Silica[310]	**SiC-Reinforced**
	Alumina-Zirconia[52]	
		High-Al_2O_3[45,46,105,192,196]
Zircon	Zircon-Mullite[92]	Mullite[105,188]
	Zircon-Pyrophyllite[90,233]	Clay-Alumina[46,48]
	Zircon-Silica[123]	Andalusite[189,190]
	Zircon-Zirconia[121]	A-Z-S[191]
		Zirconia[74]
Zirconia	Zirconia-Alumina[129]	Zirconia-Alumina[86,192]
	Zirconia-Dolime[87]	

Stainless Steel Wire-Reinforced

Chrome Ore[49]

High-Al_2O_3 & Clay-Alumina[50,51,240,290,291]

Table VIII.3 recaps and interprets all the above observations, listing refractories by type as "immune" (3), "very resistant" (2),

Table VIII.3 Thermal Stress Resistance of Various Refractory Types

REFRACTORY COMPOSITION	SHAPED & UNSHAPED	CARBON BONDED	SiC REINF.	SS WIRE REINF.
100% MgO (single phase)	1			
98-99% MgO Periclase	1-2	2		
90-95% MgO Magnesite	1-2	2		
MgO-CaO Dolime	1-2	2		
100% $MgCr_2O_4$ (single phase)	1			
50-90% MgO MgO-Chrome Ore	1-2			
30-50% MgO Chrome-Mag.	1			
Chrome Ore	1			2
100% $MgAl_2O_4$ (single phase)	1			
MgO-Spinel	1-2			
100% Mg_2SiO_4 (single phase)	0			
MgO-Forsterite	1-2			
Cordierite	3			
Cordierite-Mullite	2			
Beta-Spodumene	3			
100% Al_2O_3 (single phase)	1			
85-99% Al_2O_3 High Alumina	1-2		2	2
Al_2O_3-Cr_2O_3 (single phase)	1			
Al_2O_3-Chrome Ore	1-2			
70-85% Alumina-Mullite	1-2		2	2
70% Al_2O_3 Mullite	1-2	2	2	
60% Al_2O_3 Andalusite, etc.	1-2	2	2	2
Super- and High-Duty Fireclay	1-2			
Med.- and Low-Duty Fireclay	1-2			
100% SiO_2 Vitreous Silica	3			
90-98% SiO_2 Sintered Silica	0-1			
95-99% $ZrSiO_4$ Zircon	1			
Zircon-Silica	1-2			
Zircon-Pyrophyllite	1-2			
Zircon-Mullite (A-Z-S)	1-2	2	2	
Zircon-Zirconia	1-2			
95-99% ZrO_2-CaO Stab. Zirconia	1	2	2	
Zirconia-Magnesia	1-2			
Zirconia-Dolime	1-2			
Zirconia-Alumina	1-2		2	
Zirconia-Mullite	1-2			
Carbon (vitreous)	3			
Carbon (granular, graphite)	2-3			
SiC (Si_3N_4- or SiAlON-bonded)	2-3			
B_4C, BN, TiC (single phase)	2			

KEY TO RATINGS:
0 - Sensitive
1 - Moderately Resistant
2 - Very Resistant
3 - Immune (to ~1000°C)

"moderately resistant" (1), and "sensitive" (0), respectively, to repeated thermal cycling in the elastic temperature region. Where a range of ratings is given, viz., "1-2," the implication is that thermal cycling resistance can be purposefully varied within the type by composition adjustment and otherwise.

Table VIII.3 consistently reflects that two- and multi-phase materials generally perform better than single-phase. Where a composition type is given simply by two end-members, the end-members themselves are accordingly excluded; otherwise, the pertinent range of compositions (as well as choice of minor constituents) has to be left to more detailed inquiry. Resources for such inquiry include Chapters IV-VII, the references cited here, and product literature issued by manufacturers. While in general direct-bonded refractories are the least thermal-stress resistant and the chemically-bonded and unfired types more so, other features such as grain sizing and manner of forming or installation preclude making any further categorical observations.

One of the properties invariably tracked in product optimization is the apparent porosity, usually measured by a standardized method such as procedure no. C830 or C20 of ASTM.[9] While porosity is an unstated variable here, it is implicit for working refractories that this property is constrained in each case in Table VIII.3 by considerations of corrosion resistance sufficient for each intended duty. To the degree these considerations permit, as a rule increasing porosity yields increasing resistance to thermal stress and cycling.

Measurement of Thermal Stress Resistance

The preceding section deals at best semiquantitatively with thermal stress resistance. All of the terms used are relative. It will be recalled that all of the characterizations of thermal stress experienced in actual service in Chapter III were likewise relative: viz., "severe" or "moderate" or "minor," etc. The refractories technologist is uncomfortable in matching products to uses in this framework. When one specific application is selected and a small number of refractory products are considered, however, it becomes possible to quantify their performance somewhat through use-related *testing*. A background of field experience with one or more consistent products provides invaluable control materials for such tests; and computer-aided thermal stress analysis of the use can help in the design of realistic tests.

At least two circumstances persistently interfere, nonetheless. One is that the time duration of a test (e.g., under thermal cycling) must usually be far shorter than the service life sought in the application. Every such "accelerated" test has to impose much more severe conditions than those of use, and extrapolation of the

specimen responses back to the use conditions is risky. Another potentially invalidating circumstance is that of *alteration* of the refractory by corrosion in service. For one dramatic example of this interference, recall the slabbing failure due to freeze-thaw cycling of a penetrating slag, described under Freezing of the Penetrant Liquid in Chapter VI. Another is redox cycling of refractories containing iron oxide (Chapter V).

Quenching Tests. Rapid quenching of isothermally-heated small specimens is on the whole more severe and more reproducible than is rapid heating. For the simple ranking of different materials, it is common to pick a quenching medium such as water or oil; and to select a series of fixed temperatures to which "identical" specimens of each material are heated at steady-state, then quenched once by plunging into the cold medium. Spalling, cracking, and surface crazing are noted, visually and at low-power magnification and often using fluorescent dye penetrant techniques. The intensity of these responses is coded numerically, and the code numbers are recorded vs the heating temperature as the independent variable.

Cycling Tests. A variety of thermal cycling tests are in use,[35-37,311] with the manner, frequency, and number of cycles and their temperature extremes open to the experimenter. Tests of this type may be keyed to specific refractory usages. Measures of the specimen response can be by nondestructive means such as visual, as above, or ultrasonic; or destructively, for example by determining the modulus of rupture (tensile strength in bending) after a fixed number of cycles. The cycles are usually imposed as standard "steps," by alternately introducing the specimen into a preheated furnace and removing it to ambient air or to a cooler chamber, each for a prescribed time. Or, such cycles may be imposed solely on one face of a single brick or gang of bricks, the rear face either exposed constantly to ambient air or backed by thermal insulation. Specimens may be either bricks or the equivalent made from monolithics.

For investigations into progressive mechanical damage, *acoustic emission* or *AE* techniques have become popular.[35,37,311] Here a rugged device serving as a sensitive microphone is imbedded in or pressed against the back of a hot-face-cycled specimen. The amplified acoustic output is recorded continuously throughout a planned sequence of thermal excursions, giving "clicks" and "pops" as signals of sudden microcrack extensions and the accompanying elastic relaxations of the solid. Considerable sophistication in these "micro-seismic" techniques is possible, but other observations have to be made and correlated before the significance of acoustic signals can be fully appraised. Some work has been done in computer modelling of the gradual deterioration of refractories under an accumulation of thermal cycles.[59]

Standard Panel Spalling Test. The only industry-wide standardization of thermal stress testing in the U.S. is embodied in the *Panel Spalling Test* for bricks, given by ASTM[9] as procedure no. C38 and modified slightly for high-duty firebrick as C107 and for super-duty firebrick as C122. For this severe test every detail of equipment, test panel and procedures is rigidly specified, and some experiential data on the variance of results between tests and between laboratories are given.[9] Only the rudiments are described here as typical.

Standard "9-inch straight" bricks or their sawed equivalent are used, being 9" by 2.5" or 3" by 4.5" (228 by 64 or 76 by 114 mm) in dimensions. The 4.5" thick test panel is made up of twelve or fourteen of these, exposing an area at least 18" square (i.e., two by 9" wide and 6x3" or 7x2.5" high). The bricks are pre-weighed and mortared together, surrounded and backed by a specified insulating refractory. Two such panels are contrived in tandem as sliding doors of a specified furnace, together with provisions such that each one in turn alternately closes the furnace and is slid to one side. The furnace is thus always closed by one test panel or the other. After being preheated in place, the hot face of the panel which is then slid aside is immediately subjected to a specified blast of ambient air and fine water spray for a specified time; then this panel is moved again to close the furnace for a specified reheating time to the selected temperature. The first spray-cooling followed by reheating constitutes the first full cycle of a fixed total of twelve cycles.

The typical refractory response is a succession of accumulated small spalls, more-or-less parallel to the hot face. On conclusion of the test, the bricks are all cleaned and re-weighed. The cumulative material lost by spalling is reported as percent of the original total panel weight.

The ASTM test specifications[9] do not include the interpretation of per cent spalling loss into classifications of thermal stress resistance such as the ratings "0, 1, 2, 3" given in Table VIII.3. The per cent loss together with the top temperature used in the test is often reported in commercial product literature, however, and for a modest number of product types listed in the table we have consulted manufacturers' data to augment the other information consolidated there. The tabulated rating of "2" corresponds to panel spalling losses reported as "trace" or "none," and the rating of "1" corresponds to reported panel spalling losses ranging from about 4-5% down to about 2% or less.

The panel spalling test may in time be superseded by some other standard method. As this test is in use only for fired bricks, an even greater need exists for standardized thermal stress testing of

monolithics. At this writing no such procedure or rating scheme has found general acceptance.

CORROSION RESISTANCE

Assessments of Corrosion Resistance by Refractory Type

Resistance to corrosion is even more difficult to encapsulate than is resistance to thermal stress. Chapters V-VII encompass a large number of variables which, individually or together, can influence the durability of each refractory in any of a number of hot processing environments. The combinations of processing temperature with the chemistry of aggressive liquid environments illustrated in Chapters II and III are even more numerous.

The composition classes of Table VIII.1 allow in most cases for considerable variety of refractory overall compositions. Incorporating the subclassifications of Table VIII.2, any one composition class can encompass almost an infinite number of phase compositions, microstructures and porosities.

To organize this galaxy of materials and environments in any brief way is necessarily to focus on the *maximum* corrosion resistance that has been achieved in each composition class or type, and to cluster the corrosive environments under a few manageable headings that tend to exhibit some similarity within. A useful dependent variable in such a presentation is the *maximum temperature* at which each refractory type can be durable in each type of corrosive environment.

The very definition of durability becomes an issue. To the extent this can be normalized at all, it is normalized here against the hot processor's expectations or necessities rather than against a common time frame. The only absolute measures of refractory useful life in units of time, number of heats, etc., come from field experience. There the totality of each exposure is relatively fixed but rarely described objectively. There are virtually no parametric studies of refractory corrosion that are of any appreciable predictive value.

Fortunately in this respect, the dependency of corrosion rate on the hot-face temperature is so great -- in most cases doubling every 30°C down to every 10°C -- that it is hard to mis-state this variable by a very large interval. But there is a paucity of published data, forcing a resort in many cases to estimation or judgment. In spite of the hazards of error and the risks of over-simplification, a condensation of Chapters V-VII into brief terms should be of service to the reader. This condensation is presented in Tables VIII.4 and VIII.5.

Table VIII.4 Temperature Limits: Corrosion by Hot Process Liquids

REFRACTORY TYPE	IRON, STEEL, & Cu SLAGS; CMT.		GEN. NONFERR. METALL. SLAGS		GLASS CONTACT	REDUC. CO @ ~1 atm	OXID. CO_2 to O_2	REDOX CYCLING CO to O_2
	B[1]	A-N[1]	B-N[1]	A-N[1]	A-N[1]			
High MgO	1700°C	NR[2]	1500°C	NR[2]	1600°C	1700°C	m.p.	1700
Dolime	1700	NR	1400	NR	NR	1700	m.p.	1700
MgO or Dolime + Carb./Graph.	1800	1700°C	NR	NR	NR	1700	500°C	500
MgO-Chrome Ore	1700	1600	1500	1400°C	NR	Disint.[3]	1800[4]	1800
Chrome Ore	NR	1600	1500	1400	NR	Disint.	1800[4]	1800
MgO-Spinel	NR	1600	1500	1400	NR	1700	m.p.	1700
MgO-Forsterite	NR	1500	1400	NR	NR	1700	m.p.	1700
High Al_2O_3	1600	1600	1500	1500	1600	1900	m.p.	1900
Al_2O_3 + Carb./Graph. (+ SiC)	1700	1700	NR	NR	NR	1900	500	500
Alumina-Chrome	1600	1650	1500	1550	NR	Disint.	1800[4]	1800
Alumina-Spinel	1600	1500	1400	1400	1600	1900	m.p.	1900
Al_2O_3-Mullite (75-85% Al_2O_3)	1600	1600	1400	1400	1400	Disint.	m.p.	1900
Mullite (70% Al_2O_3)	1600	1600	1400	1400	1400	Disint.	m.p.	Debond[5]
Clay-Alumina (50-65% Al_2O_3)	NR	1500	1300	1300	NR	Disint.	m.p.	Debond
Clay-Alumina + Carb./Graph.	1600	1600	NR	NR	NR	1700	500	500
Super-Duty Firebrick	NR	NR	1200	1250	NR	Disint.	m.p.	Debond
High-Duty Firebrick	NR	NR	1150	1200	NR	Disint.	m.p.	Debond
Med.- & Low-Duty Firebrick	NR	NR	NR	1100	NR	Disint.	m.p.	Debond
High Silica	NR	NR	NR	1400	1500	1600	m.p.	1600
Zircon	1600	1600	1500	1500	1800	1800	m.p.	1800
A-Z-S (Zircon-Mullite)	1500	1600	1500	1500	1800	Disint.	m.p.	1800
Zircon-Zirconia	1600	1700	1600	1600	1900	1800	m.p.	1800
Zirconia (CaO-Stabilized)	1700	1800	1700	1700	1900	1800	m.p.	1800
Carbon, Graphite	2000+	2000+	1800	1800	NR	m.p.	500	500
SiC (Nitride-Bonded)	2000+	2000+	1800	1800	NR	m.p.	1400	1400

NOTES:
1. B = Basic; A = Acid; N = Neutral Slags. 2. NR = Not Recommended.
3. Disint. = CO Disintegration if mineral-based; disregard if synthetic.
4. 1800° = Temp. of Oxidation of Cr_2O_3 to CrO_3; ~1600° if alkalies present.
5. Debond = FeO-Fe_2O_3 Cycling Failure if mineral-based; disregard if synth.

Table VIII.4 refers to immersed or bathed contact of an enclosing refractory with liquid slags and glasses. A negative temperature gradient through the wall is presumed. The last three columns depict the *simultaneous* exposure to highly reducing and oxidizing conditions, respectively, and finally to redox cycling. Recall, for example, that the BOF is redox cycled while conditions are nominally oxidizing in the glass tank and the cement kiln and reducing in the blast furnace and the carbon baking oven.

The list of refractory types is by no means all-inclusive. The temperatures in °C in the body of the table are intended to be the maximum, in each category of exposure, of which a "better" or "best" refractory of each type is capable.

Apart from interactions with the given liquids, notations are made in the last three columns as to "disintegration" by CO (mainly in the 400°-800°C interval) and "debonding" due to FeO-Fe_2O_3 cycling (mainly in the 500°-1000°C interval), to which mineral-based refractories are liable to a greater or lesser extent. Those notations are not necessarily guarantees of failure. The phenomena are described in Chapter V.

Temperatures around 2000°C or above, cited in the bottom rows of the table, mean sufficient for practically all industrial processing of each kind. The remaining temperatures in the table, below 2000°C, range from documented to estimates but are likely within ±100°C in the worst cases. The reader is cautioned nonetheless to regard Table VIII.4 as a rough guide only.

Table VIII.5 is a similar display of the limiting temperatures for corrosion resistance in gaseous environments. The environments of the first four columns are highlights of those discussed in Chapter VII. It will be recalled from that chapter that SO_2 is unique in reacting with refractories only *below* certain limiting temperatures. The safe temperatures are accordingly above those limiting values, shown in the table by the ">" sign in the second column.

The fourth column, "Benign Atmospheres," is germane to many refractory applications: a mildly-oxidizing flame burning natural gas is a good example. The temperatures in that column are taken from the MST display of Figure VIII-3. The next three columns again deal with reducing, oxidizing, and cyclic operations. The final column of Table VIII.5 rates the listed refractory types as to dust-abrasion resistance. This table in its entirety is likewise intended for rough guidance only.

Table VIII.5 Temperature Limits: Atmospheric Corrosion/Alteration

REFRACTORY TYPE	ALKALI VAPORS Na_2O	SULFUR VAPORS SO_2+O_2	HCl & CHLORIDE VAPORS	BENIGN ATMOS-PHERES	REDUC. CO @ ~1 atm	OXID. CO_2 to O_2	REDOX CYCLING CO - O_2	DUST ABRASION All T[1]
Periclase (98-99% MgO)	1700°C	›1100[2]	NR[3]	1900°C	1600°C	m.p.	1600	Good
Magnesite (90-95% MgO)	1600	›1100°C	NR	1800	Disint.[4]	m.p.	1600	Good
Dolime (MgO-CaO)	1700	›1400	NR	1900	Disint.	m.p.	1600	Good
MgO-Chrome Ore	1700	›1200	NR	1900	Disint.	1800[5]	1800	Good
MgO-Spinel	1600	›1200	NR	1900	1600	m.p.	1600	Good
MgO-Forsterite	NR	NR	NR	1800	1600	m.p.	1600	Good
High Al_2O_3	1600	› 500	1200	1900	1900	m.p.	1900	Excel.
Alumina-Chrome	1600	› 500	NR	1900	Disint.	1800[5]	1800	Excel.
Alumina-Spinel	1600	› 600	NR	1800	1900	m.p.	1900	Excel.
Al_2O_3-Mullite (75-85% Al_2O_3)	1600	›1000	NR	1800	Disint.	m.p.	1900	Excel.
Mullite (70% Al_2O_3)	1600	›1100	1000	1800	Disint.	m.p.	Debond[6]	Good
Clay-Alumina (50-65% Al_2O_3)	1500	›1200	1000	1700	Disint.	m.p.	Debond	Good
Super-Duty Firebrick	1400	›1300	1000	1600	Disint.	m.p.	Debond	Fair
High-Duty Firebrick	1300	›1300	1000	1550	Disint.	m.p.	Debond	Fair
Med.- & Low-Duty Firebrick	NR	›1300	NR	1500	Disint.	m.p.	Debond	Poor
High Silica	1600	› 600	1400	1650	1500	m.p.	1500	Good
Zircon	1700	› 500	1400	2100	1700	m.p.	1700	Good
A-Z-S (Zircon-Mullite)	1700	› 800	NR	1900	Disint.	m.p.	1700	Good
Zircon-Zirconia	1800	› 500	1400	2200	1700	m.p.	1700	Good
Zirconia (CaO-Stabilized)	2000	› 500	1500	2200	1700	m.p.	1700	Fair
Carbon, Graphite	2000+	2000+	2000+	2000+	m.p.	500°C	500	Fair
SiC (Nitride-Bonded)	2000+	2000+	2000+	2000+	m.p.	1700	1700	Best
B_4C, TiC, TiN	2000+	2000+	2000+	2000+	m.p.	NR	NR	Excel.

NOTES:
1. Abrasion Resistance rating up to temperature of hot face softening.
2. Temps. preceded by "›" are minimum for SO_2 resistance; all others maximum.
3. NR = Not Recommended.
4. Disint. = CO Disintegration if mineral-based; disregard if synthetic.
5. 1800° = Temp. of Oxidation of Cr_2O_3 to CrO_3; ~1600° if alkalies present.
6. Debond = FeO-Fe_2O_3 Cycling Failure if mineral-based; disregard if synth.

Measurement of Corrosion Resistance

Given one particular refractory in a given zone of a given vessel or system, conducting a particular process in the manner of one given shop, how long will that refractory actually last? How fast will it wear in that unique thermal and corrosive environment? This question was evaded in the preceding section because the only data available are comparative. Yet each process operator knows how long those linings last. And the refractory manufacturer knows. As to commercial refractories actually in use, retrospective field experience is catalogued assiduously by both user and maker. A number of remarks were made about refractory life in Chapter III, drawing on these wholly empirical sources in various applications.

In addition, descriptive technical information about actual corrosion and alteration patterns is available. Postmortem examinations of used refractories, including detailed chemical and phase analyses and section-by-section profiles, make it possible for the petrologist to reconstruct their last previous condition at temperature as well as some of the chemical progression leading up to it. It remains, then, only to (a) design and conduct accelerated exposures of refractory specimens to these same kinds of chemical environment, (b) find in their postmortems the same patterns of alteration, and (c) correlate the independent and dependent test variables numerically with the real service lifetimes and wear rates of known materials. In this fashion one may create a predictive tool.

All major manufacturers of refractory products have predictive and evaluational test programs of this sort. These tests vary from the simplest "indicative" types to others that are at least well-controlled and defined if not elegant. But on the whole their quantitative correlations with service life are extremely tenuous. On the whole this is because it is extremely difficult either to know or to reproduce in the laboratory all of the many interacting circumstances in which a refractory finds itself in the field.

Standard Tests. There are a few laboratory corrosion tests whose methods of conduct and interpretation have become standardized by agreement or consent among U.S. users and makers of refractories. In all cases they are comparative, either incorporating a chosen "standard" or "control" specimen among several in the same test or else calling for successive tests on "standard" specimens and on specimens of inquiry. Their output is limited to showing that "A" performs better than "B"; but only in the test.

For recourse to these standard procedures as well as to numerous other matters of accord in the U.S. refractories industry, the serious technologist must make frequent use of Reference 9, which is updated annually by a standing ASTM Committee on Refractories.

Here a brief tabular summary of nine important standardized corrosion test procedures will suffice. Their designations are:[9]

C768 *Drip Slag Testing of Refractory Brick at High Temperature*
C874 *Rotary Slag Testing of Refractory Materials*
C621 *Isothermal Corrosion Resistance ---- to Molten Glass*
C622 *Corrosion Resistance ---- to Molten Glass: Basin Furnace*
C987 *Alkali Vapor Attack on Refractories: Glass Furnace---*
C454 *Disintegration of Carbon Refractories by Alkali---*
C863 *Oxidation Resistance of SiC Refractories---*
C288 *Disintegration of Refractories in an Atmosphere of C0*
C704 *Abrasion Resistance of Refractory Materials---*

Only the number designations are given in the table following, but in the same sequence as listed above.

Test #	Type of Specimen	Test Temp.	Corrosive Agent	Type of Contact	Test Time	Post-Test Observations
C768	Brick, oxide or composite	Open (high)	Slag, liquid, selected	Contin. flow, fresh	Open	Recession or wear; penetration
C874	Brick, oxide or composite	Open (high)	Slag, liquid, selected	Contin. rotary, fresh	Open	Recession or wear; penetration
C621	Brick, oxidic	Open (high)	Glass, liquid, selected	Static, batch	Open	Recession or wear; penetration
C622	Brick, oxidic	Open (high)	Glass, liquid, selected	Static, batch	Fixed	Recession or wear; penetration
C987	Brick, oxidic	Fixed, 1370°C	NaOH, vapor, fixed p	Closed, contin. supply	Fixed	Recession, penetration, cracking, expansion
C454	Brick, carbon	Fixed, 955°C	KOH, vapor, fixed p	Closed, contin. supply	Fixed	Cracking, expansion
C863	Brick, silicon carbide	Open (high)	H_2O, vapor, fixed p	Closed, contin. supply	Fixed	Expansion
C288	Brick or monolith, oxidic	Fixed, 500°C	C0, gas, 1 atm. p	Contin. flow, fresh	Open	Cracking, expansion
C704	Brick or monolith, oxide or nonoxide	Fixed, 25°C	SiC grit, fixed size	Contin. jet, fixed flow	Fixed	Recession or wear

"Open" and "selected" in the table refer to temperature, time, and composition of corrosive agent, chosen in the laboratory to be meaningful relative to some refractory use. Once chosen, each parameter remains fixed in testing successive refractories. Other parameters are specified in each procedure. The post-test observations are simple and capable of numerical expression. But it is readily appreciated that the only numerical result which translates into refractory life in actual service is one obtained on a "control" specimen.

Use Tests. The one remaining recourse is to install a *test panel* of a new or developmental refractory in a vessel otherwise lined with its current "standard" material. Such a test is necessarily a *proof test*, whose probability of success has to be high based on all information already available, and whose consequential cost of failure is relatively small.

On the other hand, the user often has a considerable stake in such a test. The record over the years is that the processing industries have cooperated generously with refractory manufacturers whom they trust. New and improved refractories have come through such tests as these at unflagging rates in every major industrialized country; and their ability to resist corrosive hot processing fluids has not yet ceased to advance.

QUALIFICATIONS FOR WORKING REFRACTORY SERVICE

It is an oversimplification to suggest that thermal stability or integrity and corrosion resistance are the only qualifications for mating a refractory to a use. But these two are the most critical qualifications. For orderly presentation of the subject, let them suffice for now. Other properties that figure in the selection process will be flagged later. We are now in position to describe the insulating refractory product line in Chapter IX and to illustrate the uses of both working and insulating refractories in Chapter X, then to return to those remaining properties on which both selection and design depend.

Chapter IX

The Insulating Refractory Product Line

APPLICATIONS AND APPLICATION CRITERIA

Thermally insulating refractories function by providing stagnant or "dead" gas space, which is to say they contain large volume fractions of voids. Since it is impossible to build closed-cell structures into high-void-volume ceramics, these materials are all "open": susceptible to permeation and saturation by hot process liquids and to chemical attack by aggressive gases. It follows that they are not willingly exposed directly to liquids of any kind, nor to condensible vapors, nor to gases of more than minor chemical reactivity.

Ergo, corrosion resistance is downgraded as an index of merit. The prime criterion for material selection is refractoriness and dimensional stability sufficient for the assignment. The first property needed for insulating refractory qualification is accordingly the service temperature limit, which is related to composition, sintering temperature, and void volume.

The composition classes of Table VIII.1 turn out to be more than ample. Virtually all refractories in the insulating product line are oxidic, for the obvious reason that nonoxides are on the whole innately efficient conductors of heat. Relief from the necessity of resisting corrosion by liquids eliminates some of the more expensive oxidic types and their composites.

Insulating refractories are grouped at the bottom of Table VIII.2, under Porosity -- now expanded to mean void volume fraction. But Table VIII.2 does not address the microstructures of insulating materials nor the manufacturing methods employed specifically to

create them., Some further subclassifications are needed. To put those in perspective, let us first examine where and how insulating refractories are used.

Duplex Linings; Steady-State Usage

There are two reasons for interpolating an insulating layer between a hot working lining and the "outside." These are: (a) to cool the back face, e.g., to preserve the mechanical integrity of an enclosing metal shell or for reasons of safety outside a wall or roof; and (b) to reduce the heat flux J through the lining and hence improve process fuel economy. Both motives may apply at the same time, though the second usually predominates.

In the simple case of a plane wall at steady state, where a hot-face temperature T_h is fixed by a given operation, then:

$$J = \bar{k}_w (T_h - T_i)/Z_w = \bar{k}_i (T_i - T_b)/Z_i = \bar{k}_s (T_b - T_o)/Z_s = J_o.$$

This equation is set up for a working lining "w" of mean thermal conductivity $\bar{k}_w$ and thickness Z_w, an insulating lining "i" of (low) mean thermal conductivity $\bar{k}_i$ and thickness Z_i, and metal shell "s" of (high) mean thermal conductivity $\bar{k}_s$ and thickness Z_s. T_h is the (fixed) temperature of the working hot face; T_i is that of the interface between linings "w" and "i"; T_b is the refractory back face temperature or that of the interface between lining "i" and shell "s"; and T_o is that of the outside of the shell. J_o is the heat flux to the "outside," existing by virtue of water-cooling or forced or convective air-cooling of the shell.

The equation is solvable, given all k's, once T_o or J_o is fixed. This may be done by applying practical criteria to J_o with a known relation between this and T_o, or by arbitrarily limiting T_o itself (e.g., to ~100°C if water cooled, to 40°± if exposed to human contact, or to some safe limit for mechanical integrity of the metal). Ordinarily the shell thickness Z_s will be fixed by structural design considerations; and Z_w may be limited by considerations of working lining corrosion or its end-of-life minimum allowable thickness, for example. If a metal shell is absent, delete the third equality and replace T_b by T_o. If an insulating backup refractory is absent, delete the second equality and replace T_i by T_b. If both are absent, delete both of those equalities and replace T_i by T_o. The equation is thus versatile, and comparisons may be made with it among various lining options.

Computer programs for solving this steady-state type of equation are in common use. Depending on their sophistication, provisions may be made for: (a) inserting each k as f(T) instead of estimating a mean; (b) inserting additional functions for interface conductivity or temperature drop, where applicable; and (c) inserting appropriate relations between J_o and T_o for various modes of

outside cooling. Comparable equations are suited to cylindrical or spherical geometry.

For hand calculations, reasonable estimates can be made for the independent parameters. Perhaps the only one not self-evident is the connection between J_o and T_o for air cooling. A rough empirical curve for unimpeded convective cooling of vertical exterior surfaces by ambient air at about 77°F or 25°C, used for estimating purposes, is approximated by:

$$J_o \cong 0.00525\, T_o^2 + T_o - 108 \qquad (J_o \text{ in Btu/hr ft}^2 \text{ and } T_o \text{ in °F});$$

or, in convenient metric units:

$$J_o \cong 0.193\, T_o^2 + 27.25\, T_o - 802 \qquad (J_o \text{ in kJ/h·m}^2 \text{ and } T_o \text{ in °C}).$$

This rough guide applies to a refractory cold face up to some 600°F or 300°C. It should do about as well for the outside of a steel shell.

For a conservative example of what thermal insulation can do, suppose the hot zone of a tunnel kiln, firing pottery, averages 1000°C at the hot face. Assume its working refractory sidewalls and roof are 9" or 22.86 cm thick, exposed to the air outside, constructed of super-duty firebrick whose mean thermal conductivity is 9.5 Btu · in./ft^2 hr °F or 490. kJ · cm/m^2 hr °C. By entering these quantities into the above equations and solving simultaneously:

$$J = 490\,(1000\text{-}T_o)/22.86 \quad \text{and} \quad J_o = 0.193\, T_o^2 + 27.25\, T_o - 802\ ,$$

one obtains T_o = 236°C and the heat loss J = 16,380 kJ/m^2 hr. Now add only about 2" or 5 cm of lightweight insulation to the outside, using a mean thermal conductivity of about 0.6 Btu · in./ft^2 hr°F or 30 kJ·cm/m^{2}hr°C. What will be the new T_o and heat loss? One solves:

$$J = 490\,(1000 - T_i)/22.86 = 30\,(T_i - T_o)/5$$

simultaneous with the above air-cooling equation for J_o, obtaining T_i = 804°C, T_o =105°C and the heat loss J = 4,190 kJ/m^2 hr. The saving in lost heat at steady state is (16,380 - 4,190)/16,380 or very close to 75%. If the kiln hot zone dimensions are 80 ft. by 10 ft. wide by 12 ft. high (24.4 x 3. x 3.7 meters), the total heat-loss area is about 250 m^2 and the saving in lost heat is about 3 million kJ/hour or 73 million kJ per day, or 69 million Btu per day. That is worth about $120,000 a year in 1990 U.S. dollars.

In general, interpolating an insulating refractory layer or increasing its effectiveness: (a) increases T_i and decreases J at a

fixed value of T_o; or (b) Increases T_i and decreases Z_w and T_o at a fixed value of J. These effects on T_i, which is the cold-face temperature of the working lining, make that lining increasingly vulnerable to corrosion. Of the two effects on T_i recited here, the first is much the more pronounced. Where corrosion is already economically limiting, in fact, the use of an insulating backup lining may be contra-indicated. Examples are in the O_2-blown steelmaking furnaces and the lower parts of the ironmaking blast furnace.

For the same basic reason, insulation is never placed on the *outside* of a metal shell to decrease J_o unless the shell temperature is already quite low, and never without proving analytically that the metal will not be heated above its safe limit. These same equations serve also in that proof.

Thermal Conductivity, Void Volume, and Bulk Density

Armed with the above means of computing and a list of qualified insulating refractory materials and their properties, the system designer engages iteratively in an approach to both material selection and the determination of Z_w and Z_i. The *thermal conductivity* of the insulating layer becomes both a qualifying and a design property; but it is not much used for classification. Suffice it for now that values of k_i can be had from close to those of working refractories to nearly two orders of magnitude lower. This k depends on the *void volume fraction*, f_v.

The void volume fraction is related to measurable quantities from which two corresponding densities are obtained at room temperature. Every defined solid has a *theoretical density*, ρ_{th}, obtainable by x-ray diffraction for crystalline species or by weight and volume measurements for bulk glasses. The latter method is also used for multi-phase materials after their maximum consolidation by, e.g., fusion casting or hot pressing, etc. Sectioning and counting up of pore areas under the microscope can be used to improve this measured theoretical density.

Likewise, each insulating material comprised in part of such a defined solid and in part of void space has a *bulk density*, ρ_b, obtained by measuring its weight and its "bulk volume." Measurement of the bulk volume is not always easy. In concept if not in actual practice, this is obtainable by gently shrink-wrapping or enveloping a weighed quantity of material in an infinitely thin plastic film and then measuring the volume by water displacement in a graduated cylinder or pycnometer.

Though there are standard ASTM procedures for obtaining both of these densities,[9] the above conceptual definition avoids confusion. It is important for present purposes that the "bulk volume"

shall contain *all* of the void volume within a specimen, including the interstitial packing space in the case of unconsolidated granular materials.

With these two named densities in hand and denoting the void volume fraction by f_v, this quantity is:

$$f_v = 1 - \rho_b/\rho_{th} \ .$$

But in the classification of insulating refractories, this parameter f_v is rarely stated. Instead, the *bulk density* is used for classification. Although industry practices vary, it is uncommon in the U.S. for the theoretical density to be reported, or even for the phase composition of the material to be disclosed. On the other hand, the precise computation of k from f_v is all but futile anyway; k is measured empirically vs T and is reported for each commercial and research product. We shall deal with the measurement of k along with its numerical cataloguing in Chapter XI.

Working Configurations; Cyclic Usage

Dramatic improvements in processing economy have also been made by the use of insulating refractories in the *working* configuration -- that is, directly exposed to the process environment. A first requisite is that this environment must consist only of "clean" (i.e., relatively dust-free) gases. A second is that, since high-void-volume refractories are to a greater or lesser degree friable, the usage must entail correspondingly low mechanical wear. Numerous applications meet these two requisites, however. Some that exemplify *cyclic* process operation include the walls and roofs of batch driers, ovens, and heat-treatment furnaces, batch or periodic kilns, insulating lids or "hot tops" for metal casting, the upper portions of a limited number of metallurgical furnaces, some kiln furniture, and much hot-gas ducting. Air, moist air, and clean oxidizing or neutral combustion products are generally acceptable. Redox cycling of the atmosphere disqualifies some insulating refractories, and others may not tolerate the production of soot. Chemicals vaporized from the charge are usually somewhat harmful. These have to be evaluated individually depending on chemical identity, partial pressure or transfer rate, and specific rate of attack on the selected refractory. Dust, likewise, need not always be nil but calls for careful evaluation.

What is the peculiar virtue of low-density refractories in these cyclic situations?

It is intuitive after Chapter IV that the analysis of thermal transients entails use of the thermal diffusivity, $\delta = k/c\rho_b$, where c = specific heat in kJ/kg°C or J/g°C and ρ_b = bulk density as defined

in the preceding section. Since ρ_b in high-void-volume refractories ranges from low to very low, the product $c\rho_b$ runs correspondingly low while k does likewise, relative to these properties of dense refractories. Computerized mathematical methods of performance analysis using δ are widely practiced, but can not be demonstrated here. Instead, some approximations and manual calculations will be used to illustrate the economic benefits of insulating working linings when the temperature is cycled.

Consider a periodic shuttle kiln, again firing pottery at 1000°C. Each charge of ware plus kiln furniture consumes 20 million kJ in firing, and an additional 20 million kJ goes up the stack if it is not recovered. The entire cycle occupies 22 hours, leaving two hours per day for charging and discharging. The cycle consists of 12 hours heat-up plus 4 hours steady-state at 1000°C, plus 6 hours of slow cooling (burners off).

Assume 9" thick free-standing refractory walls and roof, using super-duty firebrick, as a basis of comparison. For an insulating refractory in place of the former, take a 9" thickness backed by sufficiently heavy gauge sheet steel as to permit hanging the lightweight lining from it. The sheet steel will be ignored to simplify the heat-flow calculations.

For this illustration, except for retaining the hour as the unit of time, it is convenient to work in SI units. The needed property data for each of these refractories are tabulated below. The wall thickness Z in each case is 0.2286 m.

	Thermal Cond. k, kJ·m/m²hr°C	**Bulk Density** ρ_b, kg/m³	**Specific Heat** c, kJ/kg°C
Firebrick	4.90	2,300.	0.70
Insulating Refractory	0.30	130.	0.70

The *steady-state* portion of the operating cycle is treated for heat loss precisely as in the previous section, first for the baseline firebrick case (B) and then for the insulating refractory case (I).

(B): $J = 4.9\ (1000-T_o)/0.2286 = J_o$ and $J_o = 0.193\ T_o^2 + 27.25T_o - 802$;
(I): $J = 0.3\ (1000-T_o)/0.2286 = J_o$ and $J_o = 0.193\ T_o^2 + 27.25T_o - 802$;

Case (B) is the same as before: T_o = 236°C and J = 16,380 kJ/m²hr.
Case (I) works out as follows: T_o = 54°C and J = 1,240 kJ/m²hr.

Let this kiln be 6m by 6m by 4m in dimensions, giving a total area of sidewalls and roof of 130m². In the 4 hours of steady-state operation at 1000°C, the total heat losses to the outside are respectively:

(B) $130 \cdot 4 \cdot 16{,}380 = 8.5 \cdot 10^6$ kJ and (I) $130 \cdot 4 \cdot 1{,}240 = 0.65 \cdot 10^6$ kJ.

The *transient* (heating) portion of the cycle can be approached by an estimating device, lacking a precise analytical method. For typing convenience, we substitute Q for *J*:

$$\int_{t_1}^{t_2} Q\,dt = \int_{t_1}^{t_2} Q_{tr}\,dt + \int_{t_1}^{t_2} Q_{abs}\,dt \qquad (t = \text{time}).$$

Here it is recognized that, in a heating transient, one differential portion of the incident energy is transmitted (tr) through the refractory wall by virtue of a temperature gradient while another portion is absorbed (abs) in raising the temperature of the refractory itself. By first integrating these interactive functions over the total time of the transient (viz., t_2-t_1), we can do some useful estimating. Let us take the *absorbed* portion first, for the initial heating ramp of the periodic kiln operation. We disregard the final cooling ramp.

The reader is invited to review Figure IV-8a for visualization of the time- and z-dependent transient phenomena, bounded by an initial and a final steady-state condition. Here in the shuttle kiln, the initial condition of the refractory wall is nearly isothermal at, say, 40°C. We assume that the final steady-state condition is arrived at by the end of the 12-hour heating period, not at $t \rightarrow \infty$. We have just solved for that latter condition, above, under the *steady-state* portion of the cycle. Referring to the heating transient, then:

Case (B): Final T_h = 1000°C, final T_o = 236°C, final mean $\overline{T}_2$ = 618°C; initial mean $\overline{T}_1$ = 40°C; $\Delta\overline{T}$(mean) = 578°C. The volume of refractory of 1 m^2 hot-face area by 0.2286 m thick is 0.2286 m^3. Its density ρ_b is tabulated above as 2300 kg/m^3, and its mean specific heat c likewise as 0.70 kJ/kg°C. The heat absorbed is thus (again using Q for *J*:):

$$\int_0^{12} Q_{abs}\,dt = 0.2286 m^3 \cdot 2300\ kg/m^3 \cdot 0.70\ kJ/kg°C \cdot 578°C$$

$$= 212,730\ kJ/m^2.$$

Case (I): Final T_h = 1000°C, final T_o = 54°C, mean $\overline{T}_2$ = 527°C; initial mean $\overline{T}_1$ = 40°C; $\Delta\overline{T}$ (mean) = 487 °C. Volume of insulating refractory = 0.2286 m^3; ρ_b = 130 kg/m^3; c = 0.70 kJ/kg°C. The heat absorbed is thus:

$$\int_0^{12} Q_{abs}\,dt = 0.2286\ m^3 \cdot 130\ kg/m^3 \cdot 0.70\ kJ/kg℃ \cdot 487℃$$
$$= 10{,}130\ kJ/m^3\ .$$

Again using 130 m^2 as the total sidewall and roof area of this kiln, the total energy required to heat up the refractory is:

(B) $130 \cdot 212{,}730 = 27.6 \cdot 10^6$ kJ and (I) $130 \cdot 10{,}130 \cdot 1.32 \cdot 10^6$ kJ.

The *transmitted* portion of the incident heat flux over a 12-hour heating period is not inconsiderable. It is difficult to estimate. A very rough integrated approach is made by consulting the spirit of Figure IV-8a: averaging about one-third of the 1000°C steady-state rate in case (B), and about one-fourth of that rate in case (I). The estimated heat losses over 130 m^2 wall area and 12 hours time are accordingly:

(B) $(1/3) \cdot 130 \cdot 12 \cdot 16{,}380 = 8.5 \cdot 10^6$ kJ;
(I) $(1/4) \cdot 130 \cdot 12 \cdot 1{,}240 = 0.48 \cdot 10^6$ kJ.

The overall estimated heat consumption in a complete cycle in this kiln in cases (B) and (I) is summarized below:

Total Heat, 10^6kJ:	**9" Dense Firebrick**	**9" Insulating Refractory**
Heating/sintering the ware:	20.	20.
Lost up the stack (no regen.):	20.	20.
Lost in heating the refractory:	27.6	1.32
Lost through walls in heat-up:	8.5	0.48
Lost through walls at steady state:	8.5	0.65
Total heat consumed/cycle:	84.6	42.5
Process energy efficiency:	23.5%	47.%

The magnitudes of these numbers are such that errors of estimation cannot appreciably bias the message at the bottom line -- which in fact has been confirmed over and over again by field experience.[10] The largest single improvement made by the insulating refractory is in the third line, namely resulting from reduction in the *thermal mass* of the kiln lining. This relates directly and exclusively to its *bulk density*, since the specific heat is not discriminating. In the above examples we have used data for one of the group of *low-mass*

or *fiber* refractories which have drastically changed clean vessel lining practices over the past several decades.

A further benefit arises from this low lining mass and its correspondingly low thermal conductivity. In the periodic kiln of the above example we have assumed that both the heating and cooling ramps of the process cycle were established by the ability of the charge to withstand rapid transients. Where this is not so, low-mass refractories facilitate greatly increased rates of vessel heating and cooling because they constitute a much-reduced heat sink. Furthermore, as Figures IV-8a and b imply, the hot face itself tracks changes in the vessel interior temperature far more quickly than does that of dense refractories. Shortening of the cycle time results, and this translates directly into increased product throughput rates. Personnel can enter an insulated vessel far sooner after it is opened to the air without discomfort or risk of injury, and this translates directly into increased vessel on-line time.

Other Insulating Uses

Though fiber refractories perform exceptionally well in cyclic service,[312-317] other insulating types see useful kiln applications as well.[318] There are also other uses for insulating refractories besides those emphasized in the preceding sections. One important group, including seals for charging doors and expansion joints as well as gaskets and caulking, calls for some degree of elastic compressibility. A contrasting group of uses, mainly for "throwaway" loose fill on floors, provides both insulation and the ability to absorb spills or other reasonable amounts of process liquid waste. Still another group of applications is comprised of linings and forms used as metal-casting molds in ferrous and nonferrous metal foundries. Many other miscellaneous uses will be found in the field and in product literature.

Permeable Diffusers and Filters

A separate category of porous refractories, identified at the bottom of Table VIII.2, is the "permeable" group. Some of their uses were referenced in the text accompanying that table; another common use is as filters for molten metals. Such permeable materials are acknowledged here, inasmuch as they are microstructurally akin to insulating refractories. Since their use brings them into contact with hot process liquids, however, resistance to corrosion has to be reinstated among the service criteria. Thus the nonoxides become candidates for these uses, as well as oxidic compositions of high corrosion resistance which might be too expensive for insulation. In other respects this group of permeable materials is reasonably encompassed in the framework of this chapter.

CLASSIFICATION OF INSULATING REFRACTORIES

In the course of describing typical insulating practices, it has been noted that the service temperature limit or STL and the bulk density or ρ_b are properties by which thermally insulating refractories are classified. To say much further about those properties requires, first, some classification by other features.

Classifications by Microstructure and Form

Cellular Type. The opposite classification to fiber refractories is called *cellular*. This term starts out meaning the same as "porous." But with increasing void volume fraction, the same solid begins to take on the microstructural characteristics of a foam. The term *cellular* is intended to encompass this entire continuum.

Cellular refractories were established in the insulating product line long before the advent of modern refractory fibers. Insulating firebrick or "IFB" dates back well into the 19th century, and some of its historical predecessors go back centuries before (Table I.1). Modern cellular refractories are made using, either singly or in combination, *expanded aggregate* and an *expanded matrix*.

Expanded aggregate has several natural prototypes, of which vermiculite is one. This layered claylike mineral is expanded by flash heating or by water impregnation under hydrothermal (high-p, high-T) conditions and then letting the external pressure down suddenly. Perlite is another, naturally-expanded mineral.[319,320] Diatomite or kieselguhr is a natural low-density silica of marine origin; and natural foamed silica is of volcanic steam-expanded origin.

Steam-expansion by flash heating of highly hydroxylated compounds or their aqueous pastes is the most common synthetic process, by which low-density grain of almost any chemical composition can be made ranging from clays to silica to alumina and zirconia and their silicates. The usual technique is to spray very coarse slurry droplets into a hot air stream, either in the Spray Drier configuration of Chapter III or in the configuration of an elongate "flash drier" tube using entrained co-current flow. A further feasible synthetic method is the granulation by drying of a mud containing a particulate "burnout" additive, the latter subsequently removed by combustion in a calciner.[321] The porous grains so made are then lightly sintered, for example in rotary equipment, without appreciably collapsing their porosity. Coarse and nearly monosize grain provides for relatively open packing.[322,323]

Expanded matrix techniques include the same "burnout" method as above, most often using sawdust or other cheap cellulosic particles of somewhat controlled size. This method is common in making bricks. The other common technique is foaming, ordinarily aided by foam-stabilizing and/or gelling or setting agents.[324] Foaming may be accomplished by (a) frothing, i.e., whipping of air into the mix, using familiar beater or whisk techniques; or (b) use of a chemical gas-forming or "blowing" agent. Such agents include, e.g., aluminum powder in an acidified mix, liberating H_2,[325] and various combinations of organics or inorganics which react to generate CO_2 much like the familiar leavening agents of the bakery.[324-327]

Immediately after frothing, or before chemical foaming, the usual slurry is poured into a mold or box. Formulations are cleverly contrived to set up or solidify quickly after expansion; they are dried, calcined and/or sintered. They may be trimmed to size at any stage. This is in contrast to "burnout" mixes, which are commonly extruded and cut into bricks or may even be pressed; or can also be cast into special shapes. Burnout creates void spaces after both forming and some degree of subsequent thermal treatment, when the material is no longer appreciably plastic.

The "bloating clays" mentioned in Chapter IV in connection with ladle linings are of the expanded-matrix type. They contain natural organics from decayed vegetable matter (i.e., humus), which are further chemically decomposed on heating to yield gaseous H_20 and CO_2. Depending on atmospheric conditions, these organics may produce a porous char or else ultimately burn out; but in any event they function as blowing agents at temperatures considerably above ambient. Efforts to reproduce their function using foam-forming synthetic additives have been technically quite successful.[325-327]

The purposes of expanding grain or aggregate and of expanding a refractory matrix are essentially the same. The two differ mainly in the stage of processing at which each is carried out, different techniques being more or less convenient at one stage or the other. The highest void fractions practically achieved in commercial cellular refractories are up to the order of 0.85, or 85 vol.-%. The solid structure consists of ligaments or thin walls, largely perforated or fractured by internal gas pressurization and subsequent firing shrinkage. Hence these materials, although rigid when fired, are relatively weak and friable. They range in resistance to thermal shock from comparable to their dense counterparts at comparable density to shock-resistant at high void fractions. This latter resistance results not from any immunity to cracking, but from the isolation of small cracks from one another by empty space and the flexibility or compliance of the remaining thin ligaments.[35] Between medium and high void fractions there is a gradual transition from brittle fracture (e.g., spalling) to disconnected or isolated local tearing.

Formed and *unformed* categories apply to cellular refractories. As there is no point in installing the latter at maximum density, the majority of insulating monolithics are *castable* (or vibratory-castable), or *trowellable* plastics, phosphate or cement-bonded.[319,324,328] Cold (wet) *gunning* mixes are also made, for application in the manner of lightweight gunite concrete.

The last cellular refractory form in considerable use is *loose fill.* This employs expanded grain in the more demanding applications. For prosaic usage such as on floors, it is not unusual to see whatever crushed or granular mineral happens to be in the neighborhood, calcined enough to rid it of volatiles. The technical granular materials, on the other hand, are as carefully prepared, sized, and installed to specifications as are their consolidated counterparts. They also run up to very refractory compositions, of which "bubble alumina" is one of the longest-standing examples. "Bubble" mullite and ZrO_2 are also made.[329] Being near-monosized, loose fill gains insulating value from its approximately 30 vol.-% interstitial packing space between granules, in addition to the porosity of the grains themselves.

Fiber Type. If the cellular refractory concept is the introduction of quasi-discontinuous gas spaces into a solid continuum, the *fiber refractory* concept is the introduction of a quasi-discontinuous solid into a gaseous continuum. In the great majority of cases, molten silicates are spun or blown into long fibers in the vitreous state, a condition then preserved by rapid undercooling of the viscous liquid. This is precisely the method by which fiberglass is made, and fiberglass is the prototypical fiber refractory.

The raw materials so fiberized were first ordinary clays, then natural kaolins, then still higher-alumina mineral mixes, culminating in selected mixes of minerals and synthetics and finally in a few synthetic silicate mixtures.[313,314] Over this progression the softening point and devitrification temperature of the products increased, as did the melting and fiberizing temperature and the accompanying difficulty of manufacture.

In addition to vitreous fibers, a few cryptocrystalline fibers are made. Most notable are alumina[330,331] and zirconia,[332,333] the latter usually cubic-stabilized. One clever manufacturing method consists of impregnating a synthetic porous polymer filament with, say, aqueous aluminum or zirconium hydroxychloride; then carefully drying and heating, finally burning out the organic and crystallizing the oxide. These ceramic fibers are extremely fine, running between about 3 and 6 μm in diameter. The crystal size is of the order of a few tenths of one micrometer.

Fiber compositions in use at this writing include these expensive crystalline oxides[330-333] as well as mechanical mixtures of

crystalline and vitreous fibers;[334] and vitreous alumina-silica compositions ranging from about 70% Al_2O_3 down. Some alumina-chromia-silica vitreous fibers are also made.[335,336] Much of the "zirconia" fiber insulation made is actually A-Z-S, but genuine cubic ZrO_2 ($+Y_2O_3$) is a prominent product[332,333] and is the most refractory of all of the above.

Numerous inorganic spray-coating slurries have also been developed. These are used not only to bond fibers together as will be described next, but also to increase their resistance to gas-phase chemical attack. Thus by virtue of either fiber composition or coating, earlier restrictions of use to benign chemical environments have been considerably relieved.[313,314,330-337] For insulating fiber products used in the working refractory mode, this has been a signally important advance.

The typical immediate product of fiberization is a loose or open but tangled mass of interpenetrating filaments. This mass is compacted somewhat, yielding a "wool." This unbonded form is widely familiar by that name in fiberglass. Still further mechanically compacted, usually sprayed with a resin or with an inorganic binder as mentioned above,[338] the material becomes a bonded "felt": easily handled yet flexible and elastic. Some felts are "needled" to increase the density of tangles without bonding. Whether backed on one side with flexible sheet or foil, or not, products ranging from wool to felt are sold as *batting* and *blanket* or molded blanket, or as gasketing strips cut from the latter.

Completing the progress of densifying, thick layers of wool are rolled out, binder-sprayed, and then vacuum-pressed between large platens to make rigidly-bonded *board*. This, cut into convenient modular sizes, becomes *tile* (or, if thick enough, even bricks). Board and tile may be faced on one or both sides, or not. Spray-coating with a refractory slurry has been developed to seal the hot face. Vacuum forming has now been extended to the making of all manner of intricate and hollow yet rigid shapes such as for catalytic burners, electric heating-element embedment, cylindrical coil liners, metal hanger insulation, and custom molded components of all kinds.

An ingenious form of flexible fiber insulation for working linings is made by accordion-folding a strip of woolly material into an "N" or "M" configuration, for example, and binding the folded module tightly together (in the horizontal direction as "N" and "M" are printed here). The resulting *compressed module* may be 1 ft. by 1 ft. by 9 in. or any other convenient set of dimensions. It is installed on a wall in the following orientation:

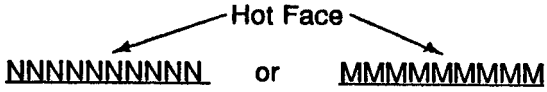

Then the bindings are cut and every module relaxes elastically against its neighbors, giving a uniform fiber density across the entire wall. The joints virtually disappear. Methods of quick installation and support are equally ingenious.

To round out the roster of most common forms, fibers are combed out as parallel bundles or yarn. These strands in turn may be either twisted together or braided into rope, or woven or knitted into fabric. Rope is widely used for gasketing and for sealing and caulking of joints. Ceramic textiles have a host of special technical uses which can justify their high price. Cut fibers are used in *gunning* mixes.[338,339]

In any of the vitreous fiber forms, it is not uncommon to find a quantity of what is called "shot." The glass which flies out from the nozzle or disc in fiberizing is in the form of tiny beads, each one trailing a fiber or filament behind it. "Shot" is the residue of these beads which were not culled out of the wool. In most applications shot does no harm beyond raising the bulk density; but it may be considered a quality defect, and products containing a low shot count are usually represented as superior.

A curious feature of fiber insulating refractories is worth noting. Wool materials are capable of being made at vanishingly low bulk densities, with void fractions up to as high as 0.98 or 0.99. But with so little solid in the way, there is almost no impedance to convection and radiation which are important components of heat transport through the gas space. There is in fact a bulk density below which the thermal conductivity of these materials increases with decreasing ρ_b. That fact restores a competitiveness to cellular refractories.

Service Temperature • Limit

The term *service temperature limit*, or *STL*, is used in this chapter in conformance with industry practice for insulating refractories. This is in contrast to the "maximum service temperature" or MST devised in Chapter VIII in the absence of uniform practice for dense working refractories. The definitions of MST and STL differ.

In the present instance, a permanent linear shrinkage of each material commences at some temperature and increases with increasing T above that limit. The contributions to this shrinkage are

several, aggravated by the large empty volume existing in insulating products. All the formed cellular materials are distinctly under-sintered. The progression of cement bonding is incomplete, as-made, whether in formed or unformed cellular refractories. Re-heating continues those unfinished processes. In fiber products, viscous relaxation starts at some softening temperature; and devitrification may occur, depending on the composition of the metastable glass.[316,335,336,340-343] Cryptocrystalline fibers are subject to thermal recrystallization and crystal growth.

The makers and users of insulating refractories in the U.S. have agreed on some maximum allowable reheat shrinkages and their measurement methods, as definitions of *service temperature limits*. These small allowables and certain arbitrary and discrete STL values have been established as standards in ASTM classification no. C155[9] for cellular insulating firebrick and classification no. C401[9] for cellular insulating aluminous or alumina-silica castables. Simultaneous maximum limits are placed on the bulk density in the classifications cited.

This is not to say that other STL values or combinations of STL and bulk density may not be achieved and marketed. Today there are numerous materials that exceed the standards. For illustration presently, we shall be largely content with the existing ASTM classifications for cellular materials insofar as the STL is concerned.

Fiber refractories are classified in similar fashion, voluntarily, by their makers. Early linear shrinkages amounting variously to about 2-5% may be anticipated in service at the recommended STL, and must be provided for in the manner of installation of rigid forms. The range of STL for fibers exceeds that for cellular refractories, starting lower and ending at least as high, namely well above 3400°F or 1870°C. Service temperature is of course a continuous variable; discrete "standard" values are for industry convenience.

Bulk Density

Cellular Products. The *bulk density*, ρ_b or *B.D.*, is also a continuous variable, at the will of the manufacturer. It is uncoupled from the STL at least to the degree that the chemical composition might be chosen arbitrarily. Note for example that the theoretical density of zircon is about 4.7 g/cm^3 or 294. lb/ft^3 (abbreviated "pcf"), while that of mullite is about 3.2 g/cm^3 or 200. pcf, and that of high-duty firebrick is about 2.56 g/cm^3 or 160 pcf. If "standard" cellular insulating bricks are made of each of these materials at a fixed bulk density of 0.96 g/cm^3 or 60 pcf, the following will be their approximate ideal respective properties. The B.D. and the STL here do not correlate:

Property	Zircon	Mullite	Firebrick
Bulk Density, pcf	60.	60.	60.
STL, °F	3300-3400	3000-3100	2800
°C	1800-1870	1650-1700	1540
Void Volume Fraction, f_v	0.80	0.70	0.62
Thermal Conductivity, kJ·cm/m^{2}hr°C	60.	100.	140.

The positive correlation between B.D. and STL that occurs in ASTM classifications nos. C155 and C401[9] presumes that the compositions of these cellular refractories are objects of industry-wide normalization -- which they may well be in fact, since price competition is intense. If the composition is the same, then the B.D. and the STL will vary together. But the above table indicates that, at a premium price, much more flexible combinations of STL and B.D. can be had than are illustrated by either ASTM standards or current industry "typicals": namely, by changing the refractory composition. Some further latitude in the B.D. arises from the method and skill employed in expanding the grain or matrix or both.

The bulk density of a cellular product can be made as close as desired to that of the dense working refractory grade, by controlling the porosity. The highest B.D. acknowledged by ASTM for insulating firebrick is 1.52 g/cm^3 or 95 pcf, corresponding to an STL of 3200°F or 1760°C. The maximum allowable B.D. values then step down, with the STL, to 0.54 g/cm^3 or 34 pcf at an STL of 1600°F or 870°C. This range of bulk densities, all of essentially the same clay-based materials, corresponds to a range of void volume fractions from about 0.40 to about 0.80 The current typical commercial products run on average about 10 pcf lower in B.D., step by step, for a corresponding range of f_v from about 0.47 to 0.85. These products are considerably better thermal insulators than is required by the ASTM classifications, each at its standard STL rating.

The same is true for the aluminous castables, though data on current commercial products are more scarce. Bulk density limits given by ASTM[9] range from 105 pcf at STL=3200°F, stepwise down to 55 pcf at STL=1700°F or 925°C. The corresponding range of f_v is from about 0.58 to about 0.78. Limited data on commercial insulating castables indicate on average (with wide scatter) about 15 pcf lower B.D., step by step. Were the average to hold, the corresponding range of f_v is from about 0.64 to about 0.84. The commercial castables not only surpass the classification standards; toward the upper end of the STL range they are significantly better thermal insulators than are the equal STL-rated firebrick. They should be. They cost more.

Above an STL of about 3200°F, high-alumina and stabilized zirconia are used, plus ZrO_2-Al_2O_3 mixtures in which the zirconia often is not stabilized or only partially so. In this last-named type, the monoclinic-tetragonal transition of ZrO_2 is made use of to create a dense population of microcracks for the sake of toughness and thermal shock resistance.[35,36,52] Owing to the very high temperatures at which these compositions serve, they are not made so porous or lightweight as are the IFB and alumina-silica types. There are at present no ASTM standards for their B.D., as these materials are off-scale of the existing STL classifications. Porous zirconia can serve up to about 3500°F or 1925°C.

Fiber Products. Discrete STL values for commercial fiber products reflect STL selections made by the industry to meet various market or user needs. They reflect compositions selected accordingly. The bulk density is all but completely uncoupled from the STL, since for any fiber composition there is an immense range of possible degrees of compaction from wool to felt to vacuum-formed board.[344] Likewise, then, any discrete values of the B.D. represent industry selections of convenience or marketability. The following ranges of B.D. are thus only typical of current practice, and are not limiting except perhaps at the lowest values.

Mineral-wool blanket and modular materials (and on up to high-Al_2O_3 compositions) can be had at bulk densities as low as about 3 lb/ft.^{3} (pcf), or 0.048 g/cm^3. Some discrete B.D. values on the market are 3, 4, 6, 8, 10, and 12 pcf. Rigid board starts at about 12 pcf or 0.19 g/cm^3, some of the discrete B.D. values being about 12, 15, 20, 30 and 45 pcf or up to 0.7 g/cm^3. There are also some alumina-fiber/cellular-alumina composites, running of the order of 90 to over 130 pcf or 1.4 to >2.1 g/cm^3.

At the present time, the principal zirconia fiber products are rigid board. Typical B.D. values run about 30, 60, and 70 pcf or 0.48 to 1.12 g/cm^3. Zirconia ceramic textiles, with STL values up to over 4500°F or 2500°C, are on the market at bulk densities as low as 15 pcf and as high as 63 pcf or 1.0 g/cm^3.

The overall fiber refractory product line, accordingly, quite overlaps the cellular in bulk density and in void volume fraction but also holds a domain of its own. Bulk densities below the order of 25 pcf or 0.4 g/cm^3, corresponding to void fractions from about 0.85 to about 0.98-0.99, are at this time the unique province of fiber products. For the most part the products in this range are of the vitreous fiber type and hence relatively inexpensive. These are the main candidates for large-scale, low-mass linings of vessels in cyclic operation. The highest STL among these runs, at present, up to about 3200°F or about 1760°C.

Classification Summary

Table IX.1 summarizes the classification scheme developed for thermally insulating refractories. The upper part of the table should serve as an adequate framework for both current and future products. The lower part, as has been discussed, conforms to current ASTM classifications and current industrial practice in the U.S. with respect to the service temperature limit and bulk density. Corresponding classifications elsewhere on the international scene reflect comparable properties for comparable compositions. Those property classifications, however, are too rigid to accept easily those future product improvements that assuredly will come.

The lower table must therefore eventually be changed. The service temperature limit is so important that it will probably be retained as a qualification; but it might profitably be divorced from any particular refractory composition, type, form, or density. The bulk density, on the other hand, could well be relegated to the category of a design property -- just like the thermal conductivity (Chapter XI), which is equally a *sine qua non* for engineering calculations. Whatever path may be taken, it seems certain that for classification purposes the lower part of Table IX.1 will not last much longer in its present form.

PHYSICAL FORM AND INSTALLATION OF LININGS

The system designer usually has several options for the installation of insulating refractories in vessel walls. Granted a preference for low k in steady-state situations and for low ρ_b in cyclic situations, the convenience and economics of installation have to be considered as well in various geometries or when comparing retrofits with original lining construction. The options available can be laid out in various geometries as follows.

Duplex Linings: Backup Insulation

Steel-Enclosed. *Insulating brick* in original construction of a vertical wall goes up first against the steel, then the working lining of either brick or monolithic is installed against it. Support of the latter is good. For thinner layers in straight runs, *insulating board* can be installed in the same sequence but is not supportive of the working lining. *Gunned* insulation can be applied to the steel and the working lining then overlaid.

Table IX.1 Classifications of Insulating Refractories

CHEMICAL COMPOSITION (see Table VIII.1)

Al_2O_3-SiO_2	High-Al_2O_3	A-Z-S
Al_2O_3-Cr_2O_3-SiO_2	Al_2O_3-ZrO_2	ZrO_2 (stab.)

CELLULAR TYPE	FIBER TYPE
Expanded Grain	Vitreous
Expanded Matrix	Cryptocrystalline
Formed	**Rigid**
BRICK, BLOCK, TILE	BOARD, TILE
Unformed	**Flexible**
CASTABLE	WOOL, BATTING
VIBRATORY-CASTABLE	MODULAR (Folded)
TROWELLABLE	BLANKET, FELT
GUNNED (wet)	ROPE
LOOSE FILL	TEXTILE
Void Volume Fraction	**Void Volume Fraction**
0.3 to 0.85	0.5 to 0.99

SERVICE TEMPERATURE LIMIT, STL, AND BULK DENSITY, B.D. (USA)

		INSULATING FIREBRICK	ALUMINOUS CASTABLES	LOW-MASS FIBER PRODUCTS
STL, °C	STL, °F	B.D., pcf	B.D., pcf	B.D., pcf
1925	3500	--	[ZrO_2 and	[ZrO_2: 30-70]
1870	3400	--	Al_2O_3: var.]	[Z, A: var.]
1815	3300	ASTM[9]	ASTM[9]	[Al_2O_3: to 45]
1760	3200	95.	105.	Al_2O_3-SiO_2
1705	3100			
1650	3000	68.	105.	
1595	2900		105.	
1540	2800	60.		
1480	2700		95.	
1425	2600	54.		
1370	2500		95.	
1315	2400			
1260	2300	48.	90.	
1205	2200			
1150	2100		75.	
1095	2000	40.		
1040	1900		65.	
980	1800			
925	1700		55.	
870	1600	34.		

Typ. commercial products avg. ~10 pcf below ASTM standards.

Typ. commercial products avg. ~15 pcf below ASTM standards.

No ASTM classifications.

Wool, Blanket, and Felt products typ. ~3-12 pcf.

Board products ~12-45 pcf.

NOTE: B.D. in g/cm^3 = 0.016 x B.D. in pcf.

When the working lining is erected first with a gap between it and the steel, *insulating castable* fills the gap, mates well to the working lining, and gives good support. *Vibratory castable* is an option. For higher insulating values but with variable remaining air gaps, the space may be filled with *board, blanket,* or *batting. Loose fill* in this situation tends to load the working lining laterally, and especially in straight runs is limited to heights of a few feet (~1 to ~2 meters) depending on the working lining strength.

In ladle and small furnace linings, *insulating brick* is most rigid and is continued over the bottom and roof as well as the sidewalls.

Unenclosed. Outside a vertical working refractory brick wall, *insulating brick* may be laid up but *gunned* insulation is fastest. *Trowelled* or *castable* insulation also goes up faster than brick, the castable requiring forms for pouring. *Board* and *blanket* are good for retrofit and in confined spaces.

Over an existing roof, all these same options can apply but the added vertical loading may be adverse in retrofit. Given sidewalls extending above the roof, *loose fill* is a further occasional option. Outdoors in the weather, all insulating roofs need protection. The same is often true of sidewalls.

Hearths of large furnaces are not often insulated due to the weight of the charge; but if so they use *insulating brick* or *castable* for rigidity and crushing strength.

Working Configuration: Direct Exposure

Vertical Walls. Load-bearing walls generally call for *insulating brick,* though reinforced *castable* can be used (requiring forms for pouring). Supported or encased walls can be *castable* or *trowelled* (e.g., as reactor linings), but lighter-weight types such as *gunned, modular, board, tile,* or even *blanket* are often more advantageous and go up more quickly. The fiber types are capable of performing better thermally; of these, modular (i.e., folded) is best for cyclic high-temperature use over large dimensions. *Insulating brick* and *board* are well suited to small kilns.

Roofs. Self-supporting arches or domes are best made of insulating brick, which is also well adapted to small kiln construction -- in all cases, laterally constrained. Supported and suspended roofs have the same options and considerations as for vertical walls, above.

Flooring. Areas taking any appreciable traffic are advantageously laid of *insulating brick,* preferably hot-face-glazed.

Brick is also convenient for small kilns, though *board* also works there in the absence of mechanical abuse. Large floor areas are quickly lined with *castable*, which is also relatively wear-resistant; *trowelled* floors are also an option. Flooring not subject to wear is effectively *gunned*. Concrete or hard refractory flooring is sometimes covered with "throwaway" *loose fill*. Other soft insulation such as modular or blanket is rarely practical on floors; and hearths are best lined with dense working refractories over an insulating backup.

Support and Reinforcement

To hold insulating refractories in place in the *working configuration*, a host of supporting devices have been contrived and more are continuing to appear. The engineer faced with decision-making is well advised to consult vendors for the spectrum available but to withhold commitment until other users have been consulted for their experience. The superficial enumeration below touches only the highlights.

Cellular monolithics, like dense monolithics, have been historically installed against steel over an open hexagonal or expanded metal grid which is welded to the shell. More recently, much more sparse arrays of deformed metal anchors have replaced metal mesh; each of these anchors is, e.g., a small "vee" or butterfly, etc., in shape and is welded to the shell. Over very small expanses, a forest of welded-on stainless steel wire bristles has been used. Some insulating bricks have borne a central hole, through which a rivet is created by welding once the brick is in place against the shell.

Such a rivet as the above is exposed at the hot face. So are many other metal studs and anchors, as well as hangers for suspended roofs. The more deformable the refractory layer, the wider the exposed flange must be which holds it in place. Stainless steel and superalloys are used accordingly; but their hot-face corrosion has been a challenge. Such fixtures are now often dense-refractory-clad and -tipped. Entire hangers made of dense refractory or ceramic have long been in use; mass-produced like electrical insulators, they are not unduly expensive. Originally devised to hang dense refractories, they manage light-weight forms readily enough. They come in various clever shapes.

Embedded fixtures also abound. Clips or stiffeners or aligning hardware may be threaded into folded fiber modules from the side before assembly, for example, then interlocked or snapped onto hidden anchors when each module is put in place. Thick tiles may be mortised in shape and their assembly indexed by hidden metal dowels, so that only one of several tiles need be anchored. The fiber refractory forms lend themselves to hidden anchoring, owing to their toughness.

The spacing of anchors must of course be carefully coordinated with the stiffness and strength of each insulating refractory material. Other than the loss of anchors by corrosion, this matter of spacing is a most critical element of design. Too many anchors waste assembly time and money. Too few risk distortion, sagging, parting or fracture of the refractory, especially after some time at temperature. "Just right" equals an installation that remains functional and workmanlike for many years. The criteria may be computed from physical properties, but in large measure are confirmed by test panels or by long experience.

Note Added in Press. There are some present suspicions of an inhalation health hazard of some refractory fibers. It seems too early to evaluate this hazard here, as information is coming in rapidly. If it exists, (a) the hazard will pertain to manufacture, handling, and disposal of fiber products; but (b) it will be controllable by well-known engineering and administrative procedures. Industry association and public health service authorities should be consulted by the interested reader.

Chapter X

Refractory Practice

REFRACTORY QUALIFICATIONS IN REVIEW

This chapter will lay out a framework for application of the refractories of Chapters VIII and IX in the vessels of Chapter III. Each processing system described there, and each zone within, presents its refractory linings with a set of functional and survival *demands*. Each process operator presents a set of *expectations* of refractory integrity and lifetime. Refractory selections made to satisfy these sets are hardly all alike; but they do fall into groups or patterns of appropriateness. Chapters VIII and IX have dealt with refractories by type. The patterns of appropriateness in each application are also recognizable by type. Our aim here is to present those patterns as founded in material behavior.

Chapters IV-IX have emphasized the most important material *qualifying* characteristics for refractory application. Qualifying characteristics for a given service are those qualities that provide or prolong the integrity of a refractory in the service environment. Since a given environment may challenge that integrity by any of thermal, chemical, and mechanical phenomena, the essential qualifications for service are accordingly thermal, chemical, and mechanical.

Thermal Qualifications

The principles underlying *refractoriness* and *microstructural and dimensional integrity* in changing thermal environments are presented in Chapter IV. Consolidation in terms of estimated Maximum Service Temperature and Thermal Stress Resistance of

working refractory classifications is given under those headings in Chapter VIII and in Figure VIII-3 and Table VIII.3. The Permanent Deformation of working refractories on heating is discussed under that heading in Chapter IV. For insulating materials the Service Temperature Limit is given in Chapter IX and Table IX.1. Fiber insulation is highly resistant to thermal stress. Resistant cellular insulating materials are found in the unfired monolithics and the lowest-density formed products.

Chemical Qualifications

Refractory corrosion phenomena and the principles underlying *corrosion resistance* are discussed in Chapters V-VII. An assessment of the Corrosion Resistance of working refractories by major classification is summarized under that heading in Chapter VIII and in Tables VIII.4 and VIII.5. Corrosion resistance as a qualification for service of insulating refractories is placed under some significant limitations in Chapter IX.

Refractory durability is a matter of both phase composition and microstructure. The microstructural and bonding criteria for maximum thermal stress resistance are on the whole opposed to those for maximum corrosion resistance. Thus any one refractory composition might display its maximum achievable thermal performance or its maximum chemical performance depending on how it is made, but not often both in the same product. This circumstance lends versatility to each composition for different assignments, as well as competitiveness of several compositions for the same assignment. This concept of designed *adaptability* has displaced some older notions, e.g., that only magnesia refractories could survive in basic environments and only silica refractories could survive in acidic environments, or that a given composition has an immutable sensitivity to thermal stress.

Mechanical Qualifications

Abrasion Resistance is treated in Chapter VII, where *hardness* is tabulated for common major refractory phases. The simultaneous importance of the matrix and of bonding is called out, however. Surface alteration by corrosion deeply influences abrasion or erosion resistance by the destruction of matrix and intergranular bonds.

A mechanical criterion for refractory service that affects material selection is the *load-bearing capability* at the service temperature. This capability may be embodied in the *hot strength*, for example, or in any of several ways of quantifying *creep*. Although we have postponed the discussion of mechanical properties, the groundwork for assessing hot strength and creep resistance has been laid in

Chapters IV and VIII. Compositions which melt progressively over a wide temperature range are deficient in these properties. The narrowest-melting compositions excel. Viscosity of the liquid fraction is of importance too; this quality was broadly characterized in those same chapters.

REFRACTORY PRACTICE FROM QUALIFICATIONS

The practical matching of operational needs with the qualifying characteristics of refractories leads toward decisions regarding *refractory practice.*

Refractory practice may be defined as the total of engineering approaches taken to the mating of refractories to a processing plant, vessel or system, zone by zone. So defined, refractory practice is equated to system design and execution for a given plant, multiplied in variety by the different plant designs, sizes, and operating methods used to accomplish the same processing purpose. This chapter is dedicated to an overview of practices in many different processes, whose whole consumes the worldwide refractory product line. This overview has to be accompanied by an immense reduction in the detail given to each process and equipment sampled. But it demonstrates that more than one kind of refractory can fulfill a given duty, and that different duties often have much in common.

Multiple Candidacy: Technical Factors

The vessel and process descriptions of Chapter III give only qualitative statements of demand, e.g., "severe" corrosion or "moderate" thermal stress. In some vessels, such as the glass melting furnace or the reverberatory or induction furnace, numerous processes of different chemistry and different operating temperatures are there consolidated under one description. The qualifying characteristics of refractories in Chapters VIII and IX are given only by class, and only broadly. There is much room for variation among products, just as there is room for a variety of demands in a particular kind of vessel. *Multiple candidacy* for each application follows.

Furthermore, refractory practice in any one situation is not static. It is an alive and dynamic thing. Long-lived vessels like the blast furnace or glass melting tank or tunnel kiln will likely embody different refractory practice in some respects each time they are rebuilt, because technological changes will have become evident in each interim. Shorter-lived vessels like blast furnace troughs and runners, torpedo ladles, oxygen furnaces, and ladle furnaces will see changes in refractory practice just as soon as improvements appear

and can be confirmed. In order to reflect this dynamism, we shall include not only (a) materials representative of current practice, but (b) some refractory types known already to have been superseded somewhere; and further, (c) materials that are objects of recent or current published research but are not necessarily in actual use at this time.

Economic Factors in Refractory Selection

Still other reasons for multiple candidacy are *economic*. In a real sense, of course, local economic factors can not be extricated from the technical in choosing a refractory. Methods are in place for sophisticated comparisons of profitability among possible courses of action. The maker and seller of refractories has to know that each product will be subjected to *cost/benefit analysis*, reaching far beyond the user's purchase cost per pound or kilogram or cubic meter. Here we shall describe a few representative economic factors that are incorporated into the user's and the refractory supplier's decisionmaking.

Mineral Sources. If two refractories of comparable type are made from different mineral raw materials, one of them may enjoy a cost advantage because its raw material is locally cheaper. If some of that saving is passed along and performance is comparable, the user may respond. One example remarked-on earlier is the use of dolomite together with or in place of magnesite in some situations. Another example has been the intensive effort in Japan to develop refractories based on roseki, or pyrophyllite, available favorably there. The historical growth of whole refractory companies at the sites of large and uniform clay deposits in the U.S.,[1,3] given precedent many times elsewhere over the world, quite parallels these two examples.

If on the other hand one mineral yields some product superiority over another, some markets may support a higher price for the better product. Early examples, dating back to two centuries ago, occurred in silica and in firebrick. A superior silica deposit in the Dinas district of Wales and several fireclay deposits of Germany earned widespread reputations and set the standards of their time for making better-performing refractories.[3] First the refractory products and ultimately the raw ores themselves were shipped elsewhere in Britain, Europe, and to the U.S.A. Increasingly high prices accompanied increasingly great distances. A more recent example was a large and superior kyanite deposit in India which spawned a family of excellent products, made by refractory manufacturers elsewhere at considerable shipping cost for the raw material. The current successor to that mineral is andalusite, presently available at a number of sites in excellent quality but also vulnerable at some future time to a decline in properties or availability. A perennial

example is magnesite, its deposits widely distributed over the earth but distinguished in crystallinity or crystal size (also in impurity content). Some magnesites are far more readily made into superior basic refractories than are others, and the better products tend to dominate their markets. Chrome ore is another example, one of deepening concern since chromium is relatively scarce in the earth's crust. Low-silica chrome is already somewhat dear.

Inventive technologies find ways of keeping up with the rise and decline of quality mineral supply. Mineral concentration or beneficiation is a case in point. Beneficiated clays, silicas, bauxites, diaspores, magnesites, dolomites, zircons, zirconias, chromites, and other minerals are on the scene, each competing with raw ore for the refractory manufacture's attention. When one of these makes possible a significant difference in refractory cost or performance, raw material preference is affected. Examples exist in every one of these named minerals, occurring over the past one to five decades and more.

A recent technology that impinges on mineral preference is that of arc-fusion of oxidic refractories. The acceptability of a given mineral source for processing into fused grain or a fused-cast refractory is not necessarily the same as for sintering. At the same time, fused-rebonded and fused-cast refractories have opened markets for themselves in every broad composition class, by virtue of higher corrosion resistance than sintered grain or bricks can achieve. The added refractory cost pays off to the user in longer refractory life in highly corrosive circumstances. Examples are scattered through several of the preceding chapters. While refractory practice is altered (and will yet be in the future), ores and minerals are re-examined as sources of feed to an arc melter rather than to a brick press.

Synthetic Raw Materials. The use of synthetics, in conjunction with or in place of mineral raw materials, certainly marks the present era in refractories. Increased cost per pound of product is a universal consequence. But whole new composition classes now compete, that could not even exist in an all-mineral-based product line. Examples range from 98+% pure periclase to all >70% aluminas, to some chromite and aluminate spinels, to zirconias, silicon carbide, other carbides and carbon. A good part of the market inroads made by synthetics have occurred while user industries were shrinking: the "effectiveness" side of the cost/effectiveness relation had to be dramatic. The use of synthetic colloids and colloid processing, like the use of graphite and silicon carbide composites, is acceptable not because it is cheaper but because it is more cost-effective in critical service situations. Meanwhile, more prosaic uses may not support the added cost.

Refractory Form. The rise of monolithics at the expense of bricks also marks the current era (and also will continue upward in market share). Early-on, each new monolithic mix was a tentative product-line addition usually made by companies whose staple business was in bricks. Monolithics were accordingly expensive. Their success illustrated what is now proverbial: it is the *installed* costs and the *installed* benefits that matter, not the refractory material cost alone. That market success has been autocatalytic. Emplacement methods are now even faster and technically more efficient and reliable than they once were, and even less labor-intensive. And with the massive changes occurring in the refractory product mix, the disparity in cost between monolithics and formed refractories has shrunk. Much of the potential user world remains to participate fully in these changes in refractory practice, where labor costs are still low but climbing and capital investment is still shifting toward the attainable.

In some ways the rise of insulating refractories now seems to have been the most sweepingly economics-driven of all. That branch of refractories which first addressed itself wholly to energy savings on a microeconomic scale (i.e., plant by plant) now seems to have a global, macroeconomic mission of the same gravity as that of world population control, world water supply, and world contamination control. The changes in refractory practice already wrought by insulating materials may saturate locally, as they grew locally; but the forces for their worldwide extension appear foreseeable for at least as long as mankind depends on a finite fossil fuel supply.

User Viewpoints. It might seem that, in any given region, the best available or cheapest refractory for each use would be identifiable categorically and would sweep its market. Though there are such cases, exceptions are the rule due to very local differences in user needs and goals. A single huge blast furnace or a single rotary kiln, supporting an entire integrated iron-and-steel plant or an entire cement plant, puts a much greater premium on refractory durability than is the case where several smaller units share the burden of continuous production. Glass melting furnaces have like considerations: a shutdown for rebuilding may close an entire integrated plant for a time interval measured in weeks or months.

Integrated plants develop a *rhythm* of operation, in which the scheduled outage of every unit is intricately coordinated. Each size and style of plant doing nominally the same thing has a different rhythm. The cost or consequences of both scheduled and unscheduled equipment outages will vary markedly among them, unit by unit. A line dedicated permanently to a single product will clearly have different needs from a plant which shifts gears periodically. Features of these kinds give rise to differences in refractory selection,

installation and repair practices in like pieces of equipment, from one plant to another.

Plant rhythm is not a continuous variable. Apart from disturbing the comfort of continuity, it is often simply not economically feasible in an interlocking set of unit operations to change schedules in one of them by a small increment, granted this change may be advantageous when regarded alone. Refractories technologists and salespeople who do not understand this are disappointed when an incrementally "better" refractory is not accepted in the face of an isolated cost/effectiveness gain. If an existing plant rhythm is already comfortable to the operator, refractory purchases may tend to go to the lowest bidder who reliably and predictably satisfies that established rhythm.

"Lowest bidder" in this context might imply a local refractory choice that differs from practice elsewhere, or it may simply imply a freight advantage. The user's call for reliability and predictability, on the other hand, is stern. This puts a floor under refractory performance, uniformity and reproducibility. But it also extends to the supplier, independent of the product. Consistent on-time delivery and responsiveness to emergency calls are a must, as is sound technical assistance in troubleshooting. In some cases the broad-spectrum supplier is favored, who can meet the needs of most or all of the equipment in a given plant. In other cases a supplier may be favored who specializes in certain product types such as monolithics alone, or gunning mixes alone, or fiber refractories alone; or who specializes in serving that one customer. Long-time supplier-user relationships of mutual confidence are an economic benefit from the user's viewpoint, or they would not be preserved. They do result in variations of refractory practice from place to place.

User industries that are themselves undergoing technological change, or the need for change, of course put immense pressure on refractory suppliers for product innovation. They also contribute much of that innovation themselves. The steel industry is the most visible example; but glass technology has to be acknowledged in the same sentence. Copper smelting is undergoing its own economic and technological revolution. Other nonferrous metal processors have been quietly employing such innovative devices as slide gate valves and continuous casting equipment for years. An innovated economic gain to the user is most often accompanied by increased refractory unit cost -- and usually by decreased refractory consumption.

The lining of an entire blast furnace bosh and stack with silicon carbide may be the single largest-scale example of expensive but cost-effective refractory selection. But the urgency of economic needs in oxygen steelmaking processes has bred decades of turbulence in

both vessel design and refractory practice, and has backed this turbulence all the way up through ladles to the troughs of the blast furnace. A striking example of the effects on variety in refractory practice is a list of lining brick being considered for steel ladles, published in 1983 together with the relative cost of each (presumably U.S. user's purchase cost per ton, uninstalled):[76]

Brick Type	Rel. Price	Brick Type	Rel. Price
Bloating Clay	1.0	Chem.-Bonded Basic	5.0-6.0
50-70% Al_2O_3	2.5-3.5	Direct-Bonded 60% MgO	6.5-7.5
Tar-Bonded Dolomite	3.5	Tar-Bonded Magnesite	8.0
80% Al_2O_3	4.5	MgO+(18-20%)Graphite	12.0

This variety would be still further multiplied if monolithic ladle linings were represented at the same time.

CATALOG OF REFRACTORY PRACTICE

Tables X.1-4, placed at the end of this chapter, present the overview of refractory types considered appropriate for each of the vessels and processes listed in Chapter III. Refractories in each use in each system are described only by major composition class, and further by notes on general manufacturing method (e.g., fused-cast or fused-rebonded) only when unusually important. Options as to physical form (bricks or monolithics) are generally indicated; and the use of insulating refractories is noted by broad type. In respect to virtually every refractory composition, appropriate patching, maintenance and repair materials are available. Notes are included of their common methods of installation instead of repeating their compositions, unless the latter are especially significant.

For all of the reasons discussed above, the reader is presented with multiple candidacy: an openness of possibilities rather than a closedness of ready-made and frozen judgments. Yet, being gleaned from finite resources, these tables cannot be complete. Most omissions should be filled by analogy or association. Local industry alternatives and preferences at any point in geography and time can be identified by consulting institutional and society colleagues, customers, refractory vendors and product data sheets. Chapters IV-IX and their references should be helpful in such a pursuit, while the references in Tables X.1-4 themselves will call out some details of usage and qualification and product differentiation.

Organization of the Catalog

Representative vessels and systems are grouped in Chapter III under four major categories. Refractory usage is presented here under those same vessel categories in the same order:

Table X.1. Continuous, Vertical
Table X.2. Continuous, Horizontal
Table X.3. Batch, Circular
Table X.4. Batch, Rectangular

Within each table the individual vessels and processes are displayed under like titles and in the same order as in Chapter III. Zoning in the tables may or may not quite correlate.

For the sake of brevity, the working temperatures and other service demands alluded to in Chapter III are not repeated here. The technologist desiring to connect a given refractory usage in one of Tables X.1-4 with the corresponding service conditions will need to refer to the corresponding vessel and process description in Chapter III. The latter can be located quickly by finding its heading in the Table of Contents.

Further Information

There is, additionally, a rich lore of information in expert technical review articles that are published from time to time. Their own bibliographies are invaluable. An efficient way of staying broadly current in a given branch of refractories technology, or of gaining an informed entree, is to seek out current reviews in the technical periodicals of the field. The storehouse of past published reviews is not so full as to be burdensome to the reader, either. A number of excellent reviews of refractory practice have been issued in the 1980s, while some of earlier date are still largely useful. Those which have come to our attention are listed below.

Reviews of Refractory Practice

By Use (alphabetical)

AOD Furnace, for foundries -- References 126, 127
Blast Furnace, ironmaking -- Ref. 111
, SiC in -- Ref. 167
, troughs & runners, castables for -- Refs. 48,198
, , installation methods -- Ref. 233
Cement Kiln, MgO-spinel bricks in -- Ref. 137
Coal Gasification, and CO disintegration in -- Ref. 106
Coke Oven, silica bricks in -- Ref. 345
Electrical Uses, nonoxides in -- Ref. 18
Glass Manufacture, continuous -- Ref. 346
, basic checkers in -- Ref. 281
Incinerators -- Ref. 116; castables in -- Ref. 240
Iron and Steel, basic bricks for -- Ref. 112
, fused-cast bricks for -- Ref. 307
, monolithics for -- References 212, 233, 240
Nonferrous Metallurgy, basic bricks, in -- Ref. 347
Petrochemical Reactors, high-alumina castables in -- Ref. 224
Steelmaking , overall reviews -- References 74, 76, 184, 189, 348
, ladles -- Ref. 349
, dolime refractories in -- References 177, 178
, oxygen process, basic linings in -- Ref. 119
, gunning mixes for -- Ref. 236
, slide gate valves and tundish nozzles -- Ref. 350

By Material (alphabetical, various uses)

Alumina and Aluminous, castables -- References 117, 240, 251
, gunning mixes -- Ref. 229
Alumina-Chrome and Mag-Chrome monolithics -- Ref. 151
Carbides, fused-cast -- Ref. 19
Dolomite, ramming mixes -- Ref. 227
Spinel-Based, monolithics -- Ref. 142
Zircon and Zirconia, bricks -- Ref. 121
Fiber Insulating Refractories -- References 312, 313, 314

Key to Symbols Used in Tables X.1-4

A = ALUMINA (85-99%)
C = CALCIA
Cl = CLAY
Cr = CHROME ORE, CHROMIA
I = INSULATING (thermally)
M = MAGNESIA (85-99%)
S = SILICA
Z = ZIRCONIA

ACr = ALUMINA-CHROME
AS = HIGH-ALUMINA-SILICA (70-85%)
AZ = ALUMINA-ZIRCONIA
ClA = CLAY-ALUMINA (50-70%)
CrM = CHROME-MAG.
FB = FIREBRICK (all classes)
FCl = FIRECLAY (monolithic)
MA = SPINEL
MC = DOLIME, MAG.-DOLIME
MCr = MAG.-CHROME
MS = FORSTERITE
SiC = SILICON CARBIDE
SS = STAINLESS STEEL (wire)
ZS = ZIRCON

And. = ANDALUSITE
Carb = CARBON
Cast = CASTABLE
Cord = CORDIERITE
Graph = GRAPHITE
Gun = GUNNED
Mull = MULLITE (65-75%)
Plast = PLASTIC
Ram = RAMMED
Vibr = VIBRATORY-CAST

ICast = INSULATING CASTABLE (ClA or AS)
IFB = INSULATING FIREBRICK (all classes)
IFCl = INSULATING FIRECLAY (monolithic)
IFib = INSULATING FIBER (all types)
IGun = GUNNED INSULATION

Fc = FUSED-CAST
fg = FUSED-GRAIN (rebonded)
rb = RESIN-BONDED
tb = TAR (PITCH)-BONDED
ti = TAR (PITCH)-IMPREG.

A-And. = ALUMINA-ANDALUSITE
A-And.-SiC = ALUMINA-AND.-SiC Composite
A-MA = SPINEL-BONDED ALUMINA
A-MA-SiC = ALUMINA-SPINEL-SiC Composite
A-SiC = ALUMINA-SiC Composite
ASCr = ALUMINA-SILICA-CHROME
AS-SiC = ALUMINA-SILICA-SiC Composite
AS-SS = SS WIRE-REINFORCED AS
AZS = ALUMINA-ZIRCONIA-SILICA
AZS-Carb = AZS-CARBON Compos.
AZ-SiC = ALUMINA-ZIRCONIA-SiC Composite
ClA-SS = SS WIRE-REINFORCED CLAY-ALUMINA
FCl-Graph = FIRECLAY-GRAPHITE Composite
M-AS = MAG.-ALUMINA-SILICA
M-MA = SPINEL-BONDED MAG.
M-Carb = MAG.-CARBON Compos.
M-Graph = MAG.-GRAPHITE Compos.
M-Z = MAGNESIA-ZIRCONIA
MA-Graph = SPINEL-GRAPHITE Composite
MCCr = DOLIME-CHROME
MC-Graph = DOLIME-GRAPHITE Composite
MC-S = DOLIME-SILICA
MC-Z = DOLIME-ZIRCONIA
SiC-Graph = SiC-GRAPHITE Composite
Z-Carb = ZIRCONIA-CARBON Composite
Z-Mull = ZIRCONIA-MULLITE
ZSCl = ZIRCON-CLAY

Table X.1 Refractory Practice: Continuous Vertical Vessels of Chapter III

VESSEL & ZONE (Fig.)	WORKING BRICK	WORKING MONOLITHIC	BACKUP INSULATION	MAINTENANCE & REPAIR
Blast Furnace (III-1,2)				
HEARTH [Refs. 10, 74,77,144]	Carb; MCr; M-Carb; FB (sub)	ACrCast; MCrCast; SiC-Graph		
TUYERE BLOCK [77]	See HEARTH	ASCrCast		
BOSH/STACK [Refs. 74,167,168]	Carb; SiC			
UPPER STACK [Refs. 10,74,167,168]	AS; SiC; FB	ASGun		ASGun
WEAR PLATE [10]	A; AS; SiC			
STOVE [Refs. 130, 351,352]	FcAS; And.; Mull; AS		ICast; IFB	
UPPER CHECKER [Refs. 10,346]	A-And.; S; AS; Mull			
LOWER CHECKER [10]	See UPPER; FB			
BUSTLE/DUCTING	AS; A-And.; FB		IFB	
TAPHOLE [Refs. 194, 195,232,351,352]	See HEARTH	rbAnd.Plast rbFCl Plast		ASGun ClAGun
TROUGH/RUNNER [Refs. 46,48,139,151,198, 200,201,232,241, 244,247,297,351-4]		ACrCast; MASCast; ASCast; And.Cast; AS-SiC Cast, Vibr, & Ram		See WORKING MONOLITHIC; also GUN
TORPEDO LADLE [45, 74,80,86,117,133, 151,189,190,193, 196,197,235,241, 247,351-2,355-6]	AS; A-And.; Mull; FB; rbA; AS-SiC; AZ-SiC; A-And.-SiC; A-MA-SiC; tiM-Carb	ASCast rbAnd.-Carb Plast	ICast; IFClCast; IFB	ASGun; AS-SiCGun
TORPEDO LANCE [Refs. 290,357]		ASPlast; AS-SSCast; ClA-SSCast		
Cupola (Fe Foundry)				
HEARTH [3,10]	FB	S Fill		S Fill
SHAFT [3,10]	carb; FB	FCl-Graph Plast		FClPlast
Blast Furnace (Lead)				
HEARTH [Ref. 3]	FB	ASCast; ClACast		

Table X.1, continued

VESSEL & ZONE (Fig.)	WORKING BRICK	WORKING MONOLITHIC	BACKUP INSULATION	MAINTENANCE & REPAIR
Heat Exchangers/Reactors (III-3)				
WALLS [Refs. 10, 117,125,224-6, 358]	AS; ClA	ACast; ASCast; ASVibr; AZSCast; ICast; IPlast; IFib		ASPlast IPlast
FLUES, DUCTS [Refs. 310,359-61]	AS; ClA; FB; S	IFClCast; SCast; IFib		
Stills & Retorts (Zinc)				
HEARTH, WALLS [3]	FB; SiC			
CONDENSERS [Ref. 3]		SiC Cast		
Aluminum Smelter				
HEARTH (Cathode)	Graph; SiC	Graph Ram		
WALLS, ROOF, DUCTS	AS; ClA; FB	ACast; ASCast	IFB	
Multiple Hearth (III-4)				
HEARTHS	AS; ClA; FB	AS; ClA, FClCast		
WALLS, CROWNS	ClA; FB; IFB		IFB	
Shaft Kiln				
WALL	A; AS; M	A, ASCast; MCast	ACast; M Fill	A, AS Gun, Ram, Plast
Spray Drier		See REACTORS		See REACTORS

Table X.2 Refractory Practice: Continuous Horizontal Vessels of Chapter III

VESSEL & ZONE (Fig.)	WORKING BRICK	WORKING MONOLITHIC	BACKUP INSULATION	MAINTENANCE & REPAIR
Rotary Kiln: Cement & Lime (III-5)				
HOT ZONE [Refs. 10, 108,136,137,150, 178,215,218,362-4]	M; MCr; M-MA MC-S; MC-Z	MC-SCast		AS, ClA Cast, Gun, Plast
HIGH-WEAR, etc. [Refs. 10,117,171, 172,243,338,339]	SiC; FB	ASCast; SiCCast; IFib/ClA Gun		See WORKING: Gun, Cast, Plast
Rotary Kiln: Other				
UNDIFFERENTIATED	M; MC-S; AS; FB	ASCast; ClACast		Gun, Cast, Plast
Glass Melting Furnace (III-6a,b)				
SUBHEARTH [365]		FCl, ZS, AZS Ram		
CONTACT (TANK, UNDIFFERENTIATED) [Refs. 10,24,27, 30,91,129,319, 365]	ZS: AZS: AZ; Cr; ACr; S; Mull; FcA; FcM; FcZ; FcAZS; FgZ; FgAZS; Fg@-A		ICast; IFib	
BREASTWALLS & UPPER STRUCTURE [Refs. 10,365]	@-A; Mull; Cr; ACr; S; M; MCr; FB; And.; ZS; FcA; Fc@-A; FcAZS; FgAZS; FcMull		ICast; IFib	
CROWN [Refs. 10, 365]	M; MCr; Mull; S; FcAZS; FgAZS		ICast; IFib	
REGENERATOR CROWN & STRUCTURE [Refs. 10,365]	M; MCr; Mull; And.; S; FB			
UPPER CHECKER [10,276,365]	M; FgAZS			
MID & LOWER CHECKER [Refs. 10, 92,275,276,282, 305,365]	M; MA; MZ; MC; MAS; AS; AZS; FB			
GLASS FORMING [Refs. 65,223,365]	S; Mull	ASVibr		

Table X.2, continued

VESSEL & ZONE (Fig.)	WORKING BRICK	WORKING MONOLITHIC	BACKUP INSULATION	MAINTENANCE & REPAIR
Reverberatory Furnace: Copper (III-7)				
BASIC, NEUTRAL [Ref. 10]	MCr; CrM		ICast; IFB	
ACID [Ref. 10]	AS	ASCast	ICast; IFB	
Reverberatory Furnace (Aluminum Remelt)				
HEARTH & SLAG LINE [Ref. 10]	AS; ZS; Mull; SiC			
SIDEWALLS & ROOF [Ref. 10]	FB; IFB	ClACast, Plast	IFB	
Reverberatory Furnace (Other Nonferrous)				
UNDIFFERENTIATED	MCr; M-MA; AS; ClA; FB		IFB	
Tunnel Kiln: Refractories (III-8)				
HOT ZONE [Ref. 10]	M; FcM; MCr; FcA			
OTHER ZONES	See TUNNEL KILN: CERAMICS & WHITEWARES			
Tunnel Kiln: Ceramics & Whitewares (III-8)				
WALLS [Refs. 10, 215,222,318]	AS; ClA; FB; IFB	ASCast	AS; IFB; IFib	Gun; Cast; Plast
ROOF [10,351,352]	See WALLS; S; And.		ICast; IFib	Gun; Plast
BAFFLES, SHIELDS	AS; And.			
KILN CAR DECK [117]		ASCast		
Heat Treatment Furnace (Ferrous)				
UNDIFFERENTIATED [Refs. 10,117,233, 315,316,351,352]	AS; FB; And.	ASCast; ClAGun; ClACast	IFib	Gun; Cast; Plast
SEALS, FLUES, DUCTS [49,310,315,316]		ClACast; SCast Cr-SSPlast	IFib	
Heat Treatment Furnace (Nonferrous & Miscellaneous)				
UNDIFFERENTIATED	FB; IFB	IFB	(See also, FERROUS)	
Continuous Driers	IFB	IFib	(May also be Unlined)	
Steam Boilers (III-9)				
INSULATING WALLS & ROOF [Refs. 10,70]	FB; IFB; IS		IFB; IFClCast	
RADIANT WALL [203]	MCr; ACr		ICast; IFB	Gun; Cast; Ram; Plast
COOLED WALL [10]	IFB	FClCast	IFib	
ASH PIT [Refs. 10, 169]	AS; FB; CrM	FClCast; SiCPlast		

Table X.3 Refractory Practice: Batch Circular Vessels of Chapter III

VESSEL & ZONE (Fig.)	WORKING BRICK	WORKING MONOLITHIC	BACKUP INSULATION	MAINTENANCE & REPAIR
Oxygen-Blown BOP & Q-BOP Vessels (III-10a,b)				
BOTTOM & BARREL [Refs. 10,43,74, 76,97,99,115,183-5,187,230-1,233, 237-9,366]	tbM-Carb; tbM-Graph; tbMC-Graph; rbM-Graph		M; MCr	Wet Gun: M; MCr; M-Graph; MC-Graph
HIGH-WEAR AREAS [Refs. 74,76,233]	See BOTTOM/ BARREL: tiM-Carb	MRam; MCrGun; M-CarbGun		Dry Gun: M-Graph; MC-Graph
BOTTOM PLUG [Refs. 76,158,162,292]	See BOTTOM/ BARREL; M; A			
LANCE [Refs. 132,140]		ACast; MACast		Flame & Plasma Gun:
Argon-Oxygen Furnace, AOD (III-10c)				
HEARTH & SIDEWALLS [Refs. 74,76,145]	See BOP/Q-BOP; MCr; MC		MCr	M; MS
TUYERES [76,146-8]	FgMCr	MCrCast		
LANCE [Refs. 132,140]		ACast; MACast		
Ladle Furnaces & Converters				
LD CONVERTER [74,241,247,367]	tbM-Carb	ACast; AZCast		ACast
BASIC [Refs. 72,74, 96,145-8,180,182, 203,228,289,368]	M; MC; MCr; CrM; A; AS; tbM-Graph; rbM-Graph	MCrGun; MCGun; MA-GraphGun		MGun; MCrGun
LANCE [Refs. 132,140]		See BOP/Q-BOP & AOD		
DIFFUSERS [Refs. 158, 162,292]		M; IM; A; IA		
Electric Arc Furnace, EAF: Steel (III-11)				
HEARTH & SLAG LINE [10,44,76,175-6]	M; tbM-Carb; rbM-Graph	MRam		M Ram, Cast, Gun
LOWER SIDEWALL & TAPHOLE	M; MCr; tbM-Carb; rbM-Graph			MCr Ram, Cast, Gun
w/c STEEL SIDEWALL [76,151,241,247]		AGun		AGun
ROOF, DELTA [10,76]	A; AS	A Ram, Cast		
LANCE, DIFFUSER [Refs. 162,192]		See LADLE FURNACES & CONVERTERS		
Electric Arc Furnace (Foundry)				
UNDIFFERENTIATED	See EAF: STEEL; A; S	ACast; SCast		

Table X.3, continued

VESSEL & ZONE (Fig.)	WORKING BRICK	WORKING MONOLITHIC	BACKUP INSULATION	MAINTENANCE & REPAIR
Coreless Induction Furnace: Steel (III-12a,b)				
UNDIFFERENTIATED [Refs. 123-4, 134,202]	M; M-MA; A; AS; Z	MRam; A, ASRam; ZSCast		MPlast; APlast; ARam, Cast
Coreless Induction Furnace: Foundry (III-12a,b)				
UNDIFFERENTIATED [Ref. 10]		M; A; S; Z; Mull	Ram, Cast Ram, Cast	See WORKING: Ram, Cast
Ladles: Steel (III-13)				
UNDIFFERENTIATED [Refs. 10,47,74, 76,87,135,143, 152,177-8,181, 233,288,351-2, 371]	M; MCr; MC; A; AS; ZS; MC-Z; A-MA; And.; ClA; ZSCl; FCl; MA-Graph; M-Graph; MC-Graph; A-SiC	ASRam; ASCast; ACrCast	AS; MCr; ICast; FB; IFB	
Ladles: Steel Teeming (III-13)				
UNDIFFERENTIATED [Refs. 88-9,120, 122,131,219,222, 287,308,323,351, 352,371-4]	M; AS; S; ZS; AZS; And.	MCast; MCCast; ACast; ASCast; ZSCast		See WORKING: Ram, Cast, Plast
Ladles: Foundry (III-13)				
IRON & STEEL	See STEEL TEEMING LADLES			
NONFERROUS [Refs. 10,117,131,291, 317,344,372]	AS; ClA; FB	ASCast; ClACast; FClCast; Fib	IFib	
FOUNDRY MOLDS		S; M; A; AS; ClA; FCl		
Continuous Casting: Steel (III-14a,b)				
TUNDISH [Refs. 89, 90,117,128,138, 192,231,233,291, 309,375-8]	AS; ClA; ZSCl	A, ASCast; M-ZGun; ClACast; M-ASCast; MGun, Plast; MCGun; MAGun, Plast; AS-SiCCast; AS-SSCast		
NOZZLE BLOCK [Refs. 74,85,191,199, 379,380]	ZS; M-Z; fgZ; Z-Carb; AZS-Carb; ZMull-Carb			
SLIDE GATE VALVE [Refs. 10,379]		MCast; M-ZCast; ACast; ZSCast; MullCast		
Copper Converter (III-15)				
UNDIFFERENTIATED [Refs. 10,73, 149,381]	MCr; CrM			MCrGun; CrMGun; MCCrGun

Table X.4 Refractory Practice: Batch Rectangular Vessels of Chapter III

VESSEL & ZONE (Fig.)	WORKING BRICK	WORKING MONOLITHIC	BACKUP INSULATION	MAINTENANCE & REPAIR
Reverberatory Furnace: Open Hearth Steel (I-5a)			(OBSOLETE[76])	
Reverberatory Furnace: Nonferrous Foundry & Roasting (I-6a,b)				
	See CONTINUOUS TYPES, Table X.2			
Arc Furnace: Oxide Melting (III-16)				
	SKULL: GRANULAR SELF-REFRACTORY			
Coke Oven				
UNDIFFERENTIATED [Refs. 10,69,115, 345,382,383]	ClA; FB; S	ClACast; FClCast	See WORKING: Cast, Plast	Plast
Carbon Baking Furnace				
UNDIFFERENTIATED	AS; ClA; A-And.; FB; IFB	See BRICK: Gun, Cast, Plast	IFB	See WORKING: Gun, Plast
Periodic Kilns: Ceramics & Whitewares (III-17a,b; III-18a,b)				
HEARTH OR CAR, WALLS & ROOF [Refs. 10,215, 222,312-314]	A; AS; S; FB; IFB	ACast; ASCast; ClACast; IFib	IFB: ICast; IFCl; IFib	See WORKING: Gun, Cast, Plast
LOW-MASS CAR TOP [Refs. 10,117]	SiC	ICast; IFib		
KILN FURNITURE [10,33,286]	A; SiC; Cord; Mull	See BRICK: Porous Cast; IFib		
Periodic Kiln: Refractories (III-18a)				
	See TUNNEL KILN: REFRACTORIES, Hot Zone			
Batch Driers	See CONTINUOUS DRIERS			

Alphabetical Equipment Index to Tables X.1-4

Chapter XI

Design Properties: Thermal and Electrical

REVERSIBLE THERMAL EXPANSION

Within narrow limits, the chemical bonds between atoms in a solid obey Hooke's Law [$f = -k(x-x_o)$]. It is readily derived from this that $dL/dH = k \cdot L$, where L is some linear dimension of a body and H is the heat or energy contained (per gram) in the vibrational motion of its atoms. Since $dH = cdT$ where c is the specific heat, the above can be rewritten:

$$dL/dT = \alpha L \qquad \text{or} \qquad d \ln L = \alpha dT \ .$$

Here α is the *coefficient of linear thermal expansion.* To the extent c is constant with temperature, so also is α. The definite integral is:

$$\ln(L/L_o) = \alpha(T - T_o) \ ,$$

where T_o is any convenient base temperature and L_o is the body length at that temperature. But for any L/L_o within several percent of 1.00, $\ln (L/L_o) = (L/L_o) - 1 = (L - L_o)/L_o = \Delta L/L_o$. Hence,

$$\Delta L_T/L_o = \alpha(T - T_o) \ .$$

Measured thermal expansion curves such as in Figures IV-9a, b and IV-10 are not often linear as the above equation might seem to suggest. Of course, c is not constant with temperature; nor are interatomic bonds always quite Hookeian springs. Their spring constants are not all alike. They are also directional, each varying azimuthally in any plane of a crystal. The curvature seen in those

figures and the anisotropy of thermal expansion of crystals are familiar manifestations of the variation of α with temperature and with direction. In polycrystalline ceramics of random crystallite orientation, anisotropy is averaged out over a whole body and then $\Delta X/X_o = \Delta Y/Y_o = \Delta Z/Z_o$ and $\Delta V/V_o \cong 3(\Delta L/L_o)$; but that condition is not always guaranteed. Isotropic body expansion is implied in most of the reference curves of Figs. IV-9a,b and -10.

Linear Thermal Expansion of Solid Substances

The figures referred to in Chapter IV give the percent body length change above a base temperature of 20°C, instead of giving the coefficient α. This is a convenience. But to read thermal expansions from plotted curves is not always convenient or accurate. Table XI.1 gives the functions from which those figures were plotted. Temperature is given in kelvin. Every function is in the same form: % expansion at $T = 100\Delta L_T/L_{293} = A + B(10^{-4}T)+C(10^{-4}T)^2 + D(10^{-4}T)^3$. The table gives the best-fit values of the constants A, B, C, and D.

The coefficient α is readily obtained by converting from percent expansion to fractional expansion and differentiating, thus:

$$\alpha = 10^{-6}B + 2 \cdot 10^{-10}CT + 3 \cdot 10^{-14}DT^2 \quad \text{and} \quad \Delta L_T/L_{293} = \int_{293}^{T} \alpha dT \ .$$

Use of these relationships to determine $\Delta L_T/L_{293}$ is more cumbersome than use of the data in Table XI.1, precisely because α is not constant.

These reference data for the thermal expansion of substances may be used for comparison with the measured thermal expansions of industrial refractories. An exception, however, is graphite. Expansions parallel and perpendicular to the "grain" (a textural feature) are tabulated here for only one grade of commercial graphite. These values have to be regarded as no more than typical; every grade exhibits its own anisotropic thermal expansions, which manufacturers can supply on request.

Linear Thermal Expansion of Refractories

There is no widely used "rule of mixtures" for the thermal expansion of heterogeneous materials.* Measurement is the only

---

*Two mixing equations are reported in Reference 385, both reputedly agreeing well with measured data. However, both require detailed knowledge of the internal stress states of materials, which is harder to acquire than the measured expansions.

Table XI.1 Linear Thermal Expansion of Solid Substances (Ref. 32)

$100\,\Delta L_T/L_{293} = A + B(10^{-4}T) + C(10^{-4}T)^2 + D(10^{-4}T)^3$ (T in K)

	M.P., K	A	B	C	D	NOTE
Al_2O_3 (hex.)	2327	-0.180	+ 5.494	+22.520	- 28.940	1
CaO	3200	-0.321	+10.590	+13.100	- 14.050	
Cr_2O_3 (hex.)	2603	-0.280	+10.380	-31.220	+106.200	2
Fe_2O_3 (trig.)	1838	-2.537	+ 7.300	+49.640	-114.000	3
MgO	3125	-0.326	+10.400	+25.810	- 28.340	
SiO_2 (lo qtz.)	tr.~873	-0.236	+ 6.912	+ 0.556	+1312.00	4
" (hi qtz.)	tr.1743	+1.040	+ 0.068	+11.660	+ 18.000	Est.
" (vitr.)	cr.~1273	-0.015	+ 0.397	+ 4.666	- 34.460	
ZrO_2 (monocl.)	2988	-0.314	+13.040	-90.920	+408.400	5
$Al_6Si_2O_{13}$	2193	-0.0929	+ 2.580	+21.530	- 45.720	
$CaAl_2O_4$	1873	-0.107	+ 2.578	+39.680	- 90.770	
Ca_2SiO_4	2403	-0.345	+11.260	+16.560	+ 27.330	
$MgAl_2O_4$	2408	-0.183	+ 5.456	+28.060	- 41.810	
$Mg_2Al_4Si_5O_{18}$	~1773	+0.00911	- 0.912	+20.640	- 3.921	6
$MgCr_2O_4$	2673	-0.176	+ 5.822	+ 5.580	+ 23.360	
$MgFe_2O_4$	2023	-0.218	+ 6.003	+52.560	- 94.040	
Mg_2SiO_4	2163	-0.238	+ 7.166	+33.810	- 37.970	
Mg_2TiO_4	~2100	-0.249	+ 8.294	+ 4.074	+ 94.300	
$ZrSiO_4$	2673	-0.136	+ 5.337	-30.420	+209.400	
AlN (hex.)	~2500	-0.0809	+ 1.806	+31.760	- 72.560	7
B_4C (rhomboh.)	2623	-0.114	+ 3.523	+12.660	- 5.085	8
BN	subl.~3273	-0.00133	- 1.278	+49.110	- 86.350	
SiC	dec.~2923	-0.0991	+ 2.970	+13.880	- 15.480	
TiC	~3410	-0.177	+ 5.710	+11.740	+ 2.412	
C (graph.) //	~3900	-0.0550	+ 1.552	+12.050	- 10.330	9
" " ⊥	"	-0.1580	+ 5.651	- 8.850	+ 35.550	9
" (vitr.)	cr.~2700	-0.0890	+ 3.015	+ 1.286	+ 17.240	
Fe	1808	-0.289	+ 7.350	+93.300	-314.000	10

NOTES: 1- Cryst. exp. c/a ~1.1 . 2- Cryst. exp. a/c ~1.3 .
3- Cryst. exp. a/c ~1.26. 4- Cryst. exp. a/c ~1.58.
5- Cryst. exp. c/b ~2.5 . 6- Cordierite refractory.
7- Cryst. exp. a/c ~1.18. 8- Cryst. exp. ~ isotrop.
9- Grade ATJ, parallel and perpendicular to the textural "grain", respectively. Cryst. exp. c/a ~10.
10- Numerous steels and SS agree with Fe within ~±15%.

practical recourse. As in many physical measurements, differences in equipment and technique as well as in specimens create uncertainties in the data. Fortunately, the uses to which thermal expansions are put are somewhat forgiving of small errors.

Representative Thermal Expansion Curves. Figure XI-1 is a compilation of illustrative linear thermal expansion curves for various refractory types, drawn from a number of different sources. Data of Reference 65 were used for stabilized cubic zirconia, zircon, and β-spodumene. Reference 74 was used for the two silicon carbides, and Reference 32 for cordierite. Most of the remainder have been reported rather generally.

It appears that a number of sources have taken some liberties in the removal of curvature. We have done some smoothing in the region below about 300°C, where behavior tends to be a little unreliable while the highest precision is rarely called for anyway. Agreement of the curves for nearly single-phase refractories with their counterparts in Figures IV-9a,b and -10 is generally satisfactory.

Silica refractories containing quartz set themselves apart: see curve 1 of Fig. XI-1. The causes and consequences have been detailed in Chapter IV: Figure IV-7 gives a quick summary. The marked slope change in curve 1 here should be repeated in other high-silica refractories such as firebrick, and it is.[3] This feature contributes to the thermal stress sensitivity of ordinary firebrick and IFB. The only firebrick represented in the present group is super-duty, curve 15. This appears to be the high-fired version, containing little crystalline silica.

Series of related refractory compositions are apparent in Figure XI-1: curves 2, 3, 4, 5, 7 and 8 for basic refractories of diminishing MgO content and curves 9, 10, 11, 14, 13 and 15 for alumina-silica refractories of diminishing Al_2O_3 content. Both series disclose a general "rule of mixtures" for thermal expansion, but not a reliable quantitative rule.

Figure XI-1 represents dense or working refractories. A body free from internal stresses exhibits no dependence of thermal expansion on porosity per se. The presence of internal stresses and microcracks complicates matters, however. Cellular insulating refractories will have somewhat different thermal expansion curves from these. Inasmuch as this figure encompasses both ranges of composition and the direct-bonded, chem-bonded and cemented versions of each, on the other hand, high-void-volume versions will be about as well represented by the same curves: namely, within modest latitudes. The next subsection will remove some of this vagueness.

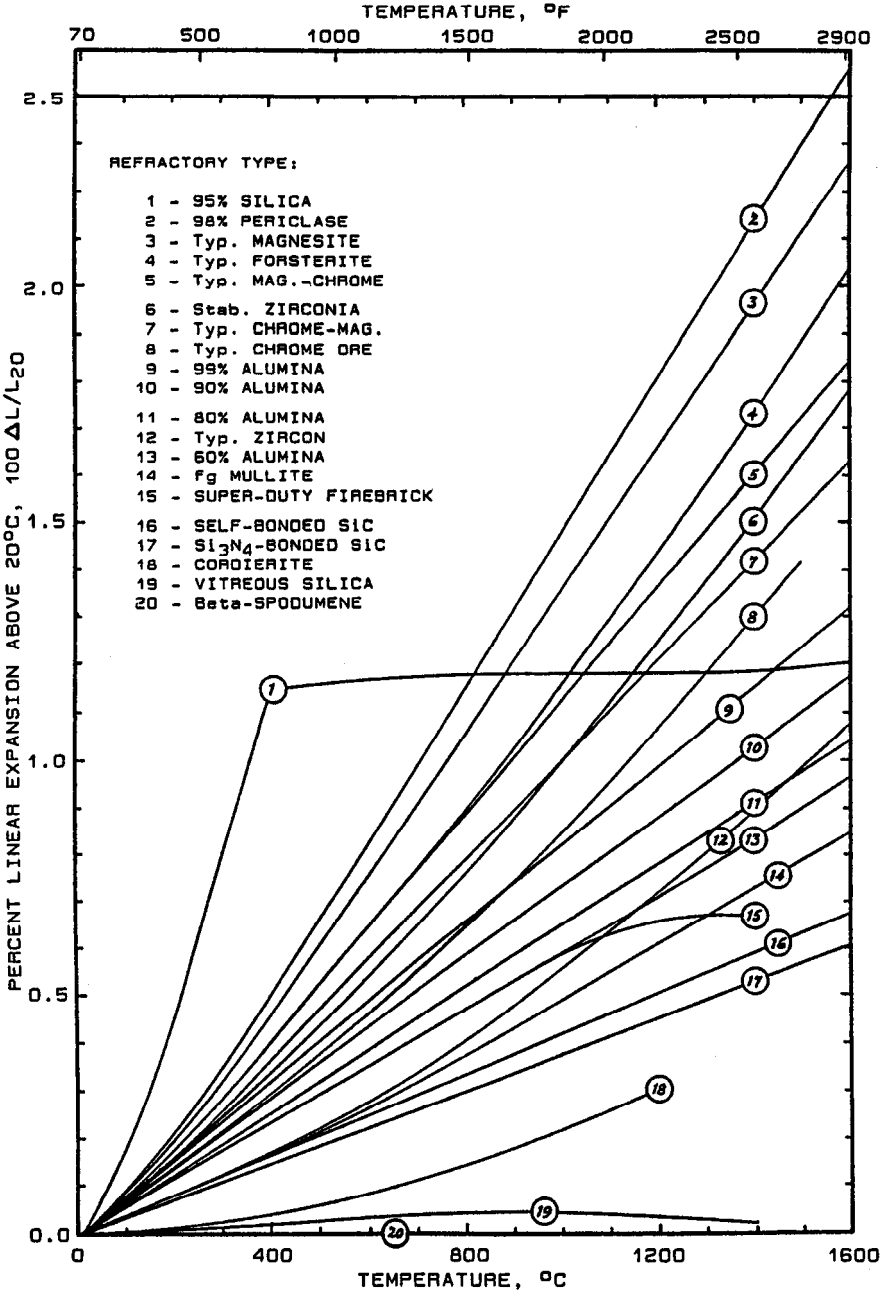

Figure XI-1 Linear Thermal Expansion of Refractories (Ref. 32)

Single-Point Data. It is common practice in the industry to report, for a given commercial refractory, only the percent linear expansion between room temperature and 1000°C. This one value of % expansion or $100\Delta L_{1000}/L_{20}$ corresponding to each of the curves of Figure XI-1 is given in the following table. The index number of each is the number of its curve in the figure.

Refractory	% Lin. Exp. at 1000°C	Refractory	% Lin. Exp. at 1000°C
1. 95% Silica	1.18	11. 80% Alumina	0.65
2. 98% Periclase	1.47	12. Typ. Zircon	0.55
3. Typ. Magnesite	1.35	13. 60% Alumina	0.58
4. Typ. Forsterite	1.16	14. fg Mullite	0.49
5. Typ. Mag. Chrome	1.12	15. Super-duty FB	0.58
6. Stab. Cubic Zirconia	0.99	16. Self-Bonded SiC	0.42
7. Typ. Chrome Mag.	0.99	17. Si_3N_4-Bonded SiC	0.375
8. Typ. Chrome (Ore)	0.84	18. Typ. Cordierite	0.22
9. 99% Alumina	0.82	19. Vitreous Silica	0.04
10. 90% Alumina	0.73	20. β-Spodumene	0.00

The technologist will want to extrapolate to higher temperatures, given only one point at 1000°C for a particular refractory product. First that product's composition class or phase composition should be identified, and the nearest of the above twenty types likewise. The product's 1000°C expansion is then compared with the appropriate entry above, and in fact should be overlaid on Figure XI-1. A reasonable slope for extrapolation can then be estimated, based on compositional similarity. No extrapolation should be carried as far as the Maximum Service Temperature of Chapter VIII, Figure VIII-3.

Dolime-based refractories should run approximately the same as their MgO-based counterparts. The above extrapolation method should suffice, given an actual percent expansion at 1000°C. All regular grades of firebrick should be extrapolated above 1000°C at zero slope, for a fair estimate in the absence of data. A-Z-S refractories should extrapolate at the steeper slopes of curves 6 and 12, or not, depending on the actual phase composition. For single-phase nonoxides, see Figure IV-10.

Alteration. Refractories in service find their thermal expansion altered, but only to the extent their phase composition is altered. Solid-state redox reactions with penetrating gases are a case in point (Chapter V). Long-term diffusional penetration in depth accompanying exposure to liquids may also occur (Chapter VI). Acute hot-face alteration is no exception, but by itself it leaves most of the refractory unchanged in the short term.

Most alteration by corrosion has such immediate damaging effects (e.g., swelling, debonding) that changes in the thermal expansion properties of the refractory tend to be regarded as secondary.

This isolated consequence of alteration can be left in the category of being physico-chemically required but overshadowed by more momentous changes.

Measurement of Reversible Thermal Expansion

The standard ASTM measurement method is the special case of C832, *Thermal Expansion and Creep of Refractories Under Load*,[9] in which the applied load is zero. The basic concepts and typical laboratory practices are described following.

A rod or bar-shaped specimen is stood vertical (to minimize external constraints) in a tube furnace. The distance between its ends is to be measured as a function of temperature ranging from ambient to at least 1000°C; for comprehensive work on oxides, to about 1500°-1600°C. The specimen length is a matter of convenience; but if this is, say, 10 cm or about 4", then a total length change of up to ~2.5 mm must be measured and with a sensitivity better than ±10 μm (±0.01% of the length). Yet the longer the specimen, the more difficult it becomes to warrant its uniformity of temperature at all temperatures.

The most convenient measurement method found has been that of a *differential comparator*. The specimen of measured room-temperature length L_o is stood upon a lower ceramic base or platen. Beside the specimen a *reference rod* is stood on the same platen. Its length L_r is sufficient to extend out of the upper extremity of the furnace, with shielding sufficient to warrant its own upper end as "cold." Then an *extensor rod*, of the same material as the reference rod, is stood atop the specimen. Its length L_e is such that $L_o + L_e \approx L_r$: it too extends out the top of the furnace. The small (or zero) vertical separation of these two upper rod ends is first measured at room temperature and becomes the "zero" of differential length corresponding to specimen length L_o. Then that vertical separation is measured at successively higher uniform specimen temperatures.

If the thermal expansion coefficient of rods "r" and "e" is zero, then the net displacement between their upper ends at each temperature is precisely ΔL_T of the specimen. Rods of vitreous silica will do up to roughly 1000°C, and it is easy to estimate corrections for their own thermal expansions (curve 19 of Figure XI-1). For higher-temperature work, high-purity dense alumina ceramic or even sapphire rods are useable; but then elegant corrections must be made for their own thermal expansions, which are unequal. One way of circumventing this problem is to use "twin" specimens (one of a reference material). Then their two extensor rods are of the same length, and no compensation is necessary.

The differential vertical separation of the upper rod ends has been measured optically, using a microscope travelling on a micrometer

screw. The more convenient method is to use an electronic transducer affixed to both rods at T_o, and whose own displacement (e.g., of capacitor plates or transformer core) is converted to a proportional electrical signal. That instrumentation is easy compared to the necessities of the remainder of the technique.

At every temperature the furnace hot zone, of length considerably greater than L_o, must be of scrupulously uniform and precisely measured T. The approach usually taken, using electric radiant heating, is to divide the helical heater into independently-controlled segments -- including guard segments at the ends to counteract end cooling. Interior shielding against end cooling and convection is also crucial, not to mention shielding against radial heat loss. The specimen temperature must be accurately and continuously measured at frequent intervals along its length, for which embedded Pt/Pt-Rh thermocouples will do. Feedback circuitry can be devised to drive the heater segments from the thermocouple outputs so as to ensure a uniform specimen temperature at every T.

One must attend carefully to the specimen and its preparation. Its diameter must be sufficient that it represents the refractory. The direction in which it is cut from the latter (e.g., relative to the pressing direction or casting geometry of a brick) often counts. It must not be damaged in cutting. Most importantly, the *permanent deformation* of the specimen must be removed thermally before reversible thermal expansion data are acquired. This is ordinarily checked by measuring ΔL successively with increasing T and then with decreasing T -- or at least, remeasuring the "zero" displacement of the two rod ends after returning to T_o.

Uses of the Data

Much of the usefulness of thermal expansion data for refractories has been alluded to in Chapter IV, having to do with the development of stresses and of dimensional mismatches. Steady-state examples include consequences of ΔT across a wall: warpage of straight runs, compressive hot-face spalling, cold-face tensile parting of mortared joints, etc., and the effects of external steel constraint. Temperature transient and cycling examples include thermal-stress fracture, thermal spalling, and internal degradation due to crystal expansion-coefficient mismatches and anisotropy.

There are still other calculations routinely performed by the system designer, which call for structural design adaptations. An unconstrained cylindrical wall, installed cold and then heated for operation, will increase in circumference by the ΔL of its thermal expansion. It will increase in radius by $1/2\pi$ of this. If its foundation does not expand likewise, the two will part company. The mating of a roof or crown to supporting walls presents a similar problem. Long

runs of refractory, as in a tunnel kiln or rotary kiln, must contain expansion joints for like reasons or risk buckling failure. Duplex refractory walls must be analyzed if the layers are of different types exhibiting different thermal expansions.

PERMANENT DEFORMATION

If a refractory specimen is subjected to the thermal expansion measurement described above, like as not it will fail to return to its original length L_o upon first returning to room temperature. Depending on the maximum temperature to which it is heated, and on how long it is soaked there, the specimen may require one or two or even more cycles before coming to reproducible room-temperature dimensions from which the thermal expansion then becomes reversible.

This phenomenon is evidence that the material has not been brought to a steady-state condition in manufacture. Reheating may continue high-temperature processes of chemical reaction and decomposition, gas evolution, phase (i.e., crystal) nucleation and growth, interphase bonding, and the consolidation of porosity, that were all started but previously left incomplete. The complex of further changes wrought by reheating may produce either a net volume increase or a net volume decrease. This volume change is sampled by measuring the *reheat linear change*: in one direction only, if isotropic behavior prevails.

Reheat Linear Change: A Tailored Property

It is evident that the reheat change is not a property of matter but a consequence of manufacture. For monolithic refractories installed unfired, the first heating in service is almost bound to cause a volume change, while a second heating may continue it. By means of formulation and treatment, this initial deformation is controllable by the manufacturer -- within limits.

It was pointed out earlier that a positive reheat change is desirable for ladle linings that are installed cold. Other installations of refractory-against-steel may call for the same, while still others may not. In lining repair, it is desirable to have neither excessive reheat expansion nor excessive shrinkage since the underlying wall has already matured in service and the new patch must adhere to it. In a word, different applications of the same refractory composition or type can call for different reheat linear change, which the manufacturer can usually provide. This reheat change will be meaningful if it is measured at a temperature comparable to that anticipated in service.

Reheat change data are contained in the technical descriptions of individual commercial products. A compilation can only sample what manufacturers actually do, which is dictated by their markets. How they achieve these ends is largely proprietary, and we shall leave that matter alone. Following are some selected reheat linear changes, representative but not limiting on what is found in product data sheets:

Composition Class & Type	Reheat T,°C	Linear Change,%
Basic (high-MgO) Brick	Typ. ≥ 1700	Typ. -1.0 to +0.5
85-99% Al_2O_3 Brick	Typ. ≥ 1650	Typ. -0.5 to +1.0
80% Al_2O_3 Brick	1600	Ex: +3.0,3.2,4.6,5.1
70% Al_2O_3 Brick	1600	Ex: +2.2,3.0,4.1,5.0,5.5.,6.5
60% Al_2O_3 Brick	1600	Ex: -0.2,+0.6,2.1,2.5.,4.5
≤50% Al_2O_3 Brick incl. BC	Typ. ≤1600	Typ. -1.0 to >5.0
Basic (hi-MgO)Monolithic	1650 or 1600	Typ. -1.5 to +0.5
75-98% Al_2O_3 Monolithic	1650 or 1600	Typ. -1.5 to +1.5
70% Al_2O_3 Monolithic	1650 or 1600	Ex: +0.1R,1.5P,3.0C, 3.1P,3.5G,4.4P
60% Al_2O_3 Monolithic	1650 or 1600	Ex: -0.7P,+0.2C,0.4P, 2.0C, 2.5P,3.0P
≤50% Al_2O_3 Mono. incl. BC	Typ. ≤1600	Typ. -0.2 to >5.0

BC = bloating clay; Ex. = examples; C = cast; G = gunned; P = plastic; R = rammed.

The percent linear change is usually reported for each product as a min-max range; the values given above are their midpoints. Where "examples" are given in the table, a high degree of both intentional and inadvertent selection is at work. These examples only illustrate the manufacturer's ability to tailor individual products. Where "typical" ranges are given, a similar array of individual values lies between the extremities. Likewise the given reheat temperatures, while consistent with these % change data, are not limiting on actual practice. Many data sheets list the reheat change at two or more temperatures because the products are in candidacy for more than one application.

The above tabulation clearly illustrates the individuation of products intended for ladle linings. It is easy to identify those products by their large positive reheat change. Other values closer to zero correspond to monolithic formulations suitable for lining repair, or to bricks suited for wall and roof construction. These data are all obtained in the laboratory under zero mechanical constraint. In a ladle lining in the field, constraint by the steel shell in the first heating limits the actual permanent expansion of the refractory but without consequent mechanical or structural damage.

Measurement of Reheat Linear Change

For a measurement such as this one to have comparative value among different refractories, it must be obtained in a strictly uniform manner. ASTM standard procedures C113, C179, C210, C436, and C605[9] apply in the U.S. Procedure C113, for fired brick, uses the standard 9" "straight," which is 9" by 4.5" by 2.5" or 3"; so also does C210 for IFB. The procedure for monolithics, C179, uses a 9" long formed bar and prescribes a drying or curing regimen prior to heating. Carbon refractory specimens, C436, are cut out of larger stock and are 3" x 1.5" x 1.5". Procedure C605 is like C113 except for the specimen shape; this is cut out of a pre-formed teeming-ladle nozzle or sleeve, to which that procedure is solely dedicated.

Basically these procedures call for (a) an initial length measurement; (b) heating under prescribed support at a prescribed rate in a prescribed oxidizing atmosphere (reducing in the case of carbon, C436) to any of a set of listed holding temperatures; (d) soaking there for a minimum of 5 hours (24 hours in the case of IFB, C210); (e) slow furnace cooling; and (f) remeasuring the length. The heating rates and soaking temperatures are indexed to certain refractory composition classes.[9] Details of all techniques are prescribed as well, and in C113 some statistics are given based on a comprehensive eight-laboratory round-robin program.

Similar standard procedures are in effect elsewhere, including the specification of sample dimensions in metric units. Such differences are trivial. What is important is that all members of a given industrial community use precisely the same version of this basically simple and reproducible routine. The result at a well-selected temperature unquestionably correlates with behavior in the field.

SPECIFIC HEAT

The specific heat, c, defined by $dH = cdT$ with H = heat content per gram, is needed with the bulk density ρ_b as a component of the thermal diffusivity for analysis of thermal transients in refractories (Chapter IV). With or without ρ_b, the specific heat figures in the computation of the "thermal mass" of a lining in the cyclic operation of a batch or periodic vessel between two fixed temperatures. One example is traced out in Chapter IX.

Multiplied by the formula weight of a substance, specific heat is converted to the molal *heat capacity at constant pressure*, here denoted by C_p. This fundamental thermodynamic property has the units of J/(mol·K) and remains defined by $dH = C_p dT$. Now, however,

H is the molal *enthalpy.* It is instructive to dwell on C_p, because this property provides the best data for the specific heat of refractories.

Heat Capacity of Solid Substances

Lattice Heat Capacity. Quantum theory shows that $C_p = 0$ at zero K, and the simple thermodynamics of atom vibration in solids gives $C_p = 3nR$ at high temperatures. Here n is the total number of all atoms in the formula. The initially rapid rise of C_p with increasing T above absolute zero is stepwise (i.e., quantized). Far below room temperature, C_p becomes a continuous variable as the allowable energy states of a solid proliferate and ultimately overlap. But its value still falls well short of 3nR at room temperature, because the allowed atomic vibrational energy states are still proliferating with increasing T. One might then expect to see C_p rising with T above room temperature and moving asymptotically toward 3nR at typical refractory use temperatures.

Often enough, this behavior is actually seen. Figures XI-2a, b, and c give measured C_p data vs T(°C) for various solid substances: simple (binary) oxides in Figure XI-2a, complex (ternary) oxides in Figure XI-2b, and selected nonoxides of interest in Figure XI-2c. The data are drawn from Vols. 4 and 5 of Reference 32. In Figure XI-2a there are three oxides of n = 2 (6R = 50), two of n = 3 (9R = 75), and three of n = 5 (15R = 125). Figure XI-2b presents two ternary oxides for which again 15R = 125, one for which 18R = 150, and a cluster of compounds for which 21R = 175. To understand all these curves better, one might first examine Figure XI-2c.

Metals. There the curves for the n = 2 compounds are well-behaved (6R = 50). But the two curves for mild steel and 18-8 stainless steel evidently march to a different drummer. For these the specific heat is plotted, using the right-hand ordinate scale, expanded so the upward concavity can be seen. On the C_p scale of the left ordinate, mild steel starts at about 10.6 J/(mol·K) at 0°C and reaches about 13. J/(mol·K) at 825°C. The SS curve starts and ends about half as high on the C_p scale. But why the upward concavity?

Specific heat data for elemental metals[11] show this feature only in the Transition Elements of the Periodic Table and a few others near them. It is thus a feature of the energy levels of underlying electron orbitals of the atom, not of the valence electrons or the lattice. As such, it might persist in the oxides of these elements, e.g., Cr_2O_3 or Fe_2O_3. In any event it represents a small and growing atomic heat sink superimposed over the lattice vibration energy at each temperature, hence an added contribution to C_p. It is important to know that this upward concavity of the C_p curve is not a property of the conduction electrons, present in all elemental metals at about one per atom. Conduction electrons per se do not add detectably to C_p.

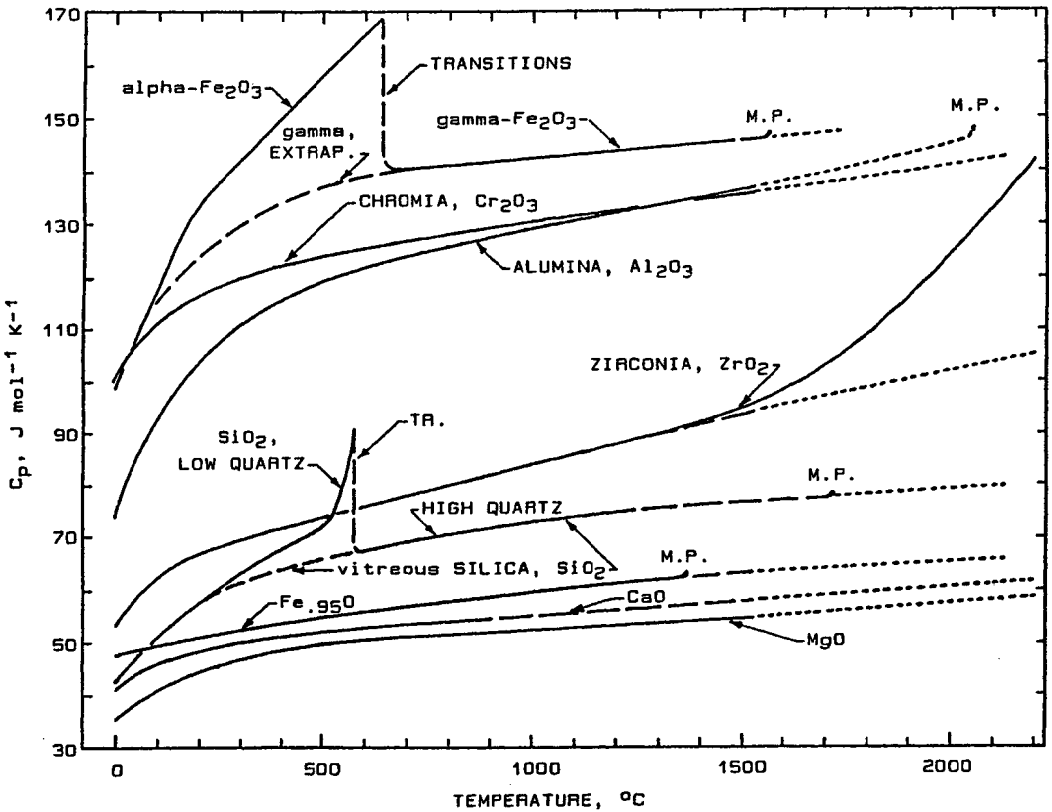

Figure XI-2a Molal Heat Capacity of Simple Oxides (Ref. 32)

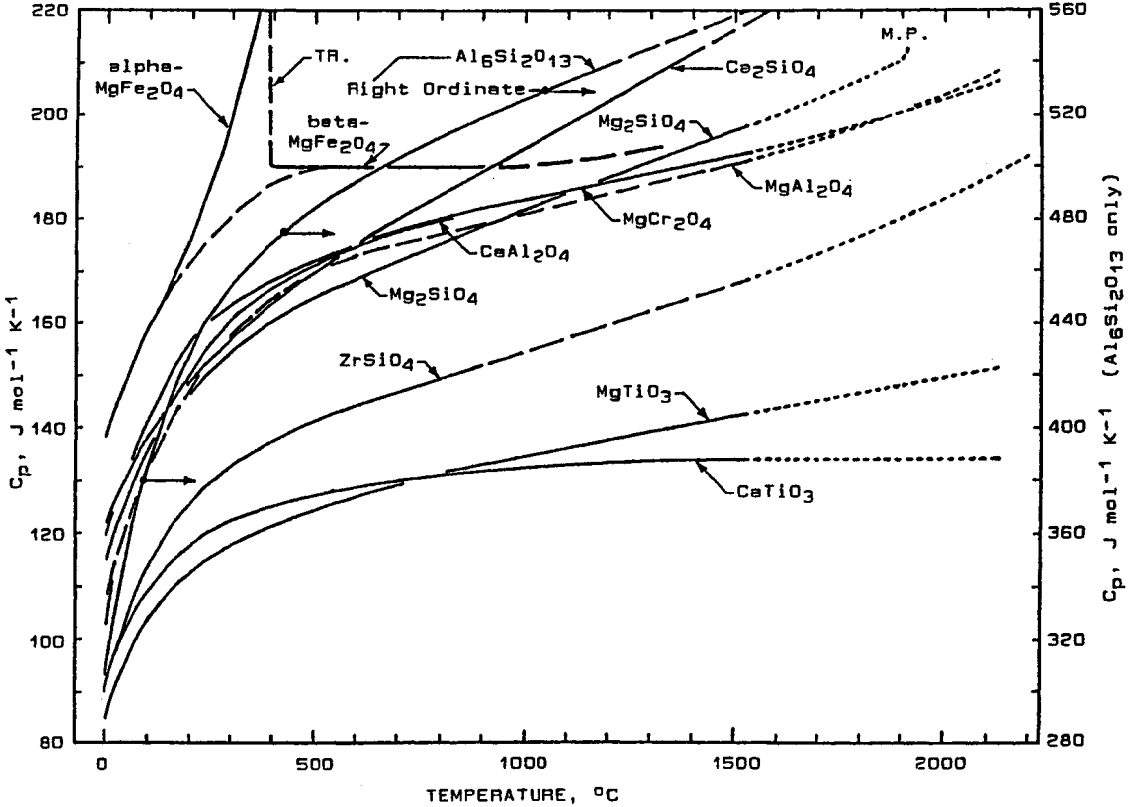

Figure XI-2b Molal Heat Capacity of Ternary Oxides (Ref. 32)

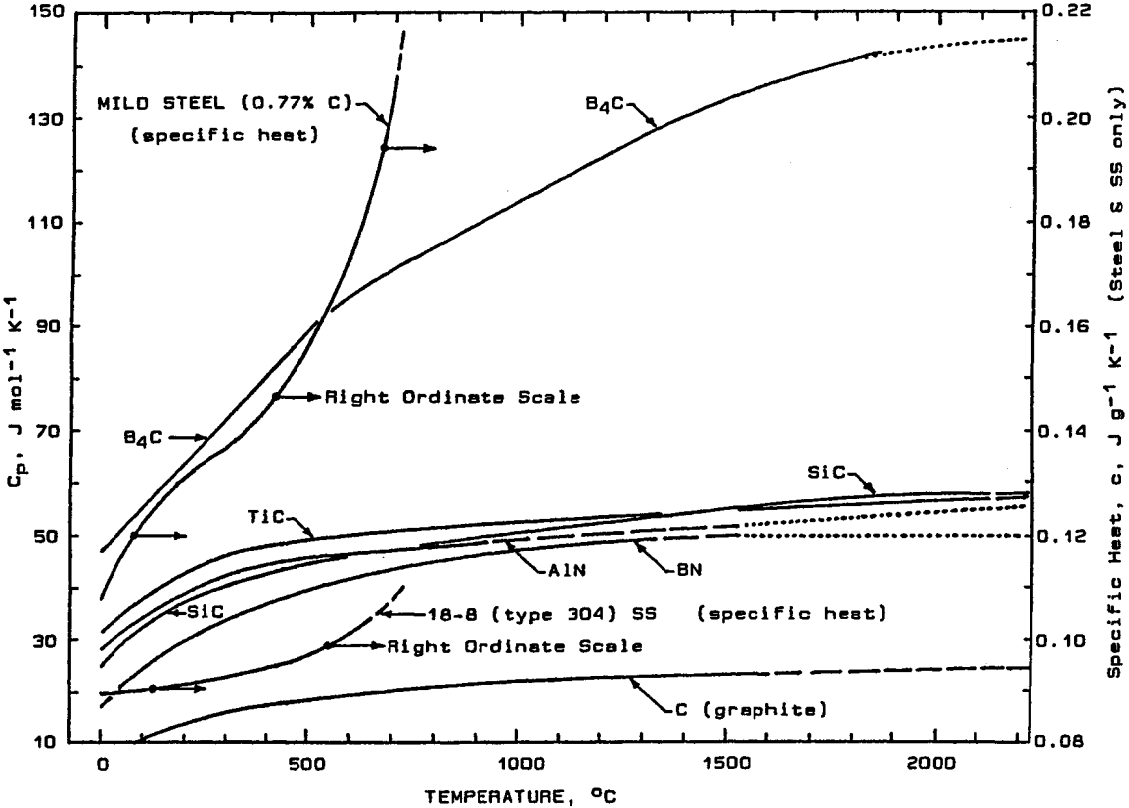

Figure XI-2c Heat Capacity of Various Nonoxides (Ref. 32)

Semiconductors. The curve for B_4C in Figure XI-2c is typical for high-temperature semiconductors, at least in that the C_p ultimately exceeds the fundamental lattice value of 3nR. This curve finally reaches about 16% above its 15R = 125.

Promotion of electron energies across the semiconducting "band gap" is endothermic and has to contribute to C_p; but the amount is probably small because the number of thus-produced conduction electrons (or "holes") is small. But all semiconductors exhibit *defect lattices*, containing either cation or anion vacancies or excess interstitial ions. It is believed that the additional contribution to C_p here arises mostly from additional allowed energy states of the defect lattice, which may be either configurational or due to added vibrational modes, or both. This observation is significant because a number of refractory oxides are important semiconductors. That is, they are distinctly *nonstoichiometric.*

Oxide Semiconductors. Returning to Figure XI-2a, C_p curves for two nonstoichiometric simple oxides are included: wüstite (FeO) and zirconia. The formula $Fe_{0.95}O$ for this wüstite is very close to the composition in equilibrium with iron. The C_p curve at the melting point is some 20% above the expected lattice value of ~50 J/(mol·K). Under controlled oxidizing conditions, wüstite in equilibrium with Fe_3O_4 is far more cation-deficient, reaching $Fe_{0.86}O$ at 1200°C.[21] The C_p curve for that composition is not known, but must lie well above the one shown here. Stoichiometric FeO does not exist.

The C_p curve for ZrO_2 in this figure was obtained in air. The Zr-O phase diagram for zirconia[21] shows a large but unknown cation deficiency in air, probably conservatively put at $Zr_{0.8}O_2$ at 1500°C. The composition in equilibrium with zirconium is substantially anion deficient, being about $ZrO_{1.8}$ at 1500°C.[21] Zirconia is a well-known high-temperature semiconductor. Titania is too, its composition at 1200°C ranging from an anion-deficient $TiO_{1.9}$ to substantially cation deficient in air.[21]

The zirconia curve in Figure XI-2a, running about 25% above the reference lattice value of C_p at 1500°C, reflects the additional heat content of the defect lattice. The further upward curvature above this temperature indicates still another large endothermic change. Contrast ZrO_2 with SiO_2, whose C_p is less than 3% above the expected lattice value at its melting-point.

CaO, MgO, Al_2O_3, Cr_2O_3 and Fe_2O_3 are all near-stoichiometric in air at all temperatures.[21] The excess of C_p over the expected value in the last two cases probably lies at least partly in atomic energy levels, as indicated previously. Plausible explanations for the first three are not immediately evident, but there are yet several aspects of lattice thermodynamics beyond those we have explored.

Additivity of Heat Capacity Per Atom Among Oxides.

Figure XI-2b describes compounds whose formulas are, in a strictly formal sense, the addition products of pairs of binary oxides. If each binary oxide of a pair exhibits only lattice heat capacity and obeys $C_p \rightarrow 3nR$, and if their addition product also exhibits only lattice heat capacity and obeys $C_p \rightarrow 3nR$ with $n_{AB} = n_A + n_B$, then clearly $C_{AB} = C_A + C_B$. That is, the heat capacity *per atom* is the same regardless of their manner of chemical combination and regardless of the crystal types of compounds A, B, and A-B.

A practical question arises: Does this additivity persist when there are further contributions to the heat capacity in either or both of binary compounds A and B? Compare the curves for $MgTiO_3$ and $CaTiO_3$, for example. Both MgO and CaO give asymptotic C_p curves (Fig. XI-2a), while from the semiconducting similarity between ZrO_2 and TiO_2 one has to infer that the curve for the latter exhibits a positive slope. Yet the C_p curve of $MgTiO_3$ is faithful to that positive slope while C_p of $CaTiO_3$ is asymptotic. On the other hand, at the point of their maximum measured divergence (1500°C) these two curves are less than 6% apart, and much closer at all lower temperatures. Would the assumption of additivity create a grievous error? Probably not.

One then tests the question where there are full sets of data. We have done this for each of the ternary compounds of Figure XI-2b, computing ΣC_p for the binary compounds and comparing the sum with C_p of the addition compound at temperatures of 0°, 500°, 1000°, and 1500°C. This comparison for mullite is: $3\ C_p\ (Al_2O_3) + 2\ C_p\ (SiO_2) - C_p\ (Al_6Si_2O_{13})$. The differences expressed as percent of the measured mullite C_p at the four listed temperatures are +1.6, +1.4, +1.0, and +0.7%, respectively. The corresponding differences for $ZrSiO_4$ are -1.7, +1.5, +1.6, and +2.7%.

The largest discrepancy is for Ca_2SiO_4: -11% at 1500°C and -5% at 1000°C. In all other cases the agreements are similar to the above two examples, or better.* The C_p data of of Figure XI-2a, for binary oxides considered as *components*, may thus be a powerful tool for computing the heat capacities of oxidic refractories by additivity.

---

*Note that each of the C_p differences examined above is the ΔC_p of a chemical reaction between two simple oxides. If $\Delta C_p \approx 0$ over a considerable temperature range, then over that same range $\Delta H°$ and $\Delta S°$ of that reaction are both nearly constant. The interested reader may want to consult the JANAF[23] or similar thermochemical tables. It is reasonable to attribute the discrepancy for Ca_2SiO_4 to the fact that CaO is the strongest of all refractory bases and SiO_2 is the strongest of all refractory acids. So founded, this discrepancy will not be repeated elsewhere.

The same is true of the nonoxide data of Figure XI-2c, useable for both nonoxide refractories and oxide-nonoxide composites. Since C_p is utterly independent of porosity, both working and insulating refractories may be treated identically.

What is at issue in the above is economy in the use of knowledge. The data presented in these figures were obtained by calorimetry, the most precise method available for determining thermochemical quantities -- and also by far the most tedious and demanding. A method somewhat commonly employed in refractories laboratories is the "hot wire" method,[386] which is able to yield k, δ and c (hence C_p) simultaneously vs T, given ρ_b of a refractory specimen. Neither this nor any other transient method can approach the precision of calorimetry in determining C_p . Hence if additivity of C_p in complex compound formation has been demonstrated within a reasonable error allowance, it is far more efficient to compute C_p for a refractory (and the specific heat from it) than to measure it.

For a simple example of the computation, suppose the heat capacity of stoichiometric cordierite is wanted but cannot be found. One writes: $2MgO + 2Al_2O_3 + 5SiO_2 = Mg_2Al_4Si_5O_{18}$. Then for each of a set of temperatures of interest for plotting, one sums: $2C_p\ (MgO) + 2C_p\ (Al_2O_3) + 5C_p\ (SiO_2) = C_p\ (Mg_2Al_4Si_5O_{18})$, using the data of Figure XI-2a for each of the binary compounds. At each temperature the specific heat of cordierite is obtained from the thus-computed C_p by dividing by the formula weight.

The same methodology applies to any complex refractory composition, whether its phases are identified or not. What is required is its *complete* chemical analysis in terms of component oxides. The computation can be no better than the chemical analysis, which must accordingly be confirmed as accurate. A wt.-% analysis cannot be transformed to mol fractions unless it adds up to 100.0%, hence any discrepancy in the summation of analyses has to be removed.

The transformation to mol fractions is best illustrated by an example. Take a mag-chrome refractory of 54.0% MgO, 22.5% Al_2O_3, 12.8% Cr_2O_3, 5.8% Fe_2O_3, 4.1% SiO_2, and 0.8% CaO. The sum of these is 100.0%. Now on a 100 gram basis, divide each weight of component oxide by its formula weight to convert grams to mols, sum these, and divide each by that sum to yield mol fraction:

	MgO	Al_2O_3	Cr_2O_3	Fe_2O_3	SiO_2	CaO
Wt. in 100 g:	54.0	22.5	12.8	5.8	4.1	0.8
Formula Wt.:	40.31	101.96	152.00	159.70	60.09	56.08
Mols in 100 g:	1.3396	0.2207	0.0842	0.0363	0.0682	0.0143
Total Mols: 1.7633						
Mol Fraction:	0.7597	0.1252	0.0478	0.0206	0.0387	0.0080
Total (check): 1.000						

Mock Formula:
$0.7597MgO{\cdot}0.1252Al_2O_3{\cdot}0.0478Cr_2O_3{\cdot}0.0206Fe_2O_3{\cdot}0.0387SiO_2{\cdot}0.0080CaO$
Mock Formula Wt.:
100.0/1.7633 = 56.71 g/mol of mock formula

One then proceeds to obtain C_p and $C_p/56.71 = c$ for this composition, at each temperature of interest, precisely as was done in the preceding example for cordierite. If the refractory composition is thermally stable (free from H_2O, CO_2, SO_2, etc.), this should be the most precise specific heat obtainable other than by calorimetry. If not thermally stable, then the refractory should be appropriately ignited and re-analyzed. Evaporation of volatiles, in particular, will create spurious dH/dT effects over the temperature range where it occurs.

Table XI.2 gives the analytical function for every C_p vs T curve of the substances identified in Figures XI-2a, b, and c. Temperatures are in kelvin. Every function is the same: $C_p = a + b(10^{-3}T) + c(10^{-3}T)^2 + d(10^{-3}T)^{-1}$. Table XI.2 gives the best-fit values of a, b, c, and d. The few spikes in the curves, caused by transitions, have been circumvented by extrapolating through them. No other way of determining the specific heat of refractories can be recommended at this time, except by direct calorimetry.

Once the specific heat has been determined as above in J g^{-1} K^{-1}, the worker preferring English units can convert by using the factor, 1 J g^{-1} K^{-1} = 0.2389 Btu lb^{-1} $°F^{-1}$.

THERMAL CONDUCTIVITY

Elements of Heat Conduction in Solids

Much of the introduction to specific heat in the preceding section serves also to introduce the complex subject of transport of heat in solids. We shall take up conduction electrons first.

Electronic Conduction in Metals. An elastic-particle collision model can show that the partition of heat energy between

Table XI.2 Molal Heat Capacity of Solid Substances (Ref. 32)

C_p (J mol^{-1} K^{-1}) = a + b(10^{-3}T) + c(10^{-3}T)^2 + d/(10^{-3}T) (T in K)

	Formula Weight	a	b	c	d	NOTE
Al_2O_3	101.96	+154.96	- 16.168	+ 7.120	-20.817	
CaO	56.08	+ 57.68	- 1.324	+ 1.560	- 4.418	
Cr_2O_3	152.00	+137.14	- 3.568	+ 3.120	- 9.585	
Fe_2O_3	159.70	+176.70	- 24.000	+ 7.200	-19.843	1
$Fe_{.95}O$	69.06	+ 45.31	+ 14.900	- 2.600	- 0.374	2
MgO	40.31	+ 63.24	- 7.632	+ 2.880	- 7.263	
SiO_2	60.09	+ 77.09	+ 3.384	- 0.160	-10.558	3
ZrO_2	123.22	+ 60.88	+ 22.320	- 1.600	- 3.370	
$Al_6Si_2O_{13}$	426.06	+607.83	- 42.752	+22.880	-81.020	
$CaAl_2O_4$	158.04	+236.00	- 39.240	+14.360	-32.120	4
Ca_2SiO_4	172.25	+182.73	+ 3.768	+11.680	-17.372	
$CaTiO_3$	135.96	+149.08	- 2.916	- 0.360	-15.051	
$MgAl_2O_4$	142.27	+233.16	- 39.244	+14.360	-32.124	4
$MgCr_2O_4$	192.31	+212.76	- 18.404	+ 8.360	-24.261	
$MgFe_2O_4$	200.01		See Figure.			5
Mg_2SiO_4	140.71	+191.48	- 4.236	+ 8.040	-21.790	6
$MgTiO_3$	120.19	+145.39	- 3.128	+ 3.520	-15.949	
$ZrSiO_4$	183.31	+179.94	- 21.380	+12.200	-22.838	
AlN	40.99	+ 61.68	- 7.344	+ 2.560	- 8.911	
B_4C	55.25	+ 35.55	+ 86.508	-16.920	- 3.145	
BN	24.82	+ 37.02	+ 19.324	- 5.560	- 6.814	
SiC	40.10	+ 55.08	- 0.876	+ 2.040	- 8.312	
TiC	59.89	+ 65.44	- 7.964	+ 2.760	- 8.911	
C (graph.)	12.01	+ 18.37	+ 8.592	- 2.480	- 3.969	7
Mild Steel (0.77% C)			See Figure.			8
18-8 (type 304) SS			See Figure.			8

NOTES:
1- Constants fit gamma-Fe_2O_3. Tr. ~630°C; m.p. 1565°C.
2- Melting point 1369°C.
3- Constants fit high-quartz. Tr. ~577°C; m.p. 1723°C.
4- Constants est. as sum of CaO+Al_2O_3 & MgO+Al_2O_3, resp.
5- Constants not det'd.; see Figure. Tr. ~390°C.
6- Melting point 1910°C.
7- No "reference" non-grephitic carbon exists.
8- See Figure. Note curves give specific heat, c, in J g^{-1} K^{-1}.

vibrating metal atoms and their mobile conduction electrons cannot favor the latter. But the *rate* of exchange of energy between an atom and its surrounding conduction-electron "sea" in metals is very rapid, while the rate at which energy is transferred from a hotter to a cooler region within the sea is likewise rapid: much faster than through the lattice. One needs only to regard the ratio of room-temperature thermal conductivities of a good metal and a good nonmetallic element to be convinced. This ratio is about 100:1 between Cu and C, and about 500:1 between Al and S.

The high atom-electron energy exchange rate and electron-electron energy transport rate can be explained, again using a particle model, because the mobile electrons "are so light, hence move so fast." Wave mechanics gives a better explanation, particularly when it comes to describing the decrease in thermal conductivity that occurs with increasing temperature whereas the electrons "move even faster." The better picture of the electron sea is one of harmonic waves, moving constantly in all directions and of constant average amplitude in an isothermal metal body. In a thermal gradient there is a net movement of energy from hotter to cooler because returning waves start out at lesser amplitudes. These waves interact with the disturbances in their space (viz., lattice atoms), constantly exchanging energy with them; hence every atom participates instantaneously in the absorption and generation of wave energy by virtue of its own vibrational motion and its incessant electromagnetic bombardment by the sea.

In a gradient (and for that matter, at uniform temperature), wave and hence energy movement is facilitated by regularity of the disturbances in the medium. Every discontinuity creates reflections or *scattering*, hence diversion of electron waves. Scatterers include solid-solution atoms of different size or different bond energies, all types of crystal imperfections, foreign particles, crystal boundaries -- all discontinuities of whatever magnitude. In particular, the random thermal vibrations of lattice atoms are irregularities in the wave-space and hence are scatterers. As atomic vibrational amplitude increases with increasing temperature, the interference with harmonic waves increases. Since those waves are the agency of energy transport in a gradient, increased scattering increasingly impedes that transport. This is basically why the electronic thermal conductivity of elemental metals decreases monotonically with increasing temperature.

Semiconduction. Semiconductors obey like rules, except the conduction electron (or "hole") waves are less concentrated by virtue of a lower density of these carriers. Electronic conduction of heat is proportional first of all to the population density of carriers, which is a variable in semiconductors but relatively fixed (and high) in metals. The carriers themselves have to contain enough thermal

energy to escape the fixed lattice sites in which they are born or trapped -- not entirely unlike the "escape velocity" of a space vehicle, required for it to leave an earth orbit. The escape velocity or required excitation energy of an electron is quantized, however, in terms of a forbidden "band gap" between bound-electron energies and the allowed energy levels in the conduction-electron sea. There is an intricate statistical relationship among the height of that band gap (which differs for each substance), the temperature, and the fraction of eligible electrons or holes which occupy the conduction band.[15]

The population of carriers increases with increasing temperature, but is significant only above some threshold T. Accordingly, it is not uncommon among high-temperature semiconductors to see a minimum or "turnaround" in thermal conductivity at some temperature above ambient. An increase in conduction above this minimum denotes rapid growth of the carrier population. At temperatures much below this minimum there are so few carriers that all that is seen is lattice-atom conduction.

Lattice Conduction. Heat conduction by lattice atom vibration is common to all solids. It is also a wave phenomenon, but of the slow, lumbering characteristics associated with acoustic frequencies and velocities. In respect to intrinsic conductivity, the atomic weight matters: "light atoms move (i.e., vibrate) more quickly." Bond lengths and strengths also matter: these are the Hookeian spring constants that also govern frequency. But among refractory compounds their variety is much less evident than the effect of atomic weight. Among simple oxides, it is foreseeable that lattice thermal conductivity should decrease in the order: BeO, MgO, Al_2O_3, SiO_2, CaO, ZrO_2, HfO_2, ThO_2, UO_2.

Lattice waves, being akin to sound waves, are called *phonons*. They are subject to basically the same rules that govern conduction-electron waves, but in a different region of wavelengths and frequencies. Lattice regularity again favors more rapid energy movement down a gradient. As example, the room-temperature thermal conductivity of quartz is about 20 times that of vitreous silica in spite of wave-scattering grain boundaries[58] in the former. As an interesting aside, phonons moving in a vitreous medium are further scattered on encountering local atomic order,[32] just as phonons in a lattice are scattered by regions of disorder.

Scattering of phonons by random lattice-atom vibrations is also in effect, also increasing with temperature. In fact, in nonconductor oxides there is a temperature region over which the thermal conductivity is theoretically proportional to 1/T: identifiable in a plot of k vs 1/T or of log k vs log T. Sometimes this region is indistinct or not discerned at all because thermal scattering is overshadowed by impurity or particle scattering.

Radiant Heat Transport. Finally, all solids interact with radiant energy. All hot body surfaces emit radiant energy at a total rate per unit area summed over all wavelengths according to the law, $E_e = KT_e^4$ (T_e in kelvin). The process of radiation emission by solids involves (a) the excitation of an electron by collision of vibrating atoms of the solid; and (b) falling-back of the electron to its normal energy state, the energy difference appearing as a quantum of radiation, $h\upsilon$ (h = Planck's constant). The frequency υ relates to the wavelength of the radiation, λ, by $\upsilon\lambda = c$ where c is the velocity of light.

Only the outermost (generally, valence shell) electrons of an atom, and especially conduction electrons, can be excited to low-overlying energy states and essentially to a continuum of these. As a body temperature is increased, the first excitations seen are of the most easily-excited electrons and to the lowest overlying levels, and the resulting radiation is of the smallest υ and the longest (infrared) wavelengths. With increasing body temperature the average energy of collisions and of excitations increases, while these are statistically distributed over a continuum of ever-shortening average emitted wavelengths. Once the visible part of the spectrum is reached, the "color temperature scale" of Figure II-1 becomes descriptive. Meanwhile the radiant energy *flux* rises proportional to T^4.

The least-disturbing medium for a radiant quantum, once emitted, is vacuum or a gas, wherein the likelihood of encounter with another atom is extremely small. We are more concerned with the fate of a quantum when it encounters another solid, a refractory in particular. There it can be (a) reflected, (b) absorbed, or (c) transmitted; generally in the aggregate, some of each.

Transmission through a solid, calling for minimal absorption, results in high apparent thermal conductivity which increases rapidly with temperature as the proportion of heat transport by this mode increases. This characteristic is seen, for example, in vitreous silica and pure coarse-crystalline colorless oxides such as quartz, alumina, magnesia and beryllia; also in large single crystals of the same. But it tends to surpass other heat-conduction modes only at high source temperatures. Its high flux dependency on temperature identifies it; this can be disclosed by a log *k* vs log T plot of measured thermal conductivity. That dependency distinguishes radiation transmission from semiconduction.

Reflection from the front face of a solid simply sends the radiation elsewhere. This is virtually never total in the aggregate. Internal reflection (e.g., at grain boundaries) in a substantially transparent solid is of greater interest. Scattering by internal reflections[58] has the effect of increasing the transmission path length, which increases the statistical probability of an absorption event.

Absorption of a quantum is exactly the reverse physical process of its emission. As the absorbing solid makeup and its temperature can differ from those of the emitter, the parameters may change but have quite the same effects on the process. The most efficient absorber is the conduction-electron sea of a metal; next, that of a semiconductor. Next is a dark-colored material: color is evidence of absorption of radiation by valence-shell or near-underlying atomic electrons. Materials of these kinds are the most opaque to thermal radiation, which accordingly penetrates but little into the solid and deposits its energy into the surface and immediate subsurface atoms as sensible heat.

Meanwhile, if the temperature of the absorbing solid is high enough, it too becomes an emitter and by the same T^4 rule. Thus if two hot solid walls face each other in a furnace but one is cooler than the other, the *net* radiant-energy flux between them is governed by the Stefan-Boltzmann Law:

$$E_{net} = E_e - E_a = K(T_e^4 - T_a^4) = K_1 T_e^3 \Delta T \quad * \qquad (\Delta T = T_e - T_a).$$

The isolation of E_{net} as almost the sole heat flux to a refractory lining can occur in radiant-heated (hence, electrically-heated) vessels. This isolation also occurs within a close-set charge on a kiln car, where radiant heat transport (between, say, bricks being fired) becomes the only means of bringing the entire charge to uniform temperature. This is why open setting is usually preferred. But the T^4 dependency of the radiation transport rate makes this mode quite efficient at very high temperatures. Refractory bricks being fired at the order of 1800°C and up are usually close-set, taking advantage of this fact and greatly increasing the kiln capacity.

Porosity or Void Space. At low temperatures the conduction of heat through a gas is governed by molecular collisions which exchange kinetic energy; by molecular velocities, whose mean-square is proportional to temperature but inversely proportional to molecular weight; and by the "mean free path" between collisions, which varies inversely with gas pressure but depends on other factors as well, including molecular size. At a fixed pressure of 1 atmosphere, gas conductivity always increases with increasing temperature; but for common gases it starts out very low at room temperature, being of the order of 1/3,000 that of dense magnesia or

---

*The "emissivity" and "absorptivity" of a solid (one and the same, but highly dependent on wavelength) have been omitted in this discussion for simplicity. No quantitative description of radiant energy transport can be obtained without knowledge of this parameter.

alumina and 1/8,500 that of graphite. By 700°C, common-gas conductivity is about 0.006 that of MgO or Al_2O_3 and about 0.0008 that of graphite.

Hence the pores in a refractory conduct but little, while in working refractories most of the heat flow is through the solid. In cellular insulating refractories heat conduction is mixed. In low-mass fiber refractories the solid phase contributes but little. In the last-named type, convection of the gas also becomes important, raising the effective gas conduction.

By 1000°C and above, radiant heat transport across pores dominates the apparent conductivity of the gas. The insulating quality of high-void-volume refractories is severely diminished at temperatures approaching 1500°C or 2700°F, by radiation transport.

Thermal Conductivity of Dense Solid Substances

Thermal conductivity, k, is defined by $J = -k(dT/dz)$, or $= -\bar{k}(\Delta T/Z)$ at steady state. Thermal conductivity measured by measuring two different temperatures in a uniform body a distance Z cm apart in the direction of plane heat flow: (a) requires that the flux J be known in watts/cm^2 (recalling that a watt is a joule per second); (b) gives an average $\bar{k}$ over the temperature interval T_2-T_1 that has then to be interpreted into point values as a function of T; and (c) represents *all* modes of heat transport that are operating in the material. So obtained, k has the units of (watts/cm^2)/(K/cm) or watt cm^{-1}K^{-1}, or equally watt cm^{-1}°C^{-1}.

The data in this section are drawn from Vols. 1, 2, and 3 of Reference 32, representing the best reference materials available prior to 1970. In necessary cases, the given k values are corrected by small margins to zero porosity, using standard approximating methods. Carbon and graphite data could not be corrected, however.

The first data set, plotted as log k vs log T in kelvin to disclose telltale slopes, is presented in Figure XI-3. The short-dashed extrapolations are ours. The characteristics of these log-log plots make it possible to identify the principal operating heat transport modes in two or more temperature domains per the prior discussion, and to relate these to each type of substance studied. Taking these curves in order from the top of the figure down, they are interpreted as follows. The code used is : D = dominant, M = minor, P = possible, Q = questionable, U = undetected, N = none. There is room in a few cases for alternative interpretations:

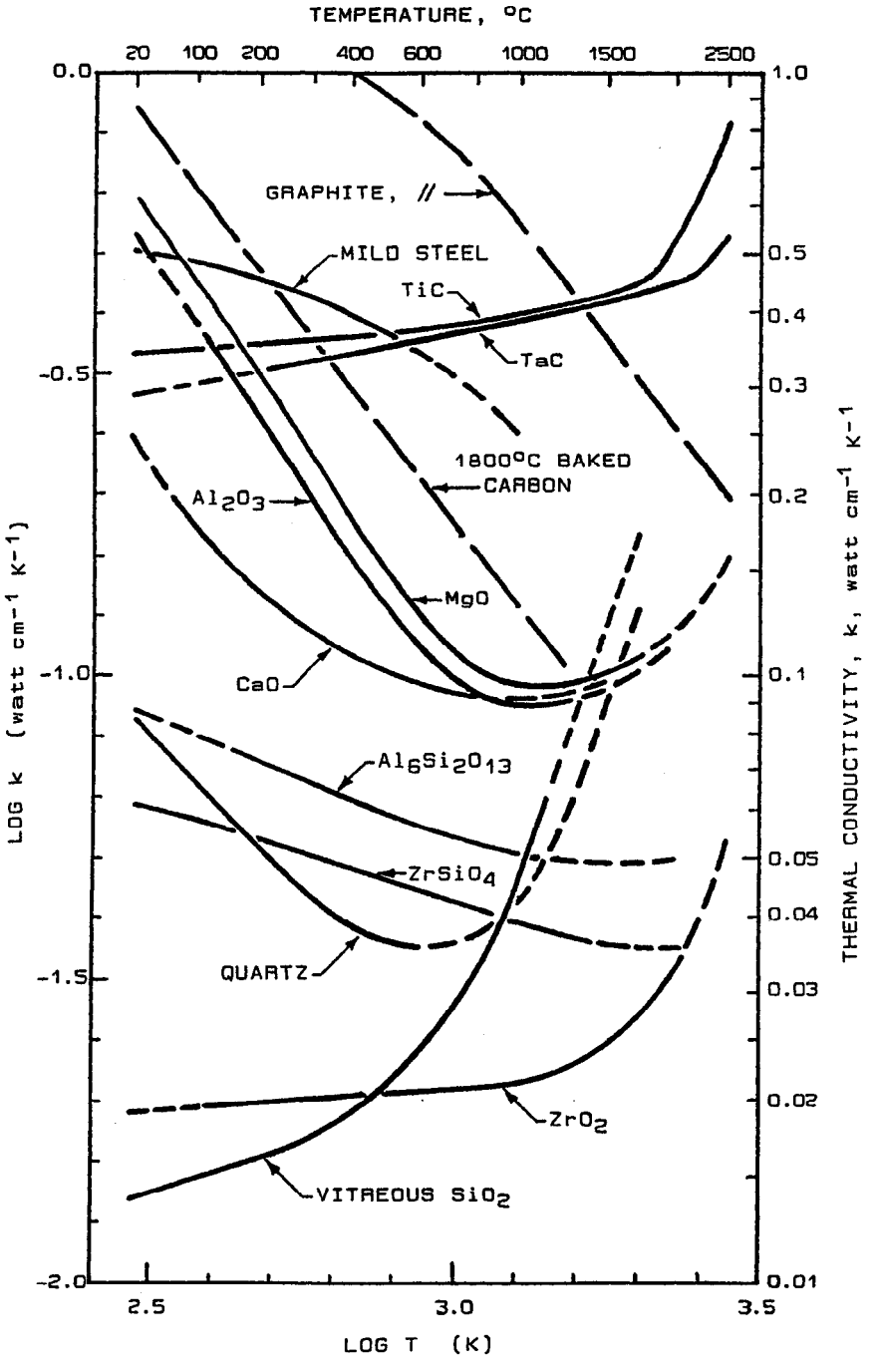

Figure XI-3 Log k vs Log T for Dense Substances (Ref. 32)

	Low T Lattice	Semi-Conduction	Metallic-Electronic	High T Radiant
Graphite	D	U	U	N
Hi-baked Carbon	D	U	U	N
Mild Steel	U	N	D	N
TiC, TaC	U	D	U	N
MgO, Al_2O_3	D	U	N	P
CaO	D	P	N	Q
$Al_6Si_2O_{13}$, Mullite	D	P	N	U
$ZrSiO_4$, Zircon	D	P	N	U
SiO_2, Quartz	D	U	N	D
Vitreous SiO_2	M	U	N	D
ZrO_2	M	D	N	D

None of the classical lattice conductors shows exactly the classical -1 slope. Quartz is close at -1.11; MgO and Al_2O_3 exceed it at about -1.15; the lime curve may start out close but is an enigma (likely due to pre-carbonation of the specimen); and the porous carbon and graphite are low at about -0.75. Mullite and zircon appear to be mixed lattice and semiconducting, while TiC, TiN, and ZrO_2 are clearly semiconducting.

Vitreous silica turns early, by hard data, into a transmitter of radiation. Its terminal curve slope is almost exactly +3. Our extrapolation of the quartz curve is made on faith to look similar, while the alumina and magnesia curves have been turned up in extrapolation based on experience of our own of several decades ago. The upturn of the ZrO_2 curve, by hard data, also appears to be due to radiant energy transmission.

Figures XI-4a and b are plotted on more familiar coordinates: log *k* vs T°C. Again the dashed extrapolations are ours. The same oxide curves of Fig. XI-3 are repeated in XI-4a, and others added. The linear T scale gives all curves a different appearance, less revealing as to heat transport mechanisms. But this figure is a good reference collection for oxidic compounds.

In Figure XI-4b the previous curves for TiC and TaC are likewise transferred and a number of other nonoxide compounds added. These curves all show one aspect or another of semiconduction, with the exception of BN.

Figures XI-5a and b are also plotted on coordinates of log *k* vs T°C. The graphite curve is the same as that of Fig. XI-3. The two baked-carbon curves illustrate the dependence of this property on baking temperature and the approach of carbon toward graphite-like behavior by 1800°C. Carbon baked at 1100°C gives *k* values about

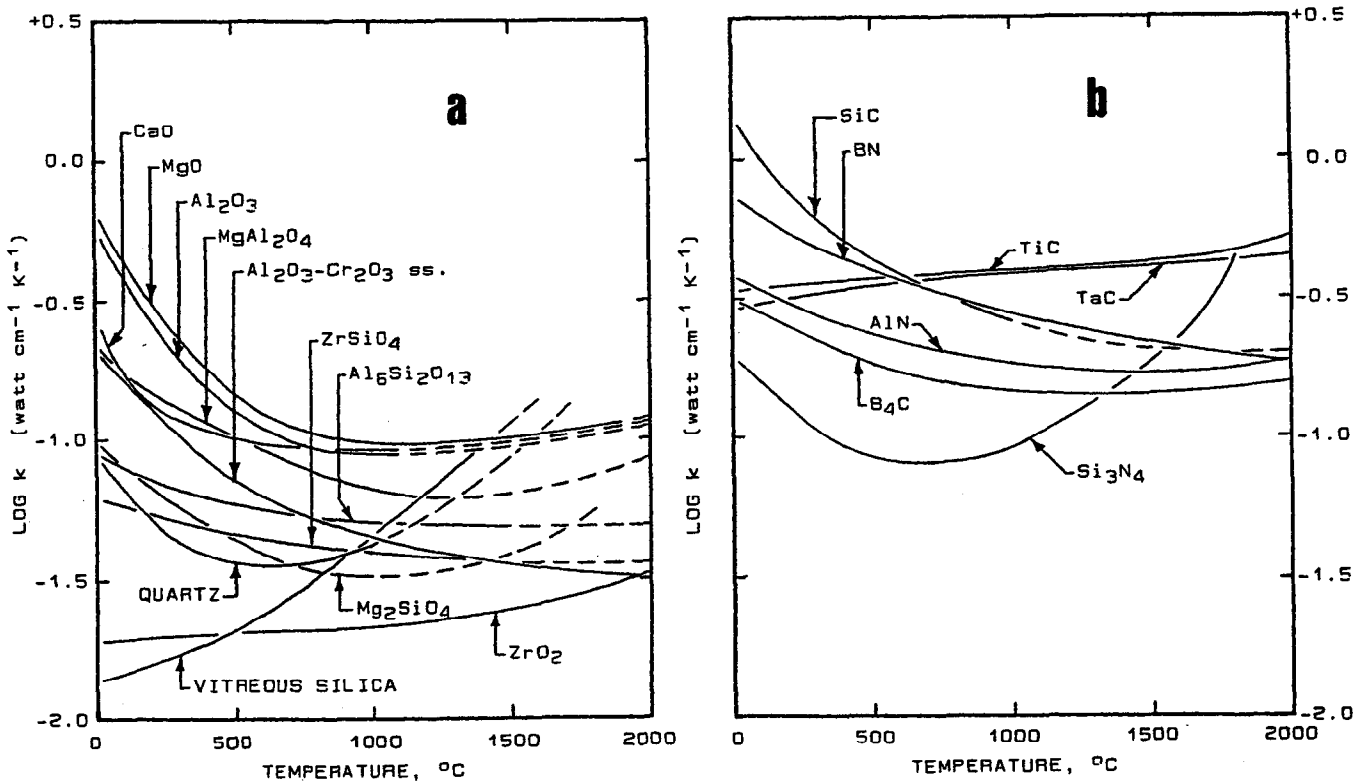

Figure XI-4 Thermal Conductivity of: a. Dense Oxides b. Dense Nonoxides (Ref. 32)

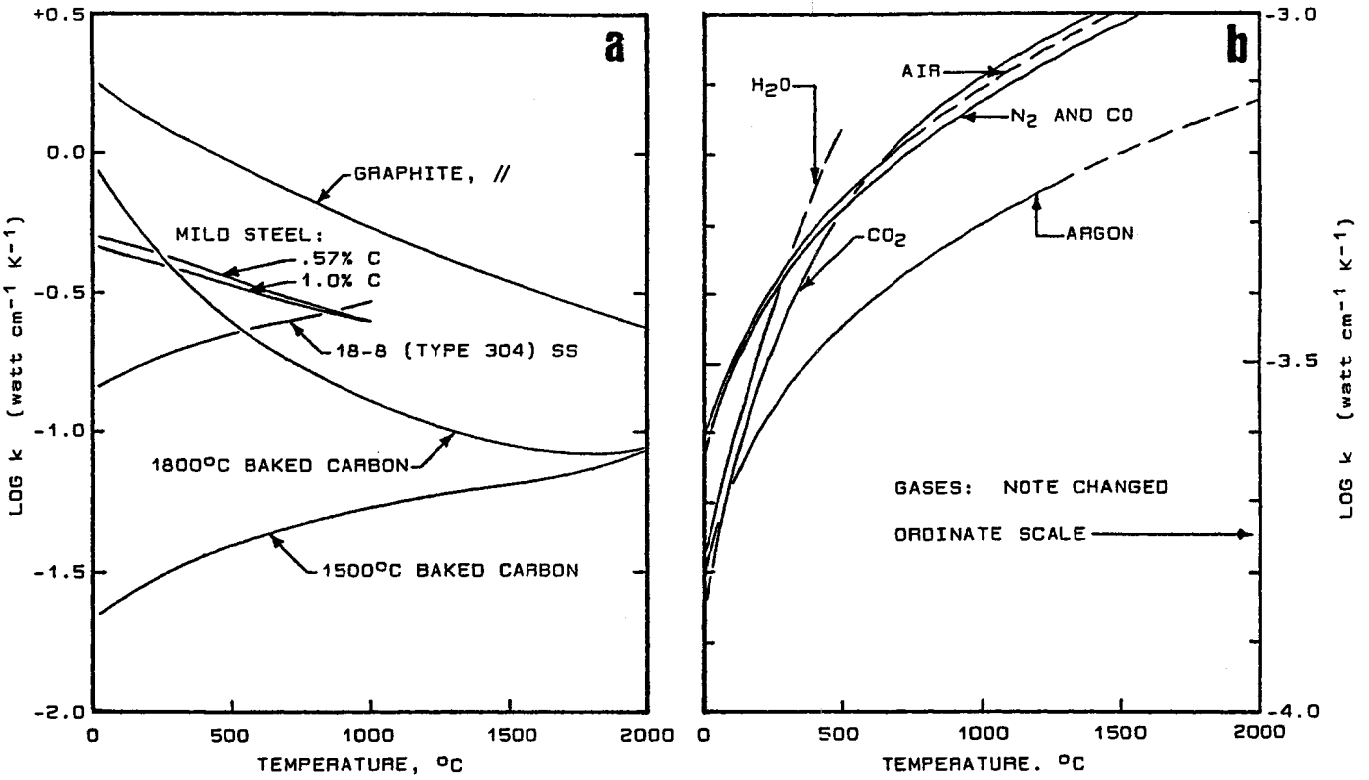

Figure XI-5 Thermal Conductivity of: a. Carbons & Steels b. Simple Gases (Ref. 32)

Table XI.3 Thermal Conductivity of Dense Solid Substances (Ref.32)

	DENSITY,[b] g cm^{-3}	THERMAL CONDUCTIVITY, k, watt cm^{-1} K^{-1}, AT TEMPERATURE IN °C [a]									
		20°C	200°C	400°C	600°C	800°C	1000°C	1200°C	1400°C	1600°C	1800°C	2000°C
Al_2O_3 (alpha)	3.97	0.537	0.266	0.156	0.110	.0933	.0891	(.089)	(.093)	(.096)	(.105)	(.112)
Al_2O_3-Cr_2O_3[c]	4.04	0.200	0.133	.0843	.0638	.0525	.0454	.0402	.0375	.0344	.0333	.0322
CaO	3.38	0.251	0.136	0.107	.0955	.0927	.0912	(.093)	(.095)	(.100)	(.106)	(.115)
MgO	3.58	0.617	0.310	0.182	0.124	0.104	.0968	.0955	.0989	0.102	0.110	(.119)
SiO_2 (quartz)[d]	2.66	.0843	.0525	.0383	.0355	.0367	(.041)	(.054)	(.072)	(.102)	(liq.)	
" (vitreous)[e]	2.19	.0137	.0160	.0189	.0238	.0320	.0452	.0708	(.097)	(.140)	(liq.)	
ZrO_2 (cubic)	5.89	.0191	.0197	.0202	.0206	.0209	.0213	.0222	.0233	.0255	.0285	.0328
$Al_6Si_2O_{13}$	3.16	.0875	.0721	.0619	.0562	.0531	.0509	.0497	.0493	(.049)	(.049)	(.050)
$MgAl_2O_4$	3.60	0.210	0.149	0.115	.0931	.0760	.0661	.0617	(.062)	(.066)	(.074)	(.085)
Mg_2SiO_4	3.21	.0942	.0673	.0501	.0390	.0336	(.033)	(.034)	(.036)	(.042)	(.056)	(liq.)
$ZrSiO_4$	4.56	.0610	.0537	.0479	.0441	.0414	.0391	.0375	.0364	(.036)	(.035)	(.035)
AlN	3.26	0.376	0.301	0.251	0.223	0.200	(.186)	(.173)	(.170)	(.172)	(.177)	(.185)
B_4C	2.52	0.309	0.251	0.203	0.170	0.156	0.148	0.143	0.142	0.146	0.150	0.156
BN	2.25	0.708	0.536	0.430	0.370	0.321	0.283	0.253	0.237	0.214	0.197	(.185)
SiC	3.22	1.318	0.759	0.518	0.389	0.310	(.262)	(.224)	(.211)	(.202)	(.200)	(.200)
Si_3N_4	3.44	0.188	0.129	.0925	.0822	.0832	.0912	0.117	0.158	0.224	(.447)	(liq.)
TaC	13.9	0.290	0.320	0.339	0.359	0.373	0.384	0.398	0.407	0.421	0.435	0.447
TiC	4.93	0.339	0.353	0.363	0.375	0.385	0.394	0.409	0.422	0.435	0.466	0.531
C (graph.), //[f]	Porous	1.738	1.324	1.035	0.836	0.671	0.562	0.447	0.380	0.324	0.273	0.238
" (1800°C) [g]	Porous	0.851	0.472	0.296	0.211	0.162	0.132	0.108	.0944	.0851	.0832	.0891
" (1500°C) [g]	Porous	.0224	.0293	.0362	.0422	.0475	.0531	.0582	.0617	.0668	.0733	.0851
Steel (.57% C)[h]	7.86	0.501	0.454	0.391	0.340	0.295	0.251	--	--	(liq.)		
Steel (1.0% C)[h]	7.86	0.456	0.406	0.372	0.331	0.293	0.251	--	--	(liq.)		
18-8 (304) SS [h]	8.02	0.145	0.178	0.210	0.236	0.264	0.290	--	--	(liq.)		
Cu (commercial)[i]	8.9	7.										

NOTES: a- Based on smooth curves through measured data. Parentheses enclose estimates.
b- Density measured at approx. 20°C. c- 6 vol.-% chromia, solid solution.
d- Data at 1600°C OK for cristobalite. e- Massive transparent silica glass.
f- Type AGOT, measured parallel to the textural "grain": For illustration only.
g- Molded coke, baked at 1800°C and 1500°C respectively: For illustration only.
h- Presumably austenitic heat-treated. i- Presumably annealed.

half those of the 1500°-baked material over this entire range of temperatures.[32]

The stainless steel curve in Figure XI-5a illustrates that the *k*-vs-T relation of metallic elements does not necessarily always hold for alloys. The curves for some common gases at 1 atm. pressure, given in Figure XI-5b, are included to complete the reference collection for substances and to provide a contrast with the thermal conductivity of solids.

Table XI.3 collects all of the above data for solid substances in a single reference, giving discrete *k* values at 20°C and at every 200°C above this to 2000°C maximum.

Thermal Conductivity of Dense Refractories

Unlike the heat capacity, the thermal conductivity of heterogeneous mixtures is intensely sensitive to variations in microstructure. The governing microstructural features being intimately dependent on processing and thus largely uncoupled from composition, there is no reliable "rule of mixtures" for thermal conductivity. One is reduced to measuring *k*, and to measuring it vs T.

Porosity is a wide-ranging variable, on which we shall isolate presently. Meanwhile it is productive to focus on dense working refractories. But "dense" is a relative term. It does not imply zero porosity, as was taken above for reference substances. Working refractories may range in apparent porosity from near-zero to well up in the twenties of percent. Under these circumstances it is impractical to normalize the data to full density.

Working Refractory Bricks. Few systematic studies of refractory thermal conductivity have been published, though every supplier possesses a storehouse of raw data. We shall be content with a few representative cases, displayed in a systematic manner. These displays are given in Figure XI-6a for some *basic refractories* and in Figure XI-6b for some *aluminous refractories.* The %Mg0 and the $\%Al_2O_3$, respectively, are assumed to be significant variables.

For plotting we have retained log *k* as the ordinate, but have adopted watts per meter per kelvin (or, °C) as the unit in place of the watt $cm^{-1}K^{-1}$ used in the preceding graphs and in Table XI.3. This conforms to much industry practice, and recognizes that *k* for refractories is on the whole well below *k* for pure reference substances. For the reader requiring English units of (Btu/hr) per ft^2 of area per (°F/inch), the conversion factor is: 1 watt $m^{-1}K^{-1}$ = 6.935 $Btu{\cdot}in.h^{-1}\ ft^{-2}\ °F^{-1}$.

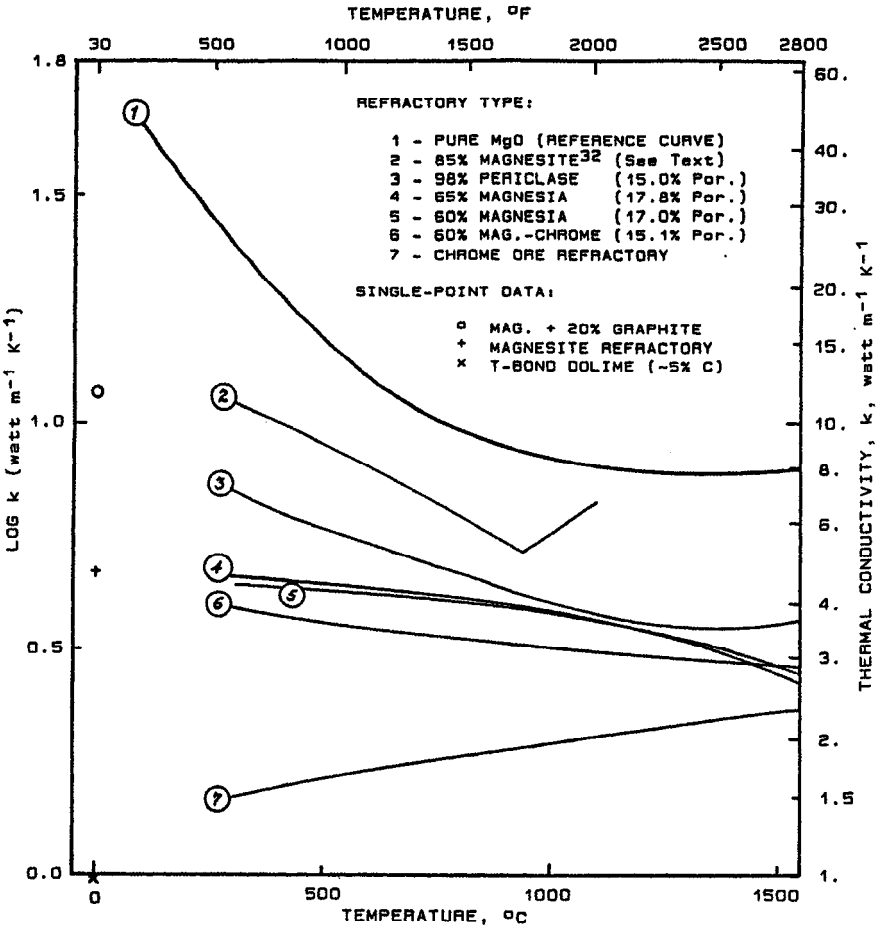

Figure XI-6a Thermal Conductivity of Basic Brick (Refs. 74, 76)

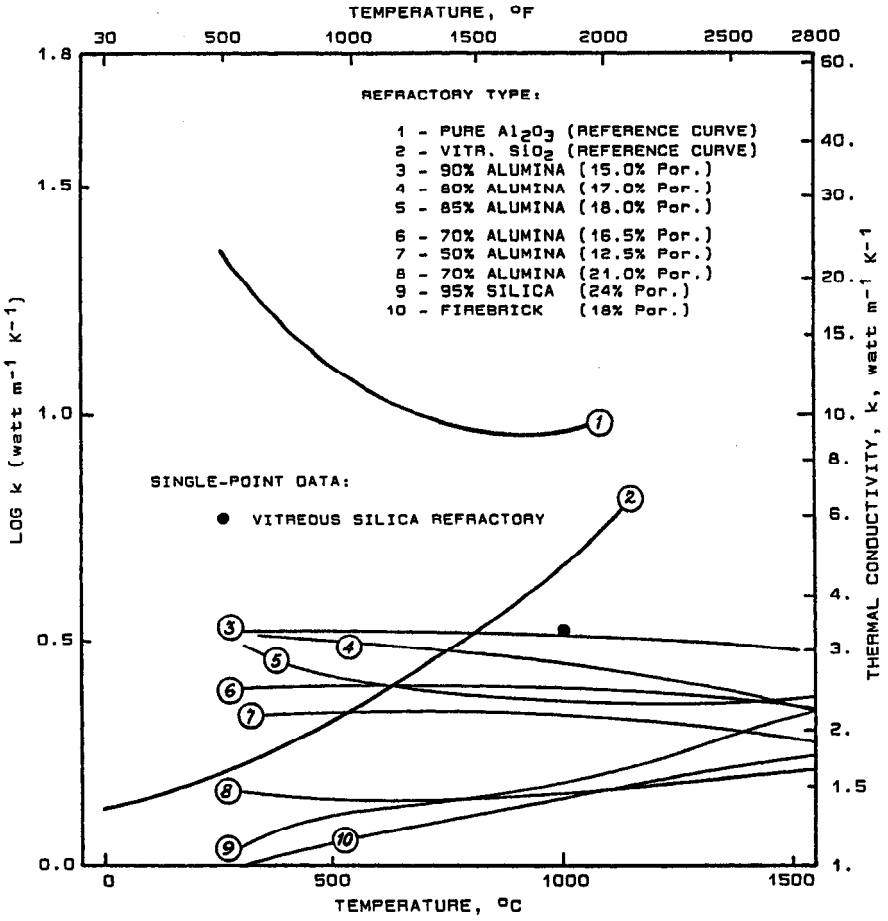

Figure XI-6b Thermal Conductivity of Aluminous Brick (Ref. 76)

The topmost curve in Figure XI-6a is the reference curve for MgO. Curves nos. 3 and following range well below it and in all cases except one have lost its upward concavity. At the low-T end that loss is due to the overshadowing of thermal phonon scattering by microstructural scattering. At the high-T end there is a loss of radiation transmission. The curve in the middle, no. 2, is taken from pre-1970 data[32] to stress the importance of comparing products of a common era (if not common *k* measuring technique). That curve should be disregarded otherwise.

In the trends the effect of %MgO (the most conductive phase) is visible but not commanding, and certainly not quantitative. In the presence of other microstructural variables, porosity does not correlate; yet independently, porosity decreases the thermal conductivity monotonically at low temperatures.

Curve no. 7, for a chrome ore brick, is placed here because chromite refractories are commonly classified as "basic." With its exception, a technologist content with approximate *k* values could well find a "rule of mixtures" at work; but not for extrapolation. A chrome-magnesite brick (<50% MgO) had better be measured.

In Figure XI-6b two reference materials are represented: Al_2O_3 and silica glass. Aluminous refractories lay themselves out in a fashion similar to the basics: the correlation of *k* with $\%Al_2O_3$ is visible but imperfect. Its correlation coefficient with porosity may be >0, but not very helpful. Curves nos. 6 and 8, both for 70% Al_2O_3 bricks of comparable porosities, illustrate the importance of unnamed other microstructural features. Yet the similarity of curves 9 and 10 suggests that most regular fireclay refractories may have comparable thermal conductivities if comparably made.

Some single-point data are included in the figures. Two of these, a magnesite and a composite of magnesite + 20% graphite at 0°C in Figure XI-6a, are of particular interest. The first point confirms the extrapolation of curves 4 and 5 to 0°C. The second raises the question of a rule of mixtures for composites, to which we shall return later.

Like the aluminous refractories, working refractory bricks in the *A-Z-S* composition triangle tend to exhibit thermal conductivities mostly in the range of 1 to 3 watt $m^{-1}\,K^{-1}$ The data are somewhat sparsely scattered in the literature.[14,85,91,92,120,121,202,287] Just two examples are tabulated below, each one compared with a like material.

An alumina-chromia-18ZrO_2 fused-grain brick of about 18% porosity[91] is first compared with a similar Al_2O_3-Cr_2O_3 or A-Cr brick without zirconia.[91] Then a fused-cast refractory of 95% ZrO_2[24] is

compared with the pure dense cubic zirconia of Table XI.3. The fused-cast refractory contained about 3.5% SiO_2, 0.5% Al_2O_3, and 1% miscellaneous incuding the order of 0.1% P_2O_5, found to prevent internal cracking in this unstabilized zirconia composition.[24] It is distinctly anisotropic. The data are:

***k*, watt $m^{-1}K^{-1}$ at:**	**500°C**	**600**	**800**	**1000**	**1200**	**1400**	**1500°C**
A-Cr-18Z[91]	1.63	1.66	1.72	1.76	1.80	1.82	1.83
A-Cr[91]	2.41	2.45	2.55	2.66	2.70	2.70	2.71
Pure ZrO_2[32]	2.04	2.06	2.09	2.13	2.22	2.33	
fc 95ZrO_2[24]	2.90	2.35	2.19	2.25	2.47	(3.2)	

Silicon carbide refractories contain enough bonding material (typically 15-25%) that they are hardly single-phase. Yet their thermal conductivity is dominated by that of the coarse-crystalline principal phase. Here the pure SiC ceramic reference material[32] is compared with a typical nitride-bonded SiC blast furnace refractory[167] and with an older 15% clay-bonded SiC refractory:[32]

***k*, watt $m^{-1}K^{-1}$ at:**	**25°C**	**400**	**600**	**800**	**1000**	**1200**	**1400°C**
Pure SiC[32]	132.	51.8	38.9	31.0	(26.2)	(22.4)	(21.1)
Nitride-bonded SiC[167]	35.0	26.3	22.8	20.0	18.3	17.5	(17.2)
Clay-Bonded SiC[32]	30.4	17.0	14.9	13.5	12.8	13.3	

Dense Monolithics. Published data for *basic monolithics* are scarce. A 95% MgO castable[386] is compared below with a 98% MgO brick, the data for the latter taken from Figure XI-6a. In like manner a magnesite-chrome castable of 54% MgO[386] is compared with the 60MgO-chrome brick from Fig. XI-6a:

k, watt $m^{-1}K^{-1}$ at:	200°C	400	600	800	1000°C
98MgO Brick (15.0% Por.)	8.03	6.38	5.37	4.62	3.98
95MgO Castable (14.7% Por.)	7.03	5.61	4.68	4.29	4.76
Difference	1.00	0.77	0.69	0.33	-0.78
60MCr Brick (15.1% Por.)	4.07	3.74	3.51	3.31	3.16
54MCr Castable (14.3% Por.)	3.09	2.87	2.87	3.07	3.28
Difference	0.98	0.87	0.64	0.24	-0.12

The two castable curves[386] are well-behaved, being of lesser negative slope than those of the bricks but giving comparable values of *k*. The sharp upturn at 1000°C for the high-mag castable is unexpected, but might have resulted from a chemical bonding reaction.

In fact, the very nature of monolithic refractories creates a serious question about how they should be prepared for thermal conductivity measurement. If they are thermally matured in advance, then the measured *k* vs T data will be reproducible but cannot reflect their actual heat transport properties in service. Conversely, lacking such preheating it is readily shown that a succession of *k* measurements made with ascending temperature is not reproduced by succeeding measurements with descending T -- nor ever again.[387] A resolution of this dilemma of specimen preparation may ultimately be agreed upon, but it has not been yet.

Alumina-silica monolithics are more often used where accurate knowledge of the thermal conductivity really matters than is the case with basics. And there are many more of them. It is virtually automatic for a manufacturer to measure *k* vs T for each new product. But different instrumental methods are used, and different approaches are taken to the above-mentioned dilemma of specimen preparation. To minimize these variables of measurement, the thermal conductivities of alumina-silica monolithics will be taken here entirely from the data of one U.S. manufacturer.* A study of castables[388] has shown that data obtained from at least four commercial suppliers are substantially parallel and overlapping.

---

*National Refractories and Minerals Corporation, 1852 Rutan Drive, Livermore, California 94550; abbreviated NRMC.

It has further been shown[388] that a strong correlation exists between the thermal conductivity and the bulk density alone. There is also a strong overall correlation between the B.D. and the wt.-% Al_2O_3. Neither of these relationships is free from interference by other variables (e.g., porosity); they are better called trends than correlations. But they do dignify the laying out of products either in compositional order as in Figures XI-6a and b, or in order of bulk density.[388]

Thirty aluminous monolithics are accordingly represented in Figure XI-7, indexed in order of decreasing wt.-% Al_2O_3 from 99% to 32%, giving for each its measured thermal conductivity vs temperature. The linear *k* scale in watt $m^{-1}K^{-1}$ is expanded so as to separate the curves; but it can be seen that the entire array conforms well to the envelope of brick data in Figure XI-6b. The curves include several for ramming mixes and several for gunning mixes, neither of which deviates appreciably from the behavior of the castable majority.

The NRMC source data for these curves consisted of discrete *k* values, in nearly all cases at three temperatures 500°F apart. The curves themselves are our own, each passing faithfully through the three data points but otherwise bearing no warranty. They do, however, correctly disclose upward and downward concavity.

Sometimes it is instructive to regard data in the mass instead of singly, because patterns emerge. Figure XI-7 is such a case. First is the matter of ranking. All of curves nos. 13-30 are found in a common group: $k \leq 2$ watt $m^{-1}K^{-1}$ Their nominal compositions are all in the mullite-silica binary system at equilibrium. Of curves nos. 1-12, the nominal compositions are all in the alumina-mullite system at equilibrium and all but nos. 3 and 10 are found in the *k* range from about 2.5 to 4 watt $m^{-1}K^{-1}$. If one discounts radiation transmission, the phases Al_2O_3, $Al_6Si_2O_{13}$, SiO_2 (quartz), and SiO_2 (vitreous) are in order of decreasing thermal conductivity (Figure XI-4a). The above trends fit this order.

Then there is the matter of concavity. A plausible reason for downward concavity is high-temperature expansion of the refractory, associated with permanent deformation, due to gas evolution and particularly from the decomposition of bonding chemicals, e.g., CA cement. Downward concavity is the rule in Figure XI-7 for all compositions in the alumina-mullite phase system and only a few others.

Upward concavity accompanied by rising *k* with increasing T is the rule in the mullite-silica phase system. Considering the curves for quartz and vitreous silica in Figure XI-4a, it is reasonable to attribute this feature in the low-alumina monolithics to a residuum of radiant

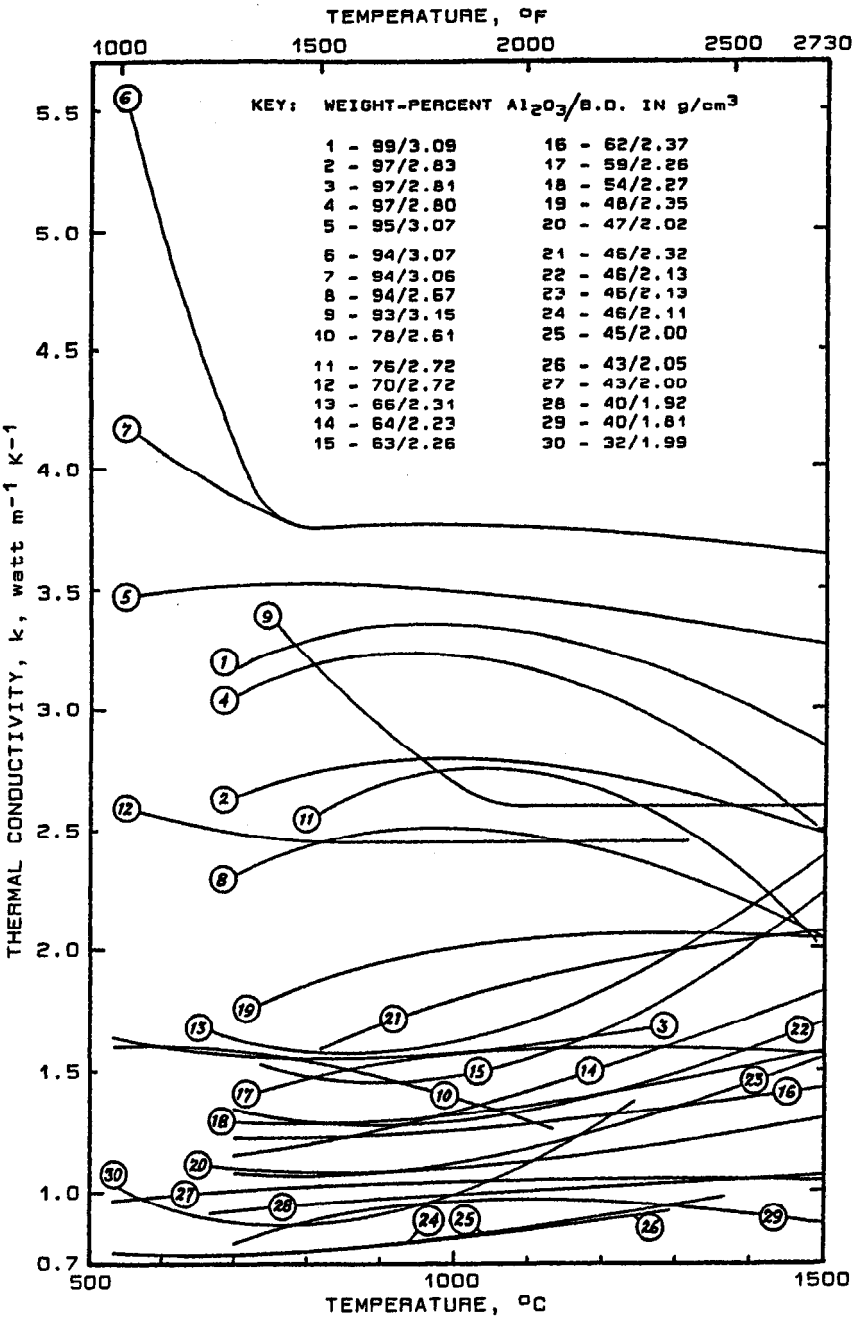

Figure XI-7 Thermal Conductivity of Aluminous Monolithics (NRMC data)

energy transmission in those two silica phases. One or both must be major.

Thus while it is necessary to measure the thermal conductivity of a refractory for its use, the conductivities of a large number of monolithics over a wide range of compositions can be broadly rationalized by only a few simple concepts. On the strength of such regularity, some "standard" castable *k* values have been recognized in Germany.[389] The corresponding range of thermal conductivities is over a factor of 5 in Figure XI-7.

Alteration. Either partial melting at the hot face of a refractory, or condensation of an intruding vapor, can raise its thermal conductivity. Although oxidic liquids are poorer thermal conductors than solids of the same composition,[32] the difference is not great. But the improvement in film coefficient between crystallites is large when microcracks are liquid-filled, compared to its value for even a hairline gas gap. Such an effect is difficult to quantify; it could account for an increase in *k* of several percent in a liquid-containing zone.

A *completely* pore-filled zone near the hot face resulting from liquid penetration, on the other hand, will experience a much larger alteration of *k*. This effect is directly proportional to the apparent porosity P in the liquid-saturated zone. If a liquid slag has a thermal conductivity of the order of 1 watt $m^{-1}K^{-1}$, this times P will be the rough order of the increase in *k*. But the removal of the film drop associated with microcracks at the same time can add still further to this. A fairly good estimate of the total Δk in the penetrated zone would lie between about P and 2P in watts m^{-1} K^{-1}, where P = vol. fraction.

This means that a refractory containing 15% porosity (P = 0.15) and exhibiting a *k* of 3 watts m^{-1} K^{-1} might, in its liquid-penetrated zone, show an increase of as much as 2·0.15 = 0.3, giving a total of 3.3 watts m^{-1} K^{-1}. If its initial conductivity is only 1.5, the new total of 1.8 is a large percentage increase.

The resulting decrease of dT/dz near the hot face is significant: further liquid penetration is encouraged. But the effect on the overall ΔT through a refractory wall should rarely be troublesome unless the penetrated zone is a large fraction of the total thickness. In that case there are much more serious troubles (Chapter XII).

Cellular Insulating Refractories

The classification and standardization of cellular insulating refractory types, discussed in Chapter IX, make it easy to display their thermal properties because of the likeness of products offered by different suppliers. Thermal conductivities are given at discrete

temperatures, most often starting at 500°F and at 500°F increments above in the U.S.A.

The thermal conductivity at 500°F varies linearly with the bulk density for both insulating firebrick and insulating aluminous castables, the two most numerous and widely used cellular types. Changes are made in their composition to provide for increasing service temperature limits; but these changes are orderly and should correlate monotonically with bulk density. Inspection of data from several suppliers leads to the following analytical connections between *k* and B.D.:

Insulating Firebrick

$$k_{500F}\ (\text{Btu in./hr.ft}^2\text{°F}) = 0.03455\ \text{B.D. (pcf)} - 0.2545$$

$$k_{260C}\ (\text{watt m}^{-1}\ \text{K}^{-1}) = 0.3110\ \rho_b\ (\text{g/cm}^3) - 0.0367$$

Insulating Castables

$$k_{500F}\ (\text{Btu in./hr.ft}^2\text{°F}) = 0.04375\ \text{B.D. (pcf)} - 0.4250$$

$$k_{260C}\ (\text{watt m}^{-1}\ \text{K}^{-1}) = 0.3939\ \rho_b (\text{g/cm}^3) - 0.0613$$

The pairs of equations are equivalent: 500°F = 260°C, "B.D." and "ρ_b" mean the same. The equations for IFB cover a range of products from about 28 to 60 pcf, agreeing with all data seen within about ±0.1 Btu or about ±0.015 watt m^{-1} K^{-1} The corresponding *k* range is from 0.8 to 2.2 Btu in./hr·ft²°F or from 0.11 to 0.32 watt m^{-1} K^{-1} The equations for insulating castables cover a range of products from about 45 to 100 pcf, giving a corresponding *k* range from 1.3 to 3.2 Btu in./hr.ft²°F or from 0.19 to 0.46 watt m^{-1} K^{-1} -- again agreeing with all data seen within about ±0.015 watt m^{-1} K^{-1}. These two overlapping ranges fall below the minimum *k* for comparable working refractories, seen in Figure XI-7 to be about 0.74 watt m^{-1} K^{-1}.

The variation of *k* with average body temperature for both insulating product groups is consolidated in Figure XI-8.* This gives a few representative examples for IFB and an envelope for castables corresponding to the above B.D. range. The typical absence of upward concavity in the latter group probably results from permanent expansion, as mentioned above for dense monolithics.

---

*Courtesy of National Refractories and Minerals Corp.

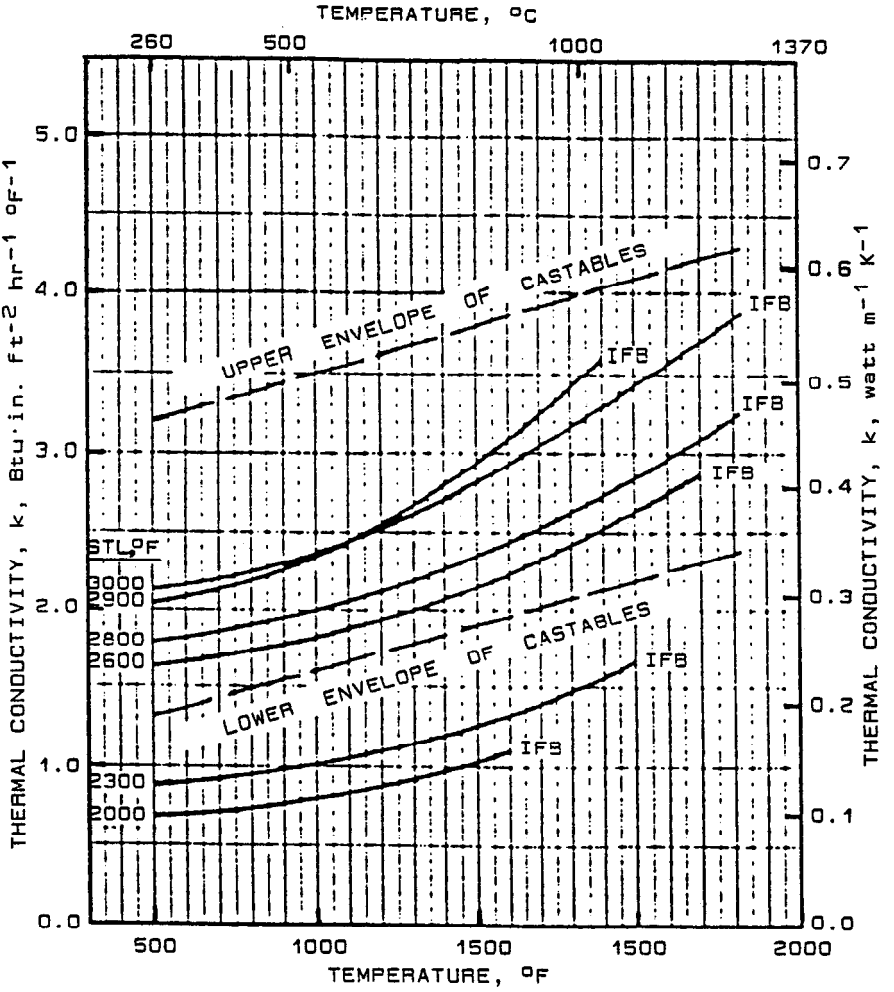

Figure XI-8 Thermal Conductivity of Cellular Insulating Refractories (courtesy of National Refractories and Minerals, Inc., by permission)

In addition to these insulating refractory types, there are a few porous high-alumina products which run still higher in B.D. and in *k*. There are also a few very-high-porosity products, made with expanded grain such as vermiculite or "bubble" synthetic oxides (see Chapter IX). Still further, reticulated foamed products are made by coating hollow polymer spheres, lightly consolidating, and then burning out the organic. Products of this type presently include alumina, several partially-stabilized zirconias, cordierite, and SiC. At present these coarse-celled materials are used more for metal filtration and as high-surface-area substrates than for thermal insulation. All manner of porous carbons should be acknowledged in the same context; manufacturers may be contacted for their data.

Finally, another workhorse insulating refractory brick or block is made of foamed vitreous silica. Two grades are recognized: a nominal 95% SiO_2 product and a 99+% product. Their porosities are determined by market needs at a given point in time; the span of bulk densities seen is about the same as for insulating castables. Thermal conductivities at 1000°F run from about 0.2 to 1 watt m^{-1} K^{-1}, i.e., a little higher than those of the castables at equal B.D. Some specific numerical values will be shown in the next section, where we attempt to establish a useable relationship between porosity and *k*.

Effects of Porosity

Workers in ceramics have sought for decades to obtain rigorous expressions for the effects of porosity on both mechanical properties and bulk transport properties of solids. The field has been rather infertile. Yet as pointed out in Chapter IX, the fundamental connection of thermal conductivity in a porous refractory is not with its bulk density per se but with its solid and void volume fractions, f_s and f_v. Here, $f_v + f_s = 1$ and $f_v = 1 - \rho_b/\rho_{th}$. Rearranging the second of these equations yields:

$$\rho_b = \rho_{th}(1 - f_v) = \rho_{th} f_s \quad .$$

That is, a property which depends literally on the solid volume fraction will indeed be proportional to the bulk density, so long as the theoretical density is held reasonably constant. But transport properties of a solid depend on how that solid is subdivided by a penetrating void network, microcracks, and boundaries. The "1-P" rule of the above equation (where $P = f_v$) was long since abandoned in ceramics. Available data were better fitted by "1-2P" or "1-3P," etc.; but those empirical functions collapse when the porosity exceeds 50% or 33%. All that has received general agreement is that, within reasonable limits, properties of the solid which depend on porosity do not depend on the pore diameter.[390]

There is no present certainty of a predictive breakthrough. An assist in extrapolating and interpolating *k* values in series of insulating refractories would be helpful, however, on a more secure footing than that of bulk density.[391] There is the further problem of mixed conduction of heat shared between two phases, solid and gas; or even more often, between two solid phases of different conductivity. There is an especial need to augment measurement with computation in particulate oxide + nonoxide composites. One needs the wherewithal to compute.

An empirical equation first proposed in 1968[392] has the appeal of simplicity together with a reasonably sound physical foundation. In its general form it relates a "mixed" transport property $\overline{X}$ of a two-phase material to that property of each phase and to their volume fractions. It is:

$$\frac{\overline{X}-X_2}{X_1-X_2}=\frac{1-f_2}{1+n(f_2)^2} \quad .$$

Figure XI-9 plots this equation for a succession of arbitrary n values, over an entire two-phase composition range. The curves are unsymmetrical; the phase labelled "1" must always be that of higher conductivity.

As applied here, the property X is the low-temperature thermal conductivity *k*; and phase "2" is void space, for which $k_2 = 0$. Reducing and rearranging at the same time, we obtain:

$$\overline{k}= k_1 (1-f_v)/(1+nf_v^2).$$

In principle, all terms are knowable except n. That quantity is variable from 0 to two-digit numbers, increasing with interface resistances to heat transport within the solid such as microcracks, unbonded intercrystalline areas, etc., which are unassociated with measurable void volume. In use of the equation, n is determined by data-fitting.

For use in refractories, phase "1" is the theoretically-dense solid, whether itself homogeneous or heterogeneous. While in principle its k_1 is knowable, in fact most porous refractories cannot be made identically in pore-free form; so the thermal conductivity of the dense solid may become a second data-fitting term. Any two porous versions of the same refractory, differing sufficiently in known f_v and each with a measured $\overline{k}$, suffice to determine the two unknown quantities k_1 and n.

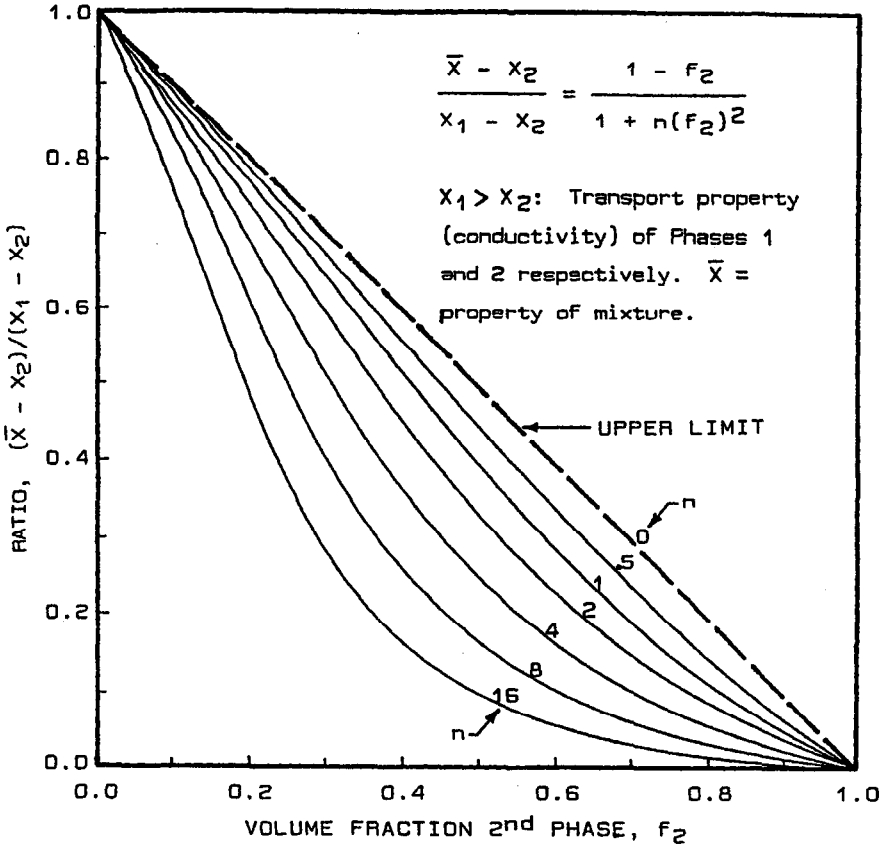

Figure XI-9 Plot of a Mixing Equation for Transport Properties of Heterogeneous Mixtures (Ref. 392)

Given a family of like materials of differing f_v, it is evident that if k_1 varies from one member to another, the equation will fail. Likewise if n varies (e.g., due to different processing from member to member), it will fail. Being utterly empirical in its manner of use and being thus rigidly restricted, this equation is in need of confirming. It has been applied to the thermal conductivity of a number of porous solids including aluminas, silicas, graphite, and minerals, with considerable success.[393] Here it will be tested against known data for commercial insulating firebrick and for commercial foamed silica. Although insulating firebricks do differ, those of various bulk densities seem to exhibit enough sameness to permit a trial. Foamed fused silica, being substantially single-phase and substantially all SiO_2, seems an excellent candidate.

A number of manufacturers report comparable if not identical physical properties and chemical compositions for each class of IFB. The chemical and density data used here were drawn from Thermal Ceramics product literature.* From each chemical composition a theoretical density was computed; f_v follows from the reported B.D. of each of seven products. Data for one more were drawn from Figure XI-6b. Iterative data-fitting by the above mixing equation produced best values of k_1 = 8.5 Btu in./hr.ft^2°F and n = 0.50. The value of k at 500°F was chosen for this procedure throughout.

Likewise for foamed silica: Harbison-Walker product data** were used for each of five insulating brick products. The theoretical density of vitreous SiO_2 was taken as 2.2 g/cm^3 from Table XI.3, from which f_v follows for each product. The best value obtained for k_1 was 13.8 Btu in/hr.ft^2°F; this compares reasonably well with the 14.8 read at 538°C from Figure XI-4a for vitreous silica. The optimum n obtained was 3.00. The 1000°F value of k was used throughout in this case.

The computed curves for the porous IFB and for foamed vitreous silica are given in Figure XI-10 (ignoring the inset for now), together with points representing the reported $\bar{k}$ of each product at 500°F and 1000°F, respectively. To distinguish the two sets of data, the f_v scale for the silicas has been reversed, as given across the top of the figure. The root-mean-square deviations of the measured from the computed $\bar{k}$ data are approximately 0.17 for the IFB and 0.44 for the foamed silica, in Btu in./hr.ft^2°F. Inspection of the figure shows

---

*Morgan Thermal Ceramics, Inc., Augusta, Georgia.

**Harbison-Walker Refractories, Dresser Industries, Inc., One Gateway Center, Pittsburgh, PA 15222

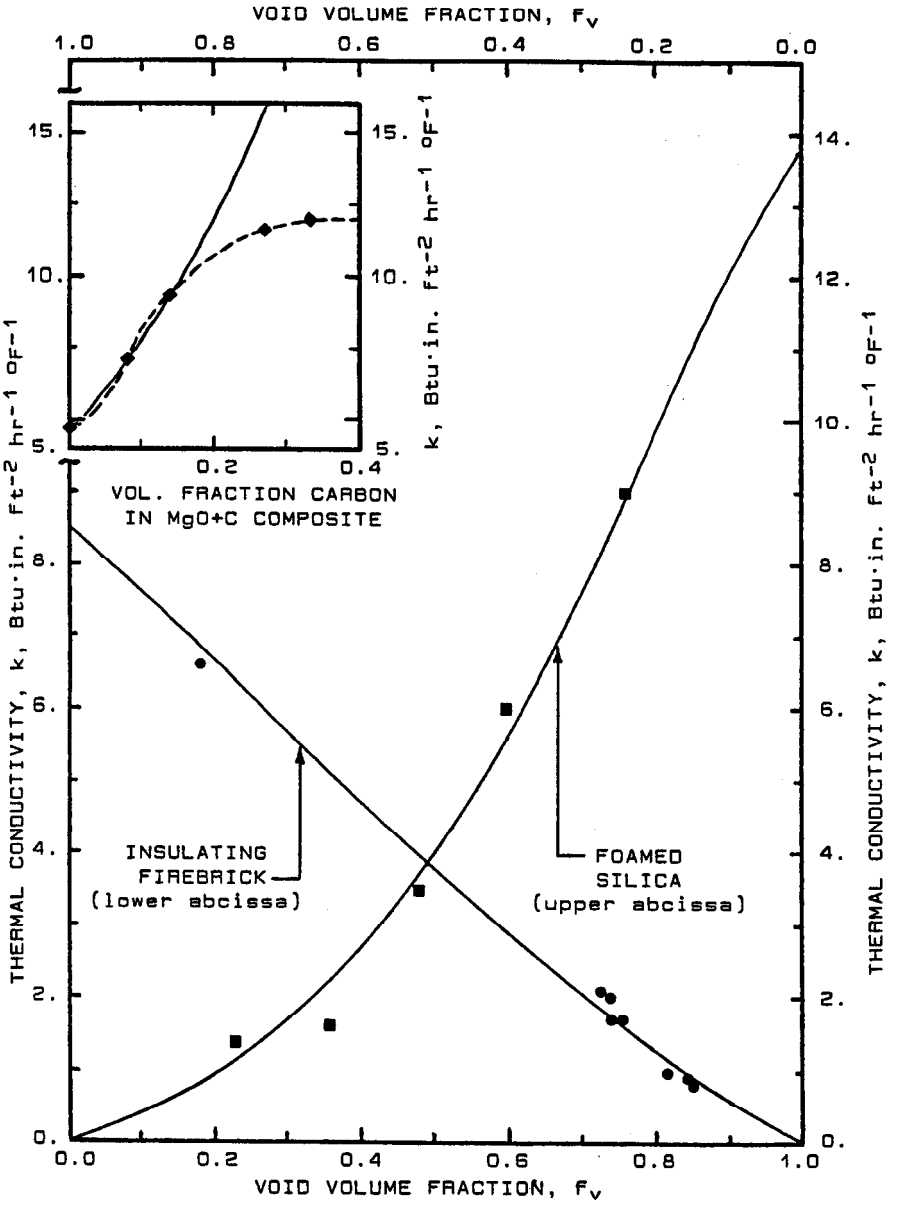

Figure XI-10 Computed vs Measured Thermal Conductivities for Two Cellular Insulating Refractories and (Inset) Magnesite + Graphite Composites

these deviations to be a matter of microstructural and compositional variety of the products, not a basic fault of the mixing equation.

This mixing equation thus has some considerable utility. One way it can be used, for example, is to predict a target B.D. for synthesis of a new cellular insulating refractory to be developed for a prescribed low-temperature thermal conductivity. Take the case of a $70Al_2O_3$-$20ZrO_2$-$10SiO_2$ refractory, hypothetically now being made at a B.D. of 206.4 pcf and having a measured apparent porosity of 17% (i.e., $f_v = 0.17$) and a measured thermal conductivity of 10.4 Btu in./hr.ft^2°F at 500°F. What should be its target bulk density to give k=1.0 in the same units?

One first computes the theoretical density from the weight fractions and densities of the three binary components (Table XI.3), or from the measured B.D. and porosity: ρ_{th} = 248.7 pcf. One next uses the above mixing equation with the "dense" refractory data and a trial value of n to determine k_1: if n = 2, k_1 turns out to be 13.25, or 13.98 if n = 4. Then one solves the mixing equation for f_v at the required $\bar{k}$ = 1.0; the result is 0.82 if n = 2, and 0.76 if n = 4. The corresponding target bulk densities are found using the computed ρ_{th}: 44.8 pcf if n = 2, or 59.7 pcf if n = 4. Lacking any independent guidelines for n, n = 2 is the more conservative choice. In any event, the mixing equation gives a far better target B.D. than would the assumption $\bar{k} \propto$ B.D., which leads to ~17. pcf. Much work remains to be done with this mixing equation before its full usefulness and its limitations for refractory calculations are established.

Composites

The need for a thermal conductivity mixing function for working oxide + nonoxide composite refractories is underscored by their susceptibility to oxidation in air at high temperatures in the course of the k measurement itself. Equipment for measuring this property in inert or reducing conditions is not common in refractories laboratories. But now we may have the ability to estimate k by calculation.

The mixing equation of the preceding section, adapted for thermal conductivity of composites, reads:

$$(\bar{k} - k_2)/(k_1 - k_2) = (1 - f_2)/(1 + nf_2^2) \quad .$$

Here phase "1" is the particulate nonoxide (viz., of higher conductivity), and phase "2" is the oxidic refractory in which it is distributed. That oxidic refractory will also have been made and characterized without any nonoxide present. That end-member oxide refractory will provide a ρ_2 = B.D.$_2$ and a k_2 (both already compensating for porosity).

The properties of end-member amorphous carbon (e.g., coked pitch) may be too elusive for use; but data are available for the graphites and silicon carbides used in composite refractories, and for other crystalline nonoxide compounds as well as metals. The ρ_1 and k_1 chosen should be consistent with the nonoxide as actually used. The weight-percentages in the composite are first converted to volume fractions; then the above equation is solved as described in the preceding section. That is, a value of n is determined by data-fitting if possible, or if not, by estimation.

Reference 74 presented a curve of $\bar{k}$ at 0°C vs percent graphite in magnesia, as the only accessible case in point. The data for 0%C and for 20%C were marked on Figure XI-6a. Thermal conductivity was read from the given curve[74] at 0%, 5.7%, 10%, 20%, and the apparently asymptotic value at >25%C.

We chose $\rho_1 = 2.2$ g/cm^3 and $k_1 = 120$ watt m^{-1} K^{-1} for graphite,[11] and $\rho_2 = 3.0$ g/cm^3 for the magnesia refractory based on curve no. 4 of Figure XI-6a. From the densities, each of the listed wt.-%C data was converted to f_1 and f_2. Then we used the above mixing equation with $k_1 = 120$.[11] and $k_2 = 4.65$ [74] to determine n at 10% C ($f_2 = 0.857$), using the reported[74] $\bar{k} = 9.3$ watt m^{-1} K^{-1}. We obtained n = 3.5.

Figure XI-10 contains an inset in which $\bar{k}$ is plotted vs f_1, the volume fraction of graphite in magnesia. The solid curve is that of the mixing equation, using the above constants. The points and the dashed curve are those obtained from Reference 74.

The discrepancy at 20 wt.-% C and above and the asymptotic S-shaped curve given in Ref. 74 have to reflect some dramatic alteration of the specimens as the graphite content was increased above 10%. Extensive cracking of the MgO due to differential thermal contraction is a possibility. Here the mixing equation may have served to flag a measurement or specimen problem. For better-behaved materials and after some experience, it should yield useful thermal conductivity data for composites. This method of estimating may merit some perseverance, as in many cases practical alternatives are not apparent.

Fiber Insulating Refractories

Now we turn to refractories in which the void space is clearly continuous, interrupted by a quasi-discontinuous solid phase. The gas conductivity as displayed in Figure XI-5b should be a factor. But if the conductivity is low, the ΔT through such a refractory is large and the driving force for *convection* is correspondingly large.

All other things being equal, gas convection is impeded in proportion to the solid volume fraction; more precisely, to the aggregate frontal area provided by the fibers to gas flow across them. In this, a dependency on bulk density alone can be confounded by such variables as the density of the solid phase itself, the fiber diameter, and the proportion of "shot" which can be up to 40-50 wt.-%. But additionally, all other things are not equal, The geometry of the lining, its orientation (walls vs roof, etc.) and the gas flow velocity and turbulence within the vessel all have important effects on convective heat transport within the insulating refractory.

Then there is the transition, with increasing temperature, ultimately to the dominance of heat transport by *radiation*. The downward concavity of the gas curves of Figure XI-5b cannot be extrapolated. Now the fibers play a dual role of (a) scattering radiation by reflection, and (b) absorbing it and re-radiating as well as transferring heat interfacially to the gas surrounding them. Their frontal area in aggregate is again a prime consideration, wherein a proportionality to B.D. alone is a little too simplistic.

Recognizing both the convective and the radiation phenomena and their dependencies, lining designers have turned increasingly to duplex or even triplex fiber insulation.[394] The most important feature of these designs is to impede both convective and radiant heat transport near the hot side by use of a relatively dense or even solid-filled fiber layer there. That layer is then backed by one or more layers of lower B.D. whose insulating quality is better retained at lower temperatures and in a confined space. This arrangement also gives better mechanical protection to the lighter materials.

The interactions among transport processes within even single-layer fiber refractories make it difficult to compute their thermal conductivity from basic mechanisms taken in isolation. Some excellent contributions have been made to the understanding of individual phenomena, for example the role of fiber volume fraction,[395] the influence of gas composition at low temperatures,[396] and the parameters governing resistance to radiant energy transport.[397] These and other studies, through systematic coverage of the variables, provide a massive data base while adding to understanding by their variety.[398-401] Manufacturers' data abound.

The tendency among suppliers remains to index fiber refractories by bulk density (see under Classification in Chapter IX). The curves of Figure XI-11 are also indexed in that fashion, each code number being the B.D. in lb/ft^3 or pcf. Several groupings are also identified in the figure: blanket and rigid (viz., board or molded), and by fiber composition. The curves are terminated approximately at the service temperature limit in each case.

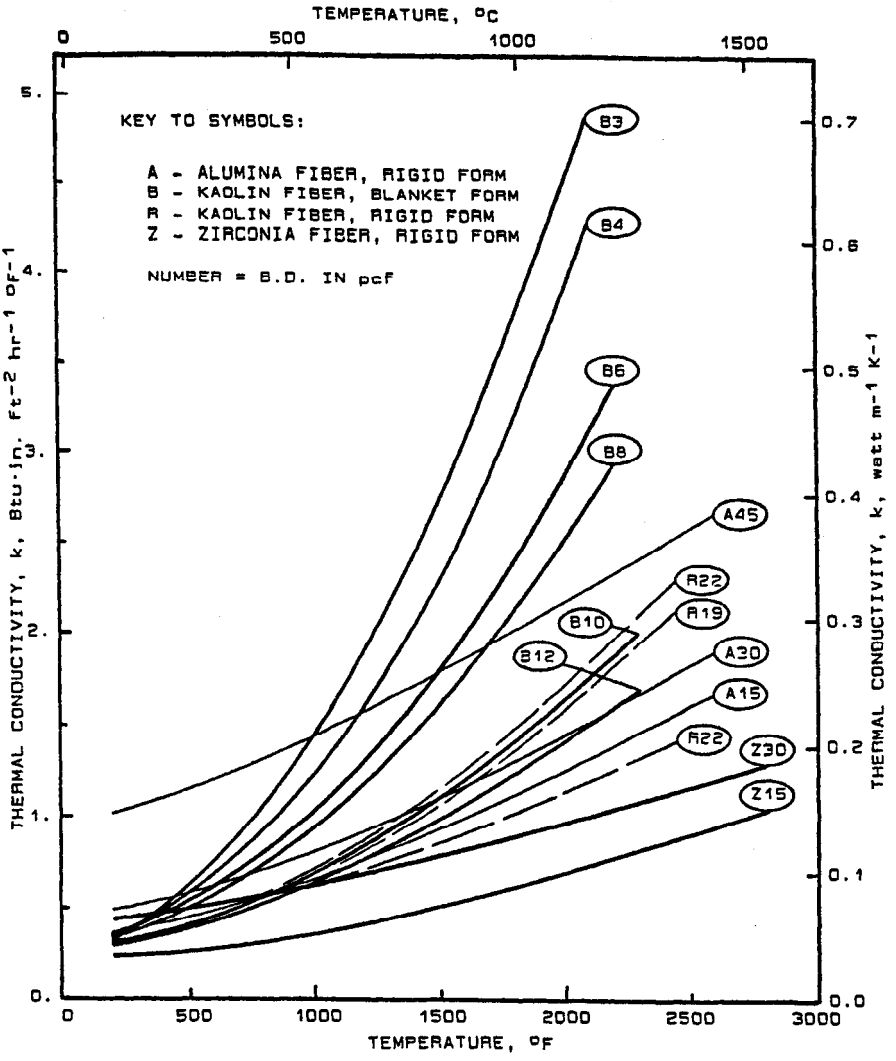

Figure XI-11 Thermal Conductivities of Fiber Refractories vs Temperature (U.S. supplier data)

Curves B3-B8 represent mean values of *k* for up to 8 different commercial blanket products of each B.D. class, all *k* values having been determined in the same way in the same laboratory.[397] The range about each curve is typically ±0.01-0.03 watt $m^{-1} K^{-1}$ and well explained;[397] in a few cases up to ±0.1-0.15 at the highest temperature. Data from Thermal Ceramics product literature* are on the whole in relative agreement, though running consistently lower in *k* for reasons of measurement method. Manufacturers in the U.S. generally use a single standard ASTM procedure (see later), and their data should be accepted at least for consistency. Thermal Ceramics product data were employed alone here for curves B10 and B12, and the gap between B8 and B10 in the figure is an artifact of that change of data source. For engineering use, curves B3-B8 should be adjusted downward.

Curves R19 and R22, for rigid materials comparable in STL to the above, were drawn from Foseco product literature.** The A-series curves and Z-series curves, representing bonded short-fiber products of cryptocrystalline alumina and zirconia, respectively, were drawn from Zircar literature.*** This small sampling of fiber types is sufficient only to point out some physical phenomena; it in no way represents the full product lines of these or other commercial suppliers.

As seen in Figure XI-11, most fiber refractories do not individuate appreciably at 100°C or 200°F and below. By 500°C they have begun to sort out, and by a mean temperature of 1000°C they make their characteristic differences relatively clear. The consistency of fiber blankets in showing decreasing *k* with increasing bulk density has been known, related to the role of fibers in interrupting heat transport by convection and radiation in the gas continuum. That trend must eventually reverse. Where it reverses depends on what refractories are compared. The A-series and Z-series refractories are closer to cellular in their microstructure, and they exhibit the conventional *k*-B.D. relationship. The lower of the two R22 curves exemplifies the industry concensus, however, that for like fiber products the minimum in *k* lies about where that curve is and the corresponding "turnaround" B.D. is in the low to mid-twenties of pcf.

Apart from the low thermal conductivites of the zirconia products, materials of considerable particulate ceramic content exhibit a relatively low slope of *k* vs T curves. The curve labelled A45 is a

---

*Morgan Thermal Ceramics, Inc., Augusta, GA.

**Foseco Technik, Ltd., Tamworth, Staffordshire, England; also Cleveland, OH.

***Zircar Products, Inc., Florida, NY.

distinctly visible example. These materials are more opaque to thermal radiation than are the open-fiber types.

If radiant energy transmission at high temperature characterizes fiber blankets, then that fact should be disclosed in a log-log plot of k vs T (in K). All of curves B3 to B12 were so plotted. All of their plots were impressively linear over some interval of temperature from 2000°F or 1093°C down. For curves B6 and B8 that interval extended down to 1000°F or 538°C, and for B3 and B4 down to about 800°F or 427°C. In that interval the thermal conductivity is accurately described by:

$$k = aT^b \quad .$$

The slopes of the log-log plots (the exponent b in the above equation) are 2.14 for B3 and B4, 1.99 for B6, and 1.97 for B8. The interested reader may want to explore this matter further. For the present, these four curves represent the averages of two dozen or so commercial products[397] which reasonably fit the equation,

$$k = aT^2 \quad ,$$

in the temperature region dominated by radiant energy transport. It is readily derived from this function that a blanket of thickness Z and of hot-face and cold-face temperatures T_h and T_c will obey the following heat transport equation:

$$Q = \frac{a}{3} \cdot \frac{(T_h^3 - T_c^3)}{Z} \quad .$$

That is, the common use of an "average" temperature $(T_h + T_c)/2$ and an "average" k at that temperature may well give misleading results.

Thermal Diffusivity of Refractories

Repeating the definition of thermal diffusivity, δ:

$$\delta = k/\rho_b c \quad ,$$

this quantity is determined at any temperature if k, ρ_b, and the specific heat c are known at that temperature. Thus the thermal diffusivity is often a computed quantity. Alternatively, it may be measured directly (see next section) and the thermal conductivity computed from it. Between the two approaches, the direct measurement of δ involves a much narrower T interval and is thus freer from uncertainties about the "average" T alluded to last above. Unfortunately, for fiber blankets where the identification of k with T is most critical, it is not practical to

measure δ. Furthermore, the occurrence of "shot" in those materials represents such a major heterogeneity that the connection between thermal conductivity and diffusivity is tenuous.

With that one exception, the relation between k and δ is straightforward. The Specific Heat is treated under that heading earlier in this chapter, while reference to the measurement of bulk density[9] was first made under Thermal Conductivity, Void Volume, and Bulk Density in Chapter IX.

Measurement of Thermal Conductivity and Diffusivity

The essential measurement methods available are of two types: (a) steady-state, and (b) transient. These can yield k and δ, respectively. Both are capable of accurate work, yet both are capable of measurement error or bias such that, to this day, respected workers using different methods can disagree by up to the better part of 0.1 watt m^{-1} K^{-1} without being able to agree on which is "right."

The usual geometry of steady-state methods is planar (i.e., of unidirectional heat flux). Ensuring uniform flux over a specified cross-section area is difficult enough, calling for various "guard" heating and insulating techniques to ensure that each of a specified T_1 and T_2 is uniform over an entire specimen area and with time. Perhaps the most difficult of all is the measurement of the flux, J. A calorimetric technique must measure the product $J \cdot A \cdot t$, where A is a confined specimen cross-section area and t is time. Restricting the collected heat to precisely that from area A is very difficult; and in any event the performance of calorimetry without feedback to the specimen is a challenge. Indirect rather than absolute techniques are sometimes employed.[388] An appealing alternative is the use of sandwich construction, in which the same flux J passes through a layer of specimen and a layer of reference material; but then contact or film resistances become impossible to eliminate and difficult to reproduce or measure.

Transient methods include sinusoidal and pulse heating within a specimen otherwise maintained isothermal. Pulse techniques include flash-heating and a resistance-heated hot wire technique[386] in appropriate geometries. The hope in pulse methods is to reduce calorimetry to a simple electrical or optical heat-input measurement, or eliminate it altogether; then to measure T vs time after the pulse in such manner as to describe heat transmission and decay out into the material in a prescribed geometry -- e.g., radially from a straight segment of heated wire in a cylindrical (or infinitely large) specimen,[386] or through the thickness of a flash-heated disc.

In all cases the heterogeneity of refractories interferes, increasingly with decreasing dimensions. So also does anisotropy.

Each method and each geometry and size have their drawbacks. Numerous workers have studied one or more measurement methods intensively, including various detailed techniques of meeting each of the challenges presented. The reader desiring to make a critical comparative evaluation should consult References 24, 32, 65, 74, 76, 91, 167, 386-389, and 395-404, and their references in turn. Further valuable data and resources are cited in Ref. 405 and one or more of ASTM standard procedures C201, C202, C182, C417, C714, C767, and C1113,[9] which are outlined next.

The industry standard for measuring the thermal conductivity of refractories in the U.S.A. has been a steady-state, plane-geometry, uniaxial heat flow, water-calorimeter method. It is described in the following ASTM procedures:[9]

C201 *Thermal Conductivity of Refractories* (basic specifications);
C202 ..... *of Refractory Brick* (details for formed working refractories);
C182 ..... *of Insulating Firebrick* (details for formed IFB);
C417 ..... *of Unfired Monolithics* (details for working castables and plastics)
C767 ..... *of Carbon and Carbon-Bearing Refractories* (conducted in argon).

A square (plan view), electrically-heated furnace is specified in the first of these. The radiant heat from above is spread evenly by a silicon carbide plate suspended over a 9" straight brick specimen (9" by 4.5" by 2.5" or 3") laid flat and surrounded by guard bricks of the same composition, then by specified peripheral insulation. Thermocouples centered in the upper and lower faces of the specimen establish its T_1, T_2, and the distance Z between them. All bricks lie on 0.5" sheets of insulating material through which the flux *J* then passes. Centered under the specimen and its insulating sheet is a 3" square copper flowing-water calorimeter, surrounded by guard calorimeters of like kind which are used to warrant the uniformity of *J*. Statistics are given based on a four-laboratory, three-refractory, four-temperature round robin program.

Each of the remaining procedures listed above specifies the heating, soaking, and measuring regimen in detail for its refractory type. Method C417 makes a provision for sweeping out water-vapor evolved from unfired monolithics, besides specifying their dimensions and details of forming, curing and drying prior to heating. While all other procedures are ordinarily conducted in air, C767 specifies sweeping with argon to protect carbon-containing refractories from oxidation. Most procedures require postmortem examination of the specimen to ensure freedom from undetected cracking. In all cases, *k* is determined by:

$$k = [Q/At] / [(T_1 - T_2)/Z] \ ,$$

where Q is the total heat collected by the calorimeter of area A in time t at steady state.

A new ASTM standard method is procedure C1113, *Thermal Conductivity of Refractories by Hot Wire (Pt Resistance Thermometer)*.[9] Although a transient technique, it is not to be confused with pulse methods: it measures *k*, not δ. Its advantages include a very narrow T interval and some automatic averaging out of anisotropy, as well as freedom from an external calorimetric measurement. A straight length of platinum wire is used both as heater and as temperature sensor along the centerline of a cylindrical volume of material within a larger (sensibly infinite) specimen. But unlike the diffusivity device,[386] this wire is heated at constant power input (i.e., V·I) with time. The thermal conductivity is computed from the Fourier equation for heat flow from a line source:

$$k = (Q/4\pi) / (dT/d \ln t) \ ,$$

where Q is the power input per unit length of wire and t is time. The details of determination of (dT/d ln t) are all prescribed in the procedure, including in-situ calibration of the same wire as a resistance thermometer at each selected temperature of measurement. Provisions are specified for maintaining an otherwise-isothermal 9-inch "straight" brick or other specimen at each T. The maximum centerline temperature rise during each measurement is less than 5°C. Some round-robin statistics are given for dense working refractories.

At present there is only one ASTM standard procedure for thermal diffusivity. This is C714, *Thermal Diffusivity of Carbon and Graphite*.[9] It is a flash-pulse method, designed to heat one face of a small, thin disc specimen uniformly and to measure, by thermocouple and CRT scanner, the time required for the temperature of the center of the back face to rise suddenly to one-half its maximum observed increase. Within generous limits, the method is independent of the Q (integrated heat) of the pulse; and only a proportionate measure of the back-face ΔT is required. The crucial measure is of the time elapsed from pulse to 1/2-maximum ΔT. The equation connecting this to the thermal diffusivity δ is:

$$\delta = kZ^2/t_{1/2} \ ,$$

where Z is the specimen thickness, $t_{1/2}$ is the elapsed time defined above, and k is a known parameter which depends on the ratio of pulse duration to $t_{1/2}$ and on the departure from adiabatic conditions. The specimen being only a few mm thick, the method is not suitable for coarse-textured refractories.

There is, at this writing, no special ASTM standard for determining the thermal conductivity of fiber insulating refractories. Most manufacturers use an adaptation of C201. Insulating castables employ procedure C417 in essence, though falling in about the same *k* domain with IFB, C182.

ELECTRICAL CONDUCTIVITY

Refractory materials see special duties as electrical insulators, dielectrics, resistors, semiconductors, and conductors, among others. The commonest use as high-temperature conductors in large equipment is of course as arc-furnace electrodes. Smaller-scale hot components include electrodes, susceptors, resistive heating elements, heat sinks, and the active elements of numerous transducers, sensors and instruments in addition to insulators. Here we shall deal solely with the function of high-temperature electrical insulation, citing only enough of conducting materials and their properties to provide a perspective. Considerable data on electronically active materials are summarized in References 8, 11, and 405.

The preceding discussion of heat transport mechanisms in solids lays a sufficient groundwork for electrical conduction as well. Radiant and phonon or lattice-wave heat transport mechanisms have no electrical counterparts at sub-kilovolt potentials, however; we are left with only metallic conduction and the electron and hole transport of semiconductors. Materials suitable for D.C. and line-frequency A.C. electrical insulation exhibit only semiconduction, and very little of that at room temperature.

By thus limiting the scope of applications in this section, we limit the properties of interest to electrical conductivity (or its inverse, resistivity) and to the effect of temperature on this property through semiconduction alone. By limiting applied potentials to sub-kilovolt levels we minimize surface conduction and can focus on the volume resistivity, ρ, whose convenient units are (ohm cm^2)/cm or ohm-cm. The resistance R of a bar or plate insulator of dimension L (cm) in the direction of current flow and of area A (cm^2) perpendicular to this is:

$$R_L = \rho(L/A) \quad .$$

For the common insulator geometry of a ring or collar of inner and outer radii r_i and r_o and cylindrical length X between an electrode and a structural shell, the resistance in the radial direction is:

$$R_r = \rho(1/2\pi X)\ln(r_o/r_i) \quad .$$

From Kirchhoff's law of parallel circuits, it is evident that the ratio of wasted leakage current to working current in an insulated electrical system is inversely proportional to the resistance of the insulator and thus (for a fixed geometrical design) inversely proportional to ρ. It is simple enough to find high-ρ materials at room temperature; but high resistivity at high temperatures is another matter.

The two principal thermally-activated quantities in solid semiconduction are (a) the promotion of electrons or holes from the valence to the conduction band, and (b) the creation or increase of lattice nonstoichiometry (hence, increase in the electron or hole population) as the lattice vibrational energy increases with increasing temperature. The latter is of higher activation energy than the former, and becomes significant in a higher temperature range. Therefore, a plot of log ρ vs 1/T (in kelvin) is likely to show a more-or-less linear low-temperature branch of lower slope, joined to a more-or-less linear high-temperature branch of steeper slope.

Resistivities taken from Reference 11 are given in Table XI.4, together with a few entries from Refs. 3 and 8 and from some early data of National Carbon Co., for a variety of materials of comparative interest. The first grouping is of metallic elements, whose electrical and thermal conductivity both decrease with increasing temperature; and with them some familiar alloys. These metals are included here to establish the general magnitude of ρ for metallic conduction. The second group, a few carbide compounds, are also essentially metallic conductors, as is also graphite shown in the group of "others" at the bottom.

Temperature-dependent data for polycrystalline insulating oxide compounds are listed in the middle of the table. In the group of "others" the data are placed under the same temperature headings shown above them for oxides. Figure XI-12 is a composite plot of log ρ vs $10^3/T$ for all of these "nonconductors." Note that the $10^3/T$ scale (top of the figure) is reversed.

The solid points in the figure are those given in Table XI.4. The solid curve branches connecting them are relatively well justified. The dashed curve segments are ours, uncertified by the data but reasonable, illustrating the near-linear branches expected in each case from the foregoing discussion of mechanisms. Finally, two shaded regions are delineated in Figure XI-12, numbers "1" and "2," representing a variety of commercial refractories named in their legends.

The most important feature to be noted in this figure is the common tendency of all insulators to become increasingly conducting at temperatures much above 1000°C. By 1500°C, most refractories

Table XI.4 Electrical Resistivity of Selected Materials (Refs. 3, 8, 11)

VOLUME RESISTIVITY, ρ, microhm cm, AT TEMPERATURE IN °C

ELEMENTS	20°C	250°C	ALLOYS	20°C
Aluminum	2.65	3.64	Al (2017, 3003)	4.
Chromium	12.96	13.65	Brass (yellow)	7.
Copper	1.68	3.24	Cu (commercial)	1.7
Gold	2.24	4.15	Hastelloy C	139.
Iron	9.71	11.21	Inconel X	122.
Magnesium	4.45	8.25	Mg (AZ31B)	9.
Molybdenum	5.2		Monel K	58.
Platinum	10.6	11.5	Ni (commercial)	10.
Silver	1.59	2.99	Steel (carbon)	10.
Tungsten	5.6		18-8 (304) SS	72.

CARBIDES	20°C
B_4C	0.3 - 0.8
SiC (beta)	100.-200.
TaC	~30.
TiC	180.-250.
ZrC	~70.

OXIDES	20°C	250°C	500°C	750°C	1000°C	1250°C	1500°C
Al_2O_3 (alpha)	$8 \cdot 10^{21}$	$5 \cdot 10^{19}$	$(2 \cdot 10^{18})$	$2 \cdot 10^{15}$	$6 \cdot 10^{12}$	$(3 \cdot 10^{11})$	$(3 \cdot 10^{10})$
Cr_2O_3	$(3 \cdot 10^{10})$	$(4 \cdot 10^{9})$	$3 \cdot 10^{8}$	$8 \cdot 10^{7}$	$3 \cdot 10^{7}$	$2 \cdot 10^{7}$	$(1 \cdot 10^{7})$
Fe_2O_3	$4 \cdot 10^{4}$	$(2 \cdot 10^{4})$	$(2 \cdot 10^{3})$				
MgO (CRC data)	$(1 \cdot 10^{23})$	$(4 \cdot 10^{20})$	$(2 \cdot 10^{19})$	$(1 \cdot 10^{16})$	$3 \cdot 10^{13}$	$5 \cdot 10^{11}$	$4 \cdot 10^{10}$
MgO (Norton)	$(1 \cdot 10^{24})$	$(3 \cdot 10^{21})$	$(4 \cdot 10^{20})$	$(9 \cdot 10^{19})$	$9 \cdot 10^{18}$	$2 \cdot 10^{17}$	$2 \cdot 10^{16}$
SiO_2	$1 \cdot 10^{21}$	$(7 \cdot 10^{18})$	$9 \cdot 10^{14}$	$3 \cdot 10^{10}$	$5 \cdot 10^{7}$	$5 \cdot 10^{5}$	$4 \cdot 10^{4}$
SiO_2 (natural)	10^{15}-10^{21}						
TiO_2	$(\sim 10^{16})$			$6 \cdot 10^{10}$	$2 \cdot 10^{8}$	$4 \cdot 10^{6}$	$4 \cdot 10^{5}$
ZrO_2	$(3 \cdot 10^{15})$	$5 \cdot 10^{13}$	$(4 \cdot 10^{12})$	$7 \cdot 10^{9}$	$5 \cdot 10^{7}$	$2 \cdot 10^{6}$	$3 \cdot 10^{5}$
OTHERS							
BN	$1 \cdot 10^{20}$	$(1 \cdot 10^{18})$	$8 \cdot 10^{13}$	$(1 \cdot 10^{10})$	$(4 \cdot 10^{8})$		
C (AGW graphite)	560.	530.	525.	555.	620.	690.	755.
C (CS graphite)	900.	675.	645.	670.	730.	790.	845.
Glass	10^{11}-10^{15}						
Porcelain (NBS)	$(1 \cdot 10^{14})$	$(3 \cdot 10^{12})$	$3 \cdot 10^{11}$	$7 \cdot 10^{10}$	$2 \cdot 10^{10}$	$1 \cdot 10^{10}$	$(7 \cdot 10^{9})$
Mineral-Based Refractory Bricks					10^{10}-10^{12}		10^{8}-10^{10}
Chrome-Ore-Based Refractory Bricks					10^{8}-10^{9}		10^{6}-10^{7}

Parentheses enclose estimates.

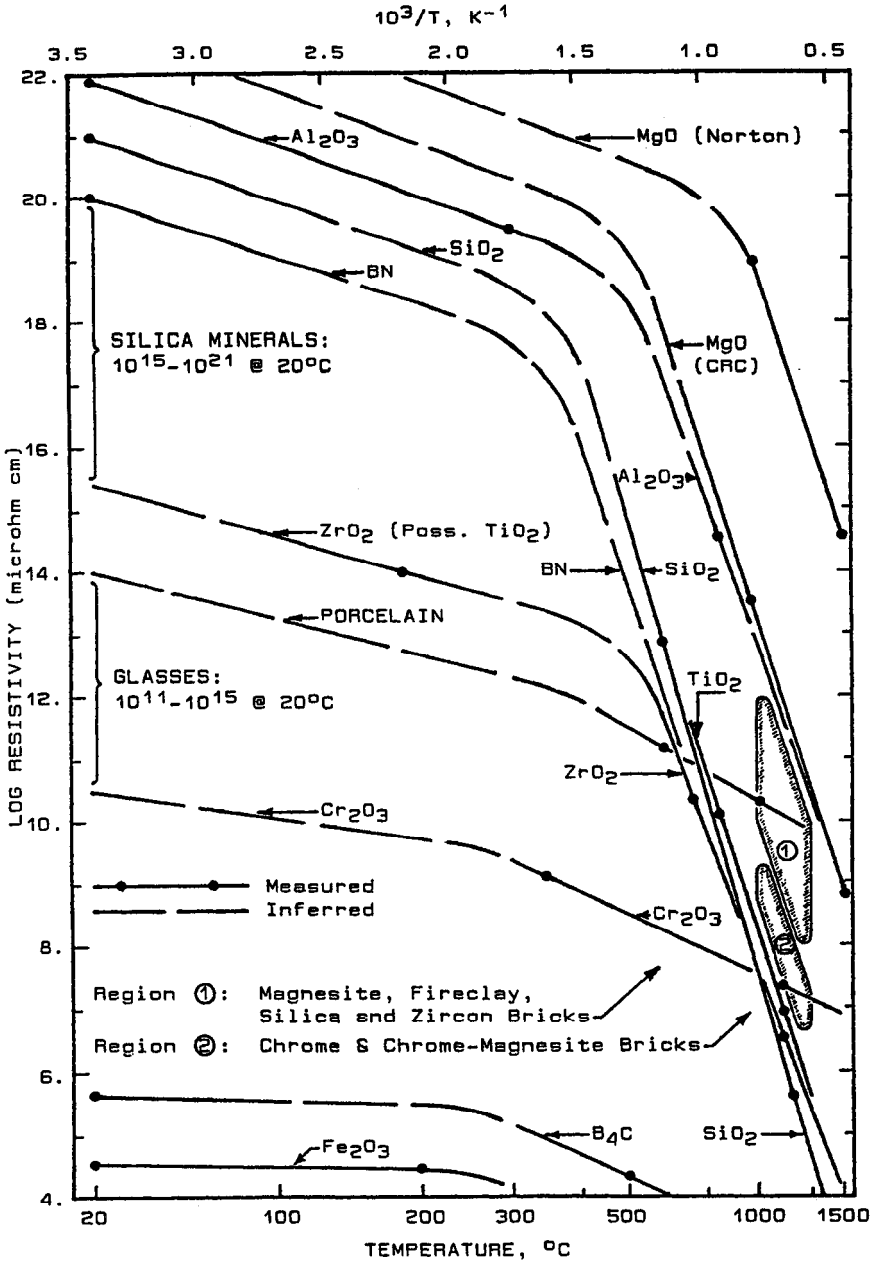

Figure XI-12 Electrical Resistivities of Insulating Materials vs Temperature (from Table XI.4)

and refractory oxides exhibit volume resistivities only a few orders of magnitude above those of metallic conductors. Thus insulator design dimensions that are entirely satisfactory at low temperatures may permit considerable current leakage in the 1000°-1500°C region and higher. Because the curve slopes are so steep, shielding or jacketing and water-cooling to, say, 500°C and below is far more effective in controlling leakage current than is simply increasing the radial thickness of a high-temperature insulator.

The figure also makes it evident that alumina and magnesia refractories have much higher resistivities at high temperatures than do those containing the oxides of Zr, Ti, Fe, and the alkali metals. Alumina performs reliably over a wide temperature span, giving way to the less-expensive steatites, other porcelains, and finally some glasses only at successively much lower temperatures. The insulating rings in the electric arc furnace, and many other high-temperature insulators, are typically made of high-alumina compositions for this reason.

Chapter XII

Design Properties: Mechanical

ELASTICITY AND PLASTICITY: CERAMICS AS A MODEL

So long as all bonds within a solid obey Hooke's Law, that solid will exhibit a linear and reversible relationship between its restoring *stress* and a mechanical deformation expressed as *strain*. The proportionality constant between the two is the *modulus of elasticity*: the *Young's modulus*, E, if the strain is compressive or tensile, or the *shear modulus*, G, if the strain is in shear or torsion. Thus,

$$\sigma = E\varepsilon \qquad \text{and} \qquad \tau = G\gamma \quad .$$

In simple loading geometries, plane strain ε is a fractional length change, $\Delta x/x$, while shear strain γ is a displacement per unit of length measured perpendicular to it, $\Delta x/y$. Both are dimensionless. Plane stress σ is a force per unit of area measured perpendicular to it, F_x/A_{yz}, while shear stress τ is a gradient of force per unit of width, $(dF_x/dy)/z$. Both have the dimensions of pressure. So also do the elastic moduli E and G. Units of convenient magnitude for these parameters are kg/mm^2 and 10^6 psi (lb/in^2). Their conversion factor is 10^6 psi = 703.1 kg/mm^2. For conversion into SI units, 10^6 psi = 6.895 GPa (gigapascals), where 1 Pa = 1 N/m^2 (Table II.1).

A dimensionless factor connecting E and G is *Poisson's ratio*, υ:

$$\upsilon = \frac{E}{2G} - 1 \quad .$$

As υ runs mostly around 0.2-0.3, the ratio E/G is typically about 2.5:1 in ceramics.

Ceramics at Room Temperature

Tensile stress-strain curves for dense ceramic materials at low temperatures are linear until they end in fracture. A high-strength polycrystalline oxide ceramic might have a fracture strength σ_f in tension of about 50,000 psi or 35 kg/mm^2 (actually measured in bending, and called the *modulus of rupture* or MOR). Its Young's modulus may be about $50 \cdot 10^6$ psi or 35,000 kg/mm^2. Thus it experiences shattering "brittle" or "catastrophic" fracture at a strain ε of about 0.001, or 0.1% elongation. There is no perceptible yield, or plastic deformation, prior to fracture. There is likewise no nondestructive mechanism for the redistribution of nonuniform stresses.

This inability to deform plastically makes any ordinary ceramic material on the one hand (a) susceptible to fracture under concentrated or "point" loading, and on the other hand (b) liable to fracture at the weakest stressed location in its own microstructure, e.g., at a pore, microcrack, weak boundary, missing grain, large grain, inclusion, machine-damaged surface feature, etc. (collectively called "flaws"). In neither case can a local high stress be relieved by local plastic deformation. Fracture stresses vary over a wide range along with the severity of flaws.[406, 407] Though ultra-fine-grained (sub-μm) ceramics and "toughened" ceramics[29] provide minor deviations, the critical size of the flaw that actually initiates catastrophic fracture is typically of the order of one to a few times the crystallite size: perhaps a few to 10 μm in length in the strongest materials.[408]

The room-temperature MOR of pure, dense, high-melting oxide ceramics is given in pascals by an adaptation of Griffith's equation:

$$\text{MOR} = K[\Gamma E/c(1-\upsilon^2)]^{1/2} \cong 1.5[\text{N/m}]^{1/2}[E/c]^{1/2} \quad ,$$

where E is Young's modulus in Pa, Γ is the "work of fracture" ($\geq$ surface energy) in N/m, υ is Poisson's ratio, and c is the critical flaw length in meters.[406] For mean grain sizes above ~20 μm or $2 \cdot 10^{-5}$ m, $\bar{c} \cong D$ (mean grain diameter).[408]

The Young's modulus applies to compression as well as to tension; but compressive strengths in ceramics run some 5 to 10 times the MOR.[409] Simplistically, this is because flaws are "pushed closed" rather than "pulled open." But ceramics in uniaxial compression typically fail in shear. It is readily shown that the maximum resolved shear stress in a uniform medium occurs at an

angle of 45° to a uniaxial compressive load, and that along such a surface, $\tau_{max} = \sigma/2$. The remaining factor in the fracture strength ratio may relate to the "closed" vs "open" crack argument. A more sophisticated analysis of compressive fracture is not needed for present purposes. Suffice it that this shear failure under compression is also elastic at low temperatures. There is still no perceptible ductility, though the macroscopic strain ε at fracture may be more like 0.005 to 0.01, or 0.5% to 1%. The stress-strain curve remains linear, hence E remains constant to the end.

Ceramics at Moderate Temperatures

Now raise the temperature by 100°C increments. In a well-behaved dense high-melting polycrystalline oxide ceramic, the Young's modulus falls gradually with increasing T. About the same rate of fall is seen in single crystals. Staying well below the Tammann temperature (Chapter IV), this decrement in E is typically only some 10-20% overall, and fairly linear with temperature.[409] In no way does it reflect a thermally-activated deformation process.

There are minor exceptions that have some parallel in refractories. A few high-melting ceramics have shown an initial small increase in E with increasing T, over the first 500°C or more, followed by the normal decrement.[408,409] This "trend reversal" has been attributed to relief of internal stresses. Similar-appearing curves of MOR vs T[409] lend weight to the argument. An exception of a different kind is found in SiC: this ceramic shows no dependency of E on T over at least 1000°-1500°C, when well-bonded.[409] Most other carbides are not this unusual.

If there is a trend in the shear modulus of oxides, it is that G falls a little faster with increasing temperature than does E, and Poisson's ratio accordingly rises. But this is by no means universal.

Meanwhile, still staying well below the Tammann temperature, the average MOR of most high-melting oxide ceramics falls comparably with E in terms of percentage loss of the room-temperature value.[409] This behavior persists variously to some 1000°-1200°C or higher. Compressive strengths fall faster, typically losing from half to 2/3 of the room temperature value by 1100°C. In fact, the usual curve of compressive strength vs T starts down somewhat steeply from room temperature, then tails out at decreasing negative slope with increasing T to temperatures of the order of 1500°C.[409]

Macroscopically speaking, in this temperature range elastic behavior is still in effect. There is no noticeable curvature in stress vs strain in the vicinity of fracture. The fracture itself tends to become

more simple, less shattering, and predominantly intergranular in its path, however, as the temperature is increased.

The term, "microplastic deformation," was coined decades ago to explain these observations from room temperature on up. In oxide ceramics as opposed to metals, even in the chemically purest case there is a marked disparity in strength and stiffness between the crystals and the intercrystalline boundaries.[110] Grain-boundary shear or tearing has to be the usual fracture-initiating process even at room temperature. By the rough order of 1000°C, there is no doubt.

Yet this is not necessarily plastic deformation in the ordinary sense, even in the limited domain of the crystal boundaries. The crystals do not appear to participate by diffusion, least of all by dislocation activity. The temperature dependence of strength is quite distinct from that of thermal activation. Though segregated impurities are undoubtedly involved,[110,408] their bulk melting is not. The finest-grained oxides, only slightly stronger at room temperature than modestly coarser ones, show evidence of pre-critical crack growth.[408] They also lose strength more rapidly with increasing temperature.[409] All this points to grain-boundary tearing as the initiator of fracture.

Ceramics at High Temperatures

In some high temperature interval the common behavior of polycrystalline ceramics is to show a "knee" in both the E vs T curve and the MOR vs T curve.[409] This "knee" is a rapid downturn, completed in about a 100°-200°C interval, beyond which either property retains only a small fraction of its original value. The corresponding stress-strain curve bends a little at first, then increasingly with increasing T. Single crystals do not show this behavior in this temperature interval.[409]

In polycrystals the temperature location of the knee depends primarily on chemical purity of the material. That temperature was historically increased some 500°C by attending to chemical purity in MgO, BeO, and Al_2O_3 ceramics.[110] But a knee always appears. Even in refractory oxides of 99.8, 99.9 and 99.9+% reported purity, the knee occurs somewhat below the Tammann temperature; and further, except for MgO there has been no evidence whatsoever of dislocation activity in the grains along fractured surfaces. Yet, at a sufficiently low rate of loading in the MOR bend test, at temperatures much above the knee specimens may show "plastic" deformations or strains up to the order of 10% before fracture -- or may not fracture at all. Fracture in the MOR test, above the knee, is by progressive tearing and is entirely intergranular.

Numerous studies of *creep* (time-dependent plastic deformation at constant load) of polycrystalline oxides have been conducted at temperatures above that of the knee in the MOR.[409] Creep is not constructively measurable below the knee because (a) there is essentially no deformation other than elastic, prior to fracture, and (b) the applied stress required to seek it is essentially the fracture stress.

Creep of polycrystalline oxide ceramics occurs in three stages nominally corresponding to those of metals, but not for the same reasons. In only rare cases does it have anything at all to do with dislocations.[410] It is primarily a matter of sliding or shear movement of grains separated by more or less continuous films of liquid of greater or lesser viscosity and greater or lesser interfacial tension. In Stage II (steady-state) creep the liquid films remain unbroken, flow is stable, and the specimen volume remains constant with increasing strain. In Stage III (pre-rupture) creep, liquid films are progressively broken or parted from the grains, voids develop and the volume increases slightly; instability develops as voids link up or coalesce, and rupture by tearing occurs where the film-bonded fraction of a stressed cross-section or shear plane becomes too small to support the load.

The effect of increasing temperature on ceramic creep is dual: (a) more liquid is produced, and (b) its viscosity decreases. The effect of increasing the load at a fixed temperature is also dual: (a) the creep or strain rate increases by $\dot{\varepsilon} \propto \sigma^a$, with $1 \leq a \leq 4$; and (b) the onset of Stage III is eventually hastened. Efforts to analyze Stage II creep of ceramics in terms of the viscosity of liquids have not worked out very well because of the wide range of non-Newtonian liquid shear rates present in an array of closely-spaced particles, the interplay of viscosity and interfacial tension in thin liquid films, and the variation of both amount and composition of the liquid with temperature. Nevertheless, it is certain that creep here is a manifestation of viscous flow in a two-phase (liquid + solid) system. The "knee" referred to above is clearly identified with the onset of grain-boundary melting.

Porosity and Grain Size Effects in Ceramics

Grain or crystallite size in ceramics affects only strength and creep. The average low-temperature MOR or fracture stress in tension tends to obey $\sigma_f = aD^{-1/2}$ in coarser textures and $\sigma_f = a'D^{-1/2} + b$ when $D < 20\ \mu m$.[408] Here D is mean grain diameter and a, a' and b are constants. Creep rates increase with decreasing grain size, as expected.[409]

Porosity affects all the mechanical properties, but not by the same amounts. The equation used in Chapter XI for transport properties will not do. Equations that have been employed for mechanical properties of ceramics are all substantially empirical, though recognizing that pores are concentrators or multipliers of stress at close range in addition to their reducing the overall solid volume fraction.[411] The two most popular and simple mathematical forms, applied to Young's modulus and MOR data in particular, are:

$$X = X_0(1 - bP) \qquad \text{and} \qquad X = X_0 \exp(-bP) \ ,$$

where X_0 is the property at zero porosity, X is that at pore volume fraction P ($=f_v$), and b is a data-fitting constant. These two forms are identical at a few percent porosity, while the second manages much better over wide ranges.[409] Values of b in the exponential equation have grouped mostly around 3 to 4 for MOR at room temperature, climbing slowly with temperature and grouping around 4 to 5 at 1000°C. Values for E appear more like 2 to 3 and 3 to 4, respectively.[409]

The following table illustrates the magnitude of adjustment made by this exponential equation for various $P = f_v$, giving the ratio X/X_0 for b = 2, 3, 4, and 5:

Porosity, P:	**0.05**	**0.10**	**0.15**	**0.20**	**0.25**	**0.30**	**0.40**	**0.50**
X/X_0, b=2:	0.90	0.82	0.74	0.67	0.61	0.55	0.45	0.37
X/X_0, b=3:	0.86	0.74	0.64	0.55	0.47	0.41	0.30	0.22
X/X_0, b=4:	0.82	0.67	0.55	0.45	0.37	0.30	0.20	0.14
X/X_0, b=5:	0.78	0.61	0.47	0.37	0.29	0.22	0.14	0.08

All of the above applies only to elastic behavior, viz., only below the temperature of the knee in MOR-T and E-T curves. Above the knee the only property of interest is creep, for which but little data exist for ceramics at high porosities.[409] The indications are that P exerts a profound effect on $\dot{\varepsilon}$, correlating positively. It is probable that porosity interacts with both the applied stress exponent ($\dot{\varepsilon} \propto \sigma^a$) and the temperature effect on creep rate.

Summary of Ceramic Behavior as a Model

This introduction to the mechanical properties of fired refractories by way of their single-phase ceramic counterparts anticipates that the two are of one kind. Their elastic moduli are of the same origins. They are elastic and brittle (and thermal stress sensitive) much below first melting by the same rules. Both are

stronger in compression than in tension for the same reasons, and both show a wide scatter in MOR for the same reasons. Both are excessively weak and subject to creep above the "knee;" and the same principles govern their Young's modulus and MOR behavior below the knee. Fired or sintered refractories differ importantly from single-oxide ceramics in both phase composition and microstructure; but they are better understood comparatively than as some new type of matter without precedent.

Unfired refractories are bound in addition to introduce reaction-bonding effects into their temperature-dependent mechanical behavior. But again it is better to view these effects as superimposed on a common foundation than as something wholly novel.

Table XII.1 summarizes the important mechanical properties of a number of "best" pertinent single-phase oxide ceramics at room temperature and extrapolated to theoretical density, drawn from the compilation of Reference 409. While ultra-fine-grained and toughened versions[29] are not represented, that source has the advantage of a contemporaneous view of a large number of different simple compositions. Effects of purity, grain size and porosity have to be inferred from the foregoing text. The characteristic effects of temperature on the Young's modulus, modulus of rupture, and stress-strain curves are illustrated schematically in Figure XII-1, representing no one particular ceramic but serving for comparison with the features to be seen next in refractories.

MECHANICAL CHARACTERIZATION OF REFRACTORIES

Young's Modulus vs Composition

For obvious economic reasons, even "single-phase" refractories are not made chemically purer than they have to be to perform their assigned functions. In such products, up to the limit of elastic response the Young's modulus at room temperature should ideally resemble that of each respective ceramic counterpart -- but subject to some critical differences to be noted presently. Heterogeneous compositions will exhibit a range of (mostly still lower) room-temperature E values; but their melting behavior will add even more variety to the temperature of onset and the temperature interval of the knee between brittle and viscous behavior. Melting temperatures and ranges were treated at length in Chapter IV.

Maximum knee temperatures are found in direct-bonded and fused single-phase refractories, in spinel-bonded basic compositions including $MgAl_2O_4$ and $MgCr_2O_4$ bonds, and in the ZrO_2-Al_2O_3 system.

Table XII.1 Room-Temperature Mechanical Properties of Dense Single-Phase Ceramics (Ref. 409)

COMPOSITION	MOR		COMPRESSIVE STR.		YOUNG'S MOD., E		SHEAR MOD., G		POISSON'S
[grain size]	kg/mm^2	10^3 psi	kg/mm^2	10^3 psi	kg/mm^2	10^6 psi	kg/mm^2	10^6 psi	RATIO, ν
Al_2O_3 [1-2 μm]	>46.	>65.	>280.	>400.	42,200.	60.	16,600.	23.6	0.27
BeO [20 μm]	>28.	>40.	>210.	>300.	40,000.	57.	15,500.	22.	0.30
MgO [1-3 μm]	29.5	42.	84.5	120.	32,300.	46.	13,000.	18.5	0.24
ZrO_2 [CaO stab.]	>25.	>35.	210.	300.	25,000.	35.5	9,500.	13.5	0.31
$MgAl_2O_4$ [10 μm]	22.5	32.	190.	270.	29,500.	42.	11,200.	16.	0.31
$Al_6Si_2O_{13}$	17.5	25.	134.	190.	17,600.	25.			
Mg_2SiO_4	14.	20.	56.	80.	(17,600.)	(25.)	(Estimated)		
$ZrSiO_4$	14.	20.	70.	100.	14,000.	20.			
B_4C	>35.	>50.	280.	400.	45,700.	65.	19,000.	27.	0.20
SiC	42.	60.	140.	200.	49,200.	70.	20,400.	29.	0.21
AlN	28.	40.	210.	300.	35,200.	50.			
BN	12.6	18.	31.5	45.	10,500.	15.			

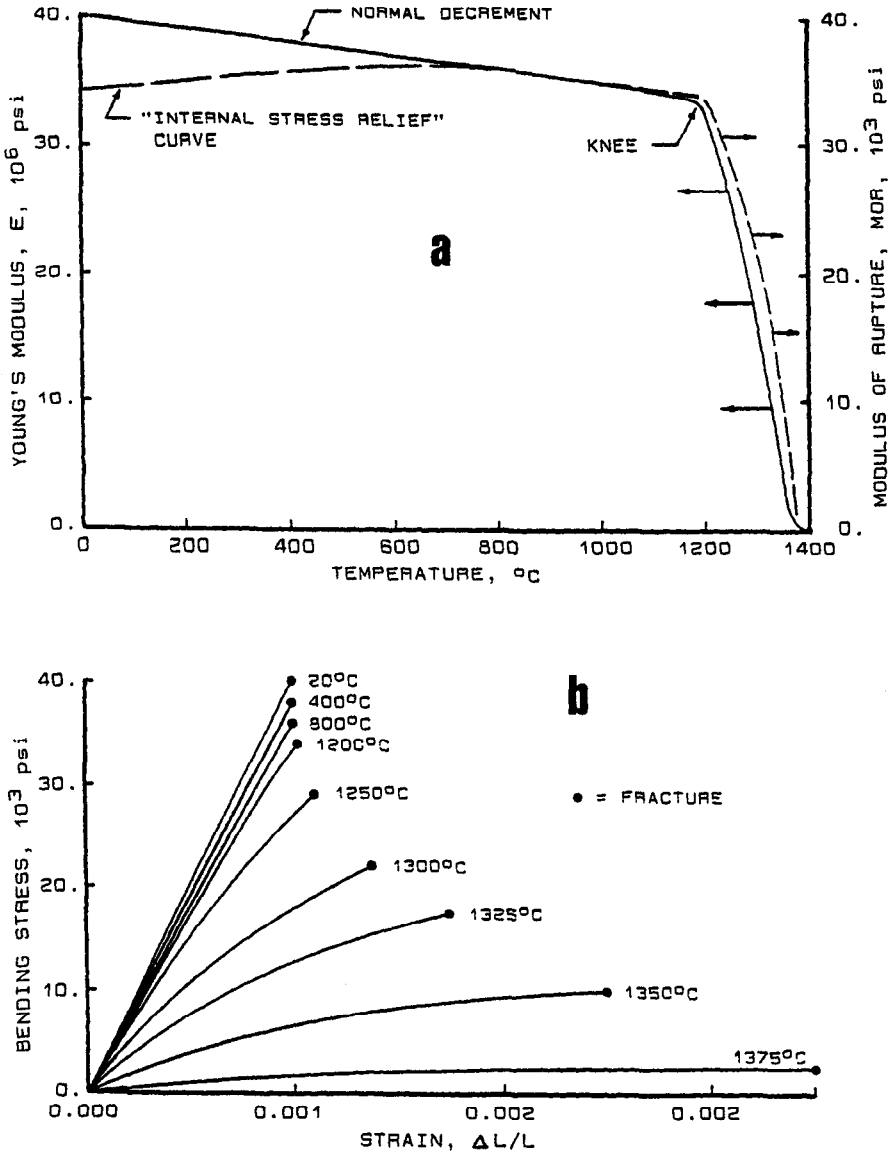

Figure XII-1 Typical Mechanical Properties of a Dense Oxide Ceramic: a. Young's Modulus and MOR vs T b. Bending Stress vs Strain vs Temperature

Highest-viscosity liquids are of high SiO_2 content, but those are generally lower-melting except for silica itself in the "super duty" (i.e., 99+% pure) version. The zircon-zirconia system, zircon-MgO system and parts of the A-Z-S system are relatively high-melting, barring alkali and alkaline earth impurities; likewise MgO-forsterite. Modern SiC bonds are extremely high-melting.

A further uniqueness may exist in heterogeneous oxidic refractories when there is a large volume of lower-melting matrix material between grains of the major phase(s). Intergranular material has its own Tammann temperature. There must then be a range of temperatures between this and the onset of bulk melting, over which plastic deformation in the matrix comes into play in stress, strain and fracture. This phenomenon is bound to be diffusion-controlled and thermally activated. It should lower the temperature of onset of the E-T knee somewhat below that of the onset of melting; but it would not be seen separately. The kinetics of this phenomenon will be put in perspective presently.

Young's Modulus vs Microstructure

Grain or crystallite size, per se, should have little effect on the low-temperature Young's modulus of refractories. But it has a very large consequential effect, namely due to *microcracking*. Chapter IV indicates that an increasing extent of microcracking must accompany increasingly coarse-crystalline microstructures and the use of still coarser-sized premanufactured grain or aggregate. Accordingly, depending on the coarseness of their texture, refractories can be expected to have (a) markedly below-ceramic Young's modulus values, and (b) a dependence of E upon P which, if still exponential, will exhibit other-than-ceramic values of b in the function $E = E_o \exp(-bP)$. A further consequence of microcracking with open porosity, which also sets refractories apart from dense fine-grained ceramics, is a sharp reduction of the "elastic limit." The mechanism of this is worth pursuing.

Effect of Method of Measuring E

It is necessary to pause, first, to examine the two different ways in which elastic moduli are measured. One is *sonic*, often called *dynamic*. The velocity of sound in an elastic medium is a known function of the bulk modulus of elasticity, which is a known function of E and G. One way of utilizing this fact is to send a brief pulse of ultrasonic vibration down a rod from one end, then electronically to sense the same pulse reflected back from the opposite end and to measure the elapsed time.[9] This method works well for dense, fine-grained ceramics. The coarse texture, microcracks and porosity of

most refractories are so scattering and damping of ultrasound as to frustrate this technique, however.

A second sonic method, which is used for both ceramics and refractories,[412] is to support a bar or brick horizontally at its two nodes and to vibrate it flexurally by use of a variable-frequency electromechanical transducer. One starts at a low frequency and works up. The fundamental flexural frequency is found by sensing the first peak in amplitude that occurs when the transducer and the specimen remain in phase. Hence the name, "resonant" technique. The frequency, wavelength, velocity of sound, and specimen dimensions are uniquely related,[9,412] and E is computed.

The limitations on the resulting "dynamic" Young's modulus are that (a) the amplitude of vibration is always extremely small, hence the stress and strain connected by the measured E are all but infinitesimal; and (b) the effects of microcracks and porosity, while averaged into that E, are not sampled over an informative range of stresses. Then, (c) neither are any inelastic deformation processes disclosed.

These limitations are overcome in principle by the *static* method of measuring E, which is to measure σ and ε simultaneously and continuously, right up to fracture, using an Instron or similar test machine. Usually the strain is increased from zero at a fixed rate. This is done in the course of measuring either the MOR (bending strength) or the compressive strength of a specimen. The *static* or *secant* Young's modulus is the locus of all σ/ε values from (0/0) to fracture. *Nonlinearities* in the σ vs ε curve are more likely to be seen or exaggerated in flexure than in compression, by the previous "pulled open" vs "pushed closed" argument concerning flaws or cracks.

There are in fact three different values of the Young's modulus of a refractory, which it is necessary to distinguish:

(1) The *intrinsic* modulus, E_i, pertaining to theoretical density and without microcracks but a function of phase composition and temperature.

(2) The *dynamic* modulus, E_d, representing purely elastic behavior but incorporating the effects of microcracks and porosity; measurable sonically, but without any known mathematical connection to E_i.

(3) The *static* modulus, E_s, superimposing on E_d the effects of inelastic deformation processes (hence nonlinearity of σ vs ε) which at least exhibit hysteresis and may be

irreversible. Measurable as macroscopic stress vs strain up to fracture but at relatively low loading or deformation rates.

In microcrack-free ceramics, E_i is computed by measuring E_d at low porosity and extrapolating to P = 0. A means of estimating E_i for refractories will be suggested presently.

Two Low-Temperature Features of Stress-Strain Curves

At modest temperatures and the lowest stress levels, an initial *upward* concavity of the static stress-strain curve is sometimes seen.[413] That feature may reflect a nonuniform elastic stress and strain distribution within the solid, which may be induced by voids or in solid phases of disparate E. Initial deformation will then be borne unequally between thin ligaments and massive volumes of the same solid, or will give rise to different stresses in bonded solid phases of different E, resulting in an *elastic* redistribution of internal stress and strain with increasing load. This response to initial deformation in a refractory is without internal friction. It is reversible and free from hysteresis. The redistribution of stress and strain soon stabilizes with increasing σ, and the stress-strain curve becomes linear at a slightly higher slope.[413]

A second possible cause of the same observed nonlinearity is a minor misalignment of the test specimen with the loading rig. In either event, if the change in slope is small the observation is inconsequential. The higher, constant value of E is the useful value.

A more meaningful and common feature of stress-strain curves of refractories is an initial *downward* concavity. At low temperatures this is ordinarily followed by some linear interval of increasing stress and strain, thus of constant E but perceptibly below its initial value.[413,414] This too is a matter of redistribution of stresses and strains within the solid. Though it is *inelastic* in outward appearance (viz., by curvature in σ vs ε), the inelastic component is permanent. That component is believed to consist of *noncatastrophic grain-boundary tearing.* In a dense ceramic, if seen, it would be called "pre-critical crack growth." The difference is that here it occurs at many locations simultaneously and at very low stresses, and the aggregate effect on macroscopic stress and strain is readily discernible.

It will be recalled that under Thermal Anisotopy and Differential Thermal Expansion in Chapter IV we left many interfacial microcracks stopped at room temperature because the length of boundary ligaments between them was just able to support the residue of shear strain originating in differential contraction. The frequency of such precariously-balanced situations in a heterogeneous refractory has

not been estimated, but it has to be very high. Now, under an externally-applied body stress or strain, the extension of such sharp-tipped microcracks must be resumed essentially without a threshold, wherever such cracks are favorably oriented relative to the local resolved tensile and shear stresses. With increasing applied stress or strain an increasing number of such microcracks will be activated, progressively including those less and less favorably oriented, until the supply of this type of internal crack configuration is exhausted.

The idealized description of each initial configuration consists of a pair of open-ended microcracks, their sharp tips facing each other in the same boundary or interfacial plane. The idealized final configuration (after the two cracks run together or "link up") consists of a single larger crack, its open ends lying in pore walls and thereby blunted. Thus the growth of each such pair of cracks is terminated pending some higher level of applied stress or strain. The cumulative progress of this noncatastrophic tearing might be monitored by acoustic emission,[34,35,37] but each individual event at low stress is unlikely to be heard. Crack extension at low temperatures is irreversible, however. The simplest confirmation of the above explanation of initial downward concavity in refractory stress-strain curves would be to unload and reload the specimen after a linear interval has been entered. At this writing there has been no published report of such a test.

Time Dependence of High-Temperature Stress-Strain Curves

To the extent that any other than purely elastic deformation processes contribute to the strain at any applied stress, the resulting ε and hence static E will be *time-dependent*. Inelastic deformation invariably produces a downward concavity in a plot of σ vs ε, and always at stress levels leading incrementally toward ultimate failure. Except for the unique case just described, it is also always associated with the knee in the E vs T curve. Three high-temperature inelastic processes are recognized, in order of increasing characteristic temperatures of onset.

The first is plastic matrix deformation, if it occurs, taking place above the Tammann temperature of the matrix. The total strain in this case is called *elastico-plastic* strain.[3] Upon a small further increase in T the matrix commences melting and *viscoelastic* deformation ensues, wherein bonded grain-boundary segments or necks in the solid alternate irregularly with pockets of viscous liquid.[415,416] At still higher temperatures *viscous* deformation is observed, wherein the liquid phase becomes essentially continuous and no further solid deformation is involved. These last two types may also evolve from one into the other with time at fixed temperature, as with increasing

strain the remaining solid-bonded necks give way successively to the intrusion of liquid from adjacent pockets.[415,416] The three deformation modes entail decreasing stress at a given strain in the order listed, and each one typically ends in fracture. In refractories, the last two modes and their progression at fixed temperature can be further complicated by simultaneous time-dependent chemical changes, including the simple dissolution of solids and the retention or formation of crystallites in the molten matrix.[189,416]

Inasmuch as the inelastic part of each of these processes is time-dependent, the measured E will always increase with increasing stress or strain *rate*, and conversely. It follows that the concave-downward portion of any high-temperature stress-strain curve is never intrinsic but has meaning only at the stress rate or strain rate employed in the test.

Low-Temperature Strength: Critical Crack Length and Grain Size Effects

The Griffith equation, focal to the discipline of brittle *fracture mechanics*,[8,417] was cited at the opening of this chapter. Reducing that equation to its shorthand approximation,

$$MOR \cong 1.5[N/m]^{1/2}[E/c]^{1/2} \quad ,$$

strips from it the whole issue of fracture toughness with which we have had several encounters earlier in this book. Taking the work of fracture Γ out as a variable in no way discounts its importance, but permits focussing in this section on the remaining vital elements of brittle fracture. These are the Young's modulus E and the critical crack length c.

A sharp-tipped crack or flaw of length L becomes thermodynamically critical (L = c) when the energy expended in its differential extension is just returned in full by the surrounding elastic relaxation which accompanies that extension. For any length L < c, crack extension costs a net energy input or might not occur at all. For any length L > c, the excess energy returned increases with the disparity: post-critical crack extension is spontaneous and violent.

The above equation relates the critical crack length c to the MOR or tensile fracture stress, σ_f. Any applied stress σ has a corresponding imagined critical crack length c at which fracture would occur at that stress. To illustrate this concept, place a refractory specimen under a test in which the strain ε and hence σ is slowly increased; and imagine one particular flaw of initial length L which is

fated ultimately to initiate fracture when a particular stress σ_f is reached.

At first, $\sigma << \sigma_f$ and $c >> L$; increasing the applied load strains the specimen elastically, storing increasing Hookeian energy in the body but doing no work on the flaw itself. That is, L remains constant. Now bring σ up close to σ_f but still $<\sigma_f$, at which point c comes close to L but is still >L. Now pause. There are two options to bring about failure:

(a) Raise σ again until $\sigma = \sigma_f$, while c decreases until c = L. This is a common circumstance in MOR testing. But the second option is the more interesting.

(b) Switch the test machine to constant load, σ remaining $<\sigma_f$ but close to it. In time the crack will undergo *precritical growth,* i.e., L increases toward the existing fixed c. As it does so the specimen relaxes elastically, becoming more compliant. The test machine responds by increasing the strain ε to hold σ constant. The work thus done by the machine, $\sigma d\varepsilon$, provides the net energy input for crack length extension dL. Over time, then, the crack length L rises to meet the existing c while the corresponding fracture stress σ_f falls to meet the existing σ, and fracture ensues. The MOR thus observed is less than that prevailing under option (a).

Precritical crack growth, also called *slow crack growth* in the language of fracture mechanics,[417] is complicated in refractories by the proximity of large numbers of microcracks and pores or voids. There it typically takes the form of a jerky, discontinuous running-together or "linking-up" of pairs of cracks,[418] observable for example by acoustic emission sensing.[34,35,37,74] This phenomenon is responsible for stress fatigue (i.e., weakening), and particularly for the cumulative effects of cyclic thermal stresses on refractories (Chapter IV). It also applies over the long periods of high steady-state stresses to which refractories are often subjected. Though the methods of isolation and study of slow crack growth have become quite sophisticated and have even been applied to refractory specimens,[418] the complexity of refractory microstructures has so far deprived fracture mechanics of any significant predictive capability. One is impelled, however, to distrust the short-time measured MOR as an index of long-time stress resistance. The practical ASTM thermal stress tests mentioned in Chapter VIII continue to fill the gap.

That same heterogeneity of most refractory microstructures also deprives Griffith's equation of the tidy energy-balance

computations on which it is based. It too loses its quantitative predictive value. The abbreviated equation given above is suitable only for order-of-magnitude relationships among E, the MOR, and the critical crack length c. Since preexisting flaws are so prolific and so large in most refractories, there is next-to-zero chance that tensile failure will ever be initiated at a critical crack size that is smaller than one of these. The characteristically low strengths and the scatter of strength values in refractories have their origins in these flaws.

What is the magnitude of these flaw sizes? Generally, the larger or more open surface microcracks on a refractory brick are visible to the naked eye. Sawing a brick to expose the interior reveals the same. The crack dimensions are comparable to the coarser features of the solid microstructure, ranging up to the 1/4" or so top size of premanufactured grain (Chapter VI). Fused-cast microstructures are usually somewhat less coarse, and so are those of fireclays and other powder-compacted refractories.

Irrespective of philosophical distinctions between crystallite size and aggregate size as a measure of texture, the larger microcracks in refractories can be imaged and can be measured. Rarely do they fall below a few hundred μm (few tenths of a millimeter). In many refractory bricks, pre-existing cracks are in the millimeter domain, ranging on occasion up to the order of 10mm.

The remaining quantity needed is the Young's modulus, and thereby hangs a trilemma. Which among the three Young's modulus values we have listed should be used? The static Young's modulus is rejected in this context, since the strain measured statically may include inelastic components which cannot store releasable energy prior to fracture. The dynamic modulus has been used,[418] on grounds that it is a truly elastic measure of E. This practice is probably carried over from dense ceramics, where the difference between the intrinsic modulus and the measured dynamic modulus is trivial.

In refractories, however, the difference between E_i and E_d is sometimes close to an order of magnitude; and it is important. A case can be made for the use of E_i instead of the dynamic modulus here, as follows:

(a) Only the solid fraction can store and release elastic energy, and that storage and release are governed by the Young's modulus of the solid, namely by E_i.

(b) In the triggering of fracture (energy-balance criterion) in these materials, it may be sufficient to consider only a small volume element which contains the critical

crack. That volume element is all solid, governed by E_i.

In support of these arguments, use of the intrinsic Young's modulus in the above abbreviated Griffith equation gives much more acceptable results than does the dynamic modulus.

Intrinsic E values for some oxide compounds are given in Table XII.1. For two-phase oxidic refractories it should be sufficiently accurate to use for E_i the volume-weighted average of those of the two major phases. The abbreviated Griffith equation rearranged explicit in c reads:

$$c \cong 2.25E/(MOR)^2 \quad .$$

Table XII.2 contains the MOR and E_d data of Reference 418 for ten aluminous refractories, the E_i for each estimated by volume-weighted averaging as above, and the critical crack length c computed for each one by the above equation using E_d and E_i, respectively. The table is filled out by adding two further high-Al_2O_3 refractories, four basic refractories, and five insulating aluminous refractories, drawing data from other sources credited in the footnotes.

The c values in the right-hand column of Table XII.2 are in good accord with the textures of the refractories represented. As such they are more acceptable than those computed using E_d. The submillimeter values of c for the low-alumina bricks reflect the presence of a vitreous silicate component in the fine-crystalline matrix which limits initial flaw size. The multiple-mm values for the basic bricks reflect the exceptionally large thermal contraction of the MgO phase on cooling in their manufacture (Figure IV-9a) and resultant coarse microcracking.[34]

The insulating refractories are listed in the table in order of increasing percent void volume. Those of $P \geq 70\%$ give computed critical crack lengths of several hundred mm, or multiple tens of centimeters. Those high-void-volume cellular materials typically fail by progressive tearing as opposed to Griffith-critical catastrophic crack propagation; the c data are quite in accord with this behavior.

On balance, it appears that this simple Griffith-derived equation can satisfactorily rationalize the low-temperature tensile strengths of refractories, leaving no major mysteries. A few systematic studies have confirmed that refining the texture of a refractory increases its strength.[38,419] Other conventional strength relations at low temperatures will be taken up later.

Table XII.2 Computed Critical Crack Length for Various Refractories from MOR, E_d and E_i

BRICKS % Al_2O_3[a]	MOR, 10^6 Pa[a]	E_d, 10^9 Pa[a,b]	E_i, 10^9 Pa[c]	c COMPUTED FROM E_d, mm[d]	c COMPUTED FROM E_i, mm[d]
42	34.1	67.0	189.	0.13	0.36
45	31.8	69.8	187.	0.155	0.42
59	22.9	46.1	180.	0.20	0.77
70	9.8	13.5	172.5	0.32	4.04
70	17.3	32.5	172.5	0.24	1.30
70	13.9	30.3	172.5	0.35	2.01
72	11.2	24.1	179.	0.43	3.22
72	27.4	75.4	179.	0.23	0.54
85	45.6	93.0	271.	0.10	0.29
91	20.0	40.0	324.	0.225	1.82
90[e]	13.7[e]	39.2[e]	320.	0.47	3.82
99[f]	26.2[f]	--	400.	--	1.31
% MgO[e]	MOR[e]	E_d[b,e]	E_i[c]	c FROM E_d[d]	c FROM E_i[d]
46 (+Cr)	6.9	--	245.	--	11.6
60 (+Cr)	8.8	40.2	265.	1.17	7.7
98	10.3	--	294.	--	6.2
98	17.2	--	294.	--	2.2
INSUL. % Al_2O_3	FORM	POROSITY, %	MOR. 10^6 Pa	E_i, 10^9 Pa[c]	c COMPUTED FROM E_i, mm[d]
82[e]	BRICK[e]	42.[e]	6.9[e]	265.	12.5
38[e]	CASTABLE[e]	70.[e]	1.0[e]	191.	430.
44[e]	CASTABLE[e]	72.[e]	1.44[e]	187.	200.
45[f]	BRICK[f]	76.[f]	1.1[f]	187.	350.
39[f]	BRICK[f]	85.[f]	0.82[f]	190.	640.

NOTES:
[a] - Data from Ref. 418 except where noted otherwise.
[b] - Dynamic Young's modulus.
[c] - Intrinsic Young's modulus: see text for estimation.
[d] - Computed by the equation: $c\ (mm) = 2250 \cdot E/(MOR)^2$.
[e] - Data from National Refractories & Minerals, Inc.
[f] - Data from Thermal Ceramics, Inc., Augusta, GA.

High-Temperature Strength

Refractories show the same knee in both strength and Young's modulus as do dense ceramics; but where matrix melting progresses over a wider temperature range, so must the early part of the knee. Systematic studies of MOR vs T and of E vs T are rare, particularly the latter; and measures of the dynamic modulus above room temperature are all but absent. Nevertheless, there appears to be no feature of the temperature-dependent downturn in E_s and σ_f that is inconsistent with the melting behavior of oxidic refractory compositions and the relative viscosities of their early-melting liquids.

Between room temperature and the knee, different refractories exhibit different modulus and strength behaviors. The normal decrement seen in dense ceramics is also sometimes in evidence here, often exaggerated beyond explaining as a simple effect of temperature on atomic bond strength and stiffness. Likewise, the early trend reversal shown dashed in Figure XII-1a for ceramics sometimes appears exaggerated in refractories, beyond explaining as relief of internal stress. In these characteristically opposed behaviors, the properties near the knee appear to be the more consistent. It is the room-temperature values of E_s and σ_f that spread widely and somewhat unpredictably for refractories of a given composition class or type, and from one type to another.

The qualitative explanation of this behavior lies in the vastly different kinds and degrees of intercrystalline bonding that are in effect in refractories. These differences begin with the different approaches taken in manufacture: thermal sintering, reaction sintering, chemical bonding and cement bonding, to name the most recognizable and conventional. The chemical composition, previous thermal history, and particle sizing of each constituent of a given refractory mix are also of major importance; a convincing example in current practice lies in the difference between colloidal silica and even the most finely-ground crystalline SiO_2. Then whatever degree of bonding may have been achieved at temperature, its extensive destruction by microcracking adds variety, depending on the thermal expansion coefficients and anisotropy and the crystal and aggregate sizing of the final phases, their amounts and distribution, and the processing temperature from which the product is cooled. Unfired refractories add still more to this variety, as does also porosity as a variable.

For the most part, strengths in the elastic temperature region are adequate for the usages of refractories. Some transient weaknesses have arisen among products that are installed unfired. It was mentioned in Chapter VI, for example, that the succession of chemical changes in calcium aluminate cement left its cemented

products mechanically vulnerable at intermediate temperatures.[220] Another example is the pitch-bonded basic refractory which, when coked in place in the BOF, became the first of the MgO+carbon composites. Industrial pitches, upon heating, first exhibit a decrease in viscosity whereby pitch-bonded bricks risk slumping under their own weight during burn-in in a BOF wall. Then at some 400°C and above, polymerization gradually stiffens the pitch until eventually it cokes and becomes permanently rigid as carbon. In both CA-cemented and pitch-bonded refractories, reformulation and the use of chemical additives have controlled this transient weakening.

Intermediate-temperature weakness and subsequent strengthening, resulting from such transient physico-chemical changes, can be effectively revealed by a laboratory procedure measuring *thermal expansion under constant load.*[9] A fixed compressive load is applied which is too small to fracture the specimen; then the temperature is raised at a constant rate and the dimensional change is measured continuously. Lacking disruptive internal changes in the specimen, a strain-vs-temperature curve is obtained which resembles a thermal expansion curve. A temperature interval of transient softening is made readily evident by a halt or reversal of this expansion, followed by its resumption on conclusion of the disturbance. The technique was described and interpreted for pitch-bonded periclase, for example, in Reference 173. Along with *DTA* and *TGA* (see under Industrial Drying in Chapter II), this technique is of broad investigative value toward the understanding of reactions that are accompanied by transient plasticity and weakness. It has recently been employed in the study of resin-bonded graphite-containing MgO+C refractories, in which polymerization stiffening commences at about 500°C.[420]

High-Temperature Creep

Upon approach to the temperature of the knee in E_s and σ_f, every refractory exhibits some plasticity under load. This is not transient but increases as a substantially exponential or thermally activated function of temperature.[410] This property, visualized in the increasingly curvilinear stress-strain plots of Figure XII-1b for dense ceramics, is directly related to the load-bearing capacity of refractories at their highest service temperatures.

Here a wide variety of behaviors is seen, depending first of all on refractory composition. Pure single-phase materials melt most sharply and, below the knee, exhibit inappreciable creep rate except at very high stresses. A notable example is 99+% silica, whose further virtue lies in the high viscosity of its liquid. Other high-purity single-phase oxide refractories follow, lacking only that high liquid viscosity. As a practical matter, nitride-bonded silicon carbide is

similar. These materials are referred to as having high *hot strength*, though what is meant is high "hot stiffness" (i.e., low creep rate), up very near to the temperature of the knee. They come closest to the dense single-phase ceramics on which this chapter opened.

Heterogeneous multi-component refractories, on the other hand, melt progressively over a broad temperature range and may further show some solid-state matrix plasticity before melting begins. Parametric studies of creep in these cases can be revealing and useful, particularly in the elastico-plastic and viscoelastic temperature regions. Some excellent work of this kind has been reported on monolithic refractories, wherein chemical reactions affecting Stage I creep were clearly distinguished from the steady-state behavior of Stage II.[410]

Such comprehensive studies of creep are laborious and costly, however. Refractories have to be used in the field long before their hot mechanical properties can be completely and accurately described. Some knowledge of hot deformation is necessary nonetheless, since sagging without actual failure may destroy the integrity of a refractory structure.

A *hot-load deformation* or *hot load subsidence* test has been devised as a convenient short-term index of hot load-bearing capacity. This is conducted as one of several standardized tests specified by ASTM[9] (see later under Methods of Mechanical Property Measurement). In concept, it locates a temperature at which a given refractory exhibits a recorded plastic deformation of from zero to at most a couple of percent in a short time (usually 1.5 hours) under a fixed low compressive stress (usually 25 psi or 1.76 kg/cm^2 or 1.72 $\cdot 10^5$ Pa, or in accord with European practice, 28.6 psi or 2.0 kg/cm^2). For refractory wall or crown design among other purposes, it is possible to transform this index of plastic deformation into practically-useful load-bearing design parameters, including an acceptable or maximum permissible mean temperature of the refractory. Though this maximum load-bearing temperature will usually be below that of the hot load deformation test itself, the downward extrapolation is much smaller and can be much more safely made than from, say, the PCE temperature as an index of plastic flow.

It will be appreciated that the hot face temperature of a refractory wall can be safely permitted, from mechanical considerations, to run somewhat hotter than this maximum permissible load-bearing temperature of the body. The permissible hot-face temperature was estimated in Chapter VIII as the Maximum Service Temperature or MST, summarized for numerous refractory types in Figure VIII-3. There is no comparable maximum load-bearing

temperature for each refractory, even in concept, because there is no single standard wall thickness or temperature profile and because structural designs and loadings as well as service lifetimes and permissible creep rates are all variables in the hands of the system designer. Fortunately, there is a large storehouse of prior field experience to go on.

ILLUSTRATIVE MECHANICAL PROPERTIES OF REFRACTORIES

The foregoing general characterizations make it evident that microstructure has an overriding influence on most mechanical properties of refractories. Yet the critical feature of microcracking, for example, is presently ill-described at best. Further, in sampling the worldwide commercial product line, it is not feasible to acquire or display even such microstructural features of each refractory as may be known to the manufacturer.

The data cited following are accordingly selected randomly, from conveniently available sources, rather than comprehensively. They have to be regarded as *illustrative* of the modern product line, not necessarily representative, and certainly not as a basis for firm correlations or limitations. We have examined several hundreds of commercial product data sets and have selected roughly one hundred, issued by only a few U.S. suppliers. These data illustrate both the variety and some commonness of mechanical properties. In no case do these data represent all of the products of any one supplier, nor in any sense the "best" of that supplier's products; nor is any implied virtue or recommendation attached to any product represented. Other products, either foreign or domestic to the U.S.A., may fall within or outside the ranges of properties shown. Their inclusion would only strengthen the central message: (a) like kinds of refractories may exhibit some likenesses in mechanical properties, yet (b) the industry is capable of achieving properties over considerable ranges by manipulating chemical and phase composition and microstructural features within each refractory class.

Room-Temperature MOR and Compressive Strength of Bricks

Tables XII.3a, b, and c present illustrative room-temperature compressive or *crushing strength* (C.S.) and *modulus of rupture* (MOR) data as obtained by appropriate ASTM procedures,[9] for "burned" or fired brick products. For identification the weight-percent of one or two key components is given, followed by the bulk density (ρ_b) and by the volume-percent apparent porosity (P) either as given

by the source or estimated from the bulk density. These identifying properties as well as the C.S. and MOR are typically given as ranges for each product; we have taken the midpoint of each range and rounded this by small amounts. The last column in each table, Hot Load Deformation, is included for convenience but should be ignored for now. Some excellent summary data are also given in References 74, 76, and 405.

Table XII.3a describes twenty-four alumina and aluminous refractories containing greater or lesser amounts of clay, but excluding the all-clay (firebrick) class. It also describes six phosphate-bonded clay-alumina products and six alumina-chromia products. In this last group, it can be discerned from the sum of % Al_2O_3 plus % Cr_2O_3 that synthetic raw materials have been used: chrome ore is not a component, nor is clay in quantity.

The reader will note some commonalities in the strength data within each grouping. Where the MOR data slip to two-digit values in kg/cm^2, note that the porosity is high ($\geq$ 20%) in every case. Fused-cast and fused-rebonded refractory types are not included in the table. On the whole nonetheless, the strengths in Table XII.3a tend to run relatively high among all oxidic refractory classes. For purposes of conversion, 100 kg/cm^2 = 1422 psi = $9.81 \cdot 10^6$ Pa.

Table XII.3b is a like display for a variety of basic refractories: twelve relatively high-MgO products and ten mag.-chrome and chrome-mag. formulations. Those ten all employ chrome ore. In the high-MgO group a very few spinel-bonded and forsterite-bonded magnesias are included, and only one (at 65% MgO) that contains dolime. Scattered through the table are a number of chemically-bonded and burned bricks, which are not greatly distinguished as a group but are usually among the stronger.

The basic refractories of Table XII.3b are more homogeneous as to percent porosity than are the aluminous products of Table XII.3a. This reflects their dedication to slag corrosion resistance. But again, fused-cast and fused-rebonded basic refractories are not included. Two-digit MOR values are the rule in the chrome-containing products, while the highest strengths tend to concentrate at about 95% MgO and up in the periclase/magnesite group. Overall the basic refractories are less strong at room temperature than are the aluminous, despite the thermal isotropy of periclase and spinels and the anisotropy of Al_2O_3. The thermal expansion curves of Figs. IV-9a and b help to make this difference credible.

Table XII.3c contains briefer samplings of firebrick, silica, and a few other working refractories, and of cellular insulating bricks of various compositions. Among these groups the two-digit MOR values

Table XII.3a Illustrative Mechanical Properties of High Alumina and Clay-Alumina Bricks (U.S. supplier data)

COMPOSITION CLASS	B.D., g/cm³	POR., %	r.t. C.S., kg/cm²	r.t. MOR, kg/cm²	HOT LOAD DEF.,[a] % @ (T°C)	
ALUMINA & ALUMINA-SILICA						
99⁺A[b]	3.09	17.	700.	265.	<1.	(1815)
99A	3.00	20.	600.	210.	0.7	(1595)
96A	3.00	16.	1580.	105.	0.8	(1760)
91A	3.02	14.	1125.	140.	0.3	(1760)
90A	2.96	16.	800.	175.	0.2	(1540)
89A	3.08	13.	875.	210.	0.6	(1815)
88A	2.93	18.	840.	255.	0.2	(1760)
84A	2.77	19.	600.	110.		
83A	2.60	25.5	385.	65.		
81A	2.82	17.5	700.	140.	0.0	(1450)
80A	2.72	19.5		110.	0.4	(1450)
80A	2.65	22.5	400.	100.	1.0	(1450)
71A	2.65	16.5	650.	125.	0.0	(1450)
71A	2.56	20.5	385.	95.	1.4	(1450)
69A	2.56	17.		125.	0.7	(1450)
69A	2.55	18.5	500.	110.	0.3	(1450)
69A	2.54	21.	350.	95.	1.5	(1450)
60A	2.41	20.	280.	85.	1.7	(1450)
59A	2.53	14.	600.		0.5	(1450)
59A	2.52	14.		210.	0.5	(1450)
59A	2.51	14.5	540.	100.	1.0	(1450)
59A	2.30	21.	175.	55.	2.5	(1450)
51A	2.45	13.	530.	150.	0.3	(1450)
51A	2.42	14.		175.	3.0	(1450)
PHOS-BONDED ALUMINOUS						
86A(P)[c]	2.86	16.	840.	200.	0.6	(1450)
82A(P)	2.84	16.	980.	220.	0.8	(1450)
82A(P)	2.80	17.5	700.	175.		
79A(P)	2.75	15.	810.	190.		
70A(P)	2.63	12.	1150.	220.	0.0	(1450)
70A(P)	2.62	13.5	765.	170.	1.5	(1450)
ALUMINA-CHROMIA						
90A-9Cr[d]	3.40	12.5	700.	450.	0.3	(1815)
90A-9Cr	3.21	18.	880.	195.	1.0	(1760)
90A-9Cr	3.18	17.5	630.	260.	0.4	(1815)
82A-17Cr	3.24	18.	700.	195.	0.3	(1760)
77A-20Cr	3.31	17.		160.		
61A-38Cr	3.60	14.5	600.	280.		

NOTES: [a] - Percent linear deformation under 1.76 kg/cm² compressive stress for 1.5 hours at fixed T.
[b] - 99⁺A = 99⁺% Al_2O_3; etc.
[c] - (P) = phosphate bonded.
[d] - 9Cr = 9% Cr_2O_3; etc.

Table XII.3b Illustrative Mechanical Properties of Basic Refractory Bricks (U.S. supplier data)

COMPOSITION CLASS	B.D., g/cm³	POR., %	r.t. C.S., kg/cm²	r.t. MOR, kg/cm²	HOT LOAD DEF.,[a] % @ (T°C)
PERICLASE & MAGNESITE					
99⁺M[b]	2.93	15.		105.	(>1850)
98M(ch)[c]	2.96	15.	525.	115.	(1760)
98M	2.92	16.	350.	140.	(>1850)
98M	2.87	17.		210.	(1760)
96M	2.95	15.5	700.	140.	(>1800)
94⁺M(ch)	2.93	16.	560.	110.	(1560)
94⁺M	2.85	17.5	650.	175.	(1510)
92M(MA)[d]	2.91	17.	350.	75.	(1700)
90M(MA)	2.95	15.		85.	(>1815)
90⁺M(M_2S)[e]	2.92	16.	560.	110.	(1510)
90⁺M(M_2S)	2.84	18.5	430.	110.	(1480)
65M(MC)[f]	2.80	20.5	450.	60.	
MAG.-CHROME & CHROME-MAG.					
81M-8Cr[g]	3.00	17.	280.	35.	(>1815)
72M-9Cr	2.98	17.	245.	30.	(1760)
70M-11Cr(ch)	3.01	16.	280.	80.	(1620)
62M-15Cr	3.20	14.		140.	(>1850)
62M-14Cr(ch)	3.08	16.5	315.	90.	(1635)
59M-22Cr	3.26	14.5		45.	
53M-19Cr	3.09	17.5		80.	(>1815)
46M-22Cr	3.08	19.	280.	70.	(>1700)
43M-32Cr	3.30	14.5		80.	(1705)
35M-25Cr	3.05	20.5	315.	75.	

NOTES:
[a] - Percent linear deformation under 1.76 kg/cm² compressive stress for 1.5 hours at fixed T. Where no % is given, T is for shear failure.
[b] - 98⁺M = 98⁺% MgO; etc.
[c] - (ch) = unspecified chemical bond.
[d] - (MA) = mag. aluminate spinel bond.
[e] - (M_2S) = forsterite (Mg_2SiO_4) bond.
[f] - (MC) = dolime (MgO·CaO) formulation.
[g] - 8Cr = 8% chrome ore as Cr_2O_3; etc.

Table XII.3c Illustrative Mechanical Properties of Various Refractory Bricks (U.S. supplier data)

COMPOSITION CLASS	B.D., g/cm³	POR., %	r.t. C.S., kg/cm²	r.t. MOR, kg/cm²	HOT LOAD DEF.,[a] % @ (T°C)	
FIREBRICK						
45A(hf)[b,c]	2.42	4.5	700.	210.	0.5	(1450)
45A	2.23	17.	280.	120.	1.0	(1450)
43A(hf)	2.32	10.5	420.	150.	1.5	(1450)
42A(hf)	2.30	10.5	395.	140.	1.8	(1450)
42A	2.29	13.5	415.	115.	2.3	(1450)
40A	2.26	12.5	525.	145.	2.0	(1450)
39A(hf)	2.24	12.0	360.	135.	2.0	(1450)
37A	2.15	17.5	220.	75.		
SILICA BRICK						
99⁺s[d]	1.94	12.	385.	90.		
99S	1.89	14.	400.	45.		
95S	1.81	22.	350.	60.	~1.	(1675)
95S	1.78	24.	280.	65.		
OTHER WORKING REFRACTORIES						
ZIRCON	3.62	21.5	630.	195.	0.4	(1595)
A-Z-S	3.14	14.		150.		
SiC(nitr)[e]	2.65	16.	1400.	385.	(0.0)	(1850)
SiC(clay)[f]	2.67	15.5	1050.	320.	~1.	(1540)
CELLULAR INSULATING BRICK						
82A	1.9	42.	350.	70.	3.5	(1760)
77A	1.3	64.	70.	35.		
61A	0.93	73.	20.	18.		
46A(IFB)[g]	0.82	74.	21.	17.		
45A(IFB)	0.77	76.	12.	11.		
45A(IFB)	0.61	81.	15.	10.		
41A(IFB)	1.5	53.	135.	60.		
39A(IFB)	0.50	84.	10.	8.		
99⁺s(fm)[h]	0.51	75.	35.	9.		
99⁺S(fm)	0.83	63.	85.	35.		
95⁺S	1.06	52.	40.	16.		
95⁺S	1.32	40.	110.	35.		

NOTES: [a] - Percent linear deformation under 1.76 kg/cm² compressive stress for 1.5 hours at fixed T.
[b] - 45A = 45% Al_2O_3; etc. [c] - (hf) = high fired.
[d] - 99⁺S = 99⁺% SiO_2; etc.
[e] - (nitr) = Si_3N_4-bonded; data from Ref. 167.
[f] - (clay) = clay-bonded.
[g] - (IFB) = insulating firebrick.
[h] - (fm) = foamed.

of the working silica bricks are noteworthy, as well as the two- and even single-digit bending strengths of the high-porosity insulating products. Those cellular products are also unique in that the C.S. and the MOR are in close approach to one another.

In fact, for all of the aluminous and silica working refractories of Tables XII.3a and 3c, the average C.S.:MOR ratio is about 4.3:1; for all of the basic refractories of Table XII.3b, that average ratio is about 4.8:1; and for twenty-one cellular insulating refractories including those of Table XII.3c plus two other bricks and seven insulating castables not shown, that average ratio is about 2.2:1. This means that, overall, the crushing strength decreases more rapidly with increasing porosity or void volume fraction than does the tensile strength in bending. Whether all three groups of refractories obey the same rules relating strength to porosity has yet to be examined.

Effects of Porosity on Room-Temperature Strength

If there is a separate and discernible relationship between the low-temperature strength of a refractory and its porosity or void volume fraction, and if such a relationship can be fitted by the same rule as was used for dense ceramics, namely:

$$\sigma_f = \sigma_o \exp(-bP) \ ,$$

it is of interest to confirm this fact and to estimate the value of b. A low correlation coefficient (or, high noise in the data) is expected, however, owing at least to the uncontrolled presence of microcracks which markedly influence refractory strength without adding appreciable void volume. The two questions above can be addressed simultaneously by plotting ln σ_f (viz., either MOR or C.S.) versus P as volume fraction (i.e., as f_v). Then,

$$\ln \sigma_f = \ln \sigma_o - bP \ .$$

Figures XII-2a and b are plots of this kind using all of the MOR and C.S. data, respectively, of the preceding three tables plus the nine additional insulating refractories mentioned above. In each figure all of the working refractories fall in a group from P = 0.05 to P = 0.26, while all of the insulating refractories fall in a readily-differentiated group from P = 0.40 to P = 0.85.

Consider Figure XII-2a (MOR data) first. Among the insulating refractories, the IFB subgroup seems relatively well-behaved. The solid curve, drawn as a median of this subgroup, is at a slope of -6 (i.e., b = 6). The insulating castables and silicas, similarly treated through considerable scatter, would give a slope of about -5 or b = 5.

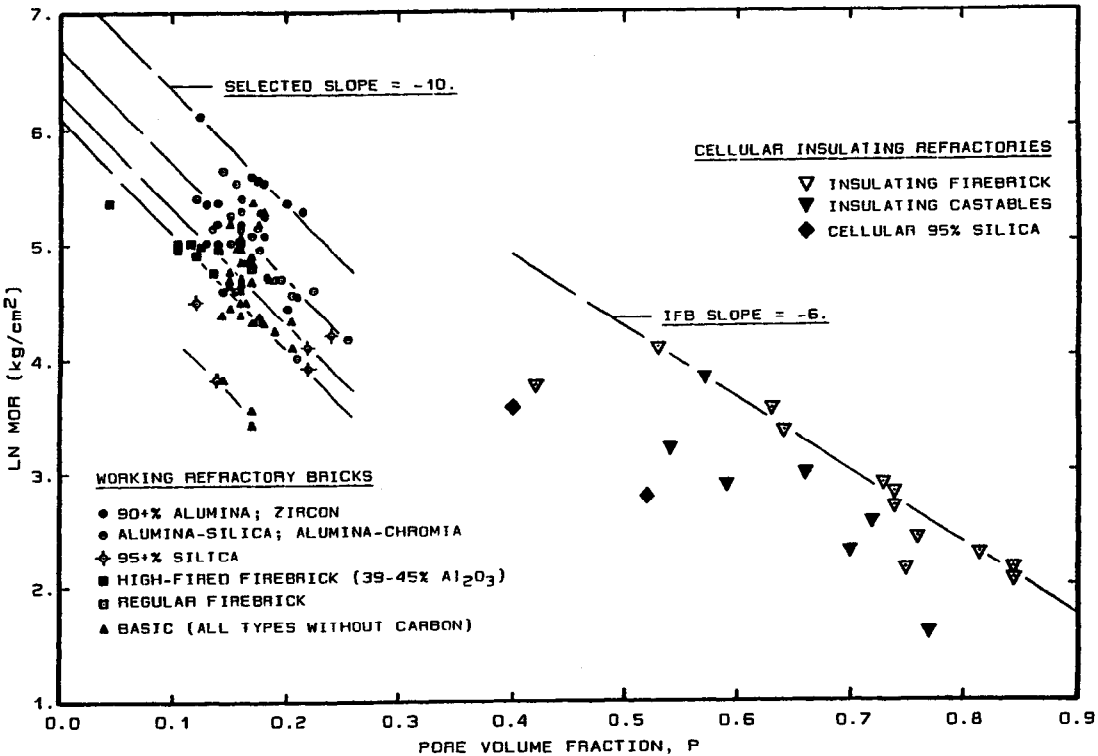

Figure XII-2a Room-Temperature MOR vs Porosity of Refractory Bricks
(from Tables XII.3a-c)

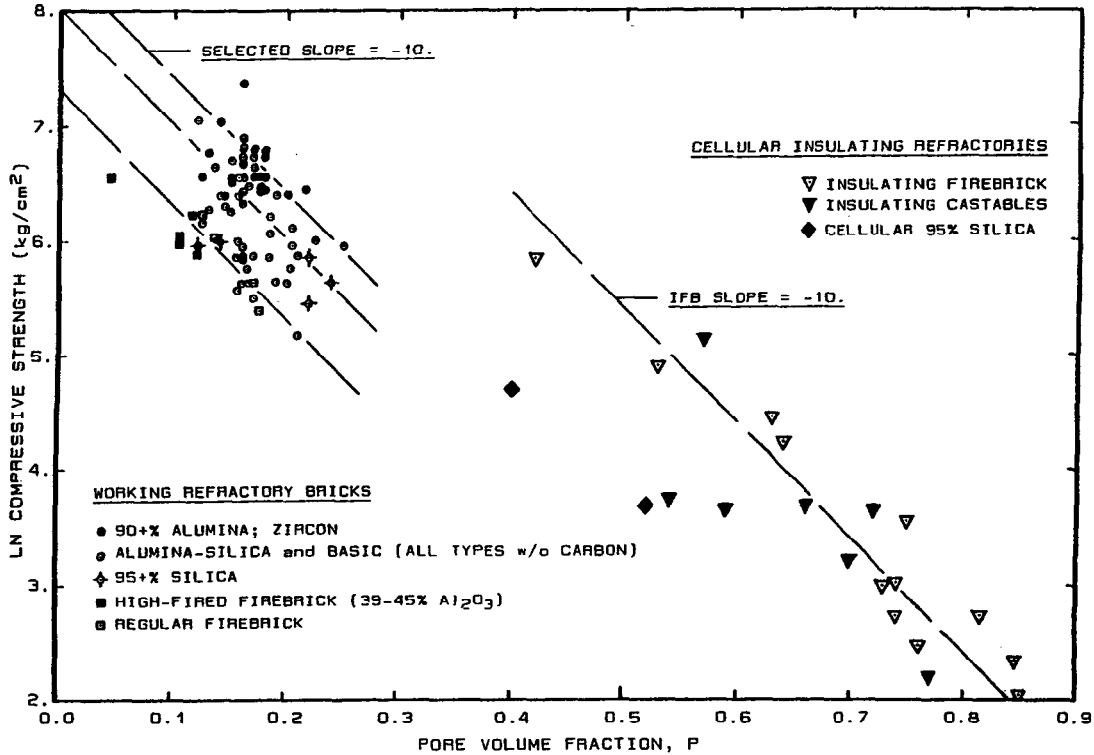

Figure XII-2b Room-Temperature Compressive Strength vs Porosity of Refractory Bricks (from Tables XII.3a-c)

The working refractories, on the other hand, can be treated by the same equation only on faith. The topmost and lowermost points seem to align at a slope of about -10 or b = 10, and parallel curves at this slope are drawn arbitrarily for the several refractory classes represented. Statistical analysis would hardly support this choice, however; at best it is only possible that this equation and this value of b apply.

Turning now to Figure XII-2b (crushing strength data), there is some support by analogy for the foregoing. The visual impact of the working-refractory data is that a slope of -10 is quite reasonable. Among the insulating refractories a slope of -10 is also a good fit for the IFB subgroup, while the remainder would call for a slope of about -8 through a wide scatter.

On balance overall, there appears some justification for use of the above equation to relate strength to porosity. Preferred values of b are as follows:

	Working Bricks	**Insulating Bricks**	**Insulating Castables, etc.**
b for MOR:	10	6	5
b for C.S.:	10	10	8

But the issue is arguable. Each inferred correlation in this uncontrolled sampling is subject to excessive noise. A further matter of interest is that the denser group and the insulating group of bricks are not of a common family, i.e., they neither meet contiguously nor extrapolate to comparable values of σ_o at $P = 0$.

A published examination of the strengths of ten different working refractories[40] has given rise to the empirical equation,

$$(C.S.) = k\,(MOR)^{1.5} \qquad \text{or} \qquad \ln (C.S.) = \ln k + 1.5 \ln (MOR)\,,$$

in which the exponent 1.5 was said to reflect the different dependencies of the C.S. and the MOR on porosity. That equation is mathematically compatible with the b values tabulated above for insulating refractories, but not for dense refractories here where the two b values appear to be about equal. Both analyses confirm a negative correlation of strength with porosity and a negative correlation of the ratio C.S.:MOR with porosity; but the best mathematical expressions of these correlations remain in doubt pending controlled studies. It is believed that the size distribution of pores does not affect strength, within limits.[390]

Modulus of Rupture vs Temperature

Bricks. Some of the data in Tables XII.3a-c were accompanied by one or more MOR values at higher temperatures (see also further summary data in References 74, 76, and 405). Though not catalogued in the tables, these high-T data are shown with the room-temperature values in Figure XII-3a. The data points are joined by straight line segments for identification only. The coding of refractories by composition is the same as that used in Tables XII.3a-c; but as indicated in those tables, details of composition are not more a determinant of strength than are microstructure and bonding. Figure XII-3a accordingly presents little more than random examples of the temperature-dependent behavior of fired bricks.

Two of those examples, 99% Al_2O_3 and 88% Al_2O_3 in the alumina-silica system, clearly show the anticipated knee in the MOR. The knee for 99% Al_2O_3 is at an inordinately low temperature; further inquiry into its chemical purity would be desirable. Knees in numerous other cases would surely be disclosed by additional data at intermediate temperatures. Below the knee, examples are seen of both rising and falling MOR with increasing temperature. Finally, at the top of the figure, the high and nearly T-independent strength of nitride-bonded SiC is seen.[167] The location of its knee is not determined, but is well off-scale of this figure: perhaps at the order of 1900°-2000°C under reducing conditions.

Castables. Data for about two dozen aluminous castables, drawn from a single U.S. manufacturer,* are displayed in Figures XII-3b and c. All but two of the MOR curves for regular calcium aluminate cemented castables (Fig. XII-3b) are remarkably similar, most showing the familiar dip in strength between room temperature and about 1000°C. Further data at 500°C would show that this dip starts at or below that temperature. The cementing reactions are completed by about 1400°-1500°C, close to the onset of the knee in strength for some compositions.

Although low- and ultra-low-cement castables were developed principally for slag corrosion resistance (Chapter VI), they often yield a gain in both room-temperature and high-temperature strength as seen in Figure XII-3c. The MOR at room temperature is above 70 kg/cm^2 or 1000 psi in all cases, and only two of the low-cement formulations show the CA cement dip in the figure. Colloidal-silica bonding reactions are quite evident by 500°C and continue to strengthen these materials to some 1000°C or higher. Some curves

---

*National Refractories and Minerals Corp., Livermore, CA.

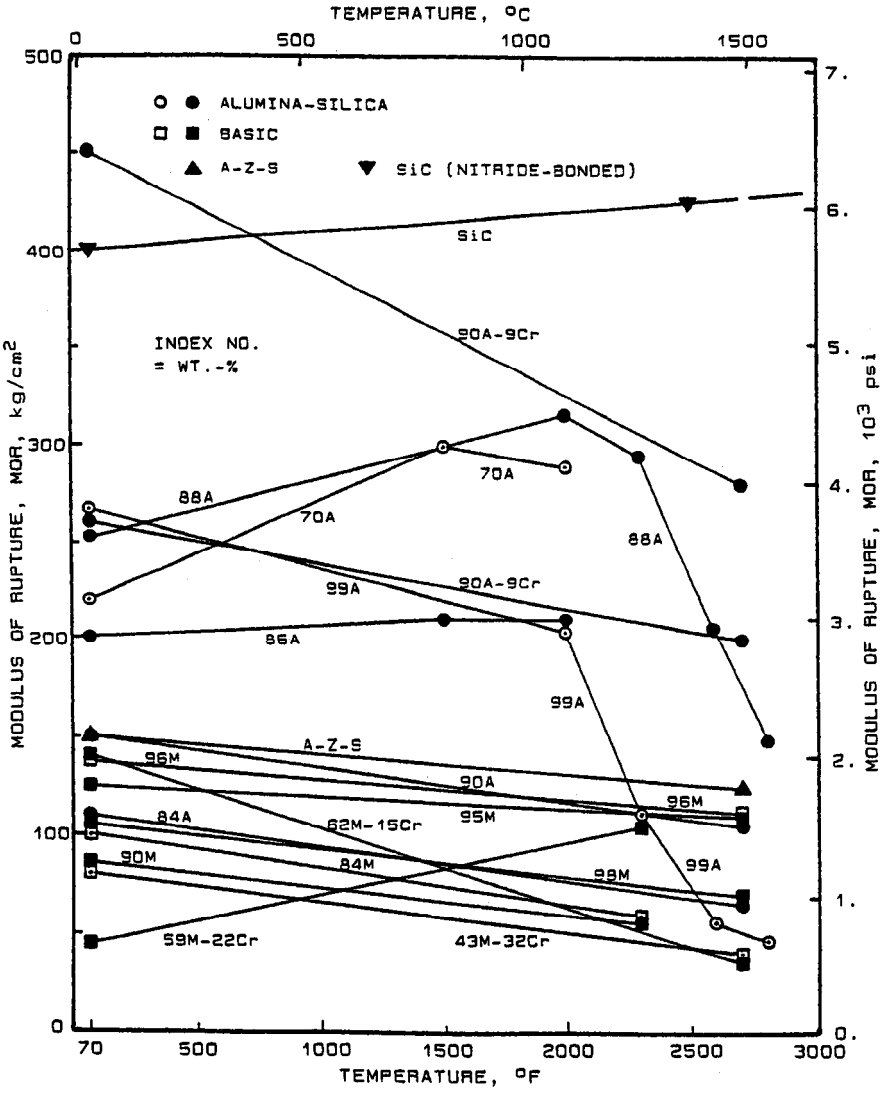

Figure XII-3a Modulus of Rupture vs Temperature for Working Refractory Bricks (U.S. supplier data)

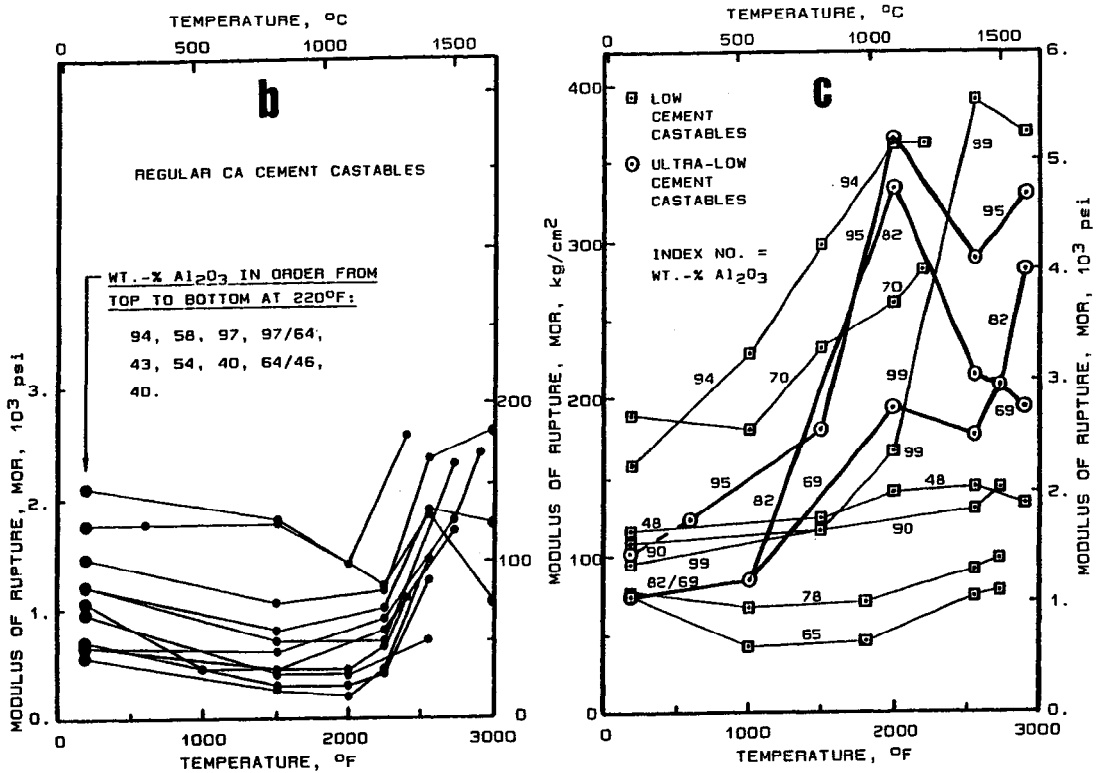

Figure XII-3b,c MOR vs T for Aluminous Castables: b. CA-Cemented c. Low and Ultra-Low Cement (NRMC data)

show a characteristic minimum in the MOR at about 1400°C, identified with silica crystallization; but they recover at still higher temperatures. The compositions of Figure XII-3c, all above 65% Al_2O_3, have in most cases not reached the knee in MOR by 1500° to 1600°C.

MgO+C Composites. Drawing on data sheets from the same sources of Tables XII.3a-c, Table XII.4 displays the MOR at several temperatures for a variety of basic steelmaking refractories containing particulate carbon or graphite. Only the pitch- or tar-bonded and resin-bonded types are represented, as the impregnated type derives its strength by conventional brick firing before pitch impregnation.

The table does not deal with initial softening over the first few hundred °C.[173,420] The room-temperature MOR describes the unburned or as-delivered organic-bonded brick; then the next column at 1095°C (2000°F) describes the fully-coked product, whose magnesia grains are bonded to each other and to graphite particles by "amorphous" carbon. The last column gives MOR data at much higher temperatures (1400°-1540°C), at which the bonding carbon has become further consolidated and -C-O-Mg- bonding fully established. The bricks described are grouped according to increasing total carbon content after coking, nominally 5, 10, 20, and 25%C (third column). Above the 5%C class, most of that carbon is graphite. As to coked porosity these products are relatively homogeneous, ranging from 8 to 12 volume percent.

The as-delivered room-temperature strengths are quite comparable to those of fired magnesia bricks. Only at 20 and 25% graphite is there a significant strength loss after coking (1095°C). This loss correlates with the below-expected thermal conductivity seen at these carbon levels (Chapter XI and Fig. XI-10 inset), but the cause is uncertain. It may be a matter of thermal expansion mismatch between graphite and MgO and of graphite anisotropy. This conjecture is supported by the failure of these same products to recover strength at higher temperatures, except for one (90% MgO) whose mineral impurities are high enough for some liquid-phase healing at 1540°C. The lower-carbon products generally show little strength change on coking and a considerable gain in strength at the highest temperatures. Some additional strength data for MgO + graphite refractories are given in References 74, 76, and 420.

Table XII.4 Illustrative Mechanical Properties of Bonded MgO+C Composite Refractory Bricks (U.S. supplier data)

MINERAL COMP'N.	INITIAL BOND	COKED % C	COKED B.D., g/cm^3	COKED POR., %	UNCOKED MOR, kg/cm^2	HOT (COKED) MOR, kg/cm^2 @ (T°C)	@ (T°C)
97M[a]	Pitch	4.9[b]	3.0	12.	85.	210. (1095)	350. (1540)
96M	Pitch	4.4[b]	3.1	9.	120.	120. (1095)	
94M	Pitch	4.5[b]	3.1	8.	105.	110. (1095)	140. (1400)
94M	Resin	9.0	3.0	8.	140.		125. (1400)
92M	Pitch	10.0	3.0	8.	105.	120. (1095)	175. (1400)
90M	Resin	9.5[c]	2.9	11.5	175.	160. (1095)	210. (1540)
97M	Resin	19.5	2.8	8.5	75.	55. (1095)	40. (1400)
94M	Resin	20.5	2.8	8.5	105.	50. (1095)	50. (1400)
90M	Resin	18.0	2.8	11.	100.	85. (1095)	125. (1540)
95M	Resin	26.5	2.7	12.	75.	65. (1095)	60. (1540)

NOTES: a - 97M = 97% MgO; etc.

b - Carbon exclusively from pitch. In all other cases, from added graphite.

c - Contains deoxidant metal powder.

Young's Modulus vs Temperature

Whether the origins of strain or stress in a refractory be thermal or mechanical, it seems self-evident that the static Young's modulus is the property needed to describe its macroscopic response up to fracture. The dynamic modulus is measured at unrealistically low deflections, and its application at high stress or strain would ignore the several other-than-elastic deformation mechanisms that may be available. If deformation happens to be purely elastic and reversible at low temperatures, then the only argument between the two measurement methods is which is the more accurate. But departures from elastic response can be detected only by making static stress-strain measurements, and once found, these departures demand the use of the static modulus.

The further element in inelastic deformation, however, is *time*. In any transient development of stress or strain, the shorter the time allowed for response the more the applicable Young's modulus shifts from the long-time static toward the dynamic. A powerful argument for use of the dynamic modulus arises in thermal shock situations. Yet refractories are not called upon to respond in microseconds, or even milliseconds. It seems reasonable in principle that the static stress-strain method can be pursued at a succession of increasing strain rates, and the resulting E be plotted vs $\dot{\varepsilon}$ and extrapolated as necessary for use in analyzing rapid thermal transients.

At this writing there is considerable interest at the other end of the time scale, viz., in the slow or truly static development of loads arising from, e.g., steel shell constraint or the thermal gradients in glass tank superstructures. Eventually the stress-strain measurement of refractories will have to address strain rate as a variable at the low end of its scale as well as at the high end. Presently, the designer must work mostly with single-point data as regards the element of time.

Admitting this temporary disadvantage, in recent years there have been a number of excellent published measurements of stress-strain-temperature relations in refractories.[413,414,421-425] Both bending and compressive loads have been employed. Purposes of the work cited are to serve various mathematical modeling exercises intended to solve dimensional-change problems in monolithic and duplex monolithic linings and design problems in furnace roofs, walls, ladles, converters, and cylindrical steel-clad vessels in general.[421-432] Reference 425 reports a particularly comprehensive study including hot crushing strength, hot MOR, and plastic relaxation in addition to Young's modulus. Its focus is on MgO and MgO-chrome steelmaking refractories. Two consecutive papers by authors-in-

common[413,414] give the static Young's modulus of a wide variety of refractory types.

A brief selection of data from References 413 and 414 illustrates the features of Young's modulus of refractories vs temperature. Stress-strain curves at several temperatures were reported for various aluminous and basic brick products and for examples of castable, vibration-cast, and gunned monolithics. Among those curves (not shown here) are found the linear and curvilinear shapes of Figure XII-1b plus a few cases of low-temperature trend reversal (Fig. XII-1a), as well as a few cases of early upward concavity and early downward concavity such as were discussed previously in this chapter. For purposes of reporting a Young's modulus at each test temperature, these authors[413,414] used a secant modulus (σ/ε) determined at one fixed value of stress. Instead, for purposes of plotting E vs T here, we have approximated a tangent to each stress-strain curve at its high-ε extremity and taken the slope ($d\sigma/d\varepsilon$) of this tangent. Our E values are thus closer to those at fracture and are generally lower than theirs; but the features of the E-T plots are comparable.

These features are displayed in Figure XII-4a for burned or fired bricks, and in Figure XII-4b for monolithics (soaked two hours at each test temperature to develop their bonding before test). The strain rates are given in the original papers;[413,414] they are not all quite the same. Note that the ordinate scales in these figures are in kg/mm^2 and 10^6 psi, instead of the kg/cm^2 and 10^3 psi used in prior figures describing strength.

The most prominent feature seen in Figure XII-4a is the knee. The sparsity of data points precludes its precise temperature estimation or that of its shape, but the curves sketched in the figure will be fairly close. Unfortunately there is no correspondence in specimens between the E-T data of this figure and the MOR-T data of Fig. XII-3a. It appears that the strength knee may occur some 50°C higher than that of the Young's modulus, but this is uncertain.

Below the knee these "elastic" constants of refractories run roughly an order of magnitude below the intrinsic E_i values of Table XII.1. Considering the superimposed effects of porosity and microcracking, this is about where they should be.

The E-T curves of Figure XII-4b for monolithics consistently exhibit a feature that has no counterpart in the MOR-T curves of Figures XII-3b and 3c: a very large fall in static Young's modulus between room temperature and the knee. In some considerable measure this feature reflects the manner in which we obtained E from the σ-ε data. Other than that, the figures contrast a tensile (MOR)

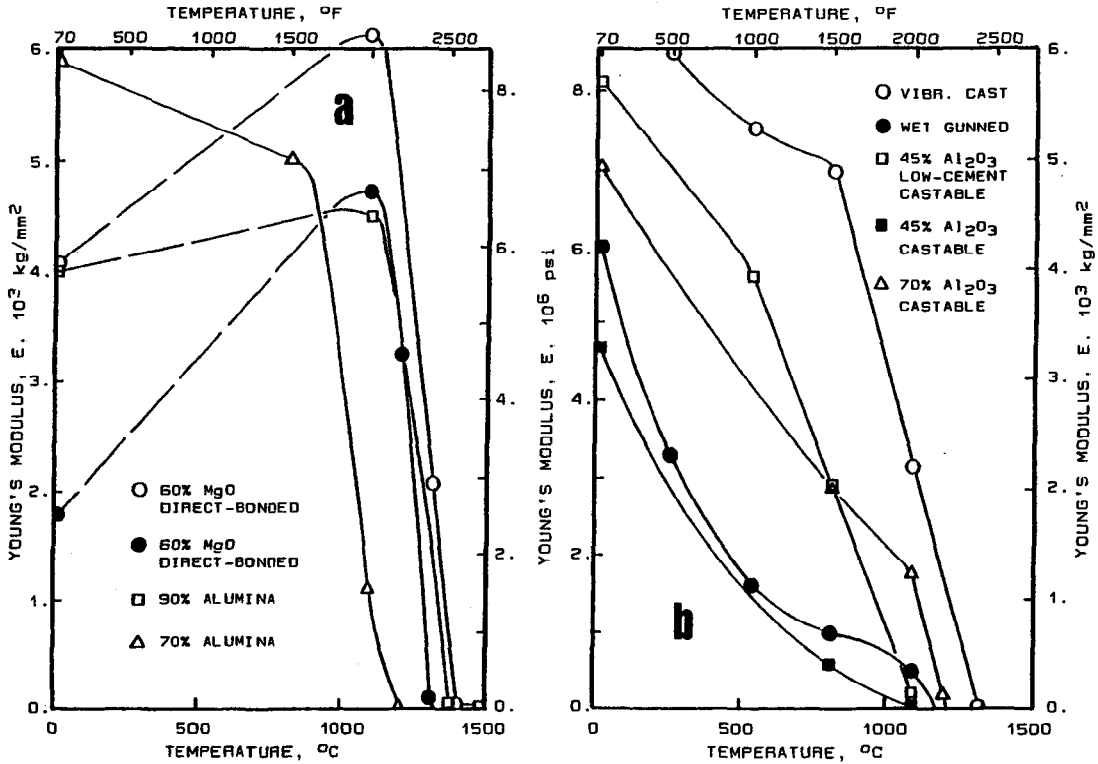

Figure XII-4 Static Young's Modulus vs Temperature (Refs. 413, 414):
a. Burned Bricks b. Monolithics

failure mode with compressive deformation, a high with a low strain rate, and probably quite different curing regimens prior to test. In any event, the monolithics of Fig. XII-4b are exceedingly deformable above about 500°C.

The prospective increased use of finite-element analytical methods, both in solving system design problems and in understanding thermal stress responses of refractories, will undoubtedly stimulate a great deal more stress-strain measurement work in the 1990s and beyond. As to both techniques and results, this will be a most interesting area of progress. Further respects in which data will be needed are in: (a) addressing loading rate as a variable, as referred to above; (b) direct comparisons of bending stress-strain with that in compression; and (c) plotting of unloading and cyclic loading-unloading curves in addition to the conventional measurements undertaken to date.

Creep of Refractories

Informative but limited studies of high-temperature creep of refractories have been reported.[189,410,433-439] One which is unusually comprehensive appeared in 1985;[410] it includes a review of mechanisms and the equations used to describe them. Experimentally, even this work is confined to a single value of compressive stress (25 psi or 1.76 kg/cm^2) and for the most part to a single temperature (1425°C). Over 100 different refractory specimens were tested, many unfired except for a 5-10 hour pre-soak at 1425°C. Deformation under constant load and temperature was tracked for 100 or 200 hours. The reader interested in actual creep data is referred to this and the other original papers;[189,433-439] here we cite only some overall findings of this work that are revealing of the essential pyroplastic nature of refractories and of the hazards of using short-time data for long-time extrapolation.

Deformation was divided into three components: (1) elastic (instantaneous reversible response); (2) primary or Stage I (transient) creep deformation; and (3) secondary or Stage II (steady state) creep deformation. The final (pre-rupture) tertiary or Stage III creep deformation was acknowledged but not emphasized in this work; it is readily recognized by a rapid increase in strain rate, ending in failure.

The elastic component of strain, ε_o, is in a sense trivial here. But it was obtained, and as such it facilitates a static estimate of the dynamic Young's modulus: $E_d \cong \sigma/\varepsilon_o$. Primary creep is characterized by a strain rate $\dot{\varepsilon}$ that decreases with time, merging asymptotically into the constant strain rate $\dot{\varepsilon} = k$ that characterizes secondary creep. The authors[410] avoided establishing a fictitious boundary between

primary and secondary stages by writing an empirical equation for the total creep strain as a function of total elapsed time, paraphrased as:

$$\varepsilon_{cr} = \varepsilon - \varepsilon_o = \varepsilon_p[1 - \exp(-t/t_k)] + \dot{\varepsilon}_{ss}t \quad .$$

Here ε without subscript is the total strain measured at any time t, and all of the constant terms ε_o, ε_p, $\dot{\varepsilon}_{ss}$, and t_k (a time constant for the decay of ε_p) are determined by fitting the equation to the whole of the experimental data. This equation was found satisfactory for a host of materials, surprisingly so since a variety of chemical (curing or aging or sintering) as well as physical changes contribute to primary creep.

Total strains recorded in 100 h of course ranged widely, depending on the refractoriness or stiffness of each specimen: running up to as much as 10 to 12% in the cases of firebrick and of CA-cemented fireclay castables. What might not have been fully appreciated prior to this work is that the time-decay constant t_k also ranged widely: some plastic and castable monolithics had not emerged out of Stage I creep in 100 hours or more, while other refractories had settled down into Stage II well within this period. Since linear extrapolation is warranted only after Stage II is established and $\dot{\varepsilon}_{ss}$ determined, the implications regarding long-term projections are obvious. Some examples taken from this work compare the total additional strain measured over a second 100-hour period with the total strain recorded in the first 100 hours:

Refractory:	**A**	**B**	**C**	**D**	**E**
ε_{100}, %:	12.	10.	8.	6.	0.7
ε_{200}-ε_{100}, %:	5.	6.5	3.6	5.	<0.2

What if the only measure of strain available had been for the first 1.5 hours?

Hot Load Deformation or Subsidence

This 1.5 h is in fact the standard duration of the Hot Load Deformation test of ASTM procedure C16.[9] Results of this abbreviated creep or plastic deformation test are given routinely by U.S. refractory manufacturers for their brick products, as shown in the last column of Tables XII.3 a, b, and c. In that test, the fixed temperature maintained under 25 psi or 1.76 kg/cm^2 compressive load for 1.5 h is selected from a standard set in accordance with the brick classification or intended use temperature; hence the inclusion of the test temperature in parentheses in that column in the tables. Some refractories fail in shear without appreciable or measurable plastic deformation; in that case the temperature of shear failure is

given in parentheses without a corresponding numerical value of plastic deformation, particularly in Table XII.3b.

In this test procedure, deformation is measured as the difference in length of the specimen between pre-test and post-test, both at room temperature. Thus ε_o in the above equation of Reference 410 is automatically backed out and ε_{cr} is the quantity directly measured. Technologists have long since known that this 1.5-hour measure of creep is not to be extrapolated linearly. Its primary value as an index of hot stiffness is relative, in comparing one brick with another for the same duty where there is already a body of field experience. For an ASTM-specified measure of long-term creep, see later under Methods of Measurement.

At a glance from Tables XII.3a-c the commercial refractory types listed can be grouped in order of decreasing temperature of zero-to-a-few-percent deformation, or decreasing "hot strength" or "hot stiffness." These groupings are:

1700°-1850°C: most magnesias of ≥90% MgO (high C:S ratio);[425] some MgO-Al_2O_3 and MgO-chrome[425]

1600°-1800°C: aluminas of ≥90% Al_2O_3, and Al_2O_3-Cr_2O_3

1450°-1600°C: some magnesias (low C:S ratio); some MgO-chrome and chrome-MgO; zircon; most conventional clay-aluminas of 50-85% Al_2O_3

1450°C down: all firebrick (largely in order of decreasing %Al_2O_3)

Nitride-bonded SiC belongs at the top of the list. Selected silica refractories go in the 1600°-1800°C category, others in the 1450°-1600°C category. It is emphasized again that the tables are a small and incomplete representation of the product line, lacking numerous well-known compositions such as zirconia and A-Z-S and in particular lacking the fused-cast and fused-rebonded refractory types. Fused mullite, for just one example, is a far cry from a conventional 70% alumina which contains at least Al_2O_3, mullite, and silica.

Finally, it has to be remarked that high hot strength per se is sought only for certain applications and is contra-indicated for others. As a rule among oxides, hot strength and thermal stress resistance correlate negatively. Hot compliance, not stiffness, permits the adaptation of a refractory lining to an external constraint or to its own differential thermal expansion under a through-wall gradient. As a rule, hot strength and refractory cost are positively correlated. As has been emphasized before, no one property of a refractory can be considered alone.

Alteration in Service

None of the mechanical properties of a refractory will likely remain unchanged, furthermore, over its service lifetime. Changes with aging and with thermal cycling are only the beginning; alteration by corrosion affects both the lower-temperature elastic and strength properties and the high-temperature load-bearing or plastic properties as well. If there is any one means by which corrosion brings an end to useful life, other than by simple recession it is by the deterioration of mechanical integrity. Whether in an hour or over twenty years, alteration is inexorable.

The ways in which corrosion damage is brought about, and deterred, are dealt with in Chapters V-VIII. Resistance to corrosion-alteration must usually be of high priority, often forcing a compromise in mechanical or other properties that has to be designed around. Only in benign environments can the system designer afford the luxury of optimizing or fine-tuning mechanical properties offhandedly. The increasing sophistication evident in mechanical property measurement and in thermo-mechanical analysis of refractory systems will surely result in better design adaptations to mechanical behavior; but in the long run engineers will take into account the service alteration of that behavior as well. There will ultimately be an upsurge in the measurement of mechanical properties of chemically-altered refractories.[167]

Methods of Mechanical Property Measurement

Most of the measurements of conventional mechanical properties of refractories have evolved into standardized or uniform procedures, specified in the U.S.A. by ASTM.[9] Every other major community of refractories technologists has recognized the same need and has responded to it either by adoption or by creating its own growing manual of uniform methods.

This need is hardly unique to the mechanical property domain; but nowhere is uniformity of technique more appropriate across-the-board. Not only are the mechanical properties of refractories excessively structure-sensitive. Both the specimen microstructures and their modes of response to mechanical loading are intricately dependent on specimen preparation, pretreatment, heating and heat treatment, and the manner and rate of application of loads. Added to this mutability of structures and responses is the difficulty of their quantitative characterization.

If the user of the test information is to have confidence in it relative to field performance, either for computation or for comparisons among products, the only recourse under present

circumstances is to standard procedures. These have taken the details of specimen preparation into account, as well as the conduct of each test. There are in fact numerous ASTM procedures which deal exclusively with specimen preparation -- a matter particularly critical for monolithics. In this chapter as previously, those auxiliary procedures are generally not cited. In the ASTM standards for refractories,[9] all pertinent auxiliary methods for every measurement or test are thoroughly indexed and cross-referenced; their extensive cataloguing here is unnecessary.

There are of course no constraints on methods used in investigative work. Researchers use their own combinations of methods. Those, described in the R & D literature, add a lore of other resources to the formal procedures. They are best assessed by consulting that literature. In the following paragraphs we present a brief entree to the ASTM procedures alone, organized according to the several properties they are designed to measure. All of these procedures specify replication. Here too, the reader is referred to the source[9] for an appreciation of their intricacy of detail.

Elastic Moduli. The following table summarizes ASTM procedures useable to obtain the room-temperature Young's modulus E and/or shear modulus G. All of these can be modified for measurement up to high temperatures. An asterisk under "Materials" indicates that suitable modifications can provide for use on other materials than those specified.

Method	ASTM Proc.	Materials	Specimen	Statistics?
E: Resonance	C885	All	Brick, Bar	Yes
E: Resonance	C747	Carbon,Graph.*	Bar, Rod	Yes
G: Resonance	C747	Carbon,Graph.*	Bar, Rod	Yes
E: Sonic Velocity	C769	Carbon,Graph.	Bar, Rod	Some
E: Static Tensile	C749	Carbon,Graph.	Gage Type	Some
E: Static Compressive	No(C133)	All	Brick, Bar	No
E: Static Bending	No(C133)	All	Brick, Bar	No

In this and the remaining sections, the following notation is used for specimen dimensions and other parameters of measurement:

L	= length or loading span	f	= resonant frequency
h	= thickness	v	= velocity of sound
b	= width	F	= applied force or load
A	= cross-section area	ΔL	= displacement parallel to L
M	= mass	ΔH	= displacement parallel to h
ρ	= bulk density	B, C, D	= tabulated functions of geometry and units[9]

Procedures C885, --- *Young's Modulus of Refractory Shapes by Sonic Resonance*, and C747, --- *Moduli of Elasticity --- of Carbon and Graphite Materials by Sonic Resonance*, employ flexural vibration in the direction of dimension h. The latter procedure also describes longitudinal vibration in the direction of L and torsional vibration normal to L. Equations for calculation are:

Flexural	Longitudinal	Torsional
$E = CMf^2$	$E = DL^2\rho f^2$	$G = BL^2\rho f^2$

The thickness h and width b (or radius r for rods) do not enter into these equations, but they do in the functions B, C, and D; and there are restrictions on relations between h, b, and L. Torsion is difficult with coarse-grained materials. Extensions of temperature call for special provisions regarding transducers and atmospheres, which are noted but not specified in the procedures. Elastic behavior is required, hence temperature as a variable is limited.

Procedure C769, --- *Sonic Velocity in --- Carbon and Graphite Materials for Use in Obtaining an Approximate Young's Modulus*, is feasible only with fine-grained materials. Most commercial refractories do not qualify. A brief longitudinal pulse is sent down a long, slender rod or bar, and the time for return of the reflected pulse is measured. Extension to high temperatures requires thermal reliability of the transducer and elastic behavior and atmospheric protection of the specimen. The approximate equation is:

$$E \cong \rho v^2 = 4\rho L^2/t^2 \quad .$$

Tensile testing of refractories is rarely practiced. The gage-type specimen shape so familiar in metals is difficult to machine in refractories without creating large flaws; and loading in pure tension without eccentricity is also difficult. For carbons and graphites (fine-grained and of relatively low E), procedure C749, --- *Tensile Stress-Strain of Carbon and Graphite*, specifies a method and the simple calculation: $E = \sigma/\varepsilon = (F/A)/(\Delta L/L)$. High-temperature modification is routine for use with these materials, which exhibit no true plasticity. Protective atmosphere is required.

At present ASTM gives no standard procedure providing separately for the determination of static Young's modulus of most refractory materials. The basic provisions of C133, --- *Cold Crushing Strength and Modulus of Rupture of Refractory Brick and Shapes,* are followed in principle, adding sensing equipment for the measurement of displacement and recording equipment for both σ and ε. High-temperature modification is not difficult; procedure C583 gives an alternative loading technique for hot three-point bending (MOR). Cylindrical (core-drilled) specimens may be used in either compression or bending. The rate of increase of the load is open, remembering that the resulting static E is rate-dependent. In compression, $E = \sigma/\varepsilon = (F/A)/(\Delta L/L)$. In bending, a small displacement is difficult to measure accurately; and the 3-point equation for a bar,

$$E = (FL^3)/(4h^3b\Delta H) \quad ,$$

is only approximate at large displacements. Other equations are available for rods and for 4-point bending.

Compressive or Crushing Strength. Three procedures are specified by ASTM[9] for the determination of strength under uniaxial compressive load. All three are basically room-temperature procedures, but can be modified for high temperatures. The crushing strength is infrequently measured above room temperature, however.[189] The methods are:

C133 --- *Cold Crushing Strength and MOR of Refractory Brick and Shapes*
C93 --- *Cold Crushing Strength and MOR of Insulating Firebrick*
C695 --- *Compressive Strength of Carbon and Graphite*

Procedure C133 is the prototype, using 9" straight bricks loaded in the direction of L. Round-robin statistics are given for this test and for C93, which modifies the specimen dimensions and loading rate for insulating bricks. Procedure C695 is a similar modification for carbons and graphites, with no statistics given. In all cases the calculation is simply:

$$C.S. = \sigma_{max.} = F_{max.}/A \quad .$$

Modulus of Rupture. A half-dozen procedures are differentiated by ASTM for determination of the MOR by 3-point bending.[9] All of these use a 9" (228 mm) long rectangular brick or equivalent-shaped specimen, with a span L of 7" (178 mm) between horizontal fixed supports. The loading ram or lever, moving down from above, carries the third "knife-edge," actually a radiused fixture, which bisects L. The specimen dimensions b and h vary somewhat among the tests, as do the loading rates:

ASTM Proc.	Materials	b x h, in.	b x h, mm	Stress Rate psi/min.	Stress Rate kg/cm^2/min.
C133	All	4.5 x 2.5	114 x 64	1493.	105.0
	All	4.5 x 3.0	114 x 76	1037.	72.9
C93	IFB	4.5 x 2.5	114 x 64	373.	26.2
	IFB	4.5 x 3.0	114 x 76	259.	18.2
C491	Monolithics	4.5 x 2.5	114 x 64	187.	13.15
C607	Coked Pitch-Bonded	3.0 x 2.5	76 x 64	2240.	157.5

The measured MOR is even more sensitive to the loading rate than is the C.S. In both cases it is important to adhere to the specified rates.

Procedures C133 and C93 are named above. Both give some statistics on reproducibility. Procedure C491, titled --- *Modulus of Rupture of Air-Setting Plastic Refractories,* prescribes the forming, drying, and firing of plastic specimens which may be tested as in C133 after drying or after firing. Castables are incorporated by reference to their specimen preparation under C860, 862, or 865. Procedure C607, *Standard Practice for Coking Large Shapes of Carbon-Bearing Material*, prescribes coking at 980°C in preparation for several tests including that of C133. See also C1025 for electrode graphite.

Procedure C583, --- *Modulus of Rupture of Refractory Materials at Elevated Temperatures*, gives a simplified loading fixture for high-temperature use, modifying C133. It prescribes heating rates and soak times, leaving the soak (and test) temperature open. Each test specimen is 6"x1"x1" (152 x 25 x 25 mm), and the 3-point test span is 5" or 127 mm. The prescribed stress rate at temperature is 1312.5 psi/min. or 92.3 kg/cm^2/min.

The equation for calculation of the MOR in 3-point bending is, for all of the above procedures and using the notation given above:

$$MOR = (3FL)/(2bh^2).*$$

A numerical factor may be required depending on the units in which the MOR is desired and in which the several test parameters of C133 are stated.[9] This equation is good for small displacements, ΔH. If a large plastic deformation is suffered, the calculated MOR is only approximate.

---

*See footnote, next page.

Four-Point Bending and Tensile Testing. The modulus of rupture or *flexural strength* in 4-point bending, popular in ceramics, is rarely used for refractories. The reader interested in how this test is set up will find a generally-applicable description under procedure C651, ---*Flexural Strength of Manufactured Carbon and Graphite Articles Using Four-Point Loading at Room Temperature.* Here, L again denotes the span of the two (outer) supports. Instead of a single concentrated load at L/2, in this test a pair of (inner) radiused loading edges is used, a distance d apart and centered over the specimen. In general the distance d is subject to some latitude at the tester's option; but in C651 it is specified: d = L/3. There are accordingly two equations for calculating the flexural strength, F.S.:

In general: $F.S. = 3F(L-d)/2bh^2$* ;

Per C651: $F.S. = (FL)/bh^2$)

Procedure C749, --- *Tensile Stress-Strain of Carbon and Graphite*, is basically designed as a strength test. As remarked previously under Elastic Moduli, it is carried out only with great difficulty on coarse-grained refractories, and at the user's risk. Although both procedures C651 and C749 are readily modified for high-temperature testing, ASTM makes no provision for the extension of either one to any refractories other than the specified carbons and graphites.

Tests of Inelastic and Plastic Behavior. ASTM procedure C832, --- *Measuring the Thermal Expansion and Creep of Refractories Under Load,* is a versatile and multi-purpose procedure for measuring linear dimensional change with constantly increasing temperature (55°C/hour) under constant compressive load or stress:

(1) If the compressive load is zero, what is measured is the Linear Thermal Expansion; see under that heading in Chapter XI. See also Permanent Deformation in that chapter, and procedures C113, C179, C210, C436, and C605 introduced there.

(2) A standard compressive stress of 25 psi (1.76 kg/cm^2 or 172 kPa) or 28.6 psi (2.0 kg/cm^2 or 197 kPa) is provided for, or other low stress at the user's option. Continuous curves of L vs T under low stress disclose intermediate-temperature regions of

---

*For round rods of radius r, these equations are,
Three-point: $MOR = FL/\pi r^3$; Four-point: $F.S. = F(L-d)/\pi r^3$.

transient plasticity, as described earlier in this chapter.

(3) At low stress as in (2) above, a plot of L vs T at 55°C/h will ultimately go through a maximum, at which the thermal expansion and the creep deformation are equal and opposite. If fracture does not intervene, above this temperature the L-T curve turns downward as the creep or plastic deformation under load exceeds the thermal expansion. The point (L_{max}, T) is called the *maximum dilation point* at the specified compressive stress; the standard 25 psi is generally employed for this purpose.

(4) A soak temperature may be selected, approached at constant rate as above, but then held fixed for 20 to 50 hours -- or longer at the user's option. The L vs T curve thus becomes a curve of L vs t (time) at constant stress, or a conventional *creep* curve; see under Creep of Refractories earlier in this chapter.

The conduct of these several measurements is specified in elaborate detail in procedure C832.[9] Some round-robin statistics are given.

Procedure C16, --- *Load Testing Refractory Brick at High Temperatures*, was referred to as the short-time (1.5 hour) "hot load deformation" or "hot load subsidence" test under High-Temperature Creep earlier in this chapter. The standard fixed compressive stress is again 25 psi, and is again applied before heating begins. The brick specimen is a standard 9" straight, stood on end and loaded in the direction of L. The difference between pre-test and post-test L includes deformations experienced in the specified heating and cooling schedules, in addition to that in the 1.5-hour soak at the selected top temperature. Some round-robin statistics are given.

Finally, as has been emphasized both in concept and by example in this chapter, much useful information on inelastic and plastic behavior is obtained by comprehensive stress-strain studies over a range of temperatures, using compressive loading. Modified procedures C133 and C93 are used, catalogued in this section under Elastic Moduli.

Chapter XIII

Refractory Manufacture

OVERVIEW: CONSOLIDATED FLOW DIAGRAM FOR REFRACTORIES

The technical *goals* of manufacture of a given refractory are embodied in its properties and performance in an intended application. The *tools* of manufacture consist of choices among raw materials and among processing methods and parameters. The *insights* of manufacture have to do with the features of phase composition and microstructure -- collectively called material *character* -- that (a) are developed through processing, and (b) are themselves responsible for product properties and behavior. The foregoing chapters have highlighted both of these connections (a) and (b), though mostly those of the second kind.

The origins of material character in manufacturing must remain somewhat fragmented until one addresses the methods and parameters of producing each individual product. The proper place for acquisition of that knowledge lies within the manufacturing plant itself. This book can not enter that privileged space. Nevertheless it is instructive to describe the approaches commonly taken in refractory synthesis, and to examine the fundamental responses of raw and in-process materials to those operations. These are the missions of this chapter.

Several revolutions in the industry across-the-board should be acknowledged first, as space will not permit giving them detailed attention. Included in these revolutions are further mechanized methods of handling tonnage solids, increased capabilities and

automation of processing equipment, and techniques for the rapid acquisition and analysis of in-process control data. These advances have transformed refractory manufacturing practice.

The first task here is to integrate sets of unit operations into generic flow diagrams illustrating how different kinds of refractories are made. A consolidation of these into a single diagram is presented in Figure XIII-1. The figure is drawn in "decision tree" style with the diverging branches keyed by numbers for identification. There are six paths, each making a particular type of refractory product:

Path (key nos.)	**Type of Product Made**
1	Unformed Refractories (monolithics, mortars, etc.)
2,3,4	Fused Grain (returned to Solid Raw Materials, SRM)
2,3,5	Fused-Cast Refractories
2,6,7	Unburned Formed Refractories (bricks, blocks)
2,6,8	Burned Formed Refractories; also Recycled Grain and Grog (returned to SRM)
2,9	Sintered and Prereacted Grain (returned to SRM)

These six generic flow diagrams stand in turn for up to thousands of specific processes, differentiated for example by their raw materials lists, the manner of preparation and the sizing and batching (meaning quantity weighed out) of each, the sequence and manner of mixing, and so on. Omissions are allowed: for example, some unformed refractories are dry-mixed and never wetted until installation. Slashes between indicated unit operations (over arrows) mean "and/or." In-process storage (not shown) will be mentioned only in sensitive cases.

Loose-fill refractories are not all covered by Figure XIII-1, though some can be made by following the Sintered Grain path (2,9). Insulating fiber refractories are not covered; their process-related descriptions in Chapter IX should suffice. With very few other such exceptions, most working and insulating refractory materials fall within this consolidated flow diagram -- including oxides, carbons and graphites, carbides, and particulate and wire-reinforced composites.

All processes start at the top left, i.e., with solid raw materials and additives, and often with liquid constituents. Attention will be given first to the two groups of starting solids and to their preparation for delivery to the forming operations. Then wet mixes will be taken up and brought to the same end. Finally, the forming and thermal treatments will be described, substantially in the order in which they occur in the six generic processes. Emphasis will be placed on oxidic

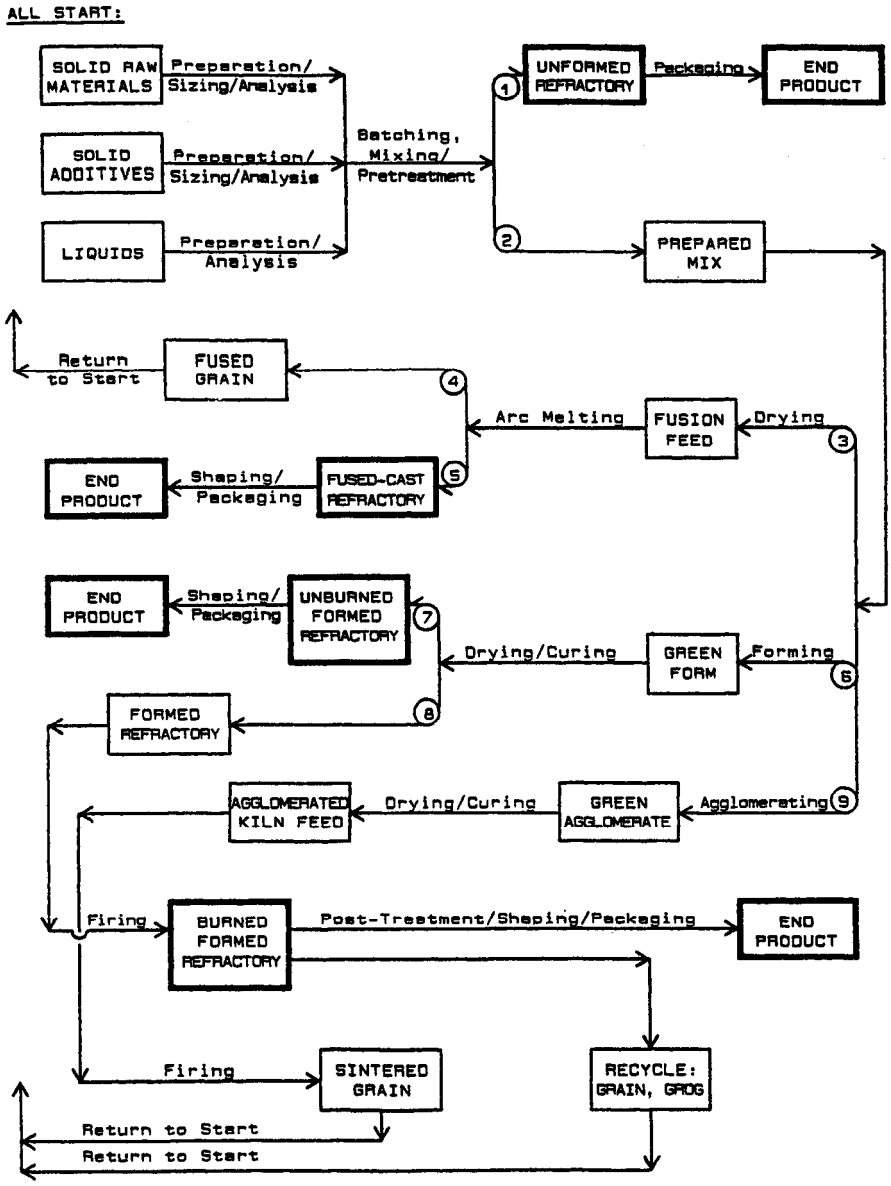

Figure XIII-1 Consolidated Refractory Manufacturing Flow Diagram

refractories, simply because that is where most of the variety is. Chapter II deals sufficiently with nonoxide synthesis.

We shall not dwell at first on chemical (i.e., compositional) analysis. This is one of the backbones of refractory formulation and quality, however, and it obviously must begin with all starting materials. It does: right at the receiving dock.

FROM RAW MATERIALS TO FORMING

Solid Raw Materials

Nomenclature. Adding a roster of ores and minerals to the compounds already encountered, mainly in Chapters IV and VIII, greatly enlarges the nomenclature. To assist the reader in recognition, a reference table of the most common minerals, chemicals, and refractory phases of interest is given as Table XIII.1. The table is subdivided into three major categories: (1) *Nonsilicates*; (2) *Anhydrous Silicas and Silicates*; and (3) *Clay and Clay-Like Minerals*. Within each category the names are in alphabetical order, including some synonyms. Table XIII.2 lists the members of the first two categories by chemical formula as locator, also for reference use.

Non-Clay Minerals. Most of the names and formulas in the first category of Table XIII.1 are familiar from prior chapters. In this category the principal mineral raw materials suitable for refractory manufacture are:

Aragonite, Calcite, Limestone (incl. oyster shells)	Dolomite
Baddeleyite (ZrO_2 ore concentrate)	Graphite
Bauxite; Boehmite, Diaspore, Gibbsite	Magnesite
Chrome Spinel, Chromite (chrome ore)	Rutile

The second category of Table XIII.1, *Anhydrous Silicas and Silicates*, includes a number of compounds previously encountered in phase diagrams and others occurring as minerals. Mentioned as pertinent mineral raw materials are:

Andalusite, Kyanite, Sillimanite	Forsterite
Cordierite	Mullite
Diatomite, Flint, Ganister, Kieselguhr, Quartzite	Olivine
Feldspars (group)	Zircon

Clays. The third category of Table XIII.1, *Clay and Clay-Like Minerals*, is comprised mainly of the products of weathering of various

Table XIII.1 Minerals and Chemicals by Name

MINERAL NAME	NOMINAL FORMULA	REMARKS
Nonsilicates		
ALUMINA, alpha	Al_2O_3	Principally synthetic.
" , beta	$(Na,K)Al_{11}O_{17}$	Other ratios also exist.
" , gamma	$Al_2O_{3-x}(OH)_{2x}$	x small. Synthetic only.
ANATASE	TiO_2	Principally synthetic.
APATITE	$Ca_5(PO_4)_3(OH,F)$	Bone, mineral deposits.
ARAGONITE	$CaCO_3$	Mineral; see also CALCITE.
BADDELEYITE	ZrO_2	Mineral; also synthetic.
BAUXITES (group)	Ores include BOEHMITE, DIASPORE, and GIBBSITE.	
BOEHMITE	AlO(OH)	Mineral; also synthetic.
BROMELLITE	BeO	Synthetic; v. rare mineral.
BRUCITE	$Mg(OH)_2$	Synthetic; rare mineral.
CALCIA	CaO	Exclusively synthetic.
CALCIOWÜSTITE	CaO-FeO ss.	Occurs esp. in slags.
CALCITE	$CaCO_3$	Mineral; also synthetic.
CARBORUNDUM	SiC	Exclusively synthetic.
CHROME SPINEL	$FeCr_2O_4$	See CHROMITE.
CHROMIA	Cr_2O_3	Synthetic only.
CHROMITE	$FeCr_2O_4$	Mineral. A SPINEL.
CORUNDUM	Al_2O_3 (impure)	Uncommon mineral.
DIASPORE	AlO(OH)	A component of BAUXITE ore.
DOLOMITE	$MgCO_3{+}CaCO_3$	Variable-ratio mineral.
GIBBSITE	$Al(OH)_3$	In BAUXITE; also synthetic.
GOETHITE	FeO(OH)	Mineral; see also HEMATITE.
GRAPHITE	C (elemental)	Mineral; also synthetic.
HEMATITE	Fe_2O_3	Mineral; also synthetic.
HERCYNITE	$FeAl_2O_4$	In refractories. A SPINEL.
HYDRARGILLITE	$Al(OH)_3$	See GIBBSITE.
HYDROMAGNESITE	$Mg_4(OH)_2(CO_3)_3{\cdot}3H_2O$	Uncommon mineral.
ILMENITE	$FeTiO_3$	Mineral. A PEROVSKITE.
LEPIDOCROCITE	FeO(OH)	Uncommon min.; cf. GOETHITE.
LIME	CaO	See CALCIA.
LIMESTONE	$CaCO_3$ (impure)	Common ore. See CALCITE.
LIMONITE	$Fe_2O_3{\cdot}xH_2O$	Mineral; cf. HEMATITE.
LODESTONE	Fe_3O_4	See MAGNETITE.
MAGNESIA	MgO	Exclusively synthetic.
MAGNESIOFERRITE	$MgFe_2O_4$	In refractories. A SPINEL.
MAGNESIOWÜSTITE	MgO-FeO ss.	Occurs in refractories.
MAGNESITE	$MgCO_3$ (impure)	Mineral. See also DOLOMITE.
MAGNETITE	Fe_3O_4	Min. & synthetic. A SPINEL.
MONAZITE	(Ce,La,R.E.,Th)PO_4	Major ore for these oxides.
PERICLASE	MgO	Esp., well-cryst. and pure.
PEROVSKITES (group)	$CaTiO_3$ et al.	Synthetic; gen. ABO_3.
PICROCHROMITE	$MgCr_2O_4$	In refractories. A SPINEL.
RUTILE	TiO_2	Mineral; also synthetic.
SAPPHIRE	Al_2O_3 (alpha)	Synthetic; minor mineral.
SIDERITE	$FeCO_3$	Mineral; see also HEMATITE.
SPINELS (group)	$MgAl_2O_4$ et al.	Mostly synthetic; gen. AB_2O_4.
THORIA	ThO_2	Mainly synth.; radioactive.
WÜSTITE	FeO, $Fe_{0.95}O$	In slags and refractories.
ZIRCITE	ZrO_2	See ZIRCONIA.
ZIRCONIA	ZrO_2	Synthetic; also BADDELEYITE.

Table XIII.1, continued

MINERAL NAME	NOMINAL FORMULA	COMPONENT OXIDE FORMULA
Anhydrous Silicas and Silicates		
ACMITE	$NaFeSi_2O_6$	$Na_2O \cdot Fe_2O_3 \cdot 4SiO_2$
AKERMANITE	$Ca_2MgSi_2O_7$	$2CaO \cdot MgO \cdot 2SiO_2$
ALBITE	$NaAlSi_3O_8$	$Na_2O \cdot Al_2O_3 \cdot 6SiO_2$
ANDALUSITE	Al_2SiO_5	$Al_2O_3 \cdot SiO_2$
ANORTHITE	$CaAl_2Si_2O_8$	$CaO \cdot Al_2O_3 \cdot 2SiO_2$
ANORTHOCLASE	$(Na,K)AlSi_3O_8$	$(Na,K)_2O \cdot Al_2O_3 \cdot 6SiO_2$
BERYL	$Be_3Al_2Si_6O_{18}$	$3BeO \cdot Al_2O_3 \cdot 6SiO_2$
CARNEGIEITE	$NaAlSiO_4$	$Na_2O \cdot Al_2O_3 \cdot 2SiO_2$
CLINOENSTATITE	$MgSiO_3$	$MgO \cdot SiO_2$
CORDIERITE	$(Mg,Fe)_2(Al,Fe)_4Si_5O_{18}$	Typ. $2MgO \cdot 2Al_2O_3 \cdot 5SiO_2$
CRISTOBALITE	SiO_2	SiO_2
CYANITE	See SILLIMANITE.	
DIATOMITE	SiO_2	SiO_2
DIOPSIDE	$CaMgSi_2O_6$	$CaO \cdot MgO \cdot 2SiO_2$
ENSTATITE	$MgSiO_3$	$MgO \cdot SiO_2$
FAYALITE	Fe_2SiO_4	$2FeO \cdot SiO_2$
FELDSPARS (group)	Include ALBITE, ANORTHITE, ANORTHOCLASE, KALIOPHYLLITE, MICROCLINE, NEPHELITE, ORTHOCLASE, PLAGIOCLASE.	
FLINT	SiO_2 (impure)	SiO_2
FORSTERITE	Mg_2SiO_4	$2MgO \cdot SiO_2$
GANISTER	SiO_2 Rock (QUARTZITE)	SiO_2
GARNETS (group)	Include GROSSULARITE, PYROPE, UVAROVITE.	
GEHLENITE	$Ca_2Al_2SiO_7$	$2CaO \cdot Al_2O_3 \cdot SiO_2$
GRANITES (group)	Rock: heterogeneous mixture of FELDSPARS, MICAS, QUARTZITE.	
GROSSULARITE	$Ca_3Al_2Si_3O_{12}$	$3CaO \cdot Al_2O_3 \cdot 3SiO_2$
JADEITE	$NaAlSi_2O_6$	$Na_2O \cdot Al_2O_3 \cdot 4SiO_2$
KALIOPHYLLITE	$KAlSiO_4$	$K_2O \cdot Al_2O_3 \cdot 2SiO_2$
KIESELGUHR	See DIATOMITE.	
KYANITE	Al_2SiO_5	$Al_2O_3 \cdot SiO_2$
LEUCITE	$KAlSi_2O_6$	$K_2O \cdot Al_2O_3 \cdot 4SiO_2$
MERWINITE	$Ca_3MgSi_2O_8$	$3CaO \cdot MgO \cdot 2SiO_2$
MICROCLINE	$KAlSi_3O_8$	$K_2O \cdot Al_2O_3 \cdot 6SiO_2$
MONTICELLITE	$CaMgSiO_4$	$CaO \cdot MgO \cdot SiO_2$
MULLITE	$Al_6Si_2O_{13}$	$3Al_2O_3 \cdot 2SiO_2$
NEPHELINE	See NEPHELITE.	
NEPHELITE	$(Na,K)(Al,Si)_2O_4$	Typ. $Na_2O \cdot Al_2O_3 \cdot 2SiO_2$
OBSIDIAN (group)	Vitreous rock of GRANITE compositions.	
OLIVINE	$(Ca,Mg,Fe)_2SiO_4$	$2(Ca,Mg,Fe)O \cdot SiO_2$
ORTHOCLASE	$KAlSi_3O_8$	$K_2O \cdot Al_2O_3 \cdot 6SiO_2$
ORTHOPYROXENE	$(Mg,Fe)SiO_3$	$(Mg,Fe)O \cdot SiO_2$
PETALITE	$LiAlSi_4O_{10}$	$Li_2O \cdot Al_2O_3 \cdot 8SiO_2$
PIGEONITE	$(Ca,Mg,Fe)(Mg,Fe)Si_2O_6$	$2(Ca,Mg,Fe)O \cdot 2SiO_2$
PLAGIOCLASE	$xNaAlSi_3O_8 \cdot yCaAl_2Si_2O_8$	
PROTOENSTATITE	$MgSiO_3$	$MgO \cdot SiO_2$
PSEUDOWOLLASTONITE	$CaSiO_3$	$CaO \cdot SiO_2$
PUMICE	Porous, vitreous SiO_2 rock.	
PYROPE	$Mg_3Al_2Si_3O_{12}$	$3MgO \cdot Al_2O_3 \cdot 3SiO_2$

(Continued)

Table XIII.1, continued

MINERAL NAME	NOMINAL FORMULA	COMPONENT OXIDE FORMULA
Anhydrous Silicas and Silicates, continued		
PYROXENES (group)	Include CLINOENSTATITE, DIOPSIDE, ENSTATITE, JADEITE, LEUCITE, PIGEONITE, PROTOENSTATITE, PSEUDOWOLLASTONITE, SPODUMENE, WOLLASTONITE.	
QUARTZ	SiO_2	SiO_2
QUARTZITE	SiO_2	SiO_2
RANKINITE	$Ca_3Si_2O_7$	$3CaO \cdot 2SiO_2$
RHYOLITE (group)	Cryptocrystalline GRANITE rock.	
SILICA	SiO_2	SiO_2
SILLIMANITE	Al_2SiO_5	$Al_2O_3 \cdot SiO_2$
SPODUMENE	$LiAlSi_2O_6$	$Li_2O \cdot Al_2O_3 \cdot 4SiO_2$
TRIDYMITE	SiO_2	SiO_2
UVAROVITE	$Ca_3Cr_2Si_3O_{12}$	$3CaO \cdot Cr_2O_3 \cdot 3SiO_2$
WOLLASTONITE	$(Ca,Fe)SiO_3$	$(Ca,Fe)O \cdot SiO_2$
ZIRCON	$ZrSiO_4$	$ZrO_2 \cdot SiO_2$
Clay and Clay-Like Minerals: Hydrated/Hydroxylated Silicates		
ACTINOLITE	$Ca_2(Mg,Fe)_5Si_8O_{22}(OH)_2$	
ALLOPHANE	$Al_2Si_2O_5(OH)_4$	Amorphous
AMPHIBOLES (group)	Include AMPHIBOLE, ANTHOPHYLLITE, CUMMINGTONITE, HORNBLENDE, TREMOLITE.	
AMPHIBOLE	$Mg_7Si_8O_{22}(OH)_2$	
ANALCITE	$NaAlSi_2O_6 \cdot H_2O$	
ANAUXITE	$Al_{2-x}Si_{2+y}O_5(OH)_4$	
ANTHOPHYLLITE	$(Mg,Fe)_7Si_8O_{22}(OH)_2$	
ASBESTOS (group)	Fibrous AMPHIBOLES, OLIVINES (anhydrous).	
ATTAPULGITE	$Mg_5Si_8O_{18}(OH)_6$	
BEIDELLITE	$NaAl_9Si_{9.5}O_{30}(OH)_6$	
BENTONITES (group)	Hydroxylated colloidal SILICAS and ALUMINUM SILICATES of various ratios. Volcanic ash.	
BIOTITE	$K(Mg,Fe)_3AlSi_3O_{10}(OH)_2$	
BRAVAISITE	$K_xAl_{4+x}Si_{8-x}O_{20}(OH)_4$	
BROMMALLITE	$Na_xAl_{4+x}Si_{8-x}O_{20}(OH)_4$	
CHABAZITE	$(Na_2,Ca)Al_2Si_4O_{12} \cdot 6H_2O$	
CHINA CLAY	See KAOLINS (group)	
CHLORITE	$(Mg,Al,Fe)_6(Al,Si)_4O_5(OH)_8$	
CHONORODITE	$Mg_5Si_2O_8(OH)_2$	
CHRYSOLITE	See SERPENTINE.	
CLINOCHLORE	See CHLORITE.	
CLINOPTOLITE	See HEULANDITE.	
CLINOZOISITE	$Ca_2Al_3Si_3O_{12}(OH)$	
CUMMINGTONITE	$(Mg,Fe)_7Si_8O_{22}(OH)_2$	
DICKITE	$Al_2Si_2O_5(OH)_4$	
ENDELLITE	$Al_2Si_2O_3(OH)_8$	
EUDIALITE	$(Na_2,Ca,Fe)_6ZrSi_6O_{18}(OH)_4$	
GLAUCONITE	Typ. $(Na_2,K_2,Ca)(Mg,Fe)_4(Al,Fe)_2Si_7O_{20}(OH)_4$	
GLAUCOPHANE	$Na_2Mg_3Al_2Si_8O_{22}(OH)_2$	
GMELINITE	$(Na_2,Ca)Al_2Si_4O_6(OH)_{12}$	
HALLOYSITE	$Al_2Si_2O_5(OH)_4$	

(Continued)

Table XIII.1, continued

MINERAL NAME	NOMINAL FORMULA
Clay and Clay-Like Minerals, continued	
HECTORITE	$LiNaMg_8Si_{12}O_{30}(OH)_6$
HEULANDITE	$(Na_2,Ca)Al_2Si_7O_{18}\cdot 6H_2O$
HORNBLENDE	Typ. $(Na_2,K_2,Ca)_2(Mg,Al,Fe)_5(Al,Si)_2Si_6O_{22}(OH)_2$
HYDROGROSSULARITE	$Ca_3Al_2Si_{3-x}O_{12-4x}(OH)_{4x}$
ILLITE	$K_{1+x}Al_{5+x}Si_{7-x}O_{20}(OH)_4$
KAOLINS (group)	Include ALLOPHANE, ANAUXITE, DICKITE, ENDELLITE, HALLOYSITE, KAOLINITE, NACRITE.
KAOLINITE	$Al_2Si_2O_5(OH)_4$
LAUMONTITE	$CaAl_2Si_4O_{12}\cdot 4H_2O$
LAWSONITE	$CaAl_2Si_2O_6(OH)_4$
LEVYNE	$(Na_2,Ca)Al_2Si_4O_{12}\cdot 6H_2O$
MESOLITE	$Na_2Ca_2Al_2Si_3O_{10}\cdot 8H_2O$
MICAS (group)	Include ATTAPULGITE, BENTONITES, BIOTITE, BRAVAISITE, BROMMALLITE, MUSCOVITE.
MONTMORILLONITES (group)	Include BEIDELLITE, HECTORITE, MONTMORILLONITE, NONTRONITE, PYROPHYLLITE, SAPONITE, TALCITE.
MONTMORILLONITE	$NaMgAl_5Si_{12}O_{30}(OH)_6$
MORDENITE	$(Na_2,K_2,Ca)Al_2Si_{10}O_{24}\cdot 7H_2O$
MUSCOVITE	$KAl_3Si_3O_{10}(OH)_2$
NACRITE	$Al_2Si_2O_5(OH)_4$
NATROLITE	$Na_2Al_2Si_3O_{10}\cdot 2H_2O$
NONTRONITE	$NaAlFe_6Si_{11}O_{30}(OH)_6$
OLIGOCLASE	$Na_{1-x}Ca_xAl_{1+x}Si_{3-x}O_8$
PARAGONITE	$NaAl_3Si_3O_{10}(OH)_2$
PIEMONTITE	Typ. $Ca_2(Al,Fe)_2AlSi_3O_{12}(OH)$
PREHNITE	$Ca_2Al_2Si_3O_{10}(OH)_2$
PYROPHYLLITE	$Al_2Si_4O_{10}(OH)_2$
SAPONITE	Typ. $(Mg,Fe)_{3+x}(Al,Fe)_{1-x}Si_{4-y}O_{10}(OH)_{3+x}$
SAPPHIRINE	$(Mg,Fe)_2Al_4SiO_{10}$
SCOLECITE	$CaAl_2Si_3O_{10}\cdot 3H_2O$
SERPENTINE	$Mg_3Si_2O_5(OH)_4$
SOAPSTONE	See TALCITE.
STEATITE	See TALCITE.
STILBITE	$(Na_2,K_2,Ca)Al_2Si_7O_{18}\cdot 7H_2O$
TALCITE	$Mg_3Si_4O_{10}(OH)_2$
TREMOLITE	$Ca_2Mg_5Si_8O_{22}(OH)_2$
VERMICULITE	Typ. $(Ca,Mg)_{0.7}(Mg,Al,Fe)_6(Al,Si)_8O_{20}(OH)_4\cdot 8H_2O$
VESUVIANITE	$Ca_{10}(Mg,Fe)_2Al_4Si_9O_{34}(OH)_4$
ZEOLITES (group)	Include ANALCITE, CHABAZITE, HEULANDITE, LAUMONTITE, LEVYNE, MESOLITE, MORDENITE, NATROLITE, SCOLECITE, STILBITE, et al.

Table XIII.2 Minerals and Chemicals by Formula

COMPONENT OXIDE FORMULA	COMMON AND MINERAL NAMES	
Simple Oxides, Hydroxides, and Carbonates		
CaO	CALCIA; LIME, QUICKLIME	
FeO	WÜSTITE	MAGNESIOWÜSTITE
MgO	MAGNESIA; PERICLASE	MAGNESIOWÜSTITE
Al_2O_3	ALUMINA; CORUNDUM, (ALUNDUM, SAPPHIRE)	
Cr_2O_3	CHROMIA	
Fe_2O_3	HEMATITE	
SiO_2	SILICA; CRISTOBALITE, DIATOMITE, FLINT, GANISTER, KIESELGUHR, PUMICE, QUARTZ, QUARTZITE, TRIDYMITE	
ZrO_2	ZIRCONIA; BADDELEYITE	
$CaO \cdot H_2O$	SLAKED LIME, HYDRATED LIME	
$CaO \cdot 2H_2O$	GYPSUM, ALABASTER	
$MgO \cdot H_2O$	MAGNESIA HYDRATE; BRUCITE	
$Al_2O_3 \cdot H_2O$	ALUMINA MONOHYDRATE; BOEHMITE, DIASPORE	
$Al_2O_3 \cdot 3H_2O$	" TRIHYDRATE; GIBBSITE, (HYDRARGYLLITE)	
$Fe_2O_3 \cdot H_2O$	LIMONITE	
$CaO \cdot CO_2$	LIMESTONE; ARAGONITE, CALCITE	
$MgO \cdot CO_2$	MAGNESITE	
$(Ca+Mg)O \cdot CO_2$	DOLOMITE	
Type $MO \cdot M_2O_3$ Compounds: Spinels		
$FeO \cdot Al_2O_3$	HERCYNITE	
$MgO \cdot Al_2O_3$	SPINEL	
$FeO \cdot Cr_2O_3$	CHROMITE; CHROME SPINEL	
$MgO \cdot Cr_2O_3$	PICROCHROMITE	
$FeO \cdot Fe_2O_3$	LODESTONE; MAGNETITE	
$MgO \cdot Fe_2O_3$	MAGNESIOFERRITE	
Type $MO \cdot xSiO_2$ Compounds		
$2CaO \cdot SiO_2$	OLIVINE	OLIVINES
$2FeO \cdot SiO_2$	FAYALITE	OLIVINES
$2MgO \cdot SiO_2$	FORSTERITE	OLIVINES
$CaO \cdot MgO \cdot SiO_2$	MONTICELLITE	OLIVINES
$3CaO \cdot MgO \cdot 2SiO_2$	MERWINITE	OLIVINES
$3CaO \cdot 2SiO_2$	RANKINITE	
$2CaO \cdot MgO \cdot 2SiO_2$	AKERMANITE	
$CaO \cdot SiO_2$	WOLLASTONITE, PSEUDOWOLLASTONITE	PYROXENES
$FeO \cdot SiO_2$	ORTHOPYROXENE, PIGEONITE	PYROXENES
$MgO \cdot SiO_2$	ENSTATITE, CLINO- & PROTOENST.	PYROXENES
$CaO \cdot MgO \cdot SiO_2$	DIOPSIDE	PYROXENES
$ZrO_2 \cdot SiO_2$	ZIRCON	
Type $M_2O_3 \cdot xSiO_2$ Compounds		
$3Al_2O_3 \cdot 2SiO_2$	MULLITE	
$Al_2O_3 \cdot SiO_2$	ANDALUSITE, SILLIMANITE, KYANITE, (CYANITE)	
Type $MO \cdot M_2O_3 \cdot xSiO_2$ Compounds		
$2CaO \cdot Al_2O_3 \cdot SiO_2$	GEHLENITE	
$CaO \cdot Al_2O_3 \cdot 2SiO_2$	ANORTHITE	
$MgO \cdot Al_2O_3 \cdot 2.5SiO_2$	CORDIERITE	
$3CaO \cdot Al_2O_3 \cdot 3SiO_2$	GROSSULARITE	GARNETS
$3MgO \cdot Al_2O_3 \cdot 3SiO_2$	PYROPE	GARNETS
Type $M_2O \cdot M_2O_3 \cdot xSiO_2$ Compounds		
$K_2O \cdot Al_2O_3 \cdot 2SiO_2$	KALIOPHYLLITE	NEPHELINE, PLAGIOCLASE FELDSPARS
$Na_2O \cdot Al_2O_3 \cdot 2SiO_2$	CARNEGIEITE, NEPHELITE	NEPHELINE, PLAGIOCLASE FELDSPARS
$K_2O \cdot Al_2O_3 \cdot 4SiO_2$	LEUCITE	PYROXENES
$Na_2O \cdot Al_2O_3 \cdot 4SiO_2$	JADEITE	PYROXENES
$Na_2O \cdot Al_2O_3 \cdot 4SiO_2$	ACMITE	PYROXENES
$K_2O \cdot Al_2O_3 \cdot 6SiO_2$	MICROCLINE	ANORTHOCLASE, ORTHOCLASE FELDSPARS
$Na_2O \cdot Al_2O_3 \cdot 6SiO_2$	ALBITE	ANORTHOCLASE, ORTHOCLASE FELDSPARS

minerals in the second category. "Weathering" in this context is the combined action of water, freeze-thaw cycles, and abrasion (e.g., glacial or wind attrition) over geologic time, in some instances followed or replaced by hydrothermal alteration. Depending on geologic circumstances, chemical and mechanical comminution has achieved sizings from those comparable to fine silt down to colloidal (≤ 1 μm). Depending on the sizing, age, and conditions of exposure, hydration of the original compositions has progressed variously together with chemical decompositions and the leaching out of water-soluble and acid-soluble components. New compounds have been formed. The result is a very wide spectrum of clay minerals, all containing at least some chemically combined water in the form of hydroxyl groups. Table XIII.1 is by no means a complete catalog of known clay minerals. It is also much-idealized as to chemical compositions.

Many clay deposits in the earth are transported, or sedimentary. They have thereby been segregated or classified by nature. As rivers slowed and spread out, the first suspended clay particles to settle were enriched in the younger, coarser, less-hydrated grains. "Flint clay" is a good example: hard, gritty, and abrasive. The last particles to settle, in sluggish or static and swampy waters and in lakes or inland seas, were the finest, most-hydrated and softest minerals. The montmorillonite group, sedimentary kaolinite, and serpentine are good examples.

One group of clay-like minerals was born ultrafine. These are the bentonites: silicas and alumina-silicas condensed in the air as volcanic ash. Settling or carried down by rainfall, these too occurred as either local or transported deposits and commenced further alteration once on the earth's crust. A group that was born relatively pure -- at least, iron-free -- is the sedimentary kaolin group. These had to originate from iron-free rock, and to endure their millennia of weathering and deposition isolated from iron-containing minerals. Groups called "residual" or "primary" clays were weathered in place and never transported from their point of origin.

For the most part, ordinary clays contain greater or lesser amounts of Fe_2O_3 and TiO_2 as well as exhibiting various Al_2O_3:SiO_2 ratios, all resulting from their rocks of origin and from chemical alteration. Further, some ancient clay deposits in swampy lowlands were hosts to lush growths of vegetation, then became buried for ages again. Some underlie coal deposits. Carbonaceous or oily and resinous residues and other decomposition products of vegetation accompany these clays, some with appreciable ferrous iron content resulting. Some contain enough resinous organics (also, carbonates and sulfur compounds) to swell or foam on heating: the so-called "bloating clays." The "plastic clays," long used for their

lubricity in fireclay forming operations, derive that quality in part from their organic components. So-called "ball clays" are sticky in part because of their organic content. But all clays of appreciable organic accompaniment are also of colloidal sizing, and these special qualities also depend in large measure on their being colloidal.

Prominent among the precursors of clays were the igneous feldspars and granites. Feldspars and other igneous minerals contain MgO, CaO, Na_2O, and/or K_2O as chemical components as well as Al_2O_3 and SiO_2 or SiO_2 alone. From these minerals many clays derive their alkaline earth and alkali components. Acid leaching tends to remove K_2O and Na_2O first, then CaO; hence MgO remains a chemical component of numerous clays, CaO less often, and the alkalies least often. Other rock sources contain none of these oxides. From them have derived clay groups consisting almost solely of hydrated alumina-silicas, such as kaolinite.

Clay minerals are infrequently classified by detailed chemical composition; yet in relation to refractoriness, at least the Al_2O_3:SiO_2 mol ratio is of interest. Scanning this category of Table XIII.1, one finds tendencies toward discrete mol ratios as follows:

Mol Ratio, Al_2O_3 : SiO_2	**Examples by Mineral Name**
0:1 = 0.000	Amphibole,Attapulgite,Beidellite,Serpentine,Talcite
1:10 = 0.100	Mordenite
1:8 = 0.125	Glaucophane, Saponite
1:7 = 0.143	Stilbite
1:6 = 0.167	Biotite, Oligoclase
5:24 = 0.208	Montmorillonite
2:9 = 0.222	Vesuvianite
1:4 = 0.250	Bravaisite,Chabazite, Gmelinite, Levyne, Pyrophyllite
7:22 = 0.318	Nontronite
1:3 = 0.333	Hydrogrossularite, Mesolite, Natrolite, Prehnite, Scolectite
5:14 = 0.357	Illite
1:2 = 0.500[a]	Dickite, Halloysite, Kaolinite, Nacrite
1:2 = 0.500[b]	Lawsonite, Muscovite, Paragonite, Piemontite, Vermiculite
2:1 = 2.000	Sapphirine (add xH_2O to formula in table)

Notes: a - MO and M_2O components absent. b - MO or M_2O present.

Three classes of minerals should be included in this series by association. *Flints* and other alumina-free silicas (0:1 ratio) are incorporated by comminution with little chemical alteration; they are found co-precipitated with clay minerals. *Bentonites* are of such

variable Al_2O_3:SiO_2 ratio as to defy placement in the above list; they run from zero to about 1:2. *Bauxites* (ores) and their component minerals *boehmite, diaspore*, and *gibbsite* (all hydrated aluminas) are of common geological or weathering origins with clays and generally occur in deposits associated with clays. They are sometimes accordingly considered as a clay-like group, though as compounds they contain no silica. As ores they are always contaminated with silica, often also seriously contaminated with Fe_2O_3 by virtue of the common chemistry of hydrated Fe_2O_3 and of hydrated Al_2O_3. "Bauxitic clay" is a term used for inter-dispersed bauxite minerals with silicate clays, e.g., kaolins, while bauxite deposits are predominantly alumina hydrates. Taken arbitrarily together as a series, these can run the Al_2O_3:SiO_2 mol ratio up from about 1:2 to about 8:1 maximum, as-mined.

Clay Crystals. The crystal lattice arrangements of the hydrated siliceous clay minerals reflect the versatility of the SiO_4 tetrahedron and of the AlO_6 octahedron in generating both three-dimensional and two-dimensional (i.e., layered) symmetries. The clay-like zeolite group we shall set aside: they are of three-dimensional structures and, though of great importance, do not figure in refractory manufacture. Set aside also the flints, but not for lack of use. Virtually all the remainder are of layered structure: their tiny crystallites are typically platelets or leaflets, sometimes curled or rolled-up leaflets, sometimes fibrous in habit.

The basal atom layers of these crystals exhibit orderly stacking sequences of several kinds; that is, they exhibit different *repeat patterns*. The chemical complexity of clays reflects these differences to begin with, plus the ability of TiO_2 to replace SiO_2 and of Fe_2O_3 to replace Al_2O_3 substitutionally, plus other defect substitutions such as Al^{+3} for Si^{+4} and Mg^{+2}, Ca^{+2}, and Fe^{+2} for Al^{+3}. These defect substitutions create charge imbalances which call for compensating intercalated or between-layer cations, principally Mg^{+2}, Ca^{+2}, Na^+ or K^+. Both intercalated and surface-sorbed ions are relatively mobile or "labile" and capable of ion-exchange reactions in aqueous media. Finally, OH^- is spatially capable of defect substitution for O^{-2}, making possible some stepwise degrees of hydration; and surface-sorbed H_2O is ubiquitous, along with surface-sorbed CO_2, SO_2, and other species present in natural waters.

It is not necessary to display structural diagrams of all these crystals. It is worthwhile, however, to examine a few for an appreciation of the nature of clays. Two common stacking sequences of layers are a-b-c-d-e and a-b-c-d-c-b-a: a 5-layer sequence of which kaolinite is prototypical and a 7-layer sequence of which pyrophyllite is prototypical. A simple illustrative section of these layers is taken, counting the minimum number of atoms in each layer

which occupy an equal distance along their parallel planes and which are stoichiometrically equivalent. Examples of this simple representation follow in Figure XIII-2, adapted from Reference 3.

A in Figure XIII-2 represents kaolinite, a prototype.
B represents serpentine, derived from **A** by substitution in layer **b**.
C represents endellite, a hydrate of **A** in which the single layer **c** is replaced by two substantially interpenetrating and hydrogen-bonded 0H layers.

D represents pyrophyllite, a prototype.
E represents talcite, derived from **D** by substitution in layer **d**.
F represents amphibole, derived from **D** by the same layer **b** substitution plus the replacement of one 0H by one 0 in both of layers **c**. The charge imbalance is compensated by intercalated Mg^{+2} as shown.
G represents attapulgite, derived from **D** by a lesser substitution in layer **d** plus replacement of one 0H by one 0 in both of layers **a** instead of **c**. The charge imbalance is again compensated by intercalated Mg^{+2}.

H is for glaucophane, derived from **D** by only a partial substitution in layer **d** plus 0-for-0H substitutions in both of layers **c**. The charge imbalance is compensated by intercalated Na^{+} as shown.
I is for muscovite, derived from **D** by the changes made in both of layers **b**. The charge-compensating intercalated ion is K^{+}.

J and **K** are compounded stacking patterns consisting of three 7-layer sequences. In case **J** the third or lowest sequence consists of the unaltered **D** pattern. The charge-compensating Na^{+} ions are shown intercalated between the first two 7-layer sequences, which are identical.

J is for montmorillonite. Its first two stacking sequences are derived from **D** by the partial substitution made in layer **d** only.
K is for nontronite. Its third sequence is derived from **D** by substitution of Fe for Al in layer **d** only. Its first two sequences bear that same substitution in **d** plus a partial substitution of Al for Si in one **b** layer.

These patterns only begin to illustrate both the regular and the disorderly crystal variety possible, hence the wide variety of clays identified in Table XIII.1. The ion-exchange capability of the labile ions makes it possible to consider the replacement of Na^{+} and K^{+} in clays, perhaps also of some Ca^{+2}, by acid washing followed by

LAYER	A	B	C
-- a --	6 OH	6 OH	6 OH
-- b --	4 Al	6 Mg	4 Al
-- c --	4 O + 2 OH	4 O + 2 OH	6 OH / 4 OH
-- d --	4 Si	4 Si	4 Si
-- e --	6 O	6 O	6 O
	REPEAT	REPEAT	REPEAT

LAYER	D	E	F	G
-- a --	6 O	6 O	6 O	5 O + OH
-- b --	4 Si	4 Si	4 Si	4 Si
-- c --	4 O + 2 OH	4 O + 2 OH	5 O + OH	4 O + 2 OH
-- d --	4 Al	6 Mg	6 Mg	4 Mg
-- c --	4 O + 2 OH	4 O + 2 OH	5 O + OH	4 O + 2 OH
-- b --	4 Si	4 Si	4 Si	4 Si
-- a --	6 O	6 O	6 O	5 O + OH
(Inter)	REPEAT	REPEAT	Mg^{+2}	Mg^{+2}
			REPEAT	REPEAT

LAYER	H	I	J	K
-- a --	6 O	6 O	6 O	6 O
-- b --	4 Si	3 Si + Al	4 Si	4 Si
-- c --	5 O + OH	4 O + 2 OH	4 O + 2 OH	4 O + 2 OH
-- d --	2 Al + 3 Mg	4 Al	3 Al + Mg	4 Fe
-- c --	5 O + OH	4 O + 2 OH	4 O + 2 OH	4 O + 2 OH
-- b --	4 Si	3 Si + Al	4 Si	3 Si + Al
-- a --	6 O	6 O	6 O	6 O
(Inter)	$2\ Na^{+}$	$2\ K^{+}$	$2\ Na^{+}$	$2\ Na^{+}$
-- a --	REPEAT	REPEAT	6 O	6 O
-- b --			4 Si	4 Si
-- c --			4 O + 2 OH	4 O + 2 OH
-- d --			3 Al + Mg	4 Fe
-- c --			4 O + 2 OH	4 O + 2 OH
-- b --			4 Si	3 Si + Al
-- a --			6 O	6 O
-- a' --			6 O	6 O
-- b' --			4 Si	4 Si
-- c' --			4 O + 2 OH	4 O + 2 OH
-- d' --			4 Al	4 Fe
-- c' --			4 O + 2 OH	4 O + 2 OH
-- b' --			4 Si	4 Si
-- a' --			6 O	6 O
			REPEAT	REPEAT

Figure XIII-2 Typical Clay Crystal Layered Structures
(data from Ref. 3)

sluicing with water. There are some viable counter-arguments, however: acid-exchanged clays are much altered in their rheology.

Another common feature of clay crystals is indicated by noting the identity of the atom layers at the upper and lower extremities of the repeat patterns of Figure XIII-2. When any of the first three sequences is repeated (i.e., stacked), a "double layer" of anions is created in the basal plane of the crystal:

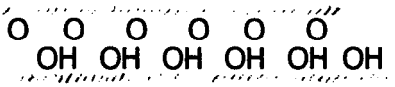

There is room for the two layers to interpenetrate a little, and hydrogen bonding occurs between them; but local dipoles are somewhat opposed. On stacking of any of the remaining eight sequences, this double layer consists rather entirely of O^{-2} ions and the opposed local dipoles are even stronger. The intercalated cation layer helps; but these basal double layers are weak planes in the crystal, and their bond lengths or layer spacings are larger than elsewhere.

When dry clays are "slaked" or soaked in water, H_20 molecules intrude into these planar spaces, creating an additional hydrogen-bonded layer in each. Lubricity results, as blocks thus separated can be readily moved in shear. Lubricating water films also collect between crystals. The resulting slipperiness can be very useful. But the swelling experienced on slaking and the subsequent shrinkage on drying can be microstructurally disruptive to a formed clay body. How processing adapts to this will be seen presently.

The readiness of slaking, the lubricity or "plastic" quality, and the drying shrinkage vary together from clay to clay. Quartz (e.g., flint or shale) is low on all three counts. Fireclays (predominantly kaolin) and pure kaolins are increasingly higher; and ball clays and bentonites run highest. For a given composition these properties all increase with decreasing particle size. A useful quantitative measure of plasticity has been developed,[440] called the "coefficient of plasticity," defined and determined as the ratio of "shrinkage water" to total water contained in a plastic clay. "Shrinkage water," occurring principally as films separating adjacent crystallites, is responsible for the shrinkage observed on drying to 105°C.[440] The remaining water fills larger pores.

Mineral Raw Materials in Perspective. The burden of managing the behavior of clays as refractory raw materials falls most heavily on the maker of fireclay refractory products. In clay-aluminas the proportion of clay in the solid mix decreases steadily with increasing weight percent Al_20_3 above 45%; and by about 60% Al_20_3 and above, the option exists to employ entirely anhydrous silicate

minerals such as andalusite or sillimanite. Bauxites and synthetics are available to complete the series.

Clays are not alone in being chemically and physically variable, nor in being susceptible to drying shrinkage. Bauxites share these qualities. Magnesites have been objects of critical scrutiny as to their impurity levels and crystal textures since basic steelmaking first made an insistent call for MgO refractories. High-quality magnesite deposits are in demand. Low-silica chromite ore is in prospect of short supply. Zircons and baddeleyite ore concentrates often have to be further upgraded. The supply of high-quality natural graphite is in danger of fading. Even good quartzite is no longer everywhere.

Part of this scenario results from the increased demands on quality made by an increasingly technical refractories industry. Partly it looms out of the finite resources of the earth's crust. Partly it has not yet taken place. But changes in ore and mineral supply -- both day-to-day and long-term -- have to be a first concern for vigilance in every plant making quality refractories. Ore dressing or beneficiation and concentration can be very helpful; yet there is hardly a mineral raw material now used in quantity in this industry that is not already so treated. Where further beneficiation ends and synthetic chemical manufacture begins may well become hazy; but by whichever means, maintaining raw material quality into the future is likely to become more costly. Synthetics now already in place -- MgO, Al_2O_3, ZrO_2 and SiC -- may next be joined in quantity by others such as mullite, spinel, zircon, chromia, silica, graphite, and other carbides.

Some excellent technical reviews and critiques of raw materials for modern refractories have been published in recent years. Examples of their coverage are:

Basic refractory raw materials[441]
Synthetic periclase[442,443]
Chrome ores[444]
Synthetic aluminas broadly[22]
Andalusite [351]
Synthetic mullite[445]
Baddeleyite and zircon[121]
Olivines[239]

The reference literature on clays is so enormous as almost to defy citing.[446] The interested reader is invited to browse.

Premanufactured Grain: A Secondary Raw Material. Figure XIII-1 includes three process paths by which in-process

products are made, themselves going back to the head end of the figure as secondary solid raw materials. *Grog* (elsewhere also called "chamotte") is one of these products. It is shown as a byproduct of the same generic path (2,6,8) by which burned clay bricks are made. It is simply a recycled fraction of those same bricks, returned, crushed and sized as part of the brickmaking feed stream. Grog was historically first introduced into clay brick manufacture (and still is), primarily for the purpose of abating the brick shrinkages experienced in drying and firing. Since it is fired at least twice in the finished brick, by virtue of further recrystallization it may also be somewhat more corrosion-resistant and thermally stable than the once-fired constituents. Finally, the size distribution of grog may be utilized to influence the size distribution of microcracks and the porosity of the finished refractory, hence the product's response to thermal cycling and thermal shock. These three considerations have figured in the use of grog in clay-alumina bricks as well, where it is always an option.

The other two paths in the figure, (2,9) and (2,3,4), yield sintered or prereacted grain and fused grain, respectively, by way of subsequent crushing and sizing. These paths represent process lines in a refractory plant that are physically separate from those lines making end products. Premanufactured grain or aggregate in these cases is usually of a different composition from the matrix components of the mix or batch. It is in some cases higher-fired by itself than is the reconstituted end product. Its purpose is always to impart corrosion resistance to the product -- though this function may be shared with other constituents, as in the case of pitch- or resin-bonded MgO + C composites, for example. Chapter VI gave an in-depth introduction to premanufactured grain or aggregate and its characterization and purpose. It is found in many high-performance refractories of both formed and unformed types. As such, it is critically important among refractory solid raw materials. Additional quantities of grain are made by recycling fired bricks, just as described above for making grog from fireclay.

Solid Additives

A distinction between Solid Raw Materials and Solid Additives in Figure XIII-1 permits us to focus on materials used in a refractory dry mix to satisfy various special needs. Some of these materials are identified as *matrix chemicals*, the remainder conveniently as *other additives*. The former are invariably finely subdivided, as they are intended to react or interact effectively with the major constituents for purposes of bonding. They may have low-temperature surface-active functions to perform as well; in fact, finely-subdivided and high-surface-area solids cannot help but influence the rheology of a mix. The "other additives" may be fine or coarse depending on their own functions.

Matrix Chemicals. The commonest constituent of any matrix mixture consists of the "fines" fraction of the same material of which the premanufactured grain is composed. The coarser size fractions of grain tend to retain their identity through heating, while below some size limit (e.g., 200 mesh or 325 mesh) the same material is expected to react in some fashion more than just to survive. The size boundary is of course hazy; but the screening out of fines while preparing grain, the production of an additional quantity by milling as necessary, and the re-introduction of an optimal quantity of these fines, are an important part of each mix formulation. In a "direct-bonded" fired refractory, these fines may constitute the entirety of the matrix. But usually not so. Other chemicals or minerals are added, for example to adjust impurity or matrix chemistry, to form new bonding phases such as spinels by reaction, or to create distinctively different chemical or cement bonding. Chapter VI explains in full.

Whereas the grain or aggregate is preferably well-crystallized and coarse-crystalline, matrix chemicals are often chosen or prepared in less chemically stable forms (as "reactive calcines," for example) as well as finely sized. In the formulation of a fireclay mix this reactivity distinction might be coincidental: between a well-calcined kaolin, some flint clay (both somewhat unreactive), and a plastic clay that provides the lubricity needed for forming but also yields the flux-producing components needed for liquid-phase sintering (i.e., reactivity). In the typical grain/matrix refractory, the grain might be well-sintered or arc-fused periclase or periclase-chrome; alpha-alumina or mullite; zirconia or zircon or A-Z-S; or crystalline SiC or BN; etc. Following are some examples of matrix chemicals used with various of these:

(1) Active calcines of periclase, magnesite, dolomite, or limestone;
(2) Fine-milled active aluminas[22,252,447] or
(3) Colloidal aluminas;[242,258,262,269,448,449]
(4) Silica flour or other silicate chemicals,[254-256] or
(5) Colloidal silicas;[117,133,240-242,246,253-258,450]
(6) Plastic or ball clays or individual soft clay minerals;[232,261,291,451]
(7) Chrome ore or synthetic Cr_2O_3;
(8) Bonding chemicals specifically qualified for use with SiC;[304]
(9) Calcium aluminate cement;[22,212,213,220,364]
(10) Barium zirconate cement for use with ZrO_2;[28]
(11) Mono-aluminum phosphate, MAP; [207] and
(12) Various inorganic phosphates, meta-, pyro-, and polyphosphates and mixtures, mainly of Na.[133-135,205-211,237,240,259,260,262,452,453]

Numerous of these solids impart some lubricity or plasticizing to dry or wet mixes, or otherwise influence rheology. Some which stabilize colloidal dispersions may be alternatively fed as aqueous solutions. The use of sodium salts probably could be avoided, and may be so in the future; presently, their amounts are small.

Other Additives. The following further solid additions exemplify other useful modifiers of refractory structure and properties:

(13) Granular graphite at, say, 20%[43,180] or 25%[74] in MgO; also in clays;
(14) SiC crystals at, say, 15% with or without graphite in castables;[46,192]
(15) Al, Si, or Al-Si metal deoxidant powder with graphite;[95]
(16) BN, Si_3N_4, AlON, or SiAlON deoxidant powder;[74,100,101]
(17) Synthetic resins used as binders and bonding agents;[193-195,299,301,303]
(18) Agents used in various ways to create porosity;[321,324,325,327]
(19) Burnout fibers to relieve the explosion hazard in castables;[295] and
(20) Wire reinforcing for thermal stress resistance.[49-51,240,290,291]

Preparation of Solids

The chemical nature and particle size distribution of each raw material constituent must be agreeable to the manufacturing process path of Figure XIII-1 which it is intended to feed, and to the characteristics wanted in the product. Following are some typical cases.

Fusion. Arc melting processes (2,3,4) and (2,3,5) call for an absolute minimum of volatiles in the prepared raw materials: no carbonates, no sulfates, no nitrates, no halides, no hydroxides, and bone-dry. Calcining to essentially zero loss on ignition (LOI) is the standard preparation of oxidic feeds.

Dense, coarse particles of a narrow size range are preferred. Air trapped in porosity can explode particles, creating fines. Fine particles of whatever origin create dust losses and nuisance. A practical envelope of particle sizes is between about 100 μm and 1-2 mm.

Chemical components do not all have to be admixed in the same particle. Feeds composed of different particles do, however, risk some segregation or fractionation if the particles are (a) of widely

disparate sizes or densities; (b) of widely disparate melting and boiling points; or (c) not uniformly co-mixed as feed. Fractionation can occur by distilling in the arc cavity, or by preferential wicking of a low-melting liquid out into the skull.

Sintered and Prereacted Grain. Process path (2,9) of Figure XIII-1 is much like that of ceramic synthesis. It calls for feed constituents that are neither too well-crystallized as oxides (hence unreactive), nor substantially of parent compositions such as hydroxides or carbonates (subject to excessive firing shrinkage). The typical preparation of a raw material constituent of the latter type accordingly consists of careful *calcination* to a time-temperature point at which most of the ultimate shrinkage has been achieved in the particles while recrystallization has not yet progressed so far as to destroy reactivity.

When hydroxide or carbonate compounds are subjected to gradually increasing temperature, decomposition of their crystals is also often gradual (see Calcining in Chapter II). Over much of the S-shaped curve of weight loss vs time-temperature, the decomposition is usually what is called *topotactic*: the residual oxide domains are pseudomorphs or skeletons of the original, i.e., occupy nearly the same volume but weigh less. Gradually the original crystals are fragmented, sometimes down to colloidal sizing. Out of those minute fragments the new oxide crystallites will ultimately be nucleated by diffusional ion rearrangement. Up to the point where oxide crystal nucleation starts, (a) the density has gone down nearly proportionate to the weight loss, (b) the microporosity has gone up nearly proportionate to the volume of atoms lost (as H_20 or $C0_2$ gas), (c) the surface area has risen enormously, and (d) the crystal skeletons are in massive atomic disorder. This is the region of maximum chemical reactivity. But decomposition may be only, say, two-thirds to three-fourths complete. Laboratory TGA curves and XRD analyses together are very informative here.

With further time-temperature progress, the remaining decomposition proceeds competitively with oxide crystal nucleation and growth. In the early part of the latter, porosity is more consolidated than eliminated: while surface area and reactivity gradually diminish, particle density does not increase much. Since particle densification is a major objective of calcining, one has to wait well toward the high-temperature end of the process when ion mobility is high and both crystal growth and the rejection of porosity are relatively rapid. The desired end-point is always a compromise, and always empirically sought. The above-described progression is not always precisely followed. Calcining in real time introduces further problems of nonuniform heating and consequent

nonuniformity of the product. If melting occurs in-process, reactivity can be further injured.

The optimally-calcined oxide is a prepared raw material constituent for the grain-making process in question. There may be two or more such constituents. If reaction is to be sought later in firing (e.g., to make prereacted mullite or spinel), it is well to consider combining the components within every particle prior to calcining. In any event, every such constituent is fine-milled to provide for intimate particle contact when the constituents are mixed and then agglomerated (step 9) before firing.

Mortars and Fireclays. The description of raw material preparation given above is applicable in principle to processes for making mortars as well. These fall under path (1) of Figure XIII-1. One or more particulate constituents may be high-fired rather than active-calcined, and may be ground to a coarser sizing; but the matrix constituents of a mortar are prepared in fine-milled and chemically-active states appropriate to their function. Mortars are made of compositions compatible with those of the masonry they join. They are typically either air-set (e.g., cement or silicate bonded) or heat-set (chemical-bonded). Important as they are, mortars are treated peremptorily here; their preparation is much like that of comparable plastic refractories.

The preceding description is also substantially applicable to the preparation of fireclay materials for manufacturing use; and for that matter to bauxites as well. Calcining is necessary not only to remove intercalated water and then collapse the hydrated crystal structures of these materials, but also to ensure that they will not slake or re-hydrate again if they are subsequently wetted. For both clays and the bauxite minerals, this means not only to decompose their hydrates but to induce a thermally-activated, irreversible phase change. The bauxite minerals undergo several series of transitions,[22] all of which end in slow, irreversible conversion to α-Al_2O_3, completed in the rough vicinity of 950°C. Above this calcining temperature the processes of crystallization and particle densification take final effect as described in the preceding section.

In the case of fireclay minerals, e.g., pure dry kaolinite, dehydration occurs fairly sharply, mostly between 550° and 650°C. But unlike the simple hydroxide compounds, kaolinite commences shrinking concurrent with its decomposition. In this respect it is much like polysilicic acid, which forms non-crystalline condensation (-Si-0-Si-) bonds coincident with the loss of water. Kaolinite then progresses into a nearly x-ray-amorphous "meta-kaolin" structure within the original platelet morphology, ending in an anhydrous glass by about 950°-1000°C. In the course of that last conversion, a

microcrystalline metastable alumina is exsolved and then slowly resorbed while mullite crystals nucleate and grow within the glass. Mullite is detected by x-ray diffraction (XRD) at about 1000°C, and microscopically at about 1200°C. Cristobalite appears just above that same threshold. The capacity of kaolinite to re-hydrate is progressively destroyed above about 800°C, but not completely so until 1000°C has been reached.

Fireclays overall are of various Al_2O_3:SiO_2 ratios and various Fe_2O_3 and other impurity contents. Their decompositions occur on the whole at lower temperatures and over wider ranges. They revert to glasses at variously lower temperatures, but all eventually yield some mullite and cristobalite. Resistance to re-hydration should be complete by about 900°C. Two papers are regarded as authoritative on these decompositions, one on kaolinite[454] and one on fireclays more broadly.[455]

Notwithstanding irreversible completion of the decomposition reactions by some 900°-1000°C, the glasses formed out of the original crystallites are extremely stiff. It becomes practically impossible to realize all the anticipated volume shrinkage of fireclays until liquid-phase sintering temperatures are reached. These may be approximated by the MST curve of Figure VIII-2. These temperatures are in the region of 1500°-1600°C. Thus while fireclays are calcined in preparation for their use, this process does not take out all of the firing shrinkage even of the particles themselves.

Calcining does take out essentially all of the lubricity. In order to reconstitute a "plastic" mix for wet forming, resort has to be made to addition of a raw plastic clay. This necessity adds a second mineral raw material to the firebrick processing line; but its quantity is smaller. The rotary-calcined fireclay fraction needs to be ground for use, but this material readily breaks down. A reasonable prepared mill-run sizing is predominantly -100m or <150 μm.

Crushing and Screening: Grain Size Distribution

Graded Grain Sizing; Particle Size Measurement. Products based on premanufactured grain comprise the majority of all high-performance working refractories. Fired and unfired, formed and unformed, they fall under process paths (2,6,7), (2,6,8) and (1) of Figure XIII-1. The creation of their dense grain or aggregate and the characterization of their matrix and other additives have been touched on. The only parameter left undefined is the sizing of their grain.

Chapter VI introduced the notion of *graded sizing* for maximum product density, strength, and corrosion resistance. The suggestion was made there that a top grain size of about 1/4" or about 6.3 mm is

commonly used in the industry. But this top size is not unique. At least 3/8", 1/4", 4-mesh and 6-mesh top sizes have been used.

Here we shall explore the principles and practices of graded sizing. To do so we express particle diameters in terms of standard sieve sizes or "mesh numbers" as given in Table II.1. For consistency we shall use the *Tyler* mesh numbers and their equivalent diameters as given there. A 16-mesh screen is denoted by "16m", for example. The equivalent diameter of its openings is 1.00 mm from the table. A particle lying on this screen (when suitably vibrated) has a diameter >1.00 mm and is designated "+16m."

A mass of dry particles might be shaken on a two-tier screen set, e.g., 16-mesh above and 32-mesh below, for size classification. Three groups of particles will result: (1) a group which lies on the upper screen, designated "+16m" and of diameters >1.00 mm; (2) a group passing through the upper and lying on the lower, designated "-16+32m" and of diameters $0.50 < d \leq 1.00$ mm; and (3) a group passing successively through both screens, designated "-32m" and of diameters ≤ 0.50 mm. Each group or fraction is weighed and expressed as percent of the total. The middle fraction above, for example, might have been weighed and designated as "2.7% -l6+32m." That percent can be taken as characteristic of the material sampled and screened.

Either size-classifying as illustrated above, or screening on an industrial scale to divert various size fractions to different storage bins, may be conducted using any convenient number of tiers and any selected set of screen sizes or mesh numbers. Little matter that particles may be irregular and jagged in shape, or elongate or oblate. Standard screens are standard; their openings are square. They pass and hold back what they will. Perhaps their diameter designations are only relative; that should be acceptable.

The system does get sticky, though, at sizes much finer than 250m. Blinding of screens may occur, preventing some or all finer particles from passing through. This is a common observation on 325m screens; and for this reason dry screening at 400m is rarely practiced at all. Wet (i.e., slurry) screening may relieve blinding for classification purposes.

Air classifiers are convenient for fine particles, down to the order of a few to 10 μm diameter. For separation, centrifugal or "cyclone" types are common. For classification, a simple laboratory device known as the "sedigraph" is much used. Both of these function based on Stokes' law, the sedigraph quite straightforwardly.

Light-scattering devices based on Rayleigh's law become useful about end-to-end with the sedigraph. Popular commercial instruments called "particle counters" employ very dilute suspensions in water; they count individual particles and measure their size by light or laser light scattering, in the size range from a few μm down to the order of 10 nm. For crystalline particles, x-ray diffraction line-broadening analysis can estimate some dimensions from roughly 5 nm down. The electron microscope can image and measure individual particles from close to 1 nm up to macroscopic sizes -- subject to severe restrictions at the low end. Other devices are available based on capacitance, electrostatics, or other physical phenomena. Even nuclear magnetic resonance (NMR) has been used to estimate particle size. BET surface area gives a good collective measure of fine sizings, quickly and economically.

Particle Size Distribution and Packing Density. With the measuring tools in hand, now start with the concept of a regular-shaped, smooth-walled, rigid vessel such as a die cavity, into which will be poured and compacted nothing but dry, size-graded refractory grain. Some axioms for a packing model are:

Axiom 1. All grains of whatever size are fully dense, rigid, incompressible and uncrushable.

Axiom 2. The size and shape distributions of grains are everywhere the same; i.e., long-range segregation is absent.

Axiom 3. There is infinite lubricity; under suitable compaction, all grains move to positions and orientations achieving minimum total volume and maximum grain-to-grain contact. As a corollary, there are no bridging or wall effects.

Axiom 4. There are no long-range inter-particle attractive or repulsive forces; and escape of gas in the course of compaction is complete.

Axiom 5. After compaction, no grain or particle will change volume during sintering; hence, fired bulk density tracks compacted bulk density.

Axiom 5, whose conclusion holds up tolerably well empirically, makes the pursuit of raw material packing worthwhile. That pursuit here entails accepting all axioms provisionally, followed later by examining their faults as well as introducing liquids.

If all grains are spherical and of a single size, the regular hexagonal (hcp) and face-centered cubic (fcc) close-packed arrays provide minimum total volume and an interstitial void volume fraction of 26%. This statement is size-independent. But such ideal packing does not occur. On the other hand, given a generous supply of all grain sizings from molecular to any chosen top size, without reference to regularity of packing it is intuitive that the void volume fraction f_v can somehow be reduced to zero.

One early model approach to packing started with hcp monosized spheres, then picked a smaller monosized set that would just fit into their interstices; then picked a still smaller monosized set to fill the larger interstices left among the first binary set; then --- ad infinitum. This is a distribution of *discrete sizings* for spheres. Again given enough liberty, it too can yield $f_v \approx 0$. We shall leave it here and come back to it.

The equally classical Andreasen semi-empirical theory of *continuous sizings* for spheres[456] is advantaged in that it allows for randomness. It is also applicable to jagged (crushed) particles. A form of Andreasen's size-distribution equation that works as well for screened size groups or increments as for continuum mathematics is:

$$\sum_{o}^{d} f(d) = (d/d_{max})^{q} \qquad \text{or} \qquad \log \sum_{o}^{d} f(d) = q \log (d/d_{max}) \ .$$

Here d is grain diameter, d_{max} is the top size, and f is the volume fraction of the total solid identified with a given size (or, screen-size cut). The summation is over all sizes from zero up to and including d; and q is an independent parameter, viz., the slope of a linear log-log plot of this equation.

Preferred values of q for maximum packing density can be identified only experimentally, using real materials which do not include zero size. For a limited span of sizes, the Andreasen equation was later modified[457] to read:

$$\sum_{o}^{d} f(d) = (d^{q} - d_{min}^{q}) \ / \ (d_{max}^{q} - d_{min}^{q}) \ .$$

This equation is a nuisance to plot, and there are no data proving that its prescribed distribution yields higher packing density than Andreasen's. An acceptable range of preferred q values in either case is from about 1/3 to 1/2,[456,457] but there may be exceptions.[458,459]

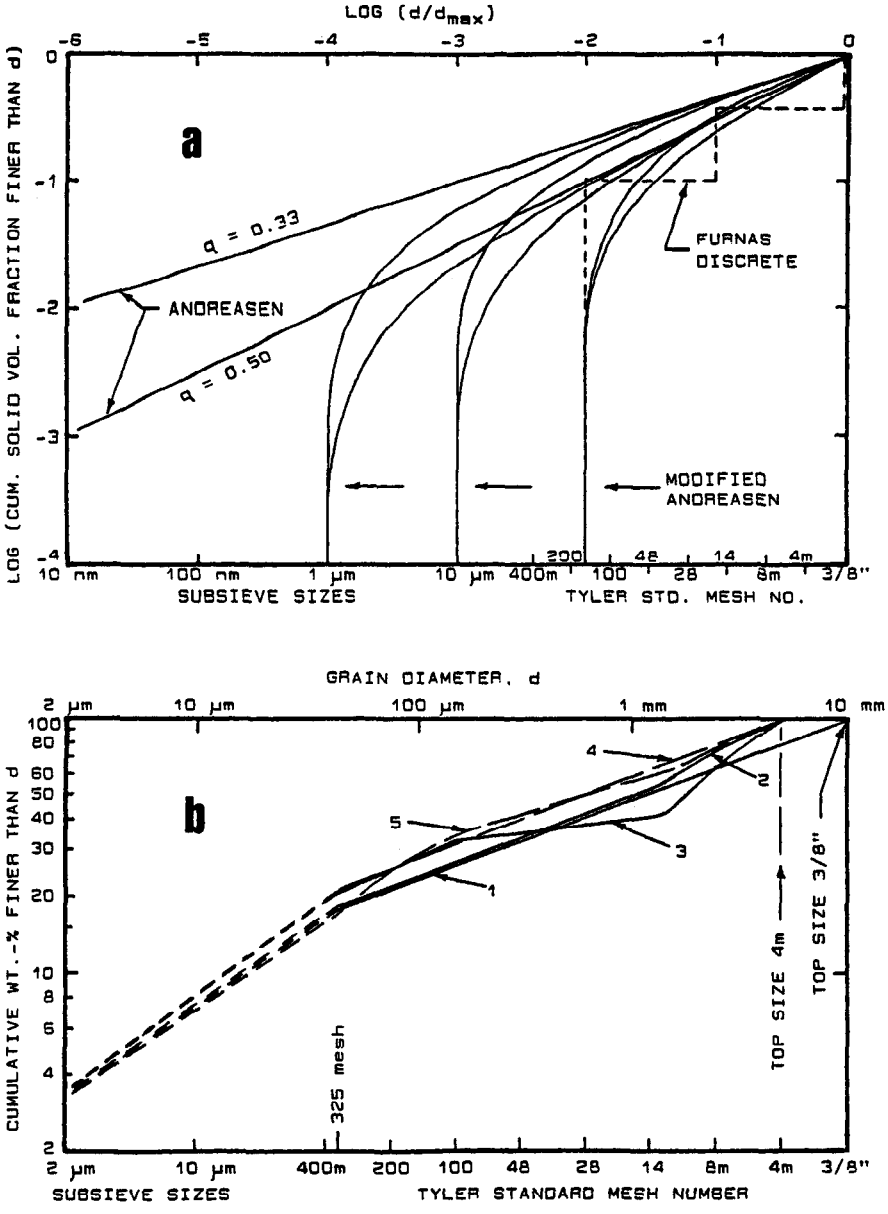

Figure XIII-3 Graded Grain Sizings for Dense Packing
a. Theoretical Models b. Periclase Brick Data

Log-log plots of these two equations are given in Figure XIII-3a for a 6-decade span of particle sizes, but cut off by d_{min} in the latter case[457] at four, three, and two decades. Each equation is plotted as the envelope of q values from 0.33 to 0.50. Please note the scale of sieve sizes at the bottom, which pertains only if the top size is 3/8".

Also shown in the figure is a plot of the semi-empirical discrete distribution due to Furnas,[460] in three monosized groups covering a two-decade size span. A four-group distribution over three size decades would be more appropriate,[461] but the Furnas distribution made up of monosized fractions is uneconomical to seek in refractory grain. Its ideal packing density appears unrealistic for our materials as well.[461,462] Its attraction for use elsewhere is that it too allows for randomness in packing and for nonspherical (e.g., crushed) particles.

Finally, another continuous distribution equation has recently appeared.[462] Called "improved" by its authors, in fact it plots precisely as do the preceding equations shown in Figure XIII-3a with a more cumbersome methodology of application.

The curves and envelopes of Figure XIII-3a accordingly embody the available guidelines for refractory grain sizing. Reliable indices of real packing density do not come out of their equations, though the best packing density always increases with increasing top size.[456-462] There is no warranty that other distributions cannot lead to equal or better density at a given d_{max}. Some members of the refractories community have approached or modified these guidelines as follows:

(a) Since all size fractions of a given grain are made by crushing and grinding the same material, volume as a measure of quantity in the above equations is replaced by weight or mass.

(b) The typical real graded grain distribution ends in a quantity of ball-milled (-325m) fines, which may include matrix additives. For economy as well as technical reasons, those fines are usually characterized by means other than by size. Since the d_{min} curve cutoff branches in Figure XIII-3a are an unevaluated formalism anyway, their equation[457] is set aside and only Andreasen's equation is used. With the above substitution of mass for volume, for log-log plotting this reads:

$$\log \sum_{o}^{d} m(d) = q \log (d/d_{max}) \ ,$$

where m(d) is the mass fraction identified with grain diameter d.

(c) With this equation in hand, grain size distributions may be optimized empirically for maximum dried and/or fired bulk density of a refractory. Distributions examined may or may not conform to this equation; and in fact, maximum density may be replaced as a goal by other considerations.[38]

Few such evaluations have been published in the refractories literature.[458,459,461] By way of example, one of us* made such a study in the early 1970s based on data collected for pilot-laboratory developmental periclase bricks made a decade before that. Five of the grain size distributions in that study are depicted in Figure XIII-3b. Curves labelled 1, 2, and 3 gave the highest (and sensibly equal) pressed and dried densities; dashed curves 4 and 5 with some twenty-five others gave from about 1% lower to still lower densities. Deficiencies in distributions nos. 4 and 5 relative to no. 1 were previously known,[456,458,461] but the equivalence of nos. 1, 2, and 3 was not foreseen.

Curve no. 3 deserves noticing. It is an example of "gap sizing:" a continuous distribution remotely resembling a two-group Furnas distribution, as previously observed.[458,461] This and the inflected curve labelled no. 2 are departures from Andreasen's linear distribution that seemed to improve on it at a top size of 4 mesh.

The short-dashed curve branches at -325m are symbolic of that ball-milled fraction but without any precise specification of its own particle size distribution. Its presence in a graded grain mix is what makes the Andreasen equation applicable in principle without a mathematical provision for d_{min}. That is, a four-decade particle size span reasonably approximates an infinite span.

The reader will rightly suspect that the preparation of a graded grain to meet some preconceived sizing recipe does not alone control its packed density. Running down the list of axioms from which we started, for example, all of them are flawed:

---

*S. C. Carniglia, unpublished work, 1972.

Axiom 1. Large grains are crushable. Grain density is often not constant.

Axiom 2. Segregation (esp., of large grains) is almost unavoidable in dry mixes.[461]

Axiom 3. This axiom is faulty on virtually every count.[456,458,461] Every mode of forming (wet casting, extrusion, vibratory casting, pressing, ramming, gunning) has its own problems in the management of particles and gives its own density.

Axiom 4. Gas entrapment is an almost universal accompaniment of compaction. Dry fines are plagued by electrostatic phenomena.

Axiom 5. With few exceptions, matrix fines, additives and chemicals are fused together and shrink on firing. If gases are evolved in firing a refractory, it may even expand.

A liquid added into a refractory mix imparts packing benefits including lubricity, the impedance of segregation, and the uniform distribution of fine particles and solutes. But liquids occupy volume and then generate gases on drying and firing. For this and all the above reasons taken as variables, a correlation between dried or fired density and grain-size distribution may well be unique to the one product formulation and process for which it is determined. Optimization is so laborious, it is little wonder that manufacturers usually regard these aspects of each product as proprietary.

It follows, of course, that packing density is decreased and porosity increased by selecting grain size distributions and matrix quantities that are removed from the optimum for dense packing.[322] A purpose in doing this deliberately is, for example, to follow empirical guidelines for improving thermal stress resistance.[37,38,41,53,54,139,308]

References 458, 461 and 462 contain further useful bibliographies on sizing. In manufacture, the grain sizing operations consist of crushing, grinding, milling, screening into convenient size fractions, and recombining these to give a calculated distribution. Descriptions of the various equipments used can be found in Reference 8.

Drying and Storage of Particulates

Solids that do not require calcining in their preparation may need to be dried. Any of three potential purposes may apply: (a) to prevent caking during storage; (b) to prepare for exclusively dry mixing, as in some of the embodiments of path (1) of Figure XIII-1; or

(c) to bring the moisture content to either a constant or a negligible level for purposes of chemical analysis and batching.

Drying of particulates may not be a matter of exceptionally high technology. But if it is to achieve a designed purpose, and uniformly, the conditions imposed should be based at least on thermogravimetric and differential thermal analysis (TGA and DTA). In some hydrated materials, e.g., raw clays, the removal of intercrystalline and interlamellar water may overlap with the thermal decomposition of chemical hydrates, making a fixed dried composition hard to achieve. Although the commonest final bed temperature used in drying is 110°C, that temperature is not always most appropriate. Some materials which contain negligible chemically-bound water (e.g., simple oxides) may be safely overdried without injury for the sake of obtaining high throughput in a given equipment. In any event, a deep bed of particles is almost as hard to dry uniformly as a consolidated solid. Particles should be dispersed, or spread in thin and rabbled beds, or tumbled. Various drying methods and equipments are described in Chapters II and III, also in Reference 8.

A challenging problem is presented by some chemically-active matrix additives after drying: sorption of H_20 and $C0_2$ from the atmosphere can cause caking or even reduce the surface activity, not all of which is necessarily recoverable by re-drying. Some active transition aluminas, for example, are subject to this "aging" phenomenon. Hermetic storage is a reasonable countermeasure.

The storage and moving of dry size-graded particulates are perennially at risk of *segregation*. Coarse particles tend to float on the finer whenever a bed is disturbed or mildly agitated -- as in filling or delivering from a vessel, for example. This risk increases with increasing span of sizings. Tumbling usually ensures some segregation, rather than overcoming it. Countermeasures usually take the form of (a) storing only the amount of an intended batch in a single vessel; or the equivalent, (b) compartmenting a storage vessel or silo in such manner that entire isolated compartments are discharged sequentially, batch by batch; or (c) providing for "plug flow" in both filling and delivery. Segregation calls for constant vigilance.

Batching

Batching of raw or starting materials is simple in concept, but not so simple in practice. Given either a dry or a wet mix whose target composition is fixed for every chemical component, and given N material constituents, each of which has been reliably analyzed for every one of the same components, then the mass M of the batch is:

$$M = \sum_{1}^{N} m_i \ ,$$

where m_i is the mass of the i^{th} constituent weighed into the batch. And the concentration (or, wt.-%) of the j^{th} chemical component in the batch, C_j, is

$$C_j = \sum_{1}^{N} (m_i/M)c_{ij} \ ,$$

where c_{ij} is the concentration (or, wt.-%) of the j^{th} chemical component in the i^{th} constituent. Simple enough, except for (a) errors in analysis, (b) losses in transfer, and (c) losses in mixing, which could be airborne fines or volatile components or segregated fines and liquids caked up on the mixing equipment.

But of the N constituents, a number N_s are size-classified solids whose proportioning must simultaneously satisfy a predetermined target particle-size distribution of the mix. It will be appreciated that an equation in m_i and d_i can also be written such that Σm_i from 1 to N_s satisfies this condition. But satisfying the compositional condition and the sizing condition simultaneously begins to be troublesome for a hand calculator.

Now consider reality in a plant. Successive lots of each raw material may be of inconstant chemical analysis or inconstant moisture content. Size fractions of graded materials will vary in their own internal size distributions, as the outputs of grinders and mills vary. Information on hour-by-hour variations of raw materials is available. But an operating plant cannot wait for batching adjustments to be calculated by hand. Nowadays all batching calculations are made by computer; and in many cases the computer output is sent directly as commands to automatic weighing equipment, whether for batchwise or continuous weigh-feeding.

Other properties have to be accounted for in wet mixes. For now, the above two -- composition and sizing -- are sufficient. But these two target characteristics of a mix have not yet been related to the phase composition and texture of its cured or fired refractory.

Those relationships are arrived at in the laboratory development of refractory formulations, to a considerable degree empirically. One part that we can illustrate as example is the relation between the overall chemical composition of a mix and the overall chemical composition of a fired brick made from it.

Suppose a clay-alumina refractory dry mix, of 1000 kg, is made up of 400 kg calcined kaolin, 400 kg calcined bauxite, and 200 kg of raw plastic clay. These will actually be wet-mixed for brick forming; but the water added will be removed in drying and in firing at 1700°C, along with the volatiles in each constituent represented by its LOI (loss on ignition to 1000°C) given as part of its analysis. Therefore we can ignore any water added in making up the mix.

The first three columns in the following table give illustrative chemical analyses of the three constituents. The next three columns give the corresponding mass of each component going into the 1000 kg dry mix, whose sum (except for LOI) is the mass of each component in (1000-23.2) or 976.8 kg of fired bricks. The last column gives the computed percent analysis of the fired bricks, whose mass of 976.8 kg is the dry mix mass minus its total LOI in kg.

Some features of this table are worth noting. First, the chemical analyses of the constituent solids are never obtained from mineral formulas, but are determined in the laboratory on representative samples of the materials actually stored in their bins or silos and ready for use. Second, the analyses tabulated here are far more tidy than are obtained in practice. Generally, each wt.-% column adds up to more or less than 100.0%, sometimes with disturbingly large discrepancies. A procedure should be in effect calling for repeat analyses when the sums do not close within prescribed limits, and for a routine arbitrary adjustment to 100.0% when they do. Third, the LOI at 1000°C does not necessarily match the mass loss at 1700°C, and a correction factor based on experience (i.e., on collected analyses of fired bricks) should be applied. The numbers here are all too neat. They have also omitted dissolved components in the added water. But they do illustrate the rationale.

	Calc. Kaolin, wt.%	Calc. Bauxite wt.%	Raw Plastic, wt.%	Kg in 400 kg Kaolin	Kg in 400 kg Bauxite	Kg in 200 kg Plastic	Kg in Fired Bricks	Fired Brick wt.%
Al_2O_3	44.4	87.9	23.4	177.6	351.6	46.8	576.0	59.0
SiO_2	52.8	6.6	58.5	211.2	26.4	117.0	354.6	36.3
TiO_2	1.4	3.2	1.4	5.6	12.8	2.8	21.2	2.2
Fe_2O_3	0.8	1.9	2.4	3.2	7.6	4.8	15.6	1.6
MgO	0.05	0.02	0.8	0.2	0.08	1.6	1.88	0.2
CaO	0.03	0.01	1.0	0.12	0.04	2.0	2.16	0.2
Na_2O	0.12	0.02	2.4	0.48	0.08	4.8	5.36	0.5
LOI	0.40	0.35	10.1	1.6	1.4	20.2	[23.2]*	---
Totals	100.0	100.0	100.0	400.0	400.0	200.0	976.8	100.0

* Not counted in total mass of fired bricks.

Batching calculations are more often performed in the reverse order, e.g., taking 400 kg kaolin and 200 kg plastic clay and computing the mass of bauxite required to achieve a target percent Al_2O_3 in the fired brick. That target in the above case is 59.0%. The weight ratio Al_2O_3:SiO_2 in the fired brick is (59.0/36.3) or 1.625:1. And the mol ratio Al_2O_3:SiO_2 is obtained by dividing each weight by the formula weight: (59.0/101.94)/(36.3/60.06) = 0.96:1. It should be noted in passing that the mol-% of any component in a material mix can not be computed from the wt.-% unless the complete chemical analysis is on hand adding up to 100.0%. But mol *ratios* can be obtained, as above.

The phase composition, porosity, and texture of the resulting refractory are determined experimentally, also in the course of laboratory development of the product. Phase composition and texture after firing are routinely interpreted by the on-site petrologist, using at least optical microscopy of polished sections. The starting compositions and particle sizings, together with the manner of compaction and the firing schedule, all affect the result.

Dry Mixing

Mixing also deeply affects the result. The efficacy, intimacy and uniformity of mixing and freedom from segregation thereafter are reflected through firing in the maximizing of interphase reactions and bonding and in uniformity of the product from one location to another -- and conversely.

Mixing is an art, punctuated by meticulous attention to detail. Mixing devices for free-flowing dry solids are usually of an open paddle type, either single or counter-rotating, preferably with a planetary head, in a relatively deep bowl. Caking or adherence to the walls must be avoided. Overfilling the mixer capacity can defeat its purpose. Dry mixing (other than by co-milling fine particles together) is an inefficient means of deagglomerating. Mixes that are prone to segregate, e.g., containing a too-coarse top size or a coarse constituent of low density, may never become or remain uniform. Arc-fusion feed, on the other hand, is well suited to dry mixing by virtue of being rather narrowly sized. Dry-mixed monolithics and mortars will be wet-mixed at the time of installation; but a dry mix must nonetheless be uniform in order to eliminate bag-to-bag variations in packaging.

Wet mixing has significant advantages over the dry operation. It is much the more common in refractory preparation. Wet mixing techniques will be discussed in the comprehensive context of rheology and plasticity.

Introduction to Wet Mixes: Surface Chemistry

It is of the nature of nonmetallic surfaces to be electrically chargeable. This phenomenon harrasses the processor of dry particulate solids. Fines become inexplicably air-borne, and they seem to stick to every surface within reach. When oxidic solid particles are placed in liquid water the mechanism of surface-charge generation becomes unique to the solid/H_20 interface; but there is nothing unexpected about the phenomenon.

Nor is the phenomenon itself uniquely associated with colloid-sized particles. To oversimplify only a little: the surface/volume ratio or surface/mass ratio of a particle is inversely proportional to its size, and hence *all* interfacial phenomena increase in importance -- relative to other factors in particle dynamics, such as mass or inertia -- with decreasing size. It is simply not true that larger particles are uncharged. What is true is that electrostatic forces become unimportant in particle dynamics at larger sizes.

It takes two observations to understand the "natural" charges on inorganic surfaces in water. Both are general for hydrophilic (water-wetted) surfaces, i.e., subject to some variations in degree but not subject to violation.

The first is that water molecules at room temperature chemisorb on oxide surfaces to give an outer, fixed layer of hydroxide groups. Schematically, this reaction is:

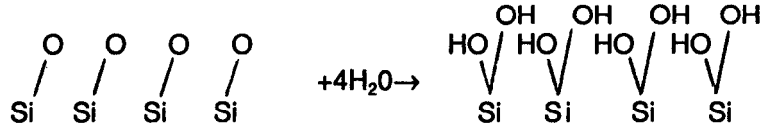

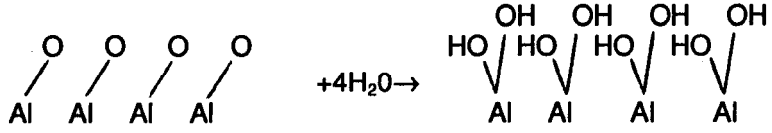

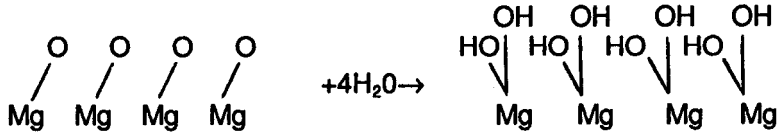

The uppermost of these three diagrams represents an Si-0 surface of solid SiO_2 (also good for silicates, clays, TiO_2, ZrO_2, etc.). The second diagram represents an Al-0 surface of solid Al_2O_3 (good for all aluminas, clays, Fe_2O_3, Cr_2O_3, Y_2O_3, etc.). The bottom diagram represents an Mg-0 surface of solid MgO (also good for NiO, PbO, ZnO, etc.). All three are alike. It is necessary only that the oxidic solid and its hydroxylated counterpart be insoluble (hence the omission of CaO). Imagine the hydroxylated surface as substantially covering each entire particle, and in turn bathed in liquid H_2O molecules.

The second observation is of a chemical relatedness between each hydroxylated surface and a simple hydroxide compound. The Si-OH surface relates to $Si(OH)_4$, also written H_2SiO_3 which is a weak acid. The Al-OH surface relates to $Al(OH)_3$, a weak base, but also written $HAlO_2$, a weak acid. $Al(OH)_3$ will be remembered as "amphoteric." And the Mg-OH surface relates to $Mg(OH)_2$, a weak base. If all insoluble hydroxide compounds are laid out in a series from strongest acid to strongest base (see opening of Chapter VI), these corresponding hydroxylated solid surfaces will lie in approximately that same order.

Now if we represent all these surfaces by M-OH (M = Si, Al, Mg, etc., etc.), the difference between an acid and a base is simply the way in which the hydroxyl group ionizes to yield an equilibrium condition in water:

$$\text{Acid} \quad \text{M-OH} = \text{MO}^- + \text{H}^+_{aq} \ ;$$

$$\text{Base} \quad \text{M-OH} = \text{M}^+ + \text{OH}^-_{aq} \ .$$

These equilibria differ from ordinary solution equilibria in that the residual charged sites, MO^- and M^+, respectively, are locked into a solid surface. The acidic or basic strength of the solid is indicated in neutral water by the surface density or nearness of these charged sites and hence the surface charge density, q/A. Amphoteric surfaces may have both kinds of sites, yielding as a net charge the difference between their respective surface densities.

The above two equations make it clear that acidic compounds have negative surfaces in water, hence yield *negative colloids* in the appropriate particle size range. And basic compounds have positive surfaces in water, hence yield *positive colloids*. A few right in the middle might yield uncharged particles. But that is so only in neutral water, i.e., at pH7. Each of the above equilibrium equations is sensitive, above all else, to pH. Acidity in the water (i.e., low pH) will suppress the first reaction, or diminish a negative charge density; and at the same time will enhance the second reaction, or increase a

positive charge density. Alkalinity in the water (i.e., high pH) has precisely the opposite two effects. Recall Le Chatelier's principle.

Curves of measured colloidal particle charge vs pH confirm the inference that any one given chemical species may be a positive colloid in one pH region, a negative colloid in another, and uncharged somewhere in between, at a pH called the *point of zero charge* or *PZC*. It is necessary only that the pH range employed be confined so as not to dissolve the particles.

Positive surface charges of course attract negative ions dissolved in the surrounding water, and are thereby partially neutralized. Likewise, negative surface charges attract positive aqueous ions and are partially neutralized. Here we are speaking of ions other than H^+ and OH^-. The neutralizing effect depends on both the concentration and the ionic charge of the dissolved ions. Thus a positive colloid is more effectively neutralized by SO_4^{-2}, for example, than by Cl^-, and a negative colloid is more effectively neutralized by Mg^{+2} or Ca^{+2} than by Na^+. A now-venerable model has it that the attracted "opposite" or counterions fall into two categories: (a) a "primary" layer, close to the charged surface (i.e., within the liquid boundary layer) and dragged along with it if the particle is moved; and (b) a diffuse "secondary" cloud which is left behind (but replaced kinetically by others) if the particle is moved.[463] The charge on the particle is taken to be adjusted by the former but not by the latter. The net or adjusted charge is expressible as a corresponding measurable electrostatic potential, called the *zeta potential*.[463,464] The zeta potential (including its sign or polarity) depends first of all on pH; then if nonzero, on the concentration of suspended solids and on the concentration and charge of dissolved ions of opposite charge. There is a comparable concentration of ions of like charge in the vicinity as well, of course, but these are repelled from the solid surface.

Curves of zeta potential vs pH are of roughly sinusoidal shape. Characteristic points on such curves for several different colloids are located approximately as tabulated below.[3,463-467] These are for low colloid particle concentration and low electrolyte concentration; the curves will move somewhat with increase of either or both. The numbers in the table are the approximate pH at which each listed feature of the zeta potential curve occurs:

pH at Feature:	Solid Dissolves	Max. Positive Zeta	PZC: Zeta = Zero	Max. Neg. Zeta	Solid Dissolves
SiO_2	--	<0	1.5	7.4	>10
Clays (var.)	0-2	1-3	2.5-5.5	7.5-8.5	>10
TiO_2	<1	3	5.5	8.2	>10.5
ZrO_2	<2	4	7.0	9.2	>10.8
Al_2O_3	<3	5	9.2	10.8	>11.5

It is true that particles of like charge repel, and the electrostatic repulsive force between isolated pairs is $F = q_1q_2/s^2$. But this equation applies only to surface separation distances s that are at least comparable to the particle radius. As s is decreased toward about a nanometer and then less, the interaction law between particles eventually turns into one of steeply increasing attraction with further decreasing distance.[463] In large part, this close interaction relates to local dipole-dipole attractions and to the formation of hydrogen bonding between -OH layers of the two particles. This branch of the potential energy vs distance law has in it a familiar steep turnaround at the "equilibrium distance of closest approach," at which two particles of appreciable abutting area are essentially bonded together. Thus the finest particles approaching each other within nanometer distance are usually fated to *agglomerate*.

Properties of Wet Mixes: Rheology

It is well to emphasize again that batched refractory raw or starting materials are typically comprised of a wide range of solid particle sizes. The boundaries placed between size ranges are arbitrary, and there are no discontinuities in behavior at these size boundaries. Nevertheless, there is some corresponding nomenclature of importance.

Range 0.1 nm to 10^+ nm. Ions and molecules, including polymeric -- *solutions* in water or other solvent. Uniformly dispersed and mobile; homogeneous.

Range 10^+ nm to 1 μm. Colloidal particles -- nonsettling suspensions called *sols* in water (or *smokes* in air). Consist of single crystals or polymeric particles, or what are called *primary agglomerates* of these.[463] Originally made mostly by chemical processes of *growth*. Primary crystals and agglomerates survive dry or wet milling and such aqueous processes as pH change; they are themselves altered in size only by chemical reactions. Colloidal particles (sols) generally pass through filters. Their larger members

can be settled by centrifuging. Sols are highly susceptible to electrostatic (surface charge) effects.

Range 1 μm to 50 μm. Typical range of ball-milled "fines," i.e., made by mechanical comminution of coarse and usually anhydrous materials. Such *comminuted* particles are either single crystals or stable *aggregates*; they generally survive aqueous processing except for possible chemical reaction.

A second category, starting in this size range and extending up through the next, consists of hydrated and relatively soft particles made by substantially-reversible *agglomeration* of finer particles in aqueous media. *Secondary agglomerates*[463] of colloidal particles are large enough to settle and to filter; they are often called *flocs*, and their formation by association or accretion is called *flocculation*. The reverse process, subdividing secondary agglomerates or flocs back to their primary colloidal particles, is called *deflocculation* or *peptizing*. Relatively huge agglomerates are made with an insufficiency of water; but these same component particles and processes can be recognized within them.

In terms of whole-particle dynamics, all particles in the 1-50 μm range are subject to surface-charge effects, but progressively less so with increasing size.

Range 50 μm to 1 cm. This is the "screen-size" range of ground or comminuted anhydrous particles, but penetrated as well by hydrated agglomerates as described above. In terms of whole-particle dynamics (viz., shear movement and hence apparent viscosity of slurries), particles in this size range are progressively still less influenced by surface charge with increasing size. Their slurry properties are progressively more dominated by the surface tension and viscosity of liquid films, i.e., by characteristics exhibited over relatively large dimensions.

Flocculation and Deflocculation. Clays were previously here characterized as natural colloids. The primary particles of kaolinite, for example, are predominantly hexagonal platelet single crystals ranging from about 0.1 μm to 10 μm across and in thickness from the rough order of 10 to 100 nm.[3,446,467] Lacking secondary agglomerates of much larger size, clays could hardly exist as sedimentary deposits in the first place, nor be wet-processed nor rotary calcined. Colloidal silicas, introduced in Chapter VI, are only one of hundreds of synthetic oxidic compounds that have now been made in submicrometer sizings. Lacking methods of their secondary agglomeration, these might all be little more than laboratory curiosities because they can not be settled or filtered.

A colloidal sol of, say, 5-10% solids is metastable indefinitely at a pH in the vicinity of a maximum in its positive or negative zeta potential (see the preceding table). There are several classical ways, singly or in combination, by which this dispersion can be flocculated:[463-468]

1. Adjust the pH near to (not necessarily at) the PZC.
2. Mix with a second sol or suspension of opposite surface charge.
3. Add electrolyte (of high counter-ion charge) to the aqueous medium.
4. Increase the slurry density (e.g., by evaporating water).
5. Simply raise the temperature.
6. Adjust the pH to incipient solubility of the solid.
7. Provide a time period of mechanical quiescence.

The first two are means of discharging the particles, permitting their approach under Brownian motion (kinetic energy acquired from liquid molecules by collisions) to nanometer separation distances and consequent agglomeration. As flocs grow they settle out, somewhat limiting the growth process. The second means is as much an admonishment against, if a sol is to be preserved, as it is an available option for flocculation. With no pH change at all, two oppositely-charged fine particles will co-flocculate, sticking together much as if they had reacted chemically. An example from the preceding table is silica with alumina at pH5.

The third means can augment either the first or the fourth, by incrementally diminishing the surface charge. In refractory mix preparation, however, adding an electrolyte will rarely be desirable. Flocs obtained under high ionic strength tend to be voluminous (excessively hydrous); and the occluded ions would have to be washed out of the consolidated material.

Means no. 4 is unqualifiedly effective, but energy-intensive. Note that the cheaper way of increasing the slurry density, namely by filtering or pressing out of water, is not accessible until flocculation has already been achieved. In a broad graded-size mix, however, sol particles may be sufficiently trapped in or electrostatically attached to larger particles as to make inexpensive water removal possible. Sol particles separated by insufficient water are forced into nanometer approach and hence may flocculate irrespective of their surface charge.

Raising the temperature (means no. 5) increases Brownian activity, driving particles together; but if a sol is not already nearly unstable, heating by itself is insufficient. On the other hand, heating is effective together with means no. 6.

No. 6, incipient dissolution by acid-base reaction, works best in fairly concentrated slurries. The process amounts to dynamic dissolution and re-precipitation of the solid, by which bridges are formed between sol particles at points of contact. This can be likened in a way to sintering. Flocculation occurs mainly by association of particles, not by growth of their size as individuals.

Means no. 7, quiescent time, is necessary particularly with no. 1 and no. 6. If particles are to flocculate by adhering, to the extent they are continually sheared over one another they will be torn apart and the intended transition will be frustrated.

With the above review comprehended, it is then easy to understand how a flocculated wet mass can be *peptized*. Consider a consolidated filter-cake as initial state, for example: perhaps 50-90% solids, depending on its particulate makeup. Two treatments are necessary, often but not always after some water addition:

1. Adjust the pH to the vicinity of maximum (±) zeta potential;
2. Provide intense mechanical shear to break up secondary agglomerates.

Two approaches to the second treatment are effective. The more common with a stiff mix is to use a device such as a mix-muller whose heavy wheels mash and extrude or "work" the material against a hard, smooth floor. A mix that is too fluid for this operation may be pug-milled, or still further thinned with pH-adjusted water, if necessary, then passed through a very-high-shear stirrer of the intensity typical of a Waring blender. Several high-shear industrial-scale devices of this kind are available. A jet mill is also useable for this purpose. In any event, without intense shear the peptizing adjustment of pH alone is in many cases totally inadequate -- unless there is infinite time.

Likewise, shearing alone under conditions of water content and pH favoring flocculation will rarely peptize a flocculated mix. One further degree of processing freedom should be mentioned, however. This is the use of *deflocculants*.[133,256,259-262,447,453,464,469] Deflocculants function in either of two ways. One, the composition of the surface of a particle can be altered by chemical reaction so as to shift the pH of its maximum zeta potential nearer to an existing pH (say, near 7 for example). Second, a naturally-colloidal polymer may be added that is preferentially adsorbed on the particle and, thus coating it, protects it from the aqueous medium. Such *protective colloids* are hydrophilic, often but not always organic. An example of an inorganic protective colloid is polyphosphate ion (hence a soluble polyphosphate compound). Another is polysilicate. Protective colloids of the hydroxylated organic kind such as gums, dextrins, and

cellulosics tend to add volume and later shrinkage, though they do burn out in firing.

Rheology of Wet Mixes. *Rheology* is a set of descriptors of the relationships among shear rate (or flow velocity in restricted geometry), shear stress (or applied force in restricted geometry), time, and stable flow as opposed to tearing -- for viscous liquids and for particulates suspended in liquids or vice versa. The independent variables in wet mixes at large are innumerable, and the responses to shear stress are not very orderly. For our purposes a *liquid* (whether homogeneous or heterogeneous) may be defined as exhibiting shear deformation or flow at any applied shear stress above zero. A *plastic* mixture exhibits a "yield stress" or some threshold stress above which deformation or flow occurs and below which it does not. But this distinction is really useful only when a yield stress is appreciable, and only when the same yield point is found both with increasing and with decreasing stress.

The observation of a yield point under increasing stress alone is very often misleading. A wet flocculated mass may on standing quiescent, for example, take on the microstructural characteristics of a *gel*. That is, van der Waals attractions and hydrogen-bonding bridges may become established between flocs in proximal contact, resulting in a continuous bonded solid network over the entire mass with an interpenetrating and no less continuous liquid network. That structure will respond elastically up to the yield point; but when flow does occur it is accompanied by disruption of the bridge bonds and at least partial reversion to individual, liquid-bathed flocs. This change is not quickly reversible.

That same structural change, both accompanying and facilitating flow, is commonly observed in fluid dispersions of fine solids in water. The rheological consequence, a time-dependent reduction of apparent viscosity at constant shear rate or a shear-rate-dependent reduction of apparent viscosity over short time, is known as *thixotropy*.[232,272,467] The proper definition of thixotropy is the former of the above two consequences;[3] but either may be observed. Either of these flow characteristics is evidence of a change in the distribution of liquid between particles and a decrease in their weak secondary or bridge bonding. This is a separate matter from deflocculation or peptizing. Sometimes it is seen in a stable, monodisperse colloidal sol, sometimes in a fine size-graded system whether containing colloidal particles or not.[232,272]

The coefficient of *viscosity* is the numerical quantity connecting shear or flow rate to the applied shear stress or shearing force. For a Newtonian liquid such as water, at fixed temperature this coefficient is a constant, independent of shear rate and of time:

$$\tau = \eta_w \dot{\gamma} \qquad \text{or in fixed geometry,} \qquad F \propto \eta_w v \ .$$

Here, τ is shear stress and $\dot{\gamma}$ is strain rate or F is shearing force and v is flow velocity, and η_w is the viscosity coefficient of water. Its SI unit is the "poise." This coefficient is measured using a viscometer which creates shear between inner and outer cylinders, the liquid being in the annular space between; or for very viscous systems, using an oscillating disc parallel to an underlying stationary base. Other viscometers and rheometers also exist; one will be mentioned presently.

Colloidal and fine-particle dispersions in water exhibit an immense variety of inconstant viscosity coefficients. For any consistent measurement at all, one must have both (a) a stable peptized dispersion or a stable dispersion of flocs, and (b) freedom from thixotropy, approached by waiting a considerable time at fixed shear rate before measuring. Given those two conditions, the apparent viscosity always increases monotonically with increasing slurry density, but in complex fashion. An equation for a monodisperse sol is:[3]

$$\eta_a = (1\text{-}f)\eta_w + k_1 f + k_2 f^3 \ ,$$

where η_a is apparent viscosity and f is the solid volume fraction in water. But size-graded slurries do not fit this neat relationship.[252-254,258,267-271]

In some instances, at constant slurry density the peptized-sol viscosity is orders of magnitude higher than the flocced viscosity. Pseudoboehmite (AlOOH) dispersions, for example, exhibit a viscosity peak at a pH near the maximum zeta potential, with minima on either side at incipient dissolving and at the PZC, respectively.[463] Clays at very high solids content, on the other hand, can be unworkably stiff at neutral pH but literally pourable when alkaline-peptized.[3,467]

Particle shape certainly influences the onset of stiffening with increasing solids content;[3,270,467] but it does not explain the above discrepancy in viscosity behavior with peptizing. Both p-boehmite and clays have platelet primary particles. Particle shape also has to influence thixotropy; but both spheroidal and platelet dispersions are thixotropic. Thixotropy, like viscosity, increases with increasing solids content.

A fairly common sequence of rheological characteristics is shown by a stable size-graded mass of particles as water is gradually added with continuous working in, say, a mix-muller or a pug mill. A

torque-rheometer in the form of a simple batch pug mill makes these changes evident.

Starting with a charge of free-flowing dry particles, the rheometer indicates a low apparent viscosity. In *Stage 1*, the first water added progressively hydrates the exterior and interior surfaces of particles and begins to substitute hydroxylated-surface interactions for dry surface interactions. The initial distribution of water being nonuniform, the first visible change is to a crumbly character while the indicated viscosity changes but little. Eventually, the whole charge becomes crumbly, and the crumbs or loose agglomerates begin to grow.

In *Stage 2*, which overlaps with *Stage 1*, further added water begins to fill the interstices between particles and to coat the exterior surfaces of crumbs with wet films. Crumbs grow by interaction and accretion and are increasingly worked or plastically deformed by the mill. The indicated viscosity rises irregularly. As interstices continue to be filled, developing some inter-particle lubricity, the growing crumbs are gradually consolidated and there is increasing interchange among them by shear and tearing. The indicated viscosity rises erratically. Visually, the charge is characterized as "caking" or "clumping." Large clumps finally ride around in the mill and are intermittently and violently deformed, and the indicated viscosity (i.e., torque) gyrates wildly. The material at this stage is "plastic," but whether it flows or tears depends on the deformation rate and magnitude. Typically, it tears in the mill.

The onset of *Stage 3* is clearly marked by the instrument. Liquid filling of inter-particle interstices becomes nearly completed and a continuous liquid film begins to develop throughout. Tearing ceases in the mill, the charge is described as "well-behaved," and a broad maximum in viscosity is recorded. The amount of water added over all of *Stage 3* is not large, however, as this stage ends when separation of particles by the intervening liquid film begins to be appreciable.

Stage 4 has its inception at this point, when the apparent viscosity begins to decline. *Stages 3* and *4* should both be described as "viscous." *Stage 4* is a long continuous stage of increasing volume, increasing separation of particles, and decreasing apparent viscosity -- ending with such descriptions of the charge as "pourable" or even "creamy." Depending on the range of particle sizes present, at various points along *Stage 4* some of the solids may settle out of the mix on standing. These four stages give criteria for the wet mixing of refractory material batches.

Wet Mixing

Wet mixing of refractory batches takes on more simultaneous purposes than does dry mixing. Included in those purposes will be up to all of the following:

(1) Mix all particles intimately and uniformly.
(2) Cope with or manage (e.g., peptize) colloidal constituents.
(3) Coat or penetrate all particles with all liquid components.
(4) Conduct initial surface reactions between solids and liquids.
(5) Develop a necessary and stable rheology for subsequent forming.

It is advisable to commence with dry mixing of all solid constituents. Equipment commonly used for wet mixing up to *Stage 3* or early *Stage 4* (above) includes the mix-muller, the pug mill, and various forms of kneaders, all well described in Reference 8. Fluid mixers for *Stage 4* include the paddle type mentioned under Dry Mixing, and numerous agitator or impeller types which combine more-or-less high-shear mixing in a small volume with continuous circulation of the whole charge through that volume.

Mixing, particle coating and deflocculation are most efficient when the shear forces exerted on the mix are highest. In the pug mill this condition prevails at the inception of *Stage 3* described above. The mix-muller, much more effective for "stiff" mixes, imparts maximum shear energy over most of the range of *Stage 2.* It has more difficulty than the pug mill, however, in managing mixes that become tacky or that include large grain sizings. A steam-jacketed pug mill is used, for example, in making up sticky pitch-bonded MgO mixes.

The details of each mixing procedure are a learned art, for which the foregoing provides background information but no fixed recipes. The same is true of adapting the final mix rheology to the forming process it is intended to feed. Additional to the matter of liquid:solids ratio, that adaptation may sometimes include prolonged agitation to stabilize or "age" the mix, or may sometimes entail a hurried conclusion and transfer to prevent aging. An example of the latter is given by mixes containing hot pitch, which stiffen with time at the mixing temperature and must be transferred and pressed before they become unworkable. Another is given by monolithic mixes containing hydraulic cement (Chapter XIV).

Liquid Additives

Aqueous Solutions and Emulsions. Apart from water alone, a number of additives can be brought into a wet mix as

aqueous solutions, sols, and emulsions. In a few cases there is no practical alternative. More often there is an option between use of a dry solid additive and use of its water solution. If the amount is quite small and the dissolved additive is unreactive toward the solid mix at room temperature, its introduction in solution may ensure its more intimate and uniform mixing with the solids than otherwise.

Aqueous agents that react or chemisorb vigorously on one of the solid constituents may, on the other hand, be far from uniformly distributed unless care is exercised in spreading a fine spray over a rapidly-moving solid bed. A further useful technique in this case is to defer adding the solution until most of the batch water has been added and well mixed in. Experience soon discloses any more than trivial deficiencies of mixing or reaction.

In any event, the number and amounts of reagents that can be added in water are limited. Following are some categories and examples of feasible aqueous additions.

Colloidal constituents such as commercial aluminas and silicas are listed as items (3) and (5) early in this chapter under Solid Additives, together with numerous cited references for each. In some cases sols are easier to handle. Aluminum hydroxychloride is a macromolecule, handled conveniently up to 50% solution. Though described in another context,[338] it has broad utility. The similar aluminum hydroxynitrate has been synthesized,[470] but there is no published record of its use in refractories. Its potential advantage over the chloride is obvious.

Bonding chemicals and deflocculants are on the whole indistinguishable: most perform both functions in a refractory. A long list of soluble phosphates and polyphosphates is given with references as item (12) under Solid Additives. Most of these can be optionally added as aqueous solutions. Further, aqueous H_3PO_4 is in very common use;[28,206,208-211,240,452] here there is no solid alternative. Some silicates and other polymeric anions offer options, while $MgCl_2$ is much more easily handled in solution than as solid.[240] Sulfuric acid and soluble sulfates are not much used anymore, except for special purposes;[327] and aqueous chromic acid, previously popular, has been all but replaced in the U.S. for reasons of toxic hazard.

Binders and lubricants for the mix itself are employed variously for plasticity in forming and for green and dried strength. Many more have been tried than are in published records; it is difficult to identify those actually in use. Included among water-compatible examples are polyalcohols, cellulosics, lignins, furans,[300] proteins and numerous other natural and synthetic gums and resins. It is believed

that, in many formulations, such additives as these may now have given way to combinations of inorganics and acids that serve the same functions without later burnout. Among further inorganics of potential interest as binders are the Al hydroxy-salts mentioned above, some related Ti and Zr compounds, and perhaps a few of the metal alkoxides that are receiving current attention in ceramics. An early review of ceramic binders[471] may suggest other candidates.

Nonaqueous Liquids. For evident reasons, there is little interest in organic liquids serving the function of water in refractory mixes. The two prominent organic families are those associated with MgO+C composite refractories, and with other binder and bonding usages.

Industrial pitches or *"tars,"* products of petroleum or coal distillation processes, have received much attention in this connection in earlier chapters. Grades of pitch with softening points above 100°C are typically used,[298,302] most often without any solvent addition. Hence pitch-bonded and pitch-impregnated refractories are processed hot, the pitch viscosity being managed by temperature selection so as to meet the needs of wetting or penetration of the refractory. A pitch-bonded carbon product was mentioned earlier, and other pitch-bonded materials are known including andalusite.[189,190] Pitch-bonded nonoxide artifacts are prolific.

Early-model pitch-bonded magnesias called for the highest possible carbon yield on coking.[115] Many chemical treatments and additives were evaluated as means of encouraging the high-temperature polymerization and coking of pitches. The only one known to have survived was a small addition of elemental sulfur. There may have been a few others. Today with the addition of graphite to these refractories, such pitch treatments probably have been discontinued; they have inconvenient side effects such as accelerated aging and stiffening of the pitch at the temperature of mixing. For general-purpose binder use such as with clays, pitches have given way considerably to the use of synthetic resins.

Synthetic thermosetting resins are viable contenders for all of the above binder and bonding uses.[115,93-195,299-301,303,472,473] Among the numerous techniques described, some employ powdered solid resins. But others such as for resin-bonded composite refractories employ liquids and mixing operations substantially like those using pitch. A current manual of thermosetting resins[474] gives a valuable overview of these materials, their properties, and how they are handled.

Sol-Gel Processing

It is fitting to close these discussions of wet mixes with a few remarks about *sol-gel* processing. Products of colloid processing are now burgeoning, exhibiting previously-unforeseen qualities of density-without-compaction, refractoriness, and corrosion resistance. Achievements in sol-gel processing of ceramics are prolific.[475-478] It seems a small enough extrapolation to suggest that further high-performance refractories might emerge from that same technology. Following is a brief outline of the basic principles.

A fairly concentrated colloidal sol may, under suitable circumstances, transform to a *gel* on standing quiescent instead of flocculating. Conditions favoring gelling over flocculation include high solids content (i.e., constant proximity of all particles), a moderate zeta potential (as opposed to near-zero), low electrolyte content, and high temperature with quiescence. Moving the pH gradually to induce gelling without stirring-in a reagent is commonly accomplished either by hydrolysis alone or by use of a soluble organic that slowly decomposes to yield an available base (i.e., OH^-).[468,479-482] One of several examples is urea, $(NH_2)_2C0$. Once gelling has taken place, neutralization and heating of the originally acid-stabilized dispersion are continued until the gel becomes quite rigid. On removal of water (usually by evaporation), condensation-polymerization takes place, resulting in -M-0-M- bonds in place of hydrogen-bonded -M-0H/H0-M-, and gelling is then reversed only with difficulty.

That sequence, called "sol-gel" processing, freezes all of the compositional and spatial uniformity of a sol -- or mixture of compatible sols -- into an extended solid mass.[475] That mass can subsequently be uniformly consolidated, ideally without developing domains of different packing density with boundaries between, which ultimately appear as shrinkage cracks. There are numerous sol-gel precedents for use toward the making of prereacted grain.[483-485] The intimacy of mixing of constituents provably reduces their reaction temperature.[478,486] At the present writing, trade-offs between grain or product qualities and cost of processing are unevaluated, but several experimental refractory syntheses have already been reported.[263,264,487] Sol-gel processing represents one more potential tool in the widening arsenal of refractory manufacturing methods. This and further advanced concepts in ceramic processing, described in current publications,[488,489] may well seed additional technology transfer into the field of refractories.

FORMING OF MASONRY AND SPECIAL SHAPES

Referring again to Figure XIII-1, batching and mixing of starting materials leads directly by process path (1) to a host of packaged monolithic products. We shall rejoin these under Installation in Chapter XIV. For now we go by the alternative path (2) to prepared feeds for further refractory manufacturing operations. We shall attend here to process paths (2,6,7) and (2,6,8) by which masonry and other engineering shapes are made, and specifically to their forming by generic operation (6). Forming has several important embodiments.

Extrusion

The so-called "stiff mud" process was one of the mainstays of firebrick manufacture well over a half-century ago. It still is. Also employed in making clay construction brick, this is an *extrusion* process whose die orifice is rectangular in shape. The die dimensions may be the larger two of a conventional brick: nominally 9" by 4.5" for making the classical 9-inch straight, for example. The continuous extrudate bar or ribbon is supported firmly on a coordinated moving belt. Periodically, a gang of taut wires transverse to the ribbon axis is brought down from above in such manner as to cut vertically through the ribbon, dividing a length of it into a set of individual bricks of equal thickness. The gang of wires is strung on a frame which moves precisely with the ribbon during the cutting and vertical retraction; then this frame returns to its upstream position, awaiting the continuous emergence of more ribbon from the die until the next cutting cycle is tripped. A rotating-wheel type of frame is also used. The continuous stream of cut bricks passes, in line, onto another belt moving slightly faster so as to separate the bricks enough for pickup.

In the simplest operation, a mechanically-coordinated robotic device then thrusts a set of fingers down around each brick in turn, clamps it gently between these fingers, picks it up, and lays or stacks it in a set pattern on a tray whose destination is the drying chamber. A single extruder so equipped has a production capacity up to the order of 2,000 bricks per hour. Extruded bricks are made slightly oversize and the dimensional imperfections (due mainly to cutting) are removed later by machining. An additional size allowance is also made for drying and firing shrinkage.

Most stiff-mud refractories are subjected to a further forming step before drying, however. Each brick picked up from the "fast belt" is placed instead in one of a gang of molds for *repressing*, using small mechanical presses at up to about 1000 psi or about 70 kg/cm^2. A common purpose is to provide for exact sizing and shape, also for

tailoring of all sides and for branding. But all sorts of special shapes are also made by repressing as a kind of forging operation: arch, wedge, key, checker brick, tile, and even sleeves, for example (see Shapes in Chapter XIV). The repressed green forms then go on to the drier.

Though the plastic extrusion mix contains considerable water, these high-clay compositions shrink in proportion to the water loss on drying.[440] Then owing to the high molten silicate content accompanying firing, they shrink again. The resultant fired porosities can be as low as about 9-13%. Since the particle sizing in the mix is fine and coalescence of pores in firing is resisted by the silicate viscosity, the final porosity is also typically of small sizing. Thus these extruded products are relatively impermeable and corrosion resistant when used within their service temperature limitations, though they are thermal shock prone for the same reasons.

Hot extrusion is one of the two standard methods of forming pitch-bonded carbon and graphite mixes for subsequent baking. The typical geometries here are long circular rods, rectangular and prismatic bars and strips, maintained straight between guides until they have cooled sufficiently to become rigid. Silicon carbide rods are similarly formed. Thus virtually all arc and other electrodes and heating elements are extruded, ranging in the thickness dimension from under 1 cm to the order of half a meter.

The Extruder. Given a mix of appropriate and stable rheology, the function of an extruder is threefold: (a) to take entrained air out of the mix so as to avoid unnecessary porosity or flaws; (b) to force the de-aired mix at a uniform rate into a plenum immediately upstream of the die; and thence, (c) by design of the die orifice profile or entrant shape, to impart uniform compression and shear to the mix over the entire orifice dimension in the process of forming. The first two functions are accomplished using a self-contained pug mill and auger or ganged augers, fed by a continuously-filled hopper and equipped with a vacuum pump. The third function depends on die design which is a highly-developed art, and depends as well on mating the mix plasticity to the throughput rate and the orifice area and shape. Figure XIII-4 is a simplified section of a typical brickmaking extruder, with the die indicated schematically at the right end. Equipment manufacturers can supply additional information.

Behavior of Plastic Mixes in Extrusion. Notwithstanding good die design, the intensity of shear imparted to the extrusion mix peaks along the die entrant walls. Water in the mix is thereby redistributed. Unless they are repressed, extrudates occasionally exhibit a somewhat hard, dense outer skin on this account. This skin may impede drying and usually persists through firing. A small elastic

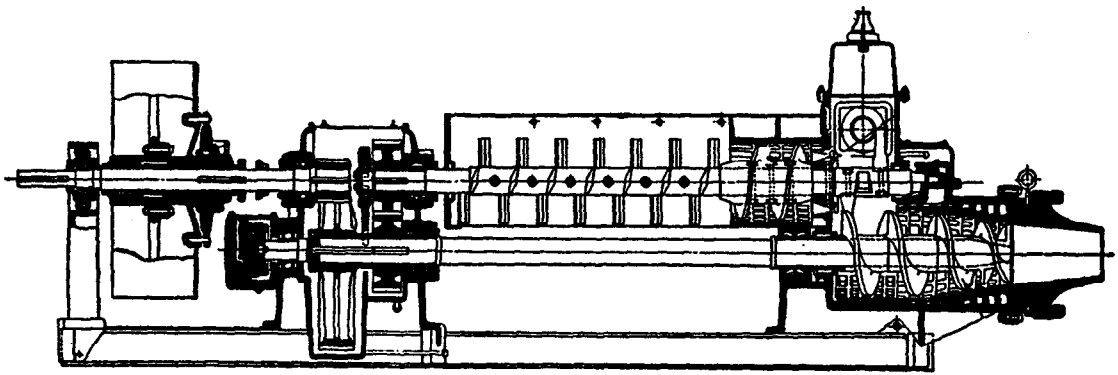

Figure XIII-4 Simplified Section of a Typical Brickmaking Extruder
(courtesy of FRH Extruding Machines, Div. of P.L.I., Inc.,
Plymouth, Ohio, by permission)

"rebound" or diametral swelling usually occurs on emerging from the die; this can in some cases cause cracking of such a hardened skin. Anisometric particles in the mix are given preferred orientation by the high shear experienced in extrusion, resulting in a net anisotropy of electrical, thermal and mechanical properties. This is particularly marked in carbons and graphites.

"Appropriate rheology" of a wet extrusion mix relates to the discussion of that subject earlier in this chapter, wherein the onset of *Stage 3* is about right for initial trial. Reliance on the ideal rheological relations of model material systems for guidance is often frustrated by the nonconforming variety of real mixes and by the nonlinear shear rates of real orifices. The practical experience of extruder engineers and rudimentary rheological information about a given type of mix will ordinarily suffice to direct small-scale pilot trials. These trials tend to give self-evident results.

Too dry a mix will tear or laminate on passing through the die. Lacking this result, an insufficiently plastic mix will overheat the die and wear it excessively. Too compliant or incohesive a mix will develop insufficient compaction with nonuniformity across a diameter, and with slumping, bending and cracking after emergence. One soon finds a workable region of rheology between these extremes, after which empirical fine-tuning can be undertaken. Mixes suitable for extrusion ordinarily exhibit a pronounced thixotropy -- a property vital to dimensional stability prior to drying, also making possible such operations as wire-cutting without excessive general deformation. Measures of green strength and of green deformation resistance or yield stress along with bulk density are helpful in monitoring extrusion.

Uniaxial Dry Pressing

Working refractory bricks and blocks have long been made by *dry pressing*, in efforts to achieve the highest possible green and fired density. The mix used is not literally dry but is variously in the crumbly *Stage 1* or *Stage 2* of mix rheology vs added water. The objects here are mutually at odds: (a) all particles are to be coated with a thin film of liquid for lubricity in the uncompacted state, yet (b) no two particles are to be separated by more than monomolecular liquid in the compacted state. Compromises are inevitable.

The optimum liquid content of a mix is always arrived at empirically. The amount needed is affected by the surface chemistry, plasticity, and particle size distribution of the solid constituents, the presence of solid lubricants, the particular techniques employed to de-air in the course of pressing, the dimensions of the pressed article (especially in the pressing direction), and the available pressing force

or pressure. Within all of these parameters, modern pressing tends to operate with insufficient liquid relative to initial lubricity.

Equally important is a set of parameters relating to uniformity: uniformity of the distribution of liquid over all solid particles; uniformity of the particle size distribution throughout the mold; uniformity of filling the mold, i.e., constant solid height and void fraction everywhere in the loose fill. These requisites put a stern obligation upon preparation of the mix in the first place, then upon the manner of filling the die cavity and of screeding or leveling the top of the charge before pressing begins. Technique is all-important -- and above all, uniformity of technique from brick to brick, cycle to cycle, shift to shift, and lot to lot.

Characteristics of Presses. Modern press design has not only achieved the exertion of ample force on the contents of the die. Ingenious feeder and screeding arrangements have markedly reduced variations in die filling. In addition, the incorporation of transducers in the pressing system now gives instant and simultaneous display of the thickness (hence, bulk density) of the compacted green brick and of the corresponding applied pressing force (hence, pressure). Heretofore, one could have either one of these as a control parameter, but not both. Now using both, and presetting an allowable variance about each, the press operator knows instantly and *for each and every brick* either (1) that it will proceed through drying and firing within specifications, or (2) that it must be crushed and returned to the mixing operation and adjustments made to the feed. In fact, by automation the press operator's judgment can be taken out of the circuit altogether. In any event, no material nor further processing need be wasted.

Figure XIII-5 gives an overview of several different means by which force has been applied to the charge in pressing. The sketches are not to any scale, and in no way do they depict the complexity or elegance of actual equipment. They are simply schematic representations of the principles employed.[490] Manufacturers will happily add details.

In the *toggle press*, it is seen in the figure that when the three pins are brought into line, (a) the downward travel of the ram is at maximum (and fixed), and (b) the mechanical advantage is all but infinite. These two characteristics also pertain to the *"Y" press*, shown next. This type is operated by forcing both arms of the "Y" to the centerline, their outer ends riding against the overlying rigid rail. These press designs both use the compacted brick thickness as a control parameter without independent command of the compacting force. The toggle press is mechanically intricate, featuring a spring-

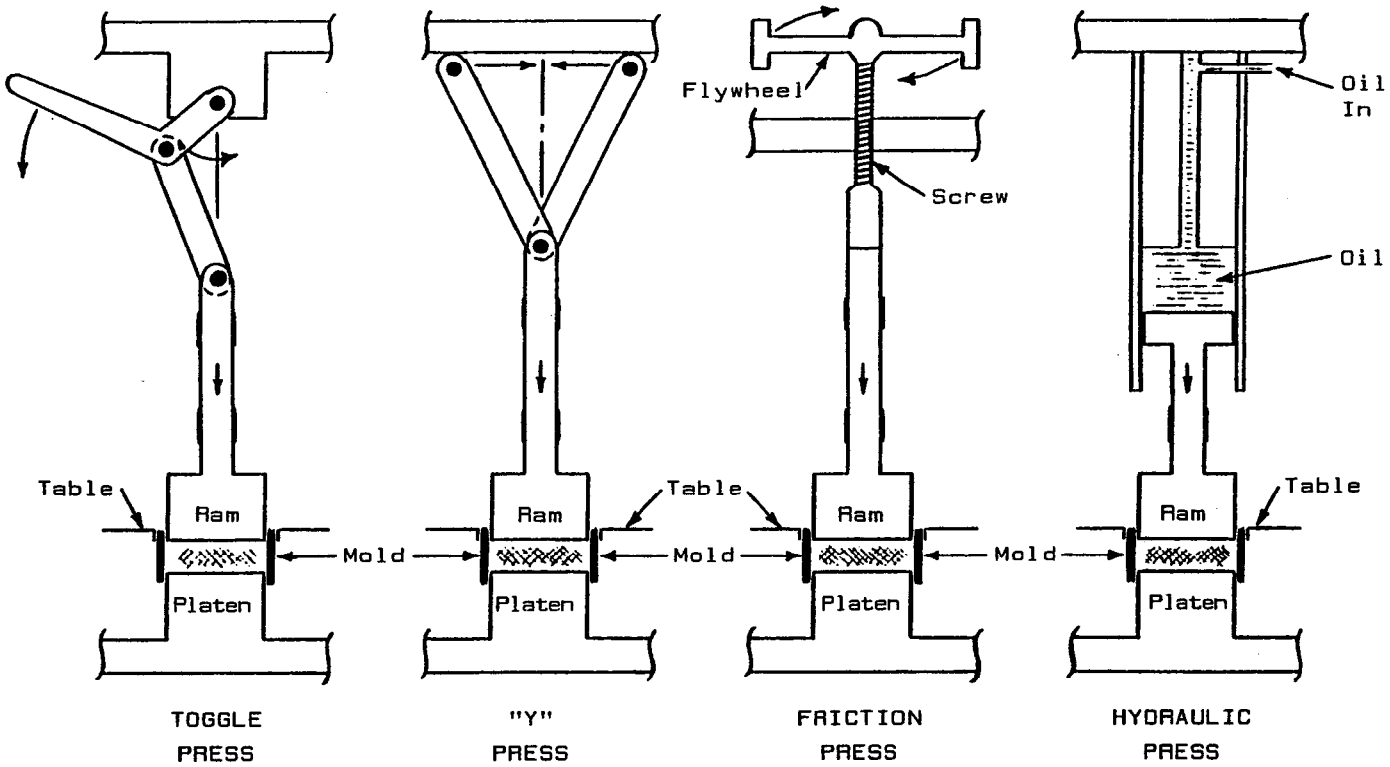

Figure XIII-5 Schematic Operating Principles of Some Refractory Brick Presses

operated lower ram. This however is seated against a stop when the upper ram is fully down. The mold is stationary.

The third type shown, the *friction press*, employs a flywheel driven to a preset speed (in free play) by a friction drive or clutch. The screw transforms this rotational motion to translation of the ram. When the charge resists, the kinetic energy stored in the flywheel (plus the driving torque) is transferred to the compacting brick and the flywheel stops. This design thus uses energy of compaction as a control parameter without independent command of the brick thickness. Its lower platen is fixed, while its mold floats during pressing.

The fourth design illustrated, the *hydraulic press*, historically used compacting force or pressure as the control parameter. But if a rigid stop is placed on the ram travel, brick thickness can be controlled instead. Or, using the instrumentation described above, both can be monitored simultaneously. The hydraulic press can be made double-acting, i.e., the platen replaced by a driven lower ram. Its mold floats in any case. Floating mold tables provide the least friction and die wear in pressing.

A detailed and current review of modern pressing equipment is given in Reference 490, and some notes on the pressure forming of large blocks are included in Ref. 346. Fully automated, the mechanical presses operate at about 6 to 8 cycles per minute. The friction and hydraulic presses run about 3 to 4 cycles per minute. Hydraulic presses can now: (a) press bricks end-on instead of flat; (b) press more than one brick per cycle; (c) press tapered shapes; and (d) using mandrels, press the parallel-bored hexagonal blast furnace heat-exchanger blocks and other tubulated shapes.

Material Behavior in Compacting. The resolved forces and flow patterns within the die cavity are complex, varying interactively with position, degree of compaction, and changing material variables. Isostatic conditions are never achieved, yet local flow transverse to the pressing axis is an important component of densification. Anisometric particles derive some preferred orientation from the predominantly uniaxial flow of the earlier stages. Some larger grains are ordinarily fractured in the process.

Disregard the fracture of grains, for simplicity. Over the entire range from an initial loose-fill void fraction of some 60-70% to a final void fraction as low as 1 to 5%, the number of grains in the mold is then constant and hence the number of interstices is roughly constant. The *size* of interstices is principally what changes. After some initial degree of compaction, the primary cause is an increase in the short-range ordering of grains -- i.e., in the efficiency of packing. Lacking

any useful mathematical model of pressing, the following is a word picture of the process from which reasonably sound inferences can be drawn.

Imagine the horizontal mid-plane of a circular mold in a double-acting press, to simplify the geometry. This plane is stationary. The particle density in this plane increases (and the void fraction f_v decreases) mainly by virtue of the motion of other particles into the plane from above and below, accompanied by particle rotation. The same is true of any other plane parallel to the rams, if taken as a plane of reference.

It is intuitive that the largest grains as individuals need not move laterally in their reference planes by more than a diameter. Their relative axial displacement is about the same. Successive reference planes separated initially by a largest-grain diameter are roughly d/3 apart after compaction. The axial, lateral, and rotational movements of the largest grains are in shear relative to their neighbors. The net effect is the gradual consumption (by occupancy) of the largest interstices. Resistance to these movements is provided by friction and by abutting and bridging; this resistance increases with increasing compaction.

Smaller grains originally lying between pairs of the largest are gradually moved out in the course of this shear. These in turn find or create interstices of at least their own size into which to move, save only those few which are blocked by bridging. By this progression of cooperating shear movements, the maximum size of remaining interstices diminishes. The grains tend to come relatively to rest in a time or compaction sequence commencing from the top size down. Relative to their own diameter, the particles must move over increasing lateral distances also in rough order from the top size down.

In the final stages of compaction, the predominant local movement is accordingly that of the finest particles and of any bulk liquid. This may be likened to extrusion. Moving out of the spaces between larger particles, the receding fines permit the ultimate approach or abutment of the latter while they themselves move into remaining smaller voids. All shear processes in effect are subject to the statistical variation of resolved shear stress with orientation and to the variation of surrounding constraints. Hence the required compacting force increases and the compaction rate decreases over time. In the ideal fully-compacted state there is only a small residue of unfilled voids. Particles of all sizes are equally abutted and with maximum areas of mutual contact.

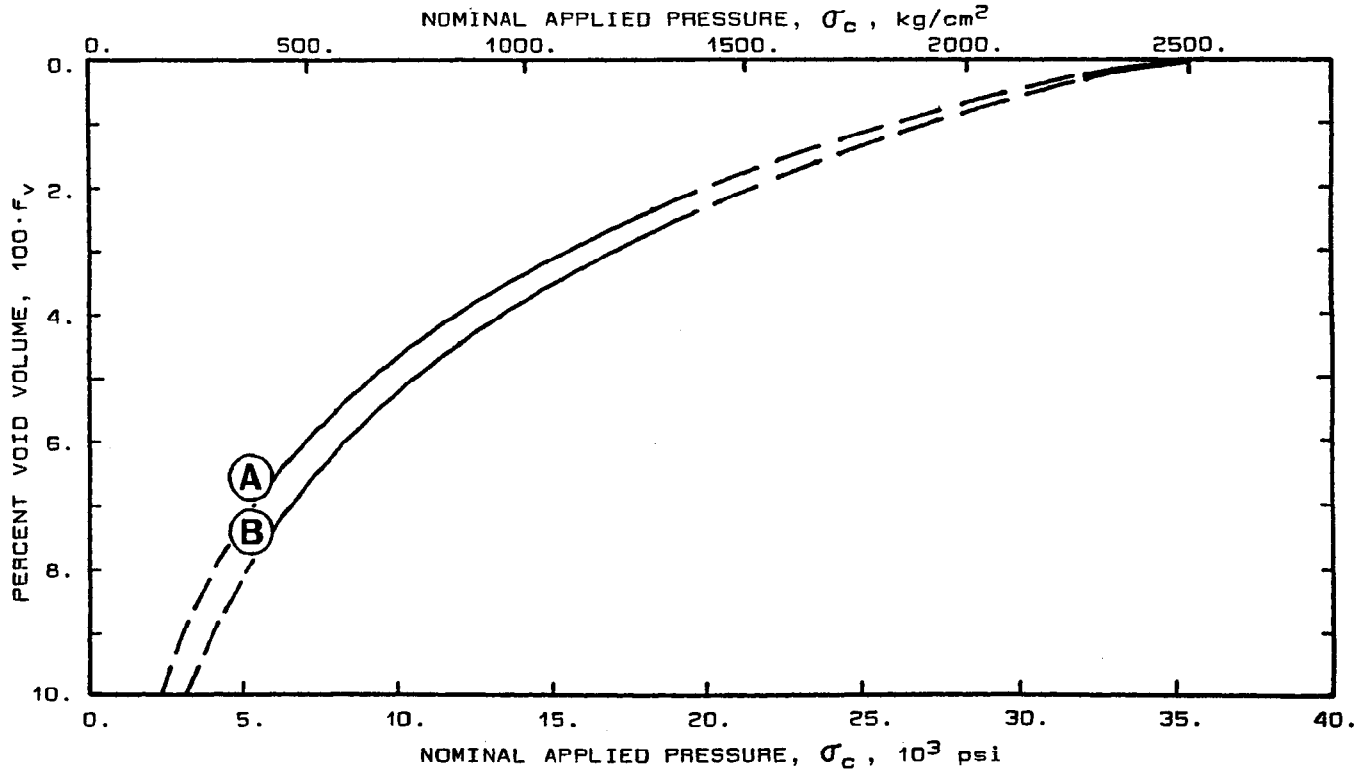

Figure XIII-6 Dry-Pressing Compaction Curves for Two Basic Bricks
(data from National Refractories and Minerals, Inc.)

The latter stages of compaction are shown in Figure XIII-6 for dry pressing of two coarse-sized nonplastic periclase-chrome formulations "A" and "B." The B.D. vs F/A or σ_c data* were taken by the instrumented hydraulic press between 6,000 and 20,000 psi, and the bulk density was converted to void fraction f_v for purposes of plotting the solid curve branches. The data were closely fitted by an empirical equation of the form:

$$f_v = a - b \log \sigma_c$$

The dashed curve branches in the figure are extrapolations of this equation. Note that the ordinate scale is reversed; $f_v = 0$ corresponds to the "theoretical" density of each damp mix.

Extrapolations are made at the maker's risk. The above equation blows up as σ_c approaches 0, and it has to fail both mathematically and physically as f_v approaches 0. These bricks are made at a final pressure of about 20,000 psi or about 1,400 kg/cm^2, where the residual void volume is about 2%. Other refractory compositions give similar-appearing curves, often at lower pressures owing to mix plasticity. The above empirical equation is not universal, but its general characteristics are.

Realities of Pressing. Not all pressing operations approach the ideal. Some origins of unwanted final porosity are:

1. Inadequate pressure;
2. Inappropriate compaction rate;
3. Inappropriate particle size distribution;
4. Nonuniform particle size distribution;
5. Edge effects;
6. Premature abutment and bridging;
7. Excess bulk liquid;
8. Trapped air.

Inadequate pressure is no longer a common limitation on pressed density.[490,491] One of several reasons for the resurgence of use of the hydraulic press in refractories, for example, resides in advances in hydraulic pumps, valves, and seals that have made possible greatly increased pressing force and durability. Dies are now much more rigidly built than was once the case. While plastic clays and clay-aluminas are pressed at only about 4,000 to 8,000 psi, high-alumina mixes employ some 8,000 to 15,000 psi and basic refractories require from 15,000 to as much as 25,000 psi to achieve maximum green density. Recall that 1,000 psi = 70.31 kg/cm^2.

---

*National Refractories and Minerals Corp., Livermore, California.

Compaction rate optimization is not always practiced, but should be in any case of persistent dissatisfaction with pressing results.[491] Since particle shear processes predominate over virtually the entire period of pressing, the imposed shear rate or the time rate of increase of pressure can markedly influence the course of compaction. Bridging, air entrapment, and lamination may be at issue in some cases; but different mixes respond differently. Compaction rate interacts strongly with the lubricity or plasticity exhibited by the mix, and optimization may be found as much in mix reformulation as in major alteration of a generally-acceptable pressing regimen.

Inappropriate or nonuniform particle sizing is avoidable. Both Andreasen and gap sizings are in common use. Jagged, angular grains do tend to pack poorly; these are sometimes rounded a little by autogenous or self-milling before use. The most sensitive deficiency consists of inadequate fines, which fail to fill the residue of porosity. Such a deficiency can lead to premature abutment and bridging of the larger grains. Too large a fines fraction interferes with compaction by caking within the mix. The fines fraction has to be optimized in its own size distribution in order to flow freely.

Edge effects have not been explained quantitatively. Where the mix impinges on the walls and especially corners of the mold, friction effects and patterns of grain movement during compaction differ from those in the bulk. The effects on texture, orientation, and increased porosity extend for several large grain dimensions into the body. Edge effects are somewhat more pronounced as the brick or block thickness is increased in the direction of pressing. Partial cures may be effected by altered sizing, pressure, or compaction rate.

Bridging is a characteristic of the somewhat larger grains of a mix, akin to the formation of arches or domes, with the grains in close abutment. It is the principal cause of fractured grains. Bridging envelops or isolates unfilled voids. By transforming the pressing (axial) force to lateral forces, a bridge further interferes with densification below it and thus can breed still more porosity. Bridging usually reflects premature abutment of larger grains, hence a fault in grain size distribution, lubricity, or compaction rate. Bridging can occur where the axial dimension of a pressing is large, due to cumulative variations in flow. Other than to correct the causative fault, a means of breaking up bridges is available in the pressing regimen. This technique is described below under *de-airing.*

Excess bulk liquid in the spaces between grains holds those grains apart. No green porosity is created thereby; but on drying, the corresponding unwanted porosity appears. Where bulk liquid films are continuous in a region undergoing compaction, the escape of gases from the void spaces may be impeded or prevented by trapping

(see below). Finally, excess liquid is often implicated in lamination. The cure is self-evident; but other measures may have to be taken to preserve plasticity in a drier mix.

Trapped air has persistently nagged brick pressing over its whole history. Reduction of the liquid content of mixes helps, but a consolidating plastic solid itself encloses air-filled voids and constricts escape routes for the gas. Not only does this entrapment promote unwanted porosity. The gas becomes compressed, ultimately to an internal pressure comparable to that exerted by the press. On removal of the pressing force, the green brick bloats or swells.

As the gas expands and distorts the surrounding microstructure, local escape routes are created. But these paths or cracks may not reach the external surface. The larger the brick dimensions, the more likely it is that the expanding gas will collect instead in lenticular spaces in the interior. This is a process of *lamination*. Today, brick lamination is rare. It has been overcome largely by attending to one or more means of *de-airing* in the course of pressing.

De-airing by the obvious means is not easy. For this purpose the faces of the hollow ram and platen are made of porous metal. Once the ram is in place in the mold, the charge within is evacuated by pumping before and during pressing.[491]

The second and more common method is based on the observation that gas escape paths can be created temporarily by imposing pulses on the pressing operation. If the ram is repeatedly relaxed or slightly withdrawn, elastic deformations in the compacting charge are relieved and shear between grains is interrupted if not actually reversed. Shock waves sent through the charge function similarly. These internal mechanical disturbances can also break up bridging within the solid mass, hence can do double duty.

Numerous ways of adding a jolting periodic motion to pressing can be imagined. Not many have survived trial. The most likely side effect is damage to the mold, or even to the pressing mechanism. The commonest technique with a mechanical press is periodically to "bump" the press: to back the ram off a little, then resume its motion forcefully to create an impact. In hydraulic pressing the technique consists of a similar periodic interruption, but little inertial effect is feasible. The floating mold is especially helpful in this circumstance.

Isostatic Pressing

In *isostatic pressing*, a body preformed otherwise is hermetically wrapped in a flexible metal foil or polymeric bag and placed in a vessel which is then filled with oil under pressure. This

method has not found favor for very large shapes. It is useful for some difficult refractory geometries such as nozzles, shrouds, and fine-tubulated gas diffusers.[492] Isostatic pressing is relatively slow and costly.

Hot Pressing

Typical *hot pressing* equipment consists of a double-acting hydraulic press system whose rams are enclosed in an electric furnace. The basic concept is to press simple disc or slab or comparable shapes at a temperature such that the material is thermally plastic. That is, forming and sintering are combined. Rams are usually graphite, bathed in inert atmosphere. This too is a costly and size-limited process, applicable to high-value compositions intended for specialty uses.[18,74,166]

A second category might better be called "warm pressing." The die parts of a conventional hydraulic press (mold, ram, and platen) may or may not be heated at all, other than by repetitive pressing of a hot charge. At the present time, pitch-bonded composite refractories are so formed in large quantities; these are principally the MgO+C refractories of oxygen-process steelmaking. Pitch-bonded carbons and graphites are also pressed in this manner into stock shapes not suitable for extrusion, in preparation for subsequent baking. Resin-bonded mixes are pressed much cooler, from room temperature to about 50°C depending on the resin system used.

Here the viscosity of liquid pitch assumes major importance. Its temperature control (140°-175°C) and aging time are critical. Liquid films are thick, air entrapment is unavoidable in pressing, mixes are tacky, and plastic deformation in the press is sluggish. Pressing cycles are from one to at most two per minute, yielding green porosities of at best about 2%. Green shapes call for firm support until they have cooled. Hot pitch fumes are toxic, and operating personnel must be protected. On the other hand, for nearly all of the composite basic refractories, pressing is the end of the process line. Process path (2,6,7) of Figure XIII-1 applies. *Tempering* of larger bricks is an oven-induced polymerization of the pitch, conducted after pressing to increase the brick stiffness during burn-in. Its use is infrequent.

Cement Casting

Refractory concretes, typically aluminous compositions plus CA cement, are formed among other ways by casting of thick slurries in the field. These castables are prominent among monolithic products. Their same forming techniques are also employed in-house by the refractory manufacturer, however, to make bricks, blocks, tuyere blocks, burner blocks, taphole blocks, ports, elbows, and other

specialty or custom shapes such as some slide-gate valve parts, concast system parts and porous diffusers.[74,132,138,140,191,199,221] Castings are near net shape, requiring only minor finish machining to meet close tolerances. The ability to cast around removable mandrels serves the needs of the several orifice designs mentioned. The evolution of low-cement and down to zero-cement castables, previously described,[117,241,242,245,247-249] has not diminished the range of feasible cast shapes or sizes.

Cement casting, thus broadened in scope, is an invaluable complement to pressing, especially where noncylindrical cavities are enclosed or where overall dimensions are too large. The *casting* and *vibratory casting* processes are described in Chapter XIV. The modern compositions are formable at far lower water content than was feasible with early conventional clays. Still further, their hydraulic setting and gelling mechanisms achieve rigidity without requiring the initial removal of water. Drying shrinkage is largely eliminated. As was mentioned in Chapter XI, by adroit chemical formulation the dimensional change on firing is also substantially controllable between modest shrinkage and permanent expansion. Porosities below 10% have been achieved, and service temperatures as high as 2000°C have been met.

These vast improvements over classical casting technology have been wrought from combinations of careful particle size grading with the mastery of rheology including colloid peptizing. They also entail the control of bonding mechanisms from initial setting over the entire thermal range up to the service temperature. The strength curves of Figure XII-3c are continuing to be exceeded. These remarks apply equally to the casting of monolithics in the field and to in-house casting, though in-house process control is potentially better.

AGGLOMERATION FOR SINTERED GRAIN

Premanufactured refractory grain made by sintering or reaction sintering is described by process path (2,9) of Figure XIII-1. Here we shall catalog the more common means of agglomeration, i.e., generic operation (9).

Agglomeration means the consolidation of particulates into any undefined shape, in the present context usually using water as carrier or agent. The interparticle bonding in an *agglomerate* is typically Van der Waals and hydrogen bonding. Upon firing, an agglomerate becomes an *aggregate* of particles or crystals whose bonding is condensed, e.g., -0-M-0-M-0- in the case of oxides. Here the purpose

of agglomerating is to produce rocklike chunks, balls, or pebbles at least as large as will be suitable for grain or aggregate.

A grain made to be as corrosion-resistant as possible must be as dense as possible after firing. The most reliable way to achieve this end is first to control its agglomeration, then separately to control the firing of the agglomerate. It is worth repeating that the feed solids for grain agglomeration are always prepared in relatively fine sizing, typically from that of fine sand down; and all preferably -325m to colloidal if prereaction is intended.[264]

Drum and Pan Nodulizing

Given a damp feed, balling up of fine particles is noticed in almost any rotating equipment whose bed tumbles or turns over. The feed end of a rotary calciner is an example. To conduct such an operation under some measure of control, however, equipment designed expressly for the purpose is more often used. Continuous feed and output are the rule, but batch operation is feasible.

One form of this equipment is a near-horizontal revolving *drum*. Solid particles are fed near one end, and water is sprayed on the rotating bed. Rolling moistened particles stick together haphazardly and begin to grow into small beads. These tend to float on the surface of the bed, where they continue to roll and to grow by accretion of the finer feed particles. At the discharge end, the floating nodules pass over a lip or low dam and are collected.

A more efficient device is the rotating *inclined pan*. This is a flat disc bounded by a low rim, of the rough order of one to three meters in diameter depending on the scale of operation. Solid particles are fed near to the elevated side; water is sprayed over their path. Here the bed remains thin and spread out. The small particles tend to move with the pan while the growing nodules roll constantly over them, rapidly picking up material. The rim speed is such as to carry the nodules centrifugally from the lower back up to the elevated side, so that they make many transits across the bed before floating over the rim at the low point. This device functions to a considerable degree as a size classifier: nodules are retained in the pan until they attain sufficient size (actually, inertia) to rise over the rim. Nodule diameters can be obtained from about 0.5 to 2.5 cm. Stationary scrapers and vanes re-direct the moving stream as desired for nodule growth and material recovery.

Numerous operating parameters call for simultaneous optimizing: tilt, rotation speed; feed, water, and vane placement; solid feed rate, and water:solids ratio. Perhaps the last of these has the most obvious effects. With increasing wetness, within limits, both the

nodule size and its density increase. The effect on density results from increased plasticity and better particle packing, while excess water tends to be rejected to the nodule surface. But the parameter limits are narrow, and the operation is sensitive to small changes. Tabular alumina[22] is an example of a refractory grain made by nodulizing.

Rotor-Augmented Pan Nodulizing

In another type of commercial rotating pan, a high-speed rotor is added. In a fixed location, this rotor bears short, heavy arms swinging just above and parallel to the floor. These arms strike and deform the nodules as they grow and circulate. This action significantly densifies the nodules, accentuating the rejection of bulk water to the surface. Though there may be somewhat restrictive limits on nodule size, for high-density agglomeration the *rotor-augmented pan* merits consideration.

Briquetting

Another means of making dense agglomerates is *briquetting.* Briquetting rolls are opposed or counter-rotating wheels whose flat steel tires carry rows of mated pockets or mold halves. The horizontal axes of the wheels are heavily spring-loaded so as to force the tires together as they rotate. Particulate material fed from above into the space between the tires is compressed into the mated pockets, the excess falling or scraped off and returned to the feeder. The pillow-shaped briquettes are ejected below, where the two tires separate.

The feed consistency for briquetting is comparable to that for dry pressing. Use of organic binders is common, and water may be absent altogether. Briquette sizes range from about 1.5 to 5 cm across, always much less thick than wide. With good choice of binder, the strength of green briquettes is sufficient even for rough handling; and they usually can go direct to firing without drying. Periclase grain is made by briquetting the hydroxide, which is then shaft-kiln fired.[442,443]

Extrusion

The process of *extrusion*, described previously for brick forming, is quite adaptable to agglomeration for making grain. The appropriate die contains a number of circular openings of a selected diameter, for the simultaneous extrusion of a number of rodlike forms. Chopping to short lengths by use of a rotating blade is an available option. Extrudates of roughly 1:1 aspect ratio can be handled comparably to spheroids or nodules for purposes of drying and firing.

Clays and clay-aluminas up to 70% Al_2O_3 are extruded in huge tonnages for rotary calcining.

Miscellaneous Other Methods

Most other agglomerating methods that are known in ceramics are less well suited to making refractory grain than are the above four. One whose appeal lies in its low cost is *granulation.* It is not known to be used at present for refractories. In this process a pourable slurry is prepared and then vacuum-filtered to give a thick filter cake. The cake is then dried without mechanical disturbance, for example by tray or belt drying. By virtue of mud-cracking due to drying shrinkage, the cake breaks up into manageable pieces, which in the present context would be fired and then crushed into granules. The main limitation is that filter cakes are always porous.

Some dense but expensive ceramic agglomerates have been made by *sol-gel* methods.[264,483-485] It is premature to describe these at length here, but this may be a technology to watch for special refractory applications in the future.

DRYING AND FIRING OF REFRACTORIES

The generic hot processes encountered in refractory manufacture were introduced in Chapter II, albeit in a broader context. Refreshers may be found there under the following headings, listed in the order given in the Table of Contents:

Industrial Drying	Sintering of Oxide Ceramics
Calcining of Hydroxides	Phosphate Decomposition
Glass Manufacture	Carbon Baking
Carbide & Nitride Synthesis	Sintering of Carbides & Nitrides
Calcining of Carbonates	Fusion of Oxidic Materials
Decomposition of Sulfates	Graphite & SiC Manufacture

And some generic hot processing equipment familiarly used in refractory manufacture was described in Chapter III under:

Shaft Kiln or Calciner	Tunnel Kiln
Multiple Hearth Furnace	Drying Ovens
Spray Drier/Calciner	Arc Furnace: Oxide Melting
Rotary Kiln	Batch or Periodic Kilns

Drying

Drying of Grain Agglomerates. Grain agglomerates, destined to be fired, will be done no technical harm if they are somewhat overdried or overheated. The two principal concerns are (1) to avoid much fracture due to shrinkage or internal steam pressure, yet (2) to accomplish drying as rapidly and as cheaply as possible.

Agglomerates made by wet nodulizing or extrusion are most likely to be fired either in a rotary kiln or in a shaft kiln. In the rotary case, one may simply provide a drying zone at the feed end and combine the drying and firing operations. If the heat balance will not permit this, or if firing is to be conducted in a shaft kiln, then drying must first be carried out as a separate unit operation. Either rotary or shaft drying suffices, though the shaft entails less mechanical attrition. Low-temperature waste heat should be available, in which case thermal breakage of agglomerates is readily minimized.

Drying of Formed Refractories. Virtually all wet-formed refractories must be dried before firing or, if not fired, before seeing their first heating in service. This need stems from (a) the three-order-of-magnitude volume expansion that occurs when water boils; (b) the constricted volume and dimensions of the gas escape paths (i.e., porosity) present in refractories; (c) the relatively large overall dimensions of formed products, within which those escape paths are long and tortuous; and (d) the characteristically low green and dried tensile strengths of refractories. A still further and more immediate destructive mechanism often looms as well: (e) in many cases a substantial overall volume shrinkage accompanies a decrease in the liquid water content. Not only do these five conditions call for drying before high heating. They also place severe restrictions on the allowable rate of drying of formed products. For this reason they demand that drying be conducted as a separate and independently-controlled unit operation.

Most drying is achieved by heating from the outside, using a stream of warmed air. There are two characteristic time periods in drying: (I) bulk liquid water is present in the solid, while later (II) no bulk liquid water remains. Period (I) is examined here first. When drying is begun, certain identifiable zones and their diffuse boundaries are soon set up. These are described schematically as follows, using slab or plane geometry and one drying surface only for simplicity:

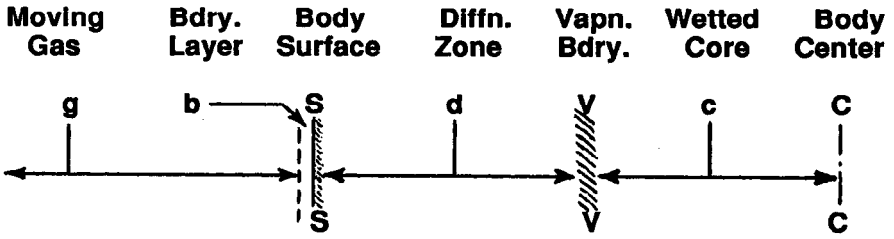

We take the moving air or gas zone **g** as being of temperature T_g and partial pressure of water vapor p_g. This air is the source of heat flow from left to right and the (infinite) sink for water-vapor flow from right to left. We recognize the existence of a gas boundary-layer **b**, and take this to include an "exchange" zone extending perhaps a few pore diameters into the solid.[8] Let the body surface, **S**, conveniently exclude that "exchange" zone.

The vapor diffusion zone in the solid, **d**, which is bounded by **V** and **S**, is a liquid-free zone. Liquid water evaporates in the vaporization boundary **V**; its movement as vapor from **V** to **S** is governed by pore diffusion or permeation. The wetted core of the solid, **c**, extending from the vaporization boundary **V** to the body center-plane **C**, contains bulk liquid water; at time zero it represents the degree of "wetness" of the entire body. Its initial temperature T_o represents the temperature of the entire body at time t = 0.

It is immediately apparent here that drying is a time-dependent set of *gradient* processes. Gradients cannot be eliminated or there will be no loss of water. The quantifying of all gradients can be done by hand calculation in infinite slab geometry or by computer methods for other geometries, using thermodynamic and physical transport properties that can all be obtained in principle. It is more important for present purposes to identify those *limiting* gradients the exceeding of which can destroy a refractory -- and to infer how these limit the parameters and rates of drying. Two extreme model cases will be examined for illustration.

Shrinkage-limited drying is typified by that of green formed refractories containing raw clay and exhibiting a large (say, 10-15%) volume shrinkage accompanying the removal of liquid water. Stiff-mud process bricks are an example. In describing wet clay raw materials earlier in this chapter, a distinction was made between "shrinkage water" and total water.[440] As the former is removed, a clay refractory shrinks. Thus a gradient in "wetness" is accompanied by a gradient in dimensions. Each such refractory has a limiting dimensional gradient, above which it will sustain large shrinkage cracks in a given geometry.

In the diagram above, the "wetness" gradient is extremely high at the vaporization boundary **V**. This circumstance is intolerable in terms of shrinkage. The tolerable circumstance is effected by maintaining the vaporization boundary continuously at (i.e., very near) the geometrical surface **S** throughout most of the first drying period. Then water vapor transport occurs solely through the boundary layer, **b**, and the ΔT of the process occurs solely in that same zone. This ΔT corresponds to heat flux J into the body; virtually all of J is consumed at the vaporization boundary by the evaporation of water. The corresponding water-vapor flux ϕ (vap) represents the drying rate. But if the vaporization boundary is to remain stationary, there must be an equal flux ϕ (liq) of liquid water from the interior or wetted core.

That flux of liquid water is provided by *wicking*, or *capillarity*. The steady-state condition near **S** may be expressed as: ϕ (liq) = ϕ (vap) $\propto \Delta T \cong (T_g - T_o)$. That is the time-independent condition for a stationary vaporization boundary. So long as this equality holds, the drying rate will be constant with time. If the drying-gas temperature T_g is too high and ϕ (liq) < ϕ(vap), the vaporization boundary will move into the body and shrinkage cracking will ensue.

Wicking of course implies a "wetness" gradient or a percent "shrinkage water" gradient within the body, and a corresponding gradient in body dimensions. Experience has shown that this is small and can be tolerated structurally. It is intuitive, also, that the initial liquid flux required for steady-state drying can not be maintained indefinitely by nature since the body wetness decreases with time. Eventually the vaporization boundary must move toward the interior. Then (unless T_g is readjusted) the distance over which ΔT occurs will increase, the temperature gradient and hence J will decrease, and the water evaporation rate will decrease with time. By then much of the body shrinkage will already have occurred, however, and its susceptibility to shrinkage cracking will have diminished.

Industrial practice employs the above principles, but uses air at over 90% relative humidity to control the evaporation rate from the wet high-clay body. This permits raising the air temperature fairly rapidly (e.g., in 5 to 10 hours) to a selected level which may be as low as 60°C or closer to 100°C -- but still maintaining >90% R.H. The body temperature follows. Its water mobility (hence wicking rate) is much increased, yielding a lesser "wetness" gradient and avoiding constriction of the near-surface pores due to shrinkage. Once the selected working temperature is reached, it is maintained steady while the humidity of the drying gas is then gradually decreased. This technique, called *humidity drying*, is far faster than low-temperature ΔT drying while exercising the same control. The end of period (I) may be reached in as little as one or two days.

Internal-pressure-limited drying is exemplified by that of green formed refractories containing size-graded fully-dense grain, whose particles are in close abutment. Near-zero drying shrinkage is exhibited; there is no risk of shrinkage cracking. There is a limit to the internal water-vapor pressure that can be withstood, however, by the tensile or cohesive strength of the material. This pressure limit can in principle be empirically discovered for each material, size and shape. Given a suitable safety factor, one thus has a knowable p_{max} which must not be exceeded in drying, and hence a knowable T_v at the boundary **V**.

For simplicity, assume in this case that wicking of the liquid is negligible. In application of the preceding diagram, the vaporization boundary **V** thus starts at the body surface at t = 0 and moves inward with drying time. Across the water-vapor diffusion zone **d** there are two simultaneous gradients at each instant: one of temperature, here simplistically approximated by $(T_g - T_v)/d$, and one of water-vapor partial pressure, simplistically approximated by $(p_{max} - p_g)/d$ where d is the thickness of zone **d**. The former determines the heat flux *J*, which in turn fixes the rate of evaporation of water per unit area of boundary **V**; and the latter determines the diffusion flux, ϕ (vap), or the area rate of drying. At steady state these two rates must be equal, and from this equality the maximum safe level of T_g can be determined as a function of increasing d.

This time-dependent problem calls for finite-element solution methods. The boundary layer **b** has to be included; so also must the consumption of *J* in sensible heat as well as in the vaporization process. But it is readily seen from the above description that if T_g is held constant over time, all of *J*, ϕ (vap), and T_v will decrease with time as the boundary **V** moves into the interior. If T_v is to be held constant over time instead, a rise in T_g will have to be programmed as d increases to give a fixed vapor diffusion gradient and drying rate.

Again there is some distinction between the above model and industrial practice; yet the model illustrates the principles which must be observed. Dry pressed refractories are relatively forgiving with respect to internal pressure in drying, owing to their low water content and their relatively coarse porosity. The severest cases of *internal-pressure-limited* drying occur in the high-density castables, and particularly those of regular CA cement content. Their as-cast permeability is extremely low. What distinguishes them from the above model, however, is that the larger part of their contained water is not bulk H_20 but chemically combined -- i.e., -0H groups -- resulting from the hydraulic cement setting reactions. This fact places the drying of castables mostly in what we have called period (II), but without relief from sensitivity to internal pressure.

Following the careful removal of bulk water up to about 100°C, this chemically combined water starts coming off above that temperature but is not completely removed until 650°C is reached and held. That is, T_v in the above model increases as the residual amount of combined H_20 in the body decreases; and further, the boundary V in the preceding figure no longer exists. This situation has a close chemical parallel in the decomposition of silicic acid hydrogel,[465] except that silica gel is very permeable while these castables are not.

Cast bodies up to 6" or so in thickness have been found to dry sufficiently at 350°C for subsequent safe use. Large EAF shapes, on the other hand, have shown the need to be dried at a final 650°C. In any case, the successful drying regimen calls for holding several hours at every 50°C or 100°F interval from 120°C to the maximum selected temperature, with a very slow rise from each interval to the next. It can be appreciated that this requirement is extremely difficult to meet in the field. It is tedious enough in an in-house drier.

Batch-operated ovens are favored equipment when precise programmed drying is necessary. Continuous tunnel drying is also used, especially for long manufacturing campaigns. Unusual drying techniques, e.g., employing infrared or microwave heating or vacuum, tend to remain unusual in refractories for economic reasons; but they are not unknown.

Firing

For the most part, firing is the culminating step in the creation of each formed refractory: process path (2,6,8) in Figure XIII-1. It also completes the making of premanufactured grain as a raw material, path (2,9). Insights of manufacture are embodied here in understanding the interactions between the character of the formed and dried material and the thermally-induced changes occurring in firing, to yield a product of expected character and properties. In this context, "firing" includes the subsequent controlled cooling.

Thermally induced changes are a mainstream subject of this book. The purposes and principles of firing -- and the nature of its consequences -- have been amply examined in previous chapters. Here we shall review the several different ways and equipments in which firing is conducted, then briefly summarize the physico-chemical processes and results.

Firing Equipment and Operations

Premanufactured Grain. Separately sintered or prereacted grain is usually fired in a rotary kiln or shaft kiln. Briquettes and large nodules are well suited to the shaft kiln, as their size provides large interstitial paths for combustion gases. Small agglomerates, high tonnage rates, or materials that become sticky due to partial melting, do better in the rotary kiln. The rotary kiln capacity for prolonged hot-zone residence time is better adapted to the conduct of pre-reaction, while the fuel efficiency of the shaft kiln is higher. The rotary can combine drying and firing; the shaft cannot. Either one can exceed 1900°C; both are best fired between neutral and oxidizing. Chapter III contains further descriptions under these two equipment headings.

Continuous feeding equipment works from under a storage silo, conveys to the kiln, and may include a weigh-feeder or volumetric feeder. An intervening day-bin is commonly used to eliminate minor interruptions. Once on line, these kilns run around the clock. Though they have cooling zones, both kilns discharge hot material which is picked up on an automatic conveyance. One way to air-cool the discharge is on its conveyor; another is to blow air up through its storage silo. The material should be cool and brittle for crushing.

Periodic product sampling and routine evaluation may include visual (color) inspection, measures of breakage and fines, chemical and petrographic (microstructure) analysis, density and apparent porosity. Permanent records are also kept of all of the kiln instrument readouts: temperatures, pressures, and flow rates.

Formed Refractory Products. Pressed or extruded or cast bricks, blocks, and special shapes, after drying, are fired in continuous tunnel kilns or batchwise in periodic kilns. These equipments are described under their respective headings in Chapter III. The tunnel kiln is effective for long campaigns. Though flexible as to temperature profiles and throughput schedules, it takes a long time to line out again if a significant change is made on-stream to accommodate a change in feed. The periodic kiln, on the other hand, may be reprogrammed between firing cycles and can handle a variety of smaller lots of different products. Either one, designed for the purpose, can exceed 1900°C and can provide any required hot-zone residence time. Both are most economically fired between neutral and oxidizing in the hot zone, though reduction firing is possible for fireclays whose peak temperature may not exceed 1500°C or so.

Firing programs are tailored to the chemistry of each refractory. Chrome ore, for example, is predominantly ferrous chromite spinel. In Chapter V the volume change accompanying oxidation of ferrous to

ferric oxide was noted, and the thermodynamic data of Table V.1 indicate that this oxidation is increasingly favored with decreasing temperature. Thus to minimize the oxidative expansion and resultant fired porosity of chrome-containing bricks, the kiln preheat zone may be operated reducing and/or made as short (i.e., rapid) as possible. This is done in firing direct-bonded periclase-chrome bricks, for example. Firing atmosphere and time-temperature programs are worked out experimentally for each different product.

Kiln cars carry the settings. An open setting suitable for prior drying may suffice unchanged for firing of moderate-duty refractories; but products fired at about 1800°C and above are close-set for maximum utilization of space and fuel. Heat transfer by radiation in the hot zone makes this feasible. Automation of the firing operation is increasingly in use and increasingly sophisticated, from handling and placement of the charge to extensive instrumentation of the kiln with feedback adjustment of burners, blowers and dampers. Continuous gas-analysis, flowrate and temperature instrumentation have brought kilns under reliable control for repetitive mass production and efficient use of fuel.

Taking in the entire product line and worldwide economic scenarios, a wider variety of firing equipment has to be encompassed. Even the beehive kiln (Fig. I-1a) is in limited operation, with its manually stacked charge. It well suits the needs of sintering silica refractories for extended periods at close to 1700°C. Smaller downdraft or other batch kilns handle small-scale and custom or unusual tasks, including the firing of odd shapes with special support furniture. Carbon and graphite and silicon carbide must be fired in the absence of air. The appropriate techniques, touched on in Chapter III, include (a) massive packings in coke in indirect-heated kiln configurations; and (b) for high-value products such as SiC and other carbides and nitrides, electric-heated furnaces with inert or selected reactive atmospheres.

Outside the most highly-industrialized areas, manual setting of charges directly on kiln hearths is often seen in place of kiln cars, and manual burner and draft control is much seen in place of automatic. Within the range of products thus made, quality need not suffer. In fact, even the most elegant firing methods still have to face two immutable facts of furnacing that may impinge on product quality. These are that:

(1) The heat flux cannot be the same near a burner (or any other heat source) as it is at a distance, even admitting bag walls and baffles; and

(2) Heating of the charge (and each article within it) is from the outside inward. Gradients and time lags are inescapable. The corresponding lags occur in reverse on cooling.

Every firing cycle can be divided simply into three parts or periods: (a) a heating ramp or period of increasing body temperature; (b) a soaking period of nominally constant temperature in the hot zone; and (c) a cooling ramp or period of decreasing body temperature. Except in special cases, the heating ramp is the steeper. Nonuniformities generated in the material by heating gradients are intended to be eradicated during the soak; but this is not necessarily entirely achieved. The cooling ramp is designed to avoid gross thermal cracking; but microcracking occurs in that period, and nonuniform cooling may yield nonuniform microcracking. The alert operator seeks evidence through product examination that these nonuniformities -- and others such as relating to burner proximity -- can be held within technically acceptable limits at the bottom line.

Theoretical Aspects of Firing

For some five decades, ceramic science has wrestled with the problem of quantitatively describing sintering. Single-oxide models have typically been assumed (i.e., absence of chemical reaction or decomposition). Solid-state diffusion has been considered exclusively in most work (i.e., absence of a liquid phase). The common particle-size models have been variously in the micrometer region (i.e., absence of graded grain sizing). Criteria for ceramic sintering have mostly been restricted to densification, or rejection of closed porosity, rather than ceramic or chemical bonding.

A "neck growth" model of isothermal solid-state crystal intergrowth between particles in contact, confirmed qualitatively by experimental work, became a pillar of the theory of sintering but did not correlate numerically with densification. Late-stage growth of crystallite diameter d, following a time law close to $d = d_o + at^{1/2}$, found limited experimental support as well as a solid-state diffusional derivation. A time law $d = d_o + at^{1/3}$, derived from a liquid-phase transport model, also found some experimental support; and the inevitable "hybrids" appeared. Not surprisingly, late-stage densification was found approximately parallel to crystallite growth, but again without numerical predictive capability.

It is hardly disparaging of that work in ceramics to suggest that firing of refractories can make but little use of it. The reader interested in pursuing the science of ceramic sintering might start with a respected reference work in the field.[493,494] But the science of firing of refractories has to be made up of its own collected observations

and rational explanations, pertinent to its own complex family of materials. The number of variables involved defies any sweeping mathematical simplification; but observations can be organized, leading to insights. The three periods of firing make a good framework for that organization, taken in order.

Material Behavior in the Heating Ramp

Decomposition and simple vaporization reactions occur mostly in the first 1000°C or so of initial heating. The sources include (a) chemisorbed hydroxyl groups and inorganic and organic skeletal hydroxides, coming off as H_20 mostly between the previous drying temperature and about 500°-700°C; (b) inorganic carbonates and nitrates and some organics (e.g., introduced as binders), coming off as $C0_2$, $N0_x$, and other small molecules mostly between the drying temperature and about 1000°-1100°C; and (c) sulfur compounds (additives or impurities), coming off largely as $S0_2$ mostly between about 1000°C and 1400°C. *Combustion* reactions also occur in this same temperature regime, yielding principally $C0_2$ and H_20. Combustion might be associated with particulate burnout additives; but all organics present, of whatever origin and purpose, must either vaporize, decompose, or burn.

The total weight loss due to these gas evolutions corresponds approximately to the dried LOI.[9] The distribution of weight losses over temperature is found by thermogravimetric analysis, or TGA. What is rarely done, however, because it is inconvenient, is (a) to use a whole dried brick as TGA specimen, and (b) to study weight-loss rate and volume change as continuous functions of rate of rise of temperature. With increasing temperature rise rate, the onset of each gas-evolving reaction is deferred to higher temperature and the evolution is compressed into a narrower range -- i.e., increasingly into a burst. The internal gas pressure peaks with this peaking of gas evolution rate.

Internal pressure also increases with increasing dimensions of the specimen, or brick. Gas evolution always leaves porosity or latent porosity, roughly equivalent to the volume of atoms lost. Internal pressurization can add to this by causing bloating or increase in the macroscopic volume, with microstructural damage possible as well. If polymeric liquids (organic resins or silicates) are present while gas evolution occurs, gas trapping and bloating are exaggerated -- better described as foaming. Therein lies the secret of "bloating clays" and of the positive permanent linear change tailored into some monolithic refractories as catalogued in Chapter XI. If minimum porosity is wanted, on the other hand, the above conditions leading to bloating must be minimized or avoided. Important among those conditions is the rate of heating.

Material Behavior During Soaking

The number one purpose of firing, whether of formed refractories or of premanufactured grain, is ceramic bonding. *Direct bonding* means the absence of added mineralizers and special chemical reagents and the absence of extensive chemical changes in firing. But the term should not be taken to imply predominantly solid-state sintering. The purest of refractories contain about 1 wt.-% of minor phases after firing, hence close to 2 vol.-% as liquid if completely molten. Simple calculations show that this amount of liquid, if uniformly distributed, would give a film thickness averaging about 1% of the grain diameter. That is about 1 μm thick on average if the mean grain diameter is 0.1 mm (150 mesh), or about 10 μm thick if the mean grain diameter is 1 mm (16 mesh). Relative to molecular dimensions, this is ample liquid indeed. Chemical purity up to 99% puts no bar on liquid-phase sintering. What differentiates a direct-bonded refractory from other sintered types is not the mechanism of sintering, but the *temperature* at which a liquid phase appears and the *kinetics* of interaction (principally, of wetting) between liquid and solid at that temperature.

Setting aside the firing of cement-bonded and chem-bonded compositions, refractory firing temperatures cannot very much exceed the Maximum Service Temperatures approximated in Figure VIII-3 and defined in its accompanying text. The reason for this is that while the highest feasible soaking temperature should yield the highest interaction rates, bricks must not be permitted to slump (i.e., creep) during firing. The permissible amount of liquid at the firing temperature accordingly depends on the viscosity of that liquid. This amount will range from a minimum in direct-bonded 99% MgO, for example, to relatively large amounts in clay-alumina, fireclay, and silica refractories. Minimum liquid might occupy only intergranular pockets, though comparable ceramic microstructures argue emphatically against this.[493] Large amounts of viscous liquid will assuredly bathe all solid grains or major-phase crystals, eventually.

To what extent major-phase inter-grain or inter-crystal neck growth occurs under these circumstances is arguable. Insofar as it does occur it is assuredly by liquid-phase transport (i.e., solution-reprecipitation), not by solid-state-diffusion sintering which is much slower. But it is certain that *all grain surfaces that are bathed by a liquid film are not bonded at all*, in the conventional sense, at the soaking temperature. To be sure, interfacial tension forces are not trivial in thin liquid films; but these forces are much weaker than solid-state chemical bonds. Creep is the incontrovertible proof.

This realization puts an unique perspective on what is superficially regarded as hot-zone "sintering." In a grain/matrix type

refractory the matrix components commence melting at an applicable eutectic composition, below the soaking temperature. As that latter temperature is approached and then held, the following are the most important changes that take place over the soaking period:

(1) The amount of liquid increases with increasing T, drawing mainly from the matrix constituents, melting and dissolving them.

(2) Porosity in the body becomes substantially enveloped by the liquid; consolidation or coalescence of porosity progresses with little volume change.

(3) The liquid gradually wets and penetrates the narrow crevices and fine interstices between the size-graded grains, locally redistributing void space as it moves by capillary action. This process is not necessarily completed by the end of the soaking period.

(4) The liquid gradually approaches a chemical composition that is in equilibrium with its surrounds; in particular, with the major-phase grains. Its liquidus thereby approaches the soaking temperature.

(5) Once saturated in the major component, the liquid can serve as a transport medium for major-phase neck growth and/or recrystallization. Other processes that are paced by crevice penetration include intercrystalline (boundary) penetration near the surfaces of grains and the solid-state dissolving of liquid components in the grains.

Changes in internal void volume and total volume occur, but with conflicting consequences. If bloating due to continued gas evolution dominates, both of these volumes increase and the hot bulk density decreases. Lacking this phenomenon, the melting of fines decreases the volume they occupy, while the interfacial tension of the penetrating liquid films tends to pull the entire structure together. If the abutted graded-grain network prevents this overall shrinkage, only the pore volume will change (i.e., increase) due separately to melting. If there is space between grains for overall shrinkage, on the other hand, that shrinkage will occur under the interfacial tension. Though this latter circumstance is common, the net effects are not easy to predict. Evidently, either some excess of fines in the original mix or previous bloating during the heating ramp will encourage

compensatory shrinkage during soaking. Some extrusion of porosity out of the body accompanies this shrinkage.

Mixes which do not contain premanufactured grain are typified by fireclays and clay-aluminas, also by some MgO-chrome compositions, for example. Firing of these mixes commonly entails (a) relatively large liquid volume fractions at the soaking temperature but (b) high viscosity of the liquid; and (c) progress of *chemical reactions* using the liquid as a mass transport medium. Thus the phase composition may change markedly during soaking; but most of the above enumerated processes still apply as well. So also does the above summary of weight and volume changes. Overall shrinkage is usual.

Finally, the calcium aluminate cemented and phosphate chem-bonded refractory types differ from the above in that their firing temperatures rarely permit any bulk melting at all. Ceramic bonding evolves mainly via solid-state changes, described for phosphate[134,135,205-211] in Chapter II and for high-purity CA cement in References 22, 214, and 220. Incomplete bonding in these cases reflects on the intimacy and uniformity of mixing of bonding chemicals with the major constituents. Changes in brick weight, overall volume and pore volume in the soaking period are small.

It has been remarked before that firing changes rarely actually reach equilibrium. One of the functions of soaking is to approach all desired end-points as uniformly as possible, not only within each brick but also from outside to inside and from top to bottom of each kiln load or setting. Some of the hot deformation tests listed in Chapter XII, conducted on previously-unfired specimens, can be useful in tracking the changes taking place in the hot zone.

Material Behavior During Cooling

Conventional descriptions of sintering do not properly attribute the ceramic bonding of refractories to the cooling ramp. If major-phase grains or crystals are separated by liquid films during the soaking period, to that extent they are technically unbonded in that period. *Bonding occurs as the intervening liquid freezes in the course of cooling.* Freezing or crystallization of the liquid commences immediately wherever the temperature begins to fall, and continues progressively until the lowest applicable eutectic temperature is reached. What finally appears to have been hot-zone neck growth may in fact be initial major-phase crystallization on cooling. The equilibrium aspects of this progressive process are properly inferred from phase equilibria[21] under Melting of Oxide Mixtures in Chapter IV; but there are obvious kinetic implications as well. However simple or complex the freezing progression may be, what is seen by the

petrologist in the cooled refractory in terms of phase distribution and bonded interfaces is the end result of this sequential crystallization. The skilled petrologist thus can not only infer the progression of freezing and of accompanying exsolution processes, but also reconstruct the phase distribution (i.e., of grains and liquid) present at the end of soaking. That skill is invaluable in guiding the whole firing process and in assessing any needed improvements in the original mix, its compaction and drying -- not to mention effects of the cooling rate itself. Insights into firing are almost wholly dependent upon the petrologist's resources. Hot-stage microscopy can help a little.

The entire progression of freezing is accompanied by volume shrinkage of that which freezes. So long as the mass remains plastic, or deformable, this shrinkage exerts a large triaxial compacting force on the overall body. Early cooling is accordingly accompanied by a decrease in overall dimensions which exceeds that of the solid thermal contraction alone -- until it becomes limited by the abutment of permanently-existing grains and previously-frozen matrix. Some increase in pore volume occurs in this period.

On cooling, the grain network soon becomes rigid. The freezing matrix ultimately loses its plasticity. The remainder of the cooling ramp is then characterized by *microcracking*, arising from differential and anisotropic thermal contractions including final freezing shrinkages and phase changes. Microcracking restores connectedness to any of the porosity which may have been isolated by liquid in the soaking period. While it adds but little to the total void volume, microcracking is a contributor to the diffusion paths joining pre-existing pores. Its characteristic frequency and dimensions lead to the observed values of room-temperature MOR, besides moderating the thermal and electrical conductivity, thermal expansion behavior, and resistance to thermal stress. See, e.g., Chapters XII, IV and XI.

Thus both bonding and subsequent debonding of each sintered refractory, as processes, are functions of the cooling regimen. Both of these processes are conditioned by the prior phase composition of each material, embodied in its character at the end of soaking; but both are influenced as well by the manner in which cooling is conducted as the final act of firing.

Arc Melting

The last visit to Figure XIII-1 for process paths (2,3,4) and (2,3,5) takes in fused grain for fused-rebonded products, and fused-cast products made to net shape. These two product types have potentially the highest corrosion resistance among all formed oxidic refractories. Growth in their use was at first impeded both by their relatively high cost and by the technical difficulties of melting and

casting. Overcoming those technical difficulties was hampered in turn by the small prospective markets: a familiar scenario in specialized products. Arc melting of oxide refractories has now turned the corner.[19,24,27,307] Fused-grain and fused-cast refractories should be found competitive in an increasing number of high-temperature and corrosive applications, assuming some persistence in developing more "best" compositions and microstructures.

The arc-melting techniques for making grain and for making cast shapes will probably converge somewhat, in time, as equipment and power utilization assumes priority. The character and properties of fused materials will also become more visible than they are now, as these materials pass from developmental to established brand-name products in increasing quantity. The essentials of arc melting of refractory oxides are discussed in Chapter II under Fusion of Oxidic Materials and, with reference to modern equipment, in Chapter III under Arc Furnace: Oxide Melting. The essentials need no further belaboring here. The excitement in coming years will lie in advances of technique and in the development and evaluation of more new products for exceptionally challenging applications. Some corollary improvements to watch for will be in methods of rebonding of fused grain and in the management of thermal stress resistance of fused-cast bodies, using reheat principles now familiar in metallurgy.

Final Shaping and Post-Treatment

Virtually all formed refractories must meet dimensional specifications on delivery to the point of use. Mortared masonry must fit. Mated parts such as in slide gate valves must be precision machined. Tapholes and plugs must mate. Burner orifices must satisfy aerodynamic requirements. Tolerances only become tighter with time: a masonry brick once enjoying a dimensional tolerance of some 1/8" or 3 to 4 mm now typically has to meet dimensions and flatness within 1 mm. Yet most refractory compositions are notoriously hard: see the hardness table in Chapter VII under Abrasive Wear. Cutting tools do not work.

Advances in *grinding* machinery and methods have enabled the industry to keep up with the need. Diamond grinding media are much used, silicon carbide where possible. Grinding to finished dimensions has to be performed after final firing or casting. That operation is called "shaping" in Figure XIII-1. To minimize cost, only those surfaces are finish-ground which require it; and in numerous cases, of course, finish grinding can still be omitted.

A brick or part to be ground must be slightly oversize as-fired. But excess material means excess grinding cost; hence attention to dimensions in processing has experienced no relaxation. In fact,

dimensional control in fired products has considerably improved over the years, resulting from tighter control and better understanding of every major operation of Figure XIII-1. It is for this reason that costly grinding can still often be done without. Unground products meet tighter tolerances, and their mortared joints are accordingly longer-lived than heretofore.

"Post-treatment" of some formed products may mean glazing of one face; cladding with a shaped steel box or steel cladding only of the hot nose, serving as a temporary spacer; mortising or drilling of a hole; or impregnation, as for example with hot pitch or wax.[178,306] Such final operations are acknowledged, but straightforward. Every product line of Figure XIII-1 is now ready for packaging, warehousing, and shipment. With each product goes an understanding that it has a certain set of properties.

QUALITY ASSURANCE IN MANUFACTURE

Product Properties and User Confidence

All usage-related properties of hot-processed refractories are of course measured at the conclusion of manufacture. For unfired products including all monolithics, the situation is confused. The use properties of every monolithic refractory are developed in the course of its installation and of the use itself. Property measurement has to be anchored somehow in a sea of user variables.

Each monolithic mix is delivered with detailed instructions for its field preparation and installation -- whether by hand-molding or trowelling of a plastic, or by casting or vibratory casting or ramming, or by any of several techniques of gunning. The quoted properties of each mix are measured by the manufacturer after using either those same installation methods or else an agreed-upon alternative, but in a standardized geometry and under controlled conditions.[387] It must be further specified whether the formed monolithic is in the set-up condition, or room-temperature aged (i.e., "cured"), or dried, or heated, after installation and before measurement.

Then there is an additional set of properties which govern the fitness of a monolithic mix for the installation method prescribed.[207,232,236,237,254,267,268,464,467] These may include a limited *storage life* (in unopened package and within temperature limits), an index of *workability* (consistency or rheology or behavior under the forming tool), a *working life* (after field preparation until no longer satisfactorily workable), a *setting time* (after installation until rigid or of some specified strength), a *drying time* (under specified

conditions, until safe to heat); or if gunned, some of the above plus *rebound loss*, or safe temperature limits on the *substrate*.

It was noted earlier that *standardization* of sample preparation procedures for monolithics presently lags behind that for formed and fired products. In another category, namely the fibrous insulating refractories, officially-sanctioned standard test procedures are not now evident. As to procedures that have been officially standardized, the role of all regional and international standards institutions in furthering worldwide intelligibility is gratefully recognized. In the property summary to follow we shall cite only ASTM standard procedures.[9] In the U.S., the Refractories Institute (address included in Ref. 10) maintains cross-references between ASTM standard procedures and those of the other major institutions; and those other standards can be obtained from ANSI.[495] In like manner, other institutions serve their constituencies with their own standards and cross-references. These include the Japanese Standards Association (JIS), Deutches Institut für Normun (DIN), British Standards Institution (BSI), L'Association Française de Normalisation (NF), Standards Association of Australia (AS), Canadian General Standards Board (CGSB), Federation Européene des Fabricants des Produits Refractaires (PRE), and the International Organization for Standardization (ISO).[285]

Table XIII.3 presents that summary, indicating property measurements made by manufacturers on their commercial products and, by asterisk, identifying those properties that are routinely reported in product data sheets. The table should lose no illustrative value for being constructed on U.S. practice. Technical data not starred are not thereby less available to users, for example; and precisely what measurement method is used in any given case can be easily learned. Properties relating to installation of monolithics have been omitted from the table to save space. Two ASTM procedures concerned with workability apply: C181 and C860.[9] There is some ambiguity regarding monolithic specimen condition prior to test; in case of doubt, the user should ask.

Table XIII.3 includes some thirty different kinds of qualities or properties of refractories. All but five are covered by ASTM procedures. Several are covered by multiple ASTM measurement methods and several by modifications for different refractory types. On the whole, both manufacturers and users accept the numerical results given by the standard procedures. For many of these procedures some statistical statements of variability have been issued and interpreted.[9] But the user can not apply those cited variances to a manufacturer's published property values for any given product. The user can not attach *confidence levels* to those published property

Table XIII.3 Commonly-Measured Properties of Refractories

PROPERTY or CHARACTERISTIC	DENSE WORKING BRICK	CELLULAR INSULATING BRICK	MONOLITHICS (All Oxidic Types) DRIED	MONOLITHICS (All Oxidic Types) HEATED	PITCH- or RESIN-BONDED OXIDE + CARBON COMPOSITES RAW	PITCH- or RESIN-BONDED OXIDE + CARBON COMPOSITES COKED	PITCH- or RESIN-BONDED OXIDE + CARBON COMPOSITES HI-T	BAKED CARBON or GRAPHITE	FIBER INSUL. PRODUCTS
CHEMICAL ANALYSIS, total	M*	M*		M*			M*	C560	M
RESIDUAL CARBON, LOI						C831*	M*		
PETROGRAPHIC ANALYSIS	M	M		M		M	M	M	
BRICK/SPECIMEN WEIGHT	M	M		M	M	M	M	M	M
BRICK/SPECIMEN DIMENSIONS	C134	C134	C134	C134	C134	C134	C134	C559,838	M
BULK DENSITY, SP. G.	C134*	C134*	C134*	C134*	C134	C134*	C134	C559,838*	M*
B.D. by Water Absorption	C20*	C20*	C20*	C20*	C20	C20*	C20	C20	
B.D. BY Waxed Immersion	C914	C914	C914	C914	C914	C914	C914	C914	
APPARENT POROSITY	C20*	C20*	C20*	C20*		C20*	C20*	C20*	
PERMEABILITY, gas	C577	C577	C577	C577		C577	C577	C577	
CRUSH/COMPR. STR., r.t.	C133*	C93,133*	C491,133*	C491,133*	C607,133	C607,133	C133	C695*	
MODULUS OF RUPTURE, r.t.	C133*	C93,133*	C491,133*	C491,133*	C607,133*	C607,133*	C133	C651,1025*	
MOR, hot (various T)	C583,133*	C583,133	C583,133	C583,133	C583,133	C583,133*	C133	C133*	
THERMAL EXPAN. UNDER LOAD	C832	C832	C832	C832	C832	C832	C832	C832	
HOT LOAD DEFORMATION	C16*	C16*	C16	C16		C16			
CREEP (var. T, var. load)	C832	C832	C832	C832					
PYROMETRIC CONE EQUIV.	C24*			C24*					
SERVICE TEMPERATURE LIMIT	M*	M*		M*		M	M		M*
REHEAT LINEAR CHANGE	C113*	C210,113*	C179,113*	C179,113*		C113	C113	C436,113*	
THERMAL EXPANSION, no load	C832	C832	C832	C832	C832	C832	C832	C832	
THERMAL CONDUCTIVITY	C201,-2,1113*	C201,-2,1113*	C417,201*	C201,1113*		C607,201	C201	C767,201	M*
THERMAL DIFFUSIVITY	M		M	M				C714	
YOUNG'S MODULUS, Sonic	C885	C885		C885		C885	C885	C747,769	
YOUNG'S MODULUS, Static	M	M		M		M	M	C749	
THERMAL STRESS RESISTANCE	M	M	M	M		M	M	M	
PANEL SPALLING LOSS	C38,439	C38	C38	C38			C38		
CORROSION, Drip Slag	C768			C768		C768			
CORROSION, Rotary Slag	C874			C874		C874			
CORROSION, Molten Glass	C621,622								
CORROSION, Alkali Vapor	C987							C454	
CO DISINTEGRATION	C288								
OXIDATION RESISTANCE	C863							M	
HYDRATION RESISTANCE	C456				C620				
ABRASION RESISTANCE	C704			C704					

NOTES: M = Measured. Cxyz = ASTM[9] Procedure No. * = Reported in Product Data Sheets.

values or to specified intervals about them, without a considerable body of data that only the manufacturer can supply.

There must be a statistically-planned sampling of each product, repetitive measurement of each property over time, and statistical analysis of the results. The importance of sound statistical bases underlying critical product property data cannot be overstressed. Not only may unanticipated deviations from property norms undermine user satisfaction. Over the years, statistical methods have also become the foundations of *process control* by the maker as a means of ensuring product quality and improving reproducibility.

Product Quality Control: An Outmoded Concept

Historically, *quality control* first consisted essentially in putting up a go/no-go gate at the point of product shipping, based on one or two simple properties. Two streams were created: "deliver," and "reject." The complexity of Table XIII.3 underscores the futility of reliable reject recognition; and lacking effective *process control*, the reject pile can bury profitability.

The earliest uses of statistics analyzed the population of data for each given product and property, collected over time in production. Norms became established, expressed in terms of the property mean and its dispersion: the range and the standard deviation. These quantities were first merely existential. The user who was made privy to them at least began to learn what to expect. But the maker began to see long-term time trends, operating-shift and other short-term differences, and aberrations. Acting on these observations did improve quality; but the inferred cause-effect connections were mostly too simple (i.e., binary) in scope. As these connections were not based on predictive knowledge, a process change had to be followed by property data collection over some time before its effect could be assessed.

Motivated by the marketplace, the refractory makers began to accumulate historical *process-parameter* data in increasing variety and detail. Until the advent of extensive computer use, this practice was painful. It also generated mountains of tabular data whose analysis by manual methods was costly and relatively unproductive. The computer changed all that. It made possible the accumulation and retrieval of massive amounts of data, and at the same time their analysis by modern statistical methods. Thus was born a refractories *database*, and with it the opportunity for *statistical process control*.

Statistical Process Control

We have previously equated the insights of manufacture to an understanding of the connections between processing and the *character* of the product, and between that *character* and its properties. Such insights are powerful; but in the real multivariable world of production they are also limited. Recall for just one example that microcracks -- an element of character -- cannot now be meaningfully described nor connected quantitatively to thermal stress resistance. There is an abundance of such quantitative uncertainties, compounded by the existence of *interactions* among possible cause-effect connections and correlations. The classical scientific experimental method of isolating variables is on the whole too simplistic and too slow in its approach to their disclosure.

Enter then *statistics*. Pure statistics takes "character" out of the above equations and seeks direct empirical connections among the parameters of processing and the product properties. Statistical methods have been put to the task of designing efficient *multivariable* data treatments for inquiring into *multivariable* relationships. Statistically-designed multivariable experimental programs distinguish between important and unimportant parametric relationships in terms of mathematical *sensitivity*. They find out the all-important *interactions* among measurable connections. They are able to ascribe the measured *variances* in properties of a repetitively-produced product to their most important antecedents in processing. Reducing a variance by acting upon this information reduces the *sampling requirement* for property measurement while increasing the *confidence levels* associated with measured values. Meanwhile, acting on the sensitivity and interaction data, one can efficiently adjust process parameters to upgrade the *mean value* of a given property. At the same time, correlations established among *dependent variables* -- different properties -- assist in avoiding upgrading one at the expense of others.

These investigational programs are in part orderly and in part ad hoc. A conceptual first step, in respect to a given property, is to remove as much as possible of the variance in it that comes from the measurement method itself. *Ruggedness* of the test method is the degree of its freedom from extraneous influences, and *ruggedness testing*[496] is a way of measuring its sensitivity to those influences. One example of such an influence consists of subtle differences in operator technique or in test equipment from shift to shift or from laboratory to laboratory. The "round-robin" exercise has long been a way of getting at these differences,[3,9,497] but by itself it does not suggest corrective measures. Differences in reproducibility between alternative measurement procedures[498] can be disclosed by ruggedness testing. The ruggedness test[496] has the best prospects

of distinguishing between measurement-method-related variance and specimen-related variance, which has long plagued efforts to deal with measurement precision in refractories.

It is patent that the influence of process parameters on a property cannot be discerned if the property measurement noise is too great. One simply must come to terms with measurement ruggedness. This implies sufficiency, however, not perfection.

The next orderly step consists of statistical *screening* experiments, aimed primarily at disclosing the important sensitivities and interaction effects between multiple process parameters and selected properties. The typical screening experiment is an explicitly designed *two-level partial-factorial* investigation of numerous parameters at once, with straightforward statistical analysis of the outcomes.[499,500] One ad hoc option following screening may consist of designing small numbers of experiments to confirm or quantify selected conclusions. Another may be to act on those conclusions in the plant. Still another, most likely a reasonable one early-on, is to design further screening experiments to take in further variables or in different combinations or over different ranges.

Still another option is to proceed to the third and last orderly step: *response surface* experiments. A response surface is a contour map (or set of them), here giving simultaneous numerical relationships of a dependent variable -- a property -- to a smaller number of most-important processing parameters already identified in screening. One of several response surface experiments is an explicitly designed *three-level partial-factorial* set,[501,502] again statistically analyzed. A process-parameter change based on a response surface has a numerically predictable effect on the product property in question.

This scanty description of statistical multivariable analysis seems abstract and hypothetical until it is vitalized by some case histories. Reference 502 is commended to the unfamiliar reader for that purpose. Its examples are real, drawn from refractories processing. They reflect both the power and the economy of the technique. The methodology has long been applied in process research: our first experience of it there dates back to the earliest 1960s. Its adoption in refractories production practice may be more recent, but has nonetheless spread rapidly. *Statistical process control* or *SPC*, based on *ruggedness testing,* [496] *screening,*[499,500] and *response surface mapping,*[501,502] is now firmly embedded in the manufacture of both bricks[503,504] and monolithics.[505] Reference 506 treats all of the above-mentioned statistical methods in mathematical depth, together with alternatives.

To understand that this approach is not a substitute for insight in processing, it is necessary only to paraphrase what the statistically-designed experiment is and does. In place of artificial isolation of variables in advance, and in ignorance of interactions, this technique combines all known important parameters in realistic ways in advance. Then, by *mathematical* instead of *physical* isolation, it tells the investigator how each independent parameter affects the outcome both singly and in combination. Knowledgeable insight is thereby most accurately served.

Nor is the design or conduct of the statistical experiment mindless. To be sure, it is rigidly *disciplined* to serve its own mathematical integrity. But the capable and insightful investigator is indispensable. Who shall decide what variables to study together, and at what levels? Who shall decide what equations to use for regression analysis in response surface mapping? Who shall decide whether a given experimental result is credible, or should be thrown out? Experiments using a production line as test-bed are fraught with risks. Product aberrations can be induced by dropping sandwich wrappers on a conveyor belt during lunch, or by dropping a tool-bit into a shaft kiln during descaling. Mindlessness in accepting data is folly, in statistical analysis as anywhere. In the hands of a discriminating investigator, SPC brings new dimensions and new efficiency into the achievement of product quality and product advancement.

Finally, it is worth mentioning again that under SPC some of the data for statistically designed experiments may come right off the production line; and process adjustments for control or compensation are made on that same line. The opportunities for involvement of the production workforce in both, and in the intervening discoveries, are rich. Modern instrumentation removes most of the drudgery from data-taking and from reacting, as was mentioned earlier regarding the hydraulic brick press. Operators can develop a positive personal stake in outcomes, as opposed to the old system in which the control organization and the production force seemed adversaries in matters of quality. Thus both the technical and the organizational prospects for SPC appear bright indeed; and the user is the ultimate beneficiary.

Table XIII.4 illustrates how SPC is implemented in terms of ongoing data collection and process monitoring in a modern refractories plant. Insofar as possible, the measurements are automated. All data are entered into computer memory. In a sophisticated system time lags are built into the retrieval program, so that a given set of data from beginning to end of a process line tracks the same raw and in-process materials and products. The table, which is constructed from the format of Figure XIII-1, can thus be a

Table XIII.4 A Refractories Database for QA and SPC in Manufacture

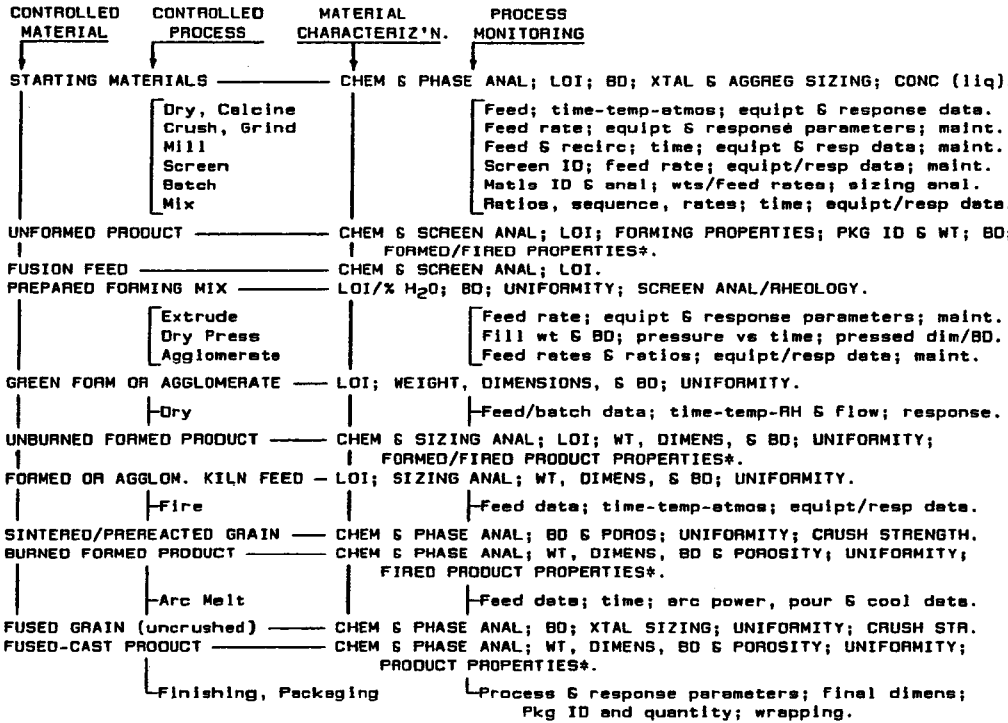

NOTE: * = Product thermal, mechanical, & corrosion properties selected from Table XIII.3.

framework for a database in real time for any process chosen from that figure.

For a statistically-designed experiment, any product property may be chosen from Table XIII.3 as the dependent variable; or for that matter, any in-process material property from Table XIII.4 may be so chosen. Most of the choices for the independent variables will be taken from among the monitored process parameters in Table XIII.4, upstream of the selected dependent variable. The experimental design[499-502] may sometimes call for running the process line as a test-bed, i.e., by fixing the independent variables at predetermined levels for long enough to obtain valid product samples. Or, experiments can be created out of real recent-historical logged data, by inspection and selection. Or, given a pilot processing facility, much fuller experiments will preferably be performed there without interfering with production. In any event, if the conclusions of such an experiment are acted upon, the indicated change will be made on the production line and the predicted results confidently monitored.

Quality Assurance Using SPC

"Quality Control" by go/no-go reject gating of products alone has long since been replaced by *quality assurance*, or *QA*. Each product is still inspected, periodically sampled, and gated by measurement of selected properties. But the characterizing of raw and in-process materials and the monitoring of unit operations in the framework of Table XIII.4 are used to ensure that products will pass. Each key on-stream-measurable quantity indicated in the table is assigned a "set-point" or target *operating value*, and in addition an *acceptable range* about this value. No matter how early in the process, any observed deviation outside the acceptable range is an immediate "alert" signal. This signal may call either (a) for removal of material from the process line or (b) for a compensating pre-planned process change, as appropriate. Not only is product quality assured. Materials removed from the line and recycled will have incorporated a minimum processing cost investment up to the point of discovery, and essentially no reject pile will be accumulated for waste disposal.

Statistical process control is seen to be superimposed on such a *quality assurance* system without conflict or inconvenience. Information gained from an SPC program is used to adjust set-points and their acceptable ranges knowledgeably, and to add confidence in product quality and reproducibility. It could even be used to eliminate some unnecessary parameter tracking.

Thus every refractory manufacturing process line merits a QA system. The more costly SPC program can be reserved for high-performance products or for trouble-shooting, but in any event can be

superimposed at will. To the extent the methodology of SPC is incorporated into new product development from the outset, then *quality assurance* and *statistical process control* in production become synonymous from the outset. Everybody gains.

Statistical descriptions of refractory properties are now spreading into manufacturers' communications accompanying shipments, and gradually into their published product literature. Examples at this writing include dimensions, B.D., porosity, and cold MOR; and for oxide + graphite composites, the percent carbon and the LOI. Statistics are creeping into purchase specifications or equivalent communications. A growing practice for variable properties is embodied in a "capability index," which focuses on the envelope of six standard deviations. These practices and the properties they encompass will continue to expand. The old idea that refractories are too mysterious to be controlled is rapidly vanishing. These products are joining the ranks of truly engineered materials.

Chapter XIV

Refractory Installation and Maintenance

STRUCTURAL ENGINEERING

In Chapter X refractories were selected for the vessels of Chapter III; and in Chapter XIII those refractories were made. Now we finally close the loop by putting them in place.

Ideally, each whole system structure is designed together so that its various elements cooperate: refractories, steel, and structural concrete. The design principles for the support and containment structures are common enough: load bearing, provisions for thermal expansion and contraction, and provisions for cooling and ventilation. These provisions have to be combined in exaggerated and uniquely interactive ways, however, in hot systems.

Engineering firms specializing in high-temperature equipment are accustomed to dealing with thermal expansion mismatches between enclosures and linings and between foundations or hearths and the structures they support. Like provisions have to be made for the steelwork used to take the lateral thrust of refractory arches or crowns. Dimensional changes due to heating and cooling have to be accommodated, while the lateral forces at the ends of an arch due to its weight must be resisted. In a tunnel kiln or reverberatory furnace, the necessary accommodation to expansion of the roof or crown varies over the length of the unit, peaking in the hot zone. Meanwhile the overall longitudinal change is exaggerated simply because this is the largest dimension of the vessel. Counterparts to these design challenges are apparent in the rotary kiln and the larger steam boilers, all elongate systems. Expansion joints with their needed

reinforcement, spaced over the length of a unit, are an answer to longitudinal mismatches; but expansion joints also mean atmospheric leakage, for which atmospheric pressure control or refractory or water-cooled sealing systems must be provided. Expansion mismatch problems in the glass furnace are also complicated, in part on account of its size.

Regenerators for the glass furnace or blast furnace suffer expansion and contraction cyclically throughout their service. In terms of cycle frequency, these are followed by the BOF and other steelmaking vessels and by transfer ladles. Every temperature transient creates a potential complex of mechanical stresses. For additional thermal mismatches occurring under conditions of shock, consider the framing and support of furnace charging doors, or the support of a slide gate valve, or the support of a removable Q-BOP bottom plug.

All in all, the design of each hot vessel for thermal mismatch alone is an intricate exercise taking both local and broad configurations into account. The thermal expansion of the particular refractory material selected enters into that exercise, as well as its wall thickness and heat conduction when new, as it wears, and at its end of life. Engineers practicing hot system design are skilled in that special discipline. They apply techniques ranging from brute force to sacrificial spacers, to expansion joints and gaps, to the use of fiber-refractory or loose-fill padding, to spring-loading of steel restraints, and to other design devices that have proved workable.

Ideally the whole structure is designed together. What then if a change in refractory practice occurs subsequently, calling for retrofit? As example, the silica crown of the open hearth furnace went over to the magnesite-chrome crown within its lifetime. Major changes in hearth and subhearth brick selection have occurred in the glass furnace. Nearly all ceramic-firing kilns have seen overlays of insulating refractory added to the working brick in both crown and walls. Duplex linings have replaced working brick alone in rotary kilns and furnaces. Such changes can not be made offhandedly. The engineering firm must recalculate. Often this means scrapping and replacing part or all of the original support structure: unaltered support design could doom the new lining. Redesign of the integrated system is part of the cost of lining conversion.

As to provisions for cooling, a large fixed hearth foundation, for example, has to be protected against overheating for its own integrity. Recall that this will in general be underground. Ordinary structural concrete deteriorates starting at about 300°C. Combinations of hearth and subhearth thickness and thermal conductivity have to be considered together with foundation cooling. One way of adapting

has been to lay a concrete base on top of which two orthogonal layers of spaced steel I-beams are placed, these beams then overlaid by a steel plate on which the subhearth rests. The I-beam lattice creates a plenum through which air is circulated. The glass furnace subhearth support is similarly designed, but above ground. Its purpose is to air-cool the subhearth itself, as a defense against glass penetration.

Cooling of upper enclosures or their refractories by circulating water has been mentioned in the arc-furnace roof and sidewalls, the blast furnace stack, and steam-boiler walls. Convective or forced-air cooling of steel vessel shells and other external steel is universal, where water is not used.

In the following sections, the structural engineering of hot systems is assumed. We proceed with descriptions of the refractory installation and maintenance operations themselves.

MASONRY CONSTRUCTION

Brick Layups and Structures

Brickwork construction has considerable load-bearing strength in compression. It is cheap for flat floors or hearths, and for straight walls where it needs support only against tilting. The price goes up a little for cylindrical walls, still more for arches, highest for domes. But in all of these configurations brickwork is reliable and long proven. One of its advantages is that parting planes under thermal expansion/contraction can be designed-in, via expansion joints or unbonded areas, with confidence that continuous cracking is unlikely to develop elsewhere. So many of the vessels of Chapter III are brick-lined as original equipment that it is more efficient to call out the exceptions later under Monolithics.

Hearths and Subhearths. Some big and heavy furnace bottoms are made up of large refractory blocks, as in the glass furnace, but never less than two courses high. Where the contained process liquid is non-viscous (e.g., in metal melting), the number of brick courses runs up to some five to eight, each course staggered over the one below in complex patterns to interrupt possible leakage paths. Figures XIV-1a and b illustrate two floor layups for less-demanding service, namely in a steam boiler. Two different expansion joint designs are shown there, the joints filled with compressible fiber board. Recall that inappreciable liquid has to be contained in this application. In many metal-melting furnaces a several-course-high brick subhearth is built up, with a monolithic hearth overlaid. But not all. BOF bottoms are all brick.

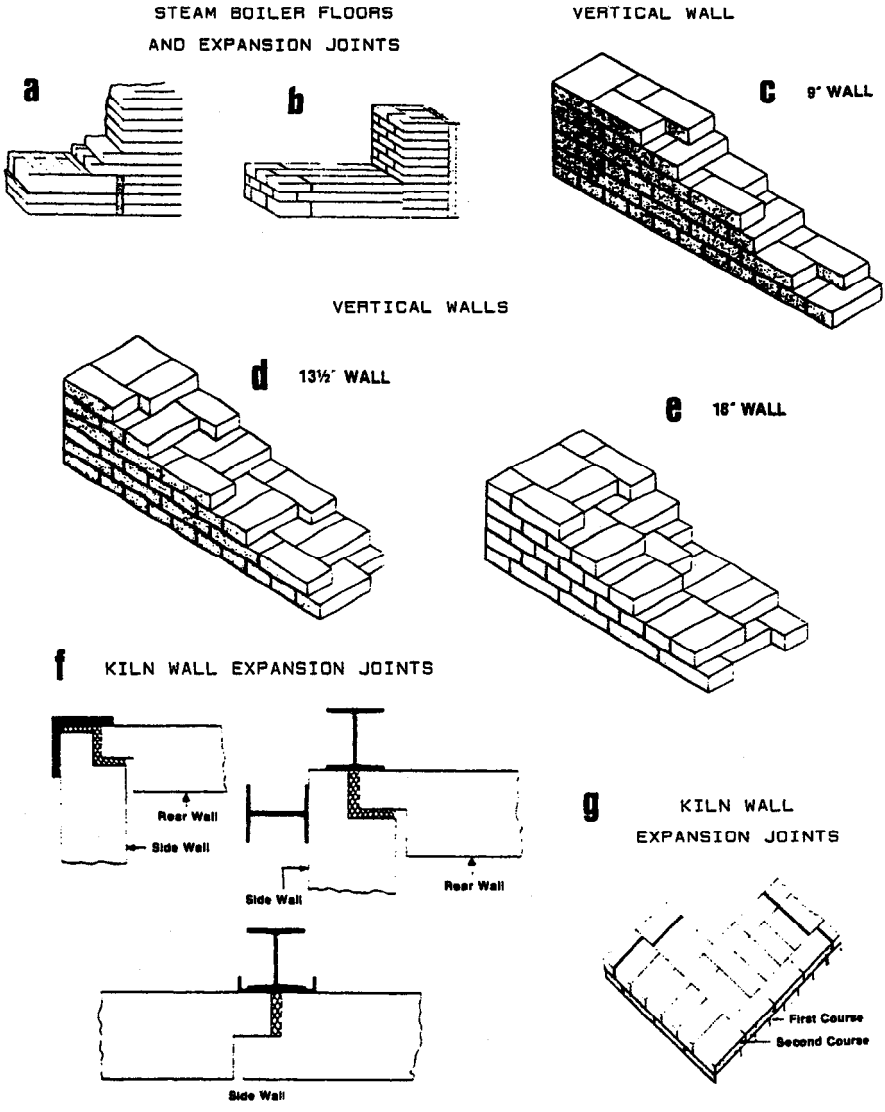

Figure XIV-1 Linear Masonry Construction
(courtesy of National Refractories and Minerals, Inc.)

Straight Walls. Straight walls that are only one brick in thickness are of limited use, generally not over about 4 feet or about 1.2 m high. Thicker walls are preferred, laid in staggered and interlocked patterns that are called *bonded* construction. Figures XIV-1c, d, and e illustrate only a few of these wall layups. The thickness dimensions given in the figure correspond to the use of "9-inch straight" bricks in the patterns shown. A 9-inch straight is 9" by 4.5" by 2.5" or 228 mm by 114 mm by 64 mm in dimensions. There are numerous other brick sizes and layup patterns.

Different names are given to different brick orientations in a wall layup. Laid flat with the brick long axis parallel to the wall is *stretcher.* Laid flat but pointed across the wall is *header.* These orientations are easily seen in Figs. XIV-1c, d and e. The on-edge course seen in Fig. XIV-1a, if in a wall, is called *orlock.* A brick standing on end is *soldier,* an orientation rarely used.

Some expansion joints incorporated into kiln wall corners and one in the middle of a straight run are shown in plan view in Figure XIV-1f. Another design leaving a structurally stronger corner is seen in Figure XIV-1g. Expansion joints interrupt a straight run every 10 to 20 feet. Just as in floors, these joints are all packed with compressible fiber mat or board.

Refractory manufacturers maintain catalogs filled with recommended wall layups, with tables of available brick dimensions, and with sound advice. There is also at least one comprehensive manual on the subject.[507]

Cylindrical Walls. Cylindrical walls and linings are readily made with "key" or other tapered bricks, also available in numerous dimensions. If a radius of curvature is wanted that is not standard, keys of two different radii can be alternated in the circle: 1-2-1-2- or 1-1-2-1-1-2- or etc., etc.

Interlocking patterns for cylinders are not convenient. But each course is staggered over the one below. A wall or lining which is two bricks thick is made up of bricks of mated radii or using different alternations as suggested above. Dozens of such patterns are worked out and tabulated in the makers' catalogs, and in Reference 507.

Arches and Domes. An arched roof or crown uses "arch" and/or "wedge" bricks, not unlike the "key" in shape. The difference is that the broad faces of the key are parallel while the long, narrow faces taper, whereas arch and wedge bricks taper in the other two directions, respectively. The following section gives their details. Figure XIV-2a shows two different styles of arch brick layup in

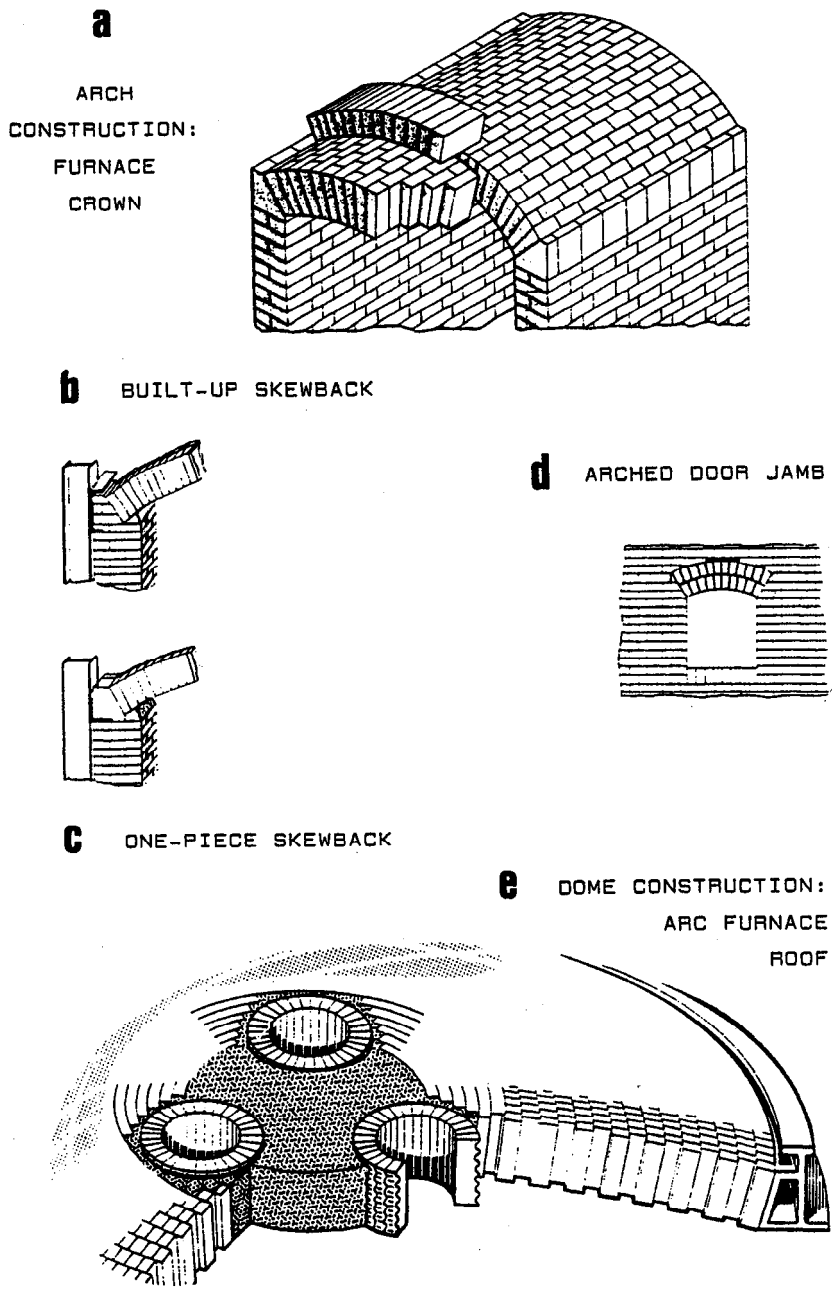

Figure XIV-2 Masonry Arches and Domes
(courtesy of National Refractories and Minerals, Inc.)

cutaway, with the inner layer staggered. The outer layer seals an expansion joint in this figure. Most arches are segments of a circular cylinder. Sometimes a high arch is catenary in curvature. Many arch dimensions are possible, characterized by (a) the span or chord, and (b) the height or arc-to-chord distance. The ratio of height to span is inversely related to the radius of curvature for a circular arch. Tables of layups abound for arches, with the resolution of forces at their extremities worked out as well. The lateral force increases with increasing arch radius.

An arch typically terminates at a *skewback* at each end. The skewback transmits the vertical force to the supporting wall and transmits the lateral or horizontal force to an external steel structure. Two of several skewback designs are shown in Figure XIV-2b and c, together with the supporting steel in cutaway. The vertical steel post extends above the top of the arch, where a tie-rod passes through it and across to the mating steel post on the opposite side. The tie-rod thus takes the lateral forces at both extremities of the arch. This is *sprung arch* construction. Tie-rod end fittings are adjustable (i.e., threaded), and may be spring-loaded. When an arch is heated, if the tie-rod does not give, the center of the arch rises with expansion. Design guidelines are worked out for managing this effect without brick failure.

A small arch framing a charging door in a brick wall is depicted in Figure XIV-2d. The fitting spaces shown in black are filled with monolithic. Arch construction within solid walls is also common, for purposes of repair beneath.

One of numerous dome designs is sketched in Figure XIV-2e. This is an electric arc furnace roof, now out of fashion in design but still in use. It is lower or flatter than most other domes would be. Its bricks taper two ways, and are called "key-arch" or "key-wedge." Three-way tapers are also employed.

Features of interest in this particular sketch are the use of vibratory-cast monolithic in the delta section, and the corrugated outside surface of the "circle" bricks through whose rings the electrodes pass. Once the monolithic is cast into the corrugations, the rings are fixed rigidly in place. Finally, the outer steel retaining ring, shown cutaway, gives the dome its lateral support. Note that the shape of this steel ring, in section, is that of the skewback. Manufacturers list several layup patterns for domes.

All roof shapes have to be supported by forms while under construction. It is for this reason that there is much interest in monolithic roofs instead of brick: once forms are in place, monolithic installation is cheaper and faster.

Brick Shapes and Sizes

Mating of brick shapes and dimensions to structure shapes and dimensions is basically a simple problem in solid geometry. Abutting brick faces must always be parallel to avoid edge or point loading. For maximum economy with design flexibility, however, construction should employ some reasonable minimum number of different brick shapes. This number is not small.

For floor and straight wall construction, it is helpful if the three dimensions of a rectangular brick are simple multiples of each other. In curved structures, the abutted faces of any two adjacent bricks should be of identical dimensions so there is no projecting lip. These two principles have given rise to the sizing of bricks in so-called *modular* or systematic series, in which the dimensions are always given as those of the brick edges (any two defining a face). A number of modular brick dimensions for rectangular and single-tapered types have been standardized in ASTM specification no. C909.[9] Resolving of these dimensions in inches with those in metric practice is treated in C861.[9] Brick makers offer a wider variety of shapes than these, but they retain the modular concept so that different series remain compatible to the greatest possible degree. Custom shapes can also be had, of course, but at higher prices.

Manufacturers' catalogs list their available size and shape series almost ad infinitum. Here we shall illustrate only enough to acquaint the reader with the more common shapes and their nomenclature. Dimensions given here are solely for orientation. Likewise where angles are given or implied: we have selected angles or tapers that are prominent enough for visual recognition, not as sole examples.

In Figure XIV-3, the concerned reader should identify the shape names with the length, width, and thickness of each brick regardless of its orientation on the page or in use. These three dimensions are always in decreasing order. In catalogs they are often given as "A," "B," and "C," respectively.

Figure XIV-3a is the *9-inch straight*, a sort of universal standard in the U.S. Its volume is 101.25 in^3 or about 1,660. cm^3. One or a quantity of bricks of any specified size is often given in terms of a number of "equivalents," obtained by dividing its volume by this standard unit volume. Elsewhere the unit of quantity is usually the metric ton. The *straight*, meanwhile, is any of a number of rectangular bricks of other dimensions as well.

The *split* and the *soap*, Figs. XIV-3b and c, respectively, are in most cases half a *straight*, made either thinner or narrower,

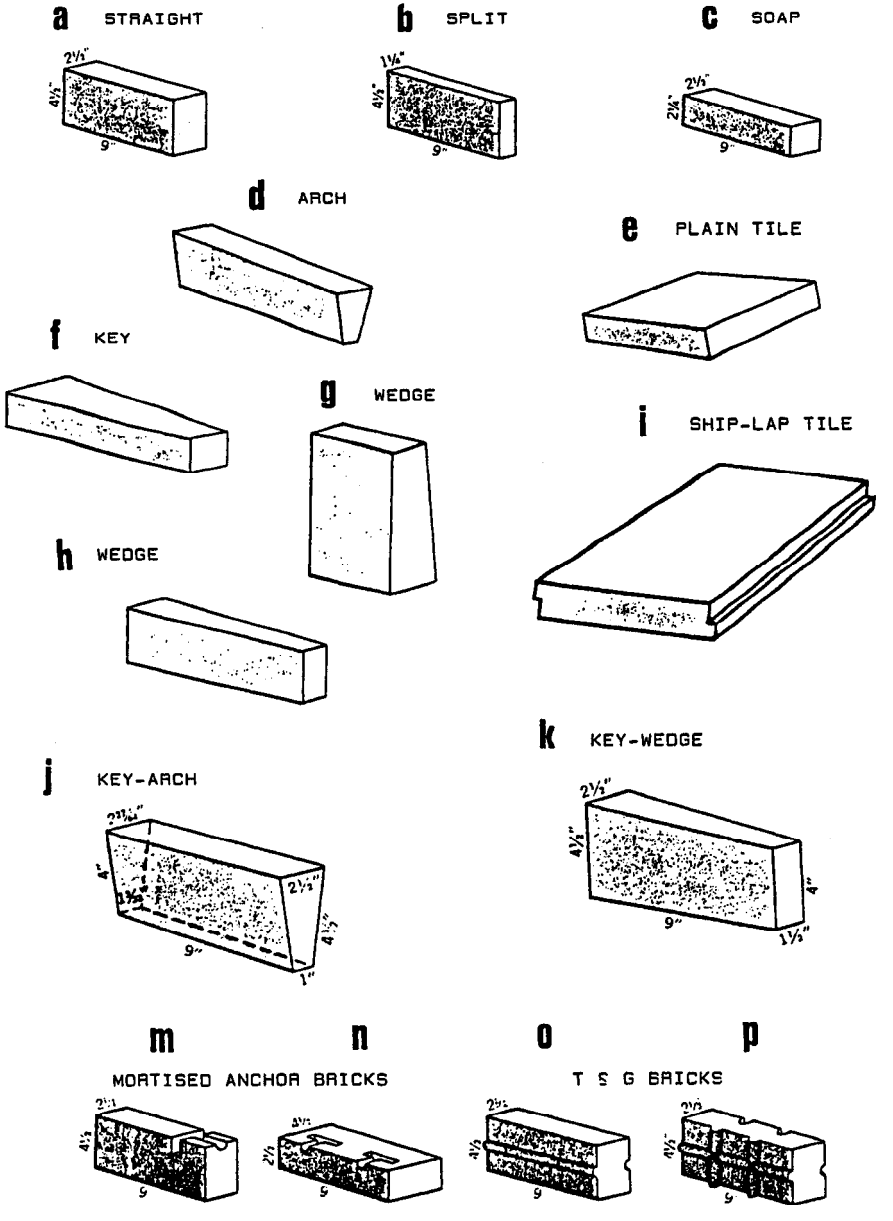

Figure XIV-3 Common Refractory Brick Shapes
(courtesy of National Refractories and Minerals, Inc.)

respectively, as shown. The third style of half-brick, easily seen in the layups of Figures XIV-1c and e, is unnamed. It is ordinarily made by diamond-sawing a straight brick on the construction site. Other rectangular shapes illustrated are *tiles*, XIV-3e and i. The former is "plain," the latter "ship-lap." Ship-lap tiles are offset on two opposite sides as shown, or on all four. Tiles are used primarily in flooring. In terms of relative thickness, when a "brick" becomes a "tile" is dealer's choice; but it is usually quite evident.

The principal brick shape used in upright cylindrical walls or linings is the *key*, Figure XIV-3f. Its longest dimension is the thickness of the wall. One basic shape for arches is the *arch* brick, Fig. XIV-3d. It is seen as the joint-sealing outer layer, cutaway, in Figure XIV-2a; but in a continuous arch its long dimension would be staggered. The other arch shape is the *wedge*, shown twice in Figure XIV-3 as g and h to point out that no tapered brick is necessarily very elongate. The wedge is seen as the staggered inner arch layer in Fig. XIV-2a.

Using A, B, and C for brick length, width, and thickness in decreasing order, the above three single-tapered shapes are defined as follows:

Key -- AC and BC faces rectangular, AB faces trapezoidal;
Arch -- AB and AC faces rectangular, BC faces trapezoidal;
Wedge -- AB and BC faces rectangular, AC faces trapezoidal.

The unfamiliar reader may want to copy Figs. XIV-3f, d, and g, respectively, append the appropriate labels A, B, and C to all of their edges, and verify the above. The fact is, these types converge as pairs of dimensions approach equality; and the further fact is, *any* of the three types can be used in *either* cylindrical wall or arch construction depending simply on the dimensions that are wanted. The wedge or arch brick, for example, is suitable for a rotary kiln or copper converter lining.

The next two shapes, Figures XIV-3j and k, are examples of double tapers for domed roof construction: the *key-arch* and *key-wedge*, respectively. These and others relate to the roof configuration of Figure XIV-2e.

Lastly in Figure XIV-3, shapes m and n are mortised for attachment to steel anchors; and o and p are tongue-and-groove shapes providing for fixed registry of successive courses. These indicate the variety of installation philosophies that can be accommodated.

Shapes a, b, and c of Figure XIV-4 are all examples of *circle brick*, differing only in dimensions. Fig. XIV-4b and c are called

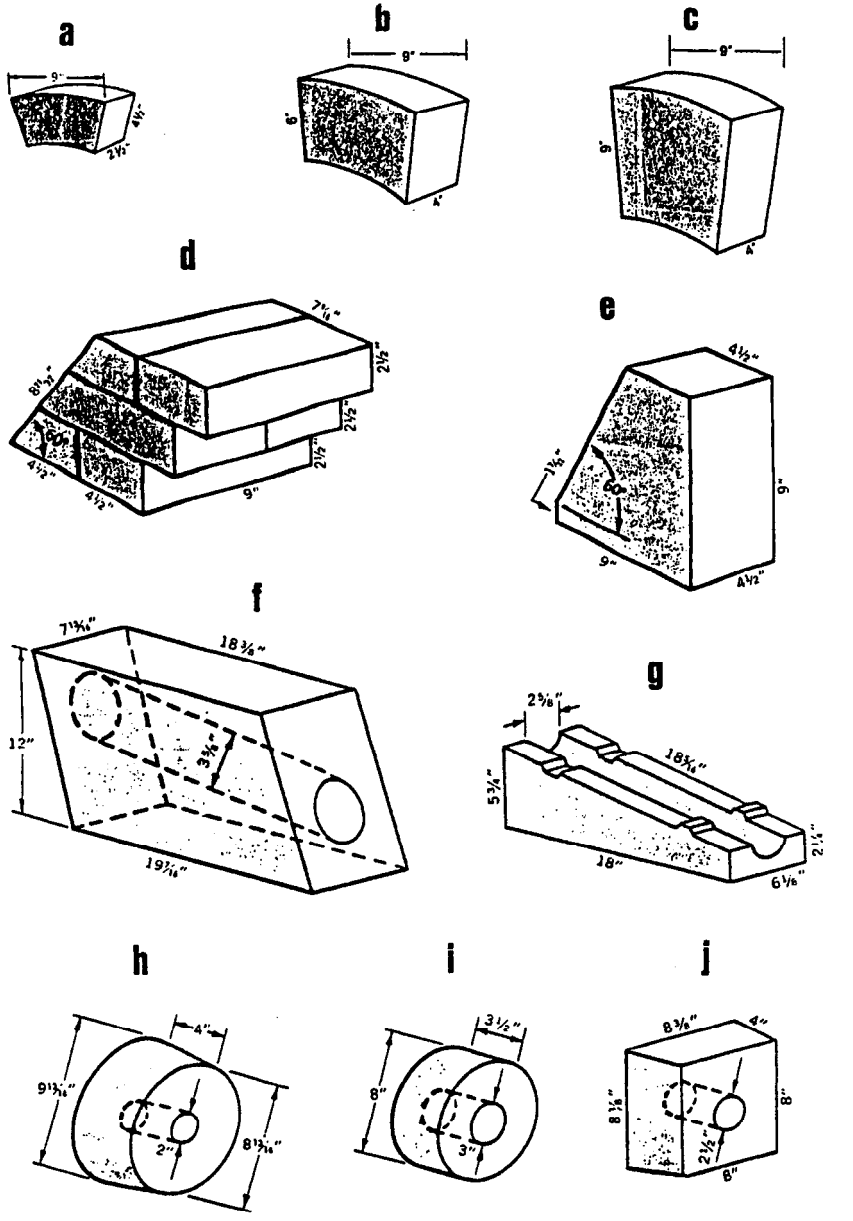

Figure XIV-4 Special Refractory Brick Shapes
(courtesy of National Refractories and Minerals, Inc.)

"cupola block" or "rotary kiln block." The corrugated brick forming the electrode rings in Figure XIV-2e is also a *circle brick*. Circle bricks, characterized by cylindrical surfaces, have evident advantages for installation inside steel shells, though at somewhat higher cost.

Figures XIV-4d and e illustrate *skewbacks*, related to the structures of Figs. XIV-2b and c. These are modular in concept: their face dimensions match those of both arches and supporting walls. Various angles of the skewed face correspond to various standard arch characteristics and are also subject to special order. Also available either standard or to order are cutouts for precise fitting to the supporting steelwork.

The remainder of Figure XIV-4 are a few examples of other special and custom shapes encountered. Many of these are cast rather than pressed. Figs. XIV-4f and g are tuyere blocks. The latter one is completed by placing a second identical block over it, inverted. Figures XIV-4h, i, and j are different taphole block configurations for furnaces. Others not too unlike them are burner blocks and the bottom-pouring orifice blocks of ladles, closed by stopper-rods or mated externally to slide gate valves. To these examples should be added the host of rods, tubes, shrouds, plugs, stoppers, diffusers, and other special refractory hardware items called for in Chapter III -- not to mention electrodes and electrical resistance and induction heating elements; muffles, baffles, condensers and pouring spouts; and an array of kiln platforms, saggers, and other support hardware.

This variety goes far beyond bricks and blocks. To return to that category, the heat-exchanger bricks of glass tank regenerators and blast furnace stoves are too important to overlook. Figure XIV-5a shows a small area of layup in the glass tank regenerator, in which one design of individual cast checker brick can be seen. Recall that the open spaces are very large, anticipating massive condensation and buildup of alkalies and dust over the long life of the heat exchanger. Figure XIV-5b illustrates the modern pressed hexagonal blocks of the blast furnace stove, whose tongue-and-groove mating at each end provides for precise registry in stacking. Lateral constraint on the honeycomb-style assembly is provided by the surrounding refractory walls of the tower, seen schematically in Figure III-2.

Finally, Figure XIV-5c illustrates the massive scale of in-house-cast shapes or "preforms" made possible by vibratory casting of the new high-strength ultra-low-cement refractory formulations. This is a one-piece domed delta section of a steelmaking EAF roof, designed for insertion into a water-cooled steel roof structure. Imagining the surrounding steel dome, contrast this current design with the brickwork structure of Figure XIV-2e. Cast refractory center sections illustrated by Fig. XIV-5c are ranging from some 10 to 13 ft. or 3-4

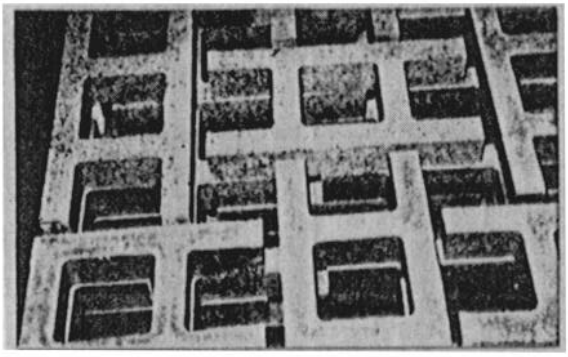

b

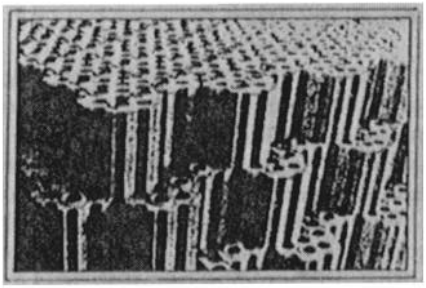

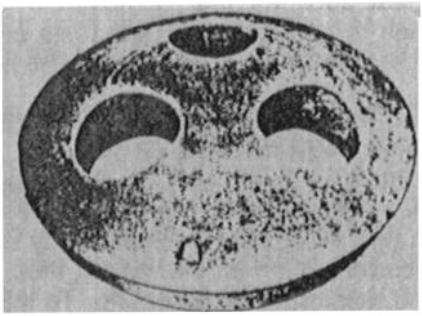

c

Figure XIV-5 Three Unique Refractory Configurations
a,b. Checkers c. Cast EAF Delta Section
(courtesy of National Refractories and Minerals, Inc.)

meters in diameter and from about 15" to 18" or 35-50 cm thick. The weight of a single casting may be from 7 to 12 tons or from 6,000 to 10,000 kg and more.

As to brick sizes available, standard *straights* range mostly from 9" long to 18". *BOF keys* are the longest pressed bricks made, giving wall thicknesses variously up to some 40". Most other bricks for curved construction, *keys*, *arches*, *wedges*, and *circle brick*, provide for single-layer wall thicknesses from a couple of inches to the order of 15". Circles can be turned from as little as 6" I.D. up to as large as >35 ft. arch span, rotary kiln diameters of 20-25 ft., and blast furnace diameters of 40-50 feet -- all in increments of from one to a few inches by specified layups of standard brick sizes. This variety can be appreciated only by consulting one or more manufacturers' catalogs or manuals.

Mortars in Brief

The old notion that the chemical composition of a mortar had to be a close match to that of the bricks it joins is no longer universally observed. Equal refractoriness remains the watchword, while chemical compatibility (embodied in phase diagrams) replaces chemical identity. High-alumina mortars now often join basic bricks on this basis, for example, as aluminous mortars are in general more readily tailored in rheology and setting characteristics than are basic mortars. Chemical bonding (e.g., by phosphate, silicate, colloidal silica, or CA cement) obviates the necessity of heating the mortar to the sintering temperature of the brick to establish a good bond. Mortars are qualified in the laboratory for a given usage by appropriately curing a bonded two-brick assembly, followed by performing a bond-strength test such as that specified in ASTM procedure C198 or C199.[9] High-temperature strength tests are also in use, as well as tests of initial setting-up or gelling time of the mortar.

Another prior practice now much-abandoned is that of trowelling the mortar onto the brick faces in laying up masonry. Heat-set mortars are trowelled to fill large gaps and for bedding, e.g., between refractory and shell. With tighter tolerances on brick, however, a superior and much thinner coating is obtained by dipping each brick face gently into the surface of an air-set mortar, then laying the brick accurately in place and tapping it into a tight fit. To this end, mortars are made up to a thick but pourable consistency, yet not subject to settling-out of solids. Their thixotropy prevents draping between brick dipping and placement. The mortar characteristics and the techniques of brick dipping and setting are matters of extreme care, as both bonding and corrosion resistance of the mortared joint are at stake. Setting time (close to 10 minutes) and water retention (resistance to water loss by wicking into the brick) are critical mortar

characteristics. Instructions for proportioning and mixing the packaged solids with water have to be rigidly observed, as well as limits on the ambient temperature and the working life of the prepared mortar.

Insulating Refractories

Cellular insulating bricks are set in place in the same manner as are working refractories and, in the case of duplex vertical walls, at the same time. Of the many wall layup patterns illustrated by Figures XIV-1c, d and e, one may choose (1) fully-independent working and backup linings, (2) occasional keying of the one into the other by a brick projecting into both, or (3) a fully-interlocked, integrated working and backup lining set. Duplex brick roofs are laid by first completing a working arch, then setting the insulating layer over it. In the case of insulation serving in the working configuration, the *sprung arch* roof of Figure XIV-2a may be replaced by a *suspended arch* or by suspended interlocking tiles or still lighter-weight forms (see Chapter IX).

INSTALLATION OF MONOLITHICS

A few notes on refractory lining maintenance, patching, repair and rebuilding might serve to introduce monolithics in perspective. Their stellar success in extending lining life, mentioned in Chapter VI, is best exemplified by their use in the steel industry and particularly in the BOF. In that use, current monolithics are not more corrosion-resistant than the original lining. But they are re-applied so frequently that the lining profile never recedes very far at one time. Gunning selectively in high-wear (e.g., trunnion) areas keeps the lining profile close to the original. Taking the vessel out of service for a complete re-lining can thereby by staved off.

Three factors in this situation combine to make the maintenance operation a success, as follows:

(1) By means of gunning, it is possible to get in and out of the vessel in a very short time in completing the application.

(2) The operating schedule of the BOF permits taking it off-line frequently for repair without a major loss in its output of steel; and at those times it is already empty and immediately accessible.

(3) The lining wear mechanism in effect is primarily one of hot-face recession, as opposed to decay of the refractory deep in its interior.

The first of these factors is an attribute of gunned monolithics that goes with them to any other type of facility. The second and third are, however, properties of the BOF that are not repeated everywhere.

Take frequent and ready accessibility, empty, without a major shutdown. Compare the blast furnace, glass melting furnace, rotary cement kiln, steam boiler, or continuous tunnel kiln with the BOF on this basis. Those facilities are simply not accessible for frequent refurbishing.

Irrespective of accessibility, the third factor is equally telling. Monolithic repair of the BOF could not succeed in the absence of its modern Mg0+C composite lining which limits slag penetration to the hot face. Slabbing would proceed underneath the overlaid repair material. For other examples in other processes, consider CO disintegration or SO_2 condensation or the slumping of carbon baking furnace walls due to reductive melting. These phenomena destroy refractories from the interior. A new hot-face repair layer could not make much difference in lining life, no matter how often applied.

The above arguments may help to explain in principle why frequent monolithic hot-face maintenance of working linings is not universal. When a repair occurs infrequently and approaches a complete lining rebuild or is accompanied by a major shutdown, then other rules apply. Then, except for innovation, a brick lining will most likely be replaced by brick and a monolithic lining most likely by monolithic. The growth of use of monolithics as original linings in that context is a history of innovation by the user. This has been equally stellar, but for its own reasons of cost/effectiveness.

Having thus disposed in broad terms of the why of repair and maintenance, we can dispose of the how by remarking oversimply that any given monolithic installation method is conducted in about the same way whether for repair or for a new lining. The methods to be discussed are casting, vibratory casting, plastic placement, ramming, and gunning.

Refractory Concrete Casting

A *concrete* is a mixture of aggregate and cement.[77-80,89,125,140,199,213-219] In this very large group of monolithics, the cement was originally only hydraulic-setting calcium aluminate.[212-214] Today the group also includes "low-cement"[133,151,152,241-250] and "ultra-low" or "zero-cement" compositions[240-242,245,246,252] in which CA cement has been partly or totally replaced at least by colloidal silica. Dry phosphate chemicals are included in some, and there may be dry soluble silicate chemicals in some. The term "cement" thus has become hazy. Over the huge range of compositions available, the implication that the remainder is solely aggregate does not hold either. Thus the term "refractory concrete," coined many years ago, is no longer descriptive of the whole group.

The industry has made the nomenclature easy, however. With no break in continuity, these materials have all been called *castables* with reference to their principal mode of placement. Whether CA-cemented or not, whether literally concretes or not, they are all installed by *casting*.

The compositions cover the whole alumina-silica range as well as zircons, zirconias and basic refractories, including chrome-bearing and high-purity. Also included are composites, variously containing organic burnout fibers, SiC, graphite, or chopped SS wire.

The following characteristics are universal: castables are packaged dry, they are mixed with water on-site, and they set up or harden at room temperature. If they are installed true to the name, they are cast within molds or forms. So cast, they are adaptable to any dimensions and any orientations (e.g., floor or hearth, wall, roof) whose forms can be fully filled without flaw. So used, they are best adaptable to new lining installation and to major or modular repair, but not to surface patching. Castables are found in petrochemical reactor linings, shaft kilns, spray driers, boilers, some furnace hearths and roofs, induction furnaces, some crucibles, ladles, troughs, platforms and tables, ports and ducts, and much of the smaller hardware of difficult geometry such as tubes, shrouds, lance and stopper-rod protection, some slide gate and concast equipment parts, and much more.[48,164,215,222]

Casting of linings often employs the shell of a vessel as part of the mold. In this situation anchors are commonly used. Figure XIV-6a shows a popular welded SS rod type of anchor used with a single and a duplex lining. Each lining layer so anchored may be up to the order of 6" or 15 cm thick. Figure XIV-6b shows one type of wall bracket anchor in cutaway, and -6c shows the same in profile for two different wall thicknesses. Anchors come in many different

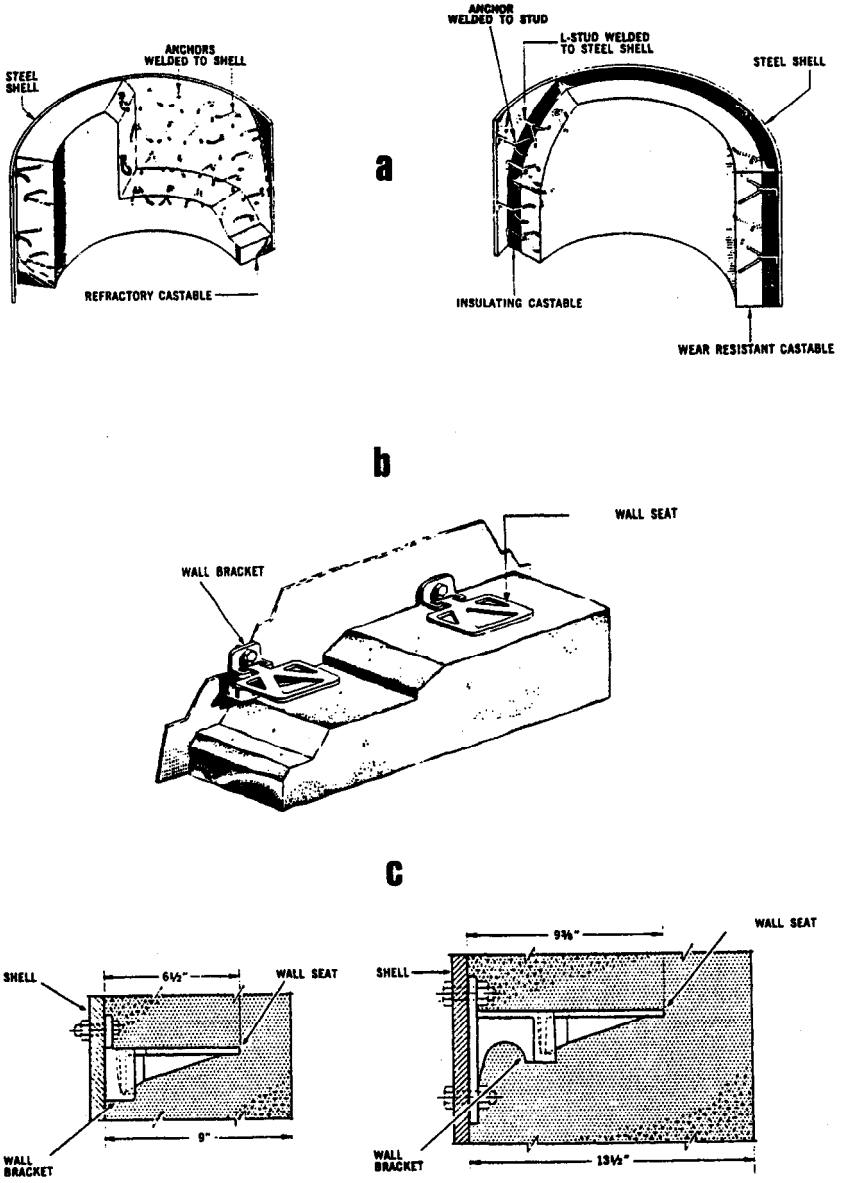

Figure XIV-6 Monolithic Wall Lining Anchors
a. Welded Rod b,c. Bolted Bracket
(courtesy of National Refractories and Minerals, Inc.)

configurations. They include hangers for suspended roofs, and numerous corrugated or deformed ceramic as well as metal types. Manufacturers' literature includes recommendations for anchor type, installation and spacing. Walls can be cast up to 15" or 40 cm thick, but curing and drying problems become severe even at 12".

CA cement has an unopened shelf life of about a year. Different mixes will vary from this. Mixing of the dry constituents with water is done, depending on scale, in an industrial paddle mixer, a plaster or cement mixer, or a continuous auger or pug mixer. Most of the prescribed water is added fairly rapidly, mixing only long enough to ensure complete uniformity. The remainder is then added more gradually, stopping when the consistency is "right" for the installation. Mixing must be thorough but not prolonged. The wet mix is delivered into the mold without delay. Dry mix left in an opened bag should not be used after about 8 hours.

The "right" amount of water (typically about 5% or less) is always the minimum convenient for the mode of installation. More than this weakens the product. Castables can be cast, or vibratory cast, or trowelled, or even rammed. Pouring into shallow molds is featured by a few special low-viscosity surface-active mixes; for the conventional formulations a literally pourable consistency that seeks a level meniscus is far too wet. A non-slumping consistency fit for trowelling is about right for casting as well. This is likely to pour from a mixer or barrow in a single slug. ASTM methods C860 and C862 provide a criterion for castable consistency.[9] Casting mixes are thixotropic.

This stiffness means the usual wet mix must be forced carefully into the mold, by rodding or spading or trowelling or tamping. Forms must accordingly be sturdy and near-rigid. It is common to coat or dampen wood forms to prevent their drawing water out of the mix. Successive batches must be poured into the same mold as soon as each previous one has been packed, or laminations may occur.

The casting is then left quiescent to set up. CA cement sets, or gels, in a couple of hours or more and then continues to harden. But additive chemicals affect the setting time; and further, since hydraulic setting is exothermic the dimensions of the casting have much to do with setting time. The manufacturer's directions should be followed rigorously. Keeping the exposed surface moist during setting is important. Removing the forms too soon can be costly. About 48 hours is average.

After mold removal, ambient air drying for 24 hours or more is common; longer does no harm. Then slow, careful warmed drying is begun, ending preferably with a dwell at some 250°C and taking at

least 24 hours. Drying time depends markedly on dimensions and on how many surfaces are unexposed. Manufacturer's directions govern.

The first heating in service should likewise be slow and careful. CA cement reactions continue over a wide temperature span;[22,214,220] so also do silicate and phosphate bonding reactions.[134,135,205-211] After the first one or two full cycles in service, the refractory should be both chemically and dimensionally stable.

Vibratory Casting

The same conventional castables, made up and placed in the same way, may be vibratory cast.[124,206,223-226,233] The consistency may be exactly the same or a little drier, but not much. The appearance of small nodules in a wad of material, separated by cracks, signifies that it is too dry.

Recalling that castable mixes are thixotropic, they can be kept fluid more or less throughout by being kept in constant shear throughout. This end is achieved by the use of ≥10 kilohertz vibrators, working either on the forms or, in channel geometry, via the top surface of the fill. Some descriptive drawings are shown in Reference 233. Whether this technique is better than those of conventional manual placement, above, may be a matter of geometry and size of casting or to some degree one of local preference and style. The delta section of the EAF roof is a dramatic example as to size. Where it is feasible, vibratory casting gives superior density and strength. Little of the art of vibrating has been codified.

Plastics and Ramming

These two kinds of monolithics, *plastic mixes* and *ramming mixes*, share in being installed with impacting equipment but are otherwise quite unlike. One name describes a rheology, hence a compositional feature; the other is a specific mode of placement. In this matter of nomenclature, in fact, it is disconcerting to the newcomer to see names on product labels like "Ram/Cast" or "Gun/Cast" or "Ram/Cast/Gun" or "Ram/Plastic," etc.; but they do exist. Here we shall take up ramming first, because it is simpler.

Ramming Mixes. There may have been a moment in history when a ramming mix was assuredly phosphate/phosphoric acid bonded and was packaged pre-mixed with its required water in a crumbly or semi-dry state. The multiplication of mixes on the market has overrun this description. Ramming mixes under single or multiple forming labels now include both dry and wet-packaged products,

phosphate or cement bonds or both at once, and clay or silicate-bonded products. What they have in common is that they are capable of effective ramming[76,134,135,165,227] if made up in the appropriate semi-dry condition. The phosphate/phosphoric acid bonded product still stands apart among these, in that (a) it cannot be packaged dry, and (b) its pH can be well below 7, giving it some unique rheological and curing properties. Its shelf life is typically a year or less.

Ramming employs a heavy hand-held pneumatic or equivalent compacting tool with a slightly-curved shoe typically some 4-6 inches across. Though subject to operator skill and judgment, ramming is capable of compacting a stiff mix to exceptionally high density. For this reason as well as the sheer weight of the tool, ramming is well-adapted to the placement of floors and hearths. Some specialized mixes for hearth ramming are accordingly the most corrosion-resistant compositions: high-alumina, alumina-chromia, and magnesite-chrome or periclase-chrome types. But floors are also rammed of less-resistant compositions, and of carbon or graphite.

The mix is spread on the base or subhearth to a depth of about 2" to 8", then rammed. The tool is "walked" repeatedly over the surface, always at an angle, so that the compacting mix is sheared or worked. Compaction at least halves the depth of the fill. Then a second layer is spread and compacted; and so on. The final depth may be up to 16-20 inches or 40-50 cm. An EAF hearth so made can be seen in Figure III-11.

Ramming is also sometimes employed for installing arches, and infrequently for vertical walls. In these cases forms have to be extremely sturdy and rigid. As all rammed structures are dense, drying has to be correspondingly slow and thorough. Manufacturers of mixes for ramming supply instructions for each step of the operation from preparing (if needed) through drying and curing.

Plastic Mixes. *Plastics* (once clays) were the earliest of all monolithic refractories other than mortars. They keep the name from the peculiar plasticity exhibited by low Al_2O_3:SiO_2-ratio clays with their natural organic accompaniment -- a combination of deformability with a remarkable tenacity or cohesive-adhesive quality. Today the family has the same kind of rheological character but runs the entire gamut of refractory composition classes: from silica to clay and clay-like, through all the clay-aluminas to high-alumina and alumina-chrome, and through all the basic classes as well, including chrome ore. Graphitic plastics were among the first of all refractory composites, and are still prominent. Add the SiC composites as well.

Many plastics are bonded by selected and carefully prepared clays. Many others are phosphate and phosphoric acid bonded,

some by proprietary additives including resins. Their particle sizings are all very fine. Acid-stabilized formulations are pre-mixed and packaged wet. Others are delivered as wet or dry mixes as the manufacturer deems best. Depending on the presence and amount of clay, the water for mixing may run up to the order of 15%. Mixing in the field can be a nuisance because the apparent viscosity is so high.

Plastic refractories have always been ideal for patching and free-form work: they can be hand-molded or trowelled, and they tenaciously adhere to clean substrates even upside-down. Their use in new lining construction is also widespread: in ferrous and nonferrous metal furnaces and ladles and as walls and roofs of heat-treating, reheat and annealing furnaces, for example.

To improve installation efficiency, for decades manufacturers have been packaging some plastics in the form of extruded ribbon cut into standard "block" sizes. Plastic blocks are placed in rows on a wall between forms, for example, and tamped in place against one another and aslant against the wall. They are thereby self-welded into a continuum.

Whether put up as block or otherwise, plastics in vertical wall and roof construction are formed around anchors of the same variety as described under Casting and in Figure XIV-6. Also regardless of the manner of laying up, wherever feasible plastics are *tamped* into place as mentioned above for blocks.

The tamping tool for plastics is pneumatic, mindful of the ramming tool but lighter, and bearing a convex shoe typically up to about 3" across. It is used in much the same way as in ramming, but the compaction is less since the as-delivered plastic is already fairly dense. Thick walls are built up layer by layer, each tamped in turn. Wall thicknesses up to 3 feet or 1 meter are not uncommon. A test for workability relating to plastic behavior in tamping is given as ASTM procedure C181.[9]

The early all-clay plastics were subject to large drying and firing shrinkage. Modern plastics have this property under control. A number of plastics are represented as to Reheat Linear Change in Chapter XI. They are not distinguished as a group from the others. The porosity of plastics runs higher than in other monolithics on the whole, though, on account of their higher green water content. On that same account, plastics are sensitive to steam explosion on drying. They must be dried with great care. The use of tubular organic fibers for steam escape from plastics is common. Manufacturers include drying precautions in their instructions.

Gunning

Gunning mixes go back to the 1930s. Gunning has evolved in importance with modern steelmaking technology, and largely because of it. Gunning was seen by farsighted steelmakers as the only practical means of maintaining their furnaces, particularly of countering the grossly uneven wear sustained by their linings. The steel industry has invested deeply in the development of gunning techniques and has been rewarded with successes. Yet the target keeps moving in its own technology. Steelmaking schedules call for furnace maintenance while still hot.

The evolution from a wet gunning method closely resembling that of Portland cement concrete to the present, where dry and semi-dry mixes have been projected onto hot surfaces, is a start. The use of flame-spraying techniques is more than a promise. But *automation* has done more than gunning methods, so far, toward successful maintenance of oxygen-blown vessels. Take the BOF for example.

Not many years ago an operator hand-held the gunning nozzle on the end of a wand and pointed it where it was thought repair was needed. Visibility of the BOF lining was remote and poor. Today the gun is held robotically inside the vessel, moved and aimed by programmed command. Today the gun is preceded into the vessel by a laser device that scans the interior and topographically maps the thickness of the entire lining.[356] By the time the gun enters, its repair task is digitized and ready for the "start" signal. No waiting for the vessel to cool. No discomfort for the operator. No uncertainty in where to traverse. No oblique trajectories. No guesswork, and no mistakes or oversights.

Not always perfect yet, perhaps. But this system is so close to trouble-free and routine realization as to dare the technology to match it with gunning methods and materials. These are coming along well too. We shall treat them briefly from the beginning, since no gunning method is obsolete.

Wet Gun Mixes. The mixing gun for spraying ordinary concrete is familiar.[8] It consists of a mixing chamber fed by a pneumatically-driven stream of dry solid particles and by jets of high-pressure water. After in-line mixing, the wet solids pass out through a nozzle and the air stream eventually disengages. Nozzle design largely controls the dispersion of the spray. The liquid feed rate, hence ratio of liquid to solids, is controlled by the liquid pressure and by valving. Auxiliary equipment upstream includes the necessary pumps and pressure regulators, pre-wetting equipment, and the solid feed regulating system where the solids flowrate is determined.

The earliest refractory *wet gunning mixes* were developed in and for this type of equipment. Advances in the equipment itself have not altered the principles of gunning mix formulation. Most modern commercial mixes have been fine-tuned or improved more than once over their predecessors, while those introduced latterly have had the benefit of the same informed viewpoints. Thus while there are hundreds of wet mixes on the market, they all perform well in gunning.

Two central concerns about every gun mix are: (1) rebound, and (2) the character of that which does not rebound, including its interface with the substrate. A third concern, the water:solids ratio, influences both. Liquid-solids mixing in the chamber is far from uniform, and slaking of particle surfaces is barely begun before deposit; so on the whole, wetter deposits have to be made than are otherwise best. The water:solids ratio is optimized empirically for each mix, but iteratively with the size distribution of the solids.

Rebound is influenced by several interactive factors. The first is particle sizing. An important component of the rebound consists of coarse-sized particles. Minimizing of rebound consistent with performance of the gunned deposit calls for a top size of about 6 mesh or 3.3 mm. Since other factors interact, this inertial criterion is somewhat flexible: a number of gun mixes are top-sized at up to 4m or 4.7 mm. Fines, on the other hand, are deflected by the general air deflection in front of the substrate; yet they are needed, and pretreatment can influence their trajectories. Moistening of the fines before feeding is practiced for other purposes, for example, and this diminishes their loss. Fines sized substantially below 325m or 44 μm are increasingly prone to deflection. Between the top size and bottom size limits, a log-linear or Andreasen distribution is reasonable (see Chapter XIII). Manufacturers do not discuss their optimized particle sizings in public, however.

All modern wet gun mixes suffer less than about 10% rebound by weight, most of them about 5% or less. The final factor in controlling rebound is *adhesion*. The wet or green particles must adhere to each other and to the substrate on arrival. Thus a major concern in wet mix formulation is the inclusion of *binders*.

The only way to deliver a binder directly to the larger particles is by feeding the binder in the water. Dry but quickly-wetted and hence activated binders can be included among the fines. Such dry agents are more often surface-active inorganics than organics. They are pre-dampened as mentioned above to increase their adhesive quality. Many have been investigated, and a few in use can be identified; but special binders are among the most guarded proprietary aspects of gunning mix formulation.

The remaining major feature of formulation is the *bond.* If not publicly advertised, the bond can often be inferred from the published chemical analysis. The commonest bond is clay, followed by CA cement.[133,229,232] Silicate chemicals are used in some cases. Phosphate bonding chemicals are found principally among the higher-performance basic gunning mixes;[230] and chrome ore is used in a few. Since some bonding chemicals serve also as green binders, in a number of mixes there is no necessary added proprietary binder. Clay-bonded mixes are an example.[232]

An *alumina-silica* gunning mix product line is evident. There are many dozens of these, ranging in percent Al_2O_3 (fired basis) at least from 30% to 95% and in service temperature limit from about 1100°C (2000°F) to about 1900°C (3400°F). A few alumina-chrome compositions are included. These materials are used not only for repair but also to build up original wall or roof linings on steel substrates. They are found in stacks, ducts, and hot dust collectors; steam boilers and incinerators; in a wide variety of petroleum and petrochemical processing vessels; in heat treatment, reheat and annealing furnaces and elsewhere in foundries and nonferrous metal plants; in rotary and ceramic kiln applications; and in pouring-pit and other areas of iron and steel manufacture. Special formulations have been addressed to special problems such as erosion resistance[229] and molten aluminum contact. Many are insulating formulations. On the whole they feature quick lining construction and repair and a minimum of required forms. They are generally not prescribed for highest-temperature slagline and metal-containment duty, e.g., in molten iron, steel, copper and nickel furnaces and ladles, nor in glass melting.

The *basic* gunning mix product line is comparably numerous, though dedicated to a lesser number of different applications. The composition range is at least from 50% to 98% MgO, including some dolime,[228,231] magnesia-chrome, and a few magnesia-spinel types. These materials are used for taphole maintenance and other local high-wear repair applications in iron, steel and copper.[381] The most corrosion-resistant formulations are used in EAF maintenance: banks, hearths, slaglines, and tapholes. And of course the largest tonnage goes to maintenance and repair of oxygen-blown steelmaking vessels, typified by the BOF.[74,228] In this connection a few graphite-containing basic gunning mixes are on the market,[230] but there is no indication of their exceptional popularity at this time.

The line is rounded out with gunned zirconia-alumina, zircon-magnesia, and others selected from the A-Z-S composition triangle and nearby; also gunned chrome ore and a few other selected

minerals. The aggregate usage of these is minor compared with that of the two principal families.

A number of commercial wet gunning mixes are claimed to be adherent on either hot or cold substrates. Applied to a cold substrate, a gunned deposit must subsequently be dried. The usual cautions about drying rate apply; but gunned deposits are a little more porous than most other monolithics and hence a little less sensitive to internal steam pressure. As to gunning on hot substrates (e.g., for furnace repair), increasingly hot means diminishing adherence to the substrate on account of flash boiling of water at the interface. The most critical circumstance is in the steelplant, because there gunning occurs on an almost daily basis. The BOF, for example, may not have to cool completely for gunned lining repair; but a severe limit is placed on the lining temperature by otherwise poor adhesion and poor material utilization in gunning. That temperature limit has not been codified. But it is sufficiently irritating to BOF operating schedules that dry and semi-dry gunning techniques have been sought.

Dry and Semi-Dry Gun Mixes. A least amount of water may be employed in a conventional wet-mixing gun, or the solids may be only moistened before feeding or not at all. In the latter two cases the wet mixing gun is replaceable by a simple tube and nozzle. The move to *semi-dry gunning* in Japanese steelplants is said to have started in the 1970s.[238]

The use of substrate temperature in place of water as the medium of binding and adhesion is appealing, but extremely difficult to carry out without downgrading the service temperature of the gunned deposit. Very few dry or semi-dry compositions have been found suitable. A broad view of Japanese experience is included in Reference 74, and a technically useful review of hot gun mixes has been published.[236] A family of dry MgO-CaO and MgO-CaO + graphite mixes has been described,[228,234] as well as phos-bonded and silicate-bonded versions of the same types.[233,238] An alumina + SiC + graphite composite has been investigated for blast furnace trough repair.[235]

Only mediocre performance has been realized, on the whole. Among commercial products in the U.S.A., dry basic gunning mixes have hardly been featured. Recognizing that even higher gunning temperatures should yield qualities of binding and adhesion by out-and-out melting of particles in flight, technologists turned to the evaluation of flame and plasma spraying.

Flame and Plasma Gun Mixes. Oxy-gas, oxy-actetylene, and oxy-hydrogen torches have long been familiar devices[8] for flame-spraying and flame-plating of refractory compounds in other contexts.

The plasma torch[8] can double to triple the gas temperature of fuel torches, but at such increased cost that it might be economically impractical for refurbishing a hot BOF. At this time it is nonetheless premature to write the plasma torch in or out of the picture. Remarks are here confined to combustion torches, with which some experience has already been accumulated.

There is no doubt that *flame gunning mixes* of interest can be torch-melted, at least partially. One starts with the phase diagrams of Chapter IV, then begins to inquire about flame heat-transfer kinetics[238] and about the cost of providing various flame temperatures. An interestingly economical torch has been devised and used, in which most of the fuel is provided as coke particles accompanying MgO particles entrained in the 0_2 stream.[184]

Progress has been made in flame gunning in the BOF or the LD converter. The subject is touched on in References 74 and 236. An $MgO\text{-}NaPO_3$ composition has been investigated,[237] while the use of $MgO\text{-}SiO_2$ compositions has been reduced to commercial practice.[233] Evaluations of the flame-gunned deposit are few at this writing; but there are good indications from actual use in basic oxygen converters that the method is superior to semi-dry gunning and that it is cost-effective for converter maintenance.[184,233,238,239] Practical oxide particle sizing guidelines have been revealed, lying between about 50 μm and 3 mm.[239] A logical and persuasive philosophy of flame-gunning maintenance of oxygen-blown steel converters has been enunciated.[239] Though the present optimism awaits much future confirmation, this particular gunning technology will unquestionably be a fascinating one to monitor throughout the 1990s.

Insulating Refractories

Monolithic mixes for all of the installation methods listed above are available in insulating as well as relatively dense versions. Rammed insulation seems something of an oxymoron, but is occasionally found. Cast, vibratory cast, plastic, and wet-gunned porous refractories are common. The installation methods described here should provide a sufficient basis for understanding, backed by Chapter IX and particularly its third section, Physical Form and Installation of insulating refractories.

This chapter brings our technical treatment of refractories to a close. Following a brief summary of the implications, Chapter XV will add one final set of information resources that the reader should find useful.

Chapter XV

Conclusion

HISTORICAL PERSPECTIVES REVISITED

Refractories technology has been divorced in this book from the macroeconomic environment of the industry. This separation was purposeful: technology is a unidirectional progression, while descriptions of the economic climate rise and fall with time and place and thus are always dated. The contemporary history of this climate is recounted in several recent papers,[74,76,189,508-511] and is brought up to date in the U.S. in a 1990 publication.[512]

The present period is not the first occasion of a substantial restructuring of the business of making refractories.[1,3] There are signs in it, though, of what could be a prolonged loss of output and profitability of the largest user industries, at least within some circumscribed national economies. That output and profitability are the ultimate wellspring of funds for refractories research and development. A telling statistic would be the total number of persons engaged in R & D in and for this industry. Whatever that statistic might say of the stability of the business, there is little doubt that substantive trends in R & D effort will be reflected five to twenty years hence in the state of the technology. Our perception is of a recent decline in the R & D level in the U.S.A. in particular.

If not stemmed, such a trend would suggest a twenty-year future technological advance that is less supportive of the user industries than the past twenty-year advance. If such a trend arises from an economy which rewards the creation of real wealth less handsomely than the redistribution of existing wealth (and

remunerates engineers and scientists inversely with academic degree), that economy would seem to be self-burdened. If productive enterprises are not encouraged as much as those that cater to affluence and leisure, then affluence and leisure will eventually dwindle.

The current competitive globalization of industry and commerce has no historical parallel, however. Globalization of refractory manufacture would address a world market of some $10 billion in 1990 U.S. currency. It is too early to distinguish between trends and turbulence in either national or international technological climates. Turbulence is not to be shunned; yet it is an uncertain bellwether. We shall make no forecasts. But a twenty-year look back provides a revealing perspective.

Not only have the user industries motivated progress in refractories by requiring better performance and by making significant changes in their own processing. Users have been remarkably willing to test and evaluate new refractories and new approaches to lining construction. Considerable credit must also be given to user companies that conducted and reported their own research on refractories, their installation, and the characteristics of their wear and deterioration in service. The recent throttling of that effort can only be lamented.

The past twenty years of progress were stimulated by both maker and user explorations going back to several decades before. Table XV.1 lists some of the most important advances made in refractories since about 1970, which have been discussed in relative isolation in the foregoing chapters. In aggregate they display far more of innovation, improvement and expansion of the product line than occurred in any prior twenty-year period in history.

The papers previously cited in this chapter[74,76,189,508-512] have knowledgeably addressed the future technical evolution of refractories, each from a particular geo-economic viewpoint. Their digestion is a must. While the specific changes to be made in the processes served will remain difficult to forecast, the forces behind them are hardly arguable. More people worldwide will clamor for more energy from a finite fuel supply. Alternatives to petroleum will simply have to be exploited. More people will need more staples -- metals and chemicals, biologicals and foodstuffs -- that must be brought economically within their reach. Environmental concerns as well as energy economy in manufacture are forces underlying the search for alternate ways of making iron and steel, nickel and copper and more. Threatened high-grade mineral supplies will call for better and multiple utilization of ores and better reprocessing of tailings. Recycling of staples will have to become commonplace. The fixing or

Table XV.1 Refractory Developments, Approx. 1970-1990

DIRECT-BONDED BRICK:

- Periclase
- Periclase-Chrome
- Dolime
- High Alumina
- Alumina-Chromia
- Zircon
- Zirconia-Alumina
- Zirconia-Magnesia

FUSED-REBONDED GRAIN:

- Improved A-Z-S
- Periclase-Chrome
- Mag. Aluminate Spinel
- Periclase (synthetic)
- Alumina (synthetic)
- Zirconia (baddeleyite)

FUSED-CAST REFRACTORIES:

- Zirconia
- Magnesia
- Alumina

ANDALUSITE REFRACTORIES:

- 50-70% Al_2O_3 Series
- Andalusite + Graphite

PROLIFERATION OF P-BOND BRICK:

- All Types

OXIDE + NONOXIDE COMPOSITES:

- MgO + Graphite
- f.g. MgO + Graphite
- Dolime + Graphite
- MgO + Graphite + Deoxidant
- Impregnated Burned Bricks
- Pitch Types (all the above)
- Resin Types (all the above)

HIGH-TEMPERATURE FIBERS:

- New Vitreous Fibers
- Crystalline Oxide Fibers
- Fiber/Ceramic Composites

HIGH-TEMPERATURE SiC:

- Si_3N_4-Bonded
- SiAlON-Bonded

SPECIAL SHAPES AND FORMS:

- Huge Preformed Blocks, etc.
- Intricate Preformed Shapes
- Thin-Wall BF Checkers
- Thin-Wall GF Checkers
- Slide Gate Valves
- Porous Plugs and Diffusers
- Lightweight Kiln Cars (platforms, furniture)
- Modular Fiber Insulation
- Hollow Insul. Oxide Spheres

NONOXIDE MONOLITHICS:

- Silicon Carbide
- Carbon and Graphite (low-temperature bonded)

OXIDIC MONOLITHICS:

- Full Composition Ranges
- Expanding Monolithics
- Proliferation of P-Bond
- Resin-Bonded Monolithics
- Low CA Cement Castables
- Ultra-Low and Zero-Cement Castables
- Vibratory Castables
- Explosion-Resistant Castables
- Pumpable Castables
- SS Fiber Reinforcing
- Composite Ram/Castables:
  - MgO + Graphite
  - Al_2O_3 + Graphite
  - Al_2O_3 + SiC
  - Al_2O_3 + SiC + Graphite
- <5%-Rebound Gun Mixes
- CrO_3-Free Gunning Mixes
- Dry (hot) Gunning and Mixes
- Flame Gunning and Mixes

CONCAST MOLD POWDERS

chemical conversion of undesirable effluents will have to expand, ultimately to all industrial practices and wherever populations congregate.

Elegance in industrial processing will continue to displace brute force. The recent trends toward sophistication in refractories and their making will have to continue apace. Global consolidation in the industry might facilitate the necessary R & D. The shape and form of the challenge will become evident enough. In a world ever socially more close-knit and materially more limited, the magnitude of the challenge is inexorable. This challenge is as it has always been: to discovery, to innovation, and to excellence.

PATENTS

The references we have cited are largely in the conventional literature. Patents in the refractories field have been kept separate. In Chapter XIII it was remarked that a book of this kind cannot enter the privileged space of the refractories plant; yet one useful feature of patents is the glimpse often given into how specific products may be preferably made. This is not the only such useful feature. Patents contain a wealth of helpful information.

Immediately following the list of References, a list of pertinent Patents is given. This list has been subdivided under several convenient refractory composition classes and subclassifications. Within each group the sequence is chronological. Each title should be sufficiently descriptive to serve the reader's interest.

These patents were collected by a DIALOG® computerized literature search based on Chemical Abstracts. No representation is made that the list is complete or accurate. In particular, no recommendation whatsoever is expressed or implied, to use any information or practice in violation of any valid patent whether included in this list or not. Having thus said what must be said, we commend refractory patents to the reader as a final resource for understanding and appreciation of this remarkable family of materials: harnessing fire in the service of man.

References

1. C. A. Krause, REFRACTORIES: THE HIDDEN INDUSTRY, 1987, The American Ceramic Society, Inc., Westerville, OH.

2. C. Singer, E. J. Holmyard, A. R. Hall, and T. I. Williams, ed., A HISTORY OF TECHNOLOGY, Vols. 1-8, 1954-84, copyright 1963 by Oxford University Press, Oxford, England.

3. F. H. Norton, REFRACTORIES, 3rd Ed., 1949; also 4th Ed., 1968; McGraw-Hill Book Co., New York.

4. J. H. Chesters, REFRACTORIES PRODUCTION AND PROPERTIES, 1973, Iron & Steel Institute, London.

5. J. H. Chesters, REFRACTORIES FOR IRON AND STEELMAKING, 1974, The Metals Society, London.

6. K. Shaw, REFRACTORIES AND THEIR USES, 1972, Halstead Press Div., John Wiley & Sons, New York.

7. J. D. Gilchrist, FUELS, FURNACES AND REFRACTORIES, 1977, Pergamon Press, New York.

8. KIRK-OTHMER ENCYCLOPEDIA OF CHEMICAL TECHNOLOGY, Vols. 1-24 & Supplement, 3rd Ed., 1984, John Wiley & Sons, New York.

9. ANNUAL BOOK OF ASTM STANDARDS, Vol. 15.01, 1990 (re-issued annually), American Society for Testing & Materials, 1916 Race Street, Philadelphia, PA 19103-1187.

10. REFRACTORIES, 1987, The Refractories Institute, 500 Wood St., Suite 326, Pittsburgh, PA 15222.

11. CRC HANDBOOK OF CHEMISTRY AND PHYSICS, 71st Ed., 1990, CRC Press, Boca Raton, FL.

12. PERRY'S CHEMICAL ENGINEERS' HANDBOOK, 6th Ed., 1984, McGraw-Hill Book Co., New York.

13. STANDARD FOR METRIC PRACTICE, Document E 380-76, 1976, American Society for Testing & Materials, Philadelphia, PA.

14. Edward R. Orton, Jr. Ceramic Foundation, Box 460, Westerville, OH 43081.

15. J. F. Shackelford, INTRODUCTION TO MATERIALS SCIENCE FOR ENGINEERS, 2nd Ed., 1988, MacMillan Publishing Co., New York.

16. International Oxide Fusion, Box 2163, Niagara Falls, Ontario, Canada; Div. of Exolon-ESK Co., P.O. Box 590, Tonawanda, New York 14151-0590.

17. Hendryx Engineers, Inc., Pittsburgh, PA.

18. Y. Kumashiro, "Electric Refractory Materials: Transition Metal Carbides, Nitrides, and Diborides," Kagaku Kogyo 38 (1987), 360.

19. P. Bardhan and R. N. McNally, "Fusion-Cast Non-Oxide Ceramics Containing Free Graphite," High Temp. Mater. Proc. 6 (1984), 195.

20. METALS HANDBOOK, Vols. 1-17, 9th Ed., 1989, American Society of Metals, Metals Park, OH.

21. E. M. Levin, C. R. Robbins, and H. F. McMurdie, ed., PHASE DIAGRAMS FOR CERAMISTS, 1964; Supplement, 1969; American Ceramic Society, Westerville, OH.

22. L. D. Hart, ed., ALUMINA CHEMICALS - SCIENCE AND TECHNOLOGY HANDBOOK, 1990, American Ceramic Society, Westerville, OH.

23. D. R. Stull and H. Prophet, ed., JANAF THERMODYNAMIC TABLES, 2nd Ed., 1971, U.S. Dept. of Commerce, Nat. Bur. of Standards, Washington, D.C. Supplements: J. Phys. Chem. Ref. Data 3 [2] (1974); 4 [1] (1975); 7 [3] (1978); 11 [3] (1982).

24. S. Kumakura, "Zirconia Fusion Cast Refractory," p. 661 in Reference 25.

25. PROCEEDINGS OF 2nd INTERNATIONAL CONFERENCE ON REFRACTORIES, Vols. 1-2, 1987, The Technical Association of Refractories, New Ginza Bldg. 4F, 7-3-13, Ginza, Chuo-ku Tokyo 104, Japan.

26. L. J. Trostel, Jr., ed., UNITECR '89 PROCEEDINGS, Vols. 1-2, 1989, American Ceramic Society, Westerville, OH.

27. S. Kumakura, "The Application of Fused High Zirconia Refractory in Glass Melting Furnaces," p.835 in Reference 26.

28. L. B. Borovkova, T. I. Borodina, G. E. Valyano, E. P. Pakhomov, A. I. Romanov, and L. G. Smirnova, "High Refractory Zirconia Lining Materials," p. 1060 in Reference 26.

29. A. G. Evans, "Perspective on the Development of High-Toughness Ceramics," Am. Ceram. Soc. J. 73 (1990), 187.

30. F. F. Lange, "Transformation Toughening. Part 2. Contribution to Fracture Toughness," J. Mater. Sci. 17 (1982), 235.

31. E. J. W. Whittaker, CRYSTALLOGRAPHY, 1981, Pergamon Press, N.Y.

32. Y. S. Touloukian et al, ed., THERMOPHYSICAL PROPERTIES OF MATTER, Vols. 1-13, 1970-79, I.F.I./Plenum Press, New York.

33. O. Terenyi, "Strength of Refractory Kiln Furniture Made of Silicon Carbide," InterCeram 32 (1983), 36.

34. M. Nagafune, I. Tsuchiya, H. Takahashi, Y. Oguchi, and T. Kawakami, "Characterization of Thermo-Mechanical Properties of Basic Refractories," p. 1017 in Reference 25.

35. K. J. Konsztowicz, "Acoustic Emission from Thermal Fracture of an Advanced Zirconia Refractory," p. 1783 in Reference 26.

36. M. Ruehle, A. G. Evans, R. M. McMeeking, P. D. Charalambides, and J. W. Hutchinson, "Microcrack Toughening in Alumina/Zirconia," Acta Metall. 35 (1987), 2701.

37. I. Elstner, P. Jeschke, W. Kroenert, and E. Protogerakis, "Thermal Shock Behavior of Zirconium Dioxide Refractory Construction Materials. II. Fracture-Mechanical Behavior," Sprechsaal 115 (1982), 288.

38. J. Homeny and R. C. Bradt,"Aggregate Distribution Effects on the Mechanical Properties and Thermal Shock Behavior of Model Monolithic Refractory Systems," p. 110 in Reference 39.

39. R. E. Fisher, ed., NEW DEVELOPMENTS IN MONOLITHIC REFRACTORIES - ADVANCES IN CERAMICS, Vol. 13, 1985, American Ceramic Society, Westerville, OH.

40. G. Routschka and L. Hagemann, "Relations Between the Compressive and Flexural Strengths of Refractory Products," Sprechsaal 120 (1987), 36.

41. D. J. Griffin and T. G. Miller, "The Effects of Long-Term Heating on the Thermal Shock Properties of Basic Refractories," Ceram. Eng. Sci. Proc. 8 (1987), 41.

42. S. C. Carniglia, W. H. Boyer, and J. E. Neely, "Chemical Properties of Refractories," p. 387 in MATERIALS SCIENCE RESEARCH, Vol. 5, W. W. Kriegel and H. Palmour, III, ed., 1971, Plenum Press, New York.

43. R. L. Nacamu and S. J. LaLama, "High-Carbon-Magnesia Refractories in Basic Oxygen Steelmaking," Refract. J. 57 (1982), 9.

44. H. M. Mikami and J. R. Martinet, "Carbon-Magnesia Bricks in Electric Arc Furnaces," IRMA J. 15 (1982), 7.

45. K. Shimada, A. Doi, and K. Kono, "Development of Refractories for Torpedo Ladles Used for Hot Metal Pretreatment," Taikabutsu 40 (1988), 145.

46. T. Ishibashi, K. Furukawa, K. Sugiyama, K. Yamada, and N. Yasuda, "Dense and High-Strength Castable Materials for Blast Furnace Troughs," ibid. 36 (1984), 467.

47. H. Sugita and T. Chikano, "The Improvement of Ladle Bricks for AOD Furnaces," ibid. 35 (1983), 500.

48. M. Chastant, "Castable Materials for Refractory Lining of Blast-Furnace Troughs and Runners," Cah. Inf. Tech./Rev. Metall. 8 (1986), 719.

49. S. N. Laha, "Steel Fiber-Reinforced Refractories," Trans. Indian Ceram. Soc. 39 (1980), 131.

50. T. Ishibashi, K. Furukawa, and N. Wada, "Effect of Stainless Steel Fiber Addition on the Properties and Acoustic Emission Characteristics of Castable Refractories," Taikabutsu 34 (1982), 115.

51. C. H. Sump, "Stainless Steel Metal Fiber Reinforcement of Refractories," J. Mater. Energy Syst. 6 (1985), 279.

52. R. C. Garvie, M. F. Goss, S. Marshall, G. T. Mayer, and C. Urbani, "The Design and Application of Dispersion Toughened Advanced Refractory Ceramics," p. 1023 in Reference 26.

53. C. A. Schacht, "Influence of Lining Restraint and Nonlinear Material Properties in Predicting Thermal Shock Fracture of Refractory Linings," p. 1286 in Reference 26.

54. T. A. Geisler, "Finite Element Analysis of Thermal Stresses in Cement Kiln Brick," p. 1317 in Reference 26.

55. D. J. Fuller, "Furnace Refractories: A Mathematical Model to Aid Selection," Br. Foundryman 76 (1983), 46.

56. I. Masakazu, S. Fujihara, M. Nakai, Y. Murai, A. Kikuchi, and K. Hikita, "A New Masonry Structure to Eliminate Thermal Stress from Blast Furnace Hearth Lining," p. 689 in Reference 25.

57. Y. Kubo, J. Yagi, K. Doi, Y. Tanno, M. Sato, and A. Mori, "Improved Design of BOF Lining," p. 712 in Reference 25.

58. F. Cabannes, "Heat Transfer at High Temperature in Ceramics," Ann. Chim. (Paris) 10 (1985), 281.

59. D. A. Bell, "A Computer Simulation of Cracking in Monolithic Refractories," Br. Ceram. Trans. J. 87 (1988), 133.

60. D. A. Bell and F. T. Palin, "Computer Modelling of Mechanical Behaviour of Refractories in Iron and Steelmaking Applications," p. 480 in Reference 26.

61. D. P. H. Hasselman, "Elastic Energy at Fracture and Surface Energy as Design Criteria for Thermal Shock," Am. Ceram. Soc. J. 46 (1963), 535.

62. D. P. H. Hasselman, "Unified Theory of Thermal Shock Fracture Initiation and Crack Propagation in Brittle Ceramics," ibid. 52 (1969), 600.

63. D. P. H. Hasselman, "Thermal Stress Resistance Parameters for Brittle Refractory Ceramics: A Compendium," Am. Ceram. Soc. Bull. 49 (1970), 1033.

64. J. A. Coppola, D. P. H. Hasselman, and R. C. Bradt, "On the Measurement of the Work-of-Fracture of Refractories," ibid. 52 (1973), 578.

65. M. K. Fishler, J. M. Vignot, M. Caruelle, and G. I. Rancoule, "Fused Silica Utilization in the Manufacture of Flat Glass," p. 677 in Reference 25.

66. S. C. Carniglia, "Limitations on Internal Oxidation-Reduction Reactions in BOF Refractories," Am. Ceram. Soc. Bull. 52 (1973), 160.

67. R. J. Leonard and R. H. Herron, "Significance of Oxidation-Reduction Reactions Within BOF (Basic Oxygen Furnace) Refractories," Am. Ceram. Soc. J. 55 (1972), 1.

68. S. C. Carniglia, "An Oxidation-Reduction Mechanism for Basic Refractory Wear in the Argon-Oxygen Vessel," Elec. Furn. Conf. ASM Proc. 30 (1972), 138.

69. V. T. Krivoshein, "Causes of Crack Formation in Coke-Oven Walls," Koks Khim. 7 (1988), 18.

70. G. Mascolo, O. Marino, and V. Sabatelli, "Refractory and Insulation Degradation in an Oil-Fired Power Plant," Sci. Ceram. 12 (1984), 411.

71. V. A. Bron, V. V. Alekseev, V. A. Perpelitsyn, and V. G. Borisov, "Wear of Periclase Refractories from Flotation-Concentrated Magnesite in the Lining of Steel Converters," Vzaimodeistvie Ogneuporov Met. Shlakami 19 (1980), 3.

72. D. H. H. Quon and K. E. Bell, "Degradation of Slagline Chrome Magnesite Bricks in Secondary Steelmaking Under Vacuum," InterCeram 32 (1983), 50.

73. R. A. Panfilov, D. S. Rutman, E. Y. Gimpel'man, and V. M. Ust'yantsev, "Dense Magnesian-Spinel Materials with Synthesized Magnesium Chromite," Ogneupory 1983, 9.

74. T. Hayashi, "Recent Development of Refractories Technology in Japan," p. 5 in Reference 75.

75. PREPRINT OF THE FIRST INTERNATIONAL CONFERENCE ON REFRACTORIES, 1983, The Technical Association of Refractories, New Ginza Bldg. 4F, 7-3-13, Ginza, Chuo-ku Tokyo 104, Japan.

76. M. L. Van Dreser and J. E. Neely, "Refractories for Steelmaking in the U.S.A. - Current Practice and Future Trends," p. 35 in Reference 75.

77. J. P. Kiehl and Y. Le Mat, "Use of Chrome-Alumina Castables and Shapes in Blast Furnace and Carbon Black Reactors," Am. Ceram. Soc. Bull. 62 (1983), 809.

78. T. Yukinawa and N. Iwase, "Rotary Slag Corrosion Test of Alumina-Chromium Oxide Parts for Repair of RH Degassing Schnorkel," Taikabutsu 35 (1983), 467.

79. H. Katayama, T. Ebisawa, and S. Yamamoto, "Improvement of RH-Degassing Refractories," ibid. 39 (1987), 523.

80. Y. T. Chien, C. C. Chou, H. C. Pan, and Y. C. Ko, "Evaluation and Selection of Refractory Materials for the Desiliconization in Torpedo Ladles," p. 254 in Reference 25.

81. Y. T. Chien and Y. C. Ko, "Causes of Refractory Disintegration in a Carbon Monoxide Environment," Am. Ceram. Soc. Bull. 62 (1983), 779.

82. J. J. Brown, "Carbon Monoxide Disintegration of Coal Gasifier Refractories," Ann. Conf. Mater. Coal Convers. Util., Proc. 6 (1981), IV/23.

83. A. Fahr, S. F. Rahman, and D. E. Day, "Properties of Refractories After Exposure to High-Temperature Gases: VI - Vapor vs Liquid Contact," Mater. Energy Syst. J. 4 (1982), 48.

84. T. Rymon-Lipinski, "Control of Carbon Oxidation Rate by Pore-Size Distribution and Porosity of Magnesite Refractories," Szilikatip. Szilikattud. Konf., Eloadasok, 13th, 1981, 347.

85. A. G. Karzalov, A. D. Malyuk, V. G. Druzhinin, and A. V. Oistrakh, "Baddeleyite Melting in an Electric Arc Furnace," Ogneupory 1983, 34.

86. K. Hiragushi, H. Shikano, I. Takita, Y. Kimura, and J. Yoshimoto, "Improvement of Corrosion Resistance of Aluminum Oxide-Silicon Carbide-Carbon Bricks," Taikabutsu 38 (1986), 758.

87. J. Stradtmann, R. Prange, and G. Wenclawiak, "Recent Development of Dolomitic Refractories for Application in the Steelmaking Process," p. 349 in Reference 25.

88. M. Nishi, M. Kobayashi, A. Miyamoto, T. Anzai, and K. Ichikawa, "Investigations on Castable Refractories for Steel Teeming Ladles," p. 475 in Reference 75.

89. J. Kärjä, "Refractory Performance in Rautaruukki's LD-KG Converter," p. 162 in Reference 25.

90. J. Mori, N. Watanabe, M. Yoshimura, Y. Oguchi, T. Kawakami, and A. Matsuo, "Material Design of Monolithic Refractories for Steel Ladle," p. 541 in Reference 26.

91. G. Aspholm and T. M. Wehrenberg, "New Refractory for Insulating Fiber Glass Electric Melters," p. 866 in Reference 26.

92. I. Kamidochi and Y. Oishi, "Regenerator Checker Brick for Glass-Melting Furnaces, with Emphasis on Borosilicate Glass-Melting Furnaces," Taikabutsu 40 (1988), 364.

93. K. Oki, M. Sugie, K. Kurihara, and Y. Aiba, "Wear Pattern of Zirconia Refractories by Molten Steel and Slag," p. 721 in Reference 75.

94. H. Kyoden, Y. Namba, and N. Tsukamoto, "Wear Mechanisms of Carbon-Containing Refractories for Continuous Casting," p. 751 in Reference 75.

95. T. Matsumura, S. Uto, K. Hosokawa, and M. Geji, "Properties of Magnesia-Carbon Bricks Containing Aluminum or Aluminum Alloys," Taikabutsu 39 (1987), 519.

96. M. Nanbu, A. Matsuo, S. Miyagawa, and K. Ogasahara, "Refractories for Use in Ladle Furnace," ibid. 38 (1986), 764.

97. A. Watanabe, H. Takahashi, T. Matsuki, and M. Takahashi, "Effects of Metallic Elements Addition on the Properties of Magnesia Carbon Bricks," p. 125 in Reference 75.

98. R. Parodi and M. Martino, "Utilization of Metallic Powders in Carbon-Containing Refractories," p. 1046 in Reference 26.

99. C. E. Semler and B. Brezny, "Magnesium Diffusion in BOF Refractories," p. 171 in Reference 75.

100. T. Yamagami, M. Takeoka, K. Fujii, K. Hiragushi, H. Shikano, H. Yamamoto, O. Nakamura, I. Tanaka, T. Tanabe, and Y. Ohnishi, "Results of Performance Tests of Magnesia-Carbon Bricks with Added Boron Nitride in a Long-Life Converter," Taikabutsu 39 (1987), 516.

101. K. Tabata, K. Ichikawa, N. Tsukamoto, and Y. Yoshimura, "A Study on Oxidation Embrittlement of Carbon-Bonded Refractories for Continuous Casting," p. 523 in Reference 25.

102. T. Rymon-Lipinski, "Reactions of Metal Additives in Magnesia-Carbon Bricks in an Oxygen Converter," Stahl Eisen 108 (1988), 1049.

103. T. Honda and A. Yamaguchi, "Thermodynamics of Refractory Applications. IX. Corrosion of Steel Plates for Basic Brick Joints in a Rotary Cement Kiln," Taikabutsu 40 (1988), 326.

104. P. L. Smith, J. White, and P. G. Whitely, "Ultra High Alumina or Silicon Carbide Refractories for Critical Areas in Blast Furnace Linings," p. 101 in Reference 25.

105. K. L. Luthra and H. D. Park, "Oxidation of Silicon Carbide-Reinforced Oxide-Matrix Composites at 1375° to 1575°C," Am. Ceram. Soc. J. 73 (1990), 1014.

106. A. Muan, "Equilibrium Relations in Systems Containing Chromium Oxide, with a Bearing on Refractory Corrosion in Slagging Coal Gasifiers," High Temp. - High Pressures 14 (1982), 653.

107. H. Reinke, H. Kern, and H. Ambs, "The Effect of Oxidizing and Reducing Atmospheres on the Mineralogical, Microstructural and Physical Properties of Chrome-Magnesia Refractories," Br. Ceram. Trans. J. 85 (1986), 188.

108. F. Tanemura and T. Honda, "Wear Pattern of Basic Refractories in the Burning Zone of a Rotary Cement Kiln," Gypsum Line 200 (1986), 20.

109. B. Clavaud, P. Meunier, and J. P. Radal, "Twenty Years of Experience with High Compactness Concretes: A Link Between Shaped Products and Electrocast Refractories," p. 1094 in Reference 26.

110. S. C. Carniglia, "Grain Boundary and Surface Influence on Mechanical Behavior of Refractory Oxides: Experimental and Deductive Evidence," p. 425 in MATERIALS SCIENCE RESEARCH, Vol. 3, W. W. Kriegel and H. Palmour, III, ed., 1966, Plenum Press, New York.

111a. T. Horio, M. Ikeda, T. Hagiwara, S. Fujiwara, and K. Aoyama, "Studies on the Wear Mechanism of Blast Furnace Refractories," Taikabutsu Overseas 2 (1982), 3.

111b. M. Miwa and T. Yamamoto, "Recent Progress in Carbon Block Characteristics for Blast Furnace Hearths," ibid., p. 42.

111c. D. Campos-Loriz, K. R. Selkregg, and Y. Tagami, "Alkali Attack Mechanisms on Blast Furnace Refractories," ibid., p. 51.

111d. Y. Sakamoto, T. Sakai, T. Yamamoto, and I. Kurashige, "Diagnosis Techniques for In-Operation Blast Furnace Linings," ibid., p. 65.

111e. T. Taniguchi, M. Otani, and I. Iwasaki, "Studies on Trough Lining Refractories for Large-Capacity Blast Furnaces," ibid., p. 78.

111f. N. Nameishi, T. Ishibashi, and T. Kitai, "The Change of Lining Materials for Torpedoes in Japan - Corresponding to the Pre-treatment of Hot Metal in Torpedoes," ibid., p. 90.

111g. T. Nishina, S. Takehara, and M. Terao, "Recent Trends of Refractories for Hot Blast Stoves," ibid., p. 98.

112. R. E. Farris, "The Use of Basic Refractories in Modern Steelmaking Practices," Int. Symp. Adv. Refract. Metall. Ind., 1st, Proc. (1988), 105.

113. I. Endo, T. Kawakami, H. Takahashi, I. Tsuchiya, and H. Ishi, "Corrosion of Basic Refractories by Various Types of Secondary Refining Slags," Taikabutsu Overseas 7 (1987), 18.

114. S. Tanaka, A. Sato, I. Tsuchiya, H. Takahashi, T. Kawakami, and Y. Kadota, "Effect of Slag Compositions and Temperature on the Corrosion Resistance of Refractories for Converters," Int. Feuerfest-Kolloq., 27th, Proc. (1984), 480.

115. H. Barthel and E. Kaltner, "The Effect of Carbon in Carbon-Containing Magnesia Bricks on the Wear in Basic Oxygen Furnaces," p. 91 in Reference 75.

116. V. D. Tsigler, "Zonal Structure Formation in Dinas Brick of Partitions in Coke Ovens," Koks Khim. 7 (1988), 15.

117. C. Richmond and C. E. Chaille, "High-Performance Castables for Severe Applications," p. 230 in Reference 39.

118. L. G. Bly and R. J. Pena, "Waste Incineration - Some Background and Furnace Refractory Design Review," p. 980 in Reference 26.

119. K. Hamano, "Corrosion and Erosion Mechanisms of Basic Refractories," Taikabutsu 255 (1979), 170.

120. K. Shimada, A. Inoue, S. Matsuo, T. Takeda, H. Nakagawa, and S. Yokoyama, "Development of Bottom Bricks for High-Temperature Steel-Teeming Ladles," ibid. 38 (1986), 771.

121. T. E. Garnar, Jr., "Zirconium Raw Materials for the Refractory Industries," Ceram. Eng. Sci. Proc. 4 (1983), 170.

122. K. Shimada, A. Inoue, S. Matsuo, T. Yagi, Y. Uchida, and Y. Suekawa, "Application of High-Zircon N-CAST Material for High-Temperature Steel Ladles," Taikabutsu 39 (1987), 8.

123. K. Fukui, T. Kamata, M. Sakaguchi, S. Moriizumi, and S. Sonoda, "Use of Quartz-Zircon Monolithic Refractories for a Low-Frequency Coreless Induction Furnace," ibid. 40 (1988), 312.

124. J. D. Parmelee and J. A. Moody, "Vibration Placement of Dry Refractories in Coreless Induction Furnaces," p. 787 in Reference 25.

125. C. N. McGarry and T. M. Wehrenberg, "New Castable Refractory Product for Catalytic Cracking Units," p. 920 in Reference 26.

126. D. A. Whitworth, "Refractory Considerations for the Foundry AOD System," Am. Foundrymen's Soc. Trans. 91 (1983), 359.

127. B. Agrawal and J. P. Wiencek, "State of the Art AOD Refractory Technology," ibid., p. 451.

128. S. Banerjee and G. L. Ramsey, "High-Fired Refractories for Continuous-Casting Tundishes," Int. Symp. Adv. Refract. Metall. Ind., 1st, Proc. (1988), 305.

129. R. Butta and L. Kleinheisterkamp, "Behavior of Fusion-Cast Refractories in Contact with Enamel and Ceramic Glazes," Sprechsaal 116 (1983), 869.

130. E. Z. Korol, V. M. Panferov, V. L. Bulakh, N. V. Pitak, and V. A. Ustichenko, "Thermomechanical Properties of Mullite-Corundum Refractories from Melted Mullite," Ogneupory 1983, 16.

131. A. Petro and R. A. Flinn, "Variables Affecting Ladle Life for Steel Castings," Am. Foundrymen's Soc. Trans. 85 (1978), 353.

132. S. Kawasaki, T. Ohnishi, H. Takagi, A. Kamimori, and T. Sato, "Life Extension by Using Unshaped Refractory for Powder Injection Lance," Taikabutsu 37 (1985), 404.

133. M. Toda, E. Yorita, T. Yamamura, and Y. Kubota, "Study of Gunning Systems for Low-Cement Castables," ibid., p. 562.

134. Y. A. Pirogov, L. V. Pamova, A. G. Belogrudov, G. A. Kalugin, and N. A. Domrachev, "Rammed Mullite-Corundum and Corundum Materials Without a Kaolinite-Containing Component," Ogneupory 1983, 28.

135. Y. X. Jian, "Use of High-Alumina Ramming Mixes in the BOF Ladles," p. 494 in Reference 75.

136. H. Grosse Daldrup and B. Scheubel, "Use of Magnesia-Spinel Refractory Bricks in Cement Kilns," Cim., Betons, Platres, Chaux 770 (1988), 20.

137. P. Bartha, "Development Status of Refractory Magnesia Spinel Bricks for Rotary Cement Kilns," TIZ 111 (1987), 526.

138. T. Yukinawa, "Development of Basic Dam Block for Tundish," Taikabutsu 38 (1986), 852.

139. M. Nishi, T. Numata, H. Katayama, H. Matsumura, T. Sumigama, H. Ueno, H. Muraoka, and C. Nishikawa, "Application of Basic Castable Refractories to the Cover for Desiliconization Trough," ibid., p. 843.

140. T. Moriimoto, A. Harita, K. Nakada, M. Shibui, M. Numata, and M. Fujisaku, "Studies on Lance Refractories for Desulfurization of Molten Steel, 2," ibid. 36 (1984), 57.

141. W. Piatkowski, W. Piatkowski, Jr., and J. Szczerba, "Some Aspects of the Spinel's Role in the Basic Refractories," p. 1814 in Reference 26.

142. A. Cisar, W. W. Henslee, and G. W. Strother, "Development of Spinel-Based Specialties: Mortars to Monoliths," p. 411 in Reference 39.

143. T. Nishitani, S. Matsuo, and T. Genba, "Application of the Alumina-Spinel Castable for BOF Ladle Lining," p. 529 in Reference 26.

144. G. Delavos and H. Winter, "Wear in the Hearth of Blast Furnace A with a Picrochromite Lining," Berg Heuttenmaenn. Monatsh. 132 (1987), 501.

145. Y. Naruse, S. Fujimoto, H. Shikano, M. Hori, T. Tanabe, and M. Kamiide, "Performance of Magnesia-Carbon Brick for LF Side-walls," Taikabutsu 36 (1984), 54.

146. Y. Watanabe, K. Sasaki, and H. Kato, "Basic Refractories for Secondary Refining Systems and their Application," p. 414 in Reference 75.

147. T. Kurisu, Y. Nezu, M. Ozawa, D. Ohtsuga, and M. Yamamoto, "Improvements of Refractories for RH Degasser," p. 431 in Reference 75.

148. T. Onishi, T. Onoye, I. Wakasugi, and M. Ohgami, "Improvements of Ladle Refractory in ASEA-SKF Process," p. 444 in Ref. 75.

149. G. Mörtl, "High Purity MgO-Cr_2O_3 Brick - A New Generation of High Performance Refractories," p. 857 in Reference 25.

150. J. A. Reyes Sanchez and O. Díaz Toledo, "New Developments of Magnesite-Chrome Brick and Magnesite-Spinel for Cement Rotary Kilns Higher Thermal Shock Resistance and Higher Coating Adherence," p. 968 in Reference 26.

151. S. Banerjee and J. Tu, "Refractories for High Temperature Application," p. 1140 in Reference 26.

152. Y. Naruse, H. Ichiyama, S. Ishimatsu, and M. Kamiide, "Performance Result of Dense High-Strength Castable Blocks for Ladle Striker Panel," Taikabutsu 34 (1982), 8.

153. H-Y. Yang and C. F. Chan, "Corrosion Resistance and Microstructure of High-Alumina Refractories, Based on the Rotary Slag Test," Am. Ceram. Soc. J. 73 (1990), 1074.

154. A. M. Segadães, N. H. Brett, and J. White, "Phase Studies in the System Magnesia-R_2O_3-Calcium Silicate," p. 197 in Ref. 75.

155. G. E. Gonçalves and J. White, "Compatibility Relationships of Periclase in the System CaO-MgO-Al_2O_3-SiO_2 in Air," p. 1110 in Reference 25.

156. A. Ohte, T. Soejima, T. Saito, I. Wakasugi, H. Kawasaki, T. Mine, and K. Horikawa, "Life-Improvement of BOF with Shell Cooling and MgO-C Brick," p. 357 in Reference 26.

157. Y. Wanibe, H. Tsuchida, T. Fujisawa, and H. Sakao, "Infiltration of Corrosive Liquids into Capillary Tubes," Iron Steel Inst. Jpn., Trans. 23 (1983), 331.

158. A. Tsuchinari and O. Shimobayashi, "Porous Plug Made of Spherical Particles for Bubbling from the Bottom of Ladles," Taikabutsu 41 (1989), 42.

159. T. Kawakami, T. Yamane, and H. Mitsui, "Permeability of Castable Refractories," ibid. 34 (1982), 69.

160. F. E. Woolley, "Prediction of Refractory Corrosion Rate from Glass Viscosity and Composition," p. 768 in Reference 26.

161. N. V. Pitak, R. M. Fedoruk, R. S. Shulyak, and T. P. Khmelenko, "Wetting of Aluminosilicate Refractories with Cast Iron," Ogneupory 1978, 35.

162. R. Ebizawa, I. Ohishi, M. Kuwayama, A. Matsuo, and E. Maeda, "Application of Basic Refractories to Teeming Ladles," p. 322 in Reference 25.

163. H. Kochi and A. Tsuchinari, "Porous Plug Made of Spherical Particles for Bubbling from the Bottom of the Ladle," p. 536 in Reference 25.

164. R. J. Milauskas, "Development and Performance of New High-Tech Monolithic Refractories for Molten Aluminum Applications," Ceram. Eng. Sci. Proc. 8 (1987), 50.

165. A. N. Sokolov, R. M. Shumeiko, and P. D. Orekhov, "Corundum Hydraulically Setting Rammed Materials for Apparatus for the Vacuum Treatment of Steel," Ogneupory 1984, 5.

166. G. W. Shaffer, "Boron Nitride Containing Composites for Molten Metal Applications," p. 645 in Reference 26.

167. R. W. Brown, "1987 World Report on Silicon Carbide Blast Furnace Refractories; Usage, Composition, Research, Support and Cooling Practices," p. 83 in Reference 25.

168. D. Y. Peng, J. H. Li, S. Z. Liu, Y. Xu, Y. L. Wang, and Z. T. Wang, "Properties and Applications of Silicon Nitride Bonded Silicon Carbide Brick for Blast Furnaces," p. 101 in Ref. 26.

169. G. S. Dhupia, W. Krönert, and E. Goerenz, "SiC Monolithics for Waste Incinerators: Experiences, Problems, and Possible Improvements," p. 395 in Reference 39.

170. M. C. Langenohl and P. A. Beaulieu, "Silicon Carbide Monoliths for Incineration," p. 1194 in Reference 26.

171. F. Tanemura, T. Honda, and H. Kozuka, "Silicon-Carbide Projected Bricks in Rotary Cement Kiln for Tumbling Raw Mix and Preventing Ring Formation," p.640 in Reference 25.

172. K. Hara, T. Shinmei, K. Otsubo, and H. Miyaoka, "SiC Based Low Cement Castable for Cement Plant Such as NSP," p. 649 in Ref. 25.

173. S. C. Carniglia, C. A. Martinek, and J. E. Neely, "Low Temperature Deformation Test for Tar-Bonded Basic Refractories," Am. Ceram. Soc. Bull. 53 (1974), 539.

174. S. C. Carniglia, W. H. Boyer, and J. E. Neely, "Magnesium Oxide Refractories in the Basic Oxygen Steelmaking Furnace," p. 57 in MATERIALS SCIENCE RESEARCH, Vol. 5, W. W. Kriegel and H. Palmour, III, ed., 1971, Plenum Press, New York.

175. S-I. Odanaka, F. Hamamoto, S. Ishii, and T. Nakanishi, "Refractories for Electric Arc Furnaces in Japan," p. 314 in Reference 75.

176. T. Nakanishi, T. Sugimoto, and R. Nakagawa, "Use of Magnesia-Carbon Bricks for an Electric Arc Furnace Bottom," Taikabutsu 39 (1987), 528.

177. Y. Hayashi, Y. Amemiya, N. Uwai, and N. Shigematsu, "Calcia-Magnesia-Dolomite Refractories in VOD Ladle," p. 461 in Ref. 75.

178. J. Sauer, L. Hundt, and G. Mlaker, "Basic Linings in Steel-Casting and Steel-Treatment Ladles," Fachber. Huettenprax. Metallweiterverarb. 24 (1986), 844.

179. D. M. Schrader and L. L. Rankovic, "The Effect of Ladle Furnace Slags on Carbon-Bonded Refractories," Iron Steelmaker 15 (1988), 23.

180. Y. Naruse, S. Fujimoto, H. Shikano, M. Hori, T. Tanabe, and M. Kamiide, "Performance of Magnesia-Carbon Brick for LF Side Walls," Taikabutsu 36 (1984), 43.

181. M. Beurotte, G. Provost, and P. Tassot, "Evolution of the Steel Ladle Linings at USINOR Aciers Dunkerque. Technical Interest - Service Performance of Dolomite Bricks," p.337 in Reference 25.

182. Y. Sasajima, T. Yoshida, and S. Hayama, "Effect of Composition and Magnesia Particle Size in Alumina-Magnesia-Carbon Refractories," p. 586 in Reference 26.

183. E. Schulz and G. Klages, "Development of the Lining Life of the BOF Vessels at Thyssen Stahl AG Since the Introduction of the TBM-Process," p. 135 in Reference 75.

184. X. Zhong, G. Li, and Z. Chen, "The Application of Carbon-Bearing Magnesitic-Dolomite Refractories for BOF Linings," p. 161 in Reference 75.

185. J. Stradtmann, G. Mlaker, and R. C. Thomas, "Dolomitic Refractories in Secondary Steelmaking and Ladle Refining Processes," p.396 in Reference 75.

186. T. Rymon-Lipinski, "Some Investigation Results on Basic Refractories Containing Carbon. Part I. Grain Composition vs Corrosion Resistance of Materials," TIZ 107 (1983), 571.

187. T. Ohnishi, S. Kawasaki, H. Takagi, and H. Sugimoto, "Development and Improvement of Refractories for Hot Metal Pretreatment Furnace," p. 225 in Reference 25.

188. H. Schneider, "Properties of Mullite and of Mullite Composite Materials," p. 1627 in Reference 26.

189. M. Koltermann, "Refractories from the European Viewpoint - Development and Trend of Refractories in the Steel Industry," p. 63 in Reference 75.

190. A. J. Brewster, P. B. Jackson, G. B. Moore, and D. L. Rush, "European Experiences with High Alumina-Graphite in Torpedo Ladles," p. 181 in Reference 26.

191. X. Zhong, G. Sun, and X. Liu, "High Temperature Properties of Carbon-Bonded Corundum-Mullite-Zirconia Materials," p. 1803 in Reference 26.

192. T. Niihari, Y. Hongo, and J. Imai, "Increased Life of Castable Refractory for Tundish Box Cover," Taikabutsu 278 (1981), 134.

193. L. Stapper, "Resin Bonded SiC-Containing High-Alumina Brick for Torpedo Ladles," Radex Rundsch. 1987, 338.

194. T. Ochiai, H. Itoj, T. Ando, and K. Oikawa, "Resin-Bonded Taphole Mixes for Blast Furnaces," Sprechsaal 112 (1979), 755.

195. J. A. Cummins, S. A. Nightingale, and I. N. Mackay, "The Development of an Improved Quick Curing High Strength Resin Bonded Blast Furnace Taphole Clay," p. 133 in Reference 25.

196. S. Uchida, H. Katayama, S. Kohira, M. Nishi, H. Kyoden, and T. Fujiwara, "Open Ladle Bricks for Hot Metal Dephosphorization," Taikabutsu 38 (1986), 755.

197. A. Matsuo, S. Miyagawa, K. Ogasahara, T. Kawakami, H. Aratani, and T. Sato, "The Effect of Graphite Grain Size on the Corrosion Resistance of Aluminum Oxide-Silicon Carbide-Carbon Bricks for Torpedo Cars," ibid., p. 764.

198. N. Hiroki, K. Marukawa, S. Anezaki, I. Yamazaki, and Y. Murakami, "Refractories for Pretreatment of Hot Metal," p. 297 in Ref. 75.

199. Y. Naruse, S. Fujimoto, and H. Shikano, "Properties and Performance of Zirconia-Containing, Carbon-Bonded Plate Bricks," p. 652 in Reference 75.

200. S. B. Bonsall and D. K. Henry, "Wear Mechanisms in Alumina-Silicon Carbide-Carbon Blast Furnace Trough Refractories," p. 331 in Reference 39.

201. Y. Kimura, H. Shikano, and K. Hiragushi, "Progress of Alumina Silicon Carbide Graphite Refractories for Hot Metal Pretreatment," p. 239 in Reference 25.

202. A. G. Karaulov, I. N. Rudyak, T. F. Grushevayav, I. Palashenko, L. F. Levchenko, and V. I. Sokur, "Zirconium Dioxide Lining in an Induction Furnace," Ogneupory 1984, 55.

203. R. N. Singh and C. R. Kennedy, "Compatibility of Refractories with Simulated MHD Environment Consisting of a Molten-Coal-Slag/Alkali-Seed Mixture," Mater. Energy Syst. J. 3 (1982), 3.

204. Y. Watanabe, T. Ono, T. Yukinawa, and S. Sakamoto, "Development and Application of Monolithic Refractory Containing Magnesia Clinker," p. 494 in Reference 25.

205. E. Aoki, J. Kishimoto, E. Hosoi, and N. Osada, "Slaking of Basic Castable Refractories," Taikabutsu 37 (1985), 148.

206. I. Teoreanu and N. Ciocea, "Relations Between Composition, Structure and Properties in Chemically Bonded Refractory Castables," Szilikatip. Szilikattud. Konf., 13th, Proc. (1981), 359.

207. A. Cisar, "Controlling the Setting Rate in Phosphate-Spinel Systems," Ceram. Eng. Sci. Proc. 8 (1987), 21.

208. G. N. Zirczy, "Evaluation of Abrasion-Resistant Monolithic Refractories," ibid., p. 9.

209. R. Hofmann, "Phosphate-Containing Auxiliary Materials in Monolithic Refractory Mixes," Br. Ceram. Trans. J. 84 (1985), 189.

210. A. Racz and Mrs. A. Racz, "Properties of Phosphate-Bonded Refractory Materials as a Function of Raw Material Quality," Epitoanyag 38 (1986), 375.

211. E. Yorita, "Phosphate-Bonded Castable Refractories," Taikabutsu 40 (1988), 218.

212. D. R. Lankard, "Evolution of Monolithic Refractory Technology in the United States," p. 46 in Reference 39.

213. G. MacZura, L. D. Hart, R. P. Heilich, and J. E. Kopanda, "Refractory Cements," Ceram. Eng. Sci. Proc. 4 (1983), 46.

214. G. MacZura, J. E. Kopanda, and F. J. Rohr, "Calcium Aluminate Cements for Emerging Castable Technology," p. 285 in Ref. 39.

215. P. H. Havranek, "Recent Developments in Abrasion- and Explosion-Resistant Castables," Am. Ceram. Soc. Bull. 62 (1983), 234.

216. V. K. Singh, "High-Alumina Refractory Castables with Calcium Aluminate Binder," Mater. Sci. Lett. J. 8 (1989), 424.

217. E. Aoki, J. Kishimoto, E. Hosoi, and N. Moritani, "Corrosion of Castable Refractories by Alkali (Potassium Carbonate)," Taikabutsu 35 (1983), 260.

218. K. Hara, E. Hosoi, and N. Moritani, "Repair of a Lime Kiln by Using Castable Refractories," ibid. 39 (1987), 398.

219. A. Matsuo, S. Miyagawa, M. Nambo, and M. Kuwayama, "Improvement of Zircon Castable for Teeming Ladle," ibid. 40 (1988), 279.

220. V. K. Singh, M. M. Ali, and U. K. Mandal, "Formation Kinetics of Calcium Aluminates," Am. Ceram. Soc. J. 73 (1990), 872.

221. D. Lankard, D. W. Lease, and P. J. Lankard, "Precast Refractory Concrete," p. 1107 in Reference 26.

222. K. Shimada, F. Isomura, and S. Matsuo, "Development of Basic Castable Refractories for Teeming Ladles," Taikabutsu 39 (1987), 629.

223. V. V. Primachenko, L. M. Kolesnikov, T. A. Zadorozhnaya, and M. M. Kostev, "Vibrationally Cast High-Alumina Feeder Refractories for Production of Glass Containers," Tekhnol. Nov. Vidov Ogneuporov 1986, 17.

224. S. Banerjee, "Application of Vibratory Castables in Petrochemical Industries," Ceram. Eng. Sci. Proc. 7 (1986), 236.

225. J. R. Peterson, P. E. Schlett, and J. J. Tanke, "Erosion Resistant, Heat Insulating Refractories for Vibration Casting in Oil Refining, Fluid Solids Applications," p. 943 in Reference 26.

226. S. F. Rahman, "Advances in Vibration-Cast Refractories for Application as Abrasion Resistant Linings," p. 955 in Ref. 26.

227. J. W. Stendera, "The Properties and Applications of Dolomite Ramming Mixes," p. 388 in Reference 39.

228. N. Hiroki, G. Muta, T. Miki, A. Watanabe, and Y. Suzuki, "Monolithic Permanent Lining of Converter by Gunning Installation," Taikabutsu 40 (1988), 492.

229. G. G. Biever and R. E. Kilgore, "Characterization of Reduced-Cement, High-Strength, Abrasion-Resistant Gunning Castable Refractories," p. 1127 in Reference 26.

230. B. Brezny and P. Schroth, "The Effect of Gunning on Magnesia-Graphite Refractories," Sprechsaal 115 (1982), 311.

231. W. M. Siegl and A. Olszewski, "Slurry Gunning Mixes for Tundishes," Fachber. Huettenprax. Metallweiterverarb. 25 (1987), 920.

232. T. Ishibashi, T. Tamehiro, K. Yamada, and T. Suzuki, "Adhesion of Gunning Material for Blast Furnaces," Taikabutsu 37 (1985), 160.

233. Y. Shinohara, H. Yaoi, and K. Sugita, "Recent Progress in Monolithic Refractories Usage in the Japanese Steel Industry," p. 1 in Reference 39.

234. J. Wojsa, "Basic Hot Gunning Materials - Study on their Bonding Mechanism," Szilikatip. Szilikattud. Konf., 13th, Proc. (1981), 381.

235. Y. Tozaki, A. Takahashi, H. Ikemiya, D. Katase, T. Yagi, and M. Kataoka, "Development of Gunning Materials for Torpedo Ladles," Taikabutsu 37 (1985), 723.

236. W. M. Siegl, "Composition and Application of Basic Refractory Maintenance Mixes," Radex Rundsch. 4 (1985), 706.

237. M. J. Rudolf, P. Steinmetz, C. Gleitzer, C. Guenard, and R. Adam, "The Repair of Steelmaking Converter Linings by Flame Gunning of Magnesia," Rev. Int. Hautes Temp. Refract. 20 (1983), 101.

238. T. Murahashi, K. Sugita, H. Ishimatsu, and K. Hamai, "Flame Gunning Repair for BOF," p. 325 in Reference 75.

239. J. J. Marino, "Future BOF Refractory Linings and Maintenance," p. 345 in Reference 75.

240. W. Krönert, "Recent Progress in the Use of Monolithic Refractories in Europe," p. 21 in Reference 39.

241. R. N. Shinmi and J. A. C. Nogueira, "Low-Cement Concretes in Iron and Steel Manufacture," Metalurgia (Sao Paulo) 44 (1988), 568.

242. U. Schuhmacher, W. Kroenert, and A. Seltveit, "Investigations on Low-Cement and Ultralow-Cement Refractory Castables," Spez. Ber. Kernforschungsanlage Juelich 446 (1988), 221.

243. P. H. Havranek and E. Olsen, "New Experiences with Monolithic Refractory Linings in Rotary Cement Kilns," Zem.-Kalk-Gips B 36 (1983), 490.

244. M. Nishi, G. Nakatani, K. Kanai, and H. Ito, "Application of Aluminum Oxide-Silicon Oxide Casting Materials for Blast Furnace Iron Trough," Taikabutsu 34 (1982), 88.

245. R. J. Volk, "Ultralow Cement Castables," Iron Steel Eng. 63 (1986), 44.

246. T. Eguchi, I. Takita, J. Yoshimoto, S. Kiritani, and M. Sato, "Low-Cement-Bonded Castable Refractories," Taikabutsu 40 (1988), 200.

247. B. Clavaud, J. P. Kiehl, and R. D. Schmidt-Whitley, "15 Years of Low Cement Castables in Steelmaking," p.589 in Reference 75.

248. E. P. Weaver, R. W. Talley, and A. J. Engel, "High-Technology Castables," p. 219 in Reference 39.

249. B. Clavaud, J. P. Kiehl, and J. P. Radal, "A New Generation of Low-Cement Castables," p. 274 in Reference 39.

250. S. Banerjee, R. V. Kilgore, and D. A. Knowlton, "Low-Moisture Castables: Properties and Applications," p. 257 in Reference 39.

251. L. P. Krietz and R. E. Fisher, "Field Performance and Fracture Behavior of Low Cement, Conventional and High Cement, Low Moisture Castables," p. 1116 in Reference 26.

252. Y. Hongo and M. Miyawaki, "Physical Properties of a Pure Alumina Castable Refractory," Taikabutsu 38 (1986), 460.

253. K. Yamamoto, "Quality Control of Microsilica and Microsilica Effects in Refractories," ibid. 39 (1987), 505.

254. T. Kawakani, M. Yoshimura, and J. Yamamoto, "Properties of Silica Flour," ibid. 37 (1985), 140.

255. T. Kawakami, M. Yoshimura, and J. Yamamoto, "Properties of Silica Flour," Taikabutsu Overseas 5 (1985), 21.

256. E. Yorita, "Silicate-Bonded Castable Refractories," Taikabutsu 40 (1988), 221.

257. A. Seltveit, G. S. Dhupia, and W. Kroenert, "Microstructural Aspects of Microsilica-Blended High Alumina Castables," Ceram. Eng. Sci. Proc. 7 (1986), 243.

258. K. Shimada and S. Sakaki, "Improvement of Tundish Weir Castable Refractories," Taikabutsu 40 (1988), 178.

259. Y. Naruse, K. Semba, S. Kiwaki, and M. Mishima, "Behavior of Deflocculants in Aluminum Oxide-Silicon Oxide Binary Disperse System," ibid. 34 (1982), 65.

260. Y. Naruse, S. Fujimoto, S. Kiwaki, and M. Mishima, "Effect of Some Deflocculants on Calcium Aluminate Cement and their Application to Castable Refractories," ibid., p. 499.

261. Y. Naruse, S. Fujimoto, S. Kiwaki, and M. Mishima, "Progress of Additives in Monolithic Refractories," p. 245 in Reference 39.

262. C-C. Chou, H. Sumimura, T. Kaneshige, Y. Hamazaki, and E. Yorita, "Fluidity and Segregation of Pure Alumina Refractory Castables," p. 904 in Reference 25.

263. V. Gottardi, M. Guglielmi, A. Tiziani, and G. Carturan, "AZSC Refractories Prepared from Gels," Non-Cryst. Solids J. 43 (1981), 105.

264. D. X. Li and W. J. Thomson, "Mullite Formation Kinetics of a Single-Phase Gel," Am. Ceram. Soc. J. 73 (1990), 964.

265. R. Pompe, R. Carlsson, and A. Sandrén, "On the Reactions Involving Refractories for Aluminum Casting," p. 906 in Reference 26.

266. D. P. Chakraborti, P. Nandi, L. Tiwari, M. S. Mukhopadhyay, and K. C. Chatterjee, "Microstructural Development and Improvements in Mechanical Properties of Reaction Sintered Alumina-Zircon Composites," p. 1652 in Reference 26.

267. S. Odanaka, K. Nakashima, M. Toh, and H. Nagata, "Effect of Alumina Powder and Silica Flour on Fluidity of Castable Refractories," Taikabutsu 40 (1988), 498.

268. S. Yoshino, K. Ichikawa, M. Katayama, and T. Kaneshige, "Flow Properties of Castable Refractories for Blast Furnace Troughs," Taikabutsu Overseas 4 (1984), 54.

269. S. Kazama and N. Kokaji, "On Microfine Calcined Alumina Powders and Flow Behavior of Prepared Unshaped Refractories," Taikabutsu 33 (1981), 630.

270. H. Kyoden, K. Ichikawa, Y. Hamazaki, and T. Kaneshige, "Effect of Grain Shape on Rheological Properties (Part 2)," Taikabutsu Overseas 5 (1985), 26.

271. T. Kawakami, T. Yamane, and N. Muroi, "Influence of Silicon Carbide Properties on Fluidity of Casting Trough Materials," Taikabutsu 35 (1983), 226.

272. J. Chappuis, J. P. Bayoux, and A. Capmas, "A Comprehensive Study of the Rheology of Aluminous Cement Pastes," p. 1171 in Ref. 26.

273. T. Kawakami, K. Aratani, S. Hasegawa, and M. Sakaguchi, "Effect of Slag Infiltration on Erosion of the Joints of Zircon Bricks," Taikabutsu 39 (1987), 632.

274. S. C. Carniglia, "Construction of the Tortuosity Factor from Porosimetry," J. Catal. 102 (1986), 401.

275. T. Ishino and A. Yamaguchi, "Wear Factors of Checker Bricks in Glass-Melting Furnace Regenerators," Taikabutsu 40 (1988), 390.

276. B. Schmalenbach and T. Weichert, "Factors Influencing Wear in Areas of Soda-Lime Glass Tanks and Lining Recommendations," Glass 65 (1988), 16.

277. C. N. Satterfield, MASS TRANSFER IN HETEROGENEOUS CATALYSIS, 1970, M.I.T. Press, Cambridge, MA.

278. M. L. Van Dreser and R. H. Cook, "Deterioration of Basic Refractories in a Glass Regenerator," A. Cer. Soc. Bull. 40 (1961), 68.

279. L. Wu, "Formation of Drops and Corrosion Cavities on Silica Crown Bricks," Boli Yu Tangci 15 (1987), 24.

280. J. B. Tak and D. J. Young, "Sulfur Corrosion of Calcium Aluminate Bonded Castables," Am. Ceram. Soc. Bull. 61 (1982), 725.

281. B. Schmalenbach and T. Weichert, "Checker Material of Regenerative Chambers in Soda-Lime Glass-Melting Furnaces - Corrosion Mechanism and Lining Recommendations," Sprechsaal 120 (1987), 386.

282. K. Nobuhara, H. Nishiyama, and K. Matsuda, "Use of Spinel Checker Bricks for Glass Melting Furnace (Regenerators)," Taikabutsu 40 (1988), 355.

283. H. Ishii, M. Nagafune, I. Tsuchiya, and T. Kawakami, "Reaction Between Magnesia and Carbon at High Temperature," p. 1704 in Reference 26.

284. E. Criado, A. Pastor, and R. Sancho, "Data Base on Refractory Materials for Iron and Steelmaking," p. 169 in Reference 26.

285. International Organization for Standardization (ISO), 1 Rue de Varembe, Case Postale 56, Geneva 20 CH-1121, Switzerland.

286. V. G. Panteleev, K. S. Ramm, and V. M. Darovskii, "Cordierite-Mullite Materials for the Porcelain-Faience Industry," Steklo Keram. 1983, 15.

287. I. Oishi, K. Ogasahara, H. Ishii, and H. Kasai, "Improvement of Zircon Bricks for Steel Ladles," Taikabutsu 35 (1983), 495.

288. E. T. Kim, M. J. Chae, I. K. Kim, J. S. Kim, and E.M. Lee, "Application Results of New Zircon Ladle Brick Utilizing Low Expansion Korean Quartzite," p. 513 in Reference 26.

289. K. Asano, H. Fukuoka, and K. Hiragushi, "Corrosion of Basic Refractories by CaO-SiO_2-Fe_2O_3-MgO Slags and Application of Magnesia-Carbon Brick to LD Converters," Int. Feuerfest-Kolloq., 27th, Proc. 1984, 453.

290. I. Oishi, K. Ogasahara, T. Yamaguchi, and Y. Sakamoto, "Transition of Lance Lining Refractories for Desulfurization in Torpedo Cars," Taikabutsu 34 (1982), 91.

291. E. Olsen and U. Randaas, "A Refractory Castable for Potline and Casthouse," Aluminium (Duesseldorf) 63 (1987), 879.

292. G. Moertl, B. Grabner, and U. Huetter, "Permeable Elements for LD Vessels and Electric Arc Furnaces," Radex Rundsch. 1 (1988), 481.

293. V. G. Stognei, V. S. Lagunov, and V. V. Trapeznikov, "Porous Cooling of Lined Baffles of Industrial Kilns," Ogneupory 5 (1988), 29.

294. T. Mimori and H. Maeno, "Development of Porous Cordierite Tubes," p. 1034 in Reference 26.

295. T. R. Kleeb and J. A. Caprio, "Properties and Service Experience of Organic Fiber-Containing Monoliths," p. 149 in Reference 39.

296. J. L. Turner, Jr., and D. M. Myers, "The Development of Dry Refractory Technology in the United States," p. 161 in Ref. 39.

297. K. N. Singh and R. S. Hoffer, "Successful Implementation of Metal-Free Low-Moisture Castables in Blast Furnace Troughs and Runners," p. 193 in Reference 26.

298. V. G. Borisov, S. A. Stegantsev, and L. L. Vanicheva, "Carbon-Containing Binders in Basic Refractories," Proizvod. Ogneuporov 9 (1981), 13.

299. E. Yorita, "Resin-Bonded Castable Refractories," Taikabutsu 40 (1988), 223.

300. N. G. Semanov, I. P. Polyakov, L. G. Grankina, V. I. Serenkov, I. M. Elshin, V. S. Kozhevnikov, K. S. Abduzhabakov, and L. V. Kamysheva, "Furan Corrosion-Resistant Materials for the Chemical Industry," Plast. Massy 3 (1983), 50.

301. A. Watanabe, T. Okamura, Y. Mizuta, M. Kusakari, and Y. Wakabayashi, "Magnesia-Carbon Monolithic Refractories Bonded with Resin," Taikabutsu 37 (1985), 150.

302. T. V. Kin, Y. A. Minaev, A. D. Sotskov, V. A. Mirko, G. V. Pol'shikov, and G. V. Yust, "Improvement of the Quality of Refractories for Converter Lining," Ogneupory 1988, 31.

303. A. Gardziella and J. Suren, "Selection Criteria for Phenolic Resins as Binders and Carbon-Forming Agents in Refractory Products," Fachber. Huettenprax. Metallweiterverarb. 26 (1988), 308.

304. O. Terenyi, "Strength of Refractory Kiln Furniture Made of Silicon Carbide," InterCeram. 32 (1983), 36.

305. W. J. Kivala and H. E. Wolfe, "Interim Study of a Chrome-Free High-Efficiency Checker Setting in a Container Glass Furnace," Ceram. Eng. Sci. Proc. 9 (1988), 315.

306. F. Tanemura, T. Honda, H. Kozuka, K. Naziri, R. D. Schmidt-Whitley, and K. Wieland, "The Behavior of Dolomite Brick Linings in the Firing Zone of Cement Rotary Kilns," Taikabutsu 40 (1988), 110.

307. H. Nishikawa, "Fusion Cast Refractories for the Iron and Steel Industry," IRMA J. 15 (1982), 15.

308. M. Nishi, H. Kato, T. Anzai, U. Nagayama, H. Kyoden, K. Ichikawa, Y. Hamazaki, and R. Nakamura, "Investigation of Basic Castable Refractories for Teeming Ladles," Taikabutsu 37 (1985), 29.

309. D. I. Gavrish, J. A. Polonskiy, and G. E. Solovushkova, "Silicon Dioxide Based Refractories for Continuous Steel Casting in Ferrous Metallurgy," p. 765 in Reference 75.

310. T. Yagi, M. Sekime, H. Hori, and Y. Matsuo, "Acid-Resistant Castable with Water Resistance," Taikabutsu 39 (1987), 394.

311. S. Takeshita, S. Hasegawa, H. Aratani, and T. Kawakami, "Evaluation of Thermal Shock Resistance of Alumina-Graphite Materials," ibid. 38 (1986), 782.

312. H. P. Zander, "Improved Energy Use and Higher Economy in the Ceramics Industry by Using Ceramic Fibers," Sprechsaal 118 (1985), 326.

313. W. Kroenert, "Evaluation and Use of Ceramic High-Temperature Fibers as a Refractory Material: Classification, Preparation, Use and Use-Limiting Temperature," Feuerfesttech.: Werkst., Rohst., Neue Entwickl., 1984, 134.

314. B. Courrier, C. Gleitzer, G. Poirson, and L. Sebillaud, "A Study of the Recrystallization of Refractory Fibers," Rev. Int. Hautes Temp. Refract. 19 (1982), 9.

315. M. Schulte, R. Klima, R. Bredehoeft, and W. Beier, "Heat Insulation of Intermittently Operated Reheating Furnaces with Ceramic Fibrous Insulating Materials," Stahl Eisen 108 (1988), 553.

316. R. Ganz and W. Kroenert, "Crystallization Behavior of High-Temperature Ceramic Fibers of the Aluminum Oxide-Silicon Dioxide System," InterCeram 31 (1982), 136.

317. J. Kutzendorfer, D. Dvorakova, and M. Kozel, "Chemical Resistance of Fibrous Aluminosilicate Refractories," Stavivo 64 (1986), 144.

318. G. Flessner and G. Spiess, "Porital 4-153, a New Lightweight Heat-Insulating Brick," Sprechsaal 116 (1983), 865.

319. I. P. Rubkevskii, "Heat-Insulating Materials for High-Temperature Apparatus," Stroit. Mater. 2 (1986), 21.

320. L. A. Dergaputskaya, A. N. Gaodu, and L. G. Litvin, "Anorthite Light-Weight Refractories for Service in Carbon-Containing Media," Ogneupory 1980, 40.

321. N. V. Pisareva, A. N. Gaodu, V. P. Rakina, S. I. Kulaenko, A. K. Gerasimenko, L. A. Inyushina, and S. A. Padalko, "Grog-Kaolin Lightweight Articles of Apparent Density 0.8-0.9 g/cm^3," ibid. 1982, 15.

322. F. F. Sigulinski, I. Stamenkovic, P. Martinovic, R. Stefanovic, and V. Vucovic, "Theoretical and Practical Approach to the Selection of the Granulometric Composition for Permeable Refractory Synthesis," Ceramurgia 9 (1979), 51.

323. V. L. Bulakh, R. F. Rud, T. S. Penzeva, and B. V. Belokon, "Tests of Unfired Siliceous Products as Linings of Steel-Teeming Ladles for Electrically Melted Steel," Ogneupory 1987, 40.

324. M. Wismer, "Inorganic Foams," Plast. Foams Monogr. 1 (1973), 805.

325. G. Popa, C. Dragomir, A. Szabo, M. Diaconescu, and C. Enastescu, "Heat-Insulating Products Prepared by Chemical Foaming," Cercet. Metal. 27 (1986), 47.

326. V. I. Kozdoba, L. D. Pilipchatin, E. Bauman, V. I. Shubin, V. I. Shabanov, V. M. Sergeeva, L. V. Gritsaenko, A. I. Ryabov, R. S. Povarova, et al., "Production of High-Strength Lightweight Refractories," Ogneupory 1985, 42.

327. V. I. Shubin, V. I. Kozdoba, and L. D. Pilipchatin, "Expansion of Refractory Clays and Kaolins Containing Metal Sulfate Additives," ibid. 1982, 48.

328. T. A. Danilova and P. G. Labozin, "Heat-Resistant Cellular Refractory," ibid. 1983, 36.

329. Y. L. Krasulin, V. T. Timofeev, A. B. Ivanov, and S. M. Barinov, "Strength of Porous Material Made from Refractory Oxides," ibid. 1978, 48.

330. H. Ninomiya and H. Itaya, "Fibrous Fire-Resistant Material," Kogyo Kanetsu 22 (1985), 25.

331. K. Zakrzewska, "Polycrystalline Alumina Fibers for Applications at Temperatures Up to 1600 Degree C," Mater. Ogniotrwale 35 (1983), 31.

332. M. Hayase, H. Asami, H. Asakura, and T. Saeki, "Development of Zirconia Fiber and its Application," Shinagawa Giho 31 (1988), 129.

333. A. Smrcek, "SIBRAL - Manufacture, Properties, and Varieties," Stavivo 63 (1985), 360.

334. R. D. Smith, "Thermal Stability of Polycrystalline Fiber/Ceramic Fiber Blended Product Forms," p. 607 in Reference 75.

335. L. E. Olds, W. C. Miller, and J. M. Pallo, "High Temperature Alumina-Silicate Fibers Stabilized with Chromic Oxide," Am. Ceram. Soc. Bull. 59 (1980), 739.

336. C. N. McGarry and T. M. Wehrenberg, "Update and Overview of Sintered Glass Contact Refractories for Fiber Glass," p.826 in Reference 26.

337. H. Ninomiya and G. Kurihara, "High-Temperature Behavior of Alumina Fiber," Taikabutsu 38 (1986), 545.

338. N. J. Rossi and W. A. Schreifels, "CERABOND II: Spray Applied Refractory Fiber Insulation," Int. Symp. Adv. Refract. Metall. Ind., 1st, Proc. 1988, 267.

339. J. Tiemann, "Unshaped Refractories for Cement Kilns," Cim., Betons, Platres, Chaux 770 (1988), 17.

340. W. Schulle, R. Wolfgang, and T. Prehl, "Industrial Use and Evaluation of Aluminosilicate Fibers," Giessereitechnik 31 (1985), 11.

341. Z. Hrabe, S. Chromy, V. Jesenak, and F. Sevcik, "Effect of the Composition of the Atmosphere in the Kiln on the Crystallinity of Aluminosilicate Fibers," Stavivo 61 (1983), 160.

342. P. Dietrichs and W. Kroenert, "The Effect of Different Gas Atmospheres on Ceramic Fiber Materials," InterCeram 31 (1982), 223.

343. J. Kutzendorfer and B. Zbuzek, "High-Temperature Shrinkage and Phase Change of Refractory Fibers," Freiberg. Forschungsh. A681 (1983), 63.

344. J. Day and F. Mucciardi, "Ladle Insulation - An Overview," p. 453 in Reference 26.

345. Y. Naruse, Y. Hoshino, and T. Tanaka, "Silica Bricks for Coke Ovens," Taikabutsu Overseas 2 (1982), 110.

346. E. A. Thomas, D. G. Patel, V. Shah, and T. Weichert, "Trends in Refractory Usage in the Glass Industry," p. 743 in Reference 26.

347. H. Ambs, "Fired and Chemically Bonded Basic Bricks in Nonferrous Metal Industry," Fachber. Huettenprax. Metallweiterverarb. 26 (1988), 429.

348. Y. Naruse, "Future Trend and Development of Refractories Industry in Japan," p. 3 in Reference 25.

349. D. H. Hubble, "Factors Affecting Life of Steel Ladles," p. 416 in Reference 26.

350. H. Le Doussal and L. Lecrivain, "Evolution in Refractory Products Used in Slide Valve Plates," p.670 in Reference 75.

351. H. J. S. Kriek, "Andalusite as a Refractory Material in Steel Making," p. 576 in Reference 75.

352. H. J. S. Kriek, "Recent Developments with Andalusite as a Refractory Material in Steelmaking," p. 480 in Reference 25.

353. T. Taniguchi, M. Ishikawa, J. Ohba, and H. Yamashita, "Development of Dense Castables for Blast Furnace Main Troughs," Taikabutsu 37 (1985), 172.

354. B. Clavaud, G. Landman, J. W. Marjerrison, and C. Turrel, "High-Performance Materials for a Blast Furnace Cast House," Refract. J. 58 (1983), 14, 16.

355. K. Shimada, A. Doi, and K. Kono, "Development of Refractories for Torpedo Ladles with Hot Metal Pretreatment," p. 266 in Reference 25.

356. A. Matsuo, S. Miyagawa, and M. Nambu, "Improvement in Refractory Lining of Torpedo Ladle for Hot Metal Pretreatment," p. 121 in Reference 26.

357. A. Kuribayashi, T. Takahashi, S. Sudo, T. Watanabe, and S. Asano, "Improvement of Steel-Desulfurization Lance Pipe," Taikabutsu 38 (1986), 219.

358. J. Q. Lu, X. G. Sun, and Y. M. Shen, "The Application of High Purity Alumina Castables in Gas Reforming Furnaces," p. 940 in Reference 26.

359. J. A. Caprio, "Third Generation FCCU Refractories," Hydrocarbon Process., Int. Ed., 65 (1986), 51.

360. J. L. Hill, A. R. Davis, P. E. Schlett, and J. R. Peterson, "Development of High Strength Insulating Castables for Hydrocarbon Industries," p. 929 in Reference 26.

361. R. Guirand and J. Garestier, "Use of Ceramic Fibers in Refineries. Part II. Experience of French Shell on the Use of Refractory Ceramic Fibers," Pet. Tech. 267 (1979), 33.

362. A. Noguchi, K. Hara, and I. Kenmochi, "Application of Dolomite Brick to Cement Rotary Kiln," Taikabutsu 40 (1988), 108.

363. J. Stradtmann, R. C. Thomas, and Y. Yasuda, "An Update on the Use of Dolomitic Refractories in the Cement Kiln," p. 597 in Reference 25.

364. T. Miller, D. Griffin, S. Ishii, and H. Kusnose, "The Development and Use of Dolomite-Zirconia Brick in Cement Rotary Kilns," p. 609 in Reference 25.

365. S. Cui, J. Li, P. Qu, W. Zhao, Q. Lu, and S. Zhao, "Reaction of Titania-Rich Slag with Magnesia-Carbon Brick," p.561 in Ref. 25.

366. J. Stradtmann, G. Mlaker, and R. C. Thomas, "Dolomitic Refractories in Secondary Steelmaking and Ladle Refining Processes," p. 396 in Reference 75.

367. S. Nagai, T. Matsumura, K. Hosokawa, M. Geji, and M. Ishizuka, "Alumina-Zircon Porous Plug," Taikabutsu 38 (1986), 785.

368. Y. Naruse, K. Furumi, T. Yagi, Y. Kamata, and I. Takita, "Effect of Gas Bubbling on the Erosion of Basic Bricks," ibid. 34 (1982), 396.

369. Y. Miyagawa, F. Hoshi, K. Fujii, and K. Koyago, "Outline of Refractories for RH Degasser in Kure Works," ibid. 36 (1984), 657.

370. E. Yorita, H. Sugimoto, and H. Kiriyama, "Development of Injection Materials for RH," ibid. 38 (1986), 854.

371. T. Nakamoto, N. Komatsu, T. Ishibashi, and T. Kitai, "High Alumina Bricks for the Bottom of Steel Ladles," ibid. 35 (1983), 502.

372. A. J. Owen and J. Ford, "Experience with Basic Linings in Steel Teeming Ladles," p. 507 in Reference 75.

373. P. Williams, P. Dawson, and T. W. Lythe, "Further Developments in the Introduction of Basic Refractories into Teeming and Secondary Steelmaking Ladles," p. 307 in Reference 25.

374. Y. A. Pirogov, "Phase Relationship and Service Behavior of Slinging Linings in Steel Teeming Ladles," p. 502 in Ref. 75.

375. T. Taniguchi, M. Otani, H. Ueno, and H. Muraoka, "Development of Dense Castable Refractories for Tundish of Steel," p. 683 in Reference 75.

376. F. Tanemura, K. Yajima, S. Ohta, and Y. Mizuno, "Properties and Applications of High-Alumina Castables for Tundishes," p. 695 in Reference 75.

377. F. Tanemura, K. Yajima, and Y. Mizuno, "Monolithic Refractories in Tundish Linings," Taikabutsu 34 (1982), 106.

378. M. Otani, H. Muraoka, H. Ueno, and K. Watanabe, "Low Cement Castables for Larger Tundish Linings," p. 425 in Reference 25.

379. I. Elstner, P. Jeschke, and H. Leistner, "New Techniques in Continuous Casting and Slide Gates Using MgO-Stabilized Zirconia Refractories," p. 639 in Reference 75.

380. N. Reitsema and P. W. Wright, "The Decomposition of Silicate Refractories in Contact with Molten Steel," p. 795 in Ref. 75.

381. O. A. Rhyzhov, L. N. Ertseva, E. I. Rukhtaeva, E. A. Algunova, and E. I. Ezhov, "Effect of the Structure of Refractories on Flame Gunning Characteristics," Ogneupory 1988, 44.

382. J. D. Panda, N. Sahoo, and S. K. Chowdhury, "High Thermal Conductivity and Abrasion Resistant Silica Bricks for Coke Ovens," p. 229 in Reference 26.

383. H. K. Koschlig, "Refractory Materials for Modern Large-Capacity Coke Oven Batteries," p.244 in Reference 26.

384. S. B. Larson and R. B. Videtto, "Improved Brick Performance in Carbon Baking Flues," Int. Symp. Adv. Refract. Metall. Ind., 1st, Proc. 1988, 215.

385. A. J. Eckel and R. C. Bradt, "Thermal Expansion of Laminated, Woven, Continuous Ceramic Fiber/Chemical-Vapor-Infiltrated Silicon Carbide Matrix Composites," Am. Ceram. Soc. J. 73 (1990), 1334.

386. K. Hayashi and M. Wakamatsu, "Measurement of Thermal Constants for Castable Refractories by Transient Hot Wire Method," p. 983 in Reference 25.

387. G. C. Padgett and F. T. Palin, "Test Methods for Monolithic Materials," p. 81 in Reference 39.

388. M. S. Crowley and J. S. Young, "Thermal Conductivity of Monolithic Refractories," Am. Ceram. Soc. Bull. 67 (1988), 1196.

389. G. Routschka, "Standard Values for the Thermal Conductivity of Refractory Castables," Keram. Z. 39 (1987), 858.

390. W. Schulle and J. Kutzendoerfer, "The Dependence of the Thermal Conductivity and Strength on the Average Pore Diameter of Lightweight Fireclay Bricks," Silikattechnik 39 (1988), 3.

391. H. W. Hennicke, P. Jeschke, and M. Neuenburg, "Properties of Lightweight Foamed Refractories: Measurement and Computation of Thermal Conductivity," Keram. Z. 39 (1987), 602.

392. M. I. Aivazov and I. A. Domashnev, "Dependence of Electrical and Thermal Conductivities of Hot-Pressed Titanium Nitride Samples on Porosity," Poroshkovaya Met. 8 (1968), 51.

393. S. K. Rhee, "Porosity-Thermal Conductivity Correlations for Ceramic Materials," Mater. Sci. Eng. 20 (1975), 89.

394. M. A. Pereyo and K. J. Moody, "Ceramic Fiber Lining Systems: Solutions to Various Heat Containment Environments," p. 1367 in Reference 26.

395. K. Hayashi, Y. Fujino, and T. Nishikawa, "Thermal Conductivity of Alumina and Zirconia Fibrous Insulators at High Temperatures," Yogio Kyokaishi 91 (1983), 449.

396. K. Hayashi, H. Okawa, and T. Nishikawa, "Prediction of Thermal Conductivity of Ceramic Fibrous Insulator," ibid. 95 (1987), 893.

397. W. C. Miller and T. A. Scripps, "Relating Apparent Thermal Conductivity to Physical Properties of Refractory Fiber," Am. Ceram. Soc. Bull. 61 (1982), 711.

398. T. W. Tong and C. L. Tien, "Analytical Models for Thermal Radiation in Fibrous Insulations," J. Thermal Insul. 4 (1980), 27.

399. D. A. Stewart and D. B. Leiser, "Characterization of the Thermal Conductivity for Fibrous Refractory Composite Insulations," Ceram. Eng. Sci. Proc. 6 (1985), 769.

400. E. V. Vazhenin, G. A. Ilyutikova, T. V. Dobrova, K. M. Shvarev, and V. A. Kudryavtsev, "Integral Emissivity and Thermal Conductivity of Fibrous Refractory Materials," Ogneupory 1984, 37.

401. M. S. Crowley, "Heat Transfer in Ceramic Fiber Systems," p. 1354 in Reference 26.

402. K. Hayashi, Y. Okamoto, M. Wakamatsu, and T. Nishikawa, "Determination of Thermal Properties of Castable Refractories by Transient Hot Wire Method," Mem. Fac. Eng. Des., Kyoto Inst. Technol., Ser. Sci. Technol. 36 (1987), 57.

403. G. Routschka, "Thermal Conductivity of Refractory Castables," InterCeram 37 (1988), 24.

404. W. Nunes Dos Santos and J. deS. Cintra Filho, "Effect of Temperature on the Thermal Conductivity and Specific Heat of Ceramic Materials ---," Ceramica (Sao Paulo) 33 (1987), 198.

405. CERAMIC SOURCE '90, pp. 290-381 (re-issued annually), American Ceramic Society, Westerville, OH.

406. F. A. McClintock, "Statistics of Brittle Fracture," p. 93 in Vol. 1 of Reference 417.

407. S. B. Batdorf, "Fundamentals of the Statistical Theory of Fracture," p. 1 in Vol. 3 of Reference 417.

408. S. C. Carniglia, "Petch Relation in Single-Phase Oxide Ceramics," Am. Ceram. Soc. J. 48 (1965), 580.

409. J. F. Lynch, C. G. Ruderer, and W. H. Duckworth, "Engineering Properties of Ceramics," BMI Report AFML-TR-66-52 (1966), Battelle Memorial Institute, Columbus, OH.

410. D. J. Bray, "Creep of Refractories: Mathematical Modeling," p. 69 in Reference 39.

411. S. C. Carniglia, "Working Model for Porosity Effects on the Uniaxial Strength of Ceramics," Am. Ceram. Soc. J. 55 (1972), 610.

412. G. R. Rigby, "Mechanical Properties of Basic Bricks," Brit. Ceram. Soc. Trans. 69 (1970), 189.

413. W. R. Alder and J. S. Masaryk, "Compressive Stress/Strain Measurement of Monolithic Refractories at Elevated Temperatures," p. 97 in Reference 39.

414. W. R. Alder and J. S. Masaryk, "Elevated Temperature Stress-Strain Measurements on Refractories,", p. 702 in Reference 25.

415. E. B. Allison, P. Brock, and J. White, "The Rheology of Aggregates Containing a Liquid Phase with Special Reference to the Mechanical Properties of Refractories at High Temperatures," Brit. Ceram. Soc. Trans. 58 (1959), 495.

416. A. Yamaguchi and E. Kato, "Liquid and Bond Structure in Refractories,", p. 209 in Reference 75.

417. R. C. Bradt, D. P. H. Hasselman, A. G. Evans, and F. F. Lange, ed., FRACTURE MECHANICS OF CERAMICS, Vols. 1-8, 1974-86, Plenum Press, New York.

418. T. E. Adams, D. L. Landini, C. A. Schumacher, and R. C. Bradt, Micro- and Macrocrack Growth in Alumina Refractories," Am. Ceram. Soc. Bull. 60 (1981), 730.

419. J. Ohba, "Particle Size Distribution of Dense Castable Refractories and Spalling Resistance," Taikabutsu 40 (1988), 181.

420. H. Ishii, I. Tsuchiya, H. Takahashi, T. Kawakami, and H. Toritani, "Deformation Behavior of Refractories for LD-Converter at High Temperature Under Load," p. 367 in Reference 75.

421. B. Jackson and T. J. Partridge, "Properties Required for Arc Furnace Roof Refractories," Iron Steel Eng. 6 (1984), 33.

422. G. C. Padgett and D. J. Bettany, "The Relaxation Behavior of Refractories," Brit. Ceram. Soc. Trans. 73 (1974), 153.

423. E. I. Greaves, "Stress Strain Properties of High Alumina and Basic Refractories and Their Use in Arc Furnace Roofs," Refract. J. 53 (1978), 13.

424. O. Buyukozturk and T-M. Tseng, "Thermomechanical Behavior of Refractory Concrete Linings," Am. Ceram. Soc. J. 65 (1982), 301.

425. F. Tomsu and M. Kozlovsky, "Microstructure and Thermomechanical Properties of Basic Refractories," Szilikatip. Szilikattud. Konf., 13th, Proc. 1 (1981), 373.

426. J. F. Wygant and M. S. Crowley, "Designing Monolithic Refractory Vessel Linings," Am. Ceram. Soc. Bull. 43 (1964), 180.

427. J. Sweeney and M. Cross, "Analyzing the Stress Response of Commercial Refractory Structures in Service at High Temperatures: I. A Simple Model of Viscoelastic Stress Response," Brit. Ceram. Soc. Trans. 81 (1982), 25.

428. A. A. Patuzzi, "Influence of Refractory Lining on Converter Vessel Construction," Iron Steel Eng. 59 (1982), 53.

429. C. A. Schacht, "Fundamental Considerations in the Structural Evaluation of Refractory-Lined Cylindrical Shells," ibid., p. 45.

430. C. A. Schacht, "Structural Behavior of Teeming Ladles Lined with High Alumina Refractories," ibid. 61 (1984), 33.

431. C. A. Schacht, "Observations on the Thermomechanical Behavior of Refractory Linings in Cylindrical Shells," Ceram. Eng. Sci. Proc. 7 (1986), 167.

432. C. A. Schacht, "Improved Analytical Procedures and Material Properties for Predicting the Thermomechanical Behavior of Refractory Linings of Teeming Ladles," ibid., p. 209.

433. J. H. Partridge, "Creep of Refractory Materials," Brit. Ceram. Soc. Trans. 53 (1954), 731.

434. B. A. Wiechula and A. L. Roberts, "The Elastic and Viscous Properties of Aluminosilicate Refractories," ibid. 51 (1952), 173.

435. C. O. Hulse and J. A. Pask, "Analysis of Deformation of a Fire Clay Refractory," Am. Ceram. Soc. J. 49 (1966), 312.

436. E. V. Degtyareva I. S. Kainarskii, and Y. Z. Shapiro, "Relation Between the Creep and Porosity of Refractories," Ogneupory 11 (1973), 41.

437. R. E. Beyer, R. D. Ek, J. L. Scott, G. A. Zeugner, and O. J. Whittemore, "Creep of Super-Duty Fire Clay Brick Under Compression," Am. Ceram. Soc. Bull. 55 (1976), 1049.

438. W. E. Snowden and J. A. Pask, "Creep Behavior of a Model Refractory System MgO-CaMgSiO$_4$," Am. Ceram. Soc. J. 61 (1978), 231.

439. D. J. Bray, J. R. Smyth, and T. D. McGee, "Creep of a 90+% Al_2O_3 Refractory Concrete," Am. Ceram. Soc. Bull. 59 (1980), 706.

440. G. L. Barna, "Plasticity of Clay Minerals," ibid. 46 (1967), 1091.

441. H. M. Mikami, "Refractory Magnesium Oxide," Ceram. Eng. Sci. Proc. 4 (1983), 97.

442. K. Nibu, Y. Takamiya, F. Kawano, and Y. Oda, "Development of High-Quality Sea Water Magnesia," p. 1072 in Reference 25.

443. Y. Takamiya, "Synthetic Magnesia," Seramikkusu 17 (1982), 823.

444. H. M. Mikami, "Refractory Chromites from Southern Africa and Other Non-Masinloc Sources," Ceram. Eng. Sci. Proc. 4 (1983), 144.

445. S. Ohta, T. Kumazawa, S. Kanzaki, and H. Tabata, "Synthesis of High Purity Mullite Powder and Its Applications," p. 1135 in Reference 25.

446. W. E. Worrall, CLAYS AND CERAMIC RAW MATERIALS, 2nd Ed., 1986, Elsevier Applied Science Publishers, London.

447. G. MacZura, V. Gnauck, and P. T. Rothenbuehler, "Fine Aluminas for High Performance Refractories," p. 560 in Reference 75.

448. Y. Hongo and M. Miyawaki, "Rho-Alumina Bonded Unshaped Refractories. 3. Spalling Resistance of Alumina Castable Refractories," Taikabutsu 34 (1982), 74.

449. Y. Hongo, "Rho-Alumina Bonded Castable Refractories," ibid. 40 (1988), 226.

450. B. Monsen, A. Seltveit, B. Sandberg, and S. Bentsen, "Effect of Microsilica on Physical Properties and Mineralogical Composition of Refractory Concretes," p. 201 in Reference 39.

451. Y. Naruse, S. Fujimoto, T. Yamato, Y. Uchida, and Y. Onishi, Properties and Construction of High Strength Clay Bond Castable," Taikabutsu 33 (1981), 508.

452. I. Teoreanu and N. Ciocea, "Composition-Structure-Property Relations in Refractory Casting Compositions," TIZ 107 (1983), 637.

453. H. Kyoden, K. Ichikawa, Y. Hamazaki, T. Kaneshige, M. Nishi, H. Kato, S. Uchida, and U. Nagayama, "Casting of Magnesia-Chrome Refractories," Taikabutsu 37 (1985), 586.

454. G. W. Brindley and M. Nakahira, "The Kaolin-Mullite Reaction Series, I, II, and III," Am. Ceram. Soc. J. 42 (1959), 311.

455. T. D. McGee, "Constitution of Fireclays at High Temperatures," ibid. 49 (1966), 83.

456. A. H. M. Andreasen and J. Andersen, "Relation Between Grain Size and Interstitial Space in Products of Unconsolidated Granules," Kolloid Z. 50 (1930), 271.

457. J. E. Funk, D. R. Dinger, and J. E. Funk, Sr., "Control Parameters for a 75 wt% Coal-Water Slurry," in Int. Symp. Coal-Slurry Combust. (DOE), 4th, Proc. 1982.

458. R. Hughan, "Theory of Particle Packing Applied to Silica and Magnesite Refractories," Refract. J. 1961, 166.

459. A. N. Talbot and F. E. Richart, Bulletin No. 137, 1923, Univ. of Illinois Eng. Experiment Station, Urbana, IL.

460. C. C. Furnas, "Grading Aggregates, I - Mathematical Relations for Beds of Broken Solids of Maximum Density," Ind. Eng. Chem. 23 (1931), 1052.

461. R. K. McGeary, "Mechanical Packing of Spherical Particles," Am. Ceram. Soc. J. 44 (1961), 513.

462. J. Zheng, P. F. Johnson, and J. S. Reed, "Improved Equation of the Continuous Particle Size Distribution for Dense Packing," ibid. 73 (1990), 1392.

463. R. J. Rigge, "Colloidal Properties of VERSAL Aluminas," Kaiser Chemicals Technical Bulletin, 1986; LaRoche Chemical Co., Baton Rouge, LA.

464. H. C. Bassalo and W. E. Worrall, "The Effect of Additives on the Physical Properties of High Alumina Cements - Part 1 - Adsorption and Zeta Potential," p. 1183 in Reference 26.

465. C. Okkerse, "Porous Silica," p. 213 in PHYSICAL AND CHEMICAL ASPECTS OF ADSORBENTS AND CATALYSTS, B. G. Lindsen, ed., 1970, Academic Press, New York.

466. H. T. Rijnten, "Formation, Preparation, and Properties of Hydrous Zirconia," p. 316 in PHYSICAL AND CHEMICAL ASPECTS OF ADSORBENTS AND CATALYSTS, B. G. Lindsen, ed., 1970, Academic Press, New York.

467. N. N. Kruglitski, "Optimizing the Deformation Properties of Ceramic Pastes by Evaluating Relevant Physical and Chemical Mechanisms," Ceram. Int. 9 (1983), 146.

468. E. G. Acker and M. E. Winyall, Brit. Patent 1,340,230 (1973); assigned to W. R. Grace & Co.

469. A. A. Rudenko and V. A. Rybkin, "Use of Porous Refractory Materials in Shell Molds Produced by Investment Casting," Liteinoe Proizvod. 1979, 18.

470. R. S. Marsden, U.S. Patent 4,297,336 (1981); assigned to Imperial Chemical Industries, Ltd.

471. J. W. Whittemore, "Industrial Use of Plasticizers, Binders and Other Auxiliary Agents in Ceramic Synthesis," Am. Ceram. Soc. Bull. 23 (1944), 427.

472. T. Darroudi, R. H. Hughes, and R. A. Landy, "Effects of Temperature and Several Gases on the Oxidation Characteristics of a Variety of Carbon-Magnesia Brick and Their Raw Materials," p. 105 in Reference 75.

473. S. I. Radchenko, E. V. Kuz'minykh, N. N. Grachev, and V. Z. Kolesnik, "Properties of Novolaks for the Plating of Sands," Liteinoe Proizvod. 1977, 14.

474. S. H. Goodman, HANDBOOK OF THERMOSET PLASTICS, 1986, Noyes Publications, Park Ridge, New Jersey.

475. R. Roy, "Ceramics by the Solution-Sol-Gel Route," Science 238 (1987), 1664.

476. T. A. Ring, "Continuous Production of Narrow Size Distribution Sol-Gel Ceramic Powders," Mater. Res. Soc. Bull. 12 (1987), 34.

477. S-M. Ho, B. E. Yoldas, and D. M. Mattox, U.S. Patent 4,357,427 (1982); assigned to Westinghouse Electric Corp.

478. P. Colomban, "Chemical and Sol-Gel Processes: The Elaboration of Ultrafine Powders," Ind. Ceram. (Paris) 792 (1985), 186.

479. B. E. Yoldas, "Transparent Porous Alumina" and "Sol Preparation from Alkoxides," Am. Ceram. Soc. Bull. 54 (1975), 286 and 289.

480. B. E. Yoldas, "Thermal Stabilization of an Active Alumina; Effect of Dopants on the Surface Area," J. Mater. Sci. 11 (1976), 465.

481. D. G. Braithwaite and V. L. Seale, U.S. Patent 3,981,979 (1976); assigned to Nalco Chemical Co.

482. E. S. Lane, Brit. Patent 1,313,750 (1973); assigned to United Kingdom Atomic Energy Authority.

483. A. P. Gerk, U.S. Patent 4,574,003 (1986); assigned to 3M Co.

484. P. A. Haas, W. W. Pitt, S. M. Robinson, and A. D. Ryon, "Preparation of Metal Oxide Gel Spheres with Hexamethylenetetramine as an Ammonia Donor," Ind. Eng. Chem. Proc. Res. Devel. 22 (1983), 461.

485. C. J. R. Gonzales-Oliver, P. F. James, and H. Rawson, "Silica and Silica-Titania Glasses Prepared by the Sol-Gel Process," J. Non-Cryst. Solids 48 (1982), 129.

486. R. Roy, "Purposive Design of Nanocomposites: Entire Class of New Materials" (1986 Conf. on Grain Boundaries and Surfaces in Ceramics), Mater. Sci. Res. 21 (1987), 25.

487. C. L. Czekaj, M. L. J. Hackney, W. J. Hurley, Jr., L. V. Interrante, G. A. Sigel, P. J. Schields, and G. A. Slack, "Preparation of SiC/AlN Ceramics Using Organometallic Precursors," Am. Ceram. Soc. J. 73 (1990), 352.

488. L. L. Hench and D. R. Ulrich, ed., SCIENCE OF CERAMIC CHEMICAL PROCESSING, 1986, John Wiley & Sons, New York.

489. J. G. P. Binner, ed., ADVANCED CERAMIC PROCESSING AND TECHNOLOGY, Vol. 1, 1990, Noyes Publications, Park Ridge, New Jersey.

490. V. Ramakrishnan, "Modern Developments in the Fabrication Process of High-Grade Refractory Bricks," Sprechsaal 120 (1987), 880.

491. V. Ramakrishnan and M. Mick, "Modern Developments in the Fabrication Process of High-Grade Refractory Bricks," p. 1052 in Reference 25.

492. G. B. Shaw, "Dense Sintered Refractories and the Role of Isostatic Pressing," Glass Technol. 19 (1978), 75.

493. R. L. Coble and J. E. Burke, "Sintering in Ceramics," p. 197 in PROGRESS IN CERAMIC SCIENCE, Vol. 3, J. E. Burke, ed., 1963, MacMillan/Pergamon Press, New York.

494. W. D. Kingery, H. K. Bowen, and D. R. Uhlmann, INTRODUCTION TO CERAMICS, 2nd Ed., 1976, John Wiley & Sons, New York.

495. American National Standards Institute (ANSI), 11 W. 42nd Street, New York, NY 10036.

496. G. Wernimount, "Ruggedness Evaluation of Test Procedures," ASTM Standardization News, 3/1977.

497. G. Routschka, "Repeatability and Reproducibility of Tests on Dense Refractory Castables: Results of Inter-Laboratory Tests," InterCeram. 36 (1987), 57.

498. R. R. Riley and S. E. Laurich, "Comparison of Castable Consistency Methods," Am. Ceram. Soc. Bull. 62 (1983), 787.

499. G. E. P. Box and J. S. Hunter, "The 2_{k-p} Fractional Factorial Designs," Technometrics 3 (1961), 311.

500. G. E. P. Box and W. G. Hunter, "Statistical Techniques for Mechanistic Modeling," Eur. Symp. Chem. React. Eng., 5th, Proc. B4 (1972), 9; Elsevier, Amsterdam.

501. G. E. P. Box and D. W. Behnken, "Some New Three Level Designs for the Study of Quantitative Variables," Technometrics 2 (1960), 455.

502. H. D. Leigh III, "Optimization of Refractory Properties Through Statistical Design," Ceram. Eng. Sci. Proc. 9 (1988), 105.

503. H. D. Leigh III, "Process Control Parameters for Refractory Brick Manufacture," ibid. 8 (1987), 1238.

504. H. S. White and F. J. Hrbolich, "SPC - The Path to Consistent Refractory Brick Quality," ibid. 9 (1988), 121.

505. D. C. Jain, "SPC at Mulcoa," ibid., p. 129.

506. A. I. Khuri and J. A. Cornell, RESPONSE SURFACES, 1987, Marcel Dekker, New York.

507. MODERN REFRACTORY PRACTICE, 1961, Harbison-Walker Refractories, Dresser Industries, Inc., Pittsburgh, PA.

508. F. Gebhardt, "The Situation of the European Refractory Industry," p. 4 in Reference 26.

509. P. R. H. M. Bittencourt, "The Challenge of the Latin American Refractories Industry in the 1990s," p. 19 in Reference 26.

510. S. Kamei, "Progress of Monolithic Refractories for Recent Ten Years in Japan," p. 46 in Reference 26.

511. Y. D. Sagalevich and A. K. Karlit, "Main Trends in Developing the Refractories Industry in the USSR," p. 87 in Reference 26.

512. E. S. Wright, "Manufacturing and Market Trends in the U.S. Refractories Industry," Am. Ceram. Soc. Bull. 69 (1990), 1155.

Refractory Patents

DENSE WORKING REFRACTORIES

DATE Mo/Da/Yr	PATENT NUMBER	TRUNCATED TITLE [PRINCIPAL FEATURE]	FIRST AUTHOR
Alumina-Based Bricks (incl. composites)			
12/31/85	Belg. BE 903167 A1	Refractory Sliding Gate for Metallurgical... [Fiber-reinf., for Expansion Joint]	Anon.
07/04/86	Jap. JP 86146773 A2/ JP 61146773	Refractory Brick Plate with... [Fiber-reinf., for Durability]	H. Kano et al.
09/12/87	Jap. JP 87207757 A2/ JP 62207757	Manuf. of Corr.-Resist. Cr_2O_3-Cont.... [Chromia for Spall- & Corr. Resistance]	S. Uto et al.
02/09/88	Jap. JP 8830363 A2/ JP 6330363	Refr. Bricks with Impr. Spalling and... [Chromia Mineralizer for Spall- & Erosion]	T. Sasaki et al.
08/25/88	Aust. AT 386406 B	Refr. Bricks Cont. an Embedded ... Tube [Molded Around Metal Tube, for Tuyere]	Anon.
09/15/88	USSR SU 1423544 A1	Fusion-Cast Refractory Material [Calcia in, for Impr. Forming Prop.]	V.A. Sokolov et al.
11/17/88	Ger. DE 3715178 A1	Manuf. of Fe- and Slag-Resist.... [Pitch-bonded Coke, for Slag Resist.]	S. Wilkening
01/04/89	Eur. EP 297827 A2	Settable Systs. for the Manuf. of Refr.... [Sol-Gel Binder, Light Org. Solvents In]	R. Shaw
Alumina-Based Castables			
06/27/80	Jap. JP 8085475	Castable Refractory Compositions [Aluminum Tripolyphosphate Binder]	Anon.
08/11/81	Jap. JP 81100174 A2	Castable Refractory Composition [Sodium Phosphate Binder]	Anon.
08/20/81	Jap. JP 81104783 A2	Castable Refractories [Sr Aluminate-bonded, for Strength]	Anon.
10/09/81	Jap. JP 81129679 A2	Castable Refractory [Aluminous Cement & Alumina Sol]	Anon.
11/02/81	Jap. JP 81140079 A2	Castable Refr. Composition for Vibr. Cast. [Sod. Silicate, Humates, Pitch Binders]	Anon.
12/16/81	Jap. JP 81164078 A2	Molded Refractory Materials [CA Cement-bonded]	Anon.
02/24/82	Jap. JP 8234084	Castable Refractory Materials [Clays, Pitch, Polyphosphates, Al Salts]	Anon.
10/04/82	Jap. JP 82160976 A2/ JP 57160976	Castable Refractories [Silica, CaO, CA Cement, for High Strength]	Anon.
12/16/82	Jap. JP 82205357 A2/ JP 57205357	Castable Amorphous Refractories [Phenolic Resin-Polyurethane Binders]	Anon.
03/01/83	Belg. BE 894917 A1	Refr. Castable Aluminous Compositions [Binder, for Foundry Castable]	Anon.
12/12/83	Jap. JP 83213673 A2/ JP 58213673	High-Strength Refractory Materials [For Flux Injection Lance]	Anon.
03/22/84	Jap. JP 8450081 A2/ JP 5950081	Castable Refr. Matls. Having High Str.... [CA Cement, for High Str. & Ther. Shock Res.]	Anon.
07/04/84	Jap. JP 84116180 A2/ JP 59116180	Castable Refractories [CA Cmt, Triethanolamine, for Forming Prop.]	Anon.
09/06/84	Jap. JP 84156966 A2/ JP 59156966	Alumina and Alumina-Chrome Castable Refr. [Cmt, Ca Carbonate, Na Polyphosphate Binders]	Anon.
04/11/85	Ger. DE 3437386 A1	Castable Refractory Composition [Chromia, for Steel & Glass Furnaces]	D.V. Stiles et al.

Alumina-Based Castables, continued

06/13/85	Jap.	JP 85108374 A2/ JP 60108374	High-Alumina Castables for Vessels for... [For Vessels for Molten Metals]	Anon.
08/04/86	Jap.	JP 86172847 A2/ JP 61172847	Basic Aluminum Lactate [Binder, for Refrs. & Fiber Refrs.]	K. Sunahara et al.
07/14/87	Jap.	JP 87158158 A2/ JP 62158158	Refractory Compositions [MgO with Al Lactate & Na Nitrile Bond]	M. Miyawaki et al.
09/12/88	Jap.	JP 88218586 A2/ JP 63218586	Alumina-Based Monolithic Refrs. [MgO & Silica, for Tapping Spout]	M. Nishi et al.
12/23/88	USSR	SU 1446127 A1	Castable Oxide Refractories [Chromia & CaO, for Corr. & Ht. Res.]	E.F. Kolomeitseva et al.

Alumina-Based Composite Castables

06/09/82	Jap.	JP 8292582 A2	Alumina-Graphite Castable Refractories [CA Cmt, Na Polyphosphate Binders]	Anon.
08/02/82	Jap.	JP 82123872 A2/ JP 57123872	Unshaped Refractory Material [Graphite-coated Al_2O_3 Particles, Pitch]	Anon.
07/26/83	Jap.	JP 83125668 A2/ JP 58125668	High-Strength Castable Refr. Materials [Surface-treated SiC, for High Strength]	Anon.
07/26/83	Jap.	JP 83125669 A2/ JP 58125669	Carbon Black-Cont. Castable Refr. Matls.... [Surface-treated Carbon Black, for Erosion]	Anon.
08/03/83	Jap.	JP 83130170 A2/ JP 58130170	Graphite Pellet-Cont. Castable Refr.... [For Erosion Resistance]	Anon.
08/03/83	Jap.	JP 83130171 A2/ JP 58130171	Castable Refr. Matls. with Impr. Erosion... [C Black-Graphite Pellets, Eros. & Spalling]	Anon.
08/03/83	Jap.	JP 83130172 A2/ JP 58130172	Graphite-Cont. Refr. Matls. with Improved... [Graphite & Silica, for Eros. & Spall. Res.]	Anon.
02/18/84	Jap.	JP 8430762 A2/ JP 5930762	Castable Refr. Matls. with High Spall.... [Al_2O_3 Rod-reinf., for Str., Spall., & Slag]	Anon.
06/22/84	Jap.	JP 84107981 A2/ JP 59107981	Castable Refractories [Cmt, Clay, & SiC, for Tundish Lining]	Anon.
10/09/84	U.S.	US 4476234 A	Refractory Cement [Si Nitride-Oxynitride Bond, Slag-resist.]	C.M. Jones et al.
12/07/84	Jap.	JP 84217679 A2/ JP 59217679	Dry Castable Refractories [SiC, with Sulfate & Tartrate Binder]	Anon.
03/06/85	Jap.	JP 8542281 A2/ JP 6042281	Castable Refractory Compositions [Cmt & Pitch, for High Corrosion Resist.]	Anon.
06/07/85	Fr.	FR 2555933 A2	Refractory Fiber-Reinf. Ceramic Matl. [Oxide Fiber & Al Nitrate, High-Str.]	L. Minjolle et al.
02/17/87	Jap.	JP 8736073 A2/ JP 6236073	Silicon Carbide-Cont. Castable Refrs. [SiC Powder, for Erosion & Spall. Resist.]	K. Furukawa et al.
10/21/86	Jap.	JP 86236656 A2/ JP 61236656	Alumina-Graphite Castable Refr. for... [Graphite & Spinel, for Gas-Blowing Lance]	M. Nishi et al.
04/20/88	Jap.	JP 8889453 A2/ JP 6389453	Aluminum Oxynitride-Alumina Castable Refrs. [Al_2O_3-SiC, Oxynitride-bonded, for Erosion]	K. Sato et al.
07/14/88	Jap.	JP 88170276 A2/ JP 63170276	Spalling-Resistant Alumina Monolithic... [Chromia, & SS Fibers, for Hot Str., Spall.]	H. Sakurai et al.

Alumina-Silica-Based Bricks (incl. composites)

12/01/81	Jap.	JP 81155073 A2	Refractory Bricks and Castables [Various Binders]	T. Iwasaki et al.
04/11/83	Jap.	JP 8360656 A2/ JP 5860656	Refractory Fiber Composites [Aluminosilicate Fibers with Clays & H_3PO_4]	Anon.
01/07/88	Jap.	JP 8802853 A2/ JP 6302853	Alumina-Carbon Bricks for Metal Melt-... [Aluminosilicate-C, for Molten Metal Resist.]	N. Kaji et al.
03/24/88	PCTI	WO 8801990 A1	Complexed Org. Hydroxyl Group-Cont. Colloids.. [Lactic Acid-Al-Oxychloride Complex Binders]	A. Adam et al.

Alumina-Silica-Based Bricks, continued

03/31/88	Pol.	PL 142879 B1	Method of Manuf. of Aluminosilicate Shapes.. [Clay Grog with Cmt & Na Tripolyphosphate]	M. Drozdz et al.
06/08/88	Eur.	EP 270377 A2	Process for the Manuf. of Refr. Articles [Phenolic Resins & Var. Solvents: Binders]	P.H. Lemon et al.
06/24/88	Jap.	JP 88151662 A2/ JP 63151662	Manuf. of Spalling-Resist. Tuyere Bricks.. [Metal Powder & Phenolic Resin Binders]	A. Okamoto et al.
07/15/88	Czech.	CS 251855 B1	Silica-Bonded Refrs. for Use in Furnaces [Colloidal-Silica-bonded]	M. Fiala et al.
10/03/88	Jap.	JP 88236783 A2/ JP 63236783	Carbon Adhesion-Preventive Refr. Bricks [Front Glazing & Var. Binders]	H. Kakimoto et al.

Alumina-Silica-Based Castables: CA Cement and Silica Bonded

09/21/81	Jap.	JP 81120578 A2	Castable Refractory Material [Grog with Coal Ash Binder]	Anon.
05/04/82	Jap.	JP 8271877	Refractory Castables for Molten Metal... [For Tundish Linings]	Anon.
02/25/84	Jap.	JP 8435067 A2/ JP 5935067	Castable Refractory Materials [CA Cement and Silica Flour Bond]	Anon.
03/23/85	Jap.	JP 8551673 A2/ JP 6051673	Castable Refractories [Ultrafine Alumina-SiO_2, -Cr_2O_3, Deflocc.]	Anon.
04/15/85	Jap.	JP 8565770 A2/ JP 6065770	Castable Refractories [CA Cmt and MgO Binder, Fine, for Fluidity]	Anon.
07/09/86	Jap.	JP 86151068 A2/ JP 61151068	Castable Refr. Matl. with Impr. Storage.. [Binder Premix of CA Cmt & SiO_2 Powder]	Y. Yamamoto et al.
12/26/86	Jap.	JP 86295276 A2/ JP 61295276	Wear-Resistant Castable Refr. Composition [CA Cement, SiO_2, and Clay Bond]	Anon.
01/31/87	Jap.	JP 8723974 A2/ JP 6223974	Heat Treatment of Shape-Complex .. Parts [Castable Packing for Metal Parts]	K. Yoshida et al.
07/23/87	Jap.	JP 87167262 A2/ JP 62167262	Binder for Low-Cement Refr. Castables [Low-Cement with Ultrafine Silica]	Y. Sasagawa et al.
08/21/87	Jap.	JP 87191476 A2/ JP 62191476	Castable Refrs. of High Str. & Durability [CA Cement-Bonded Roseki (Pyrophyllite)]	I. Sugaya et al.

Alumina-Silica-Based Castables: Phosphatic Additives

11/04/80	Jap.	JP 80140770	Castable Refractories [Alumina Cement with Sodium Phosphate]	Anon.
07/25/81	Jap.	JP 8192178 A2	Castable Refractory Material [With Sod. Ultrapolyphosphate Dispersant]	Anon.
04/23/82	Jap.	JP 8267070 A2	Ordinary Temperature-Hardenable Binders... [CA Cement with Phosphoric Acid]	Anon.
11/29/82	Hung.	HU 23994 0	Refractory Molding Matl. & Ramming Mix [With Phosphate Binder]	Z. Lebenyi et al.
12/27/84	Jap.	JP 84232975 A2/ JP 59232975	Refractory Matls. for Casting Linings [Na Silicate Binder, Phos. Glass Accelerator]	Anon.
01/21/85	Jap.	JP 8511274 A2/ JP 6011274	Castable Refrs. Having High Corr. Resist.... [CA Cmt with: SiO_2 Powder, Na Hexametaphos. Peptizer, Na Tripolyphosphate Peptizer, Silicone Oil or Sorbitan Trioleate Defoaming Agent]	Anon.
07/18/86	Jap.	JP 86158872 A2/ JP 61158872	Castable Refractory Material [With Na Hexametaphosphate, Na Sulfonate]	N. Wada et al.
12/16/86	Jap.	JP 86286269 A2/ JP 61286269	Manuf. of Castable Refr. Compositions [CA Cmt with Na Polyphosphate Peptizers]	M. Yoshimura et al.
02/23/87	Jap.	JP 8741770 A2/ JP 6241770	Amorphous Refractory Materials [Cont. CA, Na-Polyphos. Peptizers, & Al]	T. Taniguchi
02/28/87	Jap.	JP 8746970 A2/ JP 6246970	Phosphate-Bonded Castable Refractory [With Methylcellulose-coated $CaCO_3$]	M. Yoshimura et al.

Alumina-Silica-Based Castables, continued

08/09/88	U.S.	US 4762811 A	Castable Refr. with Resist. to Molten Al [Barite, Zn Borosilicate Antiadhesion Agts.]	J.T. Vayda et al.
10/25/88	U.S.	US 4780142 A	Silica Fume-Cont., Hard Setting Cast.... [Fumed-SiO_2, Na Silicate, Na Hexametaphos.]	H.L. Rechter
11/15/88	Jap.	JP 88277579 A2/ JP 63277579	Castable Refractories [Low-Cement with Citric Acid, Long Pot Life]	H. Ueno et al.

Alumina-Silica-Based Castables: Polymer and Resin Binders

03/25/80	Jap.	JP 8042223	Refr. Castables for Lining BF Tapping... [Aluminous Cement and Pitch Binder]	Y. Hamazaki et al.
03/14/81	Jap.	JP 8126775	Castable Refractories [Styrene-Maleic Acid Copolymer Binder]	Anon.
06/01/82	Jap.	JP 8288071 A2	Binder for Blast Furnace Ramming Mud [Polymer, Phenolic Resin]	Anon.
08/29/85	Jap.	JP 85166272 A2/ JP 60166272	Monolithic Refractories [Phenolic Resin, Tannin, Formaldehyde, Novolak Binders, for Ladle, Spout, Tundish]	K. Samejima et al.
11/11/85	Jap.	JP 85226461 A2/ JP 60226461	Castable Refractories [Alumina-SiC, with Hydroxymethyl Siloxanes and Silicones as Binders]	E. Yorita et al.
04/25/87	Jap.	JP 8791474 A2/ JP 6291474	Quick-Curing Castable Refractory [CA Cmt, Na Silicate, & Resol Phenolic]	T. Kosaka et al.
05/16/87	Jap.	JP 87105966 A2/ JP 62105966	Binder for Castable Refractory [Nitrile Rubber-modified Novolak Resin, Pitch]	T. Iba et al.
05/16/87	Jap.	JP 87105967 A2/ JP 62105967	Thermosetting Castable Refractories [Resol Phenolics with Furfural, Fur. Alc.]	A. Takayama et al.

Alumina-Silica-Based Castables: Other or Various Binders

12/01/81	Jap.	JP 81155073 A2	Refractory Bricks and Castables [Various Binders for]	Anon.
03/04/83	Jap.	JP 8336984 A2/ JP 5836984	Binder for Castable Refractories [Mixtures of BF Slag with Alkali Hydroxides]	Anon.
08/30/83	Jap.	JP 83145666 A2/ JP 58145666	Acid-Resistant Refractory Castables [Na Lignosulfonate]	Anon.
01/17/86	Jap.	JP 8610076 A2/ JP 6110076	Castable Refractories [Aluminous Cement & Amine Silicates]	M. Yoshimura et al.
08/11/86	Jap.	JP 86178446 A2/ JP 61178446	Refractory Binders [Calcium Aluminum Sulfur Oxide]	K. Hirano
05/09/87	Jap.	JP 87100483 A2/ JP 62100483	Castable Refractories [Bauxite with Basic Aluminum Lactate]	M. Miyawaki et al.
05/16/87	Jap.	JP 87105969 A2/ JP 62105969	Thickeners for Castable Refractory... [Boric Acid & Poly(Vinyl Alcohol]	N. Watanabe et al.
02/26/88	Jap.	JP 8895167 A2/ JP 6395167	High-Strength Castable Refractories [CA Cmt & Amine Silicate Powder]	M. Yoshimura et al.

Alumina-Silica-Based Composite Castables: Oxidic Dispersed Phase

08/20/81	Jap.	JP 81104780 A2	Alumina-Silica System Refr. Castable [Wollastonite Fibers, for High Strength]	Anon.
08/20/84	Jap.	JP 8434150 B4/ JP 5934150	Reinforcing Rods for Unshaped Refrs. [CA Cmt, Aluminosilicate Rods]	Anon.
08/20/84	Jap.	JP 8434151 B4/ JP 5934151	Unshaped Refr. Matls. with High Spall. Res.... [CA Cmt, Ceramic Fiber Reinforcing]	Anon.
01/11/85	Jap.	JP 8505080 A2/ JP 6005080	Prevention of Spalling of Monolithic Refrs. [Ceramic Fiber Reinf., for BF & Ladles]	Anon.
10/28/85	Jap.	JP 85215580 A2/ JP 60215580	Castable Refr. Matls. with Impr. Stor.... [CA Cmt, with Silica Pellets]	I. Hibino et al.

Alumina-Silica-Based Composite Castables, continued

12/05/85	Jap.	JP 85246273 A2/ JP 60246273	Castable Refractory Composition [CA Cmt, Ceramic Fibers, Flowable]	S. Sakurai et al.
12/10/85	U.S.	US 4558016 A	Ceramic Fiber-Reinforced Refractories [Phos. Binders, Alumina-Boria-Silica Fib.]	S.O. Bronson et al.
11/26/87	Ger.	DE 3715650 A1	Shaped Refractory Articles [CA Cmt, Wollastonite & Glass Fibers, for Ladles, Troughs, Pipes and Tubes]	S. Sakurai et al.

Alumina-Silica-Based Composite Castables: Nonoxide Dispersed Phase

01/07/83	Jap.	JP 8302270 A2/ JP 5802270	Silicon Carbide-Cont. Castable Refr.... [Bauxite with SiC & Silica, for Th. Shock]	Anon.
03/23/85	Jap.	JP 8551671 A2/ JP 6051671	Castable Refrs. with High Strength and... [SiC-reinf., for High Str. & Spall Resist.]	Anon.
01/22/86	Jap.	JP 8614175 A2/ JP 6114175	Castable Refrs. for BF Tapping Spouts [Al Fibers & Si Powder, for Slag Resist.]	K. Furukawa et al.
02/13/86	Jap.	JP 8631363 A2/ JP 6131363	Low Foaming Castable Refractories [CA Cmt, Lacquer-coated Al & Si Powders]	E. Maeda et al.
06/28/86	Jap.	JP 86141676 A2/ JP 61141676	Monolithic Refractories [Cellulose Paint-coated Metal Powders]	T. Kondo et al.
02/17/87	Jap.	JP 8736072 A2/ JP 6236072	Carbon-Containing Castable Refractories [C-Containing Matl., for Eros. & Spall.]	K. Furukawa et al.
07/06/88	Jap.	JP 88162579 A2/ JP 63162579	Thermally Curable Castable Refr. Matls.... [Pitches, Na Polyphosphates]	E. Yorita et al.
09/08/88	Jap.	JP 88215573 A2/ JP 63215573	Graphite-Containing Castable Refrs. [Pitch-treated Graphite, for Corrosion and Erosion Resist. to Hot Slags & Metals]	T. Sakamoto

Silica-Based Castables

03/19/85	U.S.	US 4506025 A	Silica Castables [Wollastonite and Quartzite Castables]	T.R. Kleeb et al.
11/19/86	Jap.	JP 86261276 A2/ JP 61261276	Castable Refr. for Molten-Metal Container... [Silica Sol, Amine Silicate Refrs.]	T. Kondo et al.

Aluminous Gunned Refractories (incl. composites)

09/22/82	Jap.	JP 8244636 B4/ JP 5744636	Sprayable Refractory Material [CA Cmt and Thickener, Spray/Castable]	Anon.
12/12/83	Jap.	JP 83213680 A2/ JP 58213680	Hot Spraying of Unshaped Refr. Matls. [Silica Sol & Silica Soln. Spray Medium]	Anon.
06/14/86	Jap.	JP 86127671 A2/ JP 61127671	Spraying Castable Refrs. for BF Repair [Alumina-Cordierite Spray Mix, Alkali-Res.]	T. Horio et al.
09/29/87	Can.	CA 1227359 A1	Spraying Matls. Cont. Ceramic Needle Fib.... [SiC, Si_3N_4 Whiskers, Plasma-Spray Coating]	M. Tanaka et al.
12/30/87	S.Af.	ZA 8703024 A	App. and Method for Spray Coating Refr.... [Alumina Powder and Combustible Metal (e.g., Al) Powder, Dual-Nozzle Delivery]	S. Watanabe et al.
02/11/88	Ger.	DE 3634447 C1	Refractory Sliding Plate for the Spout.. [Refr. & Fiber Flame-Spray Coatings for]	F. Schellberg et al.
07/09/88	Jap.	JP 88166770 A2/ JP 63166770	Gunning Matls. for Furnace Mending [Aluminous, with Amine Silicate, Ammon. Silicate, and Ca Salt Binders]	T. Kondo et al.
07/09/88	Jap.	JP 88166771 A2/ JP 63166771	Gunning Matls. for Desiliconization... [Aluminous or Alumina-Chromite, with Silica Flour]	T. Tamehiro

Basic Bricks

09/06/78	Jap.	JP 78102313	High-Density Magnesia Clinker [For Basic Refractory Grain]	K. Umeya et al.
11/15/79	USSR	SU 697243	Mixture for Prep. Fountain Bricks.. [Chrome-Magnesite, for Steel Ingot Bottom-Pouring]	G.V. Kashakashvili et al.
08/15/81	India	IN 149014 A	Basic Refractories [Magnesite, with Al-Cr-Phosphate Binders]	R.K. Sharma et al.
08/30/83	USSR	SU 1038323 A1	Refractory Material [MgO, with Silica-H_3PO_4 Binder]	A.N. Murashkevich et al.
04/28/86	Jap.	JP 8683654 A2/ JP 6183654	Magnesia Clinkers [Prep. for Converter Refrs., Steel]	F. Kono
06/10/86	Jap.	JP 86122158 A2/ JP 61122158	Basic Refractory Compositions [CaO & Dolime, Alkali Metal Salt Binders]	K. Ichikawa et al.
10/03/86	Jap.	JP 86222955 A2/ JP 61222955	Magnesia Refractory Materials [Spinel Coating on MgO Powder, Slag-Res.]	S. Ushigome et al.
01/30/87	Rom.	RO 90933 B1	Fabric. of Magnesite Bricks with Spin.... [Sintered Periclase-Spinel Binder]	G. Vasilescu et al.
08/15/87	Czech.	CS 240459 B1	Highly Compact Basic Refractory... [Chrome-Magnesite, Compaction of]	K. Tomasek et al.
10/22/87	Jap.	JP 87241866 A2/ JP 62241866	Calcia-Based Refrs. Having High Str.... [CaO, with $CaCO_3$ Binder, for Bricks]	K. Fujiwara et al.
11/19/87	Ger.	DE 3616168 A1	Mg and Ca Phosphinates and Basic Refrs.... [Prep. as Binders for Olivine Refractories]	K. Sommer et al.
09/08/88	Jap.	JP 88215558 A2/ JP 63215558	MgO-Spinel Refr. Bricks...Impr. Th. Shock... [MgO-Spinel for Impr. Thermal Shock Resist.]	S. Uto et al.
09/20/88	Braz.	BR 8701486 A	Manuf. of Bricks from Soapstone, and... [For Lye (Aq. NaOH) Resistance]	E.D. Vitti
11/15/88	Jap.	JP 88277557 A2/ JP 63277557	Lining Bricks for Molten Metal Cont. [MgO-CaO Clinker for]	T. Goto et al.

Basic Composite Bricks: Pitch and Resin Bonded

04/28/79	Jap.	JP 7954113	Slaking-Resist. High-Grade Dolomite Clinker [Coating with Sulfur-containing Pitch]	K. Umeya et al.
05/12/83	Jap.	JP 8379048 A2/ JP 5879048	Waterless Liquid Phenolic Binders for Refrs. [Novolak, in High-Boiling Aprotic Solvents]	Anon.
11/26/84	Jap.	JP 84207869 A2/ JP 59207869	Manufacture of Basic Refractories [With Phenol Resin, $CaCO_3$, Alkylene Carbonate]	Anon.
12/05/85	Jap.	JP 85246256 A2/ JP 60246256	Binder Compositions for Refr. Bricks [Pitches, Novolak Phenolic Resins]	E. Chinen et al.
10/29/86	Jap.	JP 86242962 A2/ JP 61242962	Hot-Repair Materials for Furnaces [Basic Refr. Block Cont. Coal Tar Pitch, Thermoplastic Resin, Org. Solvent, Glycol]	Y. Kubo et al.
04/16/87	Jap.	JP 8783356 A2/ JP 6283356	Unburned Basic Carbon-Containing Refrs. [MgO-CaO with C, Siloxanes & Silicones]	H. Ishii et al.
05/02/88	Jap.	JP 88100053 A2/ JP 63100053	Manuf. of Basic Refrs. Resist. to Slaking [With Novolak in Lipophilic Solvent]	K. Hosokawa et al.
06/24/88	Jap.	JP 88151660 A2/ JP 63151660	MgO- and C-Based Bricks for Linings... [Alumina-Graphite-MgO Bricks with Phenolic Resins & Miscellaneous Binders]	S. Uto et al.
10/17/88	Jap.	JP 88248765 A2/ JP 63248765	MgO-CaO-Carbon Refr. Bricks for Steel.... [With Al-Mg Alloy, for Oxidation Resist.]	H. Ishii et al.

Basic Composite Bricks: Added Carbon or Graphite

09/07/83	Eur.	EP 87825 A1	Refractory Elements [Basic Refrs. Cont. Carbon Black, Alkyd Resins, Coal Tar Derivs., Branched C-9-11 Fatty-Acid Glycidyl Esters, for Low-T Curing]	I. Makansi et al.
10/29/84	Jap.	JP 84190255 A2/ JP 59190255	Basic Refractory Compositions [MgO-CaO-Graphite, with Epoxy Phenolics, etc.]	Anon.

Basic Composite Bricks, continued

03/06/85	Jap.	JP 8542270 A2/ JP 6042270	Basic Refractories [MgO-Dolime-Graphite, Polyoxyalkylene Phenolics]	Anon.
06/28/86	Jap.	JP 86141663 A2/ JP 61141663	Graphitic Basic Refractories [MgO & CaO: SiO_2 Control for Slag Resist.]	Y. Imaida et al.
10/21/86	Jap.	JP 86236648 A2/ JP 61236648	Carbon-Contg. Basic Unfired Brick [MgO-Dolime-Graphite, Novolak Phenolics]	N. Tada et al.
11/26/86	Jap.	JP 86266345 A2/ JP 61266345	Carbon-Containing Basic Refr. Brick [Phenolic Resin; Ca Alloy for Oxid. Res.]	M. Geshi et al.
05/02/87	Jap.	JP 8796362 A2/ JP 6296362	Magnesia-Carbon Refractories [Ca Alloy, Al-Ca-Mg Alloy for Oxid. Res.]	A. Ikesue et al.
08/21/87	Jap.	JP 87191461 A2/ JP 62191461	Magnesia-Based Refr. Bricks...Exc. Res... [Resol Phenolics, Ca Phosphate, Silicon]	A. Shinokuma et al.
10/09/87	Jap.	JP 87230687 A2/ JP 62230687	Coating Matls. for C-Containing Refrs. [Silicone, Na Polyacrylate, Alumina-Silica Coatings/Binders]	A. Watanabe et al.
03/09/88	Jap.	JP 8855159 A2/ JP 6355159	Manuf. of Magnesia-Carbon Bricks [Al-Mg-Si Alloy, Anti-Slaking/Corr./Oxid.]	A. Ikesue et al.
04/05/88	Jap.	JP 8874956 A2/ JP 6374956	MgO-C Unburned Bricks for Vac. Degas.:.. [MgO-Graphite with Metals & Alloys]	S. Aso et al.
05/27/88	Jap.	JP 88123857 A2/ JP 63123857	Manuf. of Carbon-Containing Refrs. [Al or Al Alloy, for High Str. & Oxid. Res.]	S. Uto et al.
08/12/88	Jap.	JP 88195161 A2/ JP 63195161	Graphite-Containing Basic Refractories [MgO & MgO-Spinel Clinkers, Spall-Resist.]	K. Hayama

Basic Castables

02/19/80	Jap.	JP 8023004	Spinel-Type Castable Refractory [Mag-Aluminate, with CA Cmt: High Str., Resist.]	Anon.
11/30/80	USSR	SU 783285	Charge for Producing Refractories [Magnesite, with CA, H_3PO_4, Et. Silicate]	G.D. Semchenko et al.
01/10/83	Jap.	JP 8303910 A2/ JP 5803910	Refractory for Tuyere Repair [MgO & Clay Refrs., with Na Triphosphate]	Anon.
06/21/83	Jap.	JP 83104071 A2/ JP 58104071	Basic Refr. Matls. for Repairing... [MgO-Based Castables]	Anon.
04/12/84	Jap.	JP 8464576 A2/ JP 5964576	Magnesia-Chrome Castable Refractories [High-Alumina Cement Bonded]	Anon.
10/03/84	Jap.	JP 84174578 A2/ JP 59174578	Basic Castable Refr. Matls. Having High Str.... [MgO, with Na-Ca Phosphate & CA Cmt Binder]	Anon.
12/27/84	Jap.	JP 84232973 A2/ JP 59232973	Castable Refr. Matls. for Lances... [Mag Spinel, CA Cmt, Triethanolamine Defloc.]	Anon.
01/25/85	Jap.	JP 8516875 A2/ JP 6016875	Monolithic Refrs. for Hot Working [H_3PO_4 & Phosphates with Lactam as Binders]	Anon.
06/13/85	Jap.	JP 85108373 A2/ JP 60108373	Basic Refr. Castables with High Resist.... [Mag-Dolime, with Aluminous Binder]	Anon.
08/29/85	Jap.	JP 85166273 A2/ JP 60166273	Basic Refractory Cement Compositions [MgO, with CA Cmt & Inorg. & Org. Polymers]	Y. Sasagawa et al.
03/17/86	Jap.	JP 8653173 A2/ JP 6153173	Castable Refractory [Single-Crystal MgO Grain, CA Cement]	K. Sato et al.
06/24/86	Jap.	JP 86136955 A2/ JP 61136955	Manuf. of Magnesia Refr. with High Dig... [MgO with Borate & Phosphate & Frit]	Y. Shimamura et al.
07/02/87	Jap.	JP 87148377 A2/ JP 62148377	Fast-Curable Blowing Refr. Compositions... [Al Sulfate and Sulfamic Acid as Binders]	E. Yorita et al.
03/16/88	Jap.	JP 8860168 A2/ JP 6360168	Basic Monolithic Refractories [MgO, with Ground Siliceous Stone & Al Lactate Binder]	J. Watanabe et al.
05/21/88	Jap.	JP 88117976 A2/ JP 63117976	Basic Amorphous Refractories [Amine Silicates in, for Spalling Resist.]	J. Mori et al.
06/20/88	Jap.	JP 88147870 A2/ JP 63147870	Blowing Matl. for Repairing Tapping Spouts [Mag-Chromia, -Chrome Ore, with Phosphates]	K. Uchida et al.

Basic Composite Castables

10/08/77	India	IN 143144	Basic Refr. Ramming Mass & Fettling Mass [Containing Tar]	A. Tripathy
10/11/80	Jap.	JP 80130868	Clinker Contg. C and Its Refr. Composition [MgO-Graphite, with Na Phosphate, Anthrac..Oil]	Anon.
03/14/81	Jap.	JP 8126774	Castable Refractories [MgO-C, with Sorbitol Surfactant, Bursting Prev.]	Anon.
09/07/82	Jap.	JP 82145071 A2/ JP 57145071	Resin-Containing Refractory Castables [MgO, with Phenolics, Ca & Mg Chlorides]	Anon.
04/26/83	Jap.	JP 8369781 A2/ JP 5869781	Carbon-Containing Castable Refractories [Cont. MgO; High Str. & Resist. to Molten Fe]	Anon.
02/25/84	Jap.	JP 8435068 A2/ JP 5935068	Basic Castable Refractory Materials [MgO with Graphite & Oxidized Ferrosilicon]	Anon.
05/15/84	Jap.	JP 8483979 A2/ JP 5983979	Magnesia-Carbon Castable Refractories [MgO-Graphite, with Phenolics & Poly(Na Acrylate)]	Anon.
01/28/85	Jap.	JP 8516874 A2/ JP 6016874	Basic Monolithic Refractories [Containing Pitch & Silica Sol Binder]	Anon.
05/15/85	Jap.	JP 8586080 A2/ JP 6086080	Basic Castable Refrs. Containing Carbon [MgO-Graphite, Pitch Bonded, High Strength]	Anon.
07/22/85	Jap.	JP 85137865 A2/ JP 60137865	Castable Refr. Composition with Org. Bind. [Neutralized Resol (Phenol) Resin Binder]	Y. Kawase et al.
10/23/85	Jap.	JP 85210576 A2/ JP 60210576	Basic Monolithic Refrs. Containing Carbon [Al & Si in, Coated with Silane]	E. Maeda et al.
12/24/87	Jap.	JP 87297272 A2/ JP 62297272	Castable Refr. Compns. Cont. Self-Curing.. [Incl. Spinels, Cont. Resorcinol Resin]	H. Sugimoto et al.
12/24/87	Jap.	JP 87297273 A2/ JP 62297273	(Same Title as Above) [Resorcinol Resin & Alk. Earth Hydroxides]	H. Sugimoto et al.
09/15/88	USSR	SU 1423543 A1	Manufacture of Refractory Articles [Forsterite-Graphite Castable]	U.B. Ashimov et al.

Zirconium-Containing Bricks (incl. composites)

11/25/79	USSR	SU 698959	Charge for Manuf. Refractory Articles [Zircon, with Na Methylsilicone, Al & Cr Oxychlorides]	G.D. Semchenko et al.
04/10/87	Jap.	JP 8778151 A2/ JP 6278151	Unfired Refr. Bricks for Molten Metal... [Zircon-Roseki (Pyrophyllite) Mixtures]	K. Shimada et al.
03/16/88	Jap.	JP 8860151 A2/ JP 6360151	MgO-ZrO_2 Refr. Bricks of Exc. Th. Shock... [Thermal Shock-Resistant Formulations]	S. Uto et al.
05/21/88	Jap.	JP 88117950 A2/ JP 63117950	Manuf. of Refr. Bricks for Slide Gates... [Mullite-Baddeleyite & with Carbon]	A. Okamoto et al.
09/20/88	Jap.	JP 88225575 A2/ JP 63225575	Zircon-Based Refractory Bricks [Alone & with Cr_2O_3 or Silica, for Ladles]	M. Sakaguchi et al.
10/27/88	Ger.	DE 3736680 C1	Manuf. of C-Bonded Refr. Articles [Alumina-Mullite-Zirconia Brick, with Cellulose Fiber, Resol Phenolic & Epoxy Resins, Pitch or Tar, & Carbon (Soot)]	U. Hintzen et al.
12/29/88	Ger.	DE 3720460 A1	Manuf. of Fired Zr Silicate-Cont. MgO... [For High Thermal Shock Resistance]	T. Weichert

Zirconium-Containing Castables (incl. composites)

09/18/81	Fr.	FR 2478071 A1	Cast Refrs. of the Cr Oxide-Alumina-ZrO_2 Type Cont. Fe Oxide as Stabilizer... [For Glass Furnaces]	P. Jeanvoine et al.
04/01/83	Jap.	JP 8355368 A2/ JP 5855368	Phosphate-Bonded Siliceous Refr. Castables [Roseki & Zircon with Metaphosphate & CA]	Anon.
03/23/85	Jap.	JP 8551673 A2/ JP 6051673	Castable Refractories [Ultrafine Zircon Refr., CA Cmt, & Defloc.]	Anon.
06/20/86	Jap.	JP 86132565 A2/ JP 61132565	Refractory for Glass-Melting Tanks [A-Z-S, for Melting Tank Bottom Lining]	Anon.

Zirconium-Containing Castables, continued

02/23/87	Jap.	JP 8741771 A2/ JP 6241771	Prev. of Cracking & Spalling of Amorph.... [Size-Controlled Zircon Aggregate]	M. Kuwayama
05/16/87	Jap.	JP 87105970 A2/ JP 62105970	Castable Refractories [Al_2O_3-SiC, Cont. C Fibers, C, & ZrO_2]	K. Sato et al.
07/14/87	Jap.	JP 87158170 A2/ JP 62158170	Castable Refractory for Torpedo Car [Zircon-SiO_2-SiC-Graphite, Silicate Bond]	S. Miyagawa et al.
09/01/87	Jap.	JP 87197358 A2/ JP 62197358	Low-Sweating, White, A-Z-S Castable... [Refined Feed Materials]	S. Endo et al.
05/09/88	Jap.	JP 88103869 A2/ JP 63103869	Zirconia-Based Monolithic Refractories [Monoclinic ZrO_2 Refrs., with CA Cmt]	S. Kuwabara et al.
10/20/88	Jap.	JP 88252971 A2/ JP 63252971	Castable Monolithic Zircon-Based Refr.... [Zircon & Clay, for Ladle Lining]	H. Yaoi et al.

Nonoxide-Based Refractories

12/16/82	Jap.	JP 82205358 A2/ JP 57205358	Castable Refractories [SiC, with Novolak Phenolics & Polyisocyanates]	Anon.
02/16/83	Jap.	JP 8326079 A2/ JP 5826079	Refr. Castables with High Str. at High T [SiC-Based, with Sr Aluminate & Silica Bonds]	Anon.
08/14/84	Jap.	JP 84141463 A2/ JP 59141463	Refractory Castables [AlN Grain, with Aluminous Cement]	Anon.
10/29/86	Jap.	JP 86242963 A2/ JP 61242963	Manuf. of Refr. Fiber-Reinf. Ceramics [SiC, Reinf. by W Fiber & Refr. Wire: CVD]	M. Kayane et al.
05/26/87	U.S.	US 4668583 A	Refractory Coating [Coatings of Carbides of Hf, Si, Ta, Zr on Carbon Substrates]	D.E. Olander
03/23/88	Jap.	JP 8864979 A2/ JP 6364979	Monolithic Refractories [ZrB_2, Bonded with Alumina Cement]	S. Sakamoto
06/24/88	Jap.	JP 88151660 A2/ JP 63151660	Mag- & C-Based Bricks for Linings of Vac.... [Graphite-Based, Bonded with Phenolic Resins]	S. Uto et al.
09/06/88	U.S.	US 4769348 A	Fabric. of Refr. Insul. Matls. Consisting of a Carbon Matrix Cont. Dispersed... [Cellular Carbon, SiC or Si_3N_4 in Voids]	T.P. O'Holleran

POROUS AND INSULATING REFRACTORIES

DATE	PATENT	TRUNCATED TITLE	FIRST
Mo/Da/Yr	NUMBER	[PRINCIPAL FEATURE]	AUTHOR

Cellular Bricks: Burnout Processes

04/13/78	Ger.	DE 2543944	Ceramic Light Construction Material [Cellulose Wastes in Manuf. of]	U. Hoffmann
06/29/78	Jap.	JP 7873211	Porous Refractory Materials [Alumina, Nylon Fiber Strings in]	T. Kanemaru et al.
02/08/80	Jap.	JP 8018556	Refr. Porous Plug for Blowing of Gases... [MgO, with Carbon Black and Si Powder]	S. Oishi et al.
06/18/80	Brit.	GB 1569559	Improved Refractory Compositions [Mullite, Using Wood Flour & Polystyrene]	G.K. Sargeant et al.
07/08/82	Ger.	DE 3046791 A1	Porous Ceramic Products [Grog & Clay with Naphthalene Particles]	I. Gottsch
12/15/82	USSR	SU 981293 A1	Charge for Prod. Lightweight Refrs. [Alumina with Chalk, Pitch Coke, & Naphthalene]	Y.Z. Shapiro et al.
11/29/83	Jap.	JP 83204858 A2/ JP 58204858	Heat-Insulating Lightweight Refr. Matls. [Grog & Clay with Sawdust & Waste Oxid. Al]	Anon.
06/25/84	Pol.	PL 122885	Insulating Inserts and Tops [Alumina-Silica, with C & Sawdust]	L. Lukwinski et al.

Cellular Bricks: Burnout, continued

12/31/85	Braz.	BR 8402543 A	Low-Density Insulating Refractory [Using Aluminous Cement Bond]	P. Cordeiro
01/14/87	Jap.	JP 8707664 A2/ JP 6207664	Calcareous Refractories [Dolomitic Limestone & Acrylic Emulsion]	K. Ichikawa et al.
04/07/88	Jap.	JP 8876813 A2/ JP 6376813	Porous Refr. Plug for Gas Blowing [Silica Brick, Permeable]	H. Kano et al.
07/09/88	Jap.	JP 88166752 A2/ JP 63166752	Refractories for Gas Bubbling in Molten... [A-Z-S Compositions]	H. Kano et al.
09/20/88	Jap.	JP 88225587 A2/ JP 63225587	Porous Refr. Prods. Having...Pierced Holes [Fugitive Tubular Hole-Formers]	Y. Ozaki et al.

Cellular Brick: Foams and Reticulated Foams

10/15/76	Czech.	CS 165132	Light-Weight Refractory Material [Clay-Alumina with Polystyrene Spheres]	J. Hejda et al.
02/02/79	Belg.	BE 873918	Refractory Compositions [Alumina, with Hollow Polystyrene Spheres]	Anon.
02/06/80	Brit.	GB 1560651	Impr. in or Rel. to Foamed Refr. Matl. [Cellular Si_3N_4 etc., Polyurethane Binder, Foaming]	K.R. Cottell et al.
03/10/81	U.S.	US 4255197	Refr. Matls. with Controlled Por. & Dens. [Alumina, MgO, CA Cmt; Polyethylene, Polystyrene Expanded Beads]	A. Peralta et al.
07/27/82	U.S.	US 4341561 A	Foamed Insulating Refractory [Clay, Foaming by Phosphoric Acid]	J.M. Britt et al.
04/25/83	Pol.	PL 116443 B1	Corundum Insulating Articles [With Kaolin, Foaming by Al Sulfate & Glue & Sod. Resinate]	A. Machalica et al.
11/05/84	Belg.	BE 900093 A1	Lightweight Refractory Brick [Al Hydroxychloride Binder in, Rapid Setting]	Anon.
10/31/85	Ger.	DE 3445484 C1	Refr. or Fire-Resist. Lightweight... [Grog, Kaolin, Synth. Fibers; with Sod. Sulfonate Foaming Agent]	U. Hintzen
09/30/86	Jap.	JP 86219774 A2/ JP 61219774	Lightweight Refr. Structural Matls.... [Alumina, CA Cemented, Froth-Foamed]	Y. Sasagawa et al.
06/16/88	Ger.	DE 3642201 C1	Refr. Filter for...Molten Metals [Coarse-Cellular]	L. Doetsch et al.

Cellular Bricks: Lightweight Minerals and Various Processes

11/15/76	USSR	SU 535254	Charge, Cont. Electrocorundum & Kaolin, for Producing Porous Refractories [With Cr_2O_3 & Manganese Carbonate]	E.I. Chelnokov et al.
11/07/80	USSR	SU 777018	Charge for a Refractory Material [With Al Fluoride, Ethyl Silicate]	I.I. Nemets et al.
02/15/82	USSR	SU 830711 A1	Refr. Light-Weight Aluminophosphate... [For Thermal Insulation]	A.N. Abyzov
04/30/82	USSR	SU 923997 A1	Composition for Prod. Ltwt. Refr. Matl. [Hollow Alumina Spheres, Num. Binders]	G.V. Efimov et al.
06/15/82	USSR	SU 935493 A1	Charge for Prod. Lt.-Wt. Refr. Prods. [Sulfite Liquor & Poly(Vinyl Alc.)]	V.S. Korshunov et al.
07/13/84	Jap.	JP 84121146 A2/ JP 59121146	Refrs. Cont. Hollow Alumina Spheres [Conventional Binders]	Anon.
11/05/84	Belg.	BE 900094 A1	Lightweight Refractory Brick [Vitreous Silica and Montmorillonite]	Anon.
11/07/84	USSR	SU 1122639 A1	Charge for Prod. Lt.-Wt. Refr. Matl. [Kaolin in, for Thermal Shock Res.]	Y.I. Goncharov et al.
01/21/85	Jap.	JP 8511263 A2/ JP 6011263	Basic Refrs. Having Low Ther. Conduct. [ZrO_2-Forsterite, for Rotary Cmt Kiln]	Anon.

Cellular Bricks, continued

03/06/85	Jap.	JP 8542284 A2/ JP 6042284	Lightwt. Refr. Blocks with High Strength [Grog and Kaolin]	Anon.
04/23/86	Eur.	EP 178837 A2	Low-Density Phos.-Bonded Spinel Refrs. [For Strength & Ther. Shock Resist.]	A.J. Cisar
06/24/86	Jap.	JP 86136971 A2/ JP 61136971	Manufacture of Porous Refractories [Alumina Grain, Ultrasonic Solidif.]	S. Takeshita et al.
02/28/87	USSR	SU 1293158 A1	Raw Mixture for Prod. Refr. Ltwt. Matl. [From Gibbsite and Superphosphate]	L.A. Sheinich
07/01/87	E.Ger.	DD 247209 A1	Reinf. of Porous Ceram. by...Silicic Ac. [Cordierite-Mullite & Colloidal Silica]	F. Michaelis et al.
12/30/87	Rom.	RO 93127 B1	Manuf. of Refr. Thermal Insulators [Clay-Alumina and Aluminous Cement]	G. Popa et al.
05/02/88	Jap.	JP 88100084 A2/ JP 63100084	Inorg. Matls. & Their Manuf. for Ltwt.... [Ltwt. Minerals, Alkoxide Binders]	T. Otoma et al.

Cellular Insulating Castables

02/03/77	Ger.	DE 2632422	Light Wt. Refr. Matls. Based on Si-Oxy-N. [Cont. Si_3N_4 and Cristobalite]	M. Washburn et al.
08/25/78	USSR	SU 620462	Highly-Refr. Cold-Setting Ltwt. Matl. [ZrO_2 & Al_2O_3 with Al-Cr Phosphate]	E.P. Karpinos et al.
02/13/80	Jap.	JP 8020238	Lightweight Castable Refractories [Waterproofing with Siloxanes]	E. Horie et al.
09/09/80	U.S.	US 4221595	Insulating Hot Topping Material [Ltwt. Minerals with Fly Ash, Coke]	G.R. Zebrowski
10/21/81	Jap.	JP 81134552 A2	Aggregate with Low Water Absorption [Coating with Polyacrylic Emulsions]	Anon.
12/23/82	Jap.	JP 82209890 A2/ JP 57209890	Heat-Insulating Refractory Castables [Clay, Aluminous Cmt, Na Pyrophosphate]	Anon.
10/15/83	Jap.	JP 83176181 A2/ JP 58176181	Refr. Castables with Impr. Ht. Insul.... [Alumina, CA Cmt, & Water-Absorbing Resin]	Anon.
05/30/85	Jap.	JP 8596579 A2/ JP 6096579	Expanding Castable Refractories [Alumina-Bauxite Expanding Mix]	Anon.
11/28/85	Jap.	JP 85239370 A2/ JP 60239370	Heat Insulating Castable Refractories [Grog, Pumice, Fly Ash, Binders]	K. Ishimaki
01/17/86	Jap.	JP 8610079 A2/ JP 6110079	Castable Refractories [Fugitive Polymer Fibers in]	Y. Owada et al.
02/05/87	Jap.	JP 8727359 A2/ JP 6227359	Refractory Coating Compositions [Gibbsite, Glass, and Cement]	S. Nagashitani et al.
02/17/87	Jap.	JP 8736063 A2/ JP 6236063	Manuf. of Heat-Insulating Refractory [Flame Spray/Castable: Silicon Metal]	E. Yorita et al.
04/01/87	E.Ger.	DD 244336 A1	Method for the Manuf. of Refr. Prods. [Cont. Kaolin; Foamed with H_3PO_4]	D. Melzer et al.
02/16/88	Jap.	JP 8835462 A2/ JP 6335462	Manuf. of Castable Refractories [Hollow Sphere Aggregate]	K. Sato et al.

Refractory Fibers

03/15/80	Czech.	CS 182471	Batch for the Manuf. of Refr. Fibers [Al Silicate, Cont. Alkali & Ca,Mg Oxides]	V. Havranek et al.
12/23/82	USSR	SU 983095 A1	Refractory Fiber [Aluminosilicate, Cont. Alkali Oxide]	I.G. Subochev et al.
03/07/83	USSR	SU 1002762 A1	Refractory Fiber [Aluminosilicate]	I.G. Subochev et al.
07/07/83	PCTI	WO 8302291 A1	Inorganic Oxide Fibers [Spinning High-Alumina Fibers]	R. Bray
08/07/83	USSR	SU 1033487 A1	Produc. of Refr. Ht. Insul. from Fibrous... [Treatment with Cr Compounds]	M.N. Sorin et al.

Refractory Fibers, continued

03/21/84	Brit.	GB 2126210 A1	Aluminosilicate Fibers [Alumina-Chromia-Silica]	M. Yamamoto
05/22/85	Brit.	GB 2147925 A1	Coating of Mineral Fibers [Chromium Oxide on Aluminosilicates]	A. Briggs et al.
08/06/85	U.S.	US 4533508 A	Metal Oxide Fibers from Acrylate Salts [MgO Fiber from Mg Acrylate & Polymer]	R.R. Stevens
10/21/85	Jap.	JP 85209016 A2/ JP 60209016	Refractory Ceramic Composite Fibers [Aluminosilicate Based]	A. Ito et al.
10/07/86	Jap.	JP 86225318 A2/ JP 61225318	Alumina Fibers [From Org. Polyaluminoxanes, Spinning]	A. Yamane et al.
11/11/86	U.S.	US 4622307 A	Low Shrinkage Kaolin Refractory Fiber [From Kaolin and Zircon]	W.C. Miller et al.
01/14/87	Eur.	EP 208506 A1	Mg Aluminate Fiber Composition & Proc.... [Zr Chloride-Doped; Carriers & Stabil.]	S.L. Dahar et al.
03/22/88	U.S.	US 4732878 A	Oxid.-Resist. C-Cont. Alumina-Silica... [Composite Vitreous Fibers for Emissivity]	G.F. Everitt et al.

Insulating Fiber Products

08/09/79	Ger.	DE 2900225	Refr... Heat-Insul. Prods. Based on...Fibers [Clay & Mineral Wool, Phosphate Bonded]	Anon.
05/27/80	U.S.	US 4205032	Rigid Articles of Refractory Fibers [Alumina-Zirconia, by Impregnation]	H.G. Emblem et al.
10/30/81	Fr.	FR 2481263 A1	Use of Refr. Fibers...as Acid-Resist... [Aluminosilicate, for Effluent Stacks]	J.H. Chatillon et al.
05/15/82	Pol.	PL 113696 B1	Manuf. Molded Articles...by Vac. Form. [Fiber Pipes, Plugs, etc.]	M. Chrzeszczyk et al.
05/27/82	Belg.	BE 892072 A1	Molded Articles Having a High Th. Stabil.... [Bricks, for Rotary Kiln Expansion Joints]	Anon.
10/04/83	U.S.	US 4407969 A	Flexible Refractory Composition [Flexible Aluminosilic. Mold Liners, etc.]	J. Widener et al.
05/29/84	Jap.	JP 8492982 A2/ JP 5992982	Refr. Fiber Comps. Having Small Shrinkage [Alumina & Aluminosilicate Fiber Felts]	Anon.
05/29/85	Eur.	EP 142715 A2	Insulation System [A-Z-S Fibers, Spraying with Phos. Binder]	W.H. Smith
11/12/85	U.S.	US 4552804 A	Prevention of SiO_2 Migration in...Insul.... [Anhydrous Inorg. Acid Treatment of Fibers]	C.C. Payne
04/01/86	Jap.	JP 8663553 A2/ JP 6163553	Heat Insulating Refractories [Mixed Titanate Fibers, Insul. Mats from]	H. Inui et al.
08/04/86	Jap.	JP 86172847 A2/ JP 61172847	Basic Aluminum Lactate [Binder for Alumina Fibers]	K. Sunahara et al.

Fiber/Ceramic Composite Products

06/30/82	Brit.	GB 2089782 A	Refr. & Heat-Insul. Fibrous Compositions [Castable, Cont. Fibers & Org. Dispersant]	S. Sakurai et al.
05/22/84	Jap.	JP 8488378 A2/ JP 5988378	Lightwt. Refractory and Its Preparation [Alumina & Alumina-Silica Fiber Products]	Anon.
04/04/85	Ger.	DE 3331850 A1	Refractory Composite Blocks or Bricks [Alumina Fiber with Alumina Particulate]	K. Lepere
08/22/85	Ger.	DE 3406024 A1	Castable Refractories [Fiber & Aggregate, with Pore Formers and Phosphate, Silicate, & Org. Binders]	A. Hehl
10/15/85	USSR	SU 1184838 A1	Charge for Prod. Lightwt. Refr. Matl. [Dinas Brick, Filler, Quartz Fiber, and Silica Gel]	A.A. Dabizha et al.
01/11/86	Jap.	JP 8606170 A2/ JP 6106170	Refractory Heat-Resistant Block [Titanate Fibers with Alumina Powder]	A. Watanabe et al.

Fiber/Ceramic Composite Products, continued

04/21/86	Jap.	JP 8677675 A2/ JP 6177675	Castable Thermal Insulators [Alumina & Mullite Aggregate, Fiber, CA Cement: Moldable, Slip-Cast]	Y. Kobayashi et al.
04/21/87	U.S.	US 4659679 A	Insul. Comp. & Method of Making Articles... [Fibers with Refr. from Rice Hulls, CA Cmt]	R.A. Falk
08/21/87	Jap.	JP 87191485 A2/ JP 62191485	Porous Refr. Matl. with Exc. Ht. Resist. [Zirconia/Zirconia Fiber Coating Over Porous Alumina-Silica Fiber Mat]	K. Nagaya et al.
09/23/87	Eur.	EP 237609 A1	Castable or Moldable Insul. Refrs. for the Containment of Molten Metals [Borosilicate Coating for Non-Wetting]	D.J. Bray et al.
09/24/87	Jap.	JP 87216974 A2/ JP 62216974	Lightwt. Porous Refr. with ZrO_2 Coating [Zirconia Powder & Binder Coating for Cellular or Fiber Refractory Articles]	A. Ito et al.
10/28/87	Jap.	JP 87246881 A2/ JP 62246881	Fiber-Based Porous Refractory Materials [Alumina Fiber with Porous Refr. Aggregate, Org. Polymer Binders]	Y. Fujii et al.
12/09/87	Jap.	JP 87283885 A2/ JP 62283885	Porous Fiber-Reinf. Refrs. with...Coating... [Alumina-Based Coating, Low Permeability]	A. Ito et al.
01/07/88	Jap.	JP 8802869 A2/ JP 6302869	Adiabatic Castable Refractories [Alumina Fiber & Rods in Var. Castables]	M. Yoshimura et al.
05/17/88	Jap.	JP 88112477 A2/ JP 63112477	Heat-Resistant Inorganic Fiber Products [Molding of Alumina with Aluminosilicate Fibers, Kieselguhr, Var. Binders]	A. Ito
05/17/88	Jap.	JP 88112478 A2/ JP 63112478	Manuf. of Heat-Resist. Inorg. Fiber Prods. [Companion of Preceding Patent]	A. Ito
07/20/88	Brit.	GB 2199823 A1	Refr. Cmt. Comps., & Modules for... Furn... [Formable & Sprayable Fiber-Cement Mixes]	H. Emblem et al.
08/12/88	Fr.	FR 2610622 A1	Surface Hardening of Ceramic Articles Made from Refractory Fibers [Coating & Firing]	A.J. Farina
11/23/88	Eur.	EP 291656 A1	Molded Refr. Prods. Having Density Less than 2.0 g/cm^3, & Their Manufacture [Numerous Ceramic, Fiber, and Binder Components, Flocculating Agents and Porosity Generators]	M. Rausch et al.

Index